

ANGULAR MOMENTUM

ANGULAR MOMENTUM

An Illustrated Guide to Rotational Symmetries for Physical Systems

WILLIAM J. THOMPSON

University of North Carolina
Chapel Hill, North Carolina



**WILEY-
VCH**

WILEY-VCH Verlag GmbH & Co. KGaA

All books published by Wiley-VCH are carefully produced. Nevertheless, authors, editors, and publisher do not warrant the information contained in these books, including this book, to be free of errors. Readers are advised to keep in mind that statements, data, illustrations, procedural details or other items may inadvertently be inaccurate.

Library of Congress Card No.:

Applied for

British Library Cataloging-in-Publication Data:

A catalogue record for this book is available from the British Library

Bibliographic information published by

Die Deutsche Bibliothek

Die Deutsche Bibliothek lists this publication in the Deutsche Nationalbibliografie; detailed bibliographic data is available in the Internet at <<http://dnb.ddb.de>>.

© 1994 by John Wiley & Sons, Inc.

© 2004 WILEY-VCH Verlag GmbH & Co. KGaA, Weinheim

All rights reserved (including those of translation into other languages). No part of this book may be reproduced in any form – nor transmitted or translated into machine language without written permission from the publishers. Registered names, trademarks, etc. used in this book, even when not specifically marked as such, are not to be considered unprotected by law.

Printed in the Federal Republic of Germany

Printed on acid-free paper

Printing Strauss GmbH, Mörlenbach

Bookbinding Litges & Dopf Buchbinderei GmbH, Heppenheim

ISBN-13: 978-0-471-55264-2

ISBN-10: 0-471-55264-X



CONTENTS

Preface	xi
The Computer Interface	xiii
1 Symmetry in Physical Systems	1
1.1 Symmetries and invariances 1	
1.1.1 Symmetries and conservation laws 2	
1.1.2 Noether's theorem and Curie's principle 5	
1.2 Spatial symmetries 7	
1.2.1 Reflection symmetry in nature 8	
1.2.2 Translation symmetries; mosaics and crystals 10	
1.3 Rotational symmetries 12	
1.3.1 Active and passive rotations; Euler angles 13	
1.3.2 Coordinate systems for rotations 17	
1.3.3 Angular momentum and rotations: a cameo portrait 19	
1.4 Discrete symmetries and quantum systems 21	
1.4.1 Parity symmetry 22	
1.4.2 Charge conjugation and time reversal 25	
1.4.3 Maxwell's equations and <i>PCT</i> 30	
1.4.4 <i>PCT</i> and the Pauli principle: Lüder's theorem 32	
1.5 Broken symmetries from cosmetology to cosmology 34	
Problems on symmetry in physical systems 36	

2	Mathematical and Quantal Preliminaries	41
2.1	Matrix definitions and manipulations 42	
2.1.1	Linear spaces and operator matrix elements 42	
2.1.2	Inner and direct products of matrices 45	
2.1.3	Operations on matrices, and special properties 50	
2.1.4	Phase manipulation rules 52	
2.2	Transformations and operators 53	
2.2.1	Similarity and symmetry transformations 53	
2.2.2	Unitarity: its interpretation in quantum mechanics 57	
2.2.3	Operator exponentials and commutators 58	
2.2.4	Raising and lowering operators 59	
2.3	Eigenvalues and eigenstates 63	
2.3.1	Eigenvalues of operators and matrices 63	
2.3.2	Diagonalizing matrices 64	
2.3.3	Eigenvectors as basis states 66	
2.4	Spinors and their properties 67	
2.4.1	Definitions of spinors 67	
2.4.2	Representing spinors; rotations 69	
2.4.3	Objects that distinguish turns though 2π and 4π 72	
2.5	A primer on groups 72	
2.5.1	Group examples and definitions 73	
2.5.2	Group theory terminology 79	
2.5.3	Representations of groups 80	
2.5.4	Interesting groups and their uses 84	
2.5.5	Irreducibility of a representation 88	
2.6	Mathematics, groups, and the physical sciences 89	
	Problems on mathematical and quantal preliminaries 90	
3	Rotational Invariance and Angular Momentum	95
3.1	Infinitesimal rotations; the J operators 95	
3.1.1	Schemes for describing rotations 96	
3.1.2	Commutation relations of J operators 97	
3.1.3	The spherical-basis operators \mathbf{J}_{+1} , \mathbf{J}_0 , \mathbf{J}_{-1} 99	
3.2	Orbital angular momentum operators 100	
3.2.1	Infinitesimal rotations applied to spatial functions 100	
3.2.2	Components of L in spherical polar coordinates 103	
3.2.3	The special role of the operator L_z 105	
3.3	Other representations of J operators 105	
3.3.1	The 2×2 matrix representation: Pauli matrices 105	
3.3.2	Eigenvectors of the Pauli matrices 108	
3.3.3	Finite rotations and Pauli matrices 109	
3.3.4	Spinor space and its operators 111	
3.4	Angular momentum eigenvalues and matrix elements 113	
3.4.1	Eigenvalues of \mathbf{J}^2 and J_z ; irreducibility 113	
3.4.2	Matrix elements in the spherical basis 116	
3.4.3	Matrix elements in the Cartesian basis 117	
3.4.4	Operator matrices for $j = 1/2, 1$, and $3/2$ 119	
3.4.5	Angular momentum: geometrical and dynamical 120	

3.5	Reference frames: spin and orbital angular momenta	122
	Problems on rotational invariance and angular momentum	124
4	Angular Momentum Eigenstates	127
4.1	Orbital eigenstates and spherical harmonics	127
4.1.1	Legendre functions and their properties	129
4.1.2	Displaying Legendre functions; polar diagrams	131
4.1.3	Calculating and visualizing spherical harmonics	135
4.1.4	Solid harmonics and other variants	143
4.2	Spherical-basis vectors and angular momentum in a field	149
4.2.1	Vectors in the spherical basis	150
4.2.2	Infinitesimal rotations of vectors	152
4.2.3	The electromagnetic field and photons	155
4.3	Spin eigenstates and their representations	156
4.3.1	What is spin?	156
4.3.2	Intrinsic spin eigenstates	160
4.3.3	Spinor-space representations	162
4.3.4	Time reversal and spin	163
	Problems on angular momentum eigenstates	165
5	Angular Momentum in Quantum Systems	169
5.1	Rotational symmetry and dynamical angular momentum	170
5.1.1	Angular momentum and the role of Planck's constant	170
5.1.2	Classical angular momentum: Ehrenfest theorems	172
5.1.3	Larmor precession in magnetic fields	175
5.2	Uncertainty relations for angular momentum	179
5.2.1	Heisenberg uncertainty relations for quantum systems	180
5.2.2	Angular momentum uncertainties	183
5.2.3	Uncertainties between angular momentum and angles	186
5.3	The semiclassical vector model	189
5.3.1	Constructing the vector model of angular momentum	190
5.3.2	Uses and limitations of the vector model	192
5.4	Angular momentum and wave mechanics	193
5.4.1	Plane waves and centripetal barriers; Bessel functions	193
5.4.2	Displaying partial-wave expansions	199
5.5	The conceptual development of angular momentum	203
	Problems on angular momentum in quantum systems	206
6	Finite Rotations of Angular Momentum Eigenstates	211
6.1	Introduction to rotation matrices	211
6.1.1	Review of rotations and angle schemes	212
6.1.2	Group and factorization properties of rotations	213

- 6.2 Determining rotation matrices 213
 - 6.2.1 Rotation of eigenstates about z axes 214
 - 6.2.2 Rotations about the y axis for $j = 1$ 216
 - 6.2.3 Constructing \mathbf{d}^j from spinor representations 218
 - 6.2.4 Relation of \mathbf{d}^j elements to other functions 220
 - 6.2.5 Computing reduced rotation matrix elements 222
- 6.3 Interpreting rotated states 224
 - 6.3.1 Orbital angular momentum states 225
 - 6.3.2 Transformation amplitudes for arbitrary j 227
 - 6.3.3 Visualizing rotation matrix elements 230
- 6.4 Properties of rotation matrices 232
 - 6.4.1 Symmetry properties of \mathbf{d}^j and \mathbf{D}^j 232
 - 6.4.2 Unitarity and orthogonality properties 234
 - 6.4.3 Classical limits of rotation matrices 236
 - 6.4.4 Spherical harmonics as rotation matrix elements 239
- 6.5 Rigid-body rotations in quantum mechanics 240
 - 6.5.1 The \mathbf{D}^j as angular momentum eigenfunctions 241
 - 6.5.2 The Hamiltonian of a rigid rotator 242
 - 6.5.3 Rotational states of molecules and nuclei 245
- Problems on finite rotations of angular momentum eigenstates 247

7 Combining Two Angular Momentum Eigenstates 251

- 7.1 The semiclassical vector model for addition 252
 - 7.1.1 Vector-addition construction 252
 - 7.1.2 Triangle and projection selection rules 253
 - 7.1.3 Interpreting coupling: spin-orbit interaction 255
 - 7.1.4 Degeneracy of energy states in the Coulomb potential 258
- 7.2 Coupling coefficients: definitions and general properties 263
 - 7.2.1 Combining two angular momenta: Clebsch-Gordan coefficients 264
 - 7.2.2 Unitarity of Clebsch-Gordan coefficients 264
 - 7.2.3 Determining coefficients from spinor representations 266
- 7.3 The $3-j$ coefficients and their properties 269
 - 7.3.1 Three angular momenta coupled to zero; $3-j$ coefficients 269
 - 7.3.2 Visualizing symmetry properties 276
 - 7.3.3 Classical limits of $3-j$ coefficients 278
 - 7.3.4 Expressions for one angular momentum small 280
- 7.4 Computing coupling coefficients 280
 - 7.4.1 Tabulations of coupling coefficients 281
 - 7.4.2 Computing $3-j$ coefficients efficiently 282
- 7.5 Rotation matrices and coupling coefficients 286
 - 7.5.1 Clebsch-Gordan series for combining D^j elements 286
 - 7.5.2 Special cases of Clebsch-Gordan series 288
 - 7.5.3 Integrals of rotation functions 292
 - 7.5.4 Examples: Celestial bodies and rotator matrix elements 295
- Problems on combining two angular momentum eigenstates 300

8	Irreducible Spherical Tensors and Spin	305
8.1	Definition of irreducible tensor operators 308	
8.1.1	Defining irreducible spherical tensors 308	
8.1.2	Racah's definition and its applications 309	
8.2	Combining irreducible tensors 312	
8.2.1	Building up irreducible spherical tensors 312	
8.2.2	Contraction of irreducible tensors to scalars 315	
8.3	Wigner-Eckart theorem; reduced matrix elements 316	
8.3.1	Geometry and dynamics: The Wigner-Eckart theorem 317	
8.3.2	Conventions for reduced matrix elements 320	
8.3.3	Determining and using reduced matrix elements 320	
8.4	Density matrices and polarization tensors 325	
8.4.1	Spin density matrices and spin tensors 325	
8.4.2	Spin precession in magnetic fields: rotating frames 330	
8.4.3	Spin transport through magnetic field gradients 335	
	Problems on irreducible spherical tensors and spin 341	
9	Recombining Several Angular Momentum Eigenstates	345
9.1	Recoupling three angular momenta 345	
9.1.1	Racah and $6-j$ coefficients for three angular momenta 345	
9.1.2	Recoupling tetrahedra, quadrilaterals, and trees 348	
9.2	Formulas for $6-j$ coefficients 350	
9.2.1	Expansion in terms of $3-j$ coefficients 350	
9.2.2	Algebraic expressions for $6-j$ coefficients 352	
9.2.3	Tabulations of $6-j$ coefficients 354	
9.3	Properties of recoupling coefficients 354	
9.3.1	Orthogonality relations of $6-j$ coefficients 355	
9.3.2	Symmetries and special values of $6-j$ coefficients 355	
9.3.3	Computing $6-j$ coefficients efficiently 359	
9.4	Scalar products of irreducible tensors 361	
9.4.1	Factorization and projection theorems for tensors 361	
9.4.2	Matrix elements of multipole expansions 365	
9.4.3	Tensors in $L-S$ and $j-j$ coupling schemes 367	
9.5	Recoupling four angular momenta 370	
9.5.1	Definition and computation of $9-j$ coefficients 370	
9.5.2	Symmetries, special values, and sum rules of $9-j$ coefficients 374	
9.5.3	Tensor matrix elements in coupled schemes 376	
9.5.4	Transformations between $L-S$ and $j-j$ coupling 377	
9.5.5	Graphical and automated methods 380	
	Problems on recombining several angular momentum eigenstates 381	
	EPILOGUE	385
	APPENDIX I NOTEBOOKS FOR MATHEMATICA	387

APPENDIX II	NUMERICAL COMPUTER PROGRAMS IN C	407
C1	Program for reduced rotation matrix elements	410
C2	Program for 3- <i>j</i> coefficients	412
C3	Program for 6- <i>j</i> coefficients	415
C4	Program for 9- <i>j</i> coefficients	417
APPENDIX III	TABLES OF FORMULAS	421
T1	Legendre functions and spherical harmonics	421
T2	Rotation matrix elements	423
T3	The 3- <i>j</i> coefficients	425
T4	Irreducible spherical tensor operators	429
T5	The 6- <i>j</i> coefficients	431
T6	The 9- <i>j</i> coefficients	433
REFERENCES		437
INDEX		449



PREFACE

If a physical system has only internal interactions and if space is isotropic, then intrinsic properties of the system must be independent of its orientation and must be indistinguishable in all directions. From this fundamental rotational symmetry concept the theory of angular momentum has been developed into a sophisticated analytical and computational technique, especially when applied to quantum mechanics. I aim in this book to develop angular momentum theory in a pedagogically consistent way, starting from the geometrical concept of rotational invariance rather than from the dynamical idea of orbital angular momentum and its quantization. The latter approach, though hallowed by tradition, needlessly confuses quantum mechanics with geometry.

Topics are presented in an order so that new concepts are introduced and relevant formulas are derived in ways arising naturally in the treatment rather than by appealing to unfamiliar concepts or *ad hoc* methods. Modern notation and terminology are used in a geometric and algebraic approach. Some concepts of group theory are introduced and are related to this approach, but knowledge of group theory is not required. Those who plan to use continuous groups that are more abstract than the rotation group may thereby develop their insight and skills by practicing with rotations. I try to distinguish carefully results that depend only on rotational symmetry and are generally valid from those having their most fruitful interpretation from the viewpoint of quantum mechanics. Applications to quantum mechanics therefore usually appear toward the end of sections and chapters.

Although *Angular Momentum* is intended to be pedagogically self-contained, the treatment is not encyclopedic, since broad-ranging surveys of angular momentum theory and extensive tabulations of formulas are now available. There is also a

large research literature for further study, to which I direct you. Indeed, the field of angular momentum theory has become a mecca for algebraists. In this book, I prefer to emphasize concepts rather than techniques, because imagination is usually more important than knowledge, even in the sciences.

Visualization of objects and quantities being rotated is important for insightful and practical use of the concepts and methods of rotational symmetry. I therefore provide nearly 130 illustrations to help you understand what the mathematics is describing. If you have access to a computer software system combining mathematics and graphics, such as *Mathematica* or *Maple*, you too may explore such visualizations. There are 26 program notebooks—used to generate indicated figures in the text and for parts of the problem section at the end of each chapter—provided in Appendix I. Although written for *Mathematica* on an Apple Macintosh computer, they are readily adaptable to *Maple*.

Practical aspects are not neglected. For example, we discuss how to compute coupling coefficients efficiently, while computer programs for numerical evaluation of reduced rotation matrix elements and for $3-j$, $6-j$, and $9-j$ coefficients are given in Appendix II. These programs are written in the C language and are designed to be readily adaptable to Fortran and Pascal. Tables of formulas for practical reference are collected in Appendix III.

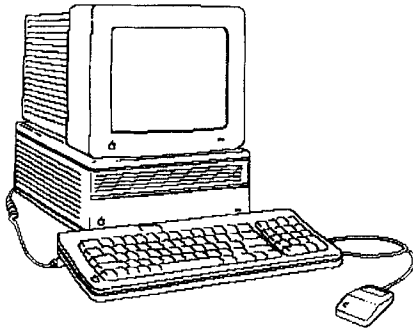
For use as a textbook, *Angular Momentum* assumes knowledge of mathematics through matrix algebra and differential equations, plus understanding of quantum mechanics usually acquired in one year of course work. Thus, I hope to make the subject of rotational symmetry accessible to advanced undergraduates in chemistry, physics, and mathematics. From several years experience of teaching courses using the materials in *Angular Momentum*, I have found that the book can readily be comprehended in less than a half year of course work, even when supplemented by detailed examples from the specific discipline in which it is taught. Emphasis is placed throughout on appropriate interpretation and use of derived results. To help with self-study and to test comprehension, 135 problems at the end of the chapters can be used to reinforce concepts and to improve skills.

Angular Momentum should provide suitable preparation for applications to research in the physical sciences—especially in physics, chemistry, and related areas of mathematical physics, such as group theory. Extensive references are given to material that is more advanced in concepts and techniques, as well as to applications of rotational symmetry aspects in research on physical systems.

Although a book may be the offspring of a single author, it has many midwives. A generation of students has helped me to refine my ideas on the subject, the U.S. Department of Energy unwittingly provided some financial support, while Ms. Word and Mac Intosh patiently retyped many drafts of the text and helped prepare the illustrations. Professors Louise Dolan and Charles Poole reviewed the manuscript and gave many suggestions for improvements. Greg Franklin and Bob Hilbert at Wiley-Interscience helped expedite the publication.

WILLIAM J. THOMPSON

Chapel Hill, February 1994



THE COMPUTER INTERFACE

The interface between angular momentum theory and computers occurs at two levels; conceptual and technical. At the conceptual level, computers are useful to visualize functions describing rotational symmetries and to produce algebraic formulas correctly and rapidly. At the technical level, we need algebraic and numerical results for functions describing these symmetries, and these results are obtained most efficiently by using computers.

Conceptual aspects of angular momentum that are helped by the interface to computers include illustration of angular momentum eigenstates (Section 4.1), of partial-wave expansions (Section 5.4), of rotation matrix elements and their classical limits (Sections 6.3 and 6.4), and of spin precession in magnetic fields (Section 8.4). Such visualizations are best produced interactively so that you can vary viewpoints and parameters in real time. These visualizations usually require computing algebraic (symbolic) expressions before numerical and graphical results are obtained.

The Mathematica Interface. The computer system we use for conceptual aspects of our treatment is *Mathematica*, a general-purpose system for doing mathematics by computer. It has convenient visualization capabilities and is available on many computers. In Appendix I we provide *Mathematica* programs in “notebook” form that are immediately usable on several small computers and on workstations. *Mathematica* is described in several books, such as Maeder’s [Mae91] and Wolfram’s [Wol91]. The programs are written to make them easy to translate to other programming environments, such as the *Maple* system for symbolic, numerical, and graphical computation. Introductions to *Maple* are provided in the book by

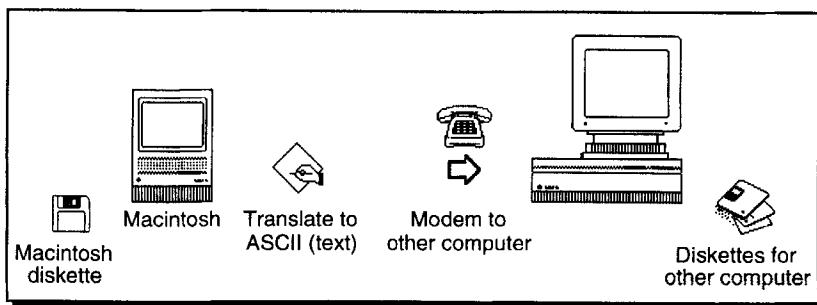
Char et al. [Cha92] and in Heck's book [Hec92]. Both *Maple* and *Mathematica* provide facilities for translating their symbolic output into C or Fortran code.

Technical aspects of rotational symmetries for physical systems typically require algebraic or numerical evaluation of functions describing eigenstates (Chapter 4), partial-wave expansions (Section 5.4), rotation matrices (Chapter 6), and coupling coefficients (Chapters 7 and 9). For exploratory use, the 26 *Mathematica* programs in Appendix I are suitable.

Problems at the end of each chapter that suggest using one of the *Mathematica* notebooks are indicated by a superscript **M**, such as 1.2^M.

The C Interface. For numerical computations, Appendix II has four programs of moderate efficiency for reduced rotation matrix elements and for $3-j$, $6-j$, and $9-j$ coefficients. These are coded in the C programming language, which is available on many computers. The C functions are intended to be incorporated into programs, so we provide just a small driver program that enables the functions to be checked for numerical correctness. If high efficiency is needed for computing coupling coefficients, then the discussions in Sections 7.4.2 (for $3-j$ coefficients), 9.3.3 (for $6-j$ coefficients), and 9.5.1 (for $9-j$ coefficients) will guide you to the technical literature.

The Program Diskette. All the *Mathematica* and C programs in Appendices I and II are provided on the diskette accompanying this book. The 3.5-inch double-density diskette can be read by Apple Macintosh computers, as well as by several other computers with appropriate hardware and software. A general-purpose way of translating from this diskette to diskettes for other computers is suggested in the following diagram.



First, read the Macintosh diskette provided, by using any Macintosh computer that is connected by modem to the other computer, then use the Macintosh to translate all the files on the diskette to ASCII text files. Next, transfer the files over a network to the other computer. Then, in this computer do any editing of the files that is needed to produce the correct format for *Mathematica* or C on that machine. Finally, make copies of the diskette for this computer system.



Chapter 1

SYMMETRY IN PHYSICAL SYSTEMS

The major topic of this book is the study of rotational symmetry applied to physical systems. The five sections in this chapter emphasize the relation between symmetries and invariances in dynamical systems (Section 1.1), the nature of spatial symmetries (Section 1.2), and particularly rotational symmetries (Section 1.3). In Section 1.4 we review the discrete symmetry operations—parity (P), charge conjugation (C), and time reversal (T)—all important in quantum mechanics. Here we also introduce the main ideas of the Pauli and Lüder PCT theorem, illustrating it with Maxwell's equations. The Pauli exclusion principle is also involved in these discussions, so we review what is known about the limits of its validity. Finally in this chapter, Section 1.5 is an excursion to look at symmetry and broken symmetries from cosmetology to cosmology.

After completing this chapter, especially if you work the problems at the end, you should have a good idea of the importance of symmetry properties for studying physical systems. In subsequent chapters we expand the concepts of this chapter, using the mathematics summarized in Chapter 2. We try throughout to distinguish considerations which are general and primarily geometrical from those which have their most fruitful applications in quantum mechanics and are primarily dynamical.

1.1 SYMMETRIES AND INVARIANCES

We begin by illustrating the relation of symmetry properties to invariances (conservation laws) of dynamical systems—using in Section 1.1.1 examples from nonrelativistic classical mechanics: linear momentum, total energy, and angular momentum. In Section 1.1.2 we discuss the generalization of these continuous symmetries to Noether's theorem, and we also discuss Curie's symmetry principle.

1.1.1 Symmetries and Conservation Laws

We present here examples of the relation between symmetries and conservation laws in the context of classical mechanics. In the following subsection these are generalized to Noether's theorem, which holds for a very wide range of continuous symmetries. What are the relations between symmetry properties of a physical system and conservation laws? To answer this, we consider the time dependence of integrals of the motion [Gol80] for several simple examples from nonrelativistic mechanics.

You should understand that the following examples are interesting because of relationships they illustrate between symmetries and conservation laws rather than because of any manipulative techniques their derivations require or because of the formal results. Indeed, you know the formulas already; it's the spin we put on them that matters. Therefore, most of the details are suggested as problems.

Momentum Conservation. Consider first the one-dimensional case of a single particle having momentum P in the x direction and moving in an *external* potential $V(x)$. Suppose that when we move the particle the potential is unchanged. The time rate of change of its momentum, \dot{P} , is then given by

$$\dot{P} = -\frac{dV}{dx} = 0 \quad \Rightarrow \quad P \text{ conserved} \quad (1.1)$$

This is fairly obvious, being an example of Newton's law of inertia.

Now consider—again in one dimension for simplicity—two particles interacting only through a *mutual* potential, $V(x_1-x_2)$, that depends only on their separation $x_{12} = x_1-x_2$, independent of the choice of origin, as shown in Figure 1.1. The total



FIGURE 1.1 If two particles interact through a mutual potential depending only on their separation x_{12} , independent of the choice of origin O , then the total momentum is conserved.

momentum of the two-particle system changes with time according to

$$\dot{P} = -\frac{dV}{dx_{12}} - \frac{dV}{dx_{21}} = 0 \quad \Rightarrow \quad P \text{ conserved} \quad (1.2)$$

This is just an example of Newton's law of action and reaction. If this system is moved as a unit through a displacement X so that

$$x'_1 = x_1 + X \quad x'_2 = x_2 + X \quad x'_{12} = x_{12} \quad (1.3)$$

then (1.2) will still hold and symmetry under spatial translation will also result in

conservation of momentum. The general case—three dimensions and a many-particle system interacting through two-body potentials satisfying the action-reaction condition—requires only technical competence with vector calculus, so we relegate it to Problem 1.1.

Total Energy Conservation. We again start with a simple example—motion of a single particle in one dimension. To consider the time evolution of the system we must assume that the particle is moving in a *time-independent* external potential, V , but now V may depend upon position x . For example, as hinted in Figure 1.2, the external potential may be gravity.

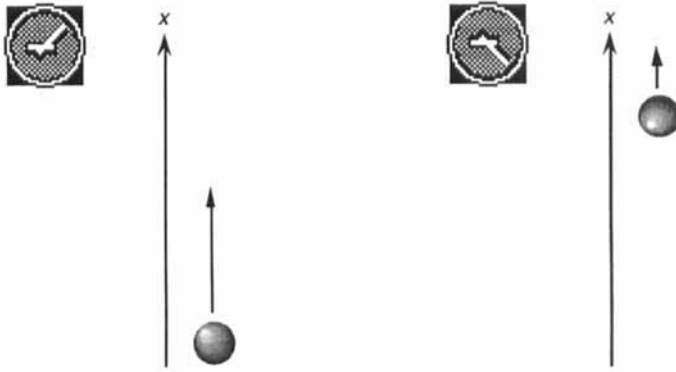


FIGURE 1.2 If a particle moves in an external time-independent potential that may depend on position x , such as gravity, its total energy is conserved.

The total energy of the particle, E , may be expressed as

$$E = \frac{1}{2} m \dot{x}^2 + V \quad (1.4)$$

Its energy therefore depends on time as

$$\dot{E} = m \dot{x} \frac{d\dot{x}}{dt} + \frac{dV}{dx} \dot{x} \quad (1.5)$$

By using Newton's force law, we can convert the first term into the negative of the second term, producing

$$\dot{E} = 0 \quad \Rightarrow \quad E \text{ conserved} \quad (1.6)$$

Thus, invariance of the potential energy under continuous time displacements pro-

duces conservation of total energy. To prove the general case in three dimensions with a many-particle system interacting through time-independent potentials is suggested in Problem 1.1.

Angular Momentum Conservation. We now turn to the topic of this book, considering the simplest case of mechanical angular momentum—a particle moving in an $x-y$ plane under a *central* potential with no explicit time dependence. This situation has $V(x, y, t) = V(r)$, where $r = \sqrt{x^2 + y^2}$. An example is that of a planet moving under the sun's gravitational attraction, as sketched in Figure 1.3.

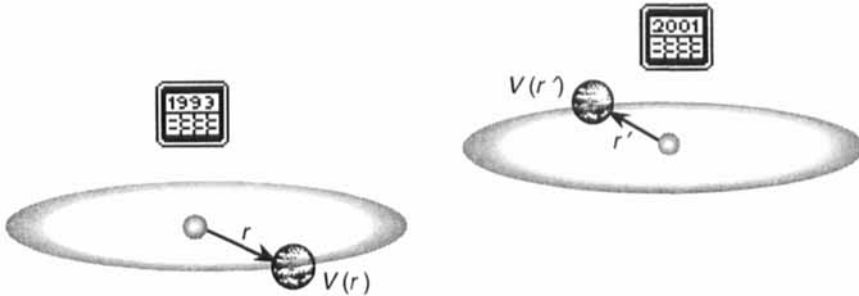


FIGURE 1.3 A planet moves under the sun's gravitational attraction, a central potential, so its angular momentum is conserved.

Note that the choice of the origin *is* important in this example, because the angular momentum depends upon the location of this reference point.

To calculate the time rate of change of the classical angular momentum, L_c , we need the derivatives

$$\frac{\partial V}{\partial x} = \frac{dV}{dr} \frac{dr}{dx} = \frac{x}{r} \frac{dV}{dr} \quad (1.7)$$

$$\frac{\partial V}{\partial y} = \frac{dV}{dr} \frac{dr}{dy} = \frac{y}{r} \frac{dV}{dr} \quad (1.8)$$

From the angular momentum of a particle moving in the $x-y$ plane,

$$L_c = m(xy\dot{y} - y\dot{x}) \quad (1.9)$$

we can readily calculate its time derivative as

$$\dot{L}_c = m \left(x \frac{d\dot{y}}{dt} - y \frac{d\dot{x}}{dt} \right) = m \left(-x \frac{\partial V}{\partial y} + y \frac{\partial V}{\partial x} \right) = 0 \quad (1.10)$$

In the second step of (1.10) we used Newton's force law, then we used (1.7) and (1.8) for the potential derivatives. We have found a conservation condition—the conservation of angular momentum. What is the symmetry condition?

If you look at the steps in the derivation of (1.10) you will see that the dependence of V on x and y —with these coordinates having equal footing, for example as they determine r —is the essential step leading to the zero in (1.10). Technically, we have assumed a Euclidean metric for the plane of the motion. Equivalently, if we performed a rotation of the plane about the same axis as the particle angular momentum, then the potential would be unaltered, since distance r rather than vector \mathbf{r} is the variable in V . Thus, the symmetry of rotational invariance of the potential leads to conservation of angular momentum of the particle. Generalization of this result for a particle in two dimensions to the result in three dimensions is suggested in Problem 1.1 and is discussed in Section 2.6 of [Gol80].

1.1.2 Noether's Theorem and Curie's Principle




We now consider two results that help organize one's thinking about symmetry in physical systems. The first, Noether's theorem, relating symmetries to conservation conditions, generalizes our examples in Section 1.1.1. It can be proved for a wide variety of systems, including classical mechanics, Maxwell's formulation of electrodynamics, and many systems (both discrete and continuous) that can be described by Lagrangians. The second result, Curie's principle—relating symmetry in causes to symmetry in effects—is just a principle, not a formal theorem.

Noether in a Nutshell. The examples in Section 1.1.1 of symmetries and their conservation laws illustrate Noether's theorem, which can be stated in nontechnical form as follows:

Noether's theorem. If a system has a continuous symmetry property, then there are corresponding quantities whose values are conserved in time.

Table 1.1 summarizes our examples of Noether's theorem on continuous symmetries and conservation laws. The examples given here can be generalized to classical mechanical systems described by Lagrangians expressed in terms of generalized coordinates. Our three examples in Table 1.1 thereby essentially collapse to a single example with different "coordinates." A proof of Noether's theorem that uses variational principles is provided in Section 2.6 of Goldstein's text on classical mechanics [Gol80]. Section 12.7 of the same text provides a more formal discussion of Noether's theorem for continuous systems and fields. Wigner [Wig27a] made similar derivations for quantum mechanics, which are more fully developed in Section IV.1 of Roman's text on elementary particles [Rom61].

TABLE 1.1 Examples of continuous symmetries of classical mechanical systems and their corresponding conservation laws, illustrating Noether's theorem.

Continuous symmetry		Conserved quantity
Spatial displacement (translation invariance)		Linear momentum
Time displacement		Total energy
Rotation about an axis		Angular momentum

Is there a converse to Noether's theorem? Is it true that if we observe conserved quantities in physical systems that there must be a related symmetry? One can construct counterexamples for special systems, but nowadays the persistent and widespread observation of conserved quantities, especially in subatomic systems, is usually taken to be a signal that there exists an underlying symmetry condition, if only we are able to find it.

Emmy Noether (1882–1935) was a leading mathematician of the early twentieth century, best known for her contributions to mathematics. Like the work of her mentor, Paul Gordan (known to physical scientists through the Clebsch-Gordan coefficients that we introduce in Section 7.2.1), Noether's work provided mathematical substance and depth to the concepts and techniques of physics. One tribute to her life and work is the biography edited by Brewer and Smith [Bre81], while another (written by her nephew) is in Grinstein and Campbell's collection of biographies of women of mathematics [Gri87].

In his essays on symmetry, Wigner—one of the founders of the use of symmetry principles in quantum mechanics and its applications—discusses [Wig67, Chapters 2 and 4] the historical development of ideas about symmetry and conservation laws. We take up this thread again in Section 5.5 when we trace the conceptual development of angular momentum.

Curie's Principle. In the pioneering investigations of piezoelectricity and pyroelectricity that he made with his brother Jacques, Pierre Curie enunciated [Cur94] the following guiding principle related to symmetry:

Curie's principle. The symmetry of an isolated system cannot decrease as the system evolves with time.

In the solid-state physics of crystals this is called *Neumann's principle*: Every point-group symmetry (Section 2.5.4) of a crystal is exhibited by every physical property of that crystal. Indeed, this is the context in which Curie first applied the

principle. Curie's principle has been generalized by Renaud [Ren35] and is discussed extensively in Section 6.2 of Rosen's primer on symmetries [Ros83].

There is no formal proof of the correctness of this principle, the major reason being that there is no quantifiable definition of the degree of symmetry of a system. However, Curie's principle is a very useful guide when investigating symmetries and their consequences.

Pierre Curie (1859–1906) made fundamental discoveries in three areas of physics: piezoelectricity, magnetism (the Curie temperature), and radioactivity. With his wife Marie (1867–1934), he discovered the elements polonium (named after her native Poland) and radium, both in 1898. They were awarded a Nobel Prize in 1903 for this work.

1.2 SPATIAL SYMMETRIES

In the following two sections we discuss spatial symmetries, beginning with general considerations in this section, then specializing to rotational symmetries—the subject of this book—in Section 1.3. These discussions and methods prepare us for the treatment of discrete symmetries, emphasizing quantum systems, in Section 1.4.

Geometry and Symmetries. Almost as soon as we encounter geometry, we are drawn to considering geometric symmetry. An overview of the relations between geometry in three dimensions and its symmetries is given in Figure 1.4.

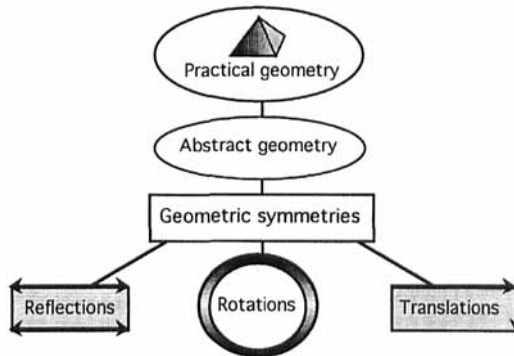


FIGURE 1.4 Overview relating geometric symmetries of three types—reflections, rotations, and translations—to abstract geometry and its origins in the practical geometry used in ancient Egypt.

As an example of the geometry–symmetry connection, in plane geometry equilateral triangles and squares are often visually more appealing than arbitrary triangles and quadrilaterals, while in three dimensions regular polyhedra such as a regular tetrahedron or a cube are usually perceived as more interesting than polyhedra with unbalanced sides. As shown in Section 1.2.2, one reason for this is that such figures can fill space (in two and three dimensions) without leaving voids.

Albert Einstein—who did so much to change concepts about space and time—provides [Ein54] an interesting discussion about the relation between practical geometry (as used for building the Egyptian pyramids), experience, and the abstraction of geometry to Euclid's system and its extensions that Einstein used in his general theory of relativity.

1.2.1 Reflection Symmetry in Nature

In the world around us we observe many examples of reflection symmetry, or close approximations to it. On the other hand, as one zooms into the microscopic scale from macroscopic through mesoscopic scales, a lack of reflection symmetry often becomes evident. We now introduce some terminology used when discussing reflection symmetry, then we discuss reflection symmetry in nature at the mesoscopic level.

Handedness, Chirality, Helicity. Several terms are used to denote that there is a distinction between left and right. One term is just *handedness*, with an obvious meaning, at least for humans when translated from English into an intelligible language. Figure 1.5 reminds you how mirror reflection is related to handedness.

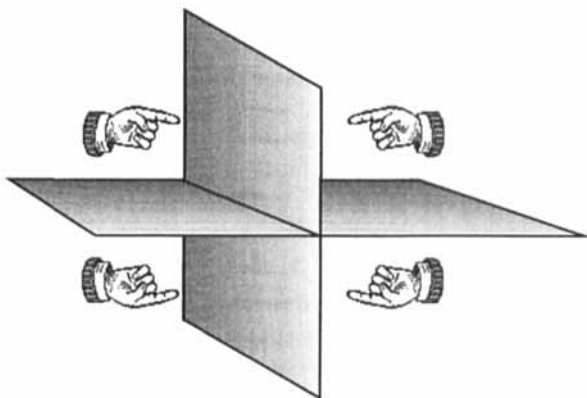


FIGURE 1.5 Hands reflected in mirrors interchange left and right if the mirror is vertical or if the mirror is horizontal. Note that reflection in two mirrors that are at right angles to each other restores the handedness, since diagonally opposite hands are either both left (top left and bottom right) or both right (top right and bottom left).

The term *chirality* (from the Greek for hand, *cheir*) is used in technical contexts, as in stereochemistry and in some areas of subatomic physics. The root word *chiro* also occurs in *chiropractor*—a physician who uses hands to manipulate (Latin *manus*, hand, as in *manuscript*, a handwritten document). Practitioners of angular momentum theory often use their hands to describe rotations; hence, their *handwaving* (nonrigorous) discussions. Molecules that have opposite handedness

are called *enantiomers*, and a mixture having the same proportion of the two enantiomers is called *racemic*.

The term *helicity* (from the same Greek root as *helix*, a spiral) is most often used by physicists when describing the projection of intrinsic spins along the direction of motion, especially in relativistic situations such as for photons. The usual definition of the helicity, h , is

$$h = \mathbf{J} \cdot \hat{\mathbf{p}} \quad (1.11)$$

where \mathbf{J} is the angular momentum of the particle and $\hat{\mathbf{p}}$ is a unit vector along the direction of motion. Sometimes h/J is used instead.

The problem of communicating with extraterrestrial life having an intelligence compatible with that of humans an indication of which side is to be labeled Left and which Right, but without sending pictures (which might accidentally be reconstructed in reverse) has been called by Martin Gardner the *Ozma problem*. It is posed in Chapter 18 of his book [Gar90], and a solution in terms of a weak-interaction experiment is given in Chapter 22.

Handedness in Nature. One of the first scientists to recognize the significance of handedness in nature—especially at the microscopic level—was Louis Pasteur (1822–1895), who in 1848 discovered the handedness of tartaric-acid molecules, as sketched in Figure 1.6. His discovery is vividly recounted in the biography of Pasteur written by Dubos [Dub76].

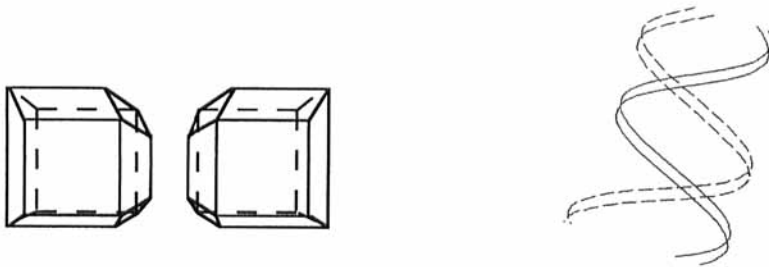


FIGURE 1.6 Handedness of the two enantiomers of tartaric acid discovered by Pasteur, and the right-handed helix of DNA discovered by Crick and Watson.

The culmination of discoveries of handedness in biological systems is that by Crick and Watson, who demonstrated the helical structure of DNA molecules in 1953. In Chapter 12 of his book on ambidexterity in the universe, Gardner [Gar90] gives an interesting presentation of Pasteur’s discovery, and in later chapters he discusses asymmetry in biological molecules. An unexplained puzzle, to which we return in Section 1.5, is why creatures on Earth have proteins that are almost exclusively left-handed, whereas DNA molecules contain only right-handed sugars.

At the subatomic level, the weak interaction exhibits violation of parity symmetry, for example in nuclear beta decay. This possibility was first suggested by Yang and Lee [Yan56] and verified experimentally by Wu et al. [Wu57].

Throughout this book, as motifs at the head of chapters, we have drawings of helical shells in both left- and right-handed varieties, just as they occur in nature. These shells characterize some aspect of the rotational symmetry and angular momentum topics in the chapter. If you look carefully at the pictures, such as Figure 1.7, you will notice that in addition to the handedness of the shell, there is also another reflection symmetry between pictures. To train yourself to recognize such kinds of symmetry, find out what it is. (Discovery favors the prepared mind.) To understand the geometry of these helices and their symmetries, do Problem 1.2.



FIGURE 1.7 Helical shells of the left- and right-handed variety (left side) and their spatial reflections (right side). (Adapted from *Mathematica* notebook Shell1.)

1.2.2 Translation Symmetries; Mosaics and Crystals

Before introducing rotational symmetries, we summarize some essential properties of geometrical symmetries resulting from translations in a plane and in three dimensions. Translations are much simpler than rotations, because (unlike the latter in three dimensions) they commute—that is, their order of application is unimportant. We consider figures whose edges are all the same size and that cover a region of the plane (regular polygons) or of three-dimensional space (regular polyhedra) without leaving space between them. They therefore have translational symmetry for discrete translations by the length of a side.

Mosaics. The regular polygons are those that can cover a plane so that no space is left unfilled, thereby forming a mosaic of tiles. Problem 1.3 leads to the proof that the only regular polygons that tile the plane are the triangle, square, and hexagon, as shown in Figure 1.8.

It is interesting to note that each of these figures has a center of reflection symmetry, whereas the pentagon, intermediate between square and hexagon, does not have such a center. An extensive discussion of fivefold symmetry is given in the

monograph edited by Hargittai [Har92], and discussions of mathematical puzzles and problems in tiling are given in Martin's book on polyominoes [Mar91].

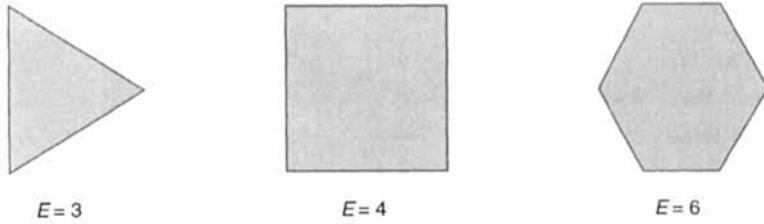


FIGURE 1.8 The three regular polygons that can tile the plane. The number of edges of each polygon is E .

Crystals. Now consider the situation in three dimensions. Suppose that we have a regular polyhedron with F faces as shown in Figure 1.9. (A polyhedron is *regular* if all its faces are the same shape and size.)

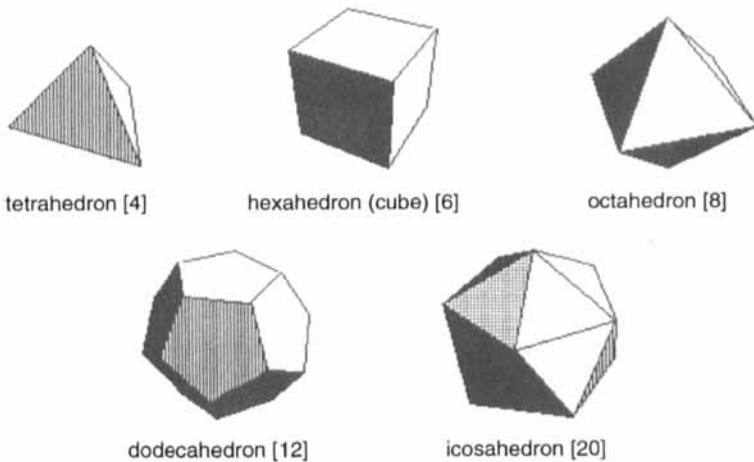


FIGURE 1.9 The five regular solids that can fill space without leaving voids. For each solid the number in brackets is the number of polyhedron faces, F . (Adapted from *Mathematica notebook Polyhedra*, which results in irregular edges.)

The appearance of a regular polyhedron will be unchanged by any rotation about the center through a discrete angle $\theta = 2\pi n/F$. Such a polyhedron might describe the filling of a region of space without voids by a crystalline material. The regular solids were described by Plato of Athens (427–347 B.C.), so they are often called the Platonic solids. Problem 1.4 leads to the proof that the only regular polyhedra have $F = 4, 6, 8, 12,$ and 20 , as shown in Figure 1.9 and summarized in Table 1.2.

TABLE 1.2 Geometric properties of the regular polyhedra (Platonic solids).

Polyhedron	F , faces	V , vertices	E , edges	N , edges at each vertex	S , edges at each face
Tetrahedron	4	4	6	3	3
Hexahedron (cube)	6	8	12	3	4
Octahedron	8	6	12	4	3
Dodecahedron	12	20	30	3	5
Icosahedron	20	12	30	5	3

A truncated icosahedron—with the same geometry as a soccer ball (in America) or football (in Europe)—has a particular interest, since it describes the molecule C_{60} , called buckminsterfullerene or the “buckyball.” The mathematics of the buckyball is described in a *Scientific American* article by Chung and Sternberg [Chu93].

Now that we have discussed symmetries and conservation laws for physical systems in Section 1.1, as well as reflection and translation symmetries in this section, we turn to the main topic of this book—rotational symmetries.

1.3 ROTATIONAL SYMMETRIES

In this section we introduce the main geometric ideas and formulas relating to rotational symmetries. One of the most important topics is the distinction between active and passive rotations, which we emphasize and clarify in Section 1.3.1. Here we also introduce Euler’s scheme for describing rotations in three dimensions and we derive the matrices that describe active rotations of the coordinates of an object. In Section 1.3.2 we develop our understanding of coordinate systems for rotations by considering rotations of the Earth as seen from a fixed point in space. Finally in this section, we provide in Section 1.3.3 a cameo portrait illustrating connections between different topics in this book.

Is Space Isotropic? To modern ways of thinking about the physical sciences, this is probably a meaningless question. I believe it to be *assumed* that space is isotropic, and you will agree with me upon reflection. In an experiment, if we observe that a phenomenon depends on orientation, we attribute this to the presence of interactions. That is, interactions are those things that give rise to a dependence on direction in space.

This viewpoint is consistent with ideas in general relativity, where “curvature” in space-time is attributed to gravitational interactions in the macroworld. Further, in experiments on fundamental symmetries in the microworld—such as breaking of reflection symmetry measured in parity-violation experiments—space is assumed to be isotropic, so the system may be rotated without changing its intrinsic properties.

When you do experiments, a constant problem is to shield the complete appara-

tus of the measurement from so-called “external” influences. Electromagnetic fields are particularly troublesome in this regard. Indeed, if the results depend on the orientation of the apparatus as a whole, this is taken as a signal that the equipment is not sufficiently shielded, rather than as a sign that space is anisotropic.

Given the assumption of the isotropy of space, the subject of rotation symmetry and angular momentum is about how our description of phenomena change when we break this symmetry by choosing a reference frame with a particular orientation. This idea is sketched in Figure 1.10.



FIGURE 1.10 Space is intrinsically isotropic (left), but this symmetry is broken upon choosing a reference axis (middle) or a reference frame (right).

The subject of angular momentum is about how our description of a system changes when we rotate the system relative to a reference frame in space. By analyzing these changes of description we may learn about the interactions within the system. It is to the study of these rotations that we now turn our attention.

1.3.1 Active and Passive Rotations; Euler Angles

A rotation can be considered from one of two viewpoints, active or passive. We now discuss this idea and develop some technical vocabulary and mathematics.

Active Rotations. The first point of view for rotations is called an *active rotation*. Here the observer is in a fixed reference frame while the object—a body in classical mechanics, a field component (\mathbf{E} , \mathbf{B} , or \mathbf{A}) in electromagnetism, or an operator in quantum mechanics—rotates with respect to this reference frame. Such dynamical rotations of objects and transformations of operators are the same as those in classical mechanics. An alternative name for an active rotation is *alibi* (from the Latin for “elsewhere”). In quantum mechanics active rotations are analogous to the Heisenberg viewpoint for time dependence, in which operators are changed by transformations while state vectors (wave functions) are unchanged thereby.

In Figure 1.11 the top half shows active rotation of an ellipsoid, with the observer’s eye being kept fixed. Active rotations can be specified by describing the relation between coordinates of a representative point of the object before rotation, $\mathbf{r} = (x, y, z)$, and after rotation, $\mathbf{r}'_A = (x', y', z')$. Geometrically, such rotations are described as indicated in Figure 1.12.

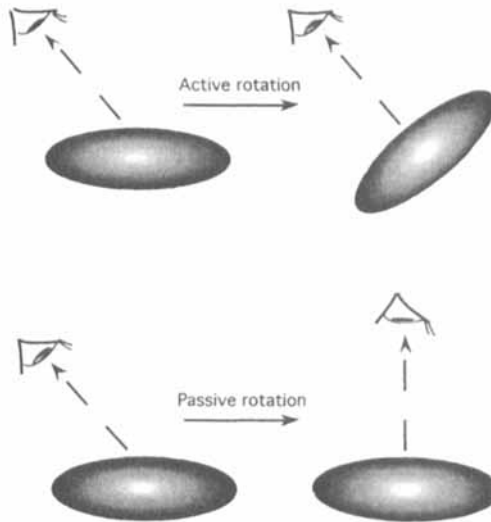


FIGURE 1.11 Active and passive rotations compared. In the top half of the figure an active rotation of the ellipsoid has been made, with the observer's eye fixed. In the bottom half of the figure the ellipsoid is fixed (passive) while the observer's eye rotates around it. Note that the two rotations are the *inverse* of each other.

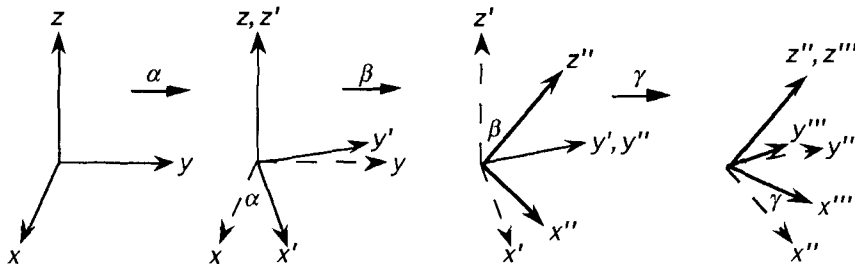


FIGURE 1.12 Active rotations in terms of the successive rotations through Euler angles α , β , then γ , with the rotations being applied in this order.

An alternative way of describing an active rotation is depicted in Figure 1.13.

Algebra of Active Rotations. Having examined rotations from the geometric viewpoint, it is now time to make an algebraic formulation. Algebraically, in order to describe the active rotation of a representative point on the object, write

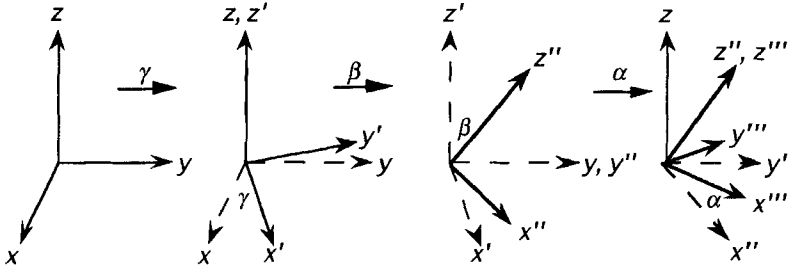


FIGURE 1.13 Alternative description of active rotations in terms of the successive rotations through Euler angles γ , β , then α . The rotations are applied in this order. They are referred to the *original* axes.

$$\mathbf{r}'_A = \mathbf{A}(\alpha, \beta, \gamma) \mathbf{r} \quad (1.12)$$

in which \mathbf{r} and \mathbf{r}'_A are column-vector representations of the coordinates and \mathbf{A} is the product of three matrices:

$$\mathbf{A}(\alpha, \beta, \gamma) \equiv \mathbf{A}_z(\alpha) \mathbf{A}_y(\beta) \mathbf{A}_z(\gamma) \quad (1.13)$$

where the subscripts specify the axis about which the rotation is made. Thus, for the z -axis rotation

$$\mathbf{A}_z(\phi) \equiv \begin{bmatrix} \cos \phi & -\sin \phi & 0 \\ \sin \phi & \cos \phi & 0 \\ 0 & 0 & 1 \end{bmatrix} \quad (1.14)$$

specifies a rotation through the z axis by an angle ϕ , taken as positive for a rotation in a right-hand screw sense. In (1.13) ϕ has the value γ for the first z -axis rotation, while $\phi = \alpha$ for the final rotation about the z axis. The second rotation is about the space-fixed y axis, namely

$$\mathbf{A}_y(\beta) \equiv \begin{bmatrix} \cos \beta & 0 & \sin \beta \\ 0 & 1 & 0 \\ -\sin \beta & 0 & \cos \beta \end{bmatrix} \quad (1.15)$$

The angles α , β , and γ are thus the Euler angles that occur in classical mechanics, as depicted in Figure 1.12.

Throughout this book, unless explicitly mentioned otherwise, we use only *active* rotations.

Passive Rotations. There is a second viewpoint for describing rotations, called a *passive rotation*. Here the object sits passively in a fixed frame while the observer rotates around it, as illustrated in the bottom half of Figure 1.11. Passive rotations are alternatively called *alias* transformations, from the Latin for otherwise-called. In quantum mechanics they are analogous to Schrödinger representations, in which state vectors and wave functions are time-dependent, whereas operators are time-independent.

For the coordinate transformation induced by a passive rotation we write

$$\mathbf{r}'_p = \mathbf{P}(\alpha, \beta, \gamma) \mathbf{r} \quad (1.16)$$

The passive-rotation matrix \mathbf{P} is given in terms of active-rotation matrices by

$$\mathbf{P}(\alpha, \beta, \gamma) \equiv \mathbf{A}(-\gamma)\mathbf{A}(-\beta)\mathbf{A}(-\alpha) = \mathbf{A}^{-1}(\alpha, \beta, \gamma) \quad (1.17)$$

If the same angles are used in (1.16) and (1.17), then in both viewpoints the rotated vectors are in the same relation to the original vectors. The proof of this is suggested as Problem 1.5. The relation between \mathbf{P} and \mathbf{A}^{-1} is illustrated in Figure 1.13, and a summary of the two viewpoints is given in Table 1.3.

TABLE 1.3 Active and passive viewpoints for rotations. In this book we use the *active* viewpoint.

Viewpoint	Euler-angle representation	Interpretation
Active (<i>alibi</i>)	$\mathbf{A}(\alpha, \beta, \gamma) \equiv \mathbf{A}_z(\alpha)\mathbf{A}_y(\beta)\mathbf{A}_z(\gamma)$	Dynamical rotations of objects and operators
Passive (<i>alias</i>)	$\mathbf{P}(\alpha, \beta, \gamma) = \mathbf{A}^{-1}(\alpha, \beta, \gamma)$	Coordinate-frame rotations

There is considerable confusion in the literature of quantum mechanics and angular momentum concerning the use of active and passive viewpoints. Occasionally, the two conventions appear mixed, resulting in errors in phases of wave functions and in the choice of rotation angles. Clarification is provided in articles by Bouten [Bou69] and by Wolf [Wol69]. For uniformity, in this book we use the *active viewpoint* when discussing rotations, unless explicitly mentioned otherwise. This usage is also consistent with most recent books on angular momentum [Bie81a, Bie81b, Zar87, Bri94].

In the group theory of rotations (Section 2.5) active rotations about axes in a space-fixed frame form a group, but passive rotations about different axes do not form a group. This distinction, which is important if group-theory methods are used to derive rotation-matrix elements, is clearly discussed by Bouten [Bou69].

Active and passive viewpoints also occur in field theories, for example for a quantum-mechanical particle in a classical electromagnetic field. In this context the symmetry of *gauge invariance* can be viewed either as active (transforming operators and potentials) or as passive (transforming momenta). Such gauge transformations may be considered as rotations in a gauge space. Alternatively, rotations in three dimensions may be considered as particular types of gauge transformations. A clear discussion of gauge invariance and electromagnetic fields is provided in the article by Kobe [Kob86].

Rotations Do Not Commute. The order of rotations about axes in three dimensions is significant; that is, *in three dimensions rotations about two different axes do not commute*. Therefore, correct specification of a rotation by the scheme (1.13) is necessary, although not necessarily unique. Note that if the successive rotations are about the *same* axis, then their order of application is unimportant. For example,

$$\mathbf{A}_y(\beta_2)\mathbf{A}_y(\beta_1) = \mathbf{A}_y(\beta_1)\mathbf{A}_y(\beta_2) = \mathbf{A}_y(\beta_1 + \beta_2) \quad (1.18)$$

By contrast with rotations, translations along axes always commute, so that the order of specifying three (for example) translations of axes is unimportant. Thus, if

$$\mathbf{r}' = \mathbf{r} + \mathbf{R} \quad (1.19)$$

then the order in which the components are displaced does not matter. This distinction between rotations and translations arises from the fact that rotations, such as (1.14), are nonlinear functions of the angle parameters, whereas translations are linear in the displacement parameters, which are the components of \mathbf{R} in (1.19). The importance of this distinction is explored further in Problem 1.6.

1.3.2 Coordinate Systems for Rotations

The purpose of this subsection is to introduce in an informal way the description of rotations and coordinates to describe them. We do this by looking at rotations of the Earth. Thus, chained to your desk by study, your mind may wander to foreign lands. Consider rotations of a sphere, such as Earth, relative to a fixed coordinate system (*active* rotations, Section 1.3.1) as shown in Figure 1.14.

Longitude and Latitude. Consider in Figure 1.14 a rotation that does not change the polar axis of the system, so that the North pole is in the same position in the two lower views. Geographically speaking, this is a change of *longitude*, which does not essentially change the description of the system. For example, one lower figure could be transformed into the other just by rotating it on the page, and both views contain essentially the same information. Clearly, rotating the page as a whole does not achieve this.

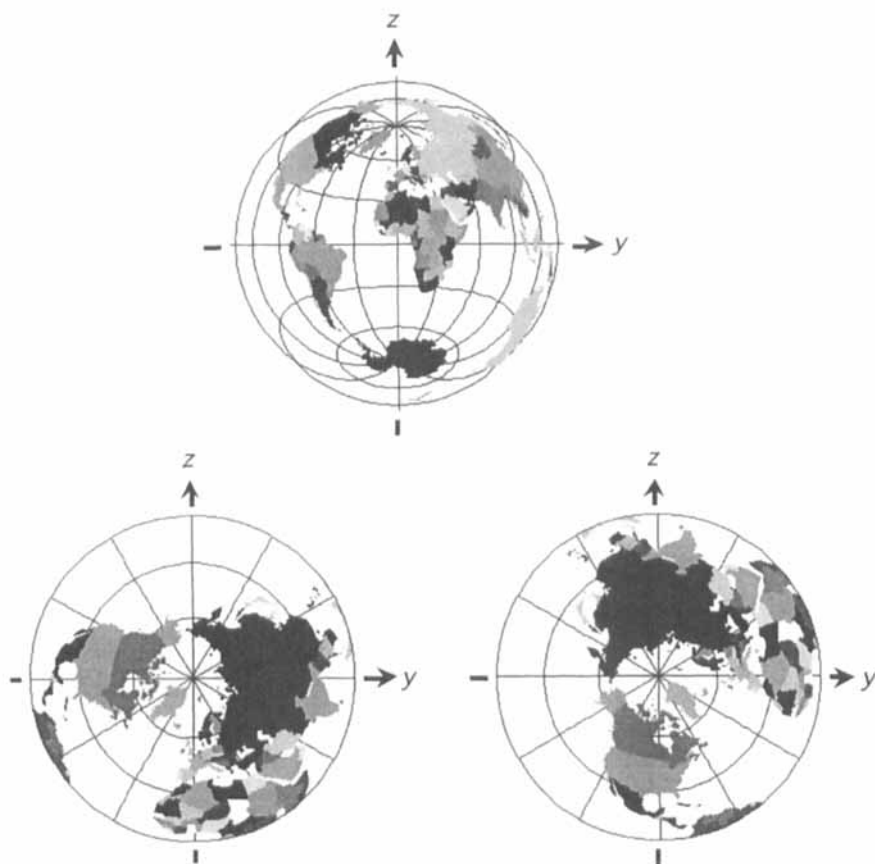


FIGURE 1.14 Rotation of a sphere in terms of latitude and longitude. All three axes pass through the center of Earth and are defined in the top view where the x axis is out of the page, passing through the prime meridian and equator. (Views beyond both poles are artifacts of *Mathematica*.) In the lower left view Earth is rotated counterclockwise about the y axis through $\pi/2$. In the lower right view Earth is rotated counterclockwise about the *new* polar axis by $\pi/2$. (Adapted from *Mathematica* notebook WorldView.)

The difficulties in the early days of global navigation of determining longitude—and thus the present-day confusion between Indians in India and Indians in the Americas—are connected to this property. The simplicity of rotations about the polar axis has its counterpart in the finite rotations of angular momentum eigenstates (Chapter 6), for which azimuthal-angle rotations ϕ that change longitude introduce only phase changes in state vectors.

On the other hand, the top view in Figure 1.14—in which the rotation about the y axis has changed the polar axis—describes an essentially different geography from those in the lower two views. Under this change of *latitude* (a change of the polar

angle, θ) there is new information because Antarctica and much of the southern hemisphere of Earth are now discovered by such a rotation. Note that the polar angle is $\theta = 0$ at the North pole and $\theta = \pi$ at the South pole, whereas latitude is zero at the equator ($\theta = \pi/2$) and has to be specified as North or South. For angular momentum eigenstates such polar-angle rotations produce mixing of state vectors and changes in their magnitudes.

In the top view in Figure 1.14 the globe is shown in its conventional orientation, with North toward the top of the page. This prejudice of mapmakers (whose craft began in the Northern hemisphere) is not always appreciated by the inhabitants of Down Under, especially in Australia and New Zealand. In these countries one can purchase maps with the opposite orientation.

Notice—as emphasized in Section 1.3.1 and Problem 1.6—that the order of applying rotations to a three-dimensional object usually has significance. For example, if you take the top view of Earth in Figure 1.14 and rotate it about the z axis as the world turns, then rotate about the *new* y axis, you will not end up with the lower-right view.

The noncommuting of rotations about different axes is the quintessential property underlying the complexity and richness of angular momentum. In classical mechanics this complexity is mostly a nuisance, whereas in quantum mechanics the essential connection between noncommuting operators and the interpretation of quantum measurements (for example, the Heisenberg uncertainty relations) makes angular momentum conceptually and technically very important. We emphasize this quantum connection in Chapter 5.

This concludes our initial discussion of coordinate systems for rotations. Schemes for describing rotations and the operators for angular momentum are considered more completely in Section 3.1.1.

1.3.3 Angular Momentum and Rotations: A Cameo Portrait

At this stage, having discussed in a preliminary way the symmetries that belong to the study of angular momentum, it is worthwhile to pause to make an overview of the subjects in this book and their relationships.

The most prominent members of the family of topics to be studied are shown in the portraits in Figure 1.15. In the first two chapters our concern (and, we hope, our interest) is with the geometry of space, techniques from linear algebra that help describe rotational transformations, spinors, and a little group theory and quantum mechanics. In Chapter 3 we develop operators describing infinitesimal rotations, which are the angular momentum operators, including orbital operators for functions of only the spatial coordinates, as well as matrix and spinor representations.

From the infinitesimal rotations studied in Chapters 3 and 4 we can proceed in several directions. One of these (Chapter 5) investigates the role of angular momentum in quantum systems, where Planck's constant (h) makes its appearance. There we emphasize the distinction between geometrical and dynamical angular momentum, and show the connection—through Ehrenfest theorems and Larmor pre-

cession—to classical angular momentum. We also derive carefully the uncertainty relations for quantum angular momentum, introduce the semiclassical vector model, and discuss the relevance of angular momentum to solutions of wave equations, including the Schrödinger equation in quantum mechanics. The historical and conceptual development of ideas about angular momentum, especially in the realm of quantum physics, is discussed in Section 5.5.

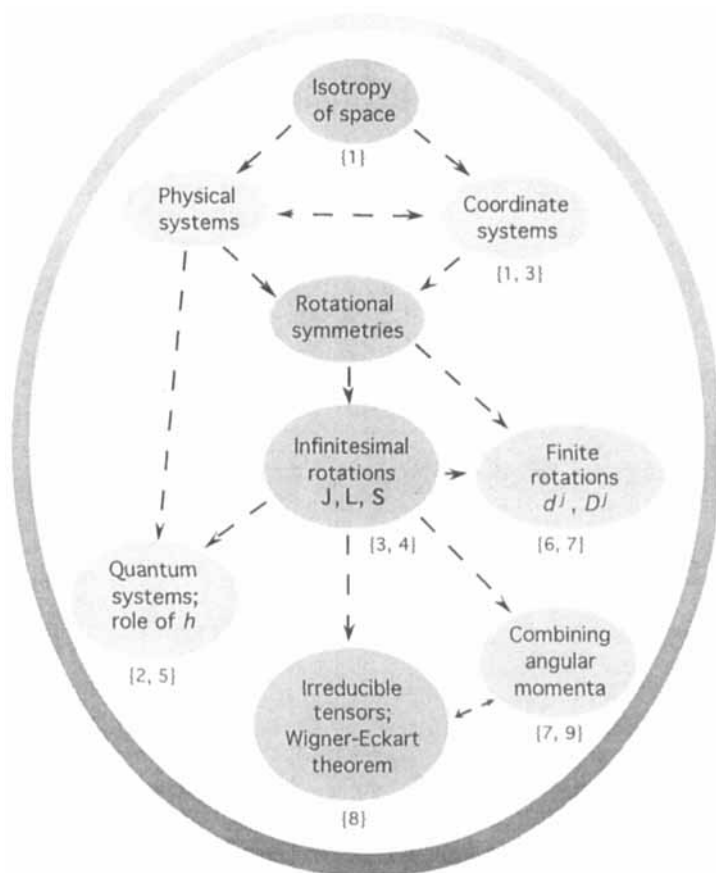


FIGURE 1.15 Portrait of relationships between topics in angular momentum, rotational symmetry applied to physical systems, and topics in this book. Cameos in the family portrait are arranged with physical systems on the left, symmetries in the middle, and geometric aspects on the right. Arrows indicate the strongest family ties and lines of descent. Numbers in braces indicate chapters with emphasis on a topic.

Chapters 6 through 9 have a more technical emphasis than in the first half of the book, although gems of physical insight will dazzle the dedicated explorer. In

Chapter 6 we develop properties of angular momentum eigenstates under finite rotations, deriving formulas, properties, and interpretations, while providing several opportunities for visualizing rotation functions with help from *Mathematica*. The combining of angular momentum states is introduced in Chapter 7. In Chapter 8 we consider the powerful irreducible tensors and the Wigner-Eckart theorem, which greatly simplify calculations in angular momentum. We also develop polarization tensors for spin and calculate the transport of spins through magnetic field gradients. Chapter 9—the technical summit of the book—emphasizes algebraic techniques for recombining several angular momentum eigenstates.

1.4 DISCRETE SYMMETRIES AND QUANTUM SYSTEMS

We now introduce three discrete symmetries that are especially interesting for quantum systems—parity, charge conjugation, and time reversal. The first of these, reflection of the coordinates or parity (Section 1.4.1), is intimately related to rotations of an object about the coordinate frame. The symmetry of time reversal becomes involved with parity because many observables are changed in similar ways by these two discrete symmetries. For example, classical linear momentum reverses sign either if its corresponding coordinate is reflected in the origin (the parity operator, P) or if the direction of time is reversed (time reversal, T), as indicated in Figure 1.16.

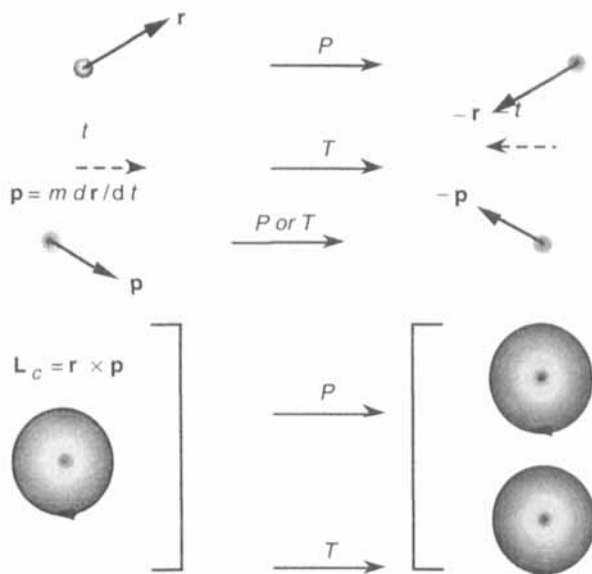


FIGURE 1.16 Parity (P) and time reversal (T) have the same effect for linear momentum, \mathbf{p} , but different effects for classical angular momentum, \mathbf{L}_c .

On the other hand, classical angular momentum $\mathbf{L}_c = \mathbf{r} \times \mathbf{p}$ is invariant under parity (since both \mathbf{r} and \mathbf{p} reverse directions), but \mathbf{L}_c reverses under time reversal, as shown in Figure 1.16.

Where does charge conjugation (sign change of all electric charges), denoted C , fit into discrete symmetries? As we show in Sections 1.4.3 and 1.4.4, any field theory (such as Maxwell's equations) is expected to have invariance under the combination PCT (applied in any order). We therefore discuss C along with P and T .

A popular exposition of symmetry aspects—from everyday life, through the sciences, to cosmology—is provided in the collection of essays by Martin Gardner [Gar90]. Another introductory-level presentation of symmetries, primarily of the geometric variety, is provided in the book by Bunch [Bun89].

1.4.1 Parity Symmetry

To relate parity to rotations, consider turning the pages of this book, as sketched in Figure 1.17.

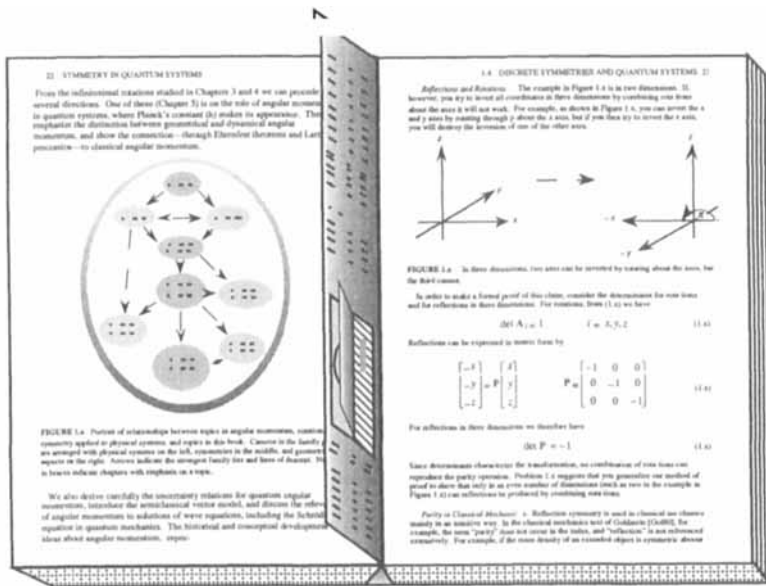


FIGURE 1.17 In two dimensions a parity inversion (flipping this page) is the same as a rotation of the back edge of the page about the spine of the book (turning the page).

If you are skimming to look over (which is not the same as to overlook) interesting topics, you are either *flipping* the pages or *turning* them. If you are flipping, then you are making an interchange between left and right sides of a leaf of the book, that is, a parity operation—just try it. What was the right edge on the previous page is now the left edge on this page, as you can see from the figure.

Reflections and Rotations. The example in Figure 1.17 is in *two* dimensions. If, however, you try to invert all coordinates in *three* dimensions by combining rotations about the axes, it will not work. For example, as shown in Figure 1.18, you can invert the x and y axes by rotating through π about the z axis, but if you then try to invert the z axis, you will destroy the inversion of one of the other axes.

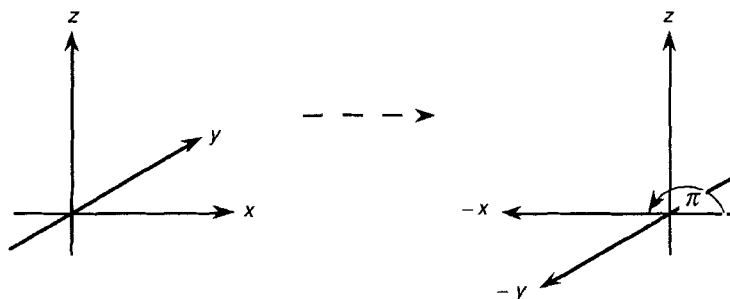


FIGURE 1.18 In three dimensions, two axes can be inverted by rotating about the axes, but the third cannot.

In order to make a formal proof of this claim, consider the determinants for rotations and for reflections in three dimensions. For rotations, from (1.14) we have

$$\det \mathbf{A}_i = 1 \quad i = x, y, z \quad (1.20)$$

Reflections can be expressed in matrix form by

$$\begin{bmatrix} -x \\ -y \\ -z \end{bmatrix} = \mathbf{P} \begin{bmatrix} x \\ y \\ z \end{bmatrix} \quad \mathbf{P} \equiv \begin{bmatrix} -1 & 0 & 0 \\ 0 & -1 & 0 \\ 0 & 0 & -1 \end{bmatrix} \quad (1.21)$$

For reflections in three dimensions we therefore have

$$\det \mathbf{P} = -1 \quad (1.22)$$

Since determinants characterize the transformation, no combination of rotations can reproduce the parity operation. Problem 1.7 suggests that you generalize our method of proof to show that in an *odd* number of dimensions (such as three in the example in Figure 1.18) reflections *cannot* be produced by combining rotations.

Parity in Classical Mechanics. Reflection symmetry is used in classical mechanics mainly in an intuitive way. In the text of Goldstein [Gol80] the term *parity* does not occur in the index, and *reflection* is not referenced extensively. As an example of intuitive use of parity symmetry, if the mass density of an extended object is symmetric about the origin of the coordinate system, then the center of mass coincides with the coordinate origin.

Parity in Quantum Mechanics. Symmetry operators such as parity and rotations have a special role in quantum mechanics because of the superposition principle for wave functions (state vectors). For example, suppose that we have a state of a given energy described by a wave function. Applying rotation or reflection operations to this state produces new states of the same energy. By contrast with classical mechanics, superposition of these wave functions produces states with quite different properties. Thus, the possibility of constructive and destructive interference of combined states depending on their relative phases adds a richness to quantum mechanics that is missing from classical mechanics.

To give a concrete example of superposition in quantum mechanics in the context of the parity operator, consider the wave function

$$\psi(x) = \cos x + (x/2 + 1)\sin x \quad (1.23)$$

We can superpose solutions to obtain combinations with properties as follows:

$$\begin{aligned} \psi_{\pm}(x) &\equiv \psi(x) \pm \psi(-x) \\ P\psi_{+}(x) &= \psi_{+}(x) = 2\cos x + x\sin x \\ P\psi_{-}(x) &= -\psi_{-}(x) = -2\sin x \end{aligned} \quad (1.24)$$

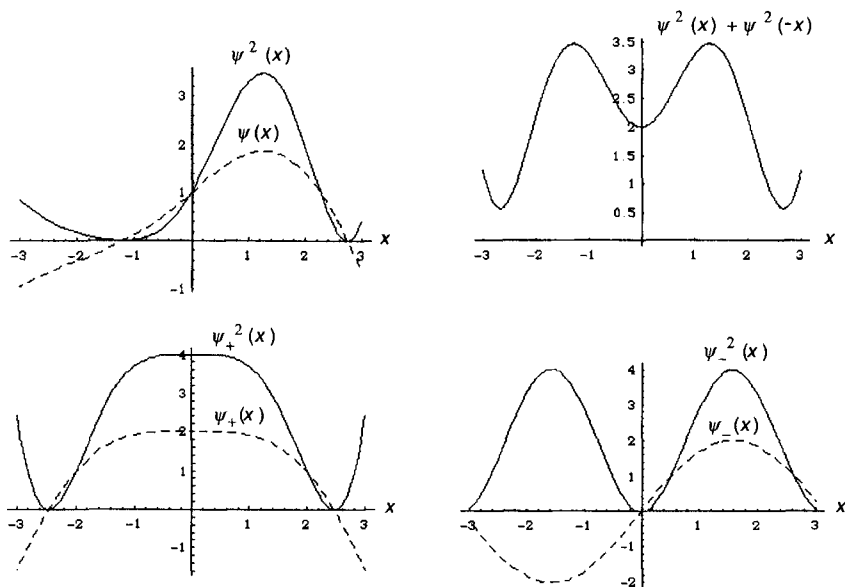


FIGURE 1.19 The wave function (1.23) and superpositions of it when acted upon by the parity operator. Wave functions are shown by dashed curves and their squares are shown by solid curves. (Adapted from *Mathematica* notebook Ppsi.)

As illustrated in Figure 1.19, such superpositions produce wave functions and probability densities that differ from each other and from the addition of probabilities given by $|\psi(x)|^2 + |\psi(-x)|^2$. From your experience with quantum mechanics, you may be surprised at the different functional forms shown, but recall that you usually deal with energy eigenstates of systems having parity-invariant Hamiltonians, so that solutions such as ψ_+ or ψ_- are most usual. Problem 1.8 suggests using the *Mathematica* notebook Ppsi to explore parity and wave functions.

Extensive discussions of the role of symmetries, invariances, and conservation laws are given in Part I of the reprint volume of essays by Wigner [Wig67]. These emphasize the difference between symmetry principles in classical and quantum physics. An extensive discussion is given in the review article by Houtappel, van Dam, and Wigner [Hou65], and it is summarized in Chapter I of Biedenharn and Louck [Bie81a].

1.4.2 Charge Conjugation and Time Reversal

We now introduce two discrete symmetries, one of which (charge conjugation) is fairly easily comprehended, while the other (time reversal) is conceptually and technically much more difficult.

Charge Conjugation. The symmetry operation of charge conjugation, C , consists of reversing the signs of all electric charges in dynamical formulas, such as in Hamiltonians or the equations of electromagnetism. When one does this, it is usual to assume that a “test charge” does not have its sign reversed. With this understanding, electric and magnetic fields reverse sign under C . In Section 1.4.3 we show (Table 1.4) the symmetry properties of quantities in the Maxwell equations under C .

Charge conjugation is particularly interesting from the viewpoint of antiparticles, such as electrons and positrons, particularly in regard to dynamical equations such as the Dirac equation. An introductory-level overview is given in Chapter 21 of Gardner’s book [Gar90], the Dirac equation is covered extensively in Chapters 14 and 15 of Landau’s text [Lan90], while Sections IV.4 and IV.5 of Roman’s text on elementary particles [Rom61] has a more advanced treatment for quantum fields. Note that even electrically neutral particles—such as neutrons and neutrinos—have antiparticles. Like the test for genuine pearls (which dissolve in vinegar), you know when you had two antiparticles, since they annihilate each other.

Time Reversal: A Simple Definition for a Subtle Subject. The operational definition of time reversal, T , is quite simple: Reverse the direction of time in all functions and operators that have a time dependence. For example, consider Newton’s equation for a particle whose mass m is constant with time: $m\mathbf{a} = \mathbf{F}$. Under time reversal we have

$$T\mathbf{r}(t) = \mathbf{r}(-t) \quad T\mathbf{v}(t) = \frac{dT\mathbf{r}(t)}{d(-t)} = -\mathbf{v}(-t) \quad T\mathbf{a}(t) = \frac{dT\mathbf{v}(t)}{d(-t)} = \mathbf{a}(-t) \quad (1.25)$$

The form of Newton's equation is therefore invariant under T —that is, we have a *covariant* equation—since

$$ma(t) = \mathbf{F}(t) \quad \Rightarrow \quad ma(-t) = \mathbf{F}(-t) \quad (1.26)$$

In classical mechanics, therefore, this equation of motion does not single out a preferred direction of time.

The Arrow of Time in the Macroworld. According to our perception, time marches on inexorably—dropping more grains of sand in the hourglass and sounding more ticks of the clock. Most of us would believe that in the macroscopic world, at about the level of human perception, there is *not* symmetry with respect to time reversal.

One way to explain this is to assume that the behavior of macroscopic systems is dominated by thermodynamic principles for which an arrow of time is imposed by the tendency of such systems to increase their disorder with time, as sketched in Figure 1.20.

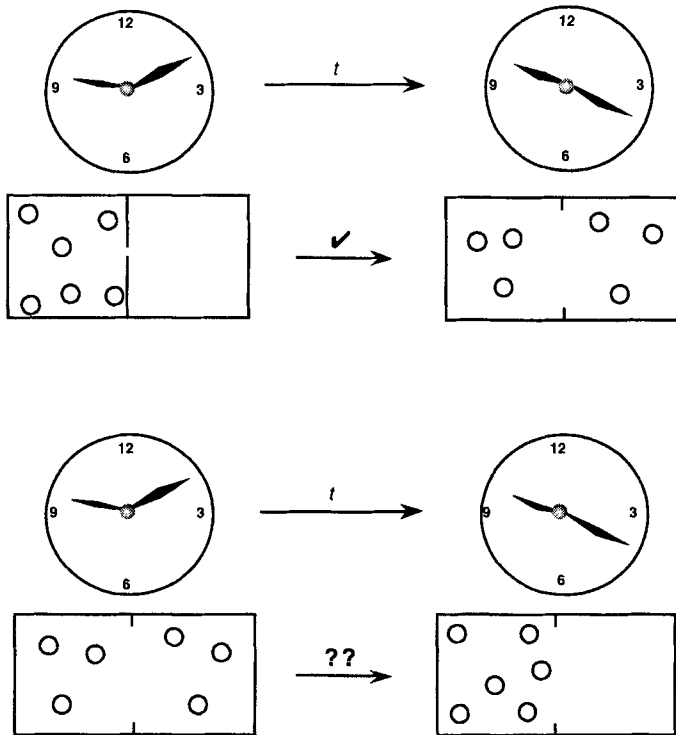


FIGURE 1.20 The arrow of time can be related to the increase of disorder in a thermodynamic system. The rearrangement of gas molecules after a partition is removed, as shown at top, is very likely. The bottom rearrangement with no partition is very unlikely.

Discussions of the arrow of time have been given by several authors. For example, at an introductory level in Chapters 28–31 of Gardner’s book on symmetries [Gar90] and at a more advanced level with a physics approach in books by Davies, such as [Dav74].

Observables and Time Reversal. As a preliminary to investigating the consequences of time reversal in quantum mechanics, it is worthwhile to summarize the behavior of observables in classical mechanics under time reversal, as shown in Table 1.4.

TABLE 1.4 Time-reversal properties of some observables for a single particle in nonrelativistic classical mechanics.

Observable	Basic relation	Behavior under time reversal
Time, t		$t \rightarrow -t$
Position, \mathbf{r}		$\mathbf{r}(t) \rightarrow \mathbf{r}(-t)$
Velocity, \mathbf{v}	$\mathbf{v} = \frac{d\mathbf{r}}{dt}$	$\mathbf{v}(t) \rightarrow -\mathbf{v}(-t)$
Kinetic energy, K	$K = \frac{1}{2}mv^2$	$K(t) \rightarrow K(-t)$
Angle, θ		$\theta(t) \rightarrow \theta(-t)$
Angular velocity, $\boldsymbol{\omega}$	$\boldsymbol{\omega} = \mathbf{r} \times \mathbf{v}$	$\boldsymbol{\omega}(t) \rightarrow -\boldsymbol{\omega}(-t)$
Rotational energy, K	$K = \frac{1}{2}I\omega^2$	$K(t) \rightarrow K(-t)$

Most of these properties are straightforward to understand, and they agree with our observation of movies showing these observables being played in reverse order. It is in the context of quantum mechanics—the Schrödinger equation, for example—that the behavior is more complicated and subtle, as we now derive.

Time Reversal and the Schrödinger Equation. We discuss here the mathematics of time reversal for a Schrödinger equation. The symbol used for the time reversal operator in quantum mechanics is \mathcal{O} , rather than the T used in most other contexts. This usually does not cause confusion with the polar angle θ .

Suppose that we have a Schrödinger equation for a Hamiltonian H , given as

$$i\hbar \frac{\partial \psi(t)}{\partial t} = H(t)\psi(t) \quad (1.27)$$

Under $t \rightarrow -t$ this becomes

$$i\hbar \frac{\partial \psi(-t)}{\partial(-t)} = H(-t)\psi(-t) \quad (1.28)$$

whose solutions generally have no simple relation to those of (1.27) because of the time dependence of the Hamiltonian. The restriction to a *time-independent Hamiltonian*—thus, by Noether's theorem in Section 1.1.2, total energy conservation—allows a solution, as follows. Apply Θ to both sides of (1.27), to obtain

$$-i\hbar \frac{\partial \Theta \psi(t)}{\partial t} = H \Theta \psi(t) \quad (1.29)$$

in which the negative sign on the left-hand side comes from replacing $\partial / \partial(-t)$ by $-\partial / \partial t$. By taking the complex conjugate of (1.27) we see that

$$-i\hbar \frac{\partial K \psi(t)}{\partial t} = H^*(t) K \psi(t) \quad (1.30)$$

in which K denotes the *complex-conjugation operator*:

$$K\psi \equiv \psi^* \quad (1.31)$$

for any function ψ . Thus, for example, $Ki = -i$, which was used to derive (1.30).

To relate the time-reversal operator Θ for a time-independent Hamiltonian H to the complex-conjugation operator K , let U be any operator for which

$$UH^*U^{-1} = H \quad (1.32)$$

If we operate on both sides of (1.30) with U , insert $U^{-1}U$ between the H^* and K , use condition (1.32), then compare the result with (1.29), we see immediately that

$$\Theta = UK \quad (1.33)$$

gives the general form of the time-reversal operator for the Schrödinger equation with time-independent Hamiltonian. In many cases it is sufficient to choose $U = I$, the unit operator, as we illustrate in the following.

Examples of Quantal Time Reversal. To show that care is needed when considering time reversal for the Schrödinger equation, consider the simplest example, a unit-amplitude plane wave with momentum expectation value \mathbf{k} . This is given by

$$\psi_{\mathbf{k}}(\mathbf{r}, t) = e^{i(\mathbf{k} \cdot \mathbf{r} - \omega t)} \quad (1.34)$$

Clearly, since H is just the kinetic-energy operator, (1.32) is satisfied with $U = I$. As Problem 1.9 suggests that you verify, we have that

$$\psi_{-\mathbf{k}}(\mathbf{r}, -t) = \psi_{\mathbf{k}}^*(\mathbf{r}, t) \quad (1.35)$$

Thus, observables that are time related, such as the wave vector \mathbf{k} , may have to be reversed if the correspondence (1.35) is to be used. This is physically reasonable, since under time reversal a particle would move in the opposite direction. Therefore, a wave packet constructed from a superposition of wave functions of the type (1.34) and peaked around some momentum $\mathbf{p} = \hbar\mathbf{k}$ should *reverse* momentum under time reversal.

What is to be done with quantum operators under time reversal? In general, for operator O under time reversal we have $O \rightarrow \Theta O \Theta^{-1} = UKOKU^{-1}$, in which we have used the fact that complex conjugation satisfies $K = K^{-1}$, since $K^2 = I$. For example, in the \mathbf{r} -space (coordinate) representation $\mathbf{r} \xrightarrow{T} \mathbf{r}$, whereas the momentum operator $\mathbf{p} = -i\hbar\nabla$ has the property (due to the factor i) that $\mathbf{p} \xrightarrow{T} -\mathbf{p}$. On the other hand, in momentum representation the Hamiltonian and coordinate operators are of the form

$$H = \frac{\mathbf{p}^2}{2m} + V(i\hbar\nabla) \quad \mathbf{r} = i\hbar\nabla \quad (1.36)$$

so that U in (1.33) must be chosen so as to undo the effect of the reversal of momentum. Then $\mathbf{p} \xrightarrow{T} -\mathbf{p}$ and $\mathbf{r} \xrightarrow{T} \mathbf{r}$, just as in the coordinate representation.

Angular Momentum and Time Reversal. Consider the angular momentum entry in Table 1.4 summarizing time-reversal properties for a particle in classical mechanics. Clearly, classical angular momentum reverses sign under time reversal. In quantum mechanics, consider the orbital angular momentum operator $\mathbf{L} = \mathbf{r} \times \mathbf{p}$, whose properties we develop in Section 3.2 and whose eigenstates we examine exhaustively in Section 4.1. As is clear by inspection, in both the \mathbf{r} and \mathbf{p} representations $\mathbf{L} \xrightarrow{T} -\mathbf{L}$, in agreement with classical mechanics. The presence of the complex-conjugation requirement for the eigenstates may lead to additional complexity, as discussed in Sections 4.1.3 and 5.4.1. The behavior of intrinsic-spin states under time reversal is very important, as well as being significantly complicated. We therefore defer its analysis until Section 4.3.4.

In Chapter 3 we develop the operators for angular momentum in terms of infinitesimal rotations. Like the linear-momentum operator, these \mathbf{J} operators have no intrinsic time dependence. Their expectation values—which are the observable quantities—may, however, be time dependent. For example, in Section 5.1.2 we derive the Ehrenfest theorem for the time evolution of angular momentum in terms of torques, while in Section 5.1.3 we derive the time dependence of Larmor precession of magnetic moments.

Time Reversal and the Dirac Equation. In relativistic quantum mechanics—such as the Dirac equation for electrons and positrons—the considerations of time reversal become much more complicated because of the constraint of relativistic covariance. A detailed discussion is given in Section IV.3 of Roman’s text on elementary particles [Rom61], while an extensive treatment emphasizing use of group theory is provided in Chapter 15 of Elliott and Dawber [Ell79].

The Microworld of Quantum Mechanics and Time Reversal. We seem to have painted ourselves into a logical corner, with the microworld being essentially time-reversal invariant and the macroworld showing an arrow of time, as indicated in Figure 1.21.

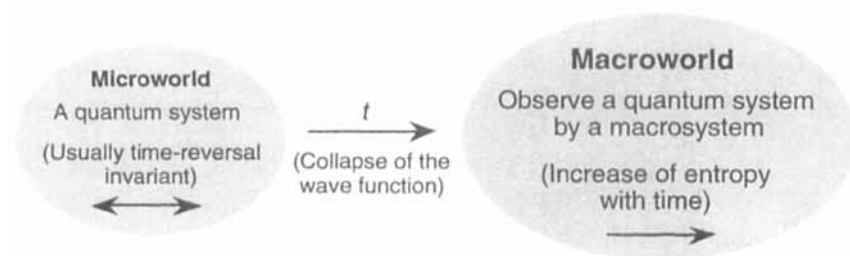


FIGURE 1.21 The microworld of a quantum system is usually time-reversal invariant. When a quantum system is observed by a macrosystem the wave function collapses. In the macroworld the general increase of entropy provides an arrow of time (Figure 1.20).

The usual way this problem is resolved is to declare that—since the probability wave function collapses when an observation is made by a macrosystem (such as a particle detector)—the time-reversal properties of the macrosystem then come into play. The discussion of this issue is part of an extensive literature on the subject of the arrow of time, such as several essays in the book edited by Flood and Lockwood [Flo86]. Landsberg [Lan82] has compiled a reprint collection of papers from 1930 to 1980, and the book by Zeh [Zeh89] has a more technical discussion on several aspects of the direction of time.

1.4.3 Maxwell’s Equations and *PCT*

Now that we understand the definition and interpretation of the discrete symmetries of *P*, *C*, and *T*, it is interesting to apply them to equations describing a field. We now do this for the electromagnetic field described by Maxwell’s equations. In Section 1.4.4 we summarize results for quantum-mechanical wave function ψ fields.

The Maxwell equations may be written (in Gaussian units) as

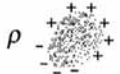
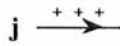
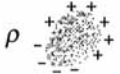

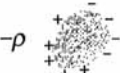
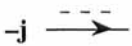
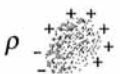

$$\begin{aligned} \nabla \times \mathbf{E} + \frac{1}{c} \frac{\partial \mathbf{B}}{\partial t} &= 0 & \nabla \cdot \mathbf{E} &= 4\pi\rho \\ \nabla \times \mathbf{B} - \frac{1}{c} \frac{\partial \mathbf{E}}{\partial t} &= \frac{4\pi}{c} \mathbf{j} & \nabla \cdot \mathbf{B} &= 0 \end{aligned} \tag{1.37}$$

We write the equations in terms of \mathbf{E} and \mathbf{B} , rather than the more symmetric potentials ϕ and \mathbf{A} , because our intuition about the symmetry properties of \mathbf{E} and \mathbf{B} is probably better. (Problem 1.10 suggests that you also write the Maxwell equations in the potential form, then carry out an analysis similar to that made for \mathbf{E} and \mathbf{B} .)

To analyze the action of P , C , and T on each quantity appearing in (1.37), consider first their effects on the source terms, the charge density ρ and the current density \mathbf{j} . By making sketches, as we show in Table 1.5, you can readily check the symmetry properties of the source terms. (Under P , volume elements do not change sign.) Note that only C affects ρ , but that \mathbf{j} is reversed by each of P , C , and T . In neither case does PCT applied sequentially return ρ or \mathbf{j} to its original sign.

The divergence and curl operators—which involve only spatial coordinates—are affected only by P . By considering their expression in Cartesian coordinates (for example), it is easy to see that they change sign under P . Finally, for the discrete-symmetry properties of the fields \mathbf{E} and \mathbf{B} , just consider a simple experimental setup and think through what happens under each symmetry operation. This will lead you to the results in Table 1.5. The actions of the parity (P), charge-conjugation (C), and time-reversal (T) operations on the dynamical quantities appearing in the Maxwell equations are summarized in Table 1.5.

TABLE 1.5 P , C , and T symmetries of electromagnetic sources and fields.

	ρ 	\mathbf{j} 	$\nabla \cdot$	$\nabla \times$	\mathbf{E}	\mathbf{B}
Symmetry operator	Effect of the symmetry operator on the source or field					
P	ρ 	$-\mathbf{j}$ 	$-\nabla \cdot$	$-\nabla \times$	$-\mathbf{E}$	\mathbf{B}
C	$-\rho$ 	$-\mathbf{j}$ 	$\nabla \cdot$	$\nabla \times$	$-\mathbf{E}$	$-\mathbf{B}$
T	ρ 	$-\mathbf{j}$ 	$\nabla \cdot$	$\nabla \times$	\mathbf{E}	$-\mathbf{B}$

Now put the pieces together and consider the effects of P , C , and T acting on each of the four Maxwell equations (1.37) in turn. What is remarkable (as Problem 1.10 suggests that you verify) is that *each* Maxwell equation is unchanged under these discrete symmetries. That is, neither the action of P , or of C , or of T changes these equations—each is invariant even though the sources and fields in them may change sign under P , C , or T . Although this may have seemed obvious to scientists in Maxwell's time, the demonstrated violation of parity in the weak interaction does not make parity invariance an obvious requirement for fields other than the electromagnetic field.

In Table 1.5 we assume that electric charges are unaffected by P and T . Further, in considering the action of C , the “test charges” that are thought of as being used to measure the fields are assumed *not* to change sign under C . Rosen [Ros73] discusses alternative valid scenarios for the action of P , C , and T .

We note further that the Maxwell equations are not the whole story on electrodynamics, since they do not describe the quantized nature of electromagnetic radiation or the consequences of the identity of photons (Bose statistics). For quantized fields what are the discrete-symmetry properties? In the next subsection we sketch an answer to this question.

1.4.4 PCT and the Pauli Principle: Lüder's Theorem

The example of Maxwell's equations and its invariance under each of P , C , and T *separately* might suggest to us that this is a property of any field that describes nature. However, this cannot be true, since experiment shows that the weak interaction giving rise to β decay violates parity symmetry. Is there any constraint on the symmetries of field equations under the *joint* action of PCT ?

Lüder's Theorem. Pauli discussed this question [Pau55] and Lüders provided a definitive answer [Lüd57]. Lüders proved by explicit examination of the actions of P , C , and T on the fields (as we do for the Maxwell equations in Section 1.4.3) that in quantum field theory—the Klein-Gordon equations for spin 0 and spin 1 and the Dirac equation for spin 1/2—the equations have the following symmetry properties:

Lüder's theorem. The Klein-Gordon and Dirac equations are invariant under the *joint* action of PCT if the following conditions are satisfied:

- (1) The interactions are local and Lorentz covariant.
- (2) Kinematically-independent fields anticommute for fermions and commute for bosons.

Now to explain the terminology in the theorem. To call an interaction “local” is, in non-technical terms, to say that the interaction at a given space-time point satisfies causality, as discussed in Section II.4b in [Rom61]. “Kinematically-independent

fields” are discussed in the context of two subsystems (kinematically independent), such as the electrons in two well-separated atoms. If the Pauli principle holds—the total system wave function changes sign under exchange of two electrons with all quantum numbers the same—then we have anticommuting fields. Similarly, if there are two boson systems (such as the pions in two atoms where electrons are replaced by pions), exchange of two bosons should leave the wave function unchanged.

There are three significant remarks to be made about Lüder’s theorem:

- The theorem does *not* claim that PCT (or any rearrangement of them) is the unit (identity) operator. As Table 1.5 shows, this does not hold even for electromagnetism.
- Lüder’s theorem establishes an intimate relation between P , C , and T and the spin-statistics of particles. For this reason it is often called the “spin-statistics theorem.” In work preceding that of Pauli and Lüders, Schwinger [Sch51, Sch53] assumed the validity of the theorem and derived the spin-statistics connection.
- Although the proof is given explicitly only for the Klein-Gordon and Dirac equations, these empirically verified equations constitute paradigms for the construction of other quantum fields. Thus, Lüder’s theorem is almost always used to constrain any field equations that may be devised.

A derivation of the theorem is given in Section IV.5 of Roman’s text [Rom61], where consequences of the theorem for elementary particle physics are discussed. For example, in the so-called T violation for the kaon system, what is measured is a violation of PC , from which (by using Lüder’s theorem) one *infers* that there is T violation. Extensive references to experimental tests of the discrete space-time symmetries are given in Commins’ resource letter [Com93].

How Valid Is the Pauli Principle? Since the Pauli principle is so intimately related to the generalized reflection invariances of P , C , and T , it is worthwhile to place limits on the validity of this principle. Its approximate validity is assured by the successive filling of shells that is required in atomic-structure or nuclear shell model calculations, and by the success of Fermi-Dirac statistics in describing the density of states of electrons in many situations—from conductivity of metals, through the balance between electron degeneracy and gravitational pressure in stars, to the equation of state of a neutron star.

The most common test of the limits of validity of the principle is to seek lower limits on the relative abundance of anomalous atoms or nuclei, having more fermions in a shell with angular momentum j than is allowed by the exclusion principle, namely, more than $2(2j + 1)$. By using accelerator mass spectrometry for precision detection of anomalous atoms and nuclei, Nolte and coworkers [Nol91] showed that the relative abundance of anomalous to normal ^{20}Ne atoms is $< 2 \times 10^{-21}$, for ^{36}Ar atoms the limit is $< 4 \times 10^{-17}$, while for anomalous nuclei of ^5Li in ^6Li the limit is $< 1 \times 10^{-17}$.

The Pauli Principle in Scattering. A dramatic demonstration of the effects of coherence, interference, and the Pauli principle is shown in low-energy nuclear

physics experiments of Coulomb scattering of the isotopes ^{12}C and ^{13}C from each other, as described by Plattner and Sick [Pla81] and shown schematically in Figure 1.22 for energies of relative motion well below the Coulomb barrier. At such energies the nuclei interact entirely by their mutual Coulomb repulsions, so the quantum mechanics of the problem is straightforward.

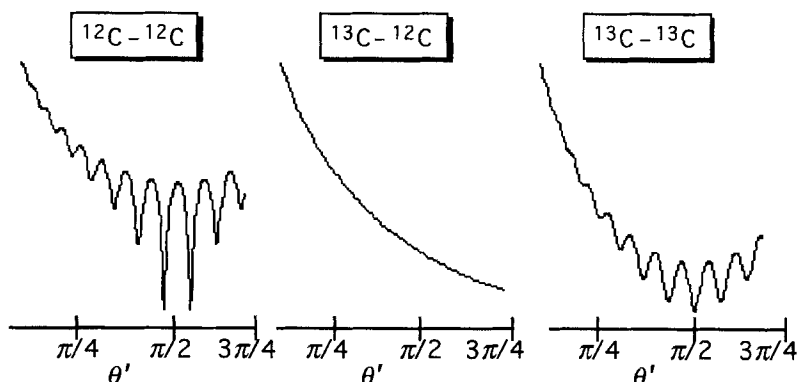


FIGURE 1.22 Identical particles scatter differently, depending on whether both are bosons (two ^{12}C nuclei), whether they are distinguishable (^{13}C - ^{12}C), or whether both are fermions (two ^{13}C nuclei). Scattering intensity as a function of laboratory scattering angle $\theta' \approx \theta/2$ is shown for each pair of nuclei for Sommerfeld parameter (Problem 1.11) $\eta = 15$, corresponding to incident energy about 4 MeV in the laboratory frame. (Adapted from *Mathematica* notebook PauliCC.)

In the scattering experiments described in [Pla81] the nuclei of ^{12}C have spin zero, so they act like bosons, whereas ^{13}C nuclei have spin $1/2$ and act like fermions under exchange. Thus, in ^{12}C - ^{12}C scattering the scattering wave function should be *symmetric* under exchange of the two nuclei. For ^{12}C - ^{13}C scattering no symmetry requirements are imposed. For ^{13}C - ^{13}C a combination of scattering with spins antiparallel ($3/4$ of the time) for an *antisymmetric* wave function and scattering with spins parallel ($1/4$ of the time) for a *symmetric* wave function is required. The data reported in their article are in very good agreement with predictions shown in Figure 1.22. Problem 1.11 suggests how to make the appropriate calculations for discrete symmetries.

1.5 BROKEN SYMMETRIES FROM COSMETOLOGY TO COSMOLOGY

Now that we have reviewed several aspects of symmetry in physical systems, it is worthwhile to pause and reflect on the observation that it is mostly asymmetry (sometimes called “broken symmetry”) that we observe in the world around us.

Symmetry and Humans. In human creations we seem to favor a high degree of geometrical symmetry, especially reflection and rotational symmetries. Examples

are found in the logos of businesses and the hubcaps of automobiles, as discussed by Gallian [Gal90] in the context of groups of symmetries (our Section 2.5). Although the human skeleton has a high degree of reflection symmetry, the internal organs are asymmetrically placed, and if a person's features (particularly the face and head) are either very regular or somewhat more irregular than the norm, we often find this unappealing. Thus, very few men will part their hair down the centerline, and people sometimes resort to cosmetology to change their facial appearance.

Juxtaposition of *cosmetology* and *cosmology* in this excursion may seem unusual. Both words, however, are immediately derived from the Greek *kosmos*, meaning order or arrangement. The first term refers to human beauty, especially of the face, whereas cosmology is the study of the general structure and evolution of the universe, with the presumption (common to all sciences) that the universe is ordered and is able to be explained rationally.

Asymmetry in Biological Systems. Broken symmetry is manifest in biological systems at several levels. As described in Section 1.2.1, chirality in biology is often manifested through a preferred direction of spiraling. The direction of such spiraling may depend upon environmental conditions. For example, the pinhead-sized sea creature *Neogloboquadrina pachyderma*, a foraminifer, forms an envelope that spirals in opposite directions depending on whether the water temperature is above or below 7°C. This property is unexplained. Figure 1.23 shows a drawing of the two chiralities observed.



FIGURE 1.23 The foraminifer *Neogloboquadrina pachyderma* develops with its four lobes in either a left-handed spiral (left sketch) or a right-handed spiral (right sketch), depending on the water temperature.

Geoscientists use the temperature dependence of the chirality of this foraminifer when examining cores of fossil sediments from the deep ocean floor in order to infer temperature variations of the oceans over geological epochs, and thereby to find clues to the presence of petroleum reservoirs. For example, in the article by Duplessy et al. [Dup91], the chirality of *Neogloboquadrina pachyderma* is used to infer the surface salinity of the North Atlantic Ocean during the last glacial maximum. The classical masterpiece on growth and form by Thompson [Tho43] provides many examples of chirality in biological systems and relates them to geometrical and physical phenomena. The polarization of sky light (thus a definite helicity) is used by bees [Fri49] and by fishes [Haw92] for orientation and navigation. It is probable that many creatures have adapted their vision to detect such polarization but that we do not yet know how to verify this.

At the molecular level, broken symmetry appears in the occurrence of only left-handed proteins and right-handed DNA in living things (Section 1.2.1). The relations between handedness, the origins of life, and evolution have been reviewed at an introductory level in an article by Avetisov, Goldanskii, and Kuz'min [Ave91]. They estimate the probabilities for simple biological systems—starting with a racemic mixture of molecules—to evolve into a chiral system over the span of several billion years since Earth was formed. They also describe a variety of physical advantage factors—such as circular polarization of scattered sunlight, geomagnetic fields plus the Coriolis force and static electric or gravitational fields—that might initiate such evolution. Even though β decay produces electrons or positrons with a definite helicity, it is now believed that this is unlikely to have a significant effect on biological evolution, as has also been summarized by Meiring [Mei87].

PROBLEMS ON SYMMETRY IN PHYSICAL SYSTEMS

1.1 The examples of Noether's theorem in Section 1.1.2 were worked out only for the simplest feasible systems exhibiting continuous symmetries—single particles in one or two dimensions. Generalize her theorem, but still use classical Newtonian mechanics, to prove the following for systems of particles in three dimensions:

- (a) A system of particles that interact by two-body, time-independent potentials that are translationally invariant (depend only on differences of particle coordinates) has a fixed total linear momentum.
- (b) The total energy of a system of particles subject to time-independent potentials is conserved.
- (c) An assembly of particles that are acted upon by time-independent central forces referred to the same force center has an angular momentum that is invariant under rotations about that force center.

1.2^M The shell motifs at the beginning of this and subsequent chapters visualize both angular momentum (rotations) and chirality (spiral sense). In order to understand the geometry of such rotations and to learn how such a shell can be described parametrically, consider the following.

- (a) Show that parametric equations generating such a shape in three dimensions are



$$\begin{aligned}x &= \phi \cos t \cos \phi \\y &= \phi \cos t \sin \phi \\z &= \phi \sin t + h\phi\end{aligned}\tag{1.38}$$

in which $0 \leq t \leq 2\pi$ generates the circular cross section of a spiral arm at a given ϕ , while ϕ generates the twist of the spiral about the central axis. For a spiral of r revolutions one has $0 \leq \phi \leq 2\pi r$. Also in this equation show that the helicity $h = +1$ for a right-handed spiral (as shown) and $h = -1$ for a left-handed spiral.

(b) By using *Mathematica*, or other system for doing mathematics by computer, generate and graph the three-dimensional spiral described by (1.38). The *Mathematica* notebook Shell in Appendix I may be used for this.

1.3 Suppose that N polygons lying in a plane and each having E edges of equal length ("regular" polygons) are to meet at a point, with no intervening space, that is, they tile the plane.

(a) By considering the angles within each polygon and the addition of angles where the polygons meet, show that

$$N = \frac{2E}{E-2} \quad \text{or} \quad E = \frac{2N}{N-2} \quad (1.39)$$

(b) Why is this relation symmetric under interchange of N and E ?

(c) By using this relation, prove that the only regular polygons that tile the plane have $E = 3, 4,$ or 6 (triangles, squares, and hexagons). These regular polygons are shown in Figure 1.8.

1.4 Consider a regular polyhedron, a three-dimensional convex solid with all F of its faces being the same. Use the result of Euler that F is related to the number of vertices, V , and the number of edges, E , by

$$V + F = 2 + E \quad (1.40)$$

Suppose that N edges meet at each vertex, then show that $E = NV/2$. Show also that if the number of edges on each face is S , then $E = FS/2$. Thus show that

$$\frac{1}{N} + \frac{1}{S} = \frac{1}{2} + \frac{2}{FS} \quad (1.41)$$

Use this result to verify Table 1.2, identifying all the regular polyhedra as shown in Figure 1.9.

1.5 Derive explicitly by using the rotation matrices the formula (1.17) for passive rotations in terms of active rotations.

1.6 Show that rotations about different axes do not commute. To do this, consider the sequences $\mathbf{A}_y(\beta)\mathbf{A}_z(\gamma)$ and $\mathbf{A}_z(\gamma)\mathbf{A}_y(\beta)$, where the matrices are given by (1.4) and (1.5).

(a) Give examples which show that for arbitrary α and β , the results depend upon the order of rotation.

(b) Show that if Maclaurin expansions of the matrix products are made and if only terms containing a single angle (α or β) are kept, the rotations *do* commute.

(c) Interpret the quantum-mechanical commutation rules for momentum-operator components, $[p_i, p_j] = 0$ (where i and j refer to $x, y,$ or z), from the viewpoint of commutation of translations. (Recall that the momentum operator generates in-

finitesimal displacements.) From this result, are the operators that generate infinitesimal rotations (they are called J_i , $i = x, y, \text{ or } z$) likely to commute?

1.7 Generalize the proof in terms of determinants for rotations and reflections, (1.20) and (1.21), to show that in a coordinate space with an odd number of dimensions—such as three—reflections cannot be produced by combining rotations.

1.8^M Explore parity and wave functions by using the *Mathematica* notebook Ppsi. The notebook is programmed with the function definition `psi` corresponding to (1.23). Modify this definition to a function of interest to you, but not necessarily of a definite parity, and run the program to produce graphics for you to interpret. Note that the program makes the various functions using the definitions in (1.23) without algebraic simplifications.

1.9 For the time-reversal (complex conjugation) of the plane wave (1.34), show the steps leading to (1.35).

1.10 The discrete-symmetry properties (P , C , and T) of Maxwell's equations (1.37) are discussed in Section 1.4.4 in terms of \mathbf{E} and \mathbf{B} fields. Check these properties by the following means.

(a) Express the divergence, $\nabla \cdot$, and the curl, $\nabla \times$, in spherical polar coordinates. Verify that under P they have the symmetry properties indicated in Table 1.5.

(b) Verify the correctness of the entries in Table 1.5 for the sources and fields by considering simple configurations of the sources ρ and \mathbf{j} .

(c) Write down Maxwell's equations in terms of the scalar potential ϕ and the vector potential \mathbf{A} , then make a similar table similar to Table 1.5 to check the symmetries of these fields under P , C , and T .

1.11^M Consider the Coulomb scattering of isotopes of the same element with boson character (spin zero) or fermion character (spin 1/2), as for ^{12}C or ^{13}C in Figure 1.22. For distinguishable particles (such as ^{13}C scattering from ^{12}C) the Coulomb-scattering amplitude, $f_c'(\theta)$, depends upon θ , the scattering angle in the center-of-mass frame, as [Lan90, Sections 4.C and 10.C]

$$f_c'(\theta) = \frac{e^{2i\eta \ln[\sin(\theta/2)]}}{\sin^2(\theta/2)} \quad (1.42)$$

in which η is the Sommerfeld Coulomb parameter, proportional to the product of the nuclear charges and inversely proportional to their relative speed. For distinguishable particles the angular dependence of the scattering intensity as a function of angle is $I_d(\theta) = |f_c'(\theta)|^2$.

(a) Show that for scattering between indistinguishable bosons (such as ^{12}C – ^{12}C) the requirement that wave functions be symmetric under exchange leads to

$$I_b(\theta) = |f_c'(\theta) + f_c'(\pi - \theta)|^2 \quad (1.43)$$

(b) Argue that for spin-1/2 particles (such as ^{13}C - ^{13}C) there is a total of four relative orientations of the spins, in only one of which the particles have all their quantum numbers equal, and it is for this that the wavefunction must be antisymmetric under exchange (Pauli principle). Show thereby that the observed intensity should be given by

$$I_f(\theta) = \frac{3}{4} |f_c'(\theta) + f_c'(\pi - \theta)|^2 + \frac{1}{4} |f_c'(\theta) - f_c'(\pi - \theta)|^2 \quad (1.44)$$

(c) Use either the *Mathematica* notebook `PauliCC` in Appendix I or a program of your own devising to calculate the angle dependences of the intensities I_b , I_d , and I_f . Compare your results with the corresponding curves shown in Figure 1.22 for Coulomb parameter $\eta = 15$. Note that the laboratory scattering angle, θ' , is related to the center-of-mass scattering angle, θ , by $\theta \approx 2\theta'$, since the masses of the two reactants are either equal or nearly equal.



Chapter 2

MATHEMATICAL AND QUANTAL PRELIMINARIES

Our purpose in this chapter is to review materials from mathematics and quantum mechanics relevant to our later treatment of angular momentum techniques and concepts. Generally speaking, mathematics provides the engines for spinning the merry-go-round of concepts and interpretation comprising quantum mechanics. Before starting this chapter, you should be familiar with standard matrix algebra, since our main emphasis in Section 2.1 is those unusual definitions and properties needed in the following chapters. Useful sources for review are Wong's introduction to mathematical physics [Won91], in which many of the matrix examples relate to rotations, and the texts by Arfken [Arf85] and by Butkov [But68]. In this chapter we review the mathematics and hint how it is applied in subsequent chapters.

In Section 2.2, on transformations and operators, the emphasis moves to applications that are particularly important in quantum mechanics. We review similarity and symmetry transformations, unitarity, the operator relations of exponentiation and commutation, and the raising and lowering (ladder) operators. Wong's book [Won91] provides introductory material on these topics. In Section 2.3 we review eigenvalues and eigenstates, with emphasis on their quantum-mechanical interpretation. The quantum-mechanics texts by Cohen-Tannoudji et al. [Coh77], by Shankar [Sha80], and by Sakurai [Sak94] provide (in order of increasing sophistication and decreasing vintage) suitable introductions to these topics.

Spinors and their properties are our topic in Section 2.4. The subject has a long and confusing history, since many ways of representing spinors have been devised. We summarize the essential ideas and uses of spinors for developing topics in angular momentum, then we show how spinors can be visualized to clarify their applications in this field. The penultimate section of this chapter (Section 2.5) is a primer on groups, with several examples and preliminary ideas. It would be helpful if you have been introduced to groups (including examples from geometry and the sciences) in a mathematics review course. For example, Wong's text [Won91] pro-

vides appropriate background. Our second excursion in this book, Section 2.6, is a philosophical digression on the relations between mathematics, group theory, and the physical sciences. It is intended to give you pause to wonder at the unreasonable effectiveness of mathematics in the sciences.

Finally in this chapter, in order to check that such mathematics have become embedded in your consciousness, there are problems on the preliminary mathematics and its applications. By the end of this chapter, we will have the basic mathematical and conceptual apparatus needed to develop our study of rotational symmetries for physical systems.

2.1 MATRIX DEFINITIONS AND MANIPULATIONS

We review highlights of matrix definitions and manipulations that are needed subsequently. We cast many of these in the language of quantum mechanics, particularly by using *bra*, $\langle \ |$, and *ket*, $| \ \rangle$, state vectors. The primary purpose of this is to provide examples, since the matrix properties are generally valid. We begin by recalling definitions from the algebra of linear spaces, including generalization of vectors in coordinate space to “vectors” described by kets in Hilbert spaces. Then we discuss relations between scalar (inner) products, matrices, and operators. Next, we review matrix *inner* products (conventional matrix products) and describe the less familiar matrix *direct* products that are so necessary for studying combinations of symmetries. Then we discuss operations on matrices and the resulting special properties, such as Hermiticity and orthogonality, and we establish the notation used for these operations. Finally at the end of this section, it is convenient to discuss rules for manipulating the phase factors that occur so frequently in the technology of angular momentum.

The relations between transformations, matrices, and linear operators are discussed more extensively in Chapter 2 of Wong’s mathematical physics text [Won91]. Linear operators in quantum mechanics are emphasized in Chapters 1 and 2 of Jordan’s treatment [Jor69], in Chapter 1 of Sakurai’s text [Sak94], and in De Lange and Raab’s book on operator methods in quantum mechanics [DeL91].

2.1.1 Linear Spaces and Operator Matrix Elements

Our purpose here is to establish the notation used in subsequent developments and to provide examples appropriate for investigating rotational symmetries. The references just cited provide detail, including proofs of results.

Linear Spaces. In a linear space one has a set of elements, called *vectors* (a generalization of vectors in coordinate space), together with two operations, one being *addition* (a generalization of addition in arithmetic and of vector addition) and the other being *scalar multiplication*. We distinguish the vectors (the *kets*, $\{ \ \} \rangle$) in a given space by labels, such as those for coordinate directions ($|x\rangle$, $|y\rangle$, $|z\rangle$) or the labels for angular momentum eigenvalues ($|\ell m\rangle$ for orbital angular momentum ℓ and its projection m).

Let us denote two representative vectors in a given space by $|s\rangle$ and $|t\rangle$, and denote by a and b two complex numbers. In a *linear* space one requires the following properties:

$$\begin{array}{ll}
 |s\rangle + |t\rangle = |t\rangle + |s\rangle & \text{commutation} \\
 |s\rangle + (|t\rangle + |u\rangle) = (|s\rangle + |t\rangle) + |u\rangle & \text{association} \\
 |s\rangle + |0\rangle = |s\rangle & \text{null vector } |0\rangle \\
 a(|s\rangle + |t\rangle) = a|s\rangle + a|t\rangle & \\
 (a + b)|s\rangle = a|s\rangle + b|s\rangle & a(b|s\rangle) = ab|s\rangle \\
 1|s\rangle = |s\rangle & 0|s\rangle = 0
 \end{array} \tag{2.1}$$

These properties are satisfied by conventional vectors in coordinate space, which we write as $|\mathbf{r}\rangle$ for a displacement vector and as $|\mathbf{p}\rangle$ for a momentum vector. Problem 2.1 (a) suggests that you demonstrate these properties. If we are concerned only with angles, rather than also with the magnitude of the vector, we sometimes use a notation such as $|(\theta\phi)\rangle$. Because our subject is *angular* momentum, we will often encounter such a state vector notation.

It is common to introduce a *bra* space, with elements $\langle s|$, $\langle t|$, $\langle u|$, and so on. This is often called the *dual space* to the ket space, as discussed in Sections 1.2 and 1.3 of Sakurai's text [Sak94]. Analogously to the required ket-space properties (2.1), we have the following requirements for a linear bra space:

$$\begin{array}{ll}
 \langle s| + \langle t| = \langle t| + \langle s| & \text{commutation} \\
 \langle s| + (\langle t| + \langle u|) = (\langle s| + \langle t|) + \langle u| & \text{association} \\
 \langle s| + \langle 0| = \langle 0| & \text{null bra vector } \langle 0| \\
 a(\langle s| + \langle t|) = a\langle s| + a\langle t| & \\
 (a + b)\langle s| = a\langle s| + b\langle s| & a(b\langle s|) = ab\langle s| \\
 1\langle s| = \langle s| & 0\langle s| = 0
 \end{array} \tag{2.2}$$

Examples of bra spaces are those whose elements are $\langle \mathbf{r}|$ or whose elements are $\langle(\theta\phi)|$.

Scalar Products. In a linear ket or bra space such as we have just discussed, we consider the generalization of scalar products of vectors in coordinate space. Scalar products are sometimes called inner products, a nomenclature that establishes a relation to inner products of matrices (Section 2.1.2). In a scalar product one forms bra-kets such as $\langle s|t\rangle$.

As with the requirement (2.1) for a set of vectors to form a linear space, the definition of the scalar product of two vectors in such a space is implicit, because any bilinear combination for the sets that has the following properties is sufficient to serve as a scalar product. If $|s\rangle$, $|t\rangle$, and $|u\rangle$ are any three vectors in the space, then scalar products involving them must have the following properties:

$$\begin{aligned} \langle s|t+u\rangle &= \langle s|t\rangle + \langle s|u\rangle \\ \langle s|at\rangle &= a\langle s|t\rangle \\ \langle t|s\rangle &= \langle s|t\rangle^* \\ \langle s|s\rangle &> 0 \quad \text{if } |s\rangle \neq |0\rangle \quad \langle 0|0\rangle = 0 \end{aligned} \tag{2.3}$$

The last property is often called the property of having a *positive-definite norm*, satisfied (for example) by conventional coordinate vectors. The quantity $\sqrt{\langle s|s\rangle}$ is usually called the *norm* of $|s\rangle$, corresponding to the magnitude of a conventional vector. State vectors labeled by s and t are said to be *orthogonal* if the scalar product $\langle s|t\rangle = 0$. Again, this is the terminology used for conventional vectors.

The scalar-product properties (2.3) are satisfied in quantum mechanics by both the general kets and by the wave functions, as Problem 2.1 (b) suggests that you show. The wave functions are the kets in a given representation, such as in configuration, \mathbf{r} , or momentum, \mathbf{p} , spaces. The connection is

$$\psi_s(\mathbf{r}) \equiv \langle \mathbf{r}|s\rangle \quad \varphi_s(\mathbf{p}) \equiv \langle \mathbf{p}|s\rangle \tag{2.4}$$

The third property in (2.3) is familiar from the properties of wave functions. Thus

$$\int \psi_t^*(\mathbf{r})\psi_s(\mathbf{r})d\mathbf{r} = \left[\int \psi_s^*(\mathbf{r})\psi_t(\mathbf{r})d\mathbf{r} \right]^* \tag{2.5}$$

Particularly for our developments in angular momentum, and independent of detailed considerations of quantum mechanics, we have the scalar product of a state vector $|jm\rangle$, where j and m are angular momentum numbers, with an angle ket $|(\theta\phi)\rangle$, expressed as

$$\langle (\theta\phi)|jm\rangle \tag{2.6}$$

The interpretation of such a scalar product is that it describes the angular momentum

state in terms of θ and ϕ . For example, when $j = \ell$ (an integer) this scalar product is proportional to a spherical harmonic, as shown in Sections 4.1, 6.3, and 6.4.

Linear Operators. Along with linear vector spaces, it is also useful to introduce linear operators. For an operator O that is linear

$$O(a|s\rangle) = a O|s\rangle \quad (2.7)$$

A clear discussion of linear operators and their matrix representations is given by Jordan in Chapter 2 of his book on linear operators for quantum mechanics [Jor69].

Antilinear Operators. Not all operators that are interesting for the physical sciences are linear. For example, as discussed in Section 1.4.2, the time-reversal operator (T) is *antilinear* (introduces at least a complex conjugate) rather than being linear. For any operator O_A that is antilinear

$$O_A(a|s\rangle) = a^* O_A|s\rangle \quad (2.8)$$

Now that we have defined linear spaces, scalar products, and operators, it is appropriate to combine the three to form operator matrix elements.

Matrix Elements of Operators. Recall that the scalar product of two kets, say $|s\rangle$ and $|t\rangle$, is written as $\langle s|t\rangle$. The state described by $|t\rangle$ may have been obtained by the effect of an operator, say O , on a state described by $|u\rangle$. Then

$$\langle s|t\rangle = \langle s|O|u\rangle = \mathbf{O}_{su} \quad (2.9)$$

in which the last equal sign indicates an abbreviation for the matrix element of O between states s and u . This subscript notation resembles that of conventional matrix algebra, but there may a difference—the “row” label s and the “column” label u may be *sets* of labels rather than single indices. The resemblance is close, as discussed in the following subsection.

In angular momentum, the operator O is often that describing rotation of a physical system through specified angles, such as the Euler angles (Section 1.3.1), while the bra and ket states are eigenstates of the angular momentum operators.

2.1.2 Inner and Direct Products of Matrices

Following on the discussion of matrix elements of operators just presented, we review the inner-product rule for matrix multiplication, then we proceed to the less familiar, but very important, direct product.

Matrix Inner Products. Recall the conventional (inner) product of two matrices and why it is so useful. Suppose that we make a succession of linear transforma-

tions, the first described by a matrix \mathbf{S} acting on a column vector \mathbf{v} , so that

$$\mathbf{v}_S = \mathbf{S}\mathbf{v} \quad (2.10)$$

If we follow this by a linear transformation of \mathbf{v}_S by matrix \mathbf{T} , we have

$$\mathbf{v}_T = \mathbf{T}\mathbf{v}_S = \mathbf{T}\mathbf{S}\mathbf{v} = \mathbf{U}\mathbf{v} \quad (2.11)$$

in which the elements of matrix \mathbf{U} are given by the inner-product rule

$$U_k = \sum_j T_{ij} S_{jk} \quad (2.12)$$

in which the sum over j is over the columns of \mathbf{T} and over the rows of \mathbf{S} , which must therefore be of the same dimension. Given this rule, one may either apply each transformation in succession in the order given (\mathbf{S} first then \mathbf{T}), or one can evaluate the matrix \mathbf{U} by rule (2.12), then apply this matrix to \mathbf{v} . The latter method is usually much simpler computationally, and it is sometimes simpler conceptually.

What is the connection between these rules of matrix algebra and the matrix representations of operators in Section 2.1.1? Suppose that we have sets of matrix elements O_{st} and P_{tu} of the operators O and P in three spaces whose representative vectors are $|s\rangle$, $|t\rangle$, and $|u\rangle$. (These vectors may be, and often are, in the same space.) By writing out in scalar-product language by using (2.12) the requirement

$$(OP)_{su} = \sum_t O_{st} P_{tu} \quad (2.13)$$

we find immediately the condition, often called the unit-operator expansion,

$$\sum_t |t\rangle\langle t| = I \quad (2.14)$$

in which the sum is over all the elements in the set and the I is a unit operator. Indeed, we subsequently take this requirement for granted and often use it to replace a unit operator by the expression on the left-hand side of (2.14). For example, in quantum mechanics this is often called “summing over intermediate states.” The property (2.14) is not a consequence of quantum dynamics, but just expresses the properties of the linear vector spaces used in quantum mechanics.

Shirt-and-Tie Theorem. Suppose that we have matrices, \mathbf{S} and \mathbf{T} , whose inner product represents successive operations, S followed by T . For example, S might be the operation of putting on a shirt, and T might be putting on a tie. Conventional dress calls for $U = TS$, in which the rightmost operation is done first. By direct multiplication of the corresponding matrices, we see that the result for \mathbf{U}^{-1} satisfies

$$\mathbf{U} = \mathbf{TS} \quad \Rightarrow \quad \mathbf{U}^{-1} = \mathbf{S}^{-1}\mathbf{T}^{-1} \quad (2.15)$$

Operationally, we can recall this relation by interpreting the right-hand-side expression for \mathbf{U}^{-1} . Namely, one takes off the tie (T^{-1}), then takes off the shirt (S^{-1}). The order of inversion usually matters, unless the original operations (S and T) commute. For example, if S is putting on shoes and T is putting on a tie, then it probably doesn't matter in what order you put them on or take them off, so $ST = TS$ and the corresponding matrices satisfy $\mathbf{ST} = \mathbf{TS}$.

In these examples the commutation property depends upon the topology of the human body and of clothing. (The shirt and tie operations for giraffes probably commute.) In quantum mechanics the successive operations usually refer to successive measurements, and noncommutation of \mathbf{S} and \mathbf{T} indicates that measurement of operator S affects the outcome of measuring T . As we discuss in detail for angular momentum in Section 5.2, this leads to uncertainty relations between noncommuting observables.

Direct Products. To introduce the direct product (sometimes called the Kronecker product), consider a 2×2 matrix \mathbf{M} and a 3×2 matrix \mathbf{N} . From these two matrices one cannot form the inner product \mathbf{MN} , since there is no matching of number of rows with number of columns. One can, however, form a *direct product*, as follows. Take any element of \mathbf{M} and associate it multiplicatively with *any* element of \mathbf{N} to obtain an element of their direct product $\mathbf{M} \otimes \mathbf{N}$:

$$(\mathbf{M} \otimes \mathbf{N})_{ij,kl} \equiv M_{ik} N_{jl} \quad (2.16)$$

The subscript notation on the left-hand side is that ij labels the super row and kl labels the super column. The dimension of a direct-product matrix is therefore the product of the dimensions of its constituent matrices, and it is therefore at least as large as either of them. For example, with the above matrices their direct product is of dimension 6×4 . Let us write out $\mathbf{M} \otimes \mathbf{N}$ explicitly, as displayed in Figure 2.1.

$$\mathbf{M} \otimes \mathbf{N} = \begin{bmatrix} M_{11}N_{11} & M_{11}N_{12} & M_{12}N_{11} & M_{12}N_{12} \\ M_{11}N_{21} & M_{11}N_{22} & M_{12}N_{21} & M_{12}N_{22} \\ M_{11}N_{31} & M_{11}N_{32} & M_{12}N_{31} & M_{12}N_{32} \\ \hline M_{21}N_{11} & M_{21}N_{12} & M_{22}N_{11} & M_{22}N_{12} \\ M_{21}N_{21} & M_{21}N_{22} & M_{22}N_{21} & M_{22}N_{22} \\ M_{21}N_{31} & M_{21}N_{32} & M_{22}N_{31} & M_{22}N_{32} \end{bmatrix}$$

FIGURE 2.1 Direct product of a 2×2 matrix \mathbf{M} with a 3×2 matrix \mathbf{N} . The dashed lines separate parts of the matrix that contain different elements of \mathbf{M} .

Although the most common notation for direct products of matrices is the symbol \otimes , as in $\mathbf{M} \otimes \mathbf{N}$, the notation $\mathbf{M} \times \mathbf{N}$ is also used, although this is easily confused with multiplication or with the vector cross product, since it may be unclear in some contexts whether \mathbf{M} and \mathbf{N} are matrices or vectors. Direct products also occur in group theory (Section 2.5), where the \times notation is more common than \otimes .

Direct Products and Spin. An example of the direct product that is particularly relevant to the treatment of spin in quantum mechanics is the following. Consider the 2×1 column matrices

$$\alpha = \begin{bmatrix} \alpha_+ \\ \alpha_- \end{bmatrix} = \alpha_+ \begin{bmatrix} 1 \\ 0 \end{bmatrix} + \alpha_- \begin{bmatrix} 0 \\ 1 \end{bmatrix} \quad \beta = \begin{bmatrix} \beta_+ \\ \beta_- \end{bmatrix} = \beta_+ \begin{bmatrix} 1 \\ 0 \end{bmatrix} + \beta_- \begin{bmatrix} 0 \\ 1 \end{bmatrix} \quad (2.17)$$

These might represent the state of a spin-1/2 system α , with probability amplitude α_+ for spin up and probability amplitude α_- for spin down, with a similar interpretation for system β . The direct product of the two matrices, $\alpha \otimes \beta$, is also a column matrix, given by

$$\alpha \otimes \beta = \begin{bmatrix} \alpha_+ \beta_+ \\ \alpha_+ \beta_- \\ \alpha_- \beta_+ \\ \alpha_- \beta_- \end{bmatrix} = \alpha_+ \beta_+ \begin{bmatrix} 1 \\ 0 \\ 0 \\ 0 \end{bmatrix} + \alpha_+ \beta_- \begin{bmatrix} 0 \\ 1 \\ 0 \\ 0 \end{bmatrix} + \alpha_- \beta_+ \begin{bmatrix} 0 \\ 0 \\ 1 \\ 0 \end{bmatrix} + \alpha_- \beta_- \begin{bmatrix} 0 \\ 0 \\ 0 \\ 1 \end{bmatrix} \quad (2.18)$$

In this direct product, following the interpretation of (2.17) for spin 1/2, the column matrices with either a one or a zero in each position may be interpreted as follows. The leftmost matrix is associated with a total spin projection of $(+1/2) + (+1/2) = 1$, the next two matrices belong to spin projection zero, and the rightmost matrix belongs to spin projection -1 . From rules that you probably know already (and which we derive in Section 3.4), the projections of magnitude 1 can belong only to a spin-1 system, while the projections of zero can belong to spin-1 or to spin-0 systems. Therefore, the direct-product matrix does not represent a state with unique total angular momentum or unique projection. One of our tasks in Chapter 7 is to find the coefficients of a unitary transformation to produce unique values from the direct product of two angular momentum states.

These coefficients are called Clebsch-Gordan coefficients or Wigner 3- j coefficients. The attribution to Clebsch [Cle72] and Gordan [Gor75] relates to their work on binary algebraic forms and direct products (as described here) in the nineteenth century, 50 years before Wigner's use of similar coefficients in quantum mechanics.

Notice that the operation of taking the direct product, like the familiar inner product of matrices, is a noncommuting operation, as can be seen in the example (2.18), where $\beta \otimes \alpha \neq \alpha \otimes \beta$. Notice that the noncommutation is rather simple,

because the same coefficients occur, but their ordering depends on the order of multiplication. This ordering dependence needs to be taken into account, for example, when combining two angular momenta, where it gives rise to phase differences, as derived in Section 7.2. The same property holds for $\mathbf{M} \otimes \mathbf{N}$ in (2.16). On the other hand, the matrix elements in the inner product \mathbf{NM} are usually quite different from those of \mathbf{MN} .

Direct Products and Separable Hamiltonians. In quantum mechanics direct-product representations occur when treating the evolution of a system with a separable Hamiltonian, H , in which $H = H_1 + H_2$, with the sub-Hamiltonians H_1 and H_2 having no (generalized) coordinates in common. The equation of evolution of the state function ψ , namely

$$i\hbar \frac{\partial \psi}{\partial t} = H\psi \tag{2.19}$$

can then be solved by $\psi = \psi_1 \psi_2$, where

$$i\hbar \frac{\partial \psi_1}{\partial t} = H_1 \psi_1 \qquad i\hbar \frac{\partial \psi_2}{\partial t} = H_2 \psi_2 \tag{2.20}$$

Those parts of ψ represented by matrices (typically, intrinsic-spin states) will appear as direct products of the spin matrices for parts 1 and 2. Even if one subsystem has no spin, a representation by a direct product is still possible if the part without spin is represented by the 1×1 unit matrix, since

$$[1] \otimes \mathbf{M} = \mathbf{M} \otimes [1] = \mathbf{M} \tag{2.21}$$

Inner Products and Direct Products. Having shown properties and some uses of direct-product matrices, it is worthwhile to summarize schematically the differences between inner products and direct products, as shown in Figure 2.2.

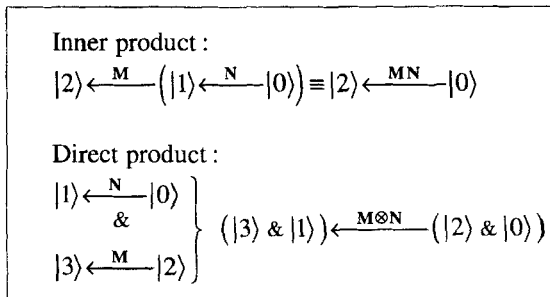


FIGURE 2.2 Schematic summary of the difference between the action of the conventional inner product \mathbf{MN} , converting state 0 to state 1 then to state 2, and the direct product $\mathbf{M} \otimes \mathbf{N}$, converting state 0 to state 1 and, *independently*, state 2 to state 3.

Problem 2.2 suggests that you prove several other interesting and useful properties of direct products of matrices. After this introduction to direct products, their potential applications, and their distinction from inner products, we review matrices with special properties that are often needed in angular momentum.

2.1.3 Operations on Matrices, and Special Properties

We now summarize the nomenclature and some properties of matrices that are relevant to symmetry investigations. First, we review operations on matrices, then symmetry properties that matrices may have under these operations, then we discuss block-diagonal matrices. A survey of the algebra of matrices, with emphasis on mathematical physics, is given in Chapter 2 of Wong's text [Won91].

Operations on Matrices. We first establish our notation for common operations, since the notation is quite variant between mathematics and the sciences. Our notation is summarized in Table 2.1.

TABLE 2.1 Operations on matrices.

Operation	Symbol and its name	Matrix-element relation
Transpose	~ tilde	$(\tilde{\mathbf{M}})_{jk} = \mathbf{M}_{kj}$
Complex conjugate	* asterisk, "star"	$(\mathbf{M}^*)_{jk} = \mathbf{M}_{jk}^*$
Hermitian conjugate	† "dagger"	$(\mathbf{M}^\dagger)_{jk} = \mathbf{M}_{kj}^*$

Note that it is common in mathematics to use a bar ($\bar{}$) for our star (*), and a star to denote the Hermitian conjugate (†), which is also called the "adjoint."

Operations on Matrix Products. Particular care needs to be taken when making the above operations on products of matrices, because the ordering of the matrices becomes inverted under transposition, inversion ("shirt-and-tie" theorem in Section 2.1.2), and Hermitian conjugation, but *not* under complex conjugation. Thus, we have

$$\begin{aligned}
 \text{transpose}(\mathbf{M}_1\mathbf{M}_2\dots) &= \dots\tilde{\mathbf{M}}_2\tilde{\mathbf{M}}_1 \\
 (\mathbf{M}_1\mathbf{M}_2\dots)^{-1} &= \dots\mathbf{M}_2^{-1}\mathbf{M}_1^{-1} \\
 (\mathbf{M}_1\mathbf{M}_2\dots)^\dagger &= \dots\mathbf{M}_2^\dagger\mathbf{M}_1^\dagger
 \end{aligned}
 \tag{2.22}$$

in which the ellipsis (...) denotes continuation to an arbitrary number of matrices.

They are written out by *inverted order* on the right-hand sides. The basic results are readily demonstrated using just two matrices, then the result for an arbitrary number of matrices can be obtained by mathematical induction, as Problem 2.3 suggests that you show.

Symmetry Properties. Matrices with special symmetries that are used extensively, especially in quantum mechanics, are summarized in Table 2.2.

TABLE 2.2 Matrices with special properties frequently used for symmetries and quantum mechanics.

If matrix \mathbf{M} has property of	then it satisfies	for which a typical application is
Diagonal	$M_{jk} = M_{jj} \delta_{jk}$	Matrix in the principal-axis system
Symmetric	$M_{jk} = M_{kj}$ $\tilde{\mathbf{M}} = \mathbf{M}$	Moment of inertia
Real	$M_{jk} = M_{jk}^*$	Bound states in quantum mechanics
Hermitian (self-adjoint)	$M_{kj}^* = M_{jk}$ $\mathbf{M}^\dagger = \mathbf{M}$	A quantum-mechanical observable
Real orthogonal	$\tilde{\mathbf{M}} = \mathbf{M}^{-1}$, $\mathbf{M}^* = \mathbf{M}^{-1}$	Spatial rotation
Unitary	$\mathbf{M}^\dagger = \mathbf{M}^{-1}$	Transformation by \mathbf{M} preserves the norm of a Hermitian matrix

Block-Diagonal Matrices. Especially important for simplifying much of the following mathematics and quantum mechanics is the property of a matrix to be *block diagonal*. An example of such a matrix is given in Figure 2.3.

$$\mathbf{M} = \begin{bmatrix} [\mathbf{M}_1] & \mathbf{0} & \mathbf{0} \\ \mathbf{0} & [\mathbf{M}_2] & \mathbf{0} \\ \mathbf{0} & \mathbf{0} & [\mathbf{M}_3] \end{bmatrix} \tag{2.23}$$

FIGURE 2.3 Block-diagonal matrix \mathbf{M} is composed of submatrices \mathbf{M}_1 , \mathbf{M}_2 , and \mathbf{M}_3 , which may be of different sizes. Large zeros indicate submatrix blocks where *all* matrix elements are zero.

Note that in a block-diagonal matrix there are no common elements between the different blocks. Therefore, if \mathbf{N} is another matrix, the product \mathbf{MN} contains \mathbf{M}_1 as a common matrix in the top positions, \mathbf{M}_2 as a common matrix in the middle

position, and \mathbf{M}_3 is common in the bottom positions. In particular, if \mathbf{N} is also block diagonal, then $\mathbf{MN} = \mathbf{NM}$ is block diagonal. Thus, block-diagonal matrices have many properties of diagonal matrices if the *blocks* are treated as if they were matrix *elements* rather than submatrices.

Irreducible Form. If the matrix in Figure 2.3 is in the form such that each diagonal block has been reduced to its smallest possible size, the matrix \mathbf{M} is said to be in a form that is irreducible. In Section 2.5.5 we discuss this in the context of matrix representations of groups. The property of irreducibility is very important for irreducible spherical tensors in Chapter 8.

As you see from Figures 2.1 and 2.3, the complexity of matrices in direct-product and irreducible forms grows very quickly with the number of elements in them. Therefore, it is not usual to exhibit the matrices in pictorial form. It is, however, conceptually and technically useful to have such pictures in your mind's eye when manipulating the elements of such matrices.

2.1.4 Phase Manipulation Rules

Although the following material on phase manipulation rules may seem trivial, you are almost sure to break the rules, especially if you don't understand the following. It is important that phase manipulation rules be applied correctly, since many symmetry effects of the kinds discussed in Chapter 1—especially those in quantum systems (Section 1.4)—are very sensitive to relative phases in formulas describing the symmetries.

Phase factors that we use multiply other expressions and are either +1 or -1. Thus, they are of the form $(-1)^n$, where n is an integer. This property will be ensured by choosing phases of angular momentum eigenstates appropriately whenever a choice must be made. Given this property, we summarize the rules for manipulating phases arising from integer exponents n_1 and n_2 by

$$(-1)^{n_1} (-1)^{n_2} = (-1)^{n_1+n_2} = (-1)^{n_1-n_2} = (-1)^{n_1} (-1)^{-n_2} \quad \text{etc.} \quad (2.24)$$

As you are probably already aware, the total angular momentum number j can take on only half-integer values such as 0, 1/2, and 1, while the corresponding projection number m may range from $-j$ to j by integer steps. Therefore, the combination $j \pm m$ is always an integer, to which the phase rules (2.24) may be applied. Even if j is a half integer, then m is a half integer and the following manipulations are allowed:

$$(-1)^{j+m} = (-1)^{-3j+m} = (-1)^{j-3m} \quad (2.25)$$

in which the equalities hold because $(-1)^{4j} = (-1)^{4m} = 1$.

If the total angular momentum number $j = \ell$, an *integer*, its projection m is therefore also an integer. Then we can mimic (2.24) and write

$$(-1)^\ell (-1)^m = (-1)^{\ell \pm m} = (-1)^\ell (-1)^{-m} \quad \text{etc.} \quad (2.26)$$

The final rule about phase manipulations relates to combinations of total angular momenta. Suppose that j_1 , j_2 , and j_3 form a triangle—denoted by $\Delta(j_1 j_2 j_3)$ —then we have the following phase rule:

$$\begin{array}{ccc} \begin{array}{c} \text{---} j_3 \text{---} \\ \backslash \quad / \\ j_1 \text{---} \quad j_2 \end{array} & \equiv & \Delta(j_1 j_2 j_3) \\ \Rightarrow & & (2.27) \\ (-1)^{j_1 \pm j_2 \pm j_3} = (-1)^{\text{integer}} & & \text{(either sign combination)} \end{array}$$

Given the triangle condition, any combination of the signs in (2.27) is allowed.

By appropriate application of phase manipulation rules in analytical and computational work, one can often simplify angular momentum formulas significantly.

2.2 TRANSFORMATIONS AND OPERATORS

In this section we review the mathematics of transformations and operators, particularly in the contexts used in quantum mechanics, in which we discuss matrix elements of quantal operators between state vectors (“wave functions”). Because there are both active and passive viewpoints of symmetry operations (Sections 1.2.1, 1.3.1), and—since the operation may be considered as applied to dynamical operators, to state vectors, or to both—it is important to describe carefully what type of transformation one is making.

We discuss the possible transformations and their matrix elements in Sections 2.2.1 (similarity transformations) and 2.2.2 (unitary transformations). From unitary operators we are led in Section 2.2.3 to their relation to exponentials of Hermitian operators, since such operators often represent observables in quantum mechanics. The question of whether or not operators commute is especially important in quantum mechanics, since in this mechanics noncommutativity implies uncertainty relations in measurements (Section 5.2). Therefore, in Section 2.2.3 we also discuss commutators of operators. Finally, in Section 2.2.4 we develop techniques for the so-called raising and lowering (ladder) operators.

2.2.1 Similarity and Symmetry Transformations

We first discuss the interpretation of three types of symmetry transformations, then present the matrix algebra of similarity transformations. Similar material is presented in Chapter 14 of Lipkin’s lecture notes on quantum mechanics [Lip73] and,

with more mathematical detail, in Jordan's text on linear operators for quantum mechanics [Jor69].

When considering state vectors and matrix elements of operators between these state vectors, there are three types of transformations. We assume that a physical system is described by its state vectors and by operators on them. The quantities that undergo transformations are therefore typically wave functions or operators. However, to maintain generality—at the expense of concreteness—we use state vectors, bras and kets such as $\langle j |$ and $|k\rangle$. General operators will be denoted by P , and they are typically dynamical operators such as Hamiltonians. Operators related to symmetries (such as rotations) will be denoted by S , or by U if they are unitary. In referring to coordinates in the following, we intend the same notion as that of generalized coordinates in classical mechanics [Gol80], rather than only spatial coordinates. We now describe and distinguish three types of transformations.

Active Transformation. As discussed in Section 1.2.1 generically and illustrated in Section 1.3.1 for rotations, an active transformation by operator S_A changes the physical system but leaves the coordinates unchanged. Thus, in the *active viewpoint*

$$|k\rangle \xrightarrow{S_A} S_A |k\rangle = |k_S\rangle \quad P \xrightarrow{S_A} P \quad (2.28)$$

in which $|k_S\rangle$ is a changed state. The operators, being expressed in terms of coordinates, are unchanged by an active transformation. What happens to matrix elements of operators? They are usually changed, since

$$\langle j | P | k \rangle \xrightarrow{S_A} \langle j_S | P | k_S \rangle \quad (2.29)$$

Compare the active viewpoint with the second viewpoint.

Passive Transformation. A passive transformation by S_P leaves the system unchanged but changes the coordinate system. Thus, in the *passive viewpoint*

$$|k\rangle \xrightarrow{S_P} |k\rangle \quad P \xrightarrow{S_P} P_S \quad (2.30)$$

in which P_S is the changed operator. Matrix elements are usually changed under a passive transformation, according to

$$\langle j | P | k \rangle \xrightarrow{S_P} \langle j | P_S | k \rangle \quad (2.31)$$

In the earlier presentations (Sections 1.2.1 and 1.3.1) this is where the discussion ended. For calculating matrix elements, there is a third type of transformation.

Canonical Transformation. What happens if we change *both* the physical system *and* the coordinates? Let us assume that the transformations—call them S_c —are unitary, $S_c = U$, with the matrix representations of U being unitary (Section 2.1.3) so that $U^\dagger = U^{-1}$. Then we may write

$$\begin{aligned} \langle j|P|k\rangle &\xrightarrow{S_c} \langle j_S|P_S|k_S\rangle = \langle Uj|UPU^{-1}|Uk\rangle \\ &= \langle j|U^\dagger UPU^{-1}U|k\rangle = \langle j|P|k\rangle \end{aligned} \tag{2.32}$$

That is, for unitary transformations the matrix elements are *invariant* under a canonical transformation, thus defined. This behavior is analogous to the invariance in classical mechanics of observables to the choice of coordinate systems. For example, a calculation (if done exactly) must give the same value in Cartesian as in spherical-polar coordinates. Notice that in (2.32) we use the transformed operator in the form UPU^{-1} , as we justify below when discussing similarity transformations.

Comparing Transformation Rules. A simple example showing the behavior of the three types of transformations clarifies the differences between them and suggests an appropriate choice for use with symmetries.

Consider a one-dimensional and time-independent system whose wave function to which a transformation is applied is $\psi(x)$, and let the operator be $P = x$, often referred to as a component of the electric dipole operator, although the electric charge is divided out. For the symmetry operator use parity, which reflects the x coordinate. Table 2.3 summarizes the effects of the transformations considered from each of the three viewpoints.

TABLE 2.3 Effects of the three types of symmetry transformations for the example of the parity operator, on wave functions in one spatial dimension, on the x component of the electric dipole operator (just x), and on matrix elements between states with wave functions ψ and ψ' .

Type of transformation	Effect on $\psi(x)$ or $\psi'(x)$	Effect on operator x	Effect on matrix element $\langle \psi' x \psi\rangle$
Active	$\psi(-x), \psi'(-x)$	x	$-\langle \psi' x \psi\rangle$
Passive	$\psi(x), \psi'(x)$	$-x$	$-\langle \psi' x \psi\rangle$
Canonical	$\psi(-x), \psi'(-x)$	$-x$	$\langle \psi' x \psi\rangle$

The transformation of matrix elements given in Table 2.3 requires discussion. Consider, for example, transformation of the matrix element in the active viewpoint, for which we have

$$\begin{aligned}
\langle \psi' | x | \psi \rangle &= \int dx \psi'(x) x \psi(x) \\
&\longrightarrow \int dx \psi'(-x) x \psi(-x) \\
&= \int d(-x') \psi'(x') (-x') \psi(x') \\
&= - \int dx \psi'(x) x \psi(x) = -\langle \psi' | x | \psi \rangle
\end{aligned} \tag{2.33}$$

It might appear that a sign has been missed between the third and fourth lines, but it is accounted for by reversing the limits of integration, assuming that the integration is over all x . Similar transformations of variables of integration are required to obtain the results in Table 2.3 for transformation of matrix elements in the passive and canonical viewpoints, as Problem 2.4 suggests that you verify.

Note that we do *not* assume that the wave functions ψ' and ψ have a definite parity symmetry (Section 1.4.1). If this were so, the matrix elements in the active and passive viewpoints would be required to be zero if ψ' and ψ had the same parity. Notice that according to the canonical-transformation viewpoint, since its matrix elements are invariant, one cannot use matrix elements to test symmetries—a very strange viewpoint! Now that we have discussed the types of transformations in the context of quantum mechanics, we revert to emphasizing the mathematics.

Similarity Transformations. Suppose that we have a vector $|k\rangle$ and that we transform it by an operator S , typically a symmetry operator such as a rotation. What is an appropriate transformation of a related operator P ? Assume that S has an inverse (for example, appropriate counter-rotations), and consider the *similarity transformation* of P by S , defined by

$$P_S = S P S^{-1} \quad \mathbf{P}_S = \mathbf{S} \mathbf{P} \mathbf{S}^{-1} \tag{2.34}$$

in which the first of these expressions is an operator relation and the second is a corresponding matrix relation. (We discuss such correspondences between operators and matrices further in Section 2.5.3 under representations of groups.)

Although the similarity transformation rule looks complicated, and is indeed if individual matrix elements are evaluated, it has the following desirable properties:

- If P is unchanged by the symmetry operation, then P and S commute, so we have $P_S = P$, since $S S^{-1} = I$, the unit operator.
- Consider the sequence of operators $Q P = R$ and the transformation of each by the *same* operator S using rule (2.34). Then we have $Q_S P_S = R_S$, so the *form* of the relation between Q , P , and R is left unchanged by application of S . Thus their relation is *covariant*, in the sense used in relativity. Clearly, this property can be generalized to the products and sums of an arbitrary number of operators and to their corresponding matrices.
- The matrix representation of P and its transform counterpart, P_S , have the same trace (sum of diagonal elements), because the trace of a matrix product is inde-

pendent of the order of its factors. In quantum mechanics a matrix trace measures an expectation value, so—especially if S is a symmetry operation—this is a desirable property.

- In the canonical-transformation viewpoint discussed in relation to (2.32), if $S = U$ and U is unitary, then the similarity transformation rule (2.34) produces invariant matrix elements.

Similarity transformations are related in the theory of groups (which we introduce in Section 2.5) to conjugate elements and classes. For a readable discussion with examples from rotations, see Sections 2.6–2.8 of Elliott and Dawber [Eli79].

We have several reasons for applying similarity transformations to operators, the last one leading us to unitary transformations, as we now discuss.

2.2.2 Unitarity: Its Interpretation in Quantum Mechanics

The term *unitary transformation* refers to a similarity transformation (2.34) by a unitary operator, that is, by an operator U described by a unitary matrix. Thus

$$P \xrightarrow{U} P_U = UPU^\dagger \quad U^\dagger = U^{-1} \quad (2.35)$$

The most important property of unitary transformations for the study of symmetries is that they leave scalar products unchanged:

$$\langle Uj|Uk \rangle = \langle j|U^\dagger U|k \rangle = \langle j|k \rangle \quad (2.36)$$

When U is a quantum-mechanical symmetry operator, we interpret this property as invariance of the scalar products of the Hilbert-space state vectors.

If the matrix elements of U are all real, then U is said to be an *orthogonal transformation*. For example, the transformation of coordinates $\mathbf{r} = (x, y, z)$ by rotation through angle γ about the z axis is the first Euler-angle rotation, as discussed in Section 1.3.1. The transformed coordinates are $\mathbf{r}' = (x', y', z')$, given by

$$\begin{bmatrix} x' \\ y' \\ z' \end{bmatrix} = \mathbf{A}_z(\gamma) \begin{bmatrix} x \\ y \\ z \end{bmatrix} = \begin{bmatrix} \cos \gamma & -\sin \gamma & 0 \\ \sin \gamma & \cos \gamma & 0 \\ 0 & 0 & 1 \end{bmatrix} \begin{bmatrix} x \\ y \\ z \end{bmatrix} \quad (2.37)$$

You can verify by inspection that $\mathbf{r}' \cdot \mathbf{r}' = \mathbf{r} \cdot \mathbf{r}$, so that $\mathbf{A}_z(\phi)$ describes an orthogonal transformation that leaves invariant the scalar product in configuration space.

Unitarity is a transitive property, in that the product of unitary transformations is unitary. Therefore, if each of two symmetry operations is unitary, then their combination is unitary. For example, rotations about successive axes describe a unitary (or orthogonal) transformation because each rotation is unitary (or orthogonal), as just shown.

2.2.3 Operator Exponentials and Commutators

We now show that there is a direct relationship of the unitary operators and matrices to the Hermitian operators and matrices described in Section 2.1.3. To do this we need to summarize properties of the exponentials of operators.

Operator Exponentials. You are sure to be familiar with the exponential function through the definition

$$E(P) = e^P \equiv \sum_{n=0} \frac{P^n}{n!} \quad (2.38)$$

Suppose that we now identify P as an *operator* rather than a number. The notation P^n will then mean the operator applied n times, with $P^0 = I$, the unit operator. The object $E(P)$ is then also an operator. A similar interpretation is to be given to matrices based on operators, in which \mathbf{P}^n is to mean the inner product of the matrix \mathbf{P} taken n times, with $\mathbf{P}^0 = \mathbf{1}$, a unit matrix of appropriate dimension.

It is easy to see, by following the proof used when P is a number, that the inverse of the exponential operator, E^{-1} , is obtained by

$$E^{-1}(P) = E(-P) \quad (2.39)$$

and that the Hermitian conjugate, E^\dagger , is given by

$$E^\dagger(P) = E(P^\dagger) \quad (2.40)$$

Suppose that $E^\dagger = E^{-1}$; then $P^\dagger = -P$, as Problem 2.5 suggests you prove in detail. Writing $P = iH$ then shows that H must be Hermitian, $H^\dagger = H$. The converse also holds, so we have the theorem

$U = e^{iH} \quad U \text{ unitary} \Leftrightarrow H \text{ Hermitian}$	(2.41)
--	--------

This result would be of interest mostly for the mathematics of our subject if it were not for the intimate connection in quantum mechanics between Hermitian operators as observables and unitary operators as transformations that leave scalar products invariant. We see from (2.41) the necessary connection between these two types of operators. So far we have discussed only the exponential of a single operator, such as P or H . In order to handle exponentials of more than one operator we have to investigate operator commutation properties.

Commutators and Exponentials of Operators. Consider two operators, P and Q , and corresponding exponentials of these operators, $E(P) = e^{\alpha P}$ and $E(Q) = e^{\alpha Q}$, where α is a real variable. Generally, there is no simple relation between these ex-

ponentials and $E(P + Q)$, since the defining series cannot be rearranged if P and Q do not commute. For most of our needs, and for much of quantum mechanics, it is sufficient to consider commutation relations for which the commutator is proportional to the unit operator. We then have the relation, for λ a number,

$$\boxed{[P, Q] = \lambda I \Rightarrow e^{P+Q} = e^P e^Q e^{\lambda I/2}} \quad (2.42)$$

The proof of this relation is suggested as Problem 2.6. Note that this relation requires that P and Q be dimensionless operators, as we will ensure in our use of it. The converse of the result (2.42) does not hold in general, since if the additional exponential $e^{\lambda I/2}$ happens to produce the unit operator, then one cannot infer that $\lambda = 0$. Examples of this behavior are given in the article by Lévy-Leblond [Lév82].

If P and Q commute, then $\lambda = 0$, so that

$$[P, Q] = 0 \Rightarrow e^P e^Q = e^{P+Q} = e^{Q+P} = e^Q e^P \quad (2.43)$$

When the commutator of P with Q is proportional to the unit operator, as in (2.42), then it can be shown directly from (2.42), as Problem 2.6 suggests you do, that

$$[P, Q] = \lambda I \Rightarrow e^Q e^P = e^P e^Q e^{\lambda I} \quad (2.44)$$

A final result that we need for commutators relates Hermitian conjugates:

$$[P^\dagger, Q^\dagger] = [P, Q]^\dagger \quad (2.45)$$

These results for operators and their exponentials are used extensively in Chapter 3 with angular momentum operators.

2.2.4 Raising and Lowering Operators

You will have noticed in beginning quantum mechanics that eigenvalues of interesting operators, such as Hamiltonians, often differ by equal steps. For example, the harmonic oscillator energy eigenvalues go by equal steps of $\hbar\omega$, where ω is the oscillator angular frequency. To avoid repetitive algebra in later sections and to provide a unity of treatment, we now consider special operators that either *raise* or *lower* eigenstates.

Collectively, such operators are called *shift* operators or *ladder* operators, because you can use a ladder to raise or to lower something. We derive here some general properties of ladder operators, following the treatment given by de la Peña and Montemayor [Pen80]. In Section 3.4 we apply these properties to the angular momentum operators.

Algebra of Ladder Operators. Suppose that we have a Hermitian operator P in a linear space having a discrete spectrum, with p_n the eigenvalue belonging to eigenstate $|n\rangle$. Thus, we have

$$P|n\rangle = p_n|n\rangle \quad (2.46)$$

Consider operators of the form

$$\eta_+ \equiv \sum_n C_n |n+1\rangle\langle n| \quad \eta_- \equiv \sum_n C_{n-1}^* |n-1\rangle\langle n| \quad (2.47)$$

in which the C_n are arbitrary complex numbers. These form ladder operators in the sense that

$$\eta_+|k\rangle = C_k|k+1\rangle \quad \eta_-|k\rangle = C_{k-1}^*|k-1\rangle \quad (2.48)$$

so that η_+ raises the k th eigenstate to the $(k+1)$ th at each application, and η_- similarly lowers the eigenstate.

The joint application of the two operators must leave the eigenvalue unchanged. Indeed, you can easily show (as Problem 2.7 suggests you do) that

$$\eta_- \eta_+ |k\rangle = |C_k|^2 |k\rangle \quad \eta_+ \eta_- |k\rangle = |C_{k-1}|^2 |k\rangle \quad (2.49)$$

Because of this property, successive applications of η_{\pm} do not move the eigenstate, so one might as well just use the lowest powers, as in (2.49). The flexibility of choice of the C_k will be exploited to make ladders for various uses. We can write

$$P = a + b\eta_- \eta_+ + c\eta_+ \eta_- \quad (2.50)$$

from which, by comparison with (2.49), we can deduce immediately that the eigenvalues of P , the p_n in (2.46), must be related to the C_n by

$$p_n = a + b|C_n|^2 + c|C_{n-1}|^2 \quad (2.51)$$

We now assume that the spectrum of P has a lower bound, which we label (but only for convenience) by $n=0$. We must therefore have

$$\eta_-|0\rangle = 0 \quad \Rightarrow \quad C_{-1} = 0 \quad (2.52)$$

An upper bound, at say $n=N$, is also a possibility. If so, we must have

$$\eta_+|N\rangle = 0 \quad \Rightarrow \quad C_N = 0 \quad (2.53)$$

In some applications the result (2.53) will lead to inconsistencies, showing that there

is not an upper bound. Figure 2.4 summarizes definitions and properties of ladder operators that we have discussed so far.

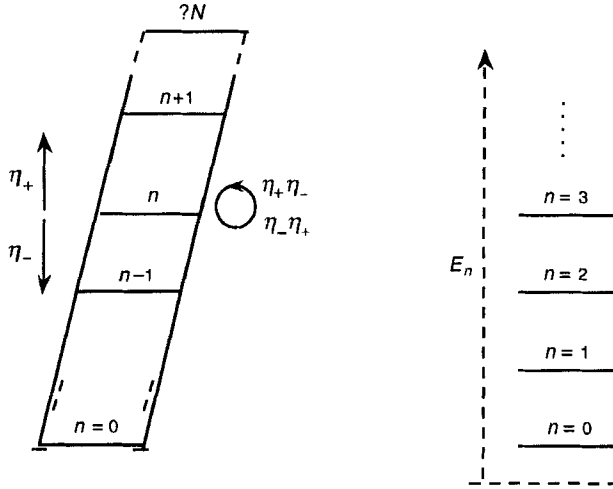


FIGURE 2.4 Ladder operators η_+ (raising) and η_- (lowering), having a lower bound labeled by $n = 0$ and perhaps an upper bound $n = N$. If the operators are applied in succession, one returns to the same state. The right side shows an example—the quantum harmonic oscillator, whose energies, E_n , are quantized by equal steps but which have no upper bound.

If the spectrum of ladder states is finite, then there are N unknown moduli of the C_n in addition to a , b , and c in (2.51), for a total of $N + 3$ unknowns. There are $N + 1$ conditions from (2.48), plus an overall normalization and a choice of origin, for a total of just $N + 3$ knowns. Therefore, representation (2.51) may be used for the spectrum of operator P .

The bilinear form (2.50) suggests alternative expressions for this operator. First, write the ladder operators in terms of new operators α and β as

$$\eta_{\pm} \equiv \frac{1}{\sqrt{2}}(\alpha \pm i\beta) \tag{2.54}$$

By solving for α and β in terms of η_+ and η_- , then constructing matrix elements of operators α and β , it is straightforward to show (as Problem 2.7 suggests doing) that α and β are Hermitian. They may thus be useful for representing observables in quantum mechanics. Further, we can express the bilinear combinations in (2.50) in terms of their antisymmetric and symmetric combinations

$$A \equiv \eta_- \eta_+ - \eta_+ \eta_- \quad S \equiv \eta_- \eta_+ + \eta_+ \eta_- \tag{2.55}$$

respectively. In terms of these operators we readily find that

$$A = -i[\alpha, \beta] \quad S = \alpha^2 + \beta^2 \quad (2.56)$$

so that the original operator

$$P = a + bA + cS = a - ib[\alpha, \beta] + c(\alpha^2 + \beta^2) \quad (2.57)$$

The second form may be convenient for identifying α and β , and thereby the other operators.

In order to calculate a spectrum of states and their eigenvalues, we need to develop relations between the eigenvalues of the various operators. Let us begin with A and S , having corresponding eigenvalues a_k and s_k , related by

$$\begin{aligned} A|k\rangle &= a_k |k\rangle = \left(|C_k|^2 - |C_{k-1}|^2 \right) |k\rangle \\ S|k\rangle &= s_k |k\rangle = \left(|C_k|^2 + |C_{k-1}|^2 \right) |k\rangle \end{aligned} \quad (2.58)$$

in which the second steps of each equation follow from (2.49). We can now derive relations for the s_k and a_k by exploiting the non-negative nature of the moduli of the C_k . Namely

$$s_k + a_k = s_{k-1} + a_{k-1} = 2|C_k|^2 \geq 0 \quad (2.59)$$

whence comes the iteration relation

$$s_{k+1} - s_k = a_{k+1} + a_k \quad (2.60)$$

and, using the bounds on the nonzero C_k from (2.52) and (2.53),

$$s_0 = a_0 \quad s_N = -a_N \quad (2.61)$$

These relations determination the structure and eigenvalues of the spectrum of operator P , as we now show by a simple example.

One-Dimensional Harmonic Oscillator. Having developed some formalism, we can now see how readily eigenvalue problems of special interest in symmetry and quantum mechanics can be solved. For example, the Hamiltonian of the harmonic oscillator in one dimension, H , may be written in terms of the momentum operator p , the particle mass m , the oscillator angular frequency ω , and the coordinate x (in classical mechanics the “displacement from equilibrium”) as

$$\begin{aligned} H &= \frac{1}{2m} p^2 + \frac{1}{2} m \omega^2 x^2 \\ &= \alpha^2 + \beta^2 = S \end{aligned} \quad (2.62)$$

where we have taken

$$\alpha \equiv \sqrt{\frac{m}{2}} \omega x \quad \beta \equiv \frac{1}{\sqrt{2m}} p \quad (2.63)$$

so that the antisymmetric operator

$$A = -i[\alpha, \beta] = -(i\omega/2)[x, p] = \frac{1}{2} \hbar \omega \quad (2.64)$$

is actually an energy. By comparison of (2.64) with (2.57), we identify

$$a = b = 0 \quad c = 1 \quad (2.65)$$

and the eigenvalues of H , E_k say, are just the eigenvalues of S , namely

$$E_k = s_k \quad a_k = \frac{1}{2} \hbar \omega \quad (2.66)$$

From (2.61) the lowest energy eigenvalue is $E_0 = \hbar \omega / 2$, while from (2.60) we see that the energies are equally spaced by $\hbar \omega$. Thus, the energy spectrum of the one-dimensional oscillator is given by $E_k = (k + 1/2)\hbar \omega$, as shown on the right-hand side of Figure 2.4. This spectrum has no upper limit, which is why the harmonic oscillator potential is eventually unrealistic—something has to give when you stretch a spring too far. To see that there is no N , note that (2.61) says that the corresponding energy would have to satisfy the contradictory requirement $E_N = -\hbar \omega / 2 < E_0$.

We return to the ladder operators in Section 3.4 to find quickly the eigenvalues of the angular momentum operators. The technique that we have developed is of quite general applicability for determining discrete spectra.

2.3 EIGENVALUES AND EIGENSTATES

Our purpose in this section is to summarize the definitions, properties, and uses of eigenvalues and eigenstates in the context of rotational symmetries. After introducing eigenvalues of systems (Section 2.3.1), we discuss the role of eigenvectors as basis states (Section 2.3.2), including the interpretation of eigenstates in quantum mechanics. Since a matrix in diagonal form exhibits the eigenvalues as its diagonal elements, it is important to know about diagonalizing matrices. We therefore state in Section 2.3.3 some theorems about diagonalization, we provide examples, and we derive consequences relevant to our applications.

2.3.1 Eigenvalues of Operators and Matrices

Suppose that we have an operator, O , that acts on a ket $|s\rangle$, where the s is just a label. For example, O may be the differential operator for rotation about the z axis in

terms of the angle ϕ , $O = -i\partial/\partial\phi$, and $\langle(\phi)|s\rangle = f_s(\phi)$ is a function of ϕ that may depend upon the label s . For an arbitrary function, the action of O on f is just to give a result proportional to its first derivative with respect to ϕ . For the particular choice

$$\langle(\phi)|s\rangle = f_s(\phi) = e^{is\phi} \quad (2.67)$$

where s is arbitrary but independent of ϕ , we have

$$O\langle(\phi)|s\rangle = -i\frac{\partial e^{is\phi}}{\partial\phi} = se^{is\phi} = s\langle(\phi)|s\rangle \quad (2.68)$$

Thus, the operator reproduces the function on which it operates just multiplied by a constant, here s . The function satisfying (2.68) is an example of an *eigenfunction*, and the number s is an *eigenvalue*.

The etymologies of *eigenvalue* and *eigenfunction* are from the German *Eigenwerte* and *Eigenfunktion*, with *eigen* being German for English *characteristic*. Therefore, on crossing the seas, one also encounters the terminology *characteristic value* and *characteristic function*. On crossing the land border into France, one may speak of *proper value* and *proper function*, from the French *propre* for *one's own*, which is the root of English *property*. Although international in its spirit, science is often nationalistic in its letters.

Why are eigenfunctions so interesting and useful? To answer this, consider the matrix elements of an operator which has state vectors $|t\rangle$ that (in a particular representation, such as that with ϕ above) are eigenfunctions with eigenvalue t . Consider the matrix elements O_{st} , which are given by

$$O_{st} = \langle s|O|t\rangle = t\langle s|t\rangle \quad (2.69)$$

Thus, the matrix elements are simply related to the eigenvalues, t , and to the scalar products $\langle s|t\rangle$. If these scalar products are those of orthogonal states, then the matrix of O will be a diagonal matrix, which can be handled very easily.

This discussion leads us to study diagonalization of matrices in more detail.

2.3.2 Diagonalizing Matrices

If a matrix is in diagonal form (Section 2.1.3), then its eigenvalues are just the diagonal elements, which clearly satisfy the eigenvalue requirement (2.68). It is therefore useful to be aware of four theorems that are derived in linear algebra.

All Unitary and Hermitian Matrices Can Be Diagonalized. The first theorem relates to the existence of unitary similarity transforms (Sections 2.2.1, 2.2.2) that diagonalize certain matrices:

- For each matrix that is unitary or Hermitian there exists a unitary similarity transformation that diagonalizes it. (2.70)

A proof of this theorem is given, for example, in Wigner's book [Wig31]. Since real orthogonal matrices are special cases of unitary matrices and real symmetric matrices are special cases of Hermitian matrices, the result (2.70) holds also for orthogonal and symmetric real matrices.

Notice that (2.70) claims that such a transformation *exists*, but it does not provide a prescription by which the required matrix can be constructed. Indeed, both analytically and numerically, the construction of such a matrix is usually very difficult, especially if the dimension of the matrix is large.

Principal-Axis Transformation. Theorem (2.70) is sometimes called the rule of the principal-axis transformation. This is the guise in which it often appears in the classical mechanics of rotating rigid bodies, as discussed (for example) in Section 5.4 of Goldstein's textbook of mechanics [Gol80], where a detailed proof of (2.70) for real matrices is given in this context. In mechanics, the inertia tensor, \mathbf{I} , is represented by a real, symmetric, 3×3 matrix. By a special choice of coordinate axes, called the *principal axes*, \mathbf{I} can be rotated into diagonal form. Its three eigenvalues are then called the *principal moments of inertia*.

As a simple example of a rotation about a principal axis, consider two point masses m kept apart by a rigid rod of negligible mass that is rotated with angular speed ω about a z axis passing through its midpoint O , as shown in Figure 2.5.

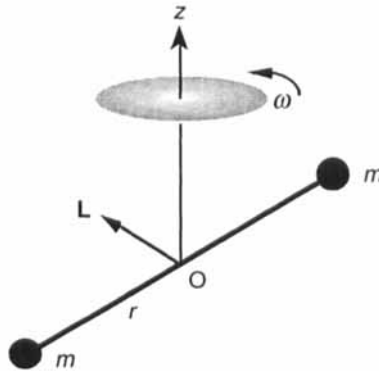


FIGURE 2.5 A rotating dumbbell has three principal axes of inertia. For one of these, the axis of rotation is parallel to the axis of the dumbbell joining the two masses m , while for the other two principal axes the axes of rotation are perpendicular to the axis of the dumbbell.

We encounter, again in the mechanics context, the principal axis transformation in Section 6.5 when investigating rigid-body rotations in quantum mechanics.

Eigenvectors and Diagonalizing Matrices. Our second theorem on matrix diagonalization states that:

- The columns of the inverse of a unitary matrix that diagonalizes a unitary or Hermitian matrix form eigenvectors of the diagonalized matrix. (2.71)

From this result, we see that once the eigenvalues of unitary or Hermitian matrices have been found, so that the matrix is in diagonal form, the matrix that produces this diagonal form by a similarity transformation exhibits all the eigenvectors. We use theorem (2.71) extensively throughout this book.

Diagonalization and Commutation. Our third theorem relates to the conditions for diagonalizing matrices:

- A series of Hermitian matrices can be diagonalized by the same unitary transformation if, and only if, the Hermitian matrices commute with each other. (2.72)

This theorem has many consequences for the discussion of the eigenfunctions of rotations (Chapters 4, 6). In particular, in quantum mechanics the Hermitian matrices represent dynamical observables, as discussed in Section 2.1.3. Moreover, also in the realm of quantum mechanics, the noncommuting of such matrices describing infinitesimal rotations gives rise to the Heisenberg uncertainty relations for angular momentum, as we derive in Section 5.2.

Normal Modes. A related context in which theorem (2.72) has an important role is in the study of the normal modes of a vibrating system, as worked out in great detail in Sections 6-2 and 6-3 of Goldstein's classical mechanics text [Gol80]. The frequency eigenvalues ("eigenfrequencies") are just the frequencies of the normal modes of vibration.

2.3.3 Eigenvectors as Basis States

The fourth and final theorem about matrix diagonalization and eigenvectors that we will need subsequently is:

- The eigenvectors of a set of commuting Hermitian matrices form a complete set of functions for the set of matrices. (2.73)

A major consequence of this theorem is that once we have eigenvectors for Hermitian operators, we have a set of basis states in terms of which other functions can be expanded. For rotational symmetries, once we have found eigenvectors for the angular momentum operators (Chapter 4), which are Hermitian operators describing infinitesimal rotations, we immediately have a basis for finite rotations (Chapter 6).

Sturm-Liouville Differential Equations. In the theory of second-order linear differential equations, as often encountered in mathematical physics, one shows that

with the appropriate choice of boundary conditions the Sturm-Liouville differential operators have eigenfunctions that form a complete set in terms of which any function that is piecewise continuous and in the same domain can be expanded. This result, which is discussed in more detail in Section 5.8 of Wong's mathematical physics text [Won91], is analogous to theorem (2.73).

An example connecting differential equations and Hermitian matrices with the completeness of eigenfunctions is provided by the eigenfunctions of the differential operator $L_z = -i\partial/\partial\phi$, which has eigenfunctions $e^{im\phi}$. For m and m' both integers, the matrix elements $\langle m'|m\rangle$ vanish if they are defined by integration over the region $0 \leq \phi \leq 2\pi$ and if m and m' are either both integers or both half integers. (Without this restriction, ϕ must range up to 4π .) The completeness result is just Fourier's theorem on the expansion of functions of ϕ in terms of the complex exponential function.

A discussion of diagonalization of linear operators that is both more general and more abstract than presented here is given in Chapter 3 of Jordan's text [Jor69]. The topic appears in many disguises in a wide variety of applied mathematics. Once the commonality of these ideas is recognized, the underlying concepts can be grasped directly.

2.4 SPINORS AND THEIR PROPERTIES

Spinors are mathematical entities that are useful when describing half-integer spins in the context of rotations of physical systems. We discuss them only in this context because there is a bewildering literature on spinors and their description.

We begin this section by defining spinors in a way appropriate for rotations, which is in terms of a sign change under a 2π rotation, then we summarize the experimental demonstrations of the spinor behavior of wave functions for neutrons. Next, we give a very simple geometrical example of a spinor and derive its properties under rotation, then we discuss other examples of spinors. Finally in this section, we give examples of physical objects that distinguish between turns through 2π and 4π .

2.4.1 Definitions of Spinors

The definition of a spinor we use is that a mathematical entity S is a spinor if it satisfies the requirement that it change sign under a 2π rotation:

$$S(\theta + 2\pi) = -S(\theta) \quad (2.74)$$

Part of this requirement is the assumption that S can have a sign associated with it. For example, a geometric figure (such as a polygon) does not have a sign, so could not be a spinor. Matrices, however, may be signed; so might be candidates for

spinors. From (2.74) it follows that a spinor returns to its original value after a 4π rotation.

Notice that this definition of a spinor is implicit; that is, you can use it only to test whether you have a spinor, since it doesn't provide a way to construct a spinor. You will be familiar with such implicit definitions from the example of a prime number—a positive integer divisible only by unity and itself—and, as you know, the task of *discovering* primes (rather than *constructing* them) is formidable.

The reason spinors are so interesting in the physical sciences is that we find in nature objects whose description by quantum mechanics requires the sign-reversal property (2.74). Although this property is assumed when discussing, for example, electron wave functions in atoms, its first direct demonstrations were provided in 1975 in experiments with neutrons [Rau75, Wer75], as we now describe.

Spinor Rotation of Wave Functions. The principle of the experimental method used to demonstrate the spinor nature of the wave functions of free spin-1/2 particles is as follows. As shown in Figure 2.6, thermal-energy neutrons strike a device at S that splits the wave front so that part is directed through a magnetic field, \mathbf{B} , transverse to the beam. This field couples to the neutron magnetic moment and rotates its spin, causing a phase difference between the parts of the neutron wave function that have gone the different routes. When the wave fronts recombine at R there will be a phase difference between them, and thus interference. Therefore, as in experiments with photons, when the count rates between detectors C_1 and C_2 are compared, there will (in principle) be maxima when the wave fronts are in phase and minima when they are out of phase.

The important question is, what is the periodicity of the interference pattern? If one converts magnetic-field changes into phase differences, the data (as sketched in Figure 2.6) show that a 4π periodicity (rather than 2π) is appropriate for neutrons.

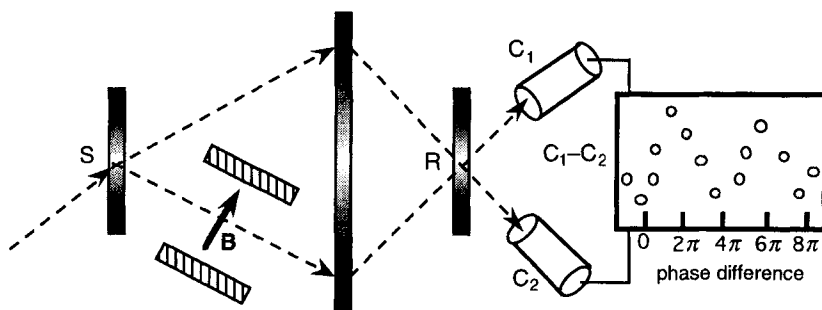


FIGURE 2.6 Schematic of experiment used to demonstrate the sign change of a fermion wave function under a 2π rotation. The setup sketched corresponds to that used by Werner et al. [Wer75].

Corresponding experiments with electrons do not seem to have been performed. We can, however, rely on the validity of calculations of atomic structure, which

assume the spinor nature of electrons, to convince us that an electron also shows the sign-reversal property of its wave function under a 2π rotation.

2.4.2 Representing Spinors; Rotations

In our general treatment of rotations of angular momentum eigenstates (Chapter 6) we will show that spin-1/2 objects (primarily electrons and subatomic particles) have wave functions that change sign if the object is rotated through 2π . At the macroscopic level of physical systems we are accustomed to an object returning to its original state upon rotation through only 2π . It is therefore instructive and interesting to seek examples of things that change sign under 2π rotations, that is, they are spinors according to our definition.

Representing Spinors. A novel way to visualize spinors that requires understanding only elementary properties of plane trigonometry is shown in Figure 2.7.

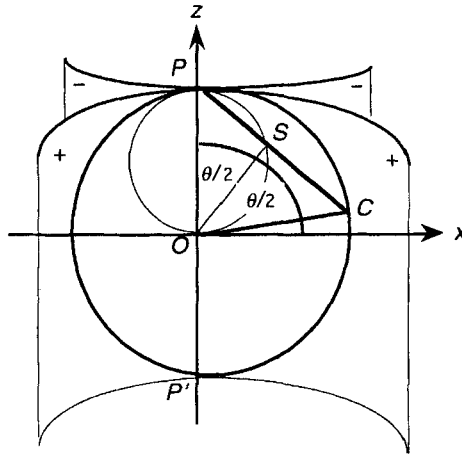


FIGURE 2.7 Geometric visualization of a spinor associated with C , described by the line segments OS and PS , including signs. As C moves through angle θ from the z axis, S rotates on the inner circle through $\theta/2$. Both signed quantities OS and PS are of opposite signs in $2\pi \leq \theta \leq 4\pi$ compared with their signs in $0 \leq \theta \leq 2\pi$. To keep track of the signs, OS and PS lie on the sheet with the appropriate sign, + or -.

Draw, as shown, the unit circle in the x - z plane centered on the origin, O , and intercepting the positive z axis at the pole P . Consider a ray OC making an angle θ with the z axis, so θ is the usual polar angle. Now, bisect the angle, so that the point S then bisects PC because $OP = OC$. Thus

$$OS(\theta) = \cos(\theta/2) \quad PS(\theta) = \sin(\theta/2) \quad (2.75)$$

Notice that OS and PS are taken to be signed quantities, although this is not obvious in Figure 2.7. To remind us that OS is negative for $\pi < \theta < 2\pi$, as is PS for $2\pi < \theta < 4\pi$, we mark two "Riemann sheets" for the signed values of OS and PS . As the control point C goes once around the unit circle, the point S goes from P to O . A second revolution of C brings S back to P . It is straightforward to show that the path of S is a circle of radius $1/2$. This path is traced out in a period of 4π of θ . Also, from (2.75), OS and PS change sign when $\theta \rightarrow \theta + \pi$. Therefore, taking our sign rule into account, the pair (OS, PS) forms a spinor associated with C .

In the two-dimensional representation shown in Figure 2.7 we may view C as marking the head of vector \mathbf{OC} , which has unity for its magnitude and θ for its direction. Then OS and PS form the components of the spinor associated with \mathbf{OC} . The vector \mathbf{OC} could also be described by giving the angle that is supplementary to θ , namely $\pi - \theta$, which is the angle from the south pole, P' , to C . The point S' that bisects $P'C$ then defines the coordinates OS' and $P'S'$ of a spinor orthogonal to the spinor in the upper half plane, and having $OS' = PS$ and $P'S' = OS$. One could therefore use OS' and OS to represent this spinor, but there does not seem to be any particular advantage to this.

The process of halving angles used to construct our diagram can, clearly, be repeated. Thereby an object with a period of 8π rather than 4π will be obtained. Such an object, although mathematically well-defined, does not appear to be of interest for understanding angular momentum.

Rotations of Spinors. The properties under rotations of the spinor (OS, PS) associated with C can be worked out simply. If C is rotated through angle β from its position at θ , then we have the following transformations:

$$\begin{aligned}\theta &\rightarrow \theta + \beta \\ OS &\rightarrow OS_\beta = \cos(\beta/2)OS - \sin(\beta/2)PS \\ PS &\rightarrow PS_\beta = \sin(\beta/2)OS + \cos(\beta/2)PS\end{aligned}\tag{2.76}$$

which follow simply from the trigonometric identities for expanding the cosine and sign of the sum of two angles. We may write (2.76) concisely in matrix form as

$$\begin{pmatrix} OS(\theta + \beta) \\ PS(\theta + \beta) \end{pmatrix} = \begin{bmatrix} \cos(\beta/2) & -\sin(\beta/2) \\ \sin(\beta/2) & \cos(\beta/2) \end{bmatrix} \begin{pmatrix} OS(\theta) \\ PS(\theta) \end{pmatrix}\tag{2.77}$$

Now we may consider the two-row column matrix on the right side of (2.77) as representing the spinor constructed geometrically in Figure 2.7. Let us name this matrix $S(\theta)$. The matrix on the left side of (2.77) then represents the spinor after rotation through angle β , $S(\theta + \beta)$.

In this matrix representation it is clear that we satisfy the basic spinor property $S(\theta + 2\pi) = -S(\theta)$. Section 6.2.3 identifies the 2×2 matrix in (2.77) as the matrix that transforms *any* spin-1/2 angular momentum eigenstate under rotation by β about the y axis, $\mathbf{d}^{1/2}(\beta)$. Although we drew the diagram in Figure 2.7 for the xz plane, it is clear that in three dimensions we could have the y coordinate perpendicular to the plane of the figure with positive direction upward. We would then be prepared to consider rotations in three dimensions.

What is an appropriate spinor in a spherical-polar coordinate system? Consider rotations about the z axis, using an angle α from the x axis as in Figure 2.8 in order to be consistent with one of the schemes for describing rotations in Section 3.1.1.

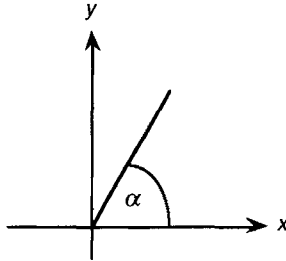


FIGURE 2.8 Rotation around the z axis (perpendicular to the figure and upward) through angle α , considered as positive for the anticlockwise direction.

What is an appropriate rotation matrix corresponding to the 2×2 matrix in (2.77)? Obviously, we may just replace θ by ϕ , say. In Sections 3.3 and 3.4 we, however, require that spinors appropriate for rotations about the z axis, S_{\pm} , be eigenfunctions of the angular momentum operator component for this axis, so that

$$J_z S(\phi) = -i \frac{\partial S}{\partial \phi} = \pm \frac{1}{2} S(\phi) \quad (2.78)$$

The linear combinations of spinors that satisfy this equation are complex, namely $OS(\phi) \pm iPS(\phi) = e^{\pm i\phi/2}$. It is straightforward to show, as Problem 2.8 suggests, that for a z -axis rotation which also satisfies (2.78), the appropriate relations are

$$S(\phi + \alpha) = \begin{bmatrix} e^{+i\alpha/2} & 0 \\ 0 & e^{-i\alpha/2} \end{bmatrix} S(\phi) \quad (2.79)$$

The price paid for gaining this property is the invention of a spinor that is complex-valued. Thus, the analog of the xz plane spinor becomes the spinor in the complex yz plane. Extensive applications of these results to angular momentum are made in Sections 3.3, 4.3, and 6.2.

Other Treatments of Spinors. There is a large and confusing variety of treatments of spinors. We categorize here some treatments most relevant to the study of rotations (especially for quantum systems) and at a level accessible to readers of this book. Geometric treatments and interpretations are provided in the articles by Payne [Pay52] and by Frescura and Hiley [Fre81]. The connection to relativity is made in Sections 41.5–41.9 of the book on gravitation by Misner, Thorne, and Wheeler [Mis73]. Spinors from the algebraic viewpoint are discussed extensively at a more advanced level in the monographs by Cartan [Car66] and also by Altmann [Alt86], who emphasizes their relations to quaternions and group theory.

Spinors are also often presented in the context of objects that distinguish between turns through 2π and 4π , as we now summarize.

2.4.3 Objects That Distinguish Turns through 2π and 4π

Discussions of spinors, the mathematical entities that we introduced in the two preceding subsections, usually go hand-in-hand with presentations of objects that distinguish turns through 2π from turns through 4π . What I mean here by “object” is something concrete (but not necessarily made from this construction material) that looks different after a 2π rotation but which can be restored to its original appearance after a 4π rotation. This is to be distinguished from *spinors*—mathematical entities such as wave functions which *change sign* after a 2π rotation.

The major purpose of inventing such objects, one of which is patented [Ada71], is to show their analogy to spinors. They are often known collectively as “Dirac’s strings.” Since their connection with spinors is by analogy rather than explanatory, I will only catalog some presentations of them. A clear discussion of Dirac’s construction is provided in Section 2.3 of Biedenharn and Louck’s treatise on angular momentum [Bie81a]. Several mechanical devices and a light prism that exhibit the 4π property are discussed by Rieflin [Rie79], whereas Bolker [Bol73] has analyzed the string entanglement and disentanglement by using topology.

2.5 A PRIMER ON GROUPS

The purpose of this section is very modest: It introduces key concepts of groups as they are used to analyze symmetry properties of physical systems, but does not prove any theorems. This is done so you can appreciate the connection between abstract group theory and the rotation group—the essential group for angular momentum. Having understood the connection for this group whose examples are concrete and intuitive, you will be better prepared to understand and use groups for systems that are more abstract.

We begin with examples of properties of physical systems that might be described by the same mathematics. For various discrete transformations we can make tables showing the effects of the transformations, and from these examples we are led to consider the mathematical definition of a group. Key terminology of group theory is introduced in Section 2.5.2, followed by the idea of a group representation

(Section 2.5.3). Interesting groups and their applications in the physical sciences are described in Section 2.5.4. Finally in this primer we introduce the notion of irreducible representations (Section 2.5.5), which is related to the block-diagonal matrices discussed in Section 2.1.3.

Our brief treatment is sufficient for this book, since we develop angular momentum by using preferentially algebraic rather than group theoretical methods. For these there are several introductory-level books, such as Armstrong's text on groups and symmetry [Arm88], the programmed-learning text by Vincent [Vin77] emphasizing group theory applied to molecular symmetry, plus two books on group theory applied to molecular structure and chemical systems by Ferraro and Ziemeck [Fer75] and by Bernal et al. [Ber72]. The latter book has many stereoscopic views of molecules that illustrate symmetry groups.

At a more technical level, the text by Hamermesh [Ham62] applies group theory to crystals, atoms, and nuclei, that by Tinkham [Tin64] emphasizes applications to condensed-matter physics, while space groups applied to solids are described in detail by Burns and Glazer [Bur90]. Extensive treatments of group theory for physical systems are given in the text by Elliott and Dawber [Ell79] and, with more emphasis on formalism, in the two books by Cornwell [Cor84].

2.5.1 Group Examples and Definitions

We begin by considering simple examples of symmetry transformations and discovering their common features. This will suggest the appropriateness of the definition of an abstract group.

Symmetry of NH_3 . The symmetry transformation we use as our working example is from geometry, namely, an equilateral triangle with an object out of plane along its symmetry axis. This example has a physical realization in the geometry of the ammonia molecule, NH_3 , as sketched in Figure 2.9.

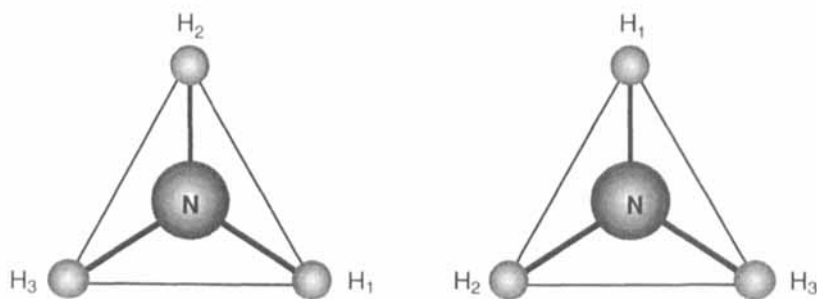


FIGURE 2.9 Geometry of ammonia molecules, NH_3 . Each nitrogen atom, N, lies above or below the center of the equilateral triangle formed by three equivalent hydrogen atoms, H. Between the left- and right-hand views H atoms have been interchanged.

In this example, as soon as we believe that all H atoms are equivalent (in spite of the labels on them) it necessarily follows that they form an equilateral triangle and that the position of the N atom must be along a line passing through the center of this triangle and perpendicular to the plane of the H atoms. Symmetry alone cannot tell us the spacing between the atoms, since this depends upon the dynamics of their average attraction.

A ball-and-stick picture such as Figure 2.9 is based on two assumptions: that each atom is treated as a particle, and that it is at rest. According to quantum mechanics, neither assumption is strictly valid. Thereby, the rigid geometric structure shown in Figure 2.9 is interpreted as describing the time-average positions of the centers of mass of the atoms. With this interpretation the equivalence of the H atoms again demands equality of the lengths of the sides of the triangle. Note that the lines joining atoms are drawn only to indicate schematically the directions of the predominant attraction between them.

The following four examples of symmetry transformations evolve from the equivalence of the vertices or the sides of an equilateral triangle. We do not invoke further symmetries in the NH_3 molecule that are implied by the position of the N atom.

Example 1 (Rotations). Discrete rotations of an equilateral triangle about the perpendicular axes through the center of the triangle are shown in Figure 2.10. Labels have been put at the vertices so you can follow the transformations the triangle has undergone.

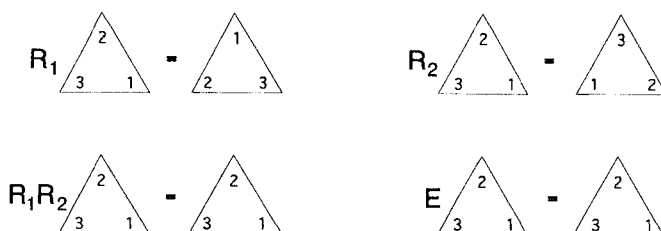


FIGURE 2.10 Discrete in-plane rotations of an equilateral triangle about its center.

The discrete rotations considered are

$$\begin{aligned}
 E &= \text{no rotation} \\
 R_1 &= \text{rotation by } 2\pi/3 \\
 R_2 &= \text{rotation by } 4\pi/3
 \end{aligned}
 \tag{2.80}$$

For purposes of checking this figure, it is helpful to notice that R_2 is the same as rotation in the opposite sense by $2\pi/3$, since $4\pi/3 = 2\pi - 2\pi/3$.

To summarize the results of these rotations, we can make a table, with each element in the table giving the result of choosing a rotation from the rows and a rotation from the columns, as shown in Table 2.4.

TABLE 2.4 Effects of consecutive discrete rotations on the equilateral triangle in Figure 2.10.

	E	R ₁	R ₂
E	E	R ₁	R ₂
R ₁	R ₁	R ₂	E
R ₂	R ₂	E	R ₁

The table is to be interpreted as follows. Choose a row, say R₂, then a column, say R₁. The order of choosing is usually important, but not so here. The element in the matrix gives the result of R₂R₁, with the rightmost element applied first. Here, as shown in Figure 2.10, the result is identical to no change at all, namely E. (We use an E that stands for the German *Einheit*, identity.) Notice the following properties in this example:

- (1) In each row of the table each element appears once and only once.
- (2) When three elements are combined in sequence it doesn't matter which combination is made first. For example, (R₁R₂)R₁ = R₁(R₂R₁), so that the operations are associative.
- (3) Combining E with any other element just gives that element.
- (4) For each element there is another element that just reverses its effect to produce no change, E.

Example 2 (Permutations). We present Example 1 (Figure 2.10) as if we are rotating the triangle. Alternatively, we could keep the triangle fixed but permute the vertex labels 1, 2, 3. (Actually, this is how the figure was drawn; who can tell otherwise?) For the NH₃ molecule in Figure 2.9 the permutations correspond to exchanging the positions of two H atoms. The permutations considered are

$$\begin{aligned}
 E &= \text{no permutation} \\
 R_1 &= \text{the cyclic permutation } 1 \rightarrow 3 \rightarrow 2 \rightarrow 1 \\
 R_2 &= \text{the cyclic permutation } 1 \rightarrow 2 \rightarrow 3 \rightarrow 1
 \end{aligned}
 \tag{2.81}$$

Clearly, Table 2.4 would be unchanged, since only the interpretation is different. Examples 1 and 2 are therefore essentially the same, in the sense that if we understood the transformation properties for one we would immediately have the properties for the other after making the translations given in (2.80) or (2.81).

Example 3 (Mirror Reflections Plus Rotations). Consider mirror reflections of the triangle as shown in Figure 2.11. In NH₃ each reflection is equivalent to a parity symmetry (Sections 1.2.1, 1.4.1) between two H atoms, as shown in the left- and right-hand views. Let M_i denote a reflection in a mirror perpendicular to

the plane of the triangle, passing through vertex $i = 1, 2,$ or 3 and through the bisector of the opposite side. The effects of such reflections are summarized in Table 2.5.

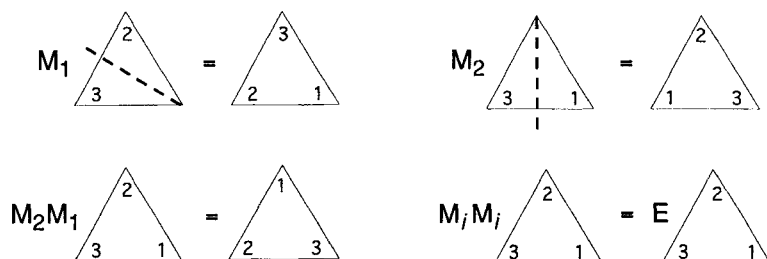


FIGURE 2.11 Reflections of an equilateral triangle in mirrors lying along the bisectors, which are shown dashed.

When a given reflection is repeated it produces thereby just the identity, that is, $M_i M_i = M_i^2 = E$. But any other combination of reflections does not give another reflection. Therefore, the properties (1)–(4) that we noticed for rotations are not satisfied, because elements other than the M_i occur in Table 2.5.

TABLE 2.5 Effects of consecutive mirror reflections on the equilateral triangle shown in Figure 2.11.

	E	M_1	M_2	M_3
E	E	M_1	M_2	M_3
M_1	M_1	E	?	?
M_2	M_2	?	E	?
M_3	M_3	?	?	E

What are the elements indicated by question marks in Table 2.5? If we look at $M_2 M_1$ in Figure 2.11, we see that it produces the same effect as the $2\pi/3$ rotation, namely R_1 . Indeed, all the elements in Table 2.5 with a ? are either R_1 or R_2 . Thus, by considering the combined set of elements of these two rotations and the three reflections we obtain a matrix of combinations, as in Table 2.6, satisfying all the properties (1)–(4) above. Problem 2.9 suggests that you verify this table for yourself.

In Table 2.6 we see a repetition of Table 2.4 embedded in the upper left corner and marked off by lines. If we comprehend the properties of the whole table we will also have found out the properties of this subtable.

TABLE 2.6 Effects of consecutive discrete rotations and reflections on an equilateral triangle.

	E	R ₁	R ₂	M ₁	M ₂	M ₃
E	E	R ₁	R ₂	M ₁	M ₂	M ₃
R ₁	R ₁	R ₂	E	M ₃	M ₁	M ₂
R ₂	R ₂	E	R ₁	M ₂	M ₃	M ₁
M ₁	M ₁	M ₃	M ₂	E	R ₂	R ₁
M ₂	M ₂	M ₁	M ₃	R ₁	E	R ₂
M ₃	M ₃	M ₂	M ₁	R ₂	R ₁	E

Example 4 (Continuous Rotations). In Examples 1 through 3 we consider a finite number of discrete actions that transform an equilateral triangle into itself. In particular, the rotations in Example 1 were through definite angles (multiples of $2\pi/3$). What properties arise if rotations about the center through *arbitrary* angles are considered, as shown in Figure 2.12?

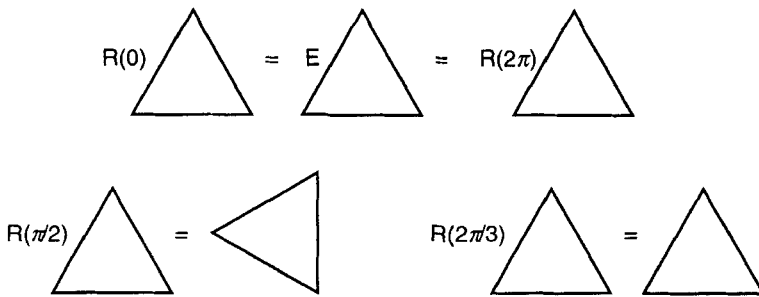


FIGURE 2.12 Continuous rotations of an equilateral triangle about its center.

For continuous rotations we note in Figure 2.12 that rotation through an arbitrary angle reproduces the shape of the triangle but does not reproduce its orientation in space. Exceptions to this occur for no rotation (top left), rotation through an integer multiple of 2π (as at top right), or for an integer multiple of $2\pi/3$ (as at bottom right). To what extent do the properties of the other examples apply to this continuous transformation?

- (1) One cannot make a table of element combinations, if we assume that different elements are described by different angles of rotation, because there are indefinitely many such angles. Imagine, however, that you had angles that were just very closely spaced, then the combination of two rotations would still be a rotation.
- (2) The operations of continuous rotations are associative, as for the other examples. (The formal proof of this is suggested as Problem 2.10.) For rotations about the *same axis*, the rotations also *commute*.

(3) The identity element (no rotation) combined with another rotation is just that rotation element.

(4) Every rotation can be inverted (by rotating through the negative of its angle) to produce the identity, E.

Thus, apart from the fact that one cannot make a finite table, continuous rotations behave similarly to the previous examples of discrete rotations, permutations, and reflections. This commonality of properties leads us to the definition of a group.

Formal Definition of a Group. We formalize the preceding examples by writing down the conditions that a set, G , of elements G_1, G_2, \dots and a relation between them (conventionally called “multiplication”) must satisfy in order that G form a group. The result of the relation between two elements is called the “product.” (Note that the *set* of elements, the group, G , is written using italics, whereas the elements are in Roman type, G_i .) The conditions that must be satisfied to form a group are summarized in Table 2.7.

TABLE 2.7 Requirements for a set of elements and an operation between them (“product”) to form a group.

(1) The product of any two elements is also an element in G .
(2) Products are associative; $(G_i G_j) G_k = G_i (G_j G_k)$ for every G_i, G_j, G_k in G .
(3) There is an <i>identity</i> element, E, whose product with any other element just gives that element; $E G_i = G_i$ for every G_i in G .
(4) For each element G_i there is an element, called the <i>inverse</i> of G_i and written as G_i^{-1} , such that $G_i G_i^{-1} = E$.

Looking back at our four examples, we see that each set indeed forms a group, as we summarize in Table 2.8.

TABLE 2.8 Elements and relations for the examples of groups.

<i>Example:</i>	1	2	3	4
Elements	Discrete rotations	Permutations of vertices	Reflections and rotations	Continuous rotations
“Multiplication” relation	Successive rotations	Successive permutations	Successive rotations	Successive rotations
Type of group	Finite Abelian	Finite Abelian	Finite non-Abelian	Continuous Abelian

Now that we have formally defined a group, we can establish some often-used terminology and apply it to our examples.

2.5.2 Group Theory Terminology

Here we define some terms used in group theory that are encountered in subsequent discussions.

Group Multiplication Table. For finite groups this is a table, such as Tables 2.4–2.6, showing the products of every pair of elements. Recall that “multiplication” is usually not arithmetic multiplication, as Table 2.8 shows.

Order of a Group. This is the number of elements in the group, including E. For example, the group in Table 2.4 is of order 3, while Table 2.6 is the group-multiplication table for a group of order 6.

The smallest group has only a single element, E by itself. The largest finite group that is simple (cannot be decomposed into smaller entities of the same kind) is the “monster group,” also called the “friendly-giant group.” It is a group of order $2^{46}3^{20}5^97^611^213^317^119^123^129^131^141^147^159^171^1 \approx 8 \times 10^{53}$. Its discovery and elucidation are discussed in an introductory-level article by Gorenstein [Gor85].

Subgroup. This is a subset of elements in the group that themselves form a group. For example, the elements in the top left corner of Table 2.6 form a subgroup of discrete rotations in the rotation-plus-reflection group. Note that a subgroup must contain the identity element, E.

Abelian Group. A group is Abelian if $G_iG_j = G_jG_i$ for every pair of elements in the group, that is, all its elements *commute* (produce a result independent of their order). Otherwise, a group is called non-Abelian. For example, the groups in Examples 1, 2, and 4 above are Abelian, but rotations and reflections don’t usually commute, as you can see in Table 2.6 and can verify for yourself using a mirror and rotating a small object near it.

In two dimensions, successive rotations about the same point commute, whereas in three dimensions rotations about different axes do not commute, as discussed in Section 1.3. Therein originates the complexity and fascination of angular momentum.

Homomorphism and Isomorphism. Suppose that two groups, G and G' , are related as shown schematically in Figure 2.13. Here two or more elements in G are mapped onto each element of G' . In the *homomorphism* shown in the upper part of the figure, elements of G map into elements of G' , with the following correspondence between elements:

$$G'_1G'_2 = G'_3 \Rightarrow G_{1a}G_{2a} = G_{3a}, \quad G_{1b}G_{2b} = G_{3b}, \dots \quad (2.82)$$

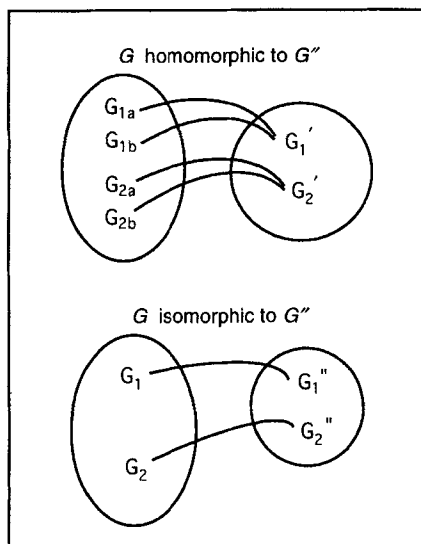


FIGURE 2.13 Homomorphism of group G onto group G' , and isomorphism of G to G'' .

Thus, the relation between G and G' is a many-to-one relation. On the other hand, if the relation of group elements between G and G'' is one-to-one, as shown in the lower part of Figure 2.13, then the two groups are said to be *isomorphic*. They are then essentially the same group, differing only by the naming of the elements, their ordering, and the operations. The ideas of homomorphism and isomorphism are important in discussion of representations of groups, introduced in Section 2.5.3.

Direct-Product Groups. In Section 2.1.2 we discuss direct products of matrices and their use in quantum mechanics to characterize independent subsystems of a total system. Further, one may often apply two or more symmetry operators independently, so their group elements commute. Thus, if one group is $G = \{G_1, G_2, \dots\}$ and the other is $G' = \{G'_1, G'_2, \dots\}$, then their direct product is $G \otimes G' = \{G_1 G'_1, G_1 G'_2, \dots, G_i G'_j, \dots\}$. Which group appears first does not matter because of their independence. The groups must have in common the identity element E , then the set of direct-product elements indeed forms a group, according to the requirements given in Section 2.5.1.

2.5.3 Representations of Groups

Many of the properties of a group of symmetry operations can be understood just by knowing the abstract group to which they belong. For applications to physical systems, however, groups are used mainly to deduce algebraic and numerical properties associated with symmetry operations. For example, when investigating symmetries of the Hamiltonian of NH_3 one will probably want to estimate the eigenenergies of its vibrational modes and the transition rates between various vibrational states.

To relate abstract groups to algebraic and arithmetic properties one therefore makes homomorphisms of groups onto *matrices*, since the latter are well understood and are very well suited to numerical calculations. More specifically, the product, or “multiplication,” of group elements required by the first condition for a group is associated with conventional inner-product matrix multiplication discussed in Section 2.1.2.

Although representations may be made in terms of any set of linear operators, the use of matrices is most common in practice because of their well-understood properties. The definition that is more general is discussed, for example, in Sections 3.3 and 4.1 in Elliott and Dawber [Ell79].

The relations between a group G and its representations (there may be several) are summarized in Figure 2.14.

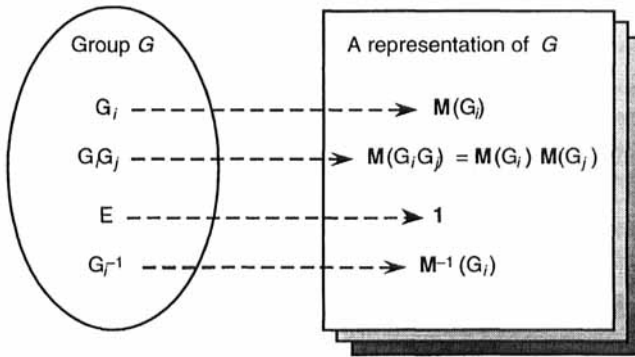


FIGURE 2.14 Correspondence between the elements of a group and matrices $\mathbf{M}(G_i)$ that form a representation of the group. There is always more than one representation of a group, so there are several layers in the right-hand panel, as indicated.

We see that the set of matrices in the figure forms a group (as you are invited to prove in detail in Problem 2.11), according to the requirements summarized in Table 2.7. First, associated with one or more group elements G_i is a single nonsingular square matrix $\mathbf{M}(G_i)$ of dimension $d \times d$, where d is called the *dimension of the representation*. Second, the product of two elements in G maps into the product of their corresponding matrices. Third, the identity element E is represented by the unit matrix of dimension d . Fourth, the inverse of a group element G_i is represented by $\mathbf{M}^{-1}(G_i)$.

A detailed proof of the third relation that $\mathbf{M}(E) = \mathbf{1}_d$ requires familiarity with matrix eigenvalues and determinants. The method of proof is indicated by, for example, Cornwell [Cor84, Section 4.1]. The relation between inverses in the group and its representation then follows directly upon using $G_j = G_i^{-1}$ in the second relation.

Note that Abelian groups have representations in which the matrices commute, as you can convince yourself from the second property in Figure 2.14. If the relation

between a group and one of its representations is an isomorphism (as discussed in Section 2.5.2), then the representation is said to be a *faithful* representation.

Examples of Representations. We now consider three simple examples of representations that involve the groups discovered in Section 2.5.1. The first example is common to all groups—the *identity representation*, in which every element of a group maps into the 1×1 matrix consisting of the single element unity. This trivial one-dimensional representation is often useful to know.

The second example is for the discrete rotations of an equilateral triangle, as introduced in Section 2.5.1. The name of this symmetry group is C_3 (cyclic group of order 3).

Note that a group of order 3 is the smallest possible group except for the group of order 1 containing only the identity, since one cannot satisfy the group conditions with only two elements of which one is E. Try it and see for yourself!

As the group-multiplication table (Table 2.4) shows, this is an Abelian group, so its representations must be commuting matrices. Since these form a group, they are either of order 1 (the identity representation) or of order 3, since order 2 is not allowed and the order of the representation cannot exceed that of the original group because the homomorphism from G goes *onto* the representation. (See Figures 2.13 and 2.14 to clarify this.)

One way to discover a representation of C_3 is to note that if we had a vector (x, y) attached to the triangle, then it would rotate through $2\pi/3$ under R_1 and under $4\pi/3$ under R_2 . Thus, one matrix representation is of dimension 2 and has $M(E)$, $M(R_1)$, and $M(R_2)$ given by

$$\begin{aligned} M(E) &= \begin{bmatrix} 1 & 0 \\ 0 & 1 \end{bmatrix} \\ M(R_1) &= \begin{bmatrix} \cos 2\pi/3 & -\sin 2\pi/3 \\ \sin 2\pi/3 & \cos 2\pi/3 \end{bmatrix} = \begin{bmatrix} -\frac{1}{2} & -\frac{\sqrt{3}}{2} \\ \frac{\sqrt{3}}{2} & -\frac{1}{2} \end{bmatrix} \\ M(R_2) &= \begin{bmatrix} \cos 4\pi/3 & -\sin 4\pi/3 \\ \sin 4\pi/3 & \cos 4\pi/3 \end{bmatrix} = \begin{bmatrix} -\frac{1}{2} & \frac{\sqrt{3}}{2} \\ -\frac{\sqrt{3}}{2} & -\frac{1}{2} \end{bmatrix} \end{aligned} \quad (2.83)$$

It is straightforward to verify, as Problem 2.12 suggests you do, that these three matrices have the same properties under inner-product multiplication as the group multiplication table given in Table 2.4. Thus, we have discovered a representation of C_3 that is of order 2.

Next, consider the reflections shown in Figure 2.11. By themselves the three reflections do not form a group, as seen by Table 2.5. However, as Table 2.6

shows, if we can find a 2×2 matrix representation of the M_i ($i = 1, 2, 3$) such that their products produce the matrices for R_1 and R_2 , then we have a representation of the group C_{3v} . Consider Figure 2.15, which is a more detailed view of the reflection M_3 , which was not shown in Figure 2.11.

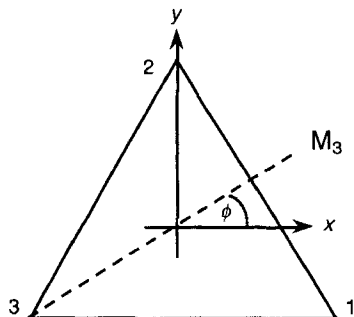


FIGURE 2.15 The reflection M_3 for a mirror (shown dashed) through vertex 3 and the center of the triangle, which is the origin of the x - y coordinate system shown. Here $\phi = \pi/6$.

There are several ways to describe the reflections, but we need to choose a matrix description that is consistent with the group multiplication, Table 2.5. Since the rotations therein are about the center of the triangle, it is clear that the origin of a Cartesian coordinate system must also be at the center. Then, to be conventional, we place the x and y axes as shown in Figure 2.15, which forces us to the following choice of 2×2 matrix for the reflections:

$$\mathbf{M}_i = \begin{bmatrix} \cos 2\phi_i & -\sin 2\phi_i \\ -\sin 2\phi_i & \cos 2\phi_i \end{bmatrix} \quad (2.84)$$

with the angles for the three reflections chosen as $\phi_1 = -\pi/6$, $\phi_2 = \pi/2$, and $\phi_3 = \pi/6$. You may readily verify (as Problem 2.12 suggests you do) that the group multiplication table, Table 2.6, coincides with that for the representation matrices (2.83) and (2.84). We have therefore found a faithful representation of C_{3v} .

After these exercises in geometry, reconsider the physical example of the ammonia molecule, as sketched in Figure 2.9. We have not yet described the full symmetry of this object, since we looked only at the symmetry in the plane of the three H atoms, that is, the symmetry of (hypothetical) H_3 . With the N atom either above or below this plane we move into three dimensions and the reflection symmetry of the N atom in the plane of the H atoms. The extended group thereby obtained is discussed in the book and articles by Wolbarst [Wol77, Wol79].

Extensive discussions of group representation theory at a level suitable for the physical sciences are given in Chapters 3–5 of [Ham62], in Chapter 3 of [Tin64], and in Chapters 4 and 5 of [Cor84]. We introduce only one more topic (irreducible representations, Section 2.5.5), but postpone this until we have discussed several

interesting groups and have glimpsed the power of this mathematics for elucidating the dynamical consequences of symmetries in physical systems.

2.5.4 Interesting Groups and Their Uses

We now make a brief tour to view groups commonly used when describing symmetries of physical systems. The first examples are geometric, beginning with discrete rotations in two dimensions (regular polygons) and advancing to three dimensions (regular polyhedra). Collectively, these are called *symmetry groups*.

We then move on to the basic continuous groups. Composite groups—common combinations of the basic groups—are then surveyed. Finally, we give examples of groups used extensively in physics, especially in quantum mechanics and relativity. Rather than characterizing each group and its applications in detail, we reference texts whose main emphasis is group theory and its applications to physical systems. Thereby you can explore in more detail those groups that you find interesting, while still having some acquaintance with most of the frequently used groups.

Point Groups. These groups describe symmetries under rotation through a definite angle about an axis and mirror reflection in a plane that leave at least one point in the body fixed. Together with translation symmetries in two and three dimensions, discussed in Section 1.2.2, they make up the symmetry group of a body. In two dimensions we have the regular polygons with E edges ($E = 3, 4, \text{ or } 6$), shown in Figure 1.8. Every rotation through a discrete angle $\theta = 2\pi n/E$ leaves the appearance of such a polygon unchanged. Therefore, the group of order n that consists of such successive rotations, called C_n (the *cyclic* group), is a symmetry group of the regular polygons. If an object, such as a molecule, also has n C_2 axes of symmetry at right angles to the principal C_n axis then the symmetry group is called D_n , the *dihedral* group.

Now consider the extension to three dimensions. Suppose that we have a regular polyhedron with F faces ($F = 4, 6, 8, 12, \text{ or } 20$), as shown in Figure 1.9 and summarized in Table 1.2. The appearance of a regular polyhedron will be unchanged by any rotation about the center through a discrete angle $\theta = 2\pi n/F$. The point groups describing the symmetries of the Platonic solids are the tetrahedral, octahedral, and icosahedral groups, T , O , and Y , respectively, since the symmetry groups of the cube and tetrahedron are isomorphic.

To the point groups may be added other discrete groups, such as reflections with an n -fold symmetry axis, S_{2n} , and the permutation of n identical objects, P_n . These discrete groups are summarized in Table 2.9 together with references to extensive treatments of them.

Continuous Groups. As discovered from the examples in Section 2.5.1, one may have groups in which the parameters (such as the angles in the above examples) are continuous rather than discrete. All that one loses thereby is the ability to make a group table and the finiteness of the number of group elements, so that the group does not have an order. Such groups are said to be continuous.

TABLE 2.9 Basic groups common in the physical sciences. The abbreviation and usual name of each group are in given the first and second columns (name in italics), then we note typical areas in physical sciences where the group is used. The rightmost column gives references with extensive discussions of the group. Chapter numbers are in parentheses.

Basic group	Name	Typical applications	References
<i>Discrete groups</i>			
C_n , $n = 1, 2, 3, 4, 6$	<i>Cyclic rotation of order n</i>	Crystals and molecules	Ham62 (2), Ell79 (9)
D_n , $n = 2, 3, 4, 6$	<i>Dihedral; C_n plus 2-fold perpendicular axis</i>		Bur90
T	<i>Tetrahedral</i>		
O	<i>Octahedral</i>		
Y	<i>Icosahedral</i>		
S_{2n} , $n = 1, 2, 3$	<i>Reflection with n-fold axis</i>		Fer75 1)
P_n or S_n	<i>Permutation of n objects</i>	Pauli principle ($n = 2$)	Ell79 (17)
<i>Continuous groups</i>			
\mathcal{T}_N , $N = 1, 2, 3$	<i>Translation in N dimensions</i>	Solids and relativity	Ell79 (15), Cor84 (17)
\mathcal{R}_N , $N = 1, 2, 3$	<i>Rotation in N dimensions</i>	Angular momentum	Ell79 (7)
\mathcal{L}	<i>Lorentz invariance</i>	Relativity	Ell79 (15), Cor84 (17)

Two geometric examples of continuous groups are \mathcal{T}_N for translations in N dimensions and \mathcal{R}_N for rotations, as summarized in Table 2.9. In the physics of special relativity, Lorentz transformations of space-time coordinates leave the length of the space-time four-vector invariant and form a group, called the Lorentz group \mathcal{L} .

Matrix Groups. Groups whose elements are matrices with some of the special properties discussed in Section 2.1.3 are of very general use in the physical sciences, especially in quantum mechanics for the subatomic physics of nuclei and elementary particles. We therefore summarize in Table 2.10 the nomenclature for matrix groups.

TABLE 2.10 Matrix groups of general use in quantum mechanics.

Matrix group	Matrix name	Property	Example
(N) or subscript N	Dimension of square matrices		
$O(N)$	Real orthogonal	$\tilde{\mathbf{o}} \mathbf{o} = \mathbf{1}_N$	$O(4)$
$U(N)$	Unitary	$\mathbf{u}^\dagger \mathbf{u} = \mathbf{1}_N$	$U(2)$
Sx	Special of type x	$\det \mathbf{s} = 1$	$SO(3)$

For each matrix group in Table 2.10 the number of elements (matrices) is not specified, but each matrix must be square and of the same dimension, N . As N changes, the properties of the group change in significant ways. For example, with N given, the set of all orthogonal matrices forms a group, as does the set of all unitary matrices. If one chooses subsets with determinant $+1$, rather than -1 (which is also allowed for orthogonal matrices) or $\exp(i\phi)$ with ϕ a real phase (which is allowed for unitary matrices), then the matrix groups $SO(N)$ and $SU(N)$ are obtained, as subgroups of $O(N)$ and $U(N)$, respectively. The proof of these claims is suggested as Problem 2.13.

Group theory in quantum mechanics and elementary particle physics is dominated by groups represented by unitary and orthogonal matrices, such as those in Table 2.10. Of course, to understand nature requires both the grammar of mathematics and the poetry of discovery and interpretation.

Composite Groups. If one combines two symmetry operations, such as rotations and reflections, one usually obtains a larger group, called a product group or composite group. For example, the cyclic group C_3 and reflections in a vertical plane (v) produce the group C_{3v} , investigated for the equilateral triangle or NH_3 molecule in Sections 2.5.1 and 2.5.3. Similarly, reflections across the plane of the triangle viewed as horizontal (h) would produce the group C_{3h} for NH_3 because of the reflection symmetry of the position of the N atom. Table 2.11 shows several composite groups similarly formed, both for the point groups and for some continuous groups used to describe symmetries in physical systems.

Groups in Physics. We now specialize our examples of groups to some used extensively in physics, especially those closely related to angular momentum and its analogs in spaces other than three dimensions. These continuous groups are summarized in Table 2.11.

The groups describing rotations in 2 and 3 dimensions, \mathcal{R}_2 and \mathcal{R}_3 , have matrix representations that are discussed in Section 1.3 and are already familiar. They are listed in Table 2.12 with other examples of symmetry groups used in subatomic and relativistic physics. The Lorentz group, \mathcal{L} , is of importance in special relativity, and Problem 2.14 suggests a simple example which shows the nature of the Lorentz group and its isomorphism to \mathcal{R}_2 .

TABLE 2.11 Composite groups used in the physical sciences. The abbreviation and usual name of each group are given in the first and second columns (name in italics), then we note typical applications in which the group is used. The rightmost column gives a textbook where the group is discussed extensively, with chapter numbers in parentheses.

Composite group	Name	Typical applications	References
<i>Point groups</i>			
X_h $X=C_n, D_n, T, O, Y$	X plus horizontal reflection	Crystals	Tin64 (4), Eli79 (9),
X_v $X=C_n, D_n, T, Y$	X plus vertical reflection		Lud88 (10), Bur90
X_d $X=D_n, T$	X plus diagonal reflection		
<i>Continuous groups</i>			
E_N $N=1, 2, 3$	<i>Euclidean</i> in N dimensions (translation plus rotation)	Solids	Eli79 (15), Cor84 (17), Bur90
\mathcal{P}	<i>Poincaré</i> group (Lorentz plus translation)	Relativity	Eli79 (15), Cor84 (17)

The special unitary group in two dimensions, $SU(2)$, and the special orthogonal group in three dimensions, $SO(3)$, are groups that form the mathematical foundations of angular momentum. For example, the degeneracy of the energy levels in a $1/r$ potential (such as in the hydrogen atom) are related to symmetries of the Schrödinger equation with this potential in a four-dimensional orthogonal space, $O(4)$, as we discuss in Section 7.1.4 and as Englfield [Eng72] describes very completely.

Subatomic Physics. Symmetry investigations in subatomic physics (nuclei and elementary particles) that assume charge independence also use the $SU(2)$ group. The model of the electromagnetic-plus-weak interaction involves this group in a direct product with the one-dimensional group of unitary transformations, $U(1)$, that is, $SU(2) \times U(1)$. Finally in Table 2.12 are the groups $SU(3)$ and $SU(6)$ which are used in the quark model of mesons and hadrons to describe the observed symmetry properties. A collection of reprints on symmetries in elementary-particle physics is provided by Froggatt and Nielsen [Fro91].

TABLE 2.12 Symmetry groups used in subatomic and relativistic physics. The rightmost column gives references (chapter numbers in parentheses) that have extensive technical discussions of the group.

Group	Applications	References
$\mathcal{R}_2, \mathcal{R}_3$	Rotation of vector and tensor operators in 2 and 3 dimensions	Ell79 (7)
\mathcal{L}	Lorentz transformations in special relativity	Ell79 (15), Cor84 (17)
$SU(2)$ $SO(3)$	Angular momentum	Ell79 (18.13), Alt86 (6)
$O(4)$	Degenerate energies of H atom	Eng72, Jud75 (3), Ell79 (18)
$SU(2)$	Isospin and charge independence	Ell79 (10), Cor84 (10)
$SU(2) \otimes U(1)$	Electromagnetic plus weak interactions (electroweak interaction)	Cor84 (19)
$SU(3)$	Spectroscopy of hadrons, Quantum Chromo Dynamics	Gib76 (10), Ell79 (11), Cor84 (10), Lud88 (14)
$SU(6)$	Quark-model symmetries	Gib76 (11), Ell79 (12)

2.5.5 Irreducibility of a Representation

In Section 2.5.3 we introduce the ideas of groups being mapped onto matrices, as schematized in Figure 2.14. We now further the connection by introducing the topic of irreducible representations and relating them to the properties of block-diagonal matrices considered in Section 2.1.3.

Suppose that the matrices forming a given representation can be expressed in a block-diagonal form in which each of the submatrices is square and of dimensions $s_1 \times s_1$, $s_2 \times s_2$, and $s_3 \times s_3$, with $s_1 + s_2 + s_3 = d$, the dimension of this representation. There should be at least two such matrices, but there may be three or more, as shown in (2.85).

$$\mathbf{M}(G_i) = \begin{bmatrix} [\mathbf{M}_1(G_i)] & \mathbf{0} & \mathbf{0} \\ \mathbf{0} & [\mathbf{M}_2(G_i)] & \mathbf{0} \\ \mathbf{0} & \mathbf{0} & [\mathbf{M}_3(G_i)] \end{bmatrix} \quad (2.85)$$

Further, the dimensions of the representation matrices must be the same for all elements G_i in the group G . It is straightforward to verify that each submatrix, \mathbf{M}_i ,

forms a representation of the group according to the requirements summarized in Figure 2.14. Thus, the matrices of the group products satisfy

$$\mathbf{M}_r(G_i G_j) = \mathbf{M}_r(G_i) \mathbf{M}_r(G_j) \quad r = 1, 2, \dots \quad (2.86)$$

so that other representations of G that are smaller (of lower dimension) have been obtained. The original representation matrices \mathbf{M} of G are therefore said to form a *reducible representation* of the group G .

To be technically more correct, in order to be a reducible representation the upper off-diagonal submatrices in \mathbf{M} need not be zero, and the representation needs only to be able to be converted to such a form by a similarity transformation. See, for example, the discussion in Section 4.4 of Cornwell [Cor84].

If the representation has been divided into block-diagonal matrices so that there are no smaller such matrices, then the representations are said to comprise *irreducible representations* of G .

Why are irreducible representations so useful for investigating symmetries of physical systems? When discussing block-diagonal matrices in Section 2.1.3 we show that for many purposes the matrix *blocks* (irreducible components) can be treated as matrix *elements* with all the simplifications inherent in diagonal matrices. This should not confuse one into thinking that the matrix blocks are themselves necessarily diagonal, since they generally are not so. This is made particularly clear in the example of the irreducible representations of the angular-momentum operator components, J_x, J_y, J_z , in Section 3.4.3. Another reason to find and use irreducible representations is that the matrices \mathbf{M}_r are smaller than those of the original representation \mathbf{M} , so manipulating them is usually less complicated. Irreducible representations are especially important for spherical tensor operators, which we introduce in Chapter 8.

Technical aspects of identifying and classifying irreducible representations are well described in Sections 4.5–4.21 of Elliott and Dawber [Eli79] and in Chapters 4 and 5 of Cornwell [Cor84].

2.6 MATHEMATICS, GROUPS, AND THE PHYSICAL SCIENCES

If you riffle through the pages of an unfamiliar book on your science library shelves, without looking at the book title, you can usually tell the discipline area just by estimating the ratio of words to figures. In a mathematics book, it is usually considered an intellectual weakness on the part of the author to provide a figure. On the other hand, from physics to chemistry to the life sciences one finds increasing use of figures. When you began to specialize your studies, you probably had to decide whether to concentrate on mathematics or on the physical sciences. Such a bifurcation of interests was probably conditioned by your predisposition toward an abstract or a visual mindset, respectively. For example, this book on rotational symmetries, written by a physicist for those in the physical sciences, has many figures because

visualizations help us to think clearly about symmetries.

Most of the mathematics you have used so far is related to quantitative measure of relative size, of rules (functions) for calculating numerical relations, and of techniques for calculating rates of change (differential calculus) or for estimating total effects (integral calculus). By contrast, much of group theory is not about *numerical* properties, but rather about common *symmetry* properties, for example, transformations under reflections or rotations. Thus, numbers measure size, whereas groups measure symmetry.

We conclude this excursion with remarks made in 1959 by Wigner (a pioneer in the use of symmetry principles and group theory in the physical sciences) on the unreasonable effectiveness of mathematics in natural sciences [Wig67, Chapter 17]:

The miracle of the appropriateness of the language of mathematics for the formulation of the laws of physics is a wonderful gift which we neither understand or deserve. We should be grateful for it and hope that it will remain valid in future research and that it will extend, for better or for worse, to our pleasure, even though perhaps to our bafflement, to wide branches of learning.

Since these ideas were expressed, an even broader range of mathematics has been adapted to and developed by physical scientists.

PROBLEMS ON MATHEMATICAL AND QUANTAL PRELIMINARIES

2.1 Consider the requirements (2.1) that must be satisfied by the elements in a linear vector space. Show that all these requirements are satisfied by:

- (a) Vectors of the conventional kind in three-dimensional coordinate space.
- (b) The wave functions that are solutions of a Schrödinger equation with a given Hamiltonian.

2.2 Direct products of matrices have several interesting and relevant properties. Prove the following results:

- (a)

$$(\mathbf{M} \otimes \mathbf{N})(\mathbf{P} \otimes \mathbf{Q}) = \mathbf{MP} \otimes \mathbf{NQ} \quad (2.87)$$

in which it is assumed that the dimensions of the matrices are appropriate for taking inner products on the left- and right-hand sides.

- (b) The direct product of two diagonal matrices is diagonal.
- (c) The direct product of two unit matrices is a unit matrix.
- (d) If the direct product of a unit matrix of dimension n with matrix \mathbf{M} is formed, then a block-diagonal matrix consisting of n replications of \mathbf{M} is obtained.
- (e) The direct product of unitary matrices is unitary.
- (f) The adjoint of a direct product of two matrices is the direct product of the adjoints, *without* reversal of the matrices:

$$(\mathbf{M} \otimes \mathbf{N})^\dagger = \mathbf{M}^\dagger \otimes \mathbf{N}^\dagger \quad (2.88)$$

2.3 Prove, in general, the inversion property for the operations on matrices described in Section 2.1.3. To do this, first prove the results for the inner products of *two* matrices, then show that if the result is true for n matrices it must be true for $n + 1$ matrices. Since the result holds for $n = 2$, it must therefore hold for $n = 3$, etc. Thus, you have used proof by induction.

2.4 For the passive and canonical transformations in Table 2.3 show in detail the steps in the transformation of the matrix elements, analogously to those in (2.33). Do *not* assume that the wave functions ψ' and ψ have a definite parity.

2.5 Consider the exponential of an operator, given by (2.38).

(a) Prove, by substituting directly in the definition the correctness of (2.40).

(b) Show that if $P = iH$ and H is Hermitian, then $U = e^{iH}$ is unitary.

(c) Prove the converse of this result. A simple way to do this is to write $U = e^{i\alpha H}$, in which α is a real parameter. Then differentiate both sides once with respect to α and use the relations (2.38) and (2.40). From this show that $H = H^\dagger$.

2.6 Consider relations between commutators of operators and their exponentials.

(a) To prove relation (2.43), consider operators $E(R) = e^{\alpha R}$. Show that $E(P + Q)$ satisfies the same first-order differential equation with respect to α as does $E(P)E(Q)E(\alpha\lambda I/2)$ and that their values coincide at $\alpha = 0$.

(b) Prove (2.44) by using (2.42) twice, first as is, then with P and Q interchanged. Note that exponentials of multiples of the unit operator commute with exponentials.

2.7 For the ladder operators in Section 2.2.4, work up the following steps in the derivations:

(a) Verify that expression (2.48) correctly gives raising and lowering of n by unity.

(b) Derive (2.49) for the result of successive applications of η_+ and η_- .

(c) Calculate matrix elements of the operators α and β , as defined by (2.54), between states n and k in order to show that these operators are Hermitian.

(d) Derive relation (2.56) between the antisymmetric and symmetric operators A and S and the Hermitian operators α and β .

2.8 Derive the relation (2.79) for z-axis rotations of a complex-valued spinor.

2.9 Verify the entries in Table 2.6 for combining rotations and reflections.

2.10 Prove that continuous rotations in a plane are associative by considering the coordinate transformations $x(\theta) = x_0 \cos \theta - y_0 \sin \theta$, $y(\theta) = x_0 \sin \theta + y_0 \cos \theta$.

(a) Show that if there are three angles of rotation θ_3 , θ_2 , θ_1 , then one can combine the third rotation after the first two or combine the last two angles first, which is the associative property.

(b) Show that for these rotations about the same axis the order of applying them does not matter (commutative property).

2.11 Prove in detail that (as stated in Section 2.5.3) any representation of a group G is itself a group in which the elements are the matrices $\mathbf{M}(G_i)$, the operation is (inner-product) multiplication, and the size of the matrix group can be no larger than the size of G . (If the representation is faithful, then the two groups are of the same

size.) Note that there is no necessary relation between the size of a representation matrix, $d \times d$, and the size of their group.

2.12 Verify the correctness of the group multiplication tables for:

- (a) The representation (2.83) of the discrete rotation group in Table 2.4.
- (b) The representations by (2.83) and (2.84) of the rotation-reflection group, C_{3v} , in Table 2.6.

2.13 Check that the matrices in Table 2.10— $O(N)$, $U(N)$, $SO(N)$, and $SU(N)$ —satisfy the conditions to form a group if the group operation is inner-product multiplication. In particular, show that each matrix has an inverse and that the identity of each group is $\mathbf{1}_N$.

2.14 Consider the Lorentz transformation for a single space dimension plus time that holds for relative motion of two reference frames having velocity β (with $|\beta| < 1$) in the same space dimension:

$$x' = \gamma(x - \beta ct) \quad ct' = \gamma(-\beta x + ct) \quad \gamma \equiv 1/\sqrt{1 - \beta^2} \quad (2.89)$$

- (a) Show that a continuous group is represented by the matrices

$$\mathbf{L}(\beta) = \begin{bmatrix} \gamma & -\beta\gamma \\ -\beta\gamma & \gamma \end{bmatrix} \quad (2.90)$$

acting on the space-time column vector as

$$\begin{pmatrix} x' \\ ct' \end{pmatrix} = \mathbf{L}(\beta) \begin{pmatrix} x \\ ct \end{pmatrix} \quad (2.91)$$

The parameter of the group is β , while the group operation is that of making successive Lorentz transformations with parameters β_i and β_j , say.

- (b) Show that the rule for combining Lorentz transformations is

$$\beta_{ij} = \frac{\beta_i + \beta_j}{1 + \beta_i \beta_j} \quad (2.92)$$

and therefore, since $\beta_{ij} = \beta_{ji}$, that the Lorentz group is Abelian.

- (c) Check that the identity of the group has $\beta = 0$.
- (d) Show that inverse transformations are obtained by $\beta \rightarrow -\beta$.
- (e) Consider the transformation in “Minkowski space”

$$\begin{pmatrix} x' \\ ict' \end{pmatrix} = \begin{bmatrix} \cos \theta & -\sin \theta \\ \sin \theta & \cos \theta \end{bmatrix} \begin{pmatrix} x' \\ ict' \end{pmatrix} \quad \beta = i \tan \theta \quad (2.93)$$

in which θ is purely imaginary in order that $\gamma \geq 1$. Show that this also describes

the Lorentz transformation and that the composition rule (2.92) is equivalent to that for obtaining the tangent of the sum of two angles. Thus, in Minkowski space the Lorentz transformation is isomorphic to \mathcal{R}_2 .



Chapter 3

ROTATIONAL INVARIANCE AND ANGULAR MOMENTUM

Our approach in this chapter is to develop the properties of the angular momentum operator, \mathbf{J} , whose three components are defined in Section 3.1 through infinitesimal rotations. Specific operators satisfying the commutation relations of J operators are devised in Section 3.2 (orbital angular momentum) and in Section 3.3 (Pauli matrices and other representations). The general problem of angular momentum eigenvalues and matrix elements is then addressed in Section 3.4, in which we use the technology of ladder operators developed in Section 2.2.4 to solve the eigenvalue problem.

By the end of this chapter, technical and algebraic aspects of angular momentum will be well in hand, but interpretation of these results will be undeveloped. Section 3.5 will help by our discussion of the importance of reference frames, leading to the distinction between spin and orbital angular momentum. In Chapter 4 we develop the interpretive aspects further by determining and illustrating angular momentum eigenstates.

3.1 INFINITESIMAL ROTATIONS; THE \mathbf{J} OPERATORS

A rotation about a given axis may be visualized as being built up from successive small rotations about that axis. Our aim in this section is therefore to understand the properties of infinitesimal rotations, particularly the operators describing such rotations—the angular momentum, or \mathbf{J} , operators.

To achieve this, we first present two schemes for describing rotations (Section 3.1.1), then we derive in Section 3.1.2 commutation relations between components of \mathbf{J} . Finally, in Section 3.1.3 we introduce ladder operators for angular momentum to simplify calculating eigenvalues and matrix elements in Section 3.4.

3.1.1 Schemes for Describing Rotations

There are two useful schemes for describing rotations. The first is simpler looking, as sketched in Figure 3.1.

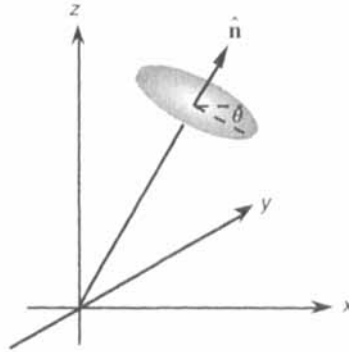


FIGURE 3.1 Scheme for describing the rotation of a system in terms of an axis of rotation, \hat{n} , and the angle of rotation about this axis, θ .

Since rotation is a unitary operation, as discussed in Sections 2.2.2 and 2.2.3, we can write it as U , given in terms of some Hermitian operator, \mathbf{J} , as

$$U(\theta, \hat{n}) = e^{-i\theta \hat{n} \cdot \mathbf{J}} \tag{3.1}$$

Here θ is the angle of rotation about the axis \hat{n} . The orientation of this unit vector must usually also be specified by two angles. The operator $\mathbf{J} = (J_x, J_y, J_z)$ is called the *angular momentum operator*. It is mostly related to angles and very little to momentum, as we discuss in detail in Chapter 5. The dimensions of \mathbf{J} , and therefore the dimensions of its components, are those of pure number.

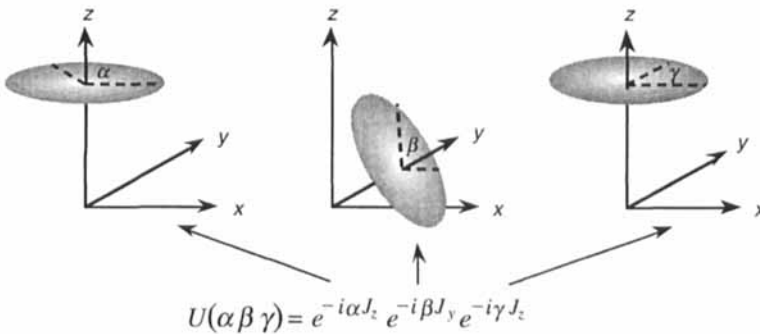


FIGURE 3.2 Euler-angle scheme for successive active rotations, with the leftmost operation applied first.

The second rotation scheme builds on (3.1) by describing rotations about each of the coordinate axes in turn. It is the Euler-angle scheme introduced in Section 1.3.1 and visualized in Figure 1.12. According to this scheme, and using *active rotations* with the same set of axes for successive rotations, we have the sequence of rotations shown in Figure 3.2.

Given the relation between rotations and angular momentum, our next task is to discover the properties of \mathbf{J} operators.

3.1.2 Commutation Relations of \mathbf{J} Operators

The angular momentum operator components, J_x, J_y, J_z are the building blocks for calculating properties of rotational symmetry. It is therefore important to acquire a clear understanding of their properties. Commutation relations among J_x, J_y, J_z can be derived by considering any convenient example, such as small rotations of an interval of unit length and initially along the x axis, as sketched in Figure 3.3.

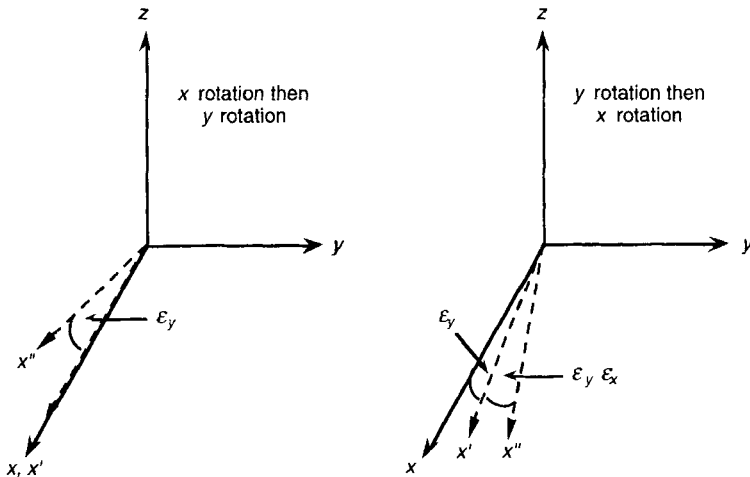


FIGURE 3.3 Effects of small rotations depend upon their order. Left, the rotation of a point initially along the x axis is first through ϵ_x about the x axis (no effect), then through ϵ_y about the y axis. Right, the same initial point is first rotated through ϵ_y about the y axis, then through ϵ_x about the x axis.

Consider a sequence of two small-angle rotations applied in two different orders:

(a) The first rotation is made through ϵ_x about the x axis to the same point on the coincident x' axis, then this point is rotated about the y axis through ϵ_y to produce a point on the x'' axis, as shown at the left side of Figure 3.3. Alternatively:

(b) The first rotation is made through angle ϵ_y about the y axis to produce a point on the x' axis [different from that in (a)], then this point is rotated about the x axis through ϵ_x to give a point on a different x'' axis, as on the right side of Figure 3.3.

As you can see by looking at Figure 3.3, the difference between the two orders of rotation, (b) minus (a), is to produce a displacement equivalent to a rotation about the z axis through angle $\epsilon_x \epsilon_y$. Write this out in terms of the rotation operators expanded through second order in the angles:

$$\begin{aligned} U(\epsilon_x, \hat{\mathbf{x}}) &= e^{-i\epsilon_x J_x} = \mathbf{1} - i\epsilon_x J_x - \epsilon_x^2 J_x^2 / 2 + \dots \\ U(\epsilon_y, \hat{\mathbf{y}}) &= e^{-i\epsilon_y J_y} = \mathbf{1} - i\epsilon_y J_y - \epsilon_y^2 J_y^2 / 2 + \dots \\ U(\epsilon_x \epsilon_y, \hat{\mathbf{z}}) &= e^{-i\epsilon_x \epsilon_y J_z} = \mathbf{1} - i\epsilon_x \epsilon_y J_z + \dots \end{aligned} \tag{3.2}$$

in which omitted terms have at least the product of three small angles. Through this order of approximation we have that

$$U(\epsilon_x, \hat{\mathbf{x}})U(\epsilon_y, \hat{\mathbf{y}}) - U(\epsilon_y, \hat{\mathbf{y}})U(\epsilon_x, \hat{\mathbf{x}}) \approx U(\epsilon_x \epsilon_y, \hat{\mathbf{z}}) - \mathbf{1} \tag{3.3}$$

If we now substitute (3.2) into this expression and simplify both sides (as Problem 3.1 suggests you do) we find that

$$\epsilon_x \epsilon_y (J_x J_y - J_y J_x) + \dots = i\epsilon_x \epsilon_y J_z + \dots \tag{3.4}$$

where omitted terms are of higher order in the angles. We may now divide both sides by $\epsilon_x \epsilon_y$, then take the limit as each angle tends to zero separately. The higher-order angle terms then vanish. Thereby we obtain the commutation relation among angular momentum operator components

$$J_x J_y - J_y J_x = iJ_z \tag{3.5}$$

Because all the axes are equivalent in a Cartesian coordinate system, by cyclic substitution of the axes labels we can summarize the commutation relations as

$$\boxed{J_r J_s - J_s J_r = i\epsilon_{rst} J_t} \tag{3.6}$$

Here we have used the permutation symbol, ϵ_{rst} , which has the properties

$$\epsilon_{rst} = \begin{cases} 0 & \text{if any two of } r, s, t \text{ are the same (e.g., } 1,1,3) \\ +1 & \text{if } r, s, t \text{ are in cyclic order (e.g., } 3,1,2) \\ -1 & \text{if } r, s, t \text{ are in odd order (e.g., } 3,2,1) \end{cases} \tag{3.7}$$

We have also assumed in (3.6) the Einstein summation convention, in which a repeated index (here the t) is to be summed over. Actually, only one term survives in

the sum—the J component that doesn't match the two on the left-hand side. After you have sorted out all this notation, you will recognize the familiar vector products, which are discussed in the context of permutation symbols and Einstein summations in Section 1.3 of Wong's text on mathematical physics [Won91].

To summarize the results in vector form: The *fundamental commutation relations among angular momentum operators* are

$$\boxed{\mathbf{J} \times \mathbf{J} = i\mathbf{J}} \tag{3.8}$$

These relations are the starting point for developments in this book that relate to rotational properties of systems. It is very important to note that the commutation relations (3.8) are completely *geometrical*, as the preceding derivation makes quite clear. They may therefore be used in (3.1) to describe any rotation, whether it be applied to a scalar function, to a vector in classical mechanics, or to a wave function in quantum mechanics.

Now that we have derived the fundamental formula of angular momentum, we can develop its consequences, both in terms of concepts and in terms of techniques.

3.1.3 The Spherical-Basis Operators J_{+1} , J_0 , J_{-1}

We define the angular momentum spherical-basis (ladder) operators as

$$\boxed{J_{\pm 1} \equiv (J_x \pm iJ_y) \quad J_0 \equiv J_z} \tag{3.9}$$

If a factor of $1/\sqrt{2}$ were included in this definition, it would give a more consistent treatment of ladder (raising and lowering) operators, as presented in Section 2.2.4. However, we bow to convention, especially to provide consistency with use of the spherical-basis operators in Chapter 8 for irreducible tensors.

Since the Cartesian-coordinate operators, J_x , J_y , and J_z , are Hermitian, the spherical-basis operators satisfy

$$J_{\pm 1}^\dagger = J_{\mp 1} \quad J_0^\dagger = J_0 \tag{3.10}$$

Justification for the terminology “spherical basis” is given in Section 3.4. The commutation relations in this basis can be obtained directly from those in the Cartesian basis, (3.6), as

$$[J_{\pm 1}, J_0] = \mp J_{\pm 1} \quad [J_{\pm 1}, J_{\mp 1}] = \pm 2J_0 \tag{3.11}$$

and the square of the total angular momentum operator becomes

$$\mathbf{J}^2 = \frac{1}{2} (J_{+1}^2 + J_{-1}^2) + J_0^2 \quad (3.12)$$

Problem 3.2 invites you to derive these two formulas. We use the spherical-basis operators extensively in Section 3.4.1 to find operator eigenvalues.

3.2 ORBITAL ANGULAR MOMENTUM OPERATORS

In this section we derive operators to describe infinitesimal rotations of functions of coordinates only, that is, of scalars. These so-called orbital angular momentum operators, \mathbf{L} , are examples of the \mathbf{J} operators whose commutation relations (3.8) are derived in Section 3.1.

Traditionally, as in the survey by Biedenharn and Louck [Bie81a], it is common to start the discussion of angular momentum by introducing the quantum-mechanical operator $\mathbf{L}_q = \mathbf{r} \times \mathbf{p}_q$, in which $\mathbf{p}_q = -i\hbar\nabla$ is the linear-momentum operator. One then verifies that \mathbf{L}_q satisfies the commutation relations (3.8), but with an extra factor of \hbar on the right-hand side. Eventually, one seeks solutions for \mathbf{J} that are more general than \mathbf{L}_q . Such an approach unnecessarily confuses the *geometrical* properties of rotations with the *quantum-mechanical* properties of operators in which \hbar appears. We discuss extensively in Chapter 5 the connections between angular momentum and quantum mechanics.

Meanwhile, we continue our logical development of the subject by deriving the form that \mathbf{L} must have (Section 3.2.1), expressing the result in spherical polar coordinates (Section 3.2.2), and emphasizing in Section 3.2.3 the special role of the operator L_z .

3.2.1 Infinitesimal Rotations Applied to Spatial Functions

Consider a continuous function of the spatial coordinates only, $f(x, y, z)$. How does f change when the system it describes is rotated through a small angle? Because we have restricted the space in which \mathbf{J} acts, we will find only a limited representation of \mathbf{J} . Let us denote this restricted \mathbf{J} by $\mathbf{L} = (L_x, L_y, L_z)$, called the *orbital angular momentum operator*, for reasons that will become clear below. We first derive the general form of the operator, then we discuss some of its properties.

Deriving the Orbital Angular Momentum Operator. To obtain the expression for the components of \mathbf{L} , say for L_z , consider rotation around the z axis by a small angle, ϵ , of the system described by f . For example, in a geophysical study f might describe the density of a fluid as a function of position near the Earth's surface. Suppose that (active) rotation of the system moves a representative point P from $\mathbf{r} = (x, y, z)$ to $\mathbf{r}_\epsilon = (x_\epsilon, y_\epsilon, z_\epsilon)$, as shown in Figure 3.4.

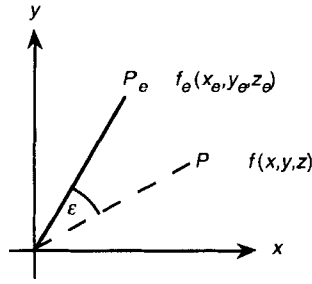


FIGURE 3.4 Rotation of a system through angle ϵ about the z axis carries a point from \mathbf{r} to \mathbf{r}_ϵ and a function describing P from $f(\mathbf{r})$ to $f_\epsilon(\mathbf{r}_\epsilon)$.

Such a rotation serves only to relabel the function, that is,

$$f_\epsilon(\mathbf{r}_\epsilon) = f(\mathbf{r}) \quad (3.13)$$

If we wish to find the effect of the rotation on f specified *at a given point in space*, we must undo the effect of transforming the coordinates. Therefore, we calculate the changed *function* as

$$f_\epsilon(\mathbf{r}) = f(\mathbf{r}_-\epsilon) \quad (3.14)$$

To relate this to angular momentum operators, we now consider that ϵ is small enough that terms in ϵ^2 and higher can be ignored in calculations, and eventually we take the limit $\epsilon \rightarrow 0$. We can use (1.14) to relate $\mathbf{r}_-\epsilon$ to \mathbf{r} according to

$$\begin{bmatrix} x_- \epsilon \\ y_- \epsilon \\ z_- \epsilon \end{bmatrix} = \begin{bmatrix} \cos(-\epsilon) & -\sin(-\epsilon) & 0 \\ \sin(-\epsilon) & \cos(-\epsilon) & 0 \\ 0 & 0 & 1 \end{bmatrix} \begin{bmatrix} x \\ y \\ z \end{bmatrix} \approx \begin{bmatrix} 1 & \epsilon & 0 \\ -\epsilon & 1 & 0 \\ 0 & 0 & 1 \end{bmatrix} \begin{bmatrix} x \\ y \\ z \end{bmatrix} \quad (3.15)$$

From the operator equation we have

$$f_\epsilon(\mathbf{r}) = e^{-i\epsilon L_z} f(\mathbf{r}) \approx (1 - i\epsilon L_z) f(\mathbf{r}) \quad (3.16)$$

We now have expressions (3.14)–(3.16), which enable $f_\epsilon(\mathbf{r})$ to be calculated two different ways—either in terms of small changes of coordinates or in terms of the operator L_z . By assuming that f is a continuous function that can be expanded in a Taylor series about \mathbf{r} , it is straightforward to show (as Problem 3.3 suggests you try) that for such functions the operator component must be expressed as

$$L_z = -i \left(x \frac{\partial}{\partial y} - y \frac{\partial}{\partial x} \right) \quad (3.17)$$

Thus, we have obtained a general expression for the z component of the operator \mathbf{J} whenever it acts on a function that depends only upon the spatial coordinates.

Because the three Cartesian coordinates are equivalent, it is clear that merely by cycling through the coordinates we immediately obtain the expressions for L_x and L_y . Expressed in vectorial form the *orbital angular momentum operators* are thus

$$\mathbf{L} = -i\mathbf{r} \times \nabla \quad (3.18)$$

This is the most general form the angular momentum operator \mathbf{J} can assume when it is applied to any continuous function that depends only upon the spatial coordinates.

The formula for \mathbf{L} does not depend in any way upon quantum mechanics. Indeed, all of the formulas were available to Taylor and Euler in the eighteenth century, long before the invention of quantum mechanics in the twentieth century. The result (3.18) was often used implicitly in developments in classical analysis and mechanics in the nineteenth century.

Notice that \mathbf{L} has the dimensions of a pure number, just as for \mathbf{J} . Further, any overall length scale is irrelevant and \mathbf{L} is purely a function of angles—genuine *angular momentum*—as also holds for \mathbf{J} .

The Mechanics Connection. For those readers in the physical sciences who crave some contact with reality, we discuss briefly the relation of formula (3.18)—a purely *geometrical* construct—to angular momentum in physical systems, which we call in Sections 3.4.5 and 5.1 *dynamical* angular momentum. We define quantum-mechanical orbital angular momentum, \mathbf{L}_q , by

$$\mathbf{L}_q \equiv \hbar \mathbf{L} \quad (3.19)$$

The dimensions of \mathbf{L}_q are those of \hbar , so its dimensions are those of mechanical angular momentum. Indeed, we may rewrite (3.19) as

$$\mathbf{L}_q = \mathbf{r} \times \mathbf{p}_q \quad \mathbf{p}_q \equiv -i\hbar \nabla \quad (3.20)$$

in which \mathbf{p}_q is the momentum operator in configuration space (\mathbf{r} coordinates). Alternatively, we have in momentum space

$$\mathbf{L}_q = \mathbf{r}_q \times \mathbf{p} \quad \mathbf{r}_q \equiv -i\hbar \nabla_p \quad (3.21)$$

where ∇_p is the position operator in momentum space (\mathbf{p} coordinates) and \mathbf{p} is a regular vector rather than a differential operator.

The operator \mathbf{L}_q induces the same type of rotational transformation as does \mathbf{L} , but with the added complication that one must write the rotation operator (3.1) when acting upon a function of only x, y, z as

$$\mathbf{U}(\theta, \hat{\mathbf{n}}) = e^{-i\theta \hat{\mathbf{n}} \cdot \mathbf{L}_q / \hbar} \quad (3.22)$$

This form gives one pause to wonder what would happen to rotations if the value of

Planck's constant were to change. Actually, \hbar may have any nonzero value and (3.22) is exactly the same. We do not presently know any connection between the isotropy of space discussed at the beginning of Section 1.3 and the value of Planck's constant, so it does not seem worthwhile to burden *rotations* with extra factors of \hbar .

The major justification for using the operator \mathbf{L}_q given by (3.19) is that it has the same appearance (but a different interpretation) as angular momentum in classical mechanics. When expectation values of \mathbf{L}_q are taken and when the angular momentum quantum number $j = \ell$ is suitably large, one obtains the same results as in classical mechanics. Angular momentum in quantum systems is developed in Chapter 5, with emphasis on its conceptual development in Section 5.5.

3.2.2 Components of \mathbf{L} in Spherical Polar Coordinates

Although the form of the orbital angular momentum operators given by (3.18) is adequate for a definition, it is not very practical because the dependence on angles is not made explicit. A suitable angle-dependent coordinate system in which to express the components of \mathbf{L} is spherical polar coordinates, where angles are explicit and for which there are many useful results from trigonometry and vector calculus.

Spherical Polar Coordinate System. To remind you of this coordinate system, we sketch it in Figure 3.5.

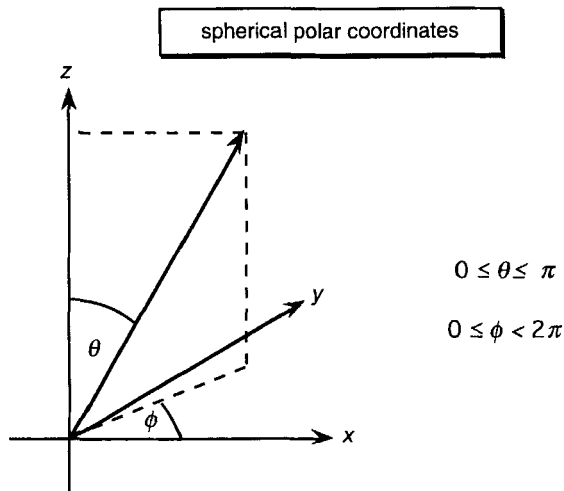


FIGURE 3.5 Spherical polar coordinate system, showing the polar angle θ , the azimuthal angle ϕ , and their ranges.

Spherical polar coordinates are related to Cartesian coordinates by

$$x = r \sin \theta \cos \phi \quad y = r \sin \theta \sin \phi \quad z = r \cos \theta \quad (3.23)$$

as can be shown easily from Figure 3.5. Given these relations, it is straightforward but tedious (so delegated to Problem 3.4) to express the components of the \mathbf{L} operator in polar coordinates as

$$\begin{aligned} L_x &= i \left(\sin \phi \frac{\partial}{\partial \theta} + \cot \theta \cos \phi \frac{\partial}{\partial \phi} \right) \\ L_y &= i \left(-\cos \phi \frac{\partial}{\partial \theta} + \cot \theta \sin \phi \frac{\partial}{\partial \phi} \right) \\ L_z &= -i \frac{\partial}{\partial \phi} \end{aligned} \quad (3.24)$$

This expression holds except at $\theta = 0$ or $\theta = \pi$, where the polar coordinate system is singular. From (3.24), and from Figure 3.5 geometrically, we see that

$$L_x(\phi) = L_y(\pi/2 + \phi) \quad (3.25)$$

In the polar coordinate expressions (3.24) there is no longer a distance scale, since r is absent. Therefore, we truly have *angular* momentum that characterizes rotations. By contrast, classical angular momentum depends both upon angles and upon distance scales, an important distinction that is emphasized in Section 5.1.

Orbital Angular Momentum in Spherical Basis. We may complete the transition to the spherical basis by casting the components into the spherical basis introduced in Section 3.1.4. By combining L_x and L_y from (3.24) we obtain directly

$$\begin{aligned} L_{\pm 1} &\equiv (L_x \pm iL_y) = e^{\pm i\phi} \left(\pm \frac{\partial}{\partial \theta} + i \cot \theta \frac{\partial}{\partial \phi} \right) \\ L_0 &\equiv L_z = -i \frac{\partial}{\partial \phi} \end{aligned} \quad (3.26)$$

Notice that operators are simpler in this basis than in the Cartesian basis, (3.24). The L_z or L_0 components are especially simple, as we investigate further in Section 3.2.3.

The expression (3.26) is useful for expressing the square of the orbital operator, \mathbf{L}^2 , in polar coordinate form as

$$\begin{aligned} \mathbf{L}^2 &= \frac{1}{2} (L_{+1}L_{-1} + L_{-1}L_{+1}) + L_0^2 \\ &= - \left[\frac{1}{\sin \theta} \frac{\partial}{\partial \theta} \left(\sin \theta \frac{\partial}{\partial \theta} \right) + \frac{1}{\sin^2 \theta} \frac{\partial^2}{\partial \phi^2} \right] \\ &= - \left[\frac{\partial}{\partial \cos \theta} \left(\frac{\partial}{\partial \cos \theta} \right) + \frac{1}{1 - \cos^2 \theta} \frac{\partial^2}{\partial \phi^2} \right] \end{aligned} \quad (3.27)$$

As usual for spherical-polar coordinates, and as the last form of L^2 in (3.27) emphasizes, these expressions are undefined at the poles, $\theta = 0$ and $\theta = \pi$. This form also shows that the basic variables for orbital angular momentum are $\cos\theta$ and ϕ rather than θ and ϕ , as the discussion of orbital eigenstates in Section 4.1 makes clear.

3.2.3 The Special Role of the Operator L_z

It is no coincidence that the z component of the angular momentum operator acting upon a function of angles, that is L_z , has an especially simple form in spherical polar coordinates. For this reason, in Section 3.4.1 we choose the axis with respect to which a component of the angular momentum operator has eigenvalues as the z axis. Then, the operator, its eigenvalues, and its eigenvectors will all be simple.

As a particular example of the simplicity of L_z , consider any function of the form $e^{i\alpha\phi}$. For any choice of α , this function is an eigenfunction of L_z , since

$$L_z e^{i\alpha\phi} = -i \frac{\partial}{\partial \phi} e^{i\alpha\phi} = \alpha e^{i\alpha\phi} \quad (3.28)$$

If α is real, then L_z will be Hermitian for matrix elements taken with respect to this function. Further, it is straightforward to show that for different values of α these functions are orthogonal for integration over the range 0 to 2π in ϕ only if α is an integer. These results obtained for L_z anticipate some of those for general angular momentum that are obtained in Section 3.4.1.

3.3 OTHER REPRESENTATIONS OF J OPERATORS

The properties of the angular momentum operators derived in Section 3.1 are—to use mathematical terminology—prescriptive rather than constructive. That is, we derived properties that *must* be satisfied by any operators that claim to describe \mathbf{J} , but we did not give any way to form such operators. Because of this, new representations of angular momentum operators are constantly being discovered. Many of them provide fresh insight into rotational symmetries, others facilitate derivations and calculations, while others serve mainly to impress readers with the genius of their discoverer.

We begin by defining the Pauli matrices and determining properties relevant to rotational symmetries. In particular, we find their eigenvectors and show how the Pauli matrices may be used to describe finite rotations. We then summarize other useful representations.

3.3.1 The 2×2 Matrix Representation: Pauli Matrices

We introduce the Pauli matrices through their algebraic properties. In Section 4.3 we show that they describe the simplest nontrivial-spin systems, namely those with intrinsic spin of $1/2$. Since so many subatomic particles (such as electrons, protons,

neutrons) are observed to have spin 1/2, the Pauli matrices are also of very general use in quantum mechanics. Further, just as one can visualize a complicated atom as being composed of many electrons, mathematically one can use Pauli matrices and other spin-1/2 descriptions to build up angular momentum and describe rotations of systems with larger angular momentum numbers.

Pauli Matrices as Angular Momentum Operator Components. In Cartesian coordinates the Pauli matrices are given by

$$\sigma_x = \begin{bmatrix} 0 & 1 \\ 1 & 0 \end{bmatrix} \quad \sigma_y = \begin{bmatrix} 0 & -i \\ i & 0 \end{bmatrix} \quad \sigma_z = \begin{bmatrix} 1 & 0 \\ 0 & -1 \end{bmatrix} \quad (3.29)$$

Collectively, these three matrices are denoted by $\sigma = (\sigma_x, \sigma_y, \sigma_z)$, although we have yet to prove that the subscripts are appropriate for x , y , and z coordinates. Define in terms of the Pauli matrices the “spin” matrices, s , as

$$\mathbf{s} \equiv \frac{1}{2} \sigma \quad (3.30)$$

It is straightforward to show that the components of s satisfy the angular momentum commutation relations (3.8).

Properties of Pauli Matrices. In terms of calculations, it is often easier to use the Pauli matrices (3.29) rather than the spin matrices (3.30) because each Pauli matrix has the property

$$\sigma_j^2 = \mathbf{1}_2 \quad j = x, y, z \quad (3.31)$$

in which $\mathbf{1}_2$ is the unit 2×2 matrix.

To explain (3.30) from a physical viewpoint, you have to know already that these 2×2 matrices describe spin-1/2 systems, as is clear if you notice that s_z has eigenvalues $+1/2$ and $-1/2$, usually called “spin-up” and “spin-down” states, respectively. These are the only possible angular momentum states for a spin-1/2 system. A repeated measurement of σ_z , corresponding to σ_z^2 , must therefore give unity for either spin up or spin down, in agreement with (3.31). Since there is nothing intrinsically special about the z direction (as discussed in Section 1.3.2), the same result must hold for the x and y directions.

Another property of the Pauli matrices is their *anticommutation* property

$$\sigma_j \sigma_k + \sigma_k \sigma_j = 0 \quad j \neq k \quad (3.32)$$

where j or k stands for one of the coordinates x , y , and z . Both properties (3.31) and (3.32) are particular among angular momentum matrices and result because the angular momentum is the simplest possible (except for complete isotropy, spin zero). Levinger and Lichtenstein [Lev79] provide an explanation of (3.32) that also

improves understanding spin, as follows. Consider a new axis relative to which the spin value is measured, say x' midway between the x and y axes, as sketched in Figure 3.6.

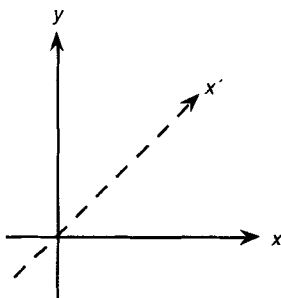


FIGURE 3.6 When the quantization axis is chosen at $\pi/4$ to the x or y axis, along x' , the x and y spin components contribute equally.

By equivalence of axes, the x and y components of spin contribute equally, so we must have

$$\sigma_{x'} = \frac{1}{\sqrt{2}}\sigma_x \pm \frac{1}{\sqrt{2}}\sigma_y \quad (3.33)$$

in which the factors before the matrices ensure that the total probability is unity. Algebraically, we can square this matrix, taking care to keep the operators in order, to obtain

$$\sigma_{x'}^2 = \frac{1}{2}[\sigma_x^2 + \sigma_y^2 \pm (\sigma_x\sigma_y + \sigma_y\sigma_x)] \quad (3.34)$$

Now, since (3.31) shows that the square of a Pauli matrix along *any* direction is a unit matrix, the cross terms in (3.34) must contribute zero, just as (3.32) claims.

Pauli Matrices in the Spherical Basis. The general spherical-basis angular momentum operators are presented in Section 3.1.3. It is interesting to discuss them for the case in which they are represented by the Pauli matrices. From definition (3.9), by letting

$$J_{\pm 1} \longrightarrow \sigma_{\pm 1} = (\sigma_x \pm i\sigma_y) \quad (3.35)$$

and recalling that $J_0 = J_z \rightarrow \sigma_0 = \sigma_z$, we obtain directly

$$\sigma_{-1} = \begin{bmatrix} 0 & 0 \\ 2 & 0 \end{bmatrix} \quad \sigma_0 = \begin{bmatrix} 1 & 0 \\ 0 & -1 \end{bmatrix} \quad \sigma_{+1} = \begin{bmatrix} 0 & 2 \\ 0 & 0 \end{bmatrix} \quad (3.36)$$

which have the properties that

$$\sigma_{\pm 1}^2 = \mathbf{0}_2 \quad \sigma_0^2 = \mathbf{1}_2 \quad (3.37)$$

where $\mathbf{0}_2$ denotes the 2×2 matrix with all elements zero. Higher powers of these spherical-basis matrices, which represent raising and lowering operators (Section 2.2.4) must similarly be zero matrices. How do we explain this property, apart from its algebraic correctness? The effect of σ_+ on a spin-down state is to raise it to a spin-up state, but if we apply σ_{+1} to this state there is not (for spin $1/2$) another state for it to be raised to, so $\sigma_{+1}^2 = 0$. Similar arguments apply for σ_{-1} .

3.3.2 Eigenvectors of the Pauli Matrices

Because of the commutation condition (3.8), for a given choice of axes we can make a diagonal representation in only one direction. From definition (3.29) of the Pauli matrices, it is clear that we have chosen the z axis as this direction. Indeed, when discussing angular momentum if one refers to “the z axis” one usually means “the direction in which the representation is diagonal.”

What are the eigenvectors (Section 2.3) of the Pauli matrix σ_z ? Clearly, to enable inner products to be formed they must be 2×1 (column) matrices. Write them with elements a_+ and a_- . Thus, as eigenvectors they must satisfy

$$\begin{bmatrix} 1 & 0 \\ 0 & -1 \end{bmatrix} \begin{bmatrix} a_+ \\ a_- \end{bmatrix} = M_{\pm} \begin{bmatrix} a_+ \\ a_- \end{bmatrix} \quad (3.38)$$

where M_{\pm} are the two eigenvalues. By multiplying out the left-hand sides, as Problem 3.5 suggests you do, it is easy to show that two eigenvectors are

$$\chi_+ \equiv \begin{bmatrix} 1 \\ 0 \end{bmatrix} \quad \chi_- \equiv \begin{bmatrix} 0 \\ 1 \end{bmatrix} \quad (3.39)$$

with corresponding eigenvalues $M_+ = +1$, $M_- = -1$. Because (3.38) is linear in the amplitudes a_{\pm} , any multiples of χ_{\pm} are also eigenvectors. The choices in (3.39) make the eigenvectors *orthonormal*, that is,

$$\tilde{\chi}_{\pm} \chi_{\pm} = 1 \quad \tilde{\chi}_{\mp} \chi_{\pm} = 0 \quad (3.40)$$

The second of these relations illustrates the orthogonality of the eigenvectors of Hermitian operators (Section 2.3).

The eigenvectors χ_{\pm} are clearly also appropriate for the angular momentum matrix $\mathbf{s}_z = \sigma_z/2$. The eigenvalues of \mathbf{s}_z , which are just the diagonal elements of this matrix, are $\pm 1/2$. It is therefore appropriate to call χ_+ and χ_- the matrices representing “spin-up” and “spin-down” states, respectively. The generalization from the simplest spin system, discussed here, to matrix eigenvectors for arbitrary spin is derived and illustrated in Sections 3.4.4 and 4.3.

3.3.3 Finite Rotations and Pauli Matrices

So far in this chapter we have discussed only *infinitesimal* rotations, which are described by the operator \mathbf{J} introduced in Section 3.1. Although you will surely agree that the algebra of such operators is fascinating, it is not of much direct practical use, since in reality we want to calculate how systems change under *finite* rotations. This can be done simply for spin-1/2 systems, because the matrices required are small (just 2×2) and have simple properties, as shown in Section 3.3.1. Therefore, by considering spin 1/2 we now illustrate one way of deriving rotation matrices for angular momentum eigenstates. Methods that are more general, as well as more abstract, are given in Section 6.2.

Finite-rotation operators are defined in terms of infinitesimal operators by (3.1). For spin-1/2 states, the rotation operator has a representation (in the group theory sense, Section 2.5.3) written as the spin-1/2 rotation matrix

$$\mathbf{D}^{1/2}(\alpha \beta \gamma) = e^{-i\alpha\sigma_z/2} e^{-i\beta\sigma_y/2} e^{-i\gamma\sigma_z/2} \quad (3.41)$$

Here we have used the full description of an active rotation in terms of Euler angles, as described in Sections 1.3.1 and 3.1.1. We have also substituted for matrices representing the angular momentum operators the spin matrices in terms of the Pauli matrices, according to (3.30).

As you see in (3.41), there are just two distinct kinds of rotations in the Euler-angle scheme—rotations about z or rotations about y . Because the z axis has been chosen for the eigenvalues, its rotation is easier to handle, so we consider it first.

Rotations About the z Axis. We have to work out the exponential of a matrix, which is not as formidable as it may seem, since the exponential is a shorthand for the series (2.38). If we plug in the exponent $-i\gamma\sigma_z/2$ there will be two distinct terms—those in which n is even, $n = 2m$ and $\sigma_z^{2m} = \mathbf{1}_2$, and those with n odd, $n = 2m + 1$ and $\sigma_z^{2m+1} = \sigma_z$. As Problem 3.6 suggests that you work out in detail, the unit matrix and σ_z then factor out of the series of even and odd terms, resulting in the spin-1/2 matrix for rotation by γ about the z axis

$$e^{-i\gamma\sigma_z/2} = \cos(\gamma/2)\mathbf{1}_2 - i\sin(\gamma/2)\sigma_z \quad (3.42)$$

By substituting for σ_z from (3.29), we have explicitly

$$e^{-i\gamma\sigma_z/2} = \begin{bmatrix} e^{-i\gamma/2} & 0 \\ 0 & e^{+i\gamma/2} \end{bmatrix} \quad (3.43)$$

The matrix elements of this z -axis rotation are thus $e^{-im\gamma}\delta_{m',m}$. In Section 6.2.1 this is shown to be the result for any value of the spin, not just for the spin-1/2 case we have just derived.

Notice that in (3.43) the transformation under rotation is unitary (Section 2.2.2), not changing total probabilities. In particular, all that the z -axis rotation does is to change the *phase* of a state vector component by $e^{\mp i\gamma/2}$, without changing its magnitude. Although this is a simple change, it often has profound consequences in quantum mechanics.

Rotations About the y Axis. For rotation about an axis orthogonal to the quantization axis, such as the y axis chosen in the Euler-angle scheme, the rotation matrices are not quite as simple as for z -axis rotations, since the Pauli y -axis matrix is not diagonal. The method of derivation is similar, however, so the details are relegated to Problem 3.6. The spin-1/2 matrix for rotation by β about the y axis is given by

$$\mathbf{d}^{1/2}(\beta) \equiv e^{-i\beta\sigma_y/2} = \begin{bmatrix} \cos(\beta/2) & -\sin(\beta/2) \\ \sin(\beta/2) & \cos(\beta/2) \end{bmatrix} \quad (3.44)$$

The matrix $\mathbf{d}^{1/2}(\beta)$ is called the *reduced rotation matrix* for spin 1/2, since it is reduced in the sense that the rotation is about a single axis (y) rather than about three axes. Its generalization to arbitrary spin is presented in Section 6.2.

As with the z -axis rotation, we notice that—consistently with the general relation (2.41) between Hermitian and unitary operators—the matrix in (3.44) is unitary. One proof of this (Problem 3.6) is by forming the Hermitian conjugate of $\mathbf{d}^{1/2}$ explicitly and multiplying out the two matrices. Alternatively, we see by inspection that the transpose of (3.44) gives the same result as the inverse rotation $\beta \rightarrow -\beta$.

If we have two successive rotations about the y axis, it is straightforward to show that

$$\begin{aligned} \mathbf{d}^{1/2}(\beta_2)\mathbf{d}^{1/2}(\beta_1) &= \mathbf{d}^{1/2}(\beta_2 + \beta_1) \\ &= \mathbf{d}^{1/2}(\beta_1 + \beta_2) = \mathbf{d}^{1/2}(\beta_1)\mathbf{d}^{1/2}(\beta_2) \end{aligned} \quad (3.45)$$

in which the first equality is obtained by multiplication of the matrices, the second equality comes from commutativity of arithmetic addition, and the third equality arises from a relabeling of the angles in the first equality. We have thus verified that successive rotations about the same axis commute.

Spinor Nature of Spin-1/2 Rotations. A striking property of both the z - and y -axis rotations is the property of the matrices in (3.43) and (3.44) that they change sign when their defining angles change by 2π . Thus

$$e^{\pm i(\alpha+2\pi)/2} = -e^{\pm i\alpha/2} \quad \mathbf{d}^{1/2}(\beta + 2\pi) = -\mathbf{d}^{1/2}(\beta) \quad (3.46)$$

Rotation matrices for spin-1/2 states are thus spinors, according to the definition in Section 2.4, so one says that spin-1/2 state vectors are spinors because of this transformation property.

The consequences of such a sign change have been observed quite directly for neutrons (Figure 2.6) and implicitly for electrons through the sign-change requirement (3.46) for electron wave functions in atomic-structure calculations. This is consistent with an assignment of 1/2 for the intrinsic spin (Section 3.5) of these particles.

General Euler-Angle Rotations for Spin 1/2. We can now combine the results of our calculations for rotations about a single axis to obtain the general Euler-angle rotation matrices for spin 1/2. From (3.43) used twice and from (3.44), we obtain the full rotation matrix

$$\mathbf{D}^{1/2}(\alpha\beta\gamma) = \begin{bmatrix} e^{-i\alpha/2} & 0 \\ 0 & e^{+i\alpha/2} \end{bmatrix} \begin{bmatrix} \cos(\beta/2) & -\sin(\beta/2) \\ \sin(\beta/2) & \cos(\beta/2) \end{bmatrix} \begin{bmatrix} e^{-i\gamma/2} & 0 \\ 0 & e^{+i\gamma/2} \end{bmatrix} \quad (3.47)$$

This matrix has the unitary and spinor properties of its component matrices, providing a complete expression for rotations of a spin-1/2 system in terms of the Euler angles. Note that since rotations about *different* axes do not generally commute, the ordering of the matrices in (3.47) is important. This is in contrast to the commutation property for rotations about the *same* axis, exemplified in (3.45).

The treatment of finite rotations for arbitrary spin is taken up in Chapter 6, where we learn that most of the properties derived here for spin-1/2 systems also hold for arbitrary angular momentum number.

3.3.4 Spinor Space and Its Operators

The eigenvectors of the Pauli matrices determined in Section 3.3.2 provide examples of spinors, according to the definition (2.74) of changing sign under rotations by 2π . This behavior of the 2×1 column matrices χ_{\pm} is apparent from the behavior of the full rotation matrix for spin 1/2, $\mathbf{D}^{1/2}(\alpha\beta\gamma)$, as given by (3.47).

It is useful in later developments to use the spin-1/2 description as a building block when constructing states and their representations for larger angular momentum numbers. For this purpose, we now introduce the spinor space and angular momentum operators in this space. At this stage it is worthwhile for you to review spinors and their properties in Section 2.4.

Spinor Space and Its Matrix Representation. Suppose that we have an abstract space whose “coordinates” are described in terms of quantities χ_+ and χ_- which act as unit vectors in the space. Technically, this is a Hilbert space, as discussed in Jordan’s introductory monograph [Jor69]. You may visualize this spinor space as shown in Figure 3.7.

We want this space to describe rotations for spin-1/2 systems, so the “coordinates” of points in this space, a_+ and a_- , are allowed to be complex and are required to satisfy

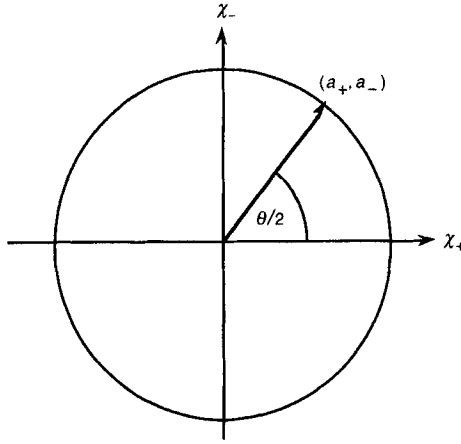


FIGURE 3.7 Spinor space for rotations, with unit vectors along the axis being χ_+ and χ_- . A representative point in the space undergoes a rotation through $\theta/2$ when the system it describes is rotated by θ .

$$|a_+|^2 + |a_-|^2 = 1$$

The points describing rotations therefore lie on a circle in spinor space, as shown in Figure 3.7.

The correspondence between rotation of a spin-1/2 system in configuration space and the trajectory of its coordinates in spinor space is to be such that a representative point in the space undergoes a rotation through $\theta/2$ when the system it describes is rotated by θ . In particular, the spinor-space coordinates change sign when $\theta = 2\pi$ and return to their origin values only under a double-angle rotation of $\theta = 4\pi$. Given this mapping from configuration space to spinor space, we are now ready to discuss angular momentum properties.

Angular Momentum Operators in Spinor Representation. We define partial differential operators in spinor space (χ_+, χ_-) just as we would for conventional variables such as (x, y) . Namely, we write

$$\partial_+ \equiv \frac{\partial}{\partial \chi_+} \quad \partial_- \equiv \frac{\partial}{\partial \chi_-} \quad (3.48)$$

and these operators have the usual differentiation properties. For spherical basis angular momentum operators we make the association

$$J_{+1} = \chi_+ \partial_- \quad J_0 = \frac{1}{2}(\chi_+ \partial_+ - \chi_- \partial_-) \quad J_{-1} = \chi_- \partial_+ \quad (3.49)$$

It is readily shown (as Problem 3.7 suggests you try) that these are indeed angular momentum operators because they satisfy the commutation rules (3.6).

They also have appropriate behavior with respect to χ_+ and χ_- , namely

$$J_{\pm 1}\chi_{\mp} = \chi_{\pm} \quad J_0\chi_{\pm} = J_z\chi_{\pm} = \pm\frac{1}{2}\chi_{\pm} \quad (3.50)$$

Note that a linear combination of χ_+ and χ_- , as shown in Figure 3.7, is usually not an eigenstate of J_z .

The above developments provide the starting point for the derivations in Section 4.3.3 (spinor-space representations of angular momentum eigenstates), Section 6.2.3 (constructing rotation matrices), and Section 7.3.1 (angular momentum coupling coefficients).

3.4 ANGULAR MOMENTUM EIGENVALUES AND MATRIX ELEMENTS

Thus far in this chapter we have derived the angular momentum operators and their commutation properties (Section 3.1), and we have found representations of these operators in terms of orbital angular momentum (Section 3.2), Pauli matrices (Sections 3.3.1, 3.3.2), and spinors (Section 3.3.4). Our goal in this section is to find general expressions for the eigenvalues and matrix elements of these operators.

Since we aim to provide general results, the derivations are elegant, making use of raising and lower operators (Section 2.2.4). Once the algebra is well under control, we show in Section 3.4.4 the operator matrices for $j = 1/2, 1$, and $3/2$. Finally in this section, we introduce in Section 3.4.5 the distinction between two descriptions of angular momentum, one as a geometrical quantity related to rotational symmetry and the other as a dynamical quantity related to mechanical motion.

3.4.1 Eigenvalues of \mathbf{J}^2 and J_z ; Irreducibility

Given the commutator relations (3.6), our task is now to find appropriate eigenvalues. We have nearly seventy years of hindsight to guide us, since the first quantum mechanics paper on angular momentum by Bohr, Heisenberg, and Jordan [Bor26] derives the general result. We take, however, a slightly different track, using the ladder-operator technology built up in Section 2.2.4.

Eigenvalues of \mathbf{J}^2 and J_z . We begin by determining eigenvalues. Consider as the Hermitian operator $P = J_z$. Thus, analogously to (2.46), we have

$$J_z|\lambda\mu\rangle = \mu|\lambda\mu\rangle \quad (3.51)$$

where $n \rightarrow \lambda\mu$, anticipating that we will have two labels for each eigenstate. (It is conventional, if there is no ambiguity, *not* to separate the labels by a comma.) Since we have the commutator relation $J_z = -i[J_x, J_y]$, it is natural to make the identifications $\alpha = J_x$, and $\beta = J_y$, so that the analogue of (2.50) has $a = 0$, $b = -1$, $c = 0$.

We then have the following translations from general ladder operators to angular momentum ladder operators:

$$\eta_{\pm} \rightarrow J_{\pm 1} = (J_x \pm iJ_y) \quad (3.52)$$

where the antisymmetric and symmetric combinations become

$$\begin{aligned} A = -[\alpha, \beta] &\rightarrow i[J_x, J_y] = -J_z \\ S = \alpha^2 + \beta^2 &\rightarrow J_x^2 + J_y^2 = \mathbf{J}^2 - J_z^2 \end{aligned} \quad (3.53)$$

respectively. We know from (2.59)–(2.61) the general relations satisfied by the eigenvalues of A and B , which are the a_k and s_k . We have therefore, through (3.51) and the first equation in (3.53), the eigenvalue equation for μ .

Rather than seeking the analogue of the eigenvalue equation for S , we seek that of $S^2 + A^2$, namely \mathbf{J}^2 . Write this as

$$\mathbf{J}^2|\lambda\mu\rangle = \lambda|\lambda\mu\rangle \quad (3.54)$$

Thus, the eigenvalue translation is $a_k = -\mu_k$, $s_k = \lambda - \mu_k^2$. Here the subscript k serves to distinguish eigenvectors that are degenerate with respect to μ , for example, by being associated with different values of λ . By inserting these results into condition (2.59), we have that $\lambda \geq \mu_k^2$, $\lambda \geq \mu_k(\mu_k \pm 1)$, while the compatibility condition (2.60) requires that $\lambda - \mu_{k+1}^2 - (\lambda - \mu_k^2) = -\mu_{k+1} - \mu_k$. The uninteresting solution of this is $\mu_{k+1} = -\mu_k$, which corresponds merely to an opposite choice of sign of the A operator. The alternative solution, $\mu_{k+1} = \mu_k + 1$, shows that the eigenvalues of J_z go by unit steps, just as for the energy of the harmonic oscillator in Section 2.2.4. By iterating this solution, we obtain

$$\mu_k = \mu_0 + k \quad k = 0, 1, 2, \dots \quad (3.55)$$

From the limit conditions (2.61) we must have $\lambda = \mu_0(\mu_0 - 1)$, $\lambda = \mu_N(\mu_N - 1)$, in which μ_0 and μ_N are related by (3.55) with $k = N$. Putting this all together and solving for λ and μ_0 (as Problem 3.9 suggests you do), we find that

$$\lambda = j(j+1) \quad (3.56)$$

where $j = N/2$ is a non-negative half integer, such as 0, 1/2, 1, Since giving j gives λ , we might as well label the eigenstate by j as by λ . Now, solving for μ_0 and μ_N in terms of λ , we find that

$$\mu_0 = -j \quad \mu_N = j \quad (3.57)$$

so that there are $2j + 1$ values of μ for each j , so μ is conventionally relabeled as m , standing for *magnetic substate*.

Let us summarize the eigenvalue properties that we have determined. Expressed algebraically, we have the eigenvalue equations for \mathbf{J}^2 and J_z :

$$\begin{aligned} \mathbf{J}^2|jm\rangle &= j(j+1)|jm\rangle & j &= 0, 1/2, 1, \dots \\ J_z|jm\rangle &= m|jm\rangle & m &= -j, -j+1, \dots, j-1, j \end{aligned} \quad (3.58)$$

The general ladder operators from Section 2.2.4 now can be displayed for the angular momentum operators, as in Figure 3.8.

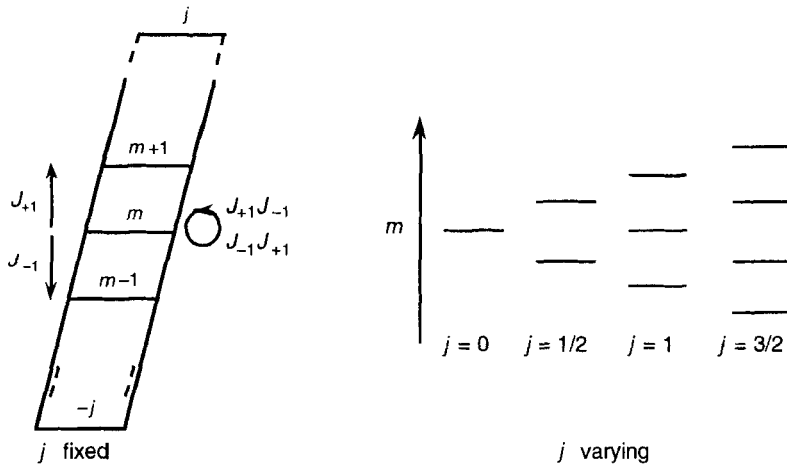


FIGURE 3.8 Angular momentum ladder operators, J_{+1} (raising) and J_{-1} (lowering), having a lower bound for given j of $m = -j$ and an upper bound of $m = j$. When the operators are applied in succession, one returns to the same state. The right side shows how the spectrum of m values changes as j increases. The value of j has no upper bound unless m is restricted.

For a given value of j there are $2j + 1$ equally spaced rungs on the ladder, as shown on the left-hand side of Figure 3.8. On the other hand, if we choose a given value of m , there is an indefinite number of j values with which it is associated, as the right-hand side of Figure 3.8 shows. This explains why an extra label, k , was made for μ below (3.54).

Irreducibility. We introduce the idea of irreducibility in Section 2.5.5 in the context of block-diagonal matrix representations of groups. The operator eigenvalues we have just determined for \mathbf{J}^2 and J_z immediately produce irreducible representations of infinitesimal rotations if the matrix elements are taken between angular momentum eigenstates, $|jm\rangle$. To see this, note that neither \mathbf{J}^2 nor J_z changes the value of j , so the matrices will be block diagonal in j , as sketched in Figure 3.9.

j/j'	0	1/2	1	3/2	...
0	[0, 0]	[0]	[0]	[0]	[0]
1/2	[0]	[1/2, 1/2]	[0]	[0]	[0]
1	[0]	[0]	[1, 1]	[0]	[0]
3/2	[0]	[0]	[0]	[3/2, 3/2]	[0]
⋮	[0]	[0]	[0]	[0]	...

FIGURE 3.9 Schematic of the block-diagonal (irreducible) representations for angular momentum, analogous to (2.85) for arbitrary group representations. The notation [0] denotes matrices of varying dimensions in which all the elements are zero.

Given the irreducibility property, we can handle each j separately when discussing eigenstates, providing a great simplification that we exploit in the following.

3.4.2 Matrix Elements in the Spherical Basis

We first obtain matrix elements of the remaining angular momentum operator components in the spherical basis, $J_{\pm 1}$, then convert these to the Cartesian basis in the next subsection. By using the identity that follows from definition (3.9) of the ladder operators in terms of J_x and J_y , namely

$$J_{\pm 1}J_{\mp 1} = (\mathbf{J}^2 - J_z^2 \pm J_z) \tag{3.59}$$

The matrix of the product of these ladder operators is diagonal in both m and j , since one operator changes the m value by unity and the other changes the m value in the other direction by unity. Let us write

$$J_{\pm 1}|jm\rangle = \Gamma_{\pm}(jm)|jm \pm 1\rangle \tag{3.60}$$

in which the Γ_{\pm} values are to be found. We then have

$$\begin{aligned} J_{\pm 1}J_{\mp 1}|jm\rangle &= \Gamma_{\pm}(jm \mp 1)\Gamma_{\mp}(jm)|jm\rangle \\ &= [j(j+1) - m^2 \pm m]|jm\rangle \end{aligned} \tag{3.61}$$

If we assume that the Γ_{\pm} values are positive, which amounts to choosing a convention for the relative phases of eigenvectors differing by unity in their m values, we can readily show that consistent solutions for the Γ_{\pm} values are

$$\begin{aligned}\Gamma_{\pm}(jm) &= \sqrt{j(j+1) - m(m \pm 1)} \\ &= \sqrt{(j \mp m)(j \pm m + 1)}\end{aligned}\quad (3.62)$$

The matrix elements of the angular momentum ladder operators $J_{\pm 1}$ can therefore be expressed as

$$\begin{aligned}\langle jm|J_{\pm 1}|j'm'\rangle &= \Gamma_{\pm}(jm')\delta_{m,m' \pm 1}\delta_{j,j'} \\ &= \sqrt{j(j+1) - m'(m' \pm 1)}\delta_{m,m' \pm 1}\delta_{j,j'} \\ &= \sqrt{(j \mp m')(j \pm m' + 1)}\delta_{m,m' \pm 1}\delta_{j,j'} \\ &= \sqrt{(j \pm m)(j \mp m + 1)}\delta_{m,m' \pm 1}\delta_{j,j'}\end{aligned}\quad (3.63)$$

One way to check that the signs in (3.63) are correct—and to recall the formulas—is to note that the matrix elements of J_{+1} must be zero if $m' \geq j$ and those of J_{-1} must vanish if $m' \leq -j$, which checks out the third equality sign in (3.63). Similar considerations hold for J_{-1} and J_{+1} in relation to m , according to the last equality.

3.4.3 Matrix Elements in the Cartesian Basis

Although the ladder-operator approach has just provided a quick derivation of angular momentum matrix elements in the spherical basis, we would often like to obtain the matrix elements of the Cartesian components of \mathbf{J} . This is straightforward, since we can immediately use (3.9). Because both J_x and J_y are linear combinations of J_{+1} and J_{-1} , we get matrix elements which contain both raising and lowering of the m values by unity. Thus, we have for the matrix elements in the Cartesian basis the x -component elements

$$\begin{aligned}\langle jm|J_x|j'm'\rangle \\ = \frac{1}{2}\left[\sqrt{(j+m)(j-m+1)}\delta_{m,m'+1} + \sqrt{(j-m)(j+m+1)}\delta_{m,m'-1}\right]\delta_{j,j'}\end{aligned}\quad (3.64)$$

which are explicitly real. For the y components the values are purely imaginary:

$$\begin{aligned}\langle jm|J_y|j'm'\rangle \\ = \frac{i}{2}\left[-\sqrt{(j+m)(j-m+1)}\delta_{m,m'+1} + \sqrt{(j-m)(j+m+1)}\delta_{m,m'-1}\right]\delta_{j,j'}\end{aligned}\quad (3.65)$$

Finally, because of our choice of quantization axis—along the z direction—we have the especially simple, diagonal, representation for the z component, namely

$$\langle jm|J_z|j'm'\rangle = m\delta_{m,m'}\delta_{j,j'} \tag{3.66}$$

It is straightforward to verify that the angular momentum representation matrices are Hermitian.

Interpreting Matrix Elements. It is important to note that these formulas for matrix elements arise *only* from the commutator properties of the \mathbf{J} operators, (3.6), and therefore hold for *any* system described by the same Lie algebra of operators. For example, in nuclear and particle physics when considering charge-independent interactions one introduces isospin operators with the same operator algebra as the rotation operators. Such isospin operators must therefore have the same matrix elements (3.64)–(3.66). What will differ for different operators (such as charge or rotations) is the *space* in which the operators act and the *interpretation* of the eigenvalues j and m .

For example, isospin operators act in a “charge space” in which the “z axis” eigenvalue m is used to indicate the electric charge of the system. In the quark model of subatomic physics, charge itself is generalized to other quantum numbers, which, like total electric charge, are conserved in interactions. Similarities and differences are summarized in Figure 3.10.

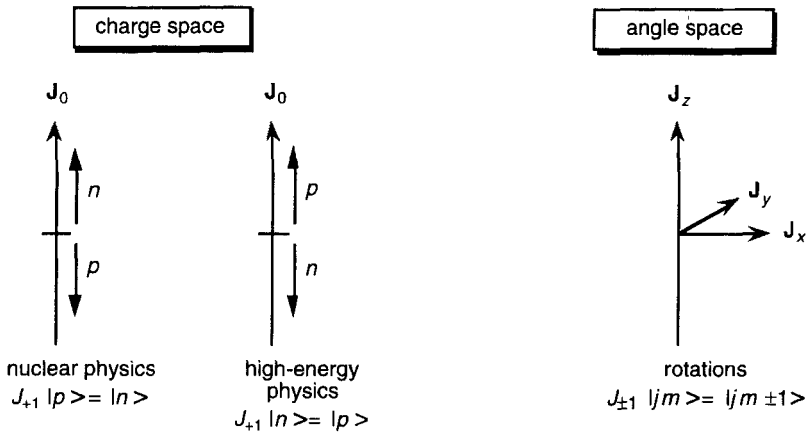


FIGURE 3.10 Charge space (isospin) and angle space (rotations) both use the same commutator algebra, but the interpretation of quantum numbers is different.

Within a given space, such as the charge or angle space in Figure 3.10, there may be differences of interpretation. For example, in nuclear physics, where nuclei generally have an excess of neutrons, the isospin quantum number m is interpreted as $+1/2$ for neutrons, $-1/2$ for protons. In high-energy physics, which often uses hydrogen targets, the opposite convention is used. Another difference of interpretation between the two spaces is the following. In angle space one can rotate the sys-

tem and one gets a superposition of m projections, as we calculate in detail in Chapter 6. In charge space the analogue of an angle, which could give superposition of charges, is not used. Thus, although there is a common mathematics (commutator algebra), there is a distinct physical application.

3.4.4 Operator Matrices for $j = 1/2, 1,$ and $3/2$

Many physical systems that we investigate have a high degree of symmetry—which is perhaps why we select them for investigation. Therefore, associated with their properties are small values of the total angular momentum number j , and therefore small values of the projection number m .

Operator Matrices. We write out in Table 3.1 the explicit operator matrices for $j = 1/2, 1,$ and $3/2$, which are the angular momentum matrices most commonly required in direct manipulations. Notice that each matrix is Hermitian, so in quantum mechanics it may represent an observable, as we discuss in Chapter 5.

TABLE 3.1 Operator matrices for $j = 1/2, 1,$ and $3/2$ in the Cartesian basis.

j	J_x	J_y	J_z
$1/2$	$\begin{bmatrix} 0 & 1/2 \\ 1/2 & 0 \end{bmatrix}$	$\begin{bmatrix} 0 & -i/2 \\ i/2 & 0 \end{bmatrix}$	$\begin{bmatrix} 1/2 & 0 \\ 0 & -1/2 \end{bmatrix}$
1	$\frac{1}{\sqrt{2}} \begin{bmatrix} 0 & 1 & 0 \\ 1 & 0 & 1 \\ 0 & 1 & 0 \end{bmatrix}$	$\frac{1}{\sqrt{2}} \begin{bmatrix} 0 & -i & 0 \\ i & 0 & -i \\ 0 & i & 0 \end{bmatrix}$	$\begin{bmatrix} 1 & 0 & 0 \\ 0 & 0 & 0 \\ 0 & 0 & -1 \end{bmatrix}$
$3/2$	$\begin{bmatrix} 0 & \sqrt{3}/2 & 0 & 0 \\ \sqrt{3}/2 & 0 & 1 & 0 \\ 0 & 1 & 0 & \sqrt{3}/2 \\ 0 & 0 & \sqrt{3}/2 & 0 \end{bmatrix}$	$\begin{bmatrix} 0 & -i\sqrt{3}/2 & 0 & 0 \\ i\sqrt{3}/2 & 0 & -i & 0 \\ 0 & i & 0 & -i\sqrt{3}/2 \\ 0 & 0 & i\sqrt{3}/2 & 0 \end{bmatrix}$	$\begin{bmatrix} 3/2 & 0 & 0 & 0 \\ 0 & 1/2 & 0 & 0 \\ 0 & 0 & -1/2 & 0 \\ 0 & 0 & 0 & -3/2 \end{bmatrix}$

Angular Momentum Eigenvectors. Matrix eigenvectors of J_z that satisfy $J_z \chi_m = m \chi_m$ are readily written down analogously to the treatment for $j = 1/2$ in Section 3.3.2. First, in order to be multiplied by a matrix having $(2j+1)$ columns, they must have $(2j+1)$ rows and there is no need to have more than one column. This is shown in Table 3.2.

In the column-vector form of the J_z eigenvectors shown in Table 3.2, note the alternation of the matrices according as $2j$ is an even or an odd integer. The two sets of representations appear distinct, so they are in different columns.

TABLE 3.2 Matrix eigenvectors χ_m for spins $j = 0, 1/2, 1,$ and $3/2$, having m projections as indicated in the columns.

j	m	$3/2$	1	$1/2$	0	$-1/2$	-1	$-3/2$
0					[1]			
1/2				$\begin{bmatrix} 1 \\ 0 \end{bmatrix}$		$\begin{bmatrix} 0 \\ 1 \end{bmatrix}$		
1			$\begin{bmatrix} 1 \\ 0 \\ 0 \end{bmatrix}$		$\begin{bmatrix} 0 \\ 1 \\ 0 \end{bmatrix}$		$\begin{bmatrix} 0 \\ 0 \\ 1 \end{bmatrix}$	
3/2		$\begin{bmatrix} 1 \\ 0 \\ 0 \\ 0 \end{bmatrix}$		$\begin{bmatrix} 0 \\ 1 \\ 0 \\ 0 \end{bmatrix}$		$\begin{bmatrix} 0 \\ 0 \\ 1 \\ 0 \end{bmatrix}$		$\begin{bmatrix} 0 \\ 0 \\ 0 \\ 1 \end{bmatrix}$

Once an m value is chosen, its matching eigenvector must have a nonzero element only in row m , in order to satisfy the above eigenvalue equation. Therefore, $(\chi_m)_{m'} = \delta_{m,m'}$, in which we have chosen that the norm of the eigenvector be unity. An alternative choice of normalization, which is more cumbersome than helpful, is to apply a factor $1/\sqrt{2j+1}$, producing a scalar product of unity over *all* the m values belonging to a given j .

3.4.5 Angular Momentum: Geometrical and Dynamical

As has become apparent throughout the previous chapters, the meaning of “angular momentum” depends upon the context in which it is used, since the term may refer either to the rotational symmetry properties of a system or to its dynamical (mechanical) angular momentum. This dual meaning gives rise to ambiguity—for example in the title and subtitle of this book. We give a preliminary discussion here, with a more complete treatment in Section 5.1 after we study angular momentum eigenstates in Chapter 4.

Geometrical Angular Momentum. Consider the rotational symmetry of an object, defined for simplicity of example in terms of a polar angle θ as the radius of its surface:

$$R(\theta) = \bar{R} \sum_{\ell=0} \beta_{\ell} P_{\ell}(\cos \theta) \quad \beta_0 = 1, \quad \beta_1 = 0 \quad (3.67)$$

in which \bar{R} is the average value of the radius, and nonzero values of the shape parameters β_ℓ for $\ell > 1$ describe deviations from a circular cross section when weighted by the Legendre polynomials $P_\ell(\cos\theta)$. (Problem 3.10 invites you to prove these assertions, to explain why we choose $\beta_1 = 0$, and to draw some of these surfaces.) Throughout the cosmos, from atoms to galaxies, the value of ℓ in (3.67) takes on only *small* values, typically only $\ell = 0, 2, 3, 4$, for many systems of interest. The ℓ values that appear in such descriptions and their associated functions, such as $P_\ell(\cos\theta)$, we call geometrical angular momentum.





System	Geometrical angular momentum $R(\theta) = \bar{R} \sum_{\ell=0} \beta_\ell P_\ell(\cos\theta)$	Dynamical angular momentum, $L_c = \ell_c \hbar$
Electrons in an atom 	$\ell = 0, 1, 2, \dots$	$\ell_c = 0, 1, 2, \dots$
Spinning ball bearing 	$\ell = 0$	$\ell_c \gg 1$
Earth rotating in space 	$\ell = 0, 2, \dots$	$\ell_c \gg 1$
Galaxy rotating about its center 	$\ell = 0, 2, \dots$	$\ell_c \gg 1$

FIGURE 3.11 Geometrical and dynamical angular momenta for various systems. Although the angular momentum ℓ_c (in \hbar units) ranges over many orders of magnitude, the degree of rotational symmetry ℓ (geometrical angular momentum) is about the same in each system.

Dynamical Angular Momentum. Consider now angular momentum defined as in classical mechanics, $\mathbf{L}_c = \mathbf{r} \times \mathbf{p}$, and write for its magnitude $L_c = \ell_c \hbar$, in which ℓ_c is a pure number because \hbar has units of angular momentum. We call L_c dynamical angular momentum. Throughout the cosmos, from atoms to galaxies, ℓ_c has a very large (even astronomical) range of values. This contrast between the values of ℓ_c for dynamical angular momentum and of ℓ for geometrical angular momentum is what leads to ambiguity and confusion.

Notice in Figure 3.11 that only for the example of electrons in an atom do the values of ℓ and ℓ_c approximately coincide for geometrical and dynamical angular momentum. A similar coincidence occurs for atomic nuclei. Historically, the use of rotational symmetry techniques was developed extensively in the 1920s and applied to the new quantum mechanics, especially to atomic and nuclear physics, as summarized in Section 5.5. Therefore, as discussed in more detail in Chapter 5, there is still a tendency to confuse methods of analysis of physical systems based on rotational symmetry with quantum-mechanical properties of these systems. Fortunately, the truth is otherwise, and almost all of the developments in this book are applicable to any physical system, whether it be large or small. This is emphasized by the agreement between the values of ℓ in the center column of Figure 3.11.

3.5 REFERENCE FRAMES: SPIN AND ORBITAL ANGULAR MOMENTA

The purpose of this section is to show that the distinction between total angular momentum, spin, and orbital angular momentum depends upon the choice of reference frames.

Small Rotations and Internal Degrees of Freedom. Consider what happens when we rotate a system through a small angle ε about the axis $i = x, y, \text{ or } z$. The center of the system is initially at \mathbf{r} with respect to the point about which the rotation is made and a representative point in the system has an internal degree of freedom ξ , which may be—but need not be—a spatial coordinate. Suppose that the system is described by a function $f(\mathbf{r}, \xi)$. We now extend the analysis made for orbital angular momentum in Section 3.2.1. For a small rotation under the action of the total angular momentum operator J_i this function is changed into $f_\varepsilon(\mathbf{r}_\varepsilon, \xi_\varepsilon)$, given by

$$f_\varepsilon(\mathbf{r}, \xi_\varepsilon) = U(\varepsilon, \hat{\mathbf{n}}_i) f(\mathbf{r}, \xi) \approx (1 - i\varepsilon J_i) f(\mathbf{r}, \xi) \quad (3.68)$$

The orbital angular momentum operator L_i also changes f , as in (3.16), so that it becomes

$$f_\varepsilon(\mathbf{r}, \xi) \approx (1 - i\varepsilon L_i) f(\mathbf{r}, \xi) \quad (3.69)$$

We can now subtract this expression from (3.68) to find the difference between the actions of operators J_i and L_i , namely

$$f_\epsilon(\mathbf{r}, \xi_\epsilon) - f_\epsilon(\mathbf{r}, \xi) \approx -i\epsilon(J_i - L_i)f(\mathbf{r}, \xi) \equiv -i\epsilon S_i f(\mathbf{r}, \xi) \tag{3.70}$$

in which the last relation defines the spin operator component S_i . Considering each of the three equivalent components $i = x, y, z$, we can write for the definition of the *spin operator* \mathbf{S}

$$\mathbf{S} \equiv \mathbf{J} - \mathbf{L} \tag{3.71}$$

The effect of the spin operator \mathbf{S} , also called the intrinsic angular momentum or *intrinsic spin*, is just the difference between the effect of the total, \mathbf{J} , and the orbital component, \mathbf{L} . One calls the corresponding total angular momentum number the *intrinsic spin* (or sometimes just *spin*), usually denoted by s . According to (3.70), if the internal degrees of freedom are unaltered by the rotation, then $\xi_\epsilon = \xi$, so that each component of the \mathbf{S} operator when acting on f produces zero. Then the total angular momentum number associated with \mathbf{S} will be zero. An example of this is for ξ to be internal spatial coordinates of a spherically symmetric object.

Planetary Rings and Intrinsic Spin. To make the discussion more concrete, consider the description of a planet with a ring system, such as Saturn, as sketched in Figure 3.12. The motion of the center of mass of the planet about the sun is described by a scalar function and therefore, according to the discussion in Section 3.2, it is described in terms of the orbital angular momentum operator \mathbf{L} . If, however, the planet is rotated about some internal axis, then the ring system will also be rotated. The total effect of rotating the system of planet-plus-rings is therefore described by operator \mathbf{J} . If it were convenient, we might first describe rotation of the planet center of mass, then make a separate calculation for the effect of rotation of the rings.



FIGURE 3.12 The difference between total angular momentum and orbital angular momentum is demonstrated by the differing effects of rotation through a small angle ϵ of a function f describing a system that has some internal degrees of freedom, such as the rings around a planet. The planet orbital angular momentum will have $\ell > 0$ if the orbit is elliptical, as shown.

For the ring system of a planet, the ξ will probably be coordinates of the ring elements and points on the planet surface (such as latitude and longitude). The in-

trinsic angular momentum will then be a composite of orbital angular momenta from bodies in the rings, plus any rotation of the planet about its poles. A planet with rings (or moons, if they are considered intrinsic to the planet) will therefore usually have nonzero intrinsic spin.

Angular Momentum Coupling. The division of the total angular momentum into orbital and spin components is not very useful—either conceptually or technically—unless \mathbf{r} and the “coordinates” ξ are independent. If this can be assured, usually as part of a dynamical model of the system, then the \mathbf{S} and \mathbf{L} operators will commute.

Under the assumption of commuting operators, one can develop an algebra in which the behavior of the subsystems under \mathbf{S} and \mathbf{L} separately is calculated, then the effect of $\mathbf{J} = \mathbf{L} + \mathbf{S}$ is derived. This “angular momentum coupling,” calculated by using Clebsch-Gordan and Racah algebra, preoccupies us in Chapters 7 and 9.

Spin in Quantal Systems. In systems described by quantum mechanics, such as atoms, nuclei, nucleons, and nucleon constituents, a complete dynamical description of the origin of the spin degrees of freedom has not yet been achieved. That is, we do not usually know the appropriate internal degrees of freedom ξ . By experiments that involve rotations, however, one can determine the quantum numbers appropriate to such internal degrees of freedom. For examples, electrons are found by experiment to have $s = 1/2$.

For subatomic systems, understanding of the dynamics is hindered by the need to describe quantal systems in a relativistically covariant framework. The extension of our analysis to a covariant analysis is given in Section I.3k of Roman’s book on elementary particles [Rom61]. Dirac’s equation for electrons and positrons is the most successful covariant quantum-mechanical equation, as described, for example, in Chapter 15 of Landau’s text [Lan90]. The problem of finding a covariant quantal description of particles of arbitrary spin was tackled by Lubanski [Lub42]. If one uses helicity (Section 1.2.1) to characterize spin states, the formalism of Jacob and Wick [Jac59] is straightforward to apply. A summary of density-matrix methods for relativistic particles is given in Section 7.7d of Biedenharn and Louck [Bie81a].

In Section 4.2 we derive in detail the unit spin associated with any vector field, and in Section 4.3 we revisit the interpretation of spin when constructing spin eigenstates.

PROBLEMS ON ROTATIONAL INVARIANCE AND ANGULAR MOMENTUM

3.1 To obtain the commutation relations of the \mathbf{J} operators, carry out the substitutions for the small-angle expansions (3.2) in (3.3).

- (a) Show that if the expansions are carried out only through terms *linear* in the angles, then the rotations commute.
- (b) Carry the expansions through terms bilinear in angles in order to verify (3.4).
- (c) Take the limit process as described in the text. Check in detail that higher terms

in angles do not contribute.

3.2 For the angular momentum operators in the spherical basis, $J_{\pm 1}$ and J_0 , derive the commutation relations (3.11) and expression (3.12) for the square of the total angular momentum operator.

3.3 To derive the orbital angular momentum operator component L_z , equate expressions (3.14) and (3.16), then use (3.15) to relate the two sets of coordinates. Now assume that ε is small enough that only terms linear in ε in the Taylor expansion of $f(x_{-\varepsilon}, y_{-\varepsilon}, z_{-\varepsilon})$ about $\mathbf{r} = (x, y, z)$ need be maintained. Thus show that in the limit $\varepsilon \rightarrow 0$, one obtains (3.17) for L_z .

3.4 Verify the correctness of the spherical-polar coordinate expression for the components of the orbital angular momentum operator \mathbf{L} as given by (3.24). The easiest way to do this is to take the given expressions and to express the angle partial derivatives in terms of Cartesian-coordinate partial derivatives. In doing so you will notice that this can be done except when $x = 0 = y$, that is, when $\theta = 0$ or $\theta = \pi$, the angles at which the polar coordinate system has a singularity.

3.5 Consider determination of the eigenvectors of the Pauli matrices.

(a) Multiply out the left-hand side of (3.38), then equate it to the right-hand side. Thereby show that the eigenvectors are as given by (3.39).

(b) Check the orthonormality relations of the Pauli matrix eigenvectors, as given by (3.40).

3.6 Consider the exponential power series of the Pauli matrices.

(a) For the z direction, σ_z , carry out the series expansion in detail, use the properties for even and odd powers to simplify the expansion, then identify the two remaining series of even and odd powers of $\gamma/2$ as power-series expansions of their cosine and sine. Thus verify (3.42) for the spin-1/2 rotation matrix.

(b) Make a similar analysis for σ_y in order to verify (3.44). To do this, show that

$$\sigma_y^{2m} = (-1)^m \mathbf{1}_2 \quad \sigma_y^{2m+1} = (-1)^m \begin{bmatrix} 0 & 1 \\ -1 & 0 \end{bmatrix} \quad (3.72)$$

then rearrange the series and collapse them to the cosine and sine functions given in (3.44).

(c) By calculating the product $\tilde{\mathbf{d}}^{1/2} \mathbf{d}$ show that the reduced rotation matrix $\mathbf{d}^{1/2}(\beta)$, (3.44), is unitary.

3.7 Consider the spinor-space representation of angular momentum.

(a) Use the definitions (3.49) for the angular momentum operators in this space to show that they satisfy the basic commutation relations (3.6).

(b) Verify the properties of these operators with respect to the states χ_+ and χ_- , as given in (3.50).

3.8 Verify that the angular momentum matrices in the Cartesian basis are Hermitian by considering the symmetry of the matrix-element formulas (3.52)–(3.58).

3.9 In the algebra of the ladder operators for angular momentum verify all steps between (3.52) and (3.58) that are used to determine the eigenvalue spectrum.

3.10^M Given the expansion of a surface in terms of the shape parameters β_ℓ in (3.67), use elementary properties of Legendre polynomials to prove the correctness of the following assertions:

- (a) The average value of $R(\theta)$ when integrated over θ from 0 to π with weight factor $\sin\theta d\theta$ is \bar{R} .
- (b) The $\ell = 1$ shape parameter describes only a translation of the whole surface, not a change in its intrinsic shape. Recall that $P_1(\cos\theta) = \cos\theta$.
- (c) Calculate and sketch some surfaces described by (3.67) for various values of the shape parameters; magnitudes of about 0.2 and parameters of both signs provide interesting results. *Mathematica* may be useful for this.



Chapter 4

ANGULAR MOMENTUM EIGENSTATES

In Chapter 3 we studied angular momentum operators, their eigenvalues, and their matrix elements, but we ignored the eigenstates that also characterize physical systems having different rotational symmetry. In this chapter we replace ignorance by enlightenment.

Orbital angular momentum eigenstates—Legendre polynomials, Legendre functions, and spherical harmonics—are the topics of Section 4.1. We discuss not only their analytical properties but also provide many visualizations, including polar diagrams for Legendre functions and three-dimensional views for spherical harmonics. If you have access to *Mathematica*, you can produce such graphics by running the notebooks given in Appendix I. Section 4.2 has a treatment of spherical-basis vectors, then uses these to discuss the angular momentum intrinsic to a vector field such as in electromagnetism.

Section 4.3 is devoted to spin eigenstates, their interpretation, and various representations, including spinor-space representations used to determine rotation matrices (Section 6.2) and the coefficients for combining two angular momentum eigenstates (Section 7.2). The relation between the time-reversal operator and spin are also considered in Section 4.3.

4.1 ORBITAL EIGENSTATES AND SPHERICAL HARMONICS

We begin this section by considering the solution of a problem that might not seem immediately relevant to rotational symmetry, namely, the solutions of the Laplace differential equation $\nabla^2 u(\mathbf{r}) = 0$. If this equation is expressed in spherical polar coordinates (Section 3.2.2), we can solve it to obtain solid harmonics and spherical harmonics. The Legendre polynomials are the simplest type of solution in this

coordinate system. The connections between the functions for orbital eigenstates that are discussed in this section are indicated schematically in Figure 4.1.

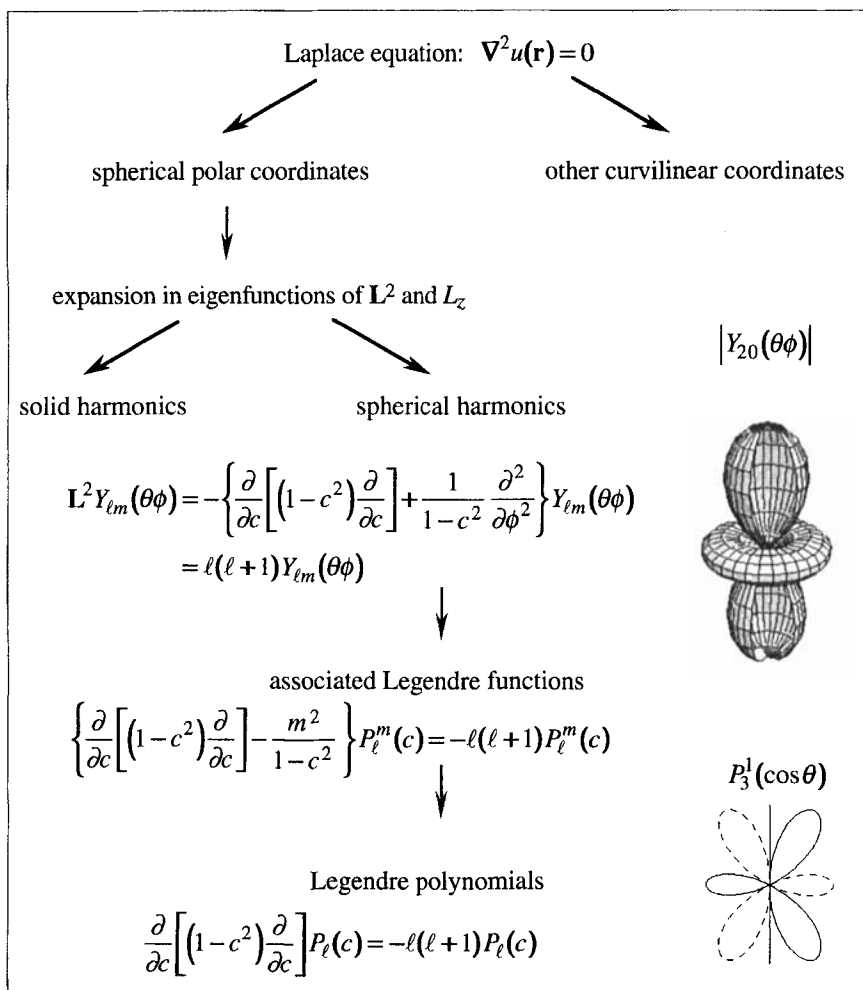


FIGURE 4.1 Connections between functions for orbital eigenstates. Separation of the Laplace equation in spherical polar coordinates and expansion in eigenfunctions of L^2 and L_z leads to the spherical harmonics, associated Legendre functions, and Legendre polynomials. The abbreviation $c = \cos\theta$ is used in each equation. Shown at right in polar-diagram views are the modulus of a spherical harmonic and an associated Legendre function.

We see that expansion in spherical polar coordinates leads to spherical harmonics, whereas other curvilinear coordinate systems—as in Table 1.2 of Wong [Won91], for example—lead to generalizations such as the ellipsoidal harmonics mentioned in Section 4.1.4. On the unit sphere, $r = 1$, the eigenfunctions of L^2

(whose equation is shown) and of L_z are spherical harmonics. Solid harmonics (Section 4.1.4) are similar to spherical harmonics but are evaluated at any \mathbf{r} .

Our development proceeds in inverse order to the scheme shown in Figure 4.1, from the simplest functions of the single parameter θ (Legendre functions), through the functions of θ and ϕ on the unit sphere that are angular momentum eigenfunctions (spherical harmonics), to variants that are solutions of the Laplace equation in spherical polar coordinates (solid harmonics) and other generalizations. We go in this order, under the assumption that you are most familiar with the simplest functions— $P_\ell(\cos\theta)$ and $e^{im\phi}$ —with just one parameter and one argument. Your experience with a function that is more complicated—such as $Y_{\ell m}(\theta\phi)$ with two parameters and two arguments—is likely to have been more limited and less agreeable.

Books on mathematical physics usually contain extensive treatments of the solution of the Laplace equation, such as in Section 4.12 of Wong's introductory text [Won91]. Older mathematics books, such as Hobson's classic [Hob31], usually contain extensive material. You should refer to such books for the analysis details of the following.

4.1.1 Legendre Functions and Their Properties

Here we summarize algebraic properties of the Legendre functions that are relevant to studying rotational symmetries, while in Section 4.1.2 we show various ways to visualize these functions.

Legendre Polynomials. The Legendre polynomial of order ℓ , $P_\ell(\cos\theta)$, is most often defined as the solution that is regular at the poles $\theta = 0, \pi$ of the differential equation for $\ell \geq 0$ written as

$$\frac{\partial}{\partial c} \left[(1-c^2) \frac{\partial}{\partial c} \right] P_\ell(c) = -\ell(\ell+1) P_\ell(c) \quad c = \cos\theta \quad (4.1)$$

where, as conventional in spherical polar coordinates, the range of θ is 0 to π . The function $P_\ell(\cos\theta)$ is a polynomial in $\cos\theta$ of order ℓ and its normalization is

$$P_\ell(1) = 1 \quad (4.2)$$

Consequently, these polynomials are *not* orthonormal, but satisfy the orthogonality condition

$$\int_0^\pi P_{\ell'}(\cos\theta) P_\ell(\cos\theta) \sin\theta \, d\theta = \frac{2\delta_{\ell'\ell}}{2\ell+1} \quad (4.3)$$

The parity property (Sections 1.2, 1.4.1) of Legendre polynomials is expressed by their symmetry under $\theta \rightarrow \pi - \theta$, so that $\cos\theta \rightarrow -\cos\theta$, namely

$$P_\ell(-\cos\theta) = (-1)^\ell P_\ell(\cos\theta) \quad (4.4)$$

Further discussion of analytical properties of Legendre polynomials is given in Section 5.2 of [Won91].

Associated Legendre Functions. The associated function, $P_\ell^m(\cos\theta)$, can be defined as the solution that is regular at the poles $\theta = 0, \pi$ of the differential equation for $\ell \geq 0, |m| \leq \ell$:

$$\left\{ \frac{\partial}{\partial c} \left[(1-c^2) \frac{\partial}{\partial c} \right] - \frac{m^2}{1-c^2} \right\} P_\ell^m(c) = -\ell(\ell+1) P_\ell^m(c) \quad c = \cos\theta \quad (4.5)$$

By comparing (4.1) and (4.5), we see that $P_\ell(\cos\theta)$ is just $P_\ell^0(\cos\theta)$, since they satisfy the same differential equations and their normalizations are suitably chosen. The function $P_\ell^m(\cos\theta)$ is a polynomial in $\cos\theta$ only when m is even, because when m is odd $P_\ell^m(\cos\theta)$ contains a factor $\sin\theta = \sqrt{1-\cos^2\theta}$. In spite of this fact, many authors mistakenly use the term “associated Legendre polynomial.”

The orthogonality property of associated Legendre functions is

$$\int_0^\pi P_{\ell'}^m(\cos\theta) P_\ell^m(\cos\theta) \sin\theta \, d\theta = \frac{2(\ell+m)! \delta_{\ell'\ell}}{(2\ell+1)(\ell-m)!} \quad (4.6)$$

of which (4.3) for $P_\ell(\cos\theta)$ is a special case. Note that there is no orthogonality property for two associated Legendre functions whose m values differ. Therefore, P_ℓ^m with $m \neq 0$ does not belong to the classical orthogonal polynomials.

At $\theta = 0$ ($\cos\theta = c = 1$) the function values are

$$P_\ell^m(1) = \delta_{m,0} \quad (4.7)$$

which is consistent with (4.2) for $m = 0$. The parity property of Legendre functions, of which (4.4) is a special case with $m = 0$, is

$$P_\ell^m(-\cos\theta) = (-1)^{\ell-m} P_\ell^m(\cos\theta) \quad (4.8)$$

Analytical properties of associated Legendre functions are discussed further in Section 5.6 of [Won91].

Formulas for Legendre Functions. In this and subsequent chapters we use the low-order Legendre functions for analytical and graphical examples. Therefore, it is useful to have a table of them at hand. As Problem 4.1 suggests, calculating the analytical expressions given in Table 4.1 is conveniently done by using built-in functions in *Mathematica*.

The first row of the table gives the Legendre polynomials for $\ell = 0 \dots 4$. The formulas illustrate properties (4.7) and (4.8), as well as showing that only for the

odd m values, 1 and 3, do the Legendre functions contain the overall factor $s = \sin\theta$, since even powers of s can be expressed as polynomials in $c = \cos\theta$ by $s^2 = 1 - c^2$.

TABLE 4.1 Legendre functions, $P_\ell^m(\cos\theta)$, in terms of $c = \cos\theta$ and $s = \sin\theta$.

$m \setminus \ell$	0	1	2	3	4
0	1	c	$-\frac{1}{2}(1-3c^2)$	$-\frac{1}{2}c(3-5c^2)$	$\frac{1}{8}(3-30c^2+35c^4)$
± 1		$\pm s$	$\pm 3cs$	$\mp \frac{3}{2}s(1-5c^2)$	$\mp \frac{5}{2}cs(3-7c^2)$
± 2			$3s^2$	$15cs^2$	$-\frac{15}{2}s^2(1-7c^2)$
± 3	$P_\ell^{-m}(\cos\theta) = (-1)^m P_\ell^{m}(\cos\theta)$ $P_\ell^m(-c) = (-1)^{\ell-m} P_\ell^m(c)$			$\pm 15s^3$	$\pm 105cs^3$
± 4					

For stretched $m = \ell$, it is straightforward to show that the Legendre function is

$$P_\ell^\ell(\cos\theta) = \frac{(2\ell)!}{2^\ell \ell!} \sin^\ell \theta \quad (4.9)$$

a property that is important for deriving spherical harmonics and that also holds for $\ell = 0$. The entries on the diagonal of Table 4.1 show these stretched- m values.

4.1.2 Displaying Legendre Functions; Polar Diagrams

We now show various ways to visualize angular momentum eigenstates as functions of angles, typically θ or (θ, ϕ) . There are several possibilities for displays, ranging from simple x - y plots of $P_\ell(\cos\theta)$ against θ for fixed ℓ to plots in three dimensions of $Y_{\ell m}(\theta, \phi)$ shown in polar coordinate form for various ℓ and corresponding allowed m values.

Conventional x - y plots are of limited usefulness in angular momentum studies, being convenient for examining purely analytical or numerical properties of functions. We therefore introduce polar diagram displays, in which angles appear in their actual positions and lengths of radius vectors indicate magnitudes of functions. Thus, there is a direct correspondence between angular location and function value. Our first visualizations are the simplest, then we gradually increase the complexity of functions and their representations.

Displaying Legendre Polynomials. Legendre polynomials are functions of two quantities—for our purposes the angle θ (which is continuous and appears only as $\cos\theta$) and the order of the polynomial, L , which is most often required at the integer values, $L = 0, 1, \dots$. It is therefore convenient to show the surface $P_L(\cos\theta)$ with θ and L as two axes, as in Figure 4.2. Because of the text-handling limitations in *Mathematica*, we temporarily use L instead of ℓ .

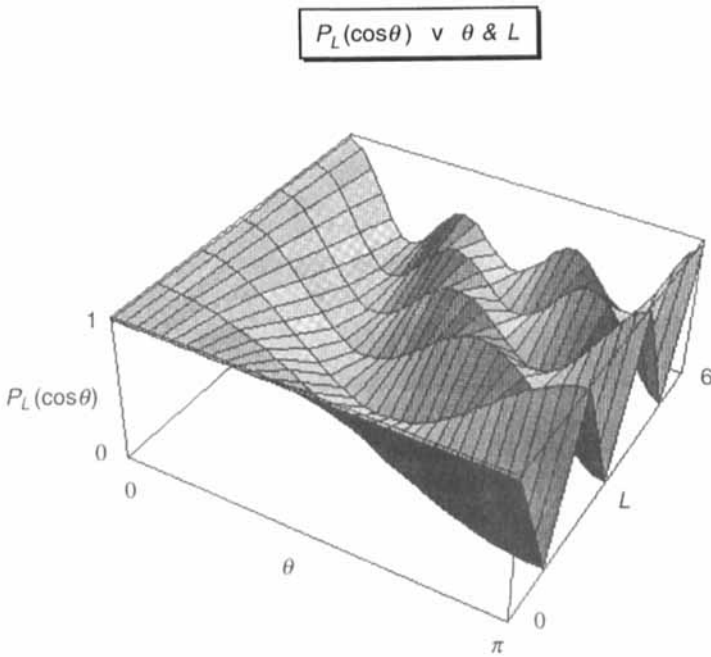


FIGURE 4.2 Legendre polynomials as a function of θ from 0 to π and for $L = 0, 1, \dots, 6$. (Adapted from *Mathematica* notebook PL.)

Note in Figure 4.2 that the standardization of the Legendre polynomial, (4.2), gives all Legendre polynomials the value unity at $\theta = 0$, as we see at the left edge of the surface. Also, since $P_L(-1) = (-1)^L$ because of the parity property (4.4), at $\theta = \pi$, the values alternate between +1 and -1 for even and odd (integer) L . As θ tends to π , the surface displayed in Figure 4.2 becomes less realistic because of this property. For $L = 0$, the isotropic function, a constant value of unity is obtained, as is seen along the front edge of the surface.

By taking cross sections through the surface in Figure 4.2, we may view P_L as a function of θ for fixed L (left panel in Figure 4.3) or as a function of L for fixed θ (right panel). The left panel shows the three zeros of P_3 , while the right panel illustrates the parity property of P_L , since the odd-parity functions (odd L) must vanish at the reflection-symmetry angle $\theta = \pi/2$.

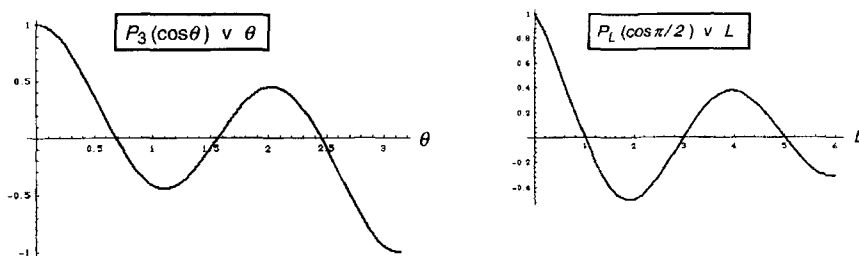


FIGURE 4.3 Legendre polynomials: The left-hand side shows $P_3(\cos\theta)$ and the right-hand side shows $P_L(\cos\pi/2) = P_L(0)$ for $L = 0$ to 6. In most applications the boundary conditions require that only the values at integer L be used. (Adapted from *Mathematica* notebook PL.)

Polar Diagrams. Having comprehended analytical properties of the Legendre polynomial, it is instructive to use polar diagram representations, which are useful for describing angular dependences. With functions that are more complicated—such as associated Legendre functions and spherical harmonics—polar diagrams greatly simplify their visualization. *Polar diagram* is the mathematical term, *radiation pattern* is the term used in physics, and *antenna pattern* is a common name in electrical engineering.

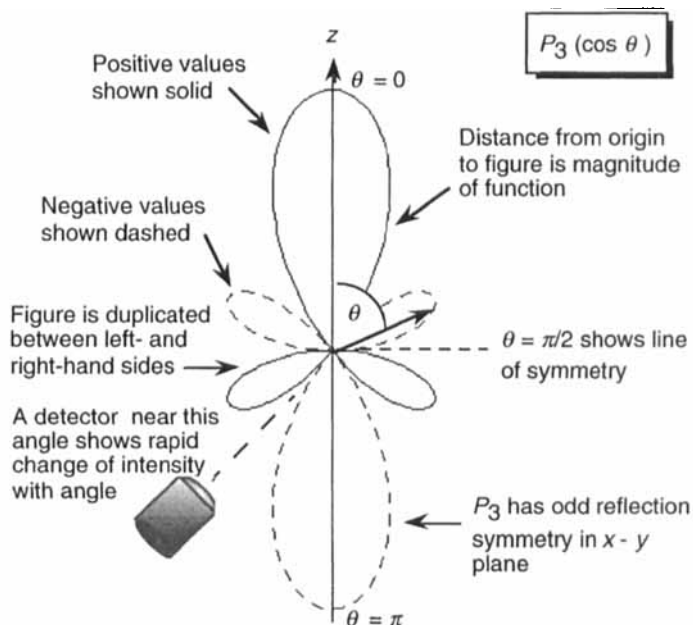


FIGURE 4.4 A polar diagram and its interpretation, displayed for the Legendre polynomial $P_3(\cos\theta)$. (Adapted from *Mathematica* notebook PLM.)

The polar diagram for $P_3(\cos\theta)$ shown with annotations in Figure 4.4 has its x - y plot representation the left-hand side of Figure 4.3. Throughout this book, polar diagrams are presented consistently in the style of Figure 4.4. Positive values are shown by solid curves, whereas negative values are shown by dashed curves.

Displaying Associated Legendre Functions. With inclusion of the z -projection number m , the variety, complexity, and interest of Legendre functions increase rapidly. Interpretation of m is clearest if polar diagrams are used, since the probability density as a function of θ should be consistent with that of a system having angular momentum projection m along z . We make a preliminary and qualitative study of this idea now, with a definitive and quantitative study being deferred to Section 6.3.

For a given ℓ , there are ℓ distinct functions, $P_\ell^m(\cos\theta)$, in addition to the polynomial $P_\ell(\cos\theta)$, of which examples and their formulas are given in Table 4.1. Note that when m is odd these are *not* polynomials in $c = \cos\theta$, because of the factor $s = \sin\theta = \sqrt{1-c^2}$. For comparison with Figure 4.4, we show in Figure 4.5 polar diagrams for $\ell = 3$, for which there are three associated Legendre functions.

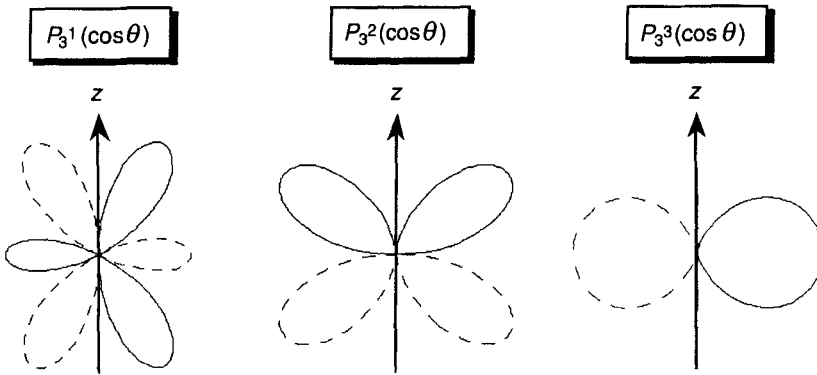


FIGURE 4.5 Polar diagrams of the three distinct associated Legendre functions for $\ell = 3$. Functions for negative m are related by the phase $(-1)^m$ to those for positive m shown here. The Legendre polynomial ($m = 0$) is shown in Figure 4.4. (Adapted from *Mathematica* notebook PLM.)

A Quantum Connection. What is the physical interpretation of the polar diagrams in Figure 4.5? From the viewpoint of quantum mechanics, we note that the square of each function indicates the probability density at θ for a system that is in angular momentum eigenstate $(3, m)$. Starting with the simplest diagram in Figure 4.5 on the right-hand side, we see that the state with projection $m = 3$ units has its probability density maximum at right angles to the axis (z) along which the projection is measured. This makes sense, since a classical particle with $\ell = m$ would move with its angular momentum \mathbf{L} perpendicular to the plane, since $\mathbf{L} = \mathbf{r} \times \mathbf{p}$ in terms of its radius vector \mathbf{r} and linear momentum \mathbf{p} .

For angular momentum projections $m = 2$ and $m = 1$ (center and left-hand diagrams in Figure 4.5) the smaller projections require motion that is more nearly in a plane containing the z axis. Finally, for $m = 0$ (Figure 4.4) the probability density and motion are predominantly in a plane containing the z axis, making the angular momentum projection as small as possible. Thus, physical insight arises from abstruse mathematics. Problem 4.2 suggests that you make calculations for $\ell = 2$ similar to those for $\ell = 3$ in order to see how closely the classical correspondence holds as ℓ decreases.

It may surprise you that a close correspondence with an interpretation in terms of classical mechanics is obtained for such a small value of ℓ , namely $\ell = 2$ or 3. As discussed in detail in Sections 5.1, 5.5, and 6.4.3, this is readily understood, and it is the main reason why we use small values of ℓ to illustrate the formalism. For $\ell > 4$ the qualitative aspects of probability densities in quantum mechanics are essentially those from classical mechanics.

4.1.3 Calculating and Visualizing Spherical Harmonics

Having summarized in Section 4.1.2 relevant properties of Legendre functions, we now turn to the problem of understanding the spherical harmonics, $Y_{\ell m}(\theta, \phi)$, the next step up the scale of functions in Figure 4.1. We emphasize the derivation and interpretation from an angular momentum viewpoint, that is, $Y_{\ell m}(\theta, \phi)$ as an eigenfunction of the orbital angular momentum operators in spherical polar coordinates in Section 3.2.2.

We derive formulas for the spherical harmonics, $Y_{\ell m}(\theta, \phi)$, from the rotational symmetry viewpoint, using raising and lowering operators (Sections 2.2.4, 3.1.2) in an approach similar to those of Andrews [And79], of Biedenharn and Louck [Bie81a, Section 3.10], and of Rose [Ros57, Appendix III].

First, we derive formulas for the $Y_{\ell m}(\theta, \phi)$ functions by using the ladder-operator techniques introduced in Section 2.2.4. Next, we derive properties of the $Y_{\ell m}$, including the addition theorem and sum rules. Then we summarize ways of calculating spherical harmonics and we give a table of formulas for those of order $\ell \leq 4$. Then we show how to visualize and interpret these functions. Finally in this subsection, we discuss zonal, tesseral, and sectorial harmonics.

Azimuthal Dependence of Spherical Harmonics. For given m we have the eigenvalue equation

$$L_z Y_{\ell m}(\theta, \phi) = -i \frac{\partial Y_{\ell m}(\theta, \phi)}{\partial \phi} = m Y_{\ell m}(\theta, \phi) \quad (4.10)$$

which is solved by inspection, to give the ϕ dependence

$$Y_{\ell m}(\theta, \phi) \propto e^{im\phi} \quad (4.11)$$

The first partial derivative of $Y_{\ell m}(\theta\phi)$ with respect to ϕ can therefore be replaced by $imY_{\ell m}(\theta\phi)$. For given ℓ , the simplest $Y_{\ell m}(\theta\phi)$ is that with $m = \ell$, namely $Y_{\ell\ell}(\theta\phi)$, as you might guess by looking at $P_\ell^\ell(\cos\theta)$ in Table 4.1. We therefore derive $Y_{\ell\ell}$ first, then we obtain the functions for smaller m by using the lowering operator L_{-1} .

The Spherical Harmonic $Y_{\ell\ell}$. Since $m = \ell$ is the largest m value on the ladder (Figure 3.8) with $2\ell + 1$ rungs starting at $m = -\ell$, L_{+1} must destroy the state:

$$L_{+1}Y_{\ell\ell}(\theta\phi) = \frac{e^{i\phi}}{\sqrt{2}} \left(\frac{\partial}{\partial\theta} + i\cot\theta \frac{\partial}{\partial\phi} \right) Y_{\ell\ell}(\theta\phi) = 0 \quad (4.12)$$

in which (3.26) has been used for the raising operator L_{+1} . If you now use the partial-derivative rule for ϕ with $m = \ell$ to convert this into an ordinary differential equation in terms of the variable $\sin\theta$, as Problem 4.3 suggests doing, then it is straightforward to show that the θ dependence of $Y_{\ell\ell}$ is $\sin^\ell\theta$.

Spherical harmonics are defined to be normalized to unity integral over the unit sphere. (We know that they are orthogonal, since they are eigenfunctions of Hermitian operators in the spherical-polar space.) It is straightforward to show (for example, by working Problem 4.4 or by using the *Mathematica* function `Integrate`) that

$$I_\ell \equiv \int_0^\pi \sin^{2\ell}\theta \sin\theta d\theta = \frac{2^{2\ell+1} \ell! \ell!}{(2\ell+1)!} \quad (4.13)$$

Since the ϕ dependence of $Y_{\ell\ell}$ contributes a factor 2π to the normalization integral, we obtain for stretched $m = \ell$ the orthonormal spherical harmonic

$$Y_{\ell\ell}(\theta, \phi) = (-1)^\ell \sqrt{\frac{(2\ell+1)!}{2^{2\ell+2} (\ell!)^2 \pi}} \sin^\ell\theta e^{i\ell\phi} \quad (4.14)$$

The phase $(-1)^\ell$ is that chosen by Condon and Shortley [Con35] in their treatise on atomic spectra and is conventional.

The General Spherical Harmonic $Y_{\ell m}$. Having obtained $Y_{\ell\ell}$, the general spherical harmonic can be found by lowering the m value by unit steps, using operator L_{-1} . If this is applied $\ell - m$ times, starting with (4.14) for $Y_{\ell\ell}$, and noting the relations (3.26), we obtain

$$Y_{\ell m}(\theta\phi) = (-1)^m \sqrt{\frac{(2\ell+1)(\ell+m)!(\ell-m)!}{4\pi}} e^{im\phi} \times \sum_x \frac{(-1)^x (\sin\theta)^{2x+m} (\cos\theta)^{\ell-2x-m}}{2^{2x+m} (m+x)! x! (\ell-m-2x)!} \quad (4.15)$$

The summation index x is over the range of integers such that none of the factorials have negative arguments. For $m \geq 0$ the range is zero to $[(\ell - m)/2]$, where $[e]$ denotes the integer part of variable e . Note that the sum of the exponents of the sine and cosine terms in (4.15) is ℓ , independent of x . The significance of this result becomes apparent in Section 4.1.4.

Properties of Spherical Harmonics. We now derive several general properties of spherical harmonics that arise from their being eigenfunctions of angular momentum operators. The mathematics of eigenstates in Section 2.3 and the angular momentum properties in Sections 3.2 and 3.4 are relevant here.

A spherical harmonic is guaranteed to have a definite parity because the parity operator P (Section 1.4.1) commutes with the angular momentum operators. The parity of $Y_{\ell m}$ can be obtained directly from (4.15), giving

$$PY_{\ell m}(\theta\phi) = Y_{\ell m}(\pi - \theta, \pi + \phi) = (-1)^\ell Y_{\ell m}(\theta\phi) \quad (4.16)$$

Recall that $Y_{\ell m}$ is an eigenfunction of L^2 , satisfying the relations

$$\begin{aligned} L^2 Y_{\ell m}(\theta\phi) &= -\left\{ \frac{\partial}{\partial c} \left[(1 - c^2) \frac{\partial}{\partial c} \right] + \frac{1}{1 - c^2} \frac{\partial^2}{\partial \phi^2} \right\} Y_{\ell m}(\theta\phi) \\ &= \ell(\ell + 1) Y_{\ell m}(\theta\phi) \end{aligned} \quad (4.17)$$

The conscientious reader may verify that (4.15) satisfies this differential equation. Because of the connection between this equation for $Y_{\ell m}$ and (4.5) for P_ℓ^m , the two functions are proportional. By comparing their orthogonality properties, for example, it is straightforward to show that

$$Y_{\ell m}(\theta\phi) = (-1)^m \sqrt{\frac{(2\ell + 1)(\ell - m)!}{4\pi(\ell + m)!}} P_\ell^m(\cos\theta) e^{im\phi} \quad m \geq 0 \quad (4.18)$$

with the definition for negative m values

$$Y_{\ell, -|m|}(\theta\phi) = (-1)^m Y_{\ell, |m|}^*(\theta\phi) \quad (4.19)$$

When $m = 0$ (4.18) simplifies to a value independent of the azimuthal angle ϕ , namely

$$Y_{\ell 0}(\theta\phi) = Y_{\ell 0}(\theta, 0) = \sqrt{\frac{2\ell + 1}{4\pi}} P_\ell(\cos\theta) \quad (4.20)$$

At the poles $\theta = 0$ and $\theta = \pi$ the azimuthal angles ϕ are indistinguishable, so $Y_{\ell m}(\theta\phi)$ cannot depend on ϕ at these angles. Therefore, the only nonzero spherical harmonic has $m = 0$. Thus

$$Y_{\ell m}(0, \phi) = \sqrt{\frac{2\ell+1}{4\pi}} \delta_{m,0} \quad Y_{\ell m}(\pi, \phi) = (-1)^\ell \sqrt{\frac{2\ell+1}{4\pi}} \delta_{m,0} \quad (4.21)$$

The first of these results is needed for the next development.

Spherical Harmonic Addition Theorem and Sum Rule. The properties just derived hold for a single $Y_{\ell m}$. There are two interesting related results arising from spherical harmonics with the same arguments but different angle pairs $(\theta'\phi')$ and $(\theta\phi)$, as shown in Figure 4.6.

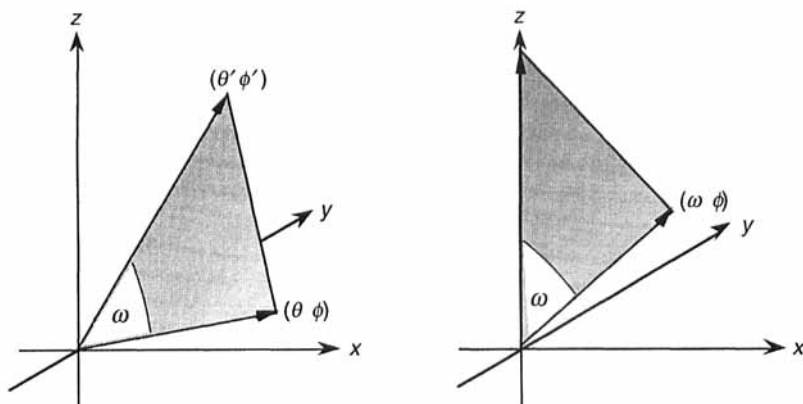


FIGURE 4.6 Unit vectors for the angle pairs $\hat{\mathbf{r}}' = (\theta'\phi')$ and $\hat{\mathbf{r}} = (\theta\phi)$ for the spherical harmonic addition theorem (4.23). The angle between the two vectors is ω . In the right panel the system has been rotated so that $\theta' = 0$.

Consider the scalar product (Section 2.1) given by $\langle(\theta'\phi')|(\theta\phi)\rangle$. This cannot depend upon the absolute orientation of the unit vectors $\hat{\mathbf{r}}'$ and $\hat{\mathbf{r}}$ that have these angles, but only upon the angle ω between the two unit vectors. To connect this to spherical harmonics, insert a unit operator between the bra and ket states, as follows:

$$\begin{aligned} \langle(\theta'\phi')|(\theta\phi)\rangle &= \langle(\theta'\phi')| \sum_m |\ell m\rangle \langle \ell m| (\theta\phi)\rangle \\ &\propto \sum_m Y_{\ell m}^*(\theta'\phi') Y_{\ell m}(\theta\phi) \end{aligned} \quad (4.22)$$

Since the absolute orientation relative to the reference frame is unimportant, we can (for example) swing $\hat{\mathbf{r}}'$ to lie along the z axis, so that $\theta = 0$ and $\theta \rightarrow \omega$, as shown in the right-hand panel of Figure 4.6. The first $Y_{\ell m}$ collapses to a delta function,

according to (4.21), from which you can discover (especially if you work Problem 4.5) the *spherical harmonic addition theorem*

$$\sum_m Y_{\ell m}^*(\theta'\phi') Y_{\ell m}(\theta\phi) = \frac{2\ell+1}{4\pi} P_\ell(\cos\omega) \quad (4.23)$$

Here the summation is over the m range $-\ell$ to ℓ , and $\cos\omega = \hat{\mathbf{r}}' \cdot \hat{\mathbf{r}}$ on the right-hand side. Note that each term in the sum is real, although the factors on the left-hand side are complex.

By setting the angles in each spherical harmonic equal, thus $\omega = 0$, and using (4.2) for the Legendre polynomial, we obtain the *sum rule for spherical harmonics*

$$\sum_m Y_{\ell m}^*(\theta\phi) Y_{\ell m}(\theta\phi) = \frac{2\ell+1}{4\pi} \quad (4.24)$$

In both (4.23) and (4.24) the complex conjugates can be replaced—through use of (4.24)—by the spherical harmonics with $-m$ times a phase, which requires more mental baggage. Both results are useful, especially in our developments in Chapters 8 and 9. We have derived most of these results on spherical harmonics without recourse to detailed expressions for $Y_{\ell m}$. Now we turn to more practical concrete results.

TABLE 4.2 Spherical harmonics, $Y_{\ell m}(\theta, \phi)$, for $0 \leq \ell \leq 4$. In terms of table entries $Y_{\ell m}(\theta, 0)$, an extra factor of $\exp(im\phi)$ is needed and $c = \cos\theta$, $s = \sin\theta$.

$m \setminus \ell$	0	1	2	3	4
0	$\sqrt{\frac{1}{4\pi}}$	$\sqrt{\frac{3}{4\pi}} c$	$-\sqrt{\frac{5}{16\pi}} (1-3c^2)$	$-\sqrt{\frac{7}{16\pi}} c(3-5c^2)$	$\sqrt{\frac{9}{256\pi}} (3-30c^2+35c^4)$
± 1		$\mp \sqrt{\frac{3}{8\pi}} s$	$\mp \sqrt{\frac{15}{8\pi}} cs$	$\pm \sqrt{\frac{21}{64\pi}} s(1-5c^2)$	$\pm \sqrt{\frac{45}{64\pi}} cs(3-7c^2)$
± 2			$\sqrt{\frac{15}{32\pi}} s^2$	$\sqrt{\frac{105}{32\pi}} cs^2$	$-\sqrt{\frac{45}{128\pi}} s^2(1-7c^2)$
± 3	$Y_{\ell, - m }(\theta, \phi) = (-1)^m Y_{\ell, m }^*(\theta, \phi)$ $Y_{\ell, m}(\pi - \theta, \phi) = (-1)^\ell Y_{\ell, m}(\theta, \phi)$			$\mp \sqrt{\frac{35}{64\pi}} s^3$	$\mp \sqrt{\frac{315}{64\pi}} cs^3$
± 4					$\sqrt{\frac{315}{512\pi}} s^4$

Formulas for Spherical Harmonics. With general expression (4.15) at hand, we can write down analytic expressions for $Y_{\ell m}$, as shown in Table 4.2 for $\ell \leq 4$. It is convenient to use the built-in *Mathematica* function `SphericalHarmonicY` with arguments `[L,m,theta,phi]` to obtain analytical expressions for the corresponding $Y_{\ell m}(\theta, \phi)$. This function is used in notebook `YLMabs` in Appendix I.

By using Table 4.2, several of the general properties of spherical harmonics can be verified explicitly. For example, entries on the diagonal—which have $m = \ell$ —illustrate formula (4.14), while (4.21) can be checked by setting $c = \pm 1$. By inspection, the parity symmetry of the $Y_{\ell m}$, given by (4.16), is also seen to be satisfied.

Visualizing and Interpreting Spherical Harmonics. In Section 4.1.2 we display Legendre functions as polar diagrams, so it might appear unnecessary to show spherical harmonics, whose θ dependence is that of Legendre functions, according to (4.18). There is, however, the extra azimuthal angle degree of freedom ϕ , which modulates the functions as $e^{im\phi}$. The absolute values of the $Y_{\ell m}$ are not affected by this, but any superposition of waves involving more than one $Y_{\ell m}$ is modified by this complex factor, unless $m = 0$.

The display method in Figure 4.7 provides easily understood figures. To include the full complexity of a spherical harmonic, imagine the right-hand surface being modulated in azimuthal angle by $e^{2i\phi} = \cos(2\phi) + i \sin(2\phi)$. The left-hand surface has $m = 0$, thus no azimuthal dependence, but note that the bulge around $\theta = \pi/2$ is negative in sign. One way to visualize azimuthal dependence is to plot a torus centered on the z axis, shown in Figure 4.8. It shows how a simple object, a torus, is modulated by the dependence on azimuthal angle, $e^{im\phi}$, in the spherical harmonic $Y_{\ell m}(\theta, \phi)$. For $m = 0$ the minor radius is independent of ϕ , while for other m values the radius goes as $\cos(m\phi)$ or $\sin(m\phi)$, depending on whether we are looking at the real or imaginary part of $Y_{\ell m}(\theta, \phi)$.

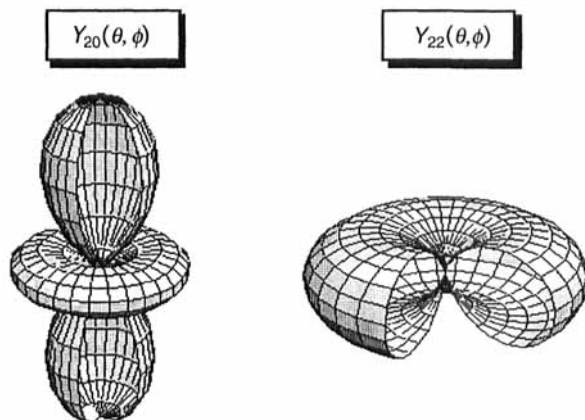


FIGURE 4.7 Absolute values of two spherical harmonics of order 2. In the azimuthal direction parts of the surfaces have been cut away from $\phi = 15\pi/8$ to $\phi = \pi/4$ to reveal the backs of the surfaces. (Adapted from *Mathematica* notebook `YLMabs`.)

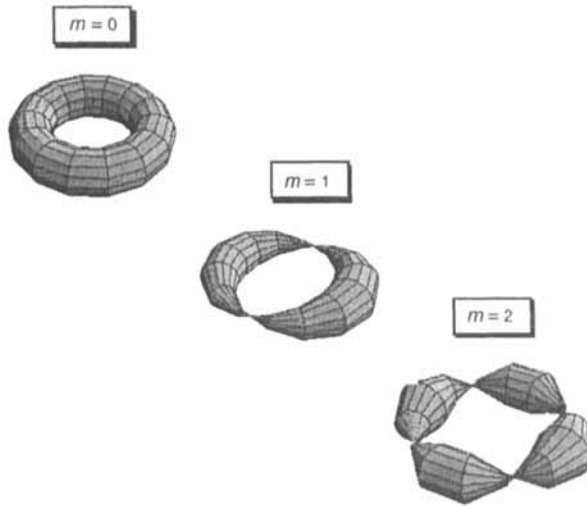


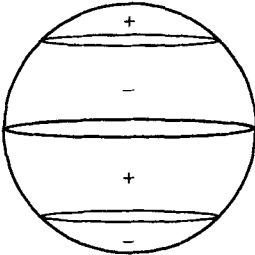
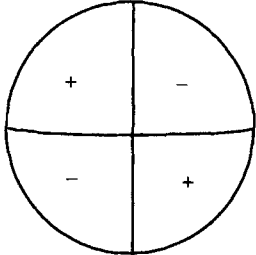
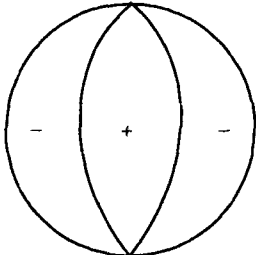
FIGURE 4.8 Aids to visualizing the azimuthal (ϕ) dependence of spherical harmonics. The torus on the left has $m = 0$, hence no ϕ dependence; the center torus has $m = 1$; the torus on the right has $m = 2$, so it depends on ϕ as $|\cos(2\phi)|$ or $|\sin(2\phi)|$. (Adapted from *Mathematica* notebook EXPi.mPHI.)

The same picture (center and right panels in Figure 4.8) serves both cosine and sine functions, since the magnitudes of these two functions differ only by a rotation through ϕ by angle $\pi/(2m)$. Problem 4.6 suggests how to construct such a figure using spherical-polar coordinates. Indeed, it is quite common to define the real and imaginary parts of the spherical harmonic (4.15), having $\cos\phi$ and $\sin\phi$ factors. The symmetries of the real harmonics are generally lower than those of the complex harmonics used here.

Zonal, Tesseral, and Sectorial Harmonics. You will occasionally encounter these three terms in discussions of spherical harmonics. By understanding the origin of the terms, you will realize another visualization of the $Y_{\ell m}$ —one emphasizing that their signs change as one navigates over the unit sphere. The terminology is best understood through formulas and diagrams on a sphere, as shown in Table 4.3.

A *zonal* harmonic is a spherical harmonic with $m = 0$. It is therefore proportional to a Legendre polynomial (Sections 4.1.1, 4.1.2) and has no dependence on the azimuthal angle (longitude) ϕ . The nodes (zeros) of a zonal $Y_{\ell m}(\theta\phi)$ therefore divide the unit sphere into zones along circles of constant latitude. If ℓ is odd (such as $\ell = 3$ in Table 4.2), the central nodal line coincides with the equator (latitude zero, colatitude $\theta = \pi/2$). Nodal circles are symmetrically arranged about the equator, because of the parity symmetry (4.16) and their number is ℓ , just the order of the zonal harmonic. Recall that in geography the region of Earth between the tropics of Cancer and Capricorn is called the “tropic zone.”

TABLE 4.3 Zonal, tesseral, and sectorial harmonics, illustrated for $\ell = 3$ for each harmonic, with $m = 2$ for the tesseral harmonic $Y_{32}(\theta, \phi)$. The sign of $\text{Im } Y_{\ell m}$ is shown for the hemisphere $\pi \leq \phi \leq 2\pi$.

Type of harmonic:		
zonal	tesseral	sectorial
$Y_{\ell 0}(\theta, \phi) \propto P_{\ell}(\cos \theta)$	$Y_{\ell m}(\theta, \phi) \propto P_{\ell}^m(\cos \theta) e^{im\phi}$	$Y_{\ell \ell}(\theta, \phi) \propto \sin^{\ell} \theta e^{i\ell\phi}$
		

A *tesseral* harmonic is the general spherical harmonic $Y_{\ell m}(\theta, \phi)$. Sometimes the term is restricted to the real and imaginary parts separately. Consider, for example, the imaginary part of this function, such as $\text{Im } Y_{32}(\theta, \phi)$. The sign changes of the associated Legendre function in the θ variable and of $\cos \phi$ or $\sin \phi$ in the ϕ variable divide the unit sphere into angular regions of alternating sign, as indicated in Table 4.3. These regions “tessellate” (tile) the sphere, although the tiles (tesserae) must be curved. Except at the poles, nodal circles intersect at right angles. In the middle figure in Table 4.3 we show the signs of the spherical harmonic, with the sign of $P_3^2(\cos \theta)$ being obtained from the center polar diagram in Figure 4.5.

A *sectorial* harmonic is a spherical harmonic for which there are no zonal circles. Thus, $m = \ell$ as given in (4.14) and Table 4.2. The azimuthal dependence of the real or imaginary part of the sectorial harmonic $Y_{\ell \ell}(\theta, \phi)$ divides the sphere into sectors, like wedges of an orange, of which there are 2ℓ in $0 \leq \phi \leq 2\pi$. For example, if we look at $\sin(3\phi)$ in the range $\pi \leq \phi \leq 2\pi$, we see in the rightmost panel of Table 4.3 three sectors of alternating sign.

Is all this nomenclature just to enlarge our vocabulary of Latin words? Partly, but there is also an interpretation in terms of deformations or vibrations of a figure about spherical equilibrium, for example the departure of a nucleus or the Earth's shape from sphericity or the pulsation modes of the surface of the sun. The tesserae indicate the regions of the surface with the same sign of the deviation from sphericity, either larger radius (+) or smaller radius (-). For deformations, these differences are constant in time, whereas for vibrations they are time-dependent and the figures correspond to snapshots. For example, compare (as Problem 4.7 suggests

you do in detail) the spherical harmonics $Y_{32}(\theta\phi)$ (left in Figure 4.9) and $Y_{63}(\theta\phi)$ (right in Figure 4.9).

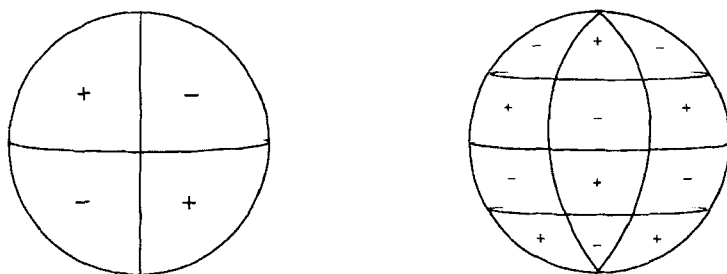


FIGURE 4.9 Signs of the imaginary part of the tesseral harmonics $Y_{32}(\theta\phi)$ (left) and $Y_{63}(\theta\phi)$ (right) over the half of the unit sphere $0 \leq \theta \leq \pi$, $\pi \leq \phi \leq 2\pi$, which is the visible half if you look along the y axis with your eye at $y < -1$.

The two spherical harmonics in Figure 4.9 have different zonal structure, with two zones for $\ell - m = 1$ but four zones for $\ell - m = 3$. They also have different sectorial structure, with 2 sectors visible on the hemisphere for $m = 2$ but 3 sectors visible for $m = 3$. For a vibrating system (whether the sun, a molecule, or a nucleus), the amplitudes $Y_{63}(\theta\phi)$ would almost certainly correspond to much higher vibrational frequencies than for $Y_{32}(\theta\phi)$.

4.1.4 Solid Harmonics and Other Variants

The spherical harmonics in Section 4.1.3, $Y_{\ell m}(\theta\phi)$, are defined in terms of the spherical polar coordinates θ and ϕ , which locate points on the surface of the unit sphere. It is also useful—particularly for applications to the quantum mechanics of molecules, to solid-state physics, and to geophysics—to be given point $\mathbf{r} = (x, y, z)$ in Cartesian coordinates, then to calculate a corresponding harmonic function, a solution of the Laplace equation directly in terms of x , y , and z , or simple combinations of them. The appropriate function, the *solid harmonic* $Y_{\ell m}(\mathbf{r}) = Y_{\ell m}(x, y, z)$, is then a solution of the Laplace equation.

Other variants of spherical harmonics can be obtained by associating vectors or tensors with points on the unit sphere. Thus, one obtains tensor harmonics. Other generalizations are to functions solving Laplace's equation on ellipsoids (ellipsoidal harmonics) and to functions defined in spaces of dimension higher than three (hyperspherical harmonics). We discuss first the solid harmonics in some detail, providing general formulas, then giving them for the same range of ℓ values as the spherical harmonics in Section 4.1.3. Then we summarize the references on the other harmonics.

Deriving the Solid Harmonics. By examining the Laplacian in spherical polar coordinates, it is easy to show—as in Section 4.12 of Wong [Won91]—that for

given ℓ and m there are two radial dependences that satisfy the equation, namely r^ℓ (which is regular as $r \rightarrow 0$) and $r^{-(\ell+1)}$ (which is irregular as $r \rightarrow 0$). In spherical polar coordinates the general solution of the Laplace equation that heads Figure 4.1 is therefore of the form

$$u(\mathbf{r}) = \sum_{\ell, m} \left[A_\ell r^\ell + B_\ell r^{-(\ell+1)} \right] Y_{\ell m}(\theta, \phi) \quad (4.25)$$

in which the A_ℓ and B_ℓ depend on the choice of boundary conditions. Because the regular solution is more commonly used, one introduces the *solid harmonic*, $Y_{\ell m}(\mathbf{r})$, defined by

$$Y_{\ell m}(\mathbf{r}) \equiv r^\ell Y_{\ell m}(\theta, \phi) \quad (4.26)$$

If left in this form, this is a complication rather than a simplification. We can, however, incorporate the r dependence within this expression by noting that

$$\begin{aligned} r^\ell (\sin \theta)^{2x'+m} (\cos \theta)^{\ell-2x'-m} e^{im\phi} \\ &= (r \sin \theta e^{i\phi})^{x'+m} (r \sin \theta e^{-i\phi})^{x'} (r \cos \theta)^{\ell-2x'-m} \\ &= (x+iy)^{x'+m} (x-iy)^{x'} z^{\ell-2x'-m} \end{aligned} \quad (4.27)$$

in which we use as summation variable x' rather than x , to avoid confusion with coordinate x . Thus we obtain the formula for the *solid harmonic*

$$\begin{aligned} Y_{\ell m}(\mathbf{r}) &\equiv r^\ell Y_{\ell m}(\theta, \phi) \\ &= (-1)^m \sqrt{\frac{(2\ell+1)(\ell+m)!(\ell-m)!}{4\pi}} \\ &\quad \times \sum_{x'} \frac{(-1)^{x'} (x+iy)^{x'+m} (x-iy)^{x'} z^{\ell-2x'-m}}{2^{2x'+m} (m+x')! x'! (\ell-m-2x')!} \end{aligned} \quad (4.28)$$

With this form one can use the Cartesian coordinates for $\mathbf{r} = (x, y, z)$, yet still have eigenfunctions of L^2 and L_z .

Spherical Harmonics in the Spherical Basis. The combinations of x , y , and z in (4.28) suggest another form of this result. Consider spherical-basis unit *coordinate* vectors, similar to the spherical-basis angular momentum operators in Section 3.1.3, namely

$$\hat{\mathbf{e}}_{\pm 1} \equiv \mp \frac{1}{\sqrt{2}} (\hat{\mathbf{e}}_x \pm i\hat{\mathbf{e}}_y) \quad \hat{\mathbf{e}}_0 \equiv \hat{\mathbf{e}}_z \quad (4.29)$$

in terms of unit vectors in the Cartesian basis. Note the extra $\mp 1/\sqrt{2}$ factor between (3.9) and this equation. If we now define the spherical-basis coordinates by

$$\xi_{\pm 1} \equiv \mp \frac{x \pm iy}{\sqrt{2} r} \qquad \xi_0 \equiv \frac{z}{r} \qquad (4.30)$$

then the length of this complex vector is unity; $|\xi_{+1}|^2 + |\xi_{+0}|^2 + |\xi_{-1}|^2 = 1$, analogously to the unit sphere in spherical polar coordinates. As you can see immediately by substituting (4.30) into (4.28), the *spherical harmonic in the spherical basis* is given by

$$Y_{\ell m}(\theta\phi) = \sqrt{\frac{(2\ell+1)(\ell+m)!(\ell-m)!}{4\pi}} \times \sum_{x'} \frac{\xi_{+1}^{x'+m} \xi_0^{\ell-2x'-m} \xi_{-1}^{x'}}{2^{x'+m/2} (m+x')! x'! (\ell-m-2x')!} \qquad (4.31)$$

which is remarkably symmetric in the three complex coordinates. Being solutions of a partial differential equation that is symmetric in the three variables, Euler’s theorem demands that each term be of the same order, namely ℓ , which is clear from inspection of (4.28) and (4.31).

Now that we have developed the analytical properties of harmonics in the solid form and in the spherical basis, it is time to see some examples and applications.

Examples of Solid Harmonics. From the general formula (4.28) for $Y_{\ell m}(\mathbf{r})$ we can give the solid harmonics corresponding to the spherical harmonics in Table 4.2. Noting that the isotropic function $Y_{00}(\theta\phi) = 1/\sqrt{4\pi}$ is the same for both kinds of harmonics, we give in Table 4.4 the solid harmonics for $\ell = 1$ and 2.

TABLE 4.4 Solid harmonics for $\ell = 1, 2$ with $w_{\pm} = x \pm iy$, $r^2 = x^2 + y^2 + z^2$.

$m \setminus \ell$	1	2
0	$\sqrt{\frac{3}{4\pi}} z$	$-\sqrt{\frac{5}{16\pi}} (r^2 - 3z^2)$
± 1	$\mp \sqrt{\frac{3}{8\pi}} w_{\pm}$	$\mp \sqrt{\frac{15}{8\pi}} z w_{\pm}$
± 2		$\sqrt{\frac{15}{32\pi}} w_{\pm}^2$

The forms used in this table are the same as in Table 4.2 for the spherical harmonics, in the sense that $Y_{\ell m}(\mathbf{r})/r^\ell$ has the same dependence on $\cos\theta$ (which is just z/r) as does $Y_{\ell m}(\theta, \phi)$. This provides a simple check between corresponding spherical and solid harmonics. Another check is that solid harmonics have the same parity symmetry (4.16) as spherical harmonics, since r (being a length) is invariant under parity. Moreover, any polynomials that form factors in $Y_{\ell m}(\mathbf{r})$ must be homogeneous, in that the degree of the terms must be the same; otherwise, the form of the polynomial would depend upon the unit of length used.

Solid harmonics for $\ell = 3$ and 4 are given in Table 4.5. Note the correspondence with the spherical harmonics in Table 4.2. In Tables 4.4 and 4.5 the signs and square-root factors before the expressions for solid harmonics agree with those for the matching spherical harmonics, and the order of factors is the same.

TABLE 4.5 Solid harmonics for $\ell = 3, 4$ with $w_\pm = x \pm iy$, $r^2 = x^2 + y^2 + z^2$.

$m \setminus \ell$	3	4
0	$-\sqrt{\frac{7}{16\pi}} z(3r^2 - 5z^2)$	$\sqrt{\frac{9}{256\pi}} (3r^4 - 30r^2z^2 + 35z^4)$
± 1	$\pm \sqrt{\frac{21}{64\pi}} w_\pm (r^2 - 5z^2)$	$\pm \sqrt{\frac{45}{64\pi}} z w_\pm (3r^2 - 7z^2)$
± 2	$\sqrt{\frac{105}{32\pi}} z w_\pm^2$	$-\sqrt{\frac{45}{128\pi}} w_\pm^2 (r^2 - 7z^2)$
± 3	$\mp \sqrt{\frac{35}{64\pi}} w_\pm^3$	$\mp \sqrt{\frac{315}{64\pi}} z w_\pm^3$
± 4		$\sqrt{\frac{315}{512\pi}} w_\pm^4$

The rule of homogeneous polynomials given above is seen in $Y_{40}(\mathbf{r})$, for example, which has the sum of the exponents of each term equal to 4. For practical applications it might be desirable to substitute for r^2 in Tables 4.4 and 4.5 its expression in terms of x , y , and z , so that $Y_{\ell m}(\mathbf{r}) = Y_{\ell m}(x, y, z)$ explicitly.

Real Forms of Harmonics. Although the complex-number forms of spherical and solid harmonics, (4.15) and (4.28), are suitable for formal work, it is often more useful to have them expressed as real quantities, especially in problems involving electrostatic potentials. As is clear from the expression in terms of Legendre functions, replacement of the complex exponential in $m\phi$ by corresponding cosines and sines would solve the problem. We therefore introduce the real forms of the spherical harmonics through the definitions

$$\begin{aligned}
 Z_\ell(\theta\phi) &\equiv \sqrt{\frac{2\ell+1}{4\pi}} P_\ell(\cos\theta) \\
 Z_{\ell m}^c(\theta\phi) &\equiv \sqrt{\frac{(2\ell+1)(\ell-m)!}{2\pi(\ell+m)!}} P_\ell^m(\cos\theta) \cos m\phi \quad m \geq 0 \\
 Z_{\ell m}^s(\theta\phi) &\equiv \sqrt{\frac{(2\ell+1)(\ell-m)!}{2\pi(\ell+m)!}} P_\ell^m(\cos\theta) \sin m\phi \quad m \geq 0
 \end{aligned} \tag{4.32}$$

Thus, the conventional spherical harmonics are given by

$$\begin{aligned}
 Y_{\ell 0} &= Z_{\ell 0} \\
 Y_{\ell m} &= \frac{(-1)^m}{\sqrt{2}} (Z_{\ell m}^c + iZ_{\ell m}^s) \quad m > 0 \\
 Y_{\ell m}^* &= \frac{(-1)^m}{\sqrt{2}} (Z_{\ell m}^c - iZ_{\ell m}^s) \quad m > 0
 \end{aligned} \tag{4.33}$$

The presence of i factors reminds us that the $Y_{\ell m}$ are complex, whereas the $Z_{\ell m}$ are real. Therefore, if the latter are expressed in terms of the former, a factor of i must appear in the definition of $Z_{\ell m}^s$. For $m < 0$ formula (4.19) can be used for $Y_{\ell m}$. As Problem 4.8 suggests verifying, the addition theorem (4.23) can be written

$$\sum_{\kappa=0,c,s} \sum_{m=0}^{\ell} Z_{\ell m}^{\kappa}(\theta'\phi') Z_{\ell m}^{\kappa}(\theta\phi) = \frac{2\ell+1}{4\pi} P_\ell(\cos\omega) \tag{4.34}$$

where each quantity is explicitly real. Figure 4.6 relates the angles on the two sides of this formula.

For the real solid harmonics, similar definitions and results hold, since they differ only by a real factor, r^ℓ , from the spherical harmonics. Tables of such solid harmonics are given, for example, in [Poo87, Section 10–7].

A Worked Example: Crystal-Field Potentials. To illustrate practical application of the real form of solid harmonics and the addition theorem (4.34), consider the problem of calculating the electrostatic potential at a point within a crystal lattice, the so-called *crystal-field potential*. A typical setup is shown in Figure 4.10.

Suppose that at point P one wants to estimate the potential $V(\mathbf{r})$ due to N charges (q_1, q_2, \dots, q_N) each of which can be approximated as a point charge, so that it has a definite position \mathbf{R}_i . The replacement of finite distributions of charge (indicated by the spherical clouds in Figure 4.10) by point charges is called the *point-charge model*. The potential is then given by

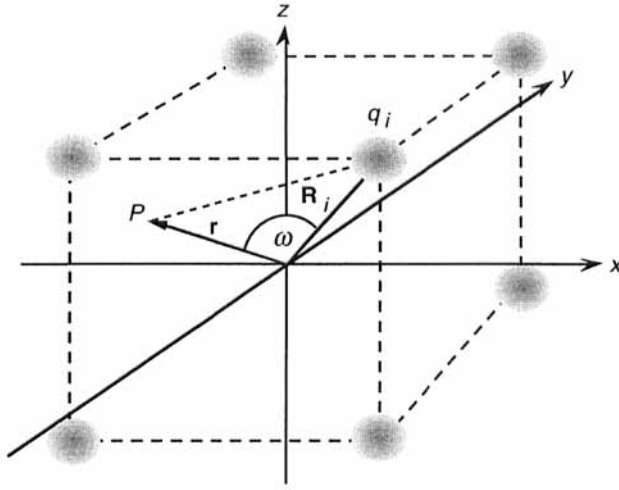


FIGURE 4.10 The electrostatic potential at point P in a crystal is to be calculated in terms of the charges q_i and their positions \mathbf{R}_i , here shown for cubic symmetry C_4 .

$$V(\mathbf{r}) = \sum_{i=1}^N \frac{q_i}{|\mathbf{r} - \mathbf{R}_i|} = \sum_{i=1}^N \frac{q_i}{R_i} \sum_{\ell=0}^{\infty} \left(\frac{r}{R_i} \right)^{\ell} P_{\ell}(\cos \omega_i) \quad (4.35)$$

in the second step of which we used the Legendre expansion, assuming that $r/R_i < 1$ for the potentials of interest. Now the addition theorem (4.10) can be used in reverse to expand the Legendre polynomials into functions of the angles (θ_i, ϕ_i) for the charges and the angles (θ, ϕ) for the field point. By using the solid form of the real harmonics, one obtains immediately

$$V(\mathbf{r}) = \sum_{\ell=0}^{\infty} \sum_{m=0}^{\ell} \sum_{\kappa=0,c,s} A_{\ell m}^{\kappa} Z_{\ell m}^{\kappa}(\mathbf{r}) \quad (4.36)$$

in which the coefficients $A_{\ell m}^{\kappa}$ depend only on the arrangement of the charges. They are defined by

$$A_{\ell m}^{\kappa} \equiv \frac{4\pi}{2\ell + 1} \sum_{i=1}^N \frac{q_i Z_{\ell m}^{\kappa}(\theta_i, \phi_i)}{R_i^{\ell+1}} \quad (4.37)$$

Expansion (4.36) is particularly convenient for calculating potentials because, once a given model determining the $A_{\ell m}^{\kappa}$ has been chosen, the field point $\mathbf{r} = (r, \theta, \phi)$ can be changed and only the sums in (4.36) need to be repeated. Poole and Farach [Poo87] provide in Sections 10–7 and 10–8 expressions for $A_{\ell m}^{\kappa}$ in various charge configurations.

Other Variants of Harmonic Functions. We begin our listing of other variants of harmonic functions by referring to the Laplace equation, which we use in Figure 4.1 to characterize the connections between functions for orbital eigenstates. If the Laplacian is expressed in a curvilinear coordinate system other than the spherical polar coordinates that lead to eigenfunctions of L^2 and L_z , one obtains functions expressing the angular dependencies in this system. For example, in ellipsoidal coordinates one obtains the *ellipsoidal harmonics* that are described extensively in Hobson's book [Hob31].

In Chapters 5 and 10 of the mathematical physics treatise by Morse and Feshbach [Mor53a] there is a complete treatment of the separability of the Laplacian in three dimensions and of solutions of the Laplace equation. Extension of the Laplace equation to the Helmholtz equation for waves is discussed in our Section 5.4 in connection with partial-wave expansions of plane waves into Legendre and Bessel functions. Spherical harmonics as rotation matrix elements are considered in Section 6.4.4, while the Gaunt integrals over three spherical harmonics are derived in Section 7.5.3 and applied in Section 7.5.4.

By combining the properties of a particular symmetry group (Section 2.5) with solid harmonics, new types of harmonics are produced. For example, the octahedral group O_h (the point group of the cube including inversion) gives rise to *Kubic harmonics*, also called lattice harmonics, discussed (for example) in Bell [Bel54].

If one combines unit vectors or unit tensors (of various ranks) with spherical harmonics, one obtains *vector harmonics* or *tensor harmonics*. An extensive treatment of tensor harmonics is provided in the monograph by Jones [Jon85]. Although he emphasizes applications to geophysics and fluid dynamics, many of the results are directly applicable to electrodynamics and to quantum mechanics. We describe vector harmonics in Section 8.2.

All the above variants of the harmonic functions involve only three dimensions. In an N -body system, especially in quantum mechanics, extension to as many as $3N$ dimensions will be needed. Such an extension introduces the *hyperspherical harmonics*. The monograph by Avery [Ave89] emphasizes their applications in quantum chemistry and also provides extensive references to their use in molecular and nuclear physics.

4.2 SPHERICAL-BASIS VECTORS AND ANGULAR MOMENTUM IN A FIELD

A major purpose of this section is to develop the concept of spin, showing (as in Section 3.5) that spin is that part of the angular momentum (rotational symmetry) remaining after orbital angular momentum effects have been taken into account.

We introduce the complex spherical-basis vectors, we show how they can be used to construct representations of angular momentum operators, and we demonstrate in Section 4.2.2 that any vector field has intrinsic angular momentum of unity. We then discuss briefly the angular momentum of the electromagnetic field and the spin of photons.

4.2.1 Vectors in the Spherical Basis

The spherical-basis operators for angular momentum, $J_{\pm 1}$ and J_0 in Section 3.1.3, are useful for determining eigenvalues and matrix elements (Section 3.4.2). Here we make a similar generalization for vectors that is also useful and provides insight.

Spherical-Basis Unit Vectors. The unit vectors in the spherical basis are defined by

$$\hat{\mathbf{e}}_{\pm 1} \equiv \mp \frac{1}{\sqrt{2}} (\hat{\mathbf{e}}_x \pm i \hat{\mathbf{e}}_y) \quad \hat{\mathbf{e}}_0 \equiv \hat{\mathbf{e}}_z \quad (4.38)$$

and are used in Section 4.1.4 to enable discussion of spherical harmonics in the spherical basis. We now show that they are of more general interest. The relations in (4.38) can also be written in matrix form as

$$\begin{bmatrix} \hat{\mathbf{e}}_{+1} \\ \hat{\mathbf{e}}_0 \\ \hat{\mathbf{e}}_{-1} \end{bmatrix} = \mathbf{U}_V \begin{bmatrix} \hat{\mathbf{e}}_x \\ \hat{\mathbf{e}}_y \\ \hat{\mathbf{e}}_z \end{bmatrix} \quad \mathbf{U}_V \equiv \frac{1}{\sqrt{2}} \begin{bmatrix} -1 & -i & 0 \\ 0 & 0 & \sqrt{2} \\ 1 & -i & 0 \end{bmatrix} \quad (4.39)$$

The matrix \mathbf{U}_V is unitary, so (according to Section 2.2.2) the vectors have the same length in both bases. The complex unit vectors defined in (4.38) have the properties

$$\hat{\mathbf{e}}_{\sigma}^* = (-1)^{\sigma} \hat{\mathbf{e}}_{-\sigma} \quad \sigma = \pm 1, 0 \quad (4.40)$$

which is analogous to property (4.16) for spherical harmonics, and they satisfy the scalar-product orthonormality conditions

$$\hat{\mathbf{e}}_{\sigma}^* \cdot \hat{\mathbf{e}}_{\sigma'} = \delta_{\sigma, \sigma'} \quad (4.41)$$

as well as the vector-product relations

$$\hat{\mathbf{e}}_{\sigma} \times \hat{\mathbf{e}}_{\sigma} = 0 \quad \hat{\mathbf{e}}_{\pm 1} \times \hat{\mathbf{e}}_{\mp 1} = \pm i \hat{\mathbf{e}}_0 \quad \hat{\mathbf{e}}_{\pm 1} \times \hat{\mathbf{e}}_0 = \pm i \hat{\mathbf{e}}_{\pm 1} \quad (4.42)$$

Therefore, if \mathbf{A} is any vector, we have

$$\mathbf{A} = \sum_{\sigma=-1}^1 A_{\sigma} \hat{\mathbf{e}}_{\sigma}^* \quad A_{\sigma} = \mathbf{A} \cdot \hat{\mathbf{e}}_{\sigma} \quad (4.43)$$

so the spherical-basis components of \mathbf{A} are related to its Cartesian components by

$$A_{\pm 1} = \mp \frac{1}{\sqrt{2}} (A_x \pm i A_y) \quad A_0 = A_z \quad (4.44)$$

Cartesian components are therefore related to spherical-basis components as

$$A_x = \frac{1}{\sqrt{2}}(A_{-1} - A_1) \quad A_y = \frac{i}{\sqrt{2}}(A_1 + A_{-1}) \quad A_z = A_0 \quad (4.45)$$

These definitions and properties are particularly useful in Section 4.2.2 and when discussing irreducible tensors in Section 8.1.

The Angular Momentum Basis. Spherical-basis unit vectors are, perhaps surprisingly, useful for constructing angular momentum operators. Define the operators $\mathbf{S}_{\pm 1}$ and \mathbf{S}_0 by

$$\mathbf{S}_{\pm 1} \equiv \mp \sqrt{2} i \hat{\mathbf{e}}_{\pm 1} \times \quad \mathbf{S}_0 \equiv i \hat{\mathbf{e}}_0 \times \quad (4.46)$$

in which \times denotes the conventional cross product. As you may show in Problem 4.9, these operators satisfy the fundamental angular momentum commutation relations (3.6). Further, when acting on the unit vectors they produce

$$\mathbf{S}_{\pm 1} \hat{\mathbf{e}}_{\sigma} = \begin{cases} 0, & \sigma = \pm 1 \\ \sqrt{2} \hat{\mathbf{e}}_0, & \sigma = \mp 1 \\ \sqrt{2} \hat{\mathbf{e}}_{\pm 1}, & \sigma = 0 \end{cases} \quad \mathbf{S}_0 \hat{\mathbf{e}}_{\sigma} = \sigma \hat{\mathbf{e}}_{\sigma} \quad (4.47)$$

as you may also choose to verify. These results are just those obtained in Section 3.4.2 for the ladder operators acting on eigenstates having eigenvalues $j = 1$ and $m = \sigma$. The $\hat{\mathbf{e}}_{\sigma}$ are therefore spin-1 eigenstates.

Angular Momentum for the Displacement Vector. By now you may believe that *any* vector has angular momentum $j = 1$. This claim must, however, be made with caution. Consider, for example, the displacement vector $\mathbf{r} = x \hat{\mathbf{e}}_x + y \hat{\mathbf{e}}_y + z \hat{\mathbf{e}}_z$. Take the z component of $\mathbf{J} = \mathbf{L} + \mathbf{S}$, where L_z is from the Cartesian-coordinate expression (3.17) and $S_z = S_0$ is from (4.46). In detail, we have

$$\begin{aligned} J_z \mathbf{r} &= -i \left(x \frac{\partial}{\partial y} - y \frac{\partial}{\partial x} \right) \mathbf{r} + i \hat{\mathbf{e}}_z \times \mathbf{r} \\ &= i (y \hat{\mathbf{e}}_x - x \hat{\mathbf{e}}_y) + i (x \hat{\mathbf{e}}_y - y \hat{\mathbf{e}}_x) \\ &= 0 \end{aligned} \quad (4.48)$$

We see that for the vector \mathbf{r} the orbital and “spin” contributions to its angular momentum exactly cancel, giving a total angular momentum component of zero. Since we made the analysis in Cartesian coordinates, which are equivalent to each other, a similar zero will hold for J_x and J_y . This result for \mathbf{r} should not be too surprising, since the field \mathbf{r} is spherically symmetric, so that a rotation leaves it unchanged. We should therefore look at rotations of vectors more closely, as we do in the following.

4.2.2 Infinitesimal Rotations of Vectors

We now tackle head-on the problem of the angular momentum of a vector field. We do this by finding the effect of small rotations on components of a vector. Since—according to the fundamental definitions in Section 3.1—operator J_i generates infinitesimal rotations about axis i (x , y , or z), we will then have determined the angular momentum properties of vectors. The results may be difficult to recognize, since they are obtained in a spherical basis, requiring a unitary transformation to recover the Cartesian basis. We therefore derive the connection between the two bases.

Transforming a Vector by Small Rotations. Suppose that we have a field of vectors. That is, at each point in space $\mathbf{r} = (x, y, z)$ there is defined a vector $\mathbf{V}(\mathbf{r}) = \mathbf{V}(x, y, z) = [V_x(x, y, z), V_y(x, y, z), V_z(x, y, z)]$. We assume that each of the functions V_x , V_y , and V_z is differentiable everywhere. Under a small rotation about an axis the behavior of \mathbf{V} will be quite complicated, since each spatial function V_x , V_y , and V_z will change under an orbital angular momentum operator, as proved in Section 3.2.1. Moreover, as vector components, these three functions will become mixed; this will be the spin of the vector field. Before becoming involved in the algebra of this problem, envision the situation, which is sketched in Figure 4.11 for rotation about the z axis.

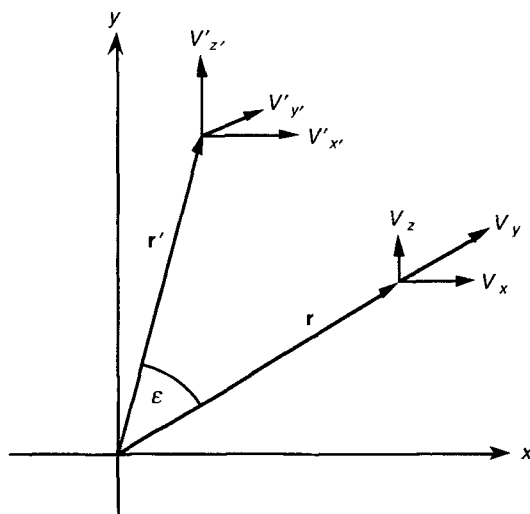


FIGURE 4.11 A vector field, with $\mathbf{V} = (V_x, V_y, V_z)$ at \mathbf{r} , is rotated through (small) angle ϵ about the z axis to \mathbf{r}' . After rotation the vector is $\mathbf{V}' = (V'_x, V'_y, V'_z)$.

Under rotation the vector \mathbf{r} is transformed into \mathbf{r}' and \mathbf{V} at \mathbf{r} is transformed into \mathbf{V}' at \mathbf{r}' . Although the lengths r and r' are equal, the three components of \mathbf{V} and of \mathbf{V}' are not so simply related, as suggested in Figure 4.11. It is our task to find the relations.

Recalling that angular momentum operators perform infinitesimal rotations (Section 3.1.2), it is sufficient to carry all calculations to only first order in the rotation angle ε , and eventually to let $\varepsilon \rightarrow 0$. In terms of the J_z operator, we can then use (3.1) to write

$$U(\varepsilon, \hat{\mathbf{z}}) \approx \mathbf{1} - i\varepsilon J_z \quad (4.49)$$

The matrix transforming the components of a vector when it is actively rotated through a small angle ε about the z axis is given approximately by

$$\mathbf{A}_z(\varepsilon) \approx \mathbf{1}_3 + \begin{bmatrix} 0 & -\varepsilon & 0 \\ \varepsilon & 0 & 0 \\ 0 & 0 & 0 \end{bmatrix} \quad (4.50)$$

where we begin with (1.14) for the matrix and expand to first order in ε . In (4.50) $\mathbf{1}_3$ denotes the 3×3 unit matrix. If we arrange the elements of \mathbf{V} in a 3-row column matrix we can write the rotated vectors for small ε as

$$\mathbf{V}'(\mathbf{r}') \approx \mathbf{A}_z(\varepsilon)\mathbf{V}(\mathbf{r}) \quad \mathbf{r}' \approx \mathbf{A}_z(\varepsilon)\mathbf{r} \quad (4.51)$$

which can be simplified to

$$\mathbf{V}'(\mathbf{r}') \approx \mathbf{A}_z \mathbf{V}(\mathbf{A}_z^{-1} \mathbf{r}') \quad (4.52)$$

for any value of \mathbf{r}' . In particular, since we want the change of the vector itself under the small rotation (*intrinsic* spin), we can replace \mathbf{r}' by \mathbf{r} . The result may be equated to the action on \mathbf{V} of U from (4.49) in a matrix representation, to obtain

$$(\mathbf{1}_3 - i\varepsilon \mathbf{J}_{z3})\mathbf{V}(\mathbf{r}) \approx \mathbf{A}_z \mathbf{V}(\mathbf{A}_z^{-1} \mathbf{r}) \quad (4.53)$$

where \mathbf{J}_{z3} is a 3×3 matrix representation of J_z applied to a vector field.

We can find the matrix representation by first making a Taylor expansion of each component of \mathbf{V} about \mathbf{r} , then using $\mathbf{A}_z^{-1}(\varepsilon) \approx \mathbf{A}_z(-\varepsilon)$. As Problem 4.10 suggests that you work out, one obtains directly

$$V_i(\mathbf{A}_z^{-1} \mathbf{r}) \approx V_i(\mathbf{r}) + \varepsilon \left(y \frac{\partial V_i}{\partial x} - x \frac{\partial V_i}{\partial y} \right) \quad i = x, y, z \quad (4.54)$$

Thus, the action of \mathbf{A}_z on the components of \mathbf{V} is given from (4.50) as

$$V'_x \approx V_x - \varepsilon V_y \quad V'_y \approx V_y + \varepsilon V_x \quad V'_z = V_z \quad (4.55)$$

Finally, we combine this with (4.54) and equate the result to (4.53) in the limit $\varepsilon \rightarrow 0$, to obtain an expression for the representation of J_z applied to a vector field, namely

$$\mathbf{J}_{zV} = -i \left(x \frac{\partial}{\partial y} - y \frac{\partial}{\partial x} \right) \mathbf{1}_3 + \mathbf{S}_{zV} \quad \mathbf{S}_{zV} \equiv \begin{bmatrix} 0 & -i & 0 \\ i & 0 & 0 \\ 0 & 0 & 0 \end{bmatrix} \quad (4.56)$$

We recognize the first part as the z component of the orbital angular momentum operator L_z derived in Section 3.2, which takes care of the change of each component, as in (4.55). What is the remaining matrix \mathbf{S}_{zV} ? To answer this, consider its eigenvectors and eigenvalues, as follows.

Eigenvectors and Eigenvalues of the Vector Spin. Suppose that \mathbf{V} , written as a column vector with three elements V_x, V_y, V_z , is an eigenvector of \mathbf{S}_{zV} with eigenvalue μ . By setting $\det(\mathbf{S}_{zV} - \mu \mathbf{1}_3) = 0$ we find that the eigenvalues are $\mu = 0$ and $\mu = \pm 1$. The elements of the eigenvectors are then obtained by writing out the elements of the matrix equation $\mathbf{S}_{zV} \mathbf{V} = \mu \mathbf{V}$, to find that

$$\mu V_x = -i V_y \quad \mu V_y = -i V_x \quad \mu V_z = 0 \quad (4.57)$$

Substituting each eigenvalue in turn gives the eigenvectors of \mathbf{S}_{zV} as

$$\begin{aligned} \mu = \pm 1: \quad \mathbf{V} &= V_{\pm} (\hat{\mathbf{e}}_x \pm i \hat{\mathbf{e}}_y) \\ \mu = \pm 0: \quad \mathbf{V} &= V_0 \hat{\mathbf{e}}_z \end{aligned} \quad (4.58)$$

in which the normalizations V_{\pm} and V_0 are arbitrary. One might as well choose them so that the eigenvectors coincide with the spherical-basis unit vectors (4.38), that is, $V_{\pm} = \mp 1/\sqrt{2}$ and $V_0 = 1$. Thus, in the representation (4.56) for \mathbf{S}_{zV} the eigenvectors are spherical-basis vectors, while the eigenvalues μ are those of a spin-1 system.

So, one operator down and two to go. Our preceding development does not use any special property of the z axis. By cyclic substitution among x, y , and z , therefore we obtain the corresponding x - and y -axis matrices. The eager reader will verify (Problem 4.10) that the triplet of matrices forms a representation (in the group-theory sense, Section 2.5.3) of the angular momentum operators, in that they satisfy the fundamental relations (3.6). Further, $\mathbf{S}_V^2 \equiv \mathbf{S}_{xV}^2 + \mathbf{S}_{yV}^2 + \mathbf{S}_{zV}^2$ has eigenvalue $2 = 1(1+1)$, showing (together with the eigenvalues $\mu = \pm 1, 0$) that we have a system with a spin of 1.

Our interpretation of (4.56) plus corresponding x and y formulas is now almost complete. The first part is orbital angular momentum \mathbf{L} , describing transformation of each component of the vector under small rotations. The second part, \mathbf{S}_V , is intrinsic to every vector; it describes mixing of components among themselves under small rotations. Following the discussion in Section 3.5 of reference frames in relation to spin and orbital angular momenta, it is appropriate to call \mathbf{S}_V the intrinsic spin operator for a vector field.

Diagonalizing the Spin Matrix. The remaining part of our analysis of angular momentum of vectors is to tidy up the spin matrices, in particular to diagonalize \mathbf{S}_{zV} . This should produce the $j = 1$ matrices in the Cartesian basis, as given in (3.64)–(3.66). By noting that matrix \mathbf{U}_V in (4.39) transforms from Cartesian to spherical-basis unit vectors, and that a vector is expanded in terms of the *complex conjugates* of the latter, according to (4.43), the appropriate matrix is seen to be \mathbf{U}_V^* . Thus, as you can verify by working Problem 4.10, we obtain the diagonal form

$$\mathbf{U}_V^* \mathbf{S}_{zV} [\mathbf{U}_V^*]^{-1} = \begin{bmatrix} 1 & 0 & 0 \\ 0 & 0 & 0 \\ 0 & 0 & -1 \end{bmatrix} \quad (4.59)$$

which leaves the eigenvalues unchanged, as required. The same similarity transformation applied to \mathbf{S}_{xV} and \mathbf{S}_{yV} produces the other $j = 1$ matrices, (3.64) and (3.65), respectively. This transformation applied to the orbital part of (4.56)—and corresponding x and y expressions—leaves them unchanged, since they are proportional to the unit matrix.

To summarize our results for the angular momentum operators appropriate to describe small-angle rotations of vectors; the operator for any vector is \mathbf{J}_V given by

$$\boxed{\mathbf{J}_V = \mathbf{L} + \mathbf{S}_V} \quad (4.60)$$

in which \mathbf{S}_V is a spin-1 operator acting on the components of the vector.

The peculiar case of the displacement vector \mathbf{r} , which we show in (4.48) is isotropic (thus $j = 0$), is such that the transformation of each coordinate by \mathbf{L} is just canceled by the transformation among its components that is made by \mathbf{S}_V . The converse to our result—that all spin-1 fields are described by vector fields—is *not* valid. For example, deuterons and ^{14}N nuclei have $j = 1$, but they are composite objects whose constituents combine to produce this angular momentum.

4.2.3 The Electromagnetic Field and Photons

The derivations made above show that *any* field described by vectors necessarily has intrinsic spin of unity associated with it. In particular, Maxwell's equations for electromagnetism (Section 1.4.3) are vector equations (for example, those describing \mathbf{E} and \mathbf{B} or the vector potential \mathbf{A}). The electromagnetic field must therefore be a spin-1 field. In this context, the vectors for circular polarization correspond to the spherical-basis vectors in Section 4.2.1, as described in Chapters 3 and 14 of Dodd's text on atoms and light [Dod91].

Angular Momentum and Light. In both classical and quantized electromagnetic field theory there is angular momentum associated with the field. A clear description

of spin in the electromagnetic field, requiring only straightforward use of Maxwell's equations, is given in an article by Ohanian [Oha86]. He shows that the ratio of intrinsic spin to energy is $1/\omega$, where ω is the angular frequency of an approximately monochromatic wave representing the electromagnetic field. Thus, if the energy is quantized in units of $\hbar\omega$, the spin will be quantized in units of \hbar .

Light also imparts mechanical angular momentum, the observable quantity being the helicity (Section 1.2.1). This was first demonstrated in an experiment by Beth [Bet36]. The details of angular momentum for the quantized electromagnetic field and its multipole decomposition are subtle. They have been elucidated by Morette-de Witt and Jensen [Mor53b] and are summarized in Section 7.6 of Biedenharn and Louck [Bie81a].

4.3 SPIN EIGENSTATES AND THEIR REPRESENTATIONS

Our purpose in this section is twofold. First, we aim to give a more refined discussion of the concept of spin than provided in Section 3.5, where the treatment is formal and discussion of spin in quantal systems is cursory. In Section 4.3.1 we survey how properties of dynamical systems are discovered and described. Then, as in the original treatment by Pauli [Pau27], we show how spin can be introduced in the Schrödinger equation.

Second, we aim to describe eigenstates of intrinsic spin, both through the common representation in terms of column matrices (Section 4.3.2) and through spinor-space representations (Section 4.3.3). A preliminary treatment of the algebra of spin-1/2 operators and eigenvectors—in terms of Pauli matrices and 2×1 column vectors, as well as spinor space—is given in Section 3.3. Finally, in Section 4.3.4, we show how spin modifies the time-reversal operator (Section 1.4.2) applied to the Schrödinger equation.

4.3.1 What Is Spin?

In Section 3.5 we discuss spin and orbital angular momenta from the viewpoint of the effect of an infinitesimal rotation of the system. If the system has internal degrees of freedom, collectively denoted by ξ , then the spin operator \mathbf{S} describes the effect of rotation on these internal degrees of freedom. This is to be contrasted with the orbital operator, \mathbf{L} , which describes behavior under small rotations of the coordinates of the center of mass of the system or some other representative point in it.

It probably surprises students, and shocks pedagogues, that we characterize (Figure 3.12) the ring system of the planet Saturn as an intrinsic spin. This is, however, consistent with our definition of spin. Thus, spin is just that part of the total angular momentum which is not described in detail. A constraint on the use of the term is that (as discussed in Section 3.5) the spin operator \mathbf{S} and the orbital operator \mathbf{L} are assumed to commute. For example, it is probably a very good approximation to assume that the spin operator for the rings of Saturn is independent of the orbital operator that describes rotation of Saturn about the sun. A coupling

between **S** and **L** that is conceivable in principle but negligible in practice is the differential effect of solar gravity (a tidal effect) on elements of the rings.



From the present viewpoint of spin, as one gradually discovers more of the internal dynamics and describes in more detail the inner workings of a system, its “spin” gradually fades away. Eventually—like the Cheshire cat of Lewis Carroll’s *Alice’s Adventures in Wonderland* [Car65]—no more than its smile remains.

To clarify ideas about spin, we summarize in Table 4.6 the typical progress of discovery for physical systems.

TABLE 4.6 The progress of discovery for five types of systems, with examples of such systems given in the second row. Properties are often discovered in about the order given by the four categories in the leftmost column.

System:	Mechanical	Electro-magnetic	Atomic	Nuclear	Particle
Category:	<i>Earth</i>	<i>Electro-magnetism</i>	<i>Electron states</i>	<i>Deuteron</i>	<i>Proton</i>
Observations and symmetries	Sun-centered orbits; daily rotation of Earth	Coulomb, Ampère, and Faraday laws	Spectroscopy; spins and parities	Spin, parity, mass, binding energy	Charge, mass, spin, parity
Phenomenology	Figure and structure of Earth; magnetism	Maxwell equations; radiation fields	Schrödinger equation plus spin-orbit coupling	Quadrupole and dipole moments; RMS radius	Charge and magnetism distributions
Dynamics	Equilibrium of cooling liquid; dynamics of core	Quantized fields and photons	Dirac equation; spin and effects of relativity	Neutron-proton interaction	Quark models of the proton and neutron
Generalizations	Structure of planets; formation of solar system	Electroweak interaction; parity violation	Quantum electro-dynamics	Meson and quark models of nucleon-nucleon force	Quark models of the strong interaction

From Observations and Symmetries to Dynamics. Table 4.6 shows steps commonly followed in the physical sciences when discovering properties, especially those at the microscopic and quantum levels. To make the generality of the approach clear, however, we give a macroscopic example similar to that for the rings of Saturn in Section 3.5, namely the dynamics of the spinning Earth. We also include the electromagnetic field, following Sections 1.4.3 and 4.2.2.

To follow the successive refinement of understanding properties of a physical system, consider in Table 4.6 the “Atomic” column. Historically and conceptually, the understanding of electron states in atoms (atomic structure) usually begins with *observations* (atomic spectroscopy experiments) on light emission from excited states of atoms and the use of *symmetries* (rotation and parity) to obtain “quantum numbers,” which we recognize as the eigenvalues of the symmetry operators.

The next step is to combine refined experiments with model equations, in which some components are *ad hoc*. In such *phenomenology* the states of an atom may be described by a Schrödinger equation in which electrons have a spin-orbit interaction, which produces the fine structure of the energies of atomic states. (We discuss the algebra of this in Section 7.1.3.) At this phenomenological stage, hyperfine coupling will be described in terms of the magnetic moments of the nucleus and electron. A more-detailed description of the *dynamics*—such as the Dirac equation—includes the effects of relativity and the relation between spin-orbit coupling and the spin-independent central Coulomb potential. A *generalization* of this description—quantum electrodynamics—includes consistently the interaction between electrons and photons, as well as the self-energy of electrons.

The refinement of comprehension that progresses from observations and discovery of symmetries, through phenomenology and dynamics, to generalizations, can also be traced for the other system examples in Table 4.6. The progress of discovery is neither uniform nor as clearly divided as these examples suggest. You can check this by tracing through an example yourself, as suggested in Problem 4.11.

Note that the level of detailed explanation one provides, and therefore the question of what part of the system is the spin, depends upon the task at hand. For example, in nuclear magnetic resonance (NMR) studies, where a nucleus as a whole participates in electromagnetic interactions predominantly through its magnetic dipole moment (as we describe in Sections 5.1.3 and 8.4.3), it is sufficient to know the spin and gyromagnetic ratio values of the nucleus. On the other hand, the nuclear structure physicist seeks a more detailed understanding, trying to explain the spin of the nucleus in terms of orbital motions and intrinsic spins of neutrons and protons. At a deeper level, a nuclear or particle physicist models these nucleon spins in terms of constituent quarks and gluons. Interestingly, particles that by present understanding appear to be elementary have spins between 0 and 2 [Geo82].

With this introduction to the concept of spin, let us work through a concrete example in quantum mechanics, showing how spin arises in a nonrelativistic context, namely in the Schrödinger equation.

Spin in the Schrödinger Equation. We adapt a discussion by Halprin [Hal78] that is very similar to the procedure first used by Dirac [Dir28] to introduce spin in

the relativistic Klein-Gordon equation. Consider a free particle with mass m and energy E that is described by a time-independent Schrödinger equation:

$$(\hbar^2 \nabla^2 + 2mE)\psi = 0 \quad (4.61)$$

Introduce an operator, σ , which is independent of space and time, and which has three components labeled by the Cartesian coordinates; $\sigma = (\sigma_x, \sigma_y, \sigma_z)$, then factorize (4.61) according to

$$\sum_{j,k} \left(\hbar \sigma_j \frac{\partial}{\partial x_j} - i\sqrt{2mE} \right) \left(\hbar \sigma_k \frac{\partial}{\partial x_k} + i\sqrt{2mE} \right) \psi = 0 \quad (4.62)$$

in which j and k each run over the x , y , and z coordinates. It is straightforward to show, as in Problem 4.12, that if

$$\sigma_j^2 = I \quad j = x, y, z \quad (4.63)$$

in which I denotes the unit operator, and if also

$$\sigma_j \sigma_k + \sigma_k \sigma_j = 0 \quad j \neq k \quad (4.64)$$

then the Schrödinger equation is recovered. If we now consult matrix representations for various spins, j , as given in Section 3.3.1 for the Pauli matrices and in Table 3.1, we see that requirements (4.63) and (4.64) are satisfied by the Pauli matrices characterizing $j = 1/2$. Indeed, a very similar procedure to that described here was used in nonrelativistic quantum mechanics by Pauli [Pau27] to describe an electron in a constant magnetic field and in a Coulomb field. Thus, by writing the Schrödinger equation in form (4.62), we have included the degrees of freedom of a spin-1/2 system. Note that it is common not to distinguish between the *operators* appearing in the preceding three equations and their representations by *matrices*.

The relation between spin and nonrelativistic quantum mechanics has been examined in terms of the Galilei group and Galilean invariance by Lévy-Leblond [Lév71]. He and others point out that the prediction of an electron g -factor of 2 does not require a relativistic wave equation such as Dirac's, although it is consistent with such. Lévy-Leblond discusses derivation of the Pauli equation—a nonrelativistic limit of the Dirac equation—using an extension of the method we use. In spite of the long history of such developments, textbooks of quantum mechanics usually claim that spin is a mysterious relativistic effect. An exception is the text by Bialynicki-Birula et al. [Bia92], where a clear derivation of the Pauli equation is given in Chapter 10. It was probably the outstanding success of Dirac's discovery [Dir28], especially its prediction of positrons, that eclipsed other descriptions of spin.

A comprehensive treatment of the Dirac equation is given in Landau's text [Lan90]. In Chapter 15 he describes the reduction to nonrelativistic approxima-

tions, such as the Schrödinger equation. A derivation of spin as circulation of energy in the wave field is given for the Dirac equation in the article by Ohanian [Oha86]. His treatment parallels the one he provides for the electromagnetic field, mentioned at the end of Section 4.2.3.

Spin and the Conservation of Angular Momentum. As a further development of spin that is relevant to the Schrödinger equation, consider the effect of a spin-orbit interaction on the rotational symmetry of the Hamiltonian. Write the Hamiltonian for a spin-half particle as

$$H = H_0 + H_{so} \mathbf{L} \cdot \mathbf{S} \quad (4.65)$$

where \mathbf{L} is the orbital angular momentum operator, which commutes with the space-independent spin operator, $\mathbf{S} = \sigma/2$. The Hamiltonian component H_0 is assumed to be of the form

$$H_0 = -\frac{\hbar^2}{2m} \nabla^2 + V_0(r) \quad (4.66)$$

which commutes with both \mathbf{L} and \mathbf{S} . The spin-orbit component H_{so} is also assumed to be rotationally invariant; for example, it can depend on the distance r or on the magnitude of the momentum, but not on angles.

Consider a component of \mathbf{L} , say L_x . As Problem 4.13 invites you to show, there are two nonzero commutators:

$$[H, L_x] = -iH_{so} (L_y S_z - L_z S_y) = -[H, S_x] \quad (4.67)$$

so that H commutes with $L_x + S_x$. Because the choice of the x component is arbitrary, the total angular momentum operator

$$\mathbf{J} = \mathbf{L} + \mathbf{S} \quad (4.68)$$

commutes with the spin-orbit Hamiltonian (4.65). Therefore, the eigenstates constructed from components of \mathbf{J} (but not those of \mathbf{L} or \mathbf{S} separately) are constants of the motion.

We develop the topic of spin-orbit coupling further in Section 7.1.3, where we consider the energy splitting under spin-orbit coupling, while in Section 7.3.1 we devise wave functions suitable for describing eigenstates of such Hamiltonians.

4.3.2 Intrinsic Spin Eigenstates

Now that we understand what spin is, we can specify intrinsic spin eigenstates. We discuss first the column-matrix representations, then (Section 4.3.3) we describe the spinor-space representations. In general, there will be no “coordinates” such as

\mathbf{r} or $(\theta\phi)$ in these eigenstates. Thus, you notice that there are many illustrations in Section 4.1 (orbital eigenstates and spherical harmonics), but there are very few in this and the preceding sections. Eigenstates may be labeled either with a symbol—such as ξ —to indicate that there are internal degrees of freedom, or sometimes this is indicated by using different symbols for different spin eigenstates.

Matrix Representations of Spin Eigenstates. It is often convenient to use matrix representations of spin eigenstates, especially since spin operators are usually expressed in matrix form (Sections 3.3, 3.4). In the former section we have a preliminary treatment of the algebra of spin-1/2 operators and eigenvectors, both in terms of Pauli matrices and 2×1 column vectors, as well as in terms of spinor space. We now generalize to the column-vector representation for arbitrary spin.

For the $j = 1/2$ case, the derivation in Section 3.3.2 shows that

$$\chi_+ = \begin{bmatrix} 1 \\ 0 \end{bmatrix} \quad \chi_- = \begin{bmatrix} 0 \\ 1 \end{bmatrix} \quad (4.69)$$

are orthonormal eigenvectors of the Pauli matrix σ_z , and therefore of the spin-1/2 matrix for z , since the spin matrices are just one half the Pauli matrices, according to (3.30). The spin projections in (4.69) are $m = \pm 1/2$ for χ_{\pm} , respectively. In Section 3.4.4 we have the operator matrices for $j = 1/2, 1,$ and $3/2$ (Table 3.1), with the corresponding eigenvectors χ_m of the J_z matrices in Table 3.2.

As is clear from these examples, the column-matrix representation for the eigenvector of \mathbf{J}^2 having eigenvalue $j(j+1)$ and of J_z having eigenvalue m is χ_{jm} given by

$$\chi_{jm} = \begin{bmatrix} \delta_{j,m} \\ \delta_{j-1,m} \\ \vdots \\ \delta_{-j,m} \end{bmatrix} \quad (\chi_{jm^*})_{m'} = \delta_{m',m^*} \quad (4.70)$$

Detailed proof of this and related results is suggested as Problem 4.14. In (4.70) the conventional labeling of angular momentum matrices—largest m values at the top—is followed. There is no reference to any spatial coordinates in these matrix representations. This makes them ideally suited for describing the rotational properties of systems whose internal workings we either do not wish to describe or do not know how to describe, as discussed in Sections 3.5 and 4.3.1.

Combining Orbital and Spin States. When combining orbital and spin states there are mathematical niceties that we should acknowledge, then put to rest. The orbital eigenstates covered in Section 4.1 are *scalar functions* of θ and ϕ , such as $Y_{\ell m}(\theta\phi)$, whereas the spin eigenstates are *matrices*. Therefore, whereas we often write $\mathbf{J} = \mathbf{L} + \mathbf{S}$ for combining the operators, mathematically more correct is

$$\mathbf{J} = \mathbf{L} \otimes \mathbf{1}_S + \mathbf{1}_L \otimes \mathbf{S} \quad (4.71)$$

in which $\mathbf{1}_S$ is a unit operator in the spin space, $\mathbf{1}_L$ is a unit operator in the orbital space, and \otimes denotes the direct product described in Section 2.1.2. The space in which \mathbf{J} acts is therefore the direct-product space of those of \mathbf{L} and \mathbf{S} . For example, the vector field equation (4.60) could be rewritten more completely in this way.

What happens to the eigenstates in such a direct-product space? As discussed in Section 2.1.2, every element in the spin space can be multiplied by any element in the orbital space. We follow up on this idea in Chapter 7 when constructing appropriate eigenstates of the combined system.

4.3.3 Spinor-Space Representations

In Section 2.4 we introduce spinors and their properties, particularly the spinorial nature of fermion wave functions in quantum mechanics, while angular momentum operators in spinor representation are introduced in Section 3.3.4. We now show how such representations can be used to describe spin eigenstates. As a relief from the mathematics of the preceding sections, we introduce the spinor representation with a pictorial view, shown in Figure 4.12.

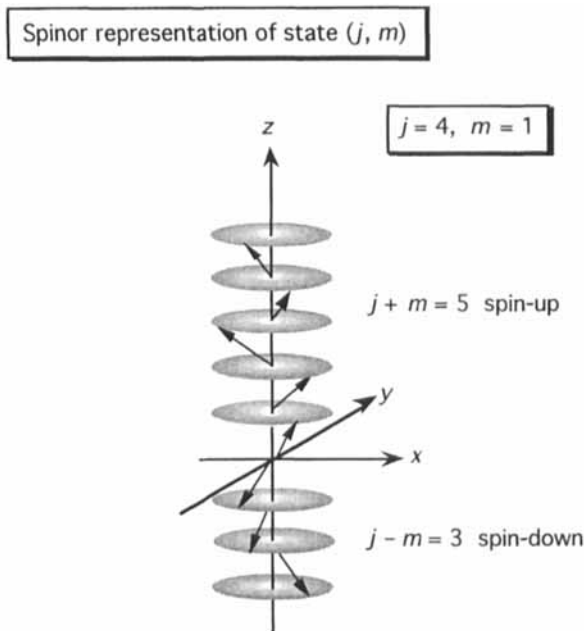


FIGURE 4.12 Semiclassical vector model view of the spinor-space representation of a state with total angular momentum number $j = 4$ and projection number $m = 1$; thus there are $j + m = 5$ spin-up spinors and $j - m = 3$ spin-down spinors. For the spinor vectors their lengths are in the appropriate proportion, $\sqrt{3}$, to their projections.

In the figure each arrow and disk represent a spin-1/2 angular momentum vector precessing uniformly about the z axis so that the diagonal elements (expectation values) of the x and y components of the angular momentum are zero, while the z -component values are either $+1/2$ (spin-up) or $-1/2$ (spin-down). This picture—the semiclassical vector model—we develop extensively in Section 5.3.

The mathematics corresponding to Figure 4.12 is as follows. Represent each of the $j+m$ spin-up states by spinor χ_+ and each of the $j-m$ states by χ_- . It is straightforward to show, as Problem 4.15 suggests trying, that the *spinor-space representations* given by

$$u(jm) = \frac{\chi_+^{j+m} \chi_-^{j-m}}{\sqrt{(j+m)! (j-m)!}} \quad (4.72)$$

are orthonormal and behave under the angular momentum operators as eigenfunctions of J^2 and J_z with eigenvalues $j(j+1)$ and m , respectively. These are the states labeled as (j, m) .

These spinor-space representations are very useful. Spin-1/2 operators and eigenfunctions can be used to generate those for arbitrary spin, as shown originally by Majorana [Maj32], as we describe in Section 5.1.3. They enable clear and concise determination of rotation matrices (Section 6.2.3) and of coupling coefficients (Section 7.2.3). They have the further advantage of being easy to visualize (as in Figure 4.12), especially when used in quantum mechanics with the semiclassical vector model (Section 5.3). Note that actual states of spin-1/2 particles (such as electrons and nucleons) must additionally include the effects of the Pauli principle (Section 1.4.4).

4.3.4 Time Reversal and Spin

In Section 1.4.2 the effect of time reversal ($t \rightarrow -t$) on systems in classical and quantum mechanics is introduced. There we discuss some consequences of time reversal for angular momentum, but discussion of time-reversal properties of angular momentum states is deferred. We now consider this topic, which has important consequences for systems of spin-1/2 particles—particularly the Kramers degeneracy for electron states in atoms.

We adapt a treatment by Brink and Satchler [Bri94, Section 4.9], which is sufficient for our needs. The original treatment by Wigner [Wig31, Chapter 26] is much more detailed, while the analysis in Elliott and Dawber's text [Eli79, Sections 15.7.4, 15.7.5] uses group theory methods in a relativistically covariant description.

Time Reversal and Angular Momentum Eigenstates. We assume that the time-reversal property that is appropriate for the angular momentum operator \mathbf{J} is the same as for classical angular velocity (Table 1.4) and angular momentum. This be-

havior is not obvious, since we define (Section 3.1) \mathbf{J} in terms of infinitesimal rotations, with no explicit reference to time. We therefore write

$$\Theta \mathbf{J} \Theta^{-1} = -\mathbf{J} \quad (4.73)$$

The angular momentum operators in the spherical basis (Sections 3.1.3, 3.4.2) therefore have the following action on the time-reversed states $\Theta|jm\rangle$:

$$\begin{aligned} J_0 \Theta|jm\rangle &= -\Theta J_0|jm\rangle = -m \Theta|jm\rangle \\ J_{\pm 1} \Theta|jm\rangle &= -\Theta J_{\mp 1}|jm\rangle = -\sqrt{(j \mp m + 1)(j \pm m)} \Theta|jm \mp 1\rangle \end{aligned} \quad (4.74)$$

in which the sign reversal between the ladder operators arises from complex conjugation in (3.10).

Suppose that a system has a time-reversal-invariant Hamiltonian, H ; then we can choose eigenstates of H , \mathbf{J}^2 , and J_z such that

$$\Theta|jm\rangle = (-1)^{p-m} |j, -m\rangle \quad (4.75)$$

since then (4.74) is satisfied for any p . This unspecified exponent is usually chosen as $p = j$, which makes combined angular momenta (Chapter 7) satisfy (4.75) if the component angular momenta have this time-reversal property. Thus, we write time-reversed angular momentum eigenstates as

$$\Theta|jm\rangle = (-1)^{j-m} |j, -m\rangle \quad (4.76)$$

If the time-reversal operator is applied twice, we then obtain

$$\begin{aligned} \Theta^2|jm\rangle &= (-1)^{2m}|jm\rangle = (-1)^{2j}|jm\rangle \\ &= \begin{cases} |jm\rangle & j \text{ an integer: } 0, 1, \dots \\ -|jm\rangle & j \text{ a half integer: } 1/2, \dots \end{cases} \end{aligned} \quad (4.77)$$

in which the second equality in the top line follows from the phase manipulation rules in Section 2.1.4. Notice that introduction of the negative sign in (4.77) does not contradict intuition that scalar products of time-reversed states should be invariant. The sign has an immediate consequence for a many-particle system.

Systems of Particles: Kramers Degeneracy. Suppose that we have a system of N particles, each of spin s . The state vector of the system can be written in terms of direct products (Section 2.1.2) of one-particle states of the type (4.77); then these can be further decomposed (Chapter 7) into products of orbital and intrinsic-spin states. Under Θ^2 each orbital state gives a positive sign in (4.77), whereas each

spin state gives a factor of $(-1)^{2s}$, thus a positive sign for integer spins (such as deuterons) and a negative sign for half-integer spins (such as electrons). For N such particles the system state $|sN, M\rangle$ therefore has the time-reversal property

$$\Theta^2 |sN, M\rangle = (-1)^{2sN} |sN, M\rangle \quad (4.78)$$

Therefore, for a time-reversal-invariant Hamiltonian the system will have two states of the same energy if sN is a half integer, that is, if s is a half integer and N is odd.

For example, an electron system with an *odd* number of electrons has (assuming time-reversal invariance of its Hamiltonian) a double degeneracy of its energy eigenvalues. This result is called Kramers' theorem or *Kramers' degeneracy*, after its discoverer [Kra30]. Notice that—and this applies particularly to atomic nuclei—attempting to hide the degeneracy by clustering the particles into higher-spin subsystems will not succeed, since only the product $sN = (sn)(N/n)$, where n is the number of particles in a cluster (assumed to be a factor of N), is operative in (4.78).

Our mention of angular momentum in a quantized field in Section 4.2.3 and our discussion of spin-1/2 states in this section lead us to inquire further into the role of angular momentum in quantum systems. We have been remarkably silent on this subject, except for discussing discrete symmetries and quantum systems in Section 1.4 and introducing the distinction between geometrical and dynamical angular momentum in Section 3.4.5. Now that we have covered the basic material on rotational symmetries in Chapter 3 and this chapter, we should be ready, willing, and able to consider angular momentum in quantum systems, which is the main topic of Chapter 5.

PROBLEMS ON ANGULAR MOMENTUM EIGENSTATES

4.1^M Evaluate analytically the Legendre functions for $0 \leq \ell \leq 4$ and all relevant m , as in Table 4.1, by using the built-in *Mathematica* functions `LegendreP[ℓ , c]` for the polynomials, or `LegendreP[ℓ , m , c]`, which can be used for both the polynomials ($m = 0$) and the associated functions ($m \neq 0$). To obtain the forms in Table 4.1, the substitution $\sqrt{1-c^2} = s$ will need to be made, since $c = \cos\theta$ and $s = \sin\theta$.

4.2^M Work out the analytical and numerical properties of the Legendre functions for $\ell = 2$, similarly to the examples in Figures 4.4 and 4.5 for $\ell = 3$. If you have access to *Mathematica*, use the notebook `PLM` in Appendix I to derive the formulas and present visualizations of the three distinct functions $P_2^m(\cos\theta)$ for $m = 0, 1, 2$. Interpret your results from the viewpoint of classical angular momentum.

4.3 To determine the θ dependence for the stretched- m spherical harmonic function $Y_{\ell\ell}(\theta\phi)$, replace the ϕ dependence in (4.12) by i^ℓ , then transform the variable to $\sin\theta$. Show that you have a separable differential equation in this variable, which for $\ell > 0$ can be integrated directly to produce the $\sin^\ell\theta$ dependence of $Y_{\ell\ell}$ on θ .

4.4 Calculate the integral for the normalization of the m -stretched spherical harmonic, I_ℓ given by (4.13), as follows.

(a) Integrate I_ℓ by parts, integrating on the $\sin\theta$ factor and differentiating on the 2ℓ power of $\sin\theta$. Thus derive the recurrence relation

$$I_\ell = \frac{2\ell}{2\ell+1} I_{\ell-1} \quad \ell > 0 \quad (4.79)$$

(b) Show by direct integration that $I_0 = 2$, then use upward recurrence on ℓ repeatedly in (4.79), inserting factors in the numerator and denominator until suitable factorials are obtained. Thus obtain (4.13).

4.5 Consider the spherical harmonic addition theorem (4.24).

(a) Show the steps between (4.22) and (4.23).

(b) Starting with the addition theorem (4.23), derive the sum rule (4.24).

(c) Verify the sum rule (4.24) for $\ell = 2$ by using the spherical harmonics in Table 4.2. The symmetry (4.19) shows that it is sufficient to add the $m = 0$ term to twice the sum over the $m > 0$ terms.

4.6^M Figure 4.8 displays three tori illustrating the m and ϕ dependences in the exponential factor $e^{im\phi}$ of the spherical harmonic $Y_{\ell m}(\theta, \phi)$.

(a) Show that in cylindrical coordinates in which ϕ is the azimuthal angle, the minor radius of the torus, r , is given by

$$r(\phi) = \cos(m\phi) \quad (4.80)$$

if we assume unit radius at $\phi = 0$. Thence show that the Cartesian coordinates of a point on the torus are given by

$$x = [R + r(\phi)\cos t]\cos\phi \quad y = [R + r(\phi)\cos t]\sin\phi \quad z = r(\phi)\sin t \quad (4.81)$$

in which R is the major radius of the torus and the angle t parametrizes the circular cross section of the torus, $0 \leq t \leq 2\pi$.

(b) Show that the real and imaginary parts in $e^{im\phi}$ are described by tori that differ in magnitude merely by rotation about the z axis through $\pi/(2m)$.

(c) Sketch the torus for various values of m . If you have access to *Mathematica* the notebook EXPIMPHI is useful for this.

4.7^M Consider the spherical harmonics in Figure 4.9, $Y_{32}(\theta\phi)$ and $Y_{63}(\theta\phi)$, and the way in which they tessellate the unit sphere.

(a) Use *Mathematica* notebooki PLM to derive the formulas for $P_3^2(\cos\theta)$ and $P_6^3(\cos\theta)$, and to make a two-dimensional plot of each function so that you can locate its zeros approximately. Determine the signs of the θ (zone) dependence of these $Y_{\ell m}$.

(b) In Figure 4.9 we consider the imaginary parts of the two spherical harmonics,

thus a ϕ dependence $\sin(m\phi)$, and we view the hemisphere with $\pi \leq \phi \leq 2\pi$. Determine the signs of the ϕ (sector) dependence of the $Y_{\ell m}$.

(c) Combine the signs of the θ and ϕ dependences to verify the signs of the two tesseral harmonics in Figure 4.9.

4.8 The spherical harmonics are related to those in real form by (4.33). Use these relations in the spherical harmonic addition theorem (4.23) to derive the real form of the addition theorem, (4.34). Show that the symmetry properties between m and $-m$ of the terms that depend on ϕ result in no cross terms between the different κ terms.

4.9 Prove the following properties of matrices, vectors, and operators for the spherical basis:

(a) Verify the unitarity of the matrix \mathbf{U}_V in (4.39).

(b) Prove the scalar-product relation (4.41) for the three projections of ± 1 and 0.

(c) Check the vector-product relations (4.42) for the three projections.

(d) Verify that the angular momentum results (4.47) agree with (3.60) for $j = 1$ and $m = \sigma$, with $\sigma = \pm 1$ or 0.

4.10 Consider the algebra of deriving the infinitesimal rotations of vectors.

(a) Show in detail the steps leading from (4.53) to (4.56).

(b) Use the determinant equation given in the text to show that the eigenvalue equation is $\mu(\mu^2 - 1) = 0$, so that the eigenvalues are $\mu = 0, \mu = \pm 1$.

(c) Obtain the spin matrices for x and y by cyclic substitution on the z matrix.

(d) Show that \mathbf{S}_V^2 is diagonal with eigenvalue 2.

(e) Carry out the similarity transformation indicated by (4.57) on \mathbf{S}_{zV} to show that it comes to the standard diagonal form. Do the same for the x and y matrices from (d) to verify agreement with the $j = 1$ entry in Table 3.1.

4.11 The progress of discovery—from symmetries to dynamics—is indicated for five examples in Table 4.6. Consider a column for a system of interest to you (other than “Atomic,” which is discussed in the text) and trace through in some detail the refinement of understanding that is indicated in successive rows. Feel free to disagree with my characterizations, but justify your arguments.

4.12 For the inclusion of spin in the Schrödinger equation, show in detail the steps leading from (4.61) to the requirements (4.63) and (4.64) on the σ -operator components.

4.13 Show that the commutators of the orbital and spin operator x components with the Hamiltonian (4.65) are nonzero, as given in (4.67).

4.14 Derive the following properties of the column vectors (4.70) to show that they form an orthonormal basis for angular momentum states of a given j .

(a) Show that when acted upon by the J_z matrix with elements (3.66), the column matrix whose elements are the second entry in (4.70) produces eigenvalue m .

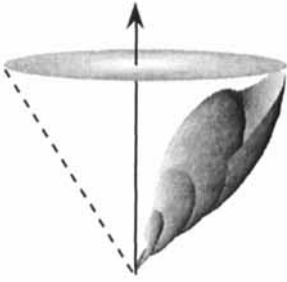
(b) By considering the matrix elements of the scalar product of χ_{jm} and $\chi_{jm'}$, prove formally that their scalar product $\tilde{\chi}_{jm} \chi_{jm'} = \delta_{mm'}$, that is, they are orthonormal.

(c) Show that the set of matrices χ_{jm} forms a basis (complete set) for column matrices with the same value of j , in agreement with the completeness theorem (2.73) for Hermitian operators. To do this, show an arbitrary column matrix with $2j + 1$ rows as a linear combination of the χ_{jm} .

4.15 Prove the following properties of the spinor representation $u(j, m)$ given by (4.72).

(a) Show by using the angular momentum operators \mathbf{J}^2 and J_z that the $u(j, m)$ are eigenfunctions with eigenvalues $j(j + 1)$ and m , respectively.

(b) Show that with the factors in the denominator of (4.72) the functions are orthonormal.



Chapter 5

ANGULAR MOMENTUM IN QUANTUM SYSTEMS

In this chapter we emphasize interpreting angular momentum in quantum systems, with less emphasis on rotational-symmetry aspects than in the previous chapters. The distinction between geometrical and dynamical angular momentum is explained in Section 3.4.5, and we show in this chapter its implications for quantum mechanics. The mathematics-physics relationship is summarized in Figure 5.1.

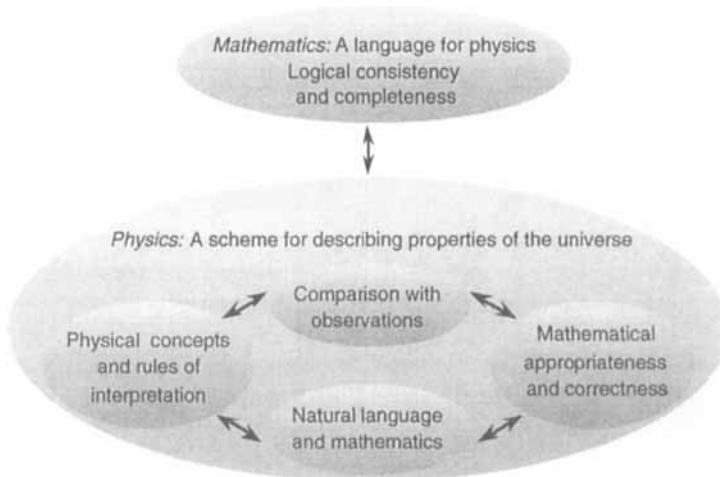


FIGURE 5.1 Schematic of the relationship between mathematics and physics.

The preceding four chapters and later chapters relate primarily to geometry, with connection to the physical world requiring mainly the assumption of isotropy of

space, which is at least partially validated by the consistency of observations. By contrast, this chapter relies heavily on ideas of physics (particularly quantum mechanics) and agreement with physical observations (experiments).

We use the term “physics” to encompass any of the physical sciences, such as physics, chemistry, and engineering. Our usage is justified historically by the fact that a majority of the concepts described in this chapter originated in physics, although they have often been developed extensively in other physical sciences, especially in chemistry.

Physics uses several kinds of language: natural language (such as English), graphical language (schematics such as Figure 5.1, diagrams, and graphs), and mathematics. When mathematics is used in physics it must be both appropriate and correct. Section 5.3.1 emphasizes that paradoxical results can be obtained if physical concepts are not expressed appropriately and manipulated by the mathematics. As summarized in Figure 5.1, physics involves a loop of four themes: concepts, language, mathematics, and observations.

We begin the chapter by discussing in Section 5.1 rotational symmetry and dynamical angular momentum, especially the role of Planck’s constant. In Section 5.2 we progress to the uncertainty relations for angular momentum as interpreted in quantum mechanics. We show that the semiclassical vector model (Section 5.3) is useful for visualizing angular momentum. The model also helps when considering how to combine two angular momenta (Section 7.1). Waves, particularly Schrödinger wave mechanics, and their relation to angular momentum are discussed extensively in Section 5.4, where we also derive and present visualizations of partial-wave expansions involving Bessel functions. Section 5.5 summarizes the conceptual development of angular momentum from a historical perspective. The inevitable problems round out the chapter.

5.1 ROTATIONAL SYMMETRY AND DYNAMICAL ANGULAR MOMENTUM

Our aim in this section is to develop the connection between rotational symmetry (geometry) and dynamical angular momentum (physics). We begin by showing in Section 5.1.1 the correspondence between geometrical, quantal, and classical angular momentum. Then we consider in Section 5.1.2 the particular case of orbital angular momentum and the quantum-classical correspondence through an Ehrenfest theorem for orbital angular momentum, analogous to that often derived for the quantum analogue of Newton’s force equation. Finally, in Section 5.1.3 we consider magnetic moments in magnetic fields, deriving by quantum mechanics the equations for Larmor precession in a uniform magnetic field and also using the Majorana construction to relate systems of arbitrary spin to those for spin $1/2$.

5.1.1 Angular Momentum and the Role of Planck’s Constant

Having studied angular momentum operators and their eigenstates (Chapters 3 and 4), we are ready to summarize the relations between geometrical and dynamical an-

gular momenta (introduced in Section 3.4.5) and to explicate the relations between quantal and classical aspects.

The Role of Planck's Constant. Especially relevant to understanding connections is the role of Planck's constant h , as $\hbar = h/2\pi$, which distinguishes geometrical and dynamical angular momenta. Further, if in dynamical angular momentum we replace quantal angular momentum operators by their expectation values and let $\hbar \rightarrow 0$ in such a way that its product with ℓ remains finite, say L_c , then we have classical angular momentum values. Of course, since \hbar is not under our control, this limiting process is merely a formal device to show the quantal-classical correspondence. Relevant relations and connections are summarized in Table 5.1.

TABLE 5.1 Connections between geometrical, quantal, and classical angular momenta.

Geometrical angular momentum (rotational symmetry)	Dynamical angular momentum	
	Quantum mechanics	Classical mechanics
<i>Operators</i>		
\mathbf{J}	$\mathbf{J}_q \equiv \hbar \mathbf{J}$	
$[J_r, J_s] = i\epsilon_{rst} J_t$	$[J_{qr}, J_{qs}] = i\hbar \epsilon_{rst} J_{qt}$	
<i>Expectation values</i>		
$\langle J_z \rangle = m$	$\langle J_{qz} \rangle = m\hbar$	
$m = -j, -j+1, \dots, j$	$m = -j, -j+1, \dots, j$	
$\langle \mathbf{J}^2 \rangle = j(j+1)$	$\langle \mathbf{J}_q^2 \rangle = j(j+1)\hbar^2$	
<i>Orbital angular momentum</i>		
$\mathbf{L} = -i\mathbf{r} \times \nabla$	$\mathbf{L}_q = -i\hbar \mathbf{r} \times \nabla = \mathbf{r} \times \mathbf{p}_q$	$\mathbf{L}_c = \mathbf{r} \times \mathbf{p}$
$j \rightarrow \ell$, integer	$j \rightarrow \ell$, integer	for a single particle
	$\lim_{\substack{\ell \rightarrow \infty, \\ \hbar \rightarrow 0}} (\ell\hbar) = L_c$	

Two interpretative remarks need to be made about Table 5.1. The first, which is a preoccupation of physicists, concerns the dimensions (units) of the quantities—geometrical angular momenta are dimensionless, but dynamical angular momenta (quantal or classical) have the same dimensions as \hbar , namely mass \times (length)²/time. It is common in quantum mechanics and in subatomic physics to state that one is using units such that $\hbar = 1$, a confusing practice which makes expressions in geometrical and dynamical quantal angular momenta *algebraically* the same, but *physically* quite different, as Figure 3.11 emphasizes.

The second remark about Table 5.1 is that the classical limit of the quantum commutator is obtained by taking expectation values, then letting $\hbar \rightarrow 0$, which results in a vanishing commutator. Thus, as examined in more detail in Section 5.2, in the transition from quantum to classical mechanics, expectation values replace eigenvalues and the order of measuring classical angular momentum components becomes unimportant.

5.1.2 Classical Angular Momentum: Ehrenfest Theorems

We now concentrate on understanding orbital angular momentum, which derives in the geometric viewpoint from infinitesimal rotations of spatial functions, as shown in Section 3.2. We refine the discussion of operators given below Table 5.1 by quantifying the relation between quantal and classical orbital angular momentum as an Ehrenfest theorem for quantum expectation values.

Quantum Analogues of Classical Equations of Motion. We summarize here results from quantum mechanics that demonstrate the origin of classical equations of motion in terms of expectation values of quantum operators. Such results are generally known as Ehrenfest theorems, from the analysis published by Ehrenfest in 1927 of the quantum analogue of Newton's force equation [Ehr27].

As you will recall from wave mechanics, if the wave function of a state, ψ , evolves according to the time-dependent Schrödinger equation of motion

$$i\hbar \frac{\partial \psi}{\partial t} = H\psi \quad (5.1)$$

where H is the Hamiltonian operator (assumed to be Hermitian), then the expectation value of an operator O taken in the state ψ evolves in time according to

$$\frac{d\langle O \rangle}{dt} = \left\langle \frac{\partial O}{\partial t} \right\rangle + \frac{1}{i\hbar} \langle [O, H] \rangle \quad (5.2)$$

in which $[O, H]$ is the commutator of O with H .

The most common example of this relation in describing the quantal-classical connection is to consider the time evolution of the expectation value of the momentum operator for a single particle moving nonrelativistically. In configuration space we then have $O = \mathbf{p}_q = -i\hbar \nabla$. Since this operator has no intrinsic time dependence, the first term on the right-hand side is zero. For the Hamiltonian

$$H = \frac{\mathbf{p}_q^2}{2m} + V \quad (5.3)$$

in which V is the potential acting on the particle, it is easy to show that the required commutator is $[O, H] = [\mathbf{p}_q, H] = -i\hbar \nabla V$. We thus obtain by substitution in (5.2) the usual Ehrenfest theorem for momentum:

$$\frac{d\langle \mathbf{p}_q \rangle}{dt} = \langle -\nabla V \rangle = \langle \mathbf{F} \rangle \quad (5.4)$$

where we introduce the relation between potential and force. This is the quantum expression corresponding to Newton's force equation. No particular assumption is made about the state ψ , except for the convergence of the expectation-value integrals. Neither is there any $\hbar \rightarrow 0$ limit required—(5.4) is a quantal equation.

An Ehrenfest Theorem for Orbital Angular Momentum. Now that we understand the goals and methods for establishing quantal-classical connections, let us choose in (5.2) for a single particle $O = \mathbf{L}_q = \mathbf{r} \times \mathbf{p}_q = -i\hbar \mathbf{r} \times \nabla$. With the Hamiltonian (5.3) and considering a representative component of \mathbf{L}_q , it is straightforward to show (as Problem 5.1 suggests you do) that

$$\boxed{\frac{d\langle \mathbf{L}_q \rangle}{dt} = \langle \boldsymbol{\tau} \rangle \quad \boldsymbol{\tau} \equiv \mathbf{r} \times \mathbf{F} = -\mathbf{r} \times \nabla V} \quad (5.5)$$

in which $\boldsymbol{\tau}$ is the torque operator. This Ehrenfest relation for angular momentum corresponds to the torque equation in classical mechanics. The conservation equation for each component $\langle L_{qi} \rangle$, with $i = x, y, z$, is that this component is conserved in time (a constant of the motion) if the expectation value of τ_i is zero. Note that $\langle \boldsymbol{\tau} \rangle \neq \langle \mathbf{r} \rangle \times \langle \mathbf{F} \rangle$ and that no particular assumption is made about the state ψ . Again we have a completely quantum-mechanical result, with no $\hbar \rightarrow 0$ limit required.

These results are not in conflict with the orbital angular momentum eigenvalue properties derived in Section 4.1 without reference to quantum mechanics and using only the geometry of rotations. There we choose the ket state, of which ψ is an example, to be an eigenstate of L_z and we develop the consequences.

Central Forces and Constants of the Motion. We discuss this topic in Sections 1.1.1 and 1.1.2 in the context of symmetries, conservation laws, and Noether's theorem for classical mechanics. Now suppose that also in quantum mechanics we define a central force as one in which the potential acting on a particle is only a function of the distance from the center of rotation, r , and is independent of angle. Thus $V(\mathbf{r}) = V(r)$ only, which is the same definition as in classical mechanics, for example, Newtonian gravitation and Coulomb's law of electrostatic interaction. It is quite direct to show—Problem 5.2 indicates the steps—that $\mathbf{r} \times \nabla V = 0$, so that, from (5.5), $\langle \mathbf{L}_q \rangle$ is independent of time. That is, the expectation value of the quantal orbital angular momentum operator of a particle is a constant of the motion for a central force operator. This is the same result as in classical mechanics if operator expectation values are equated to the corresponding classical observables.

From the above considerations, we can summarize the correspondences between geometrical angular momentum and dynamical quantal or classical angular momentum, as shown in Figure 5.2.

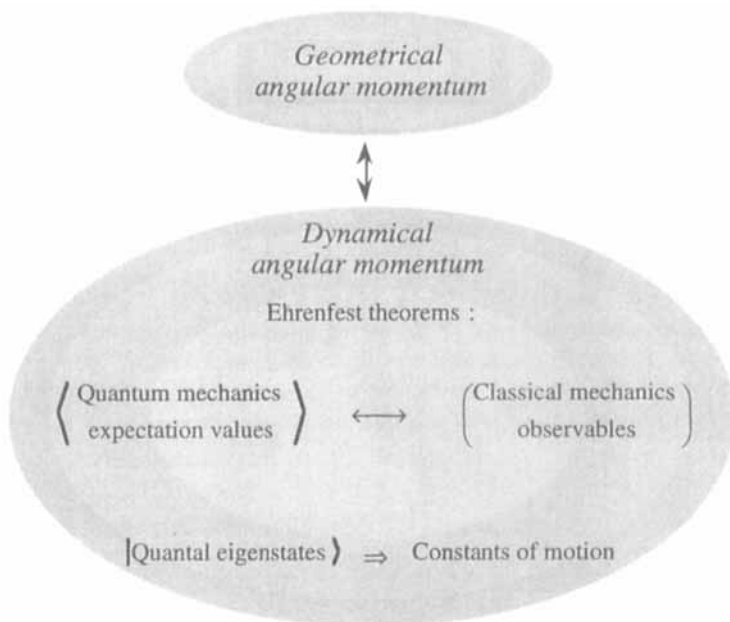


FIGURE 5.2 Correspondence between the three types of angular momentum—geometrical, quantum-dynamical, and classical. See also Table 5.1.

We now switch our attention from the dynamical operators, such as force and torque, to the state ψ with respect to which the expectation values are taken.

Choice of the Quantum State. So far we have assumed only that ψ is mathematically appropriate for calculating expectation values. Suppose, however, that ψ is an eigenstate of one of the angular momentum components, conventionally chosen as L_z . (We are assured from the purely geometric properties of rotations derived in Section 3.1.2 that only one component can be in an eigenstate.) From Section 3.2.3 we have that $L_{qz}\psi = \hbar L_z\psi = m\hbar\psi$, with ψ the normalized eigenfunction

$$\psi = \frac{1}{\sqrt{2\pi}} e^{im\phi} \quad (5.6)$$

By a direct calculation, with the scalar product that is needed for the expectation value being integration over ϕ from 0 to 2π , it is easy to show that $\langle L_{qz} \rangle = m\hbar$, which is time-independent, so the expectation value of this component of operator \mathbf{L} is a constant of the motion. This relation is also summarized in Figure 5.2.

For the L_{qx} and L_{qy} expectation values taken in this eigenstate, the integration over θ from 0 to π in calculating with the expressions in (3.24) automatically gives zero, since the eigenfunction does not depend upon θ . Thus, $\langle L_{qx} \rangle = 0 = \langle L_{qy} \rangle$. A more general proof of this result is in Section 5.2.2.

5.1.3 Larmor Precession in Magnetic Fields

We can understand the quantal-classical correspondence more completely by considering the behavior of a magnetic dipole with moment \mathbf{M} in a magnetic field, \mathbf{B} , with all other effects on the motion of the particle being ignored. We emphasize here the quantal-classical connection, with quantal aspects that are more applied being deferred to Section 8.4.

The interaction Hamiltonian for a quantal system is assumed to be just that used in classical mechanics, namely

$$H = -\mathbf{M} \cdot \mathbf{B} = -g\mu_0 \mathbf{J} \cdot \mathbf{B} \quad (5.7)$$

in which \mathbf{J} is the angular momentum operator, g is called the g -factor, and μ_0 is the unit for the magnetic moment:

$$\mu_0 = \frac{e\hbar}{m} \quad (5.8)$$

where e is the magnitude of the electron charge. For atoms and electrons the appropriate value for the mass m is the electron mass, so $\mu_0 = \mu_B$, the Bohr magneton. For nuclei and nucleons one uses the proton mass, so that $\mu_0 = \mu_N$, the nuclear magneton. Numerical values of μ_0 and representative g values are given in Table 5.2.

TABLE 5.2 Units and values for magnetic moments of electrons (e), protons (p), neutrons (n), and deuterons (d).

	Electron / Atom	Nucleus
Unit for magnetic moment	Bohr magneton: $\mu_B = 9.2740 \times 10^{-24} \text{ J T}^{-1}$	Nuclear magneton: $\mu_N = 5.0508 \times 10^{-27} \text{ J T}^{-1}$
g -factors:		
g_e	-2.0023	
g_p		5.5857
g_n		-3.8261
g_d		0.8574

For electrons or atoms the sign of the Bohr magneton unit is often given as negative to account for the negative charge of the electron. The electron g -factor is then positive. Although the magnetic dipole moment may arise from complicated internal dynamics (which is often of intrinsic interest), we treat it as an internal degree of freedom. Thus, \mathbf{J} is a spin, in the sense discussed in Section 3.5. In conformity with common usage, we use \mathbf{J} rather than \mathbf{S} in this section.

Larmor precession of spins in magnetic fields has a very broad range of applications. Nuclear magnetic resonance (NMR) techniques are used in physics and

chemistry to probe magnetic fields in condensed-matter systems, while in medical diagnosis the technique of magnetic resonance imaging (MRI) is now widely used. Introductions to magnetic resonance in the physical sciences are provided in books by Poole and Farach [Poo87] and by Slichter [Sli89].

We use two methods for deriving spin-precession quantities. The first uses the time-evolution equation for expectation values, (5.2), and therefore has a direct correspondence to classical mechanics, whereas the second (Majorana's formulation) evolves the wave function in time.

Spin Precession in a Magnetic Field. To find the time evolution of expectation values of the spin operator \mathbf{J} we can use (5.2), which requires the commutator $[\mathbf{J}, H]$, where H for a single particle is given by (5.3). It is straightforward to show (Problem 5.3 suggests the steps) that

$$[\mathbf{J}, \mathbf{J} \cdot \mathbf{B}] = -i\mathbf{J} \times \mathbf{B} \quad (5.9)$$

In the equation of motion (5.2) we therefore need the expectation value of the operator on the right-hand side. Since \mathbf{B} is assumed to be an external field whose components are established independently of the behavior of the spins, it can be factored out of expectation values, which are usually taken over volumes of atomic dimensions or smaller, within which \mathbf{B} may be considered constant. By combining (5.2), (5.7), and (5.9), we obtain the *Larmor precession equation*

$$\frac{d\langle \mathbf{J} \rangle}{dt} = \frac{g\mu_0}{\hbar} \langle \mathbf{J} \rangle \times \mathbf{B} = \frac{ge}{m} \langle \mathbf{J} \rangle \times \mathbf{B} \quad (5.10)$$

The second form shows the immediate correspondence between the quantal and classical expressions, since there is no \hbar in (5.10).

This correspondence may be more apparent than real, because quantum mechanics is required in order to understand why particles (such as nuclei) have a particular g -factor, and quantum physics is usually needed to explain the mechanism for providing an appropriately large \mathbf{B} field, especially if superconducting magnets are involved. Thus—as for the classical physics of dielectric constants, magnetic moments, refractive indexes, and other properties of matter—there is a more fundamental underlying description whose elucidation requires quantum mechanics applied to atoms and nuclei. Such layers of explanation are discussed in relation to Table 4.6.

It is shown in classical mechanics texts, as in Section 5-9 of Goldstein [Gol80], that if \mathbf{B} in (5.10) is constant in time, then $\langle \mathbf{J} \rangle$ makes a uniform precession about the direction of \mathbf{B} at the Larmor precession angular frequency, ω_L , given by

$$\omega_L = \frac{geB}{m} \quad (5.11)$$

To visualize Larmor precession, look at Figure 5.3, in which we see that at any instant the rate of change of $\langle \mathbf{J} \rangle$, proportional to $\langle \mathbf{J} \rangle \times \mathbf{B}$ according to (5.10), is perpendicular to both $\langle \mathbf{J} \rangle$ and to $\mathbf{B}(t)$.

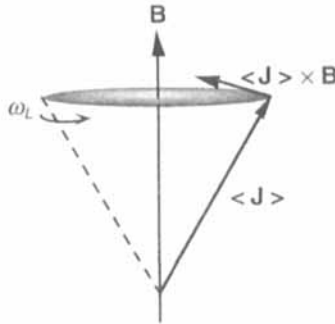


FIGURE 5.3 Classical picture of Larmor precession of spin \mathbf{J} about the direction of the magnetic field \mathbf{B} at precession frequency ω_L .

In the semiclassical vector model for angular momentum in Section 5.3 we replace the expectation value $\langle \mathbf{J} \rangle$ in Figure 5.3 by the operator \mathbf{J} . Although the simple precession pictured here is correct for a time-independent magnetic field, if \mathbf{B} changes slowly compared with the instantaneous precession frequency, then $\langle \mathbf{J} \rangle$ will precess about this time-dependent field. In Section 8.4 we show that $\langle \mathbf{J} \rangle$ changes in magnitude as well as in direction if the time dependence of the magnetic field is not relatively negligible.

We have derived the Larmor formula for precession of spins in magnetic fields, having obtained (5.10) for expectation values of spin operators. It is also instructive to consider evolution of spin wave functions for the same Hamiltonian, as we do in the following.

The Majorana Formulation. In 1932, Majorana [Maj32] provided the conceptual basis for reducing the problem of the behavior of a spin- j system to that of the superposition of $2j$ subsystems each of spin $1/2$. Although we discuss his ideas in the context of magnetic moments in \mathbf{B} fields, it is significant as the basis for spinor-space representations (Section 4.3.3), for describing rotations in general (Section 6.2.3), and for determining coefficients for combining two angular momentum eigenstates (Section 7.2.3).

Consider an assembly of $2j$ spin- $1/2$ particles each precessing about the field \mathbf{B} , as shown in Figure 5.4, where there are eight such particles, five with spin up and three with spin down. The maximum angular momentum they could represent is $8 \times (1/2) = 4$, and the net projection is $5 \times (+1/2) + 3 \times (-1/2) = 1$, as indicated to scale on the right-hand side of the figure. Although consideration of spin projections is not important at this stage, it is significant for the developments in Chapters 6 and 7.

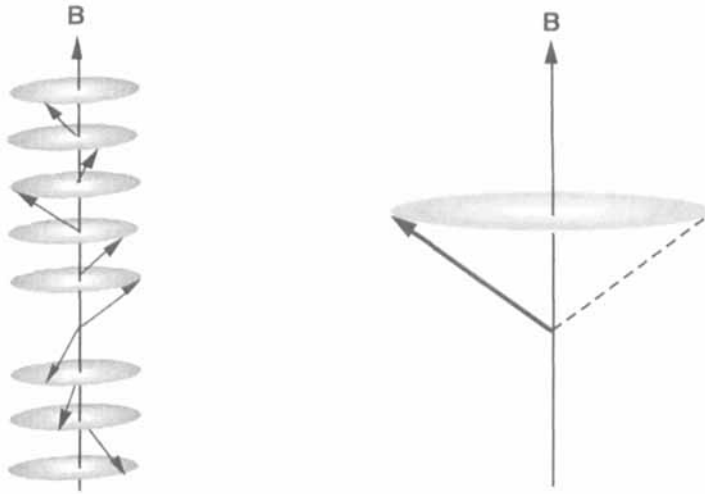


FIGURE 5.4 In Majorana's formulation, a system with spin j (right-hand side) can be represented as $2j$ subsystems each of spin $1/2$ (left-hand side). See also Figure 4.12.

Let the time-dependent wave function of the spin- j system be denoted by χ_j , so for a spin- $1/2$ subsystem the wave function is $\chi_{1/2}$. It is *not* assumed that the system has a definite m value. Also, let us call the angular momentum operator for the k th spin- $1/2$ subsystem \mathbf{s}_k , with $k = 1, 2, \dots, 2j$. The Schrödinger equation is then

$$i\hbar \frac{\partial \chi_j}{\partial t} = H \chi_j = -g\mu_0 \mathbf{J} \cdot \mathbf{B} \chi_j \quad (5.12)$$

Imagine the state χ_j evolving with time by the action of a unitary time-evolution operator, $U(t)$, on the state at $t = 0$. Thus

$$\chi_j(t) = U(t) \chi_j(0) \quad (5.13)$$

Our visualization in Figure 5.4 suggests writing the angular momentum operator as

$$\mathbf{J} = \sum_{k=1}^{2j} \mathbf{s}_k \quad (5.14)$$

so that $U(t)$ evolves in time according to

$$i\hbar \frac{\partial U(t)}{\partial t} = \sum_{k=1}^{2j} (-g\mu_0 \mathbf{s}_k \cdot \mathbf{B}) U(t) \quad (5.15)$$

Suppose that we now write the time-evolution operator U in product form:

$$U(t) = \prod_{k=1}^{2j} U_k(t) \quad (5.16)$$

in which each of the operators U_k acts only on the k th subsystem. It is then straightforward to show (as Problem 5.4 suggests you verify) that

$$i\hbar \frac{\partial U_k(t)}{\partial t} = -g\mu_0 \mathbf{s}_k \cdot \mathbf{B} U_k(t) \quad (5.17)$$

for each of the $2j$ spin-1/2 subsystems. We have thus obtained Majorana's result that the magnetic-dipole interaction between a spin- j system and a magnetic field is for calculation purposes equivalent to that of $2j$ subsystems each having spin-1/2 and the same magnetic moment as the spin- j system.

From the viewpoint of angular momentum and rotational symmetries, the Majorana formulation establishes the following relationships. In Section 2.2.3 we discuss operator exponentials and commutators, and in Section 3.1.1 we relate U as a rotation operator to \mathbf{J} the angular momentum operator. We may therefore write

$$U(\theta, \hat{\mathbf{n}}) = e^{-i\theta \hat{\mathbf{n}} \cdot \mathbf{J}} \quad U_k(\theta, \hat{\mathbf{n}}) = e^{-i\theta \hat{\mathbf{n}} \cdot \mathbf{s}_k} \quad (5.18)$$

By using (5.14), we obtain directly the relation between system operator \mathbf{J} and subsystem operators \mathbf{s}_k given by (5.14).

Majorana's construction enables us to describe the angular momentum operator for a complicated spin- j system in terms of much simpler spin-1/2 systems. The form (5.14) also justifies one aspect of Figure 5.4, namely that only the sum of the $2j$ spin components on the left-hand side has to match up to a spin component on the right-hand side, so the spin-half vectors are drawn with various x and y components and with z components consistent with an eigenvalue of J_z .

We return to the interesting physical problem of precessing spins in Section 8.4, where we derive the rotating-frame transformation and solve the equations for spin transport of a polarized beam passing through a magnetic field gradient.

5.2 UNCERTAINTY RELATIONS FOR ANGULAR MOMENTUM

Our purpose in this section is to derive and interpret uncertainty relations for angular momentum in the context of quantum mechanics. Thus, unlike most other material in this book, the operators are \mathbf{J}_q rather than \mathbf{J} , and there are factors of \hbar appearing in expressions for commutators. Further, the bra-ket states are those satisfying quantal equations of motion, so they are denoted by $\langle \psi | - | \psi \rangle$ and various modifications. As emphasized in Figure 5.1, the relevance of these results to physical systems depends upon the correctness of quantum mechanics formalism, observations, and interpretation, in addition to the presumed isotropy of space (discussed in relation to Figure 1.10) that leads to geometrical angular momentum.

In Section 5.2.1 we derive generally the Heisenberg uncertainty relations between noncommuting quantal operators and the equation for the state that produces

minimum uncertainty. We apply these relations and equations in Section 5.2.2 to situations in which both operators are angular momentum operators; then in Section 5.2.3 one operator is a quantal angular momentum and the other is constructed from angles.

5.2.1 Heisenberg Uncertainty Relations for Quantum Systems

We establish the Heisenberg uncertainty relations between any two noncommuting operators in quantum systems by deriving the relation between the product of the operator standard deviations in an arbitrary (but normalized) quantum state, $|\psi\rangle$. Then we derive the equation that a state must satisfy if the product is as small as possible; this is state $|\psi_m\rangle$. As examples of these uncertainty products and minimal states, we consider linear momentum and position operators.

Noncommuting Operators Imply Uncertainties. We summarize the derivation of the relation between noncommuting operators and uncertainties in their measurements. Suppose that we have two Hermitian operators, P and Q , and that their commutator satisfies

$$[P, Q] = i\hbar R \quad (5.19)$$

Consider their expectation values taken in a particular normalized state ψ and the difference operators, δP and δQ , defined by

$$\delta P \equiv P - \langle \psi | P | \psi \rangle I \quad \delta Q \equiv Q - \langle \psi | Q | \psi \rangle I \quad (5.20)$$

in which I is the unit operator. The expectation values of these difference operators in state ψ are both zero; $\langle \psi | \delta P | \psi \rangle = 0 = \langle \psi | \delta Q | \psi \rangle$. The real numbers

$$\Delta P \equiv \sqrt{\langle \delta P \psi | \delta P \psi \rangle} \quad \Delta Q \equiv \sqrt{\langle \delta Q \psi | \delta Q \psi \rangle} \quad (5.21)$$

thus measure standard deviations (in the sense of statistics) when P and Q are measured in the same quantum state ψ .

In order to relate these two standard deviations, we use the *Schwarz inequality* for inner products in linear spaces (Section 2.1.1):

$$\langle s | s \rangle \langle t | t \rangle \geq |\langle s | t \rangle|^2 \quad (5.22)$$

in which equality holds only if $|s\rangle$ and $|t\rangle$ are linearly dependent. A concise proof of the inequality is given, for example, in Section 2 of [Jor69]. Setting $s = \delta P \psi$ and $t = \delta Q \psi$, we have

$$\begin{aligned} (\Delta P)^2 (\Delta Q)^2 &\geq |\langle \delta P \psi | \delta Q \psi \rangle|^2 \\ &= \frac{1}{4} |\langle \psi | \delta P \delta Q | \psi \rangle|^2 = \frac{1}{4} |\langle \psi | [P, Q] + (PQ + QP) | \psi \rangle|^2 \quad (5.23) \\ &\geq \frac{1}{4} |\langle \psi | [P, Q] | \psi \rangle|^2 = \frac{\hbar^2}{4} |\langle \psi | R | \psi \rangle|^2 \end{aligned}$$

Thus, since standard deviations are positive, we obtain the general *Heisenberg uncertainty relations*

$$\Delta P \Delta Q \geq \frac{\hbar}{2} |\langle \psi | R | \psi \rangle| \quad (5.24)$$

in which P , Q , and R are related through (5.19).

As a familiar application of this relation, choose $P = p_x$, the momentum operator component, and $Q = x$, the position operator component in the same direction. Since the commutator $[p_x, x] = -i\hbar I$, we have $R = -I$, the negative of the unit operator. The Heisenberg momentum-position uncertainty relation is then obtained directly from (5.24) as

$$\Delta p_x \Delta x \geq \frac{\hbar}{2} \quad (5.25)$$

In Sections 5.2.2 and 5.2.3 we apply (5.24) to uncertainty relations among angular momentum components and between angular momentum components and functions of angles.

States with Minimum Uncertainties. So far in this section we have not specified the state ψ with respect to which uncertainties are calculated. We now find equations that ψ must satisfy if the uncertainty products are to be minimized. To obtain a minimum product, we must have equality in the first line of (5.23); thereby we require that the minimum state ψ_m satisfies the linear-dependence condition

$$\delta P |\psi_m\rangle = \lambda \delta Q |\psi_m\rangle \quad (5.26)$$

in which λ is a constant. Also, we can write the condition that the second inequality in (5.23) becomes an equality, as

$$\langle \psi_m | (\delta P \delta Q + \delta Q \delta P) | \psi_m \rangle = 0 \quad (5.27)$$

By combining these two relations and reordering the operators in the second equation by using the commutator relation $[\delta P, \delta Q] = i\hbar R$, which follows from (5.21), it is simple to show (as Problem 5.5 suggests doing) that

$$\begin{aligned} (\Delta P)_m^2 &= \langle \delta P \psi_m | \delta P \psi_m \rangle = \frac{i\hbar \langle \psi_m | R | \psi_m \rangle \lambda}{2} \\ (\Delta Q)_m^2 &= \langle \delta Q \psi_m | \delta Q \psi_m \rangle = \frac{-i\hbar \langle \psi_m | R | \psi_m \rangle}{2\lambda} \end{aligned} \quad (5.28)$$

in which subscripts denote minimum-uncertainty values. If R is Hermitian—for example, if P and Q are Hermitian—then its expectation value is real, so λ must be

purely imaginary:

$$\lambda = -i\gamma \quad \text{sgn}(\gamma) = \text{sgn}(\langle R \rangle) \quad (5.29)$$

Clearly, the product of the two uncertainties satisfies (5.24) with *equality*:

$$\Delta P_m \Delta Q_m = \frac{\hbar}{2} \langle R \rangle_m \quad (5.30)$$

The quotient of the minimum uncertainties satisfies, according to (5.28),

$$(\Delta P)_m / (\Delta Q)_m = \gamma \quad (5.31)$$

For the state producing the minimum uncertainty product, substitute for λ in (5.28) from (5.29) and (5.31), then use (5.20) to recover the original operators, thus yielding the equation for the *minimum-uncertainty state* $|\psi_m\rangle$:

$$\left[P - \langle P \rangle + i \frac{\Delta P}{\Delta Q} \text{sgn}(\langle R \rangle) (Q - \langle Q \rangle) \right] |\psi_m\rangle = 0 \quad (5.32)$$

This equation is quite general and can be applied to any quantum system.

As an example of a minimum-uncertainty state, choose (as above) $P = p_x$ and $Q = x$, and work out the wave function in configuration space, $\psi_m(x) = \langle x | \psi_m \rangle$. In x space $p_x = -i\hbar \partial / \partial x$ and its commutator with x gives $R = -I$. The differential equation for $\psi_m(x)$ is then obtained from (5.32) as

$$\left[-i\hbar \frac{\partial}{\partial x} - \langle p_x \rangle - i \frac{\Delta p_x}{\Delta x} (x - \langle x \rangle) \right] \psi_m(x) = 0 \quad (5.33)$$

which has the well-known solution with envelope a Gaussian centered on $\langle x \rangle$ and spatially modulated at a frequency determined by $\langle p_x \rangle / \hbar$, namely

$$\psi_m(x) = \left[\frac{\Delta p_x}{\pi \hbar \Delta x} \right]^{1/4} \exp \left[- \left(\frac{\Delta p_x (x - \langle x \rangle)^2}{2 \hbar \Delta x} + \frac{i \langle p_x \rangle x}{\hbar} \right) \right] \quad (5.34)$$

In this expression Δp_x , Δx , $\langle p_x \rangle$, and $\langle x \rangle$ are to be interpreted as parameters, with the two standard deviations being related by (5.30).

We have now derived for Hermitian operators P and Q the general Heisenberg uncertainty relations given by (5.24), and we have derived equation (5.32), which must be satisfied by the state $|\psi_m\rangle$, giving the minimum uncertainty product. The relationships between mathematics and physics that are given as a general paradigm in Figure 5.1 can be exemplified for the Heisenberg uncertainty relations that we have derived, as shown in Figure 5.5.

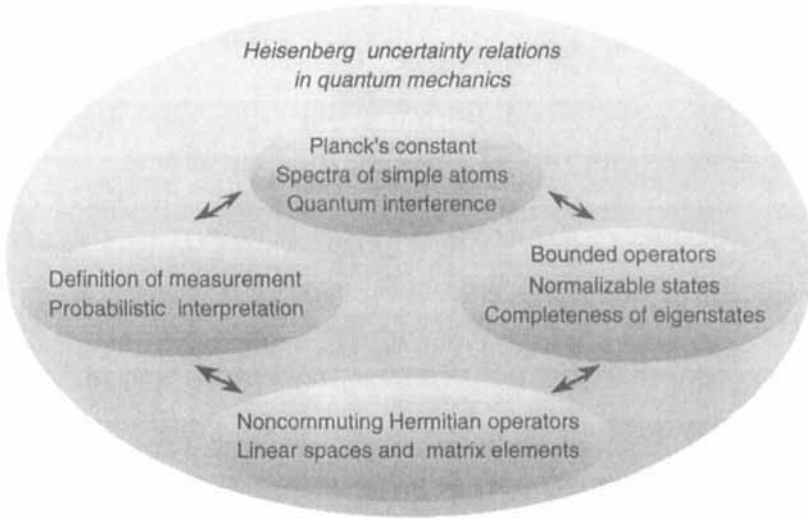


FIGURE 5.5 The Heisenberg uncertainty relations in quantum mechanics are examples of the general paradigm relating mathematics and physics. The topics in the four bubbles match those at corresponding positions in Figure 5.1.

Having illustrated using the results with familiar momentum and position operators, we turn to the objects of our desire, the quantum angular momentum operators.

5.2.2 Angular Momentum Uncertainties

We now discuss Heisenberg uncertainty relations when operators P and Q in the general uncertainty relation (5.24) are angular momenta, either measured in arbitrary states or measured in eigenstates of angular momentum with eigenvalues $j\hbar$ and $m\hbar$. Following this development, we then consider minimum uncertainty states for measuring the orbital angular momenta L_{qx} and L_{qy} .

The commutation relations for quantal angular momentum operator components can be written in terms of the permutation symbol ϵ_{rst} as

$$[J_{qr}, J_{qs}] = i\hbar \epsilon_{rst} J_{qt} \tag{5.35}$$

so that the operator $R = J_{qrst}$. (Note that the subscript q is for “quantal,” while $r, s,$ and t are choices of $x, y,$ and z .) Therefore, for any state ψ the uncertainty relations for angular momentum become

$$\Delta J_{qr} \Delta J_{qs} \geq \frac{\hbar \epsilon_{rst}}{2} |\langle \psi | J_{qrst} | \psi \rangle| \tag{5.36}$$

We now consider examples of this relation.

Uncertainties in J_{qz} with J_{qx} or J_{qy} . By choosing in (5.36) $r = z$, $s = x$, and $t = y$, we have r , s , and t in cyclic order, so $\epsilon_{rst} = 1$; therefore,

$$\Delta J_{qz} \Delta J_{qx} \geq \frac{\hbar}{2} |\langle \psi | J_{qy} | \psi \rangle| \quad (5.37)$$

If ψ is an *arbitrary* quantum-mechanical state, this is all one can say. Suppose, however, that ψ is an eigenstate of \mathbf{J}^2 and J_z with eigenvalues $j(j+1)$ and m , respectively, which we write as $|\psi\rangle = |jm\rangle$. The developments in Section 3.4.3 then show that

$$\Delta J_{qz}(jm) \Delta J_{qx}(jm) \geq \frac{\hbar}{2} |\langle jm | J_{qy} | jm \rangle| = 0 \quad (5.38)$$

in which (jm) indicates that the uncertainties are calculated in the eigenstates with these quantum numbers. Therefore, at least one of the uncertainties on the left-hand side may be zero. For such an angular momentum eigenstate

$$\Delta J_{qz}(jm) = 0 \quad (5.39)$$

On the other hand, use of (3.64) and (3.65) in the defining equations (5.20) and (5.21) for uncertainties shows (as Problem 5.6 suggests you try) that in such a state

$$\begin{aligned} [\Delta J_{qx}(jm)]^2 &= \langle jm | J_x^2 | jm \rangle = \frac{\hbar^2}{2} [j(j+1) - m^2] \geq \frac{\hbar^2 j}{2} \\ [\Delta J_{qy}(jm)]^2 &= \langle jm | J_y^2 | jm \rangle = \frac{\hbar^2}{2} [j(j+1) - m^2] \geq \frac{\hbar^2 j}{2} \end{aligned} \quad (5.40)$$

so that, except for the usually uninteresting case that $j = 0$, these uncertainties are not zero even if that for J_{qz} is zero. As j increases, the uncertainties in these two components *relative* to that in $\sqrt{j(j+1)}\hbar$ range from $1/\sqrt{2(j+1)}$ for $|m| = j$ to $1/\sqrt{2}$ for $m = 0$. These ratios are independent of \hbar .

Although (5.40) gives the uncertainties in x and y components in any state (jm) , there are new aspects when they are measured simultaneously, as we now discover.

Simultaneous Measurement of J_{qx} and J_{qy} . If we set in (5.36) $r = x$, $s = y$, $t = z$, again $\epsilon_{rst} = 1$, so for simultaneous measurements of x and y components,

$$\Delta J_{qx} \Delta J_{qy} \geq \frac{\hbar}{2} |\langle \psi | J_{qz} | \psi \rangle| \quad (5.41)$$

For a (jm) eigenstate the left-hand side of this relation is, according to (5.40), $\hbar^2 [j(j+1) - m^2] / 2 \geq \hbar^2 j / 2 \geq \hbar^2 |m| / 2$, thus verifying (5.41) whose right-hand side is just $\hbar^2 |m| / 2$. The sum of x and y mean-square uncertainties in a (jm) eigenstate is

$$\begin{aligned} [\Delta J_{qx}(jm)]^2 + [\Delta J_{qy}(jm)]^2 &= \hbar^2 [j(j+1) - m^2] \\ &= \langle jm | (\mathbf{J}_q^2 - J_{qz}^2) | jm \rangle \end{aligned} \quad (5.42)$$

which is just the contribution from $J_{qx}^2 + J_{qy}^2$. Such relations among the uncertainties in the components of \mathbf{J}_q are useful for devising the semiclassical vector model of angular momentum in Section 5.3.

Minimum-Uncertainty States for L_{qx} and L_{qy} . In Section 5.2.1 we derive the Gaussian minimum-uncertainty states (5.24) for linear momentum. It is interesting to discover the states ψ_m for which the orbital angular momentum components L_{qx} and L_{qy} have a minimum uncertainty product. As shown in Section 3.2, these operators are realizations for spatial functions of the operators J_{qx} and J_{qy} , whose uncertainties we investigate immediately above.

Consider a state for which the z component has the well-defined value $m\hbar$. Then, even if there is a superposition of ℓ states making up ψ_m , (5.40) shows that the uncertainties in x and y components of \mathbf{L}_q will be equal and the component expectation values will be zero. The expressions for L_{qx} and L_{qy} in spherical polar coordinates are given from (3.24). Thus, the general equation for the state with minimum uncertainty, (5.32), can be simplified to

$$\left[\tan \theta \frac{\partial}{\partial \theta} + i \operatorname{sgn}(m) \frac{\partial}{\partial \phi} \right] \psi_m(\theta, \phi) = 0 \quad (5.43)$$

in which $\psi_m(\theta, \phi) = \langle (\theta\phi) | \psi_m(m) \rangle$ is the minimum-uncertainty state of definite m expressed in polar coordinates. As such, it must contain $\exp(im\phi)$ for its dependence on ϕ , so that (5.43) simplifies to

$$\left[\tan \theta \frac{\partial}{\partial \theta} - |m| \right] \psi_m(\theta, \phi) = 0 \quad (5.44)$$

This can be integrated readily (as suggested in Problem 5.7) to produce the wave function for the minimum-uncertainty quantum state associated with z projection $m\hbar$, given by

$$\psi_m(\theta, \phi) = \sqrt{\frac{(2|m|+1)!!}{2^{2|m|+2} \pi (|m|)!}} \sin^{|m|} \theta e^{im\phi} \quad (5.45)$$

It is instructive to visualize the probability density corresponding to the wave function (5.44) in a polar diagram (Section 4.1.2). According to (5.44), this density is just proportional to $\sin^{2|m|} \theta$ and is independent of the azimuthal angle ϕ , since we have a state with definite angular momentum z projection, $m\hbar$. Figure 5.6 shows the density for two representative values of m .

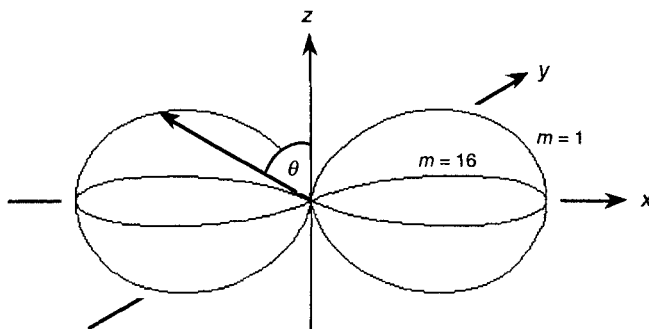


FIGURE 5.6 Probability densities corresponding to the minimum-uncertainty state (5.45) for x and y components of orbital angular momentum, given an eigenstate of L_{qz} with $m = 1$ or $m = 16$. The densities are normalized to unity at $\theta = \pi/2$.

To interpret the behavior of the minimum-uncertainty state shown in Figure 5.6, note that as m increases, the distribution becomes more concentrated into the x - y plane, just as for a classical particle whose angular momentum is primarily along the z axis. Section 6.4.3 continues the discussion of such classical limits in the context of rotation matrices.

Now that we understand the uncertainty relations between noncommuting angular momentum operators, it would seem to be merely a swing through the park to treat uncertainty relations between operators and angles. In reality—which is where we dwell—the treatment is fraught with technical difficulties.

5.2.3 Uncertainties between Angular Momentum and Angles

We begin our study of uncertainties between angular momentum and angles by making an obvious translation from a linear momentum component to an orbital angular momentum component and from displacement x to angle ϕ . Puzzling results from this will suggest replacing ϕ by functions of ϕ , such as $\cos \phi$ and $\sin \phi$. Finally, we discuss (but do not resolve) the problem of several angular momentum components and angles.

Uncertainties for Azimuthal Orbital Angular Momentum and Angle. We first consider the special case of rotations generated by the quantal orbital rotation operator L_{qz} . The geometrical version of this operator, L_z , is considered in detail in Section 3.2. The quantum-mechanical operator is

$$L_{qz} = -i\hbar \frac{\partial}{\partial \phi} \quad (5.46)$$

What is the variable conjugate to L_{qz} , the Q in the commutator (5.19)? If one chooses $Q = \phi$, then one has

$$[L_{qz}, \phi] = -i\hbar I \quad (5.47)$$

Superficially, this is satisfactory, except perhaps that ϕ is a number, not the usual kind of operator. Disaster strikes if you attempt to calculate the matrix elements of the relation (5.47) in an (ℓm) state; namely

$$(m' - m)\langle \ell m' | \phi | \ell m \rangle = \delta_{m' m} \quad (5.48)$$

which, when $m' = m$, claims that $0 = 1$. The origin of this problem is mathematically quite sophisticated, for which Biedenharn and Louck [Bie81b, pp. 314–316] provide a complete discussion.

One possible solution is to deny that it is appropriate to calculate with an (ℓm) state and initially to leave the state unspecified. We can then merely relabel the x variable in the momentum-position example worked out above as the variable ϕ , then the momentum component $p_x \rightarrow L_{qz}$. Since the commutator $R = -1$, as previously, the analogue of (5.25) is

$$\Delta L_{qz} \Delta \phi \geq \frac{\hbar}{2} \quad (5.49)$$

and the minimum-uncertainty state is obtained by relabeling (5.34) to obtain

$$\psi_m(\phi) = \left[\frac{\Delta L_{qz}}{\pi \hbar \Delta \phi} \right]^{1/4} \exp \left[- \left(\frac{\Delta L_{qz} (\phi - \langle \phi \rangle)^2}{2 \hbar \Delta \phi} + \frac{i \langle L_{qz} \rangle \phi}{\hbar} \right) \right] \quad (5.50)$$

Such relations have no mathematical problems and are intuitively satisfying.

Uncertainties for Angular Momentum and Functions of Angle. Another way around the problem presented by (5.48) is to use a different angle operator, such as the real or imaginary parts of $e^{i\phi}$, as $\cos \phi$ or $\sin \phi$, respectively. The commutation relation corresponding to (5.49) is

$$[L_{qz}, e^{i\phi}] = \hbar e^{i\phi} \quad (5.51)$$

to be interpreted as the pair of relations for Hermitian operators

$$[L_{qz}, \cos \phi] = i \hbar \sin \phi \quad [L_{qz}, \sin \phi] = -i \hbar \cos \phi \quad (5.52)$$

Uncertainty relations for $P = L_{qz}$ with $Q = \cos \phi$ or $Q = \sin \phi$ are then given from (5.24) as

$$\Delta L_{qz} \Delta(\cos \phi) \geq \frac{\hbar}{2} |\langle \psi | \sin \phi | \psi \rangle| \quad \Delta L_{qz} \Delta(\sin \phi) \geq \frac{\hbar}{2} |\langle \psi | \cos \phi | \psi \rangle| \quad (5.53)$$

for suitable states ψ . Consider the minimum-uncertainty state, ψ_m , for the first of these relations. By substituting in (5.32), you can obtain the equation for the wave

function in azimuthal angle variable ϕ , $\psi_{cm}(\phi) = \langle (\phi) | \psi_m \rangle$:

$$\left[-i\hbar \frac{\partial}{\partial \phi} - \langle L_{qz} \rangle + i \frac{\Delta L_{qz}}{\Delta(\cos \phi)} (\cos \phi - \langle \cos \phi \rangle) \right] \psi_{cm}(\phi) = 0 \quad (5.54)$$

By inspection, it is verified easily that a solution for $\psi_{cm}(\phi)$ is

$$\psi_{cm}(\phi) = N_c \exp \left[i \langle L_z \rangle \phi - \frac{i \Delta L_z}{\Delta(\cos \phi)} (\sin \phi - \langle \cos \phi \rangle \phi) \right] \quad (5.55)$$

in which N_c is the normalization constant. A similar expression obtains for the minimum state corresponding to the second solution in (5.53), namely

$$\psi_{sm}(\phi) = N_s \exp \left[i \langle L_z \rangle \phi - \frac{i \Delta L_z}{\Delta(\sin \phi)} (\cos \phi + \langle \sin \phi \rangle \phi) \right] \quad (5.56)$$

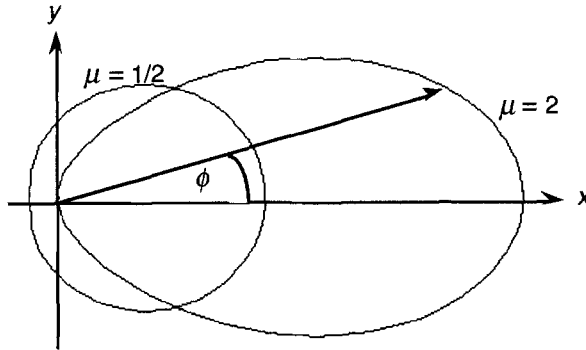


FIGURE 5.7 Probability distribution for the ϕ distribution of the function with minimum uncertainty product given by (5.57). The distributions are shown for $\mu = 1/2$ and for $\mu = 2$.

Let us develop the interpretation of this state. Remarking that ψ_{sm} describes a spatial function, we can insist that $\psi_{sm}(\phi + 2\pi) = \psi_{sm}(\phi)$. By making the abbreviation $\mu = \Delta L_z / \Delta(\sin \phi) > 0$, we then obtain

$$\psi_{sm}(\phi) = N_s \exp[\mu \cos \phi + im\phi] \quad m = 0, \pm 1, \pm 2, \dots \quad (5.57)$$

Because of the $\cos \phi$ factor in the exponent, this state is not an eigenstate of L_{qz} , thus avoiding the problems with the first attempt to develop an uncertainty relation between L_{qz} and ϕ rather than $\sin \phi$. It is, however, straightforward to show (as suggested in Problem 5.8) that

$$\langle L_{qz} \rangle = m\hbar \quad \langle \sin \phi \rangle = 0 \quad (5.58)$$

To visualize the interpretation, make a polar diagram (Section 4.1.2) of the probability density from $\psi_{sm}(\phi)$ given by (5.57), as shown in Figure 5.7. These densities have the same normalization when integrated over the angle ϕ rather than over Cartesian coordinates. As μ increases, the probability distribution becomes peaked in the $\phi = 0$ direction and the expectation value of $\cos \phi$ tends toward unity. On the contrary, as μ decreases the distribution becomes more uniform with angle ($\mu = 1/2$ diagram in Figure 5.7), so the average value of $\cos \phi$ over 0 to 2π decreases. These graphical results can be verified by analytical evaluation (Problem 5.8 suggests how), which produces the limiting behaviors of relevant expectation values shown in Table 5.3.

TABLE 5.3 Expectation values and uncertainties for minimum-uncertainty states of the operators L_{qz} and $\sin \phi$.

Limit	$\langle \cos \phi \rangle$	$\langle \sin \phi \rangle$	ΔL_{qz}	$\Delta L_{qz} \Delta(\sin \phi)$
$\mu \rightarrow \infty$	$1 - \frac{1}{4\mu}$	$\frac{1}{\sqrt{2\mu}}$	$\sqrt{\frac{\mu}{2}} \hbar$	$\frac{\hbar}{2}$
$\mu \rightarrow 0$	μ	$\frac{1}{\sqrt{2}}$	$\frac{\mu\hbar}{\sqrt{2}}$	$\frac{\mu\hbar}{2} = \frac{\langle \cos \phi \rangle \hbar}{2} \rightarrow 0$

Having analyzed the uncertainty relations for azimuthal-angle rotations, it might seem simple to generalize to rotations about all three axes.

Uncertainties between Operators and Angles in Three Dimensions. For rotations in three dimensions, appropriate choice of angle variables, analogous to the $\cos \phi$ and $\sin \phi$ used above, is much more difficult to justify. The discussion occupies 26 pages in Biedenharn and Louck's treatise [Bie81b, pp. 323–349] and requires much mathematics and physics wrangling. We refer the interested reader to their treatment and to references therein.

5.3 THE SEMICLASSICAL VECTOR MODEL

In this section we combine ideas from the geometry of small rotations (especially Section 3.4), Larmor precession in quantum mechanics (Section 5.1.3), and precession of tops in classical mechanics—for example, [Gol80, Chapter 5]—to produce the semiclassical vector model for angular momentum. We set up the model in Section 5.3.1, then we discuss its uses and limitations in Section 5.3.2. Our discussion will show that the model is mostly a mnemonic device for recalling some of the properties of the operators for small rotations.

5.3.1 Constructing the Vector Model of Angular Momentum

Historically, the vector model of angular momentum was introduced in quantum mechanics by Sommerfeld [Som16], a master of the theory of tops, with his assumption of the spatial quantization of angular momentum. In 1919, Landé [Lan19] developed this idea to include addition of angular momentum vectors. Because these ideas were produced before the full development of quantum mechanics from 1926 onward and ignored the geometric aspects of rotations that we develop in Chapters 3 and 4, they were mostly heuristics for guiding the interpretation of atomic spectra. Their role in the conceptual development of angular momentum is discussed in Section 5.5.

Analogies in the Vector Model. Let us relate quantities from the geometry of rotations to angular momentum precession in quantum and classical mechanics, as summarized in Figure 5.8.

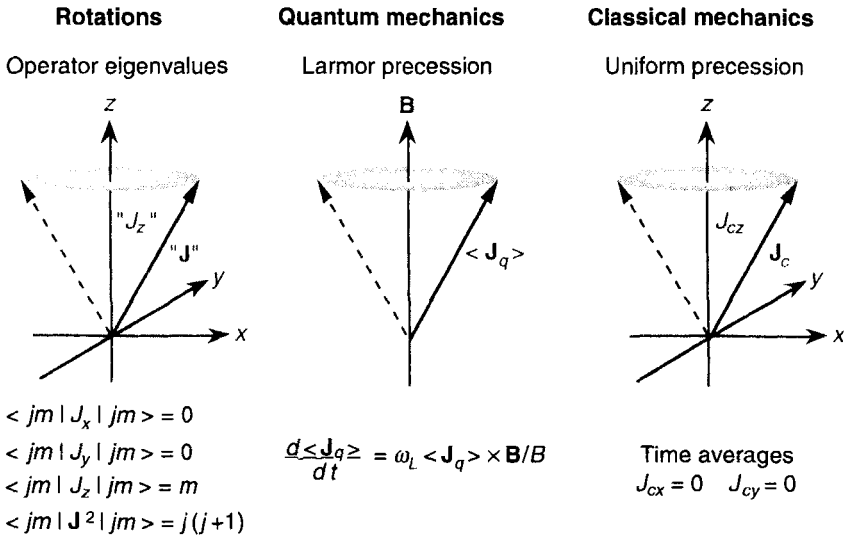


FIGURE 5.8 Related quantities from the geometry of rotations (left), Larmor precession in quantum mechanics (center), and uniform precession in classical mechanics (right).

From a first glance at the figure we see that there is close correspondence between operator expectation values in (jm) eigenstates for geometric rotations, expectation values of these operators in Larmor precession around a constant magnetic field, and uniform precession of a top in classical mechanics. In proceeding from left to right—from geometry through quantum mechanics to classical mechanics—we make correspondences between expectation values in a (jm) state, expectation values in an arbitrary state (as derived in Section 5.1.3), and time averages, respectively.

The uniform-precession viewpoint can help us to understand the $j(j+1)$ expectation value of \mathbf{J}^2 , using an argument due to Feynman [Fey63]. Assume it is known that m lies between $-j$ and j and that an average over all values of m is equivalent to an average over all spatial directions, so that $\langle J_x^2 \rangle = \langle J_y^2 \rangle = \langle J_z^2 \rangle$. Thus

$$\begin{aligned} \langle \mathbf{J}^2 \rangle &= 3 \langle J_z^2 \rangle / (2j+1) = 3 \sum_{m=-j}^j m^2 / (2j+1) \\ &= 3j(j+1)(2j+1) / 3(2j+1) = j(j+1) \end{aligned} \quad (5.59)$$

There is therefore no mystery to the expectation value being $j(j+1)$. Indeed, as Problem 5.9 suggests that you verify, if the expectation value is constructed by integrating over m rather than summing over it, then $\langle \mathbf{J}^2 \rangle \rightarrow j^2$. As j increases, the discreteness of the m values therefore becomes relatively less significant.

Analogy with a Precessing Top. The requirement that the average J_z value should be nonzero in general, but that the time-average values of J_x and J_y should both be zero, suggests an analogy with a uniformly precessing top, as indicated in Figure 5.9. Notice that only the two mechanics examples have time as a parameter, since rotation (geometrical angular momentum) does not necessarily refer to time evolution. It is interesting—and it will amuse some readers—to use *Mathematica* to visualize the analogy with the precessing top, as shown.

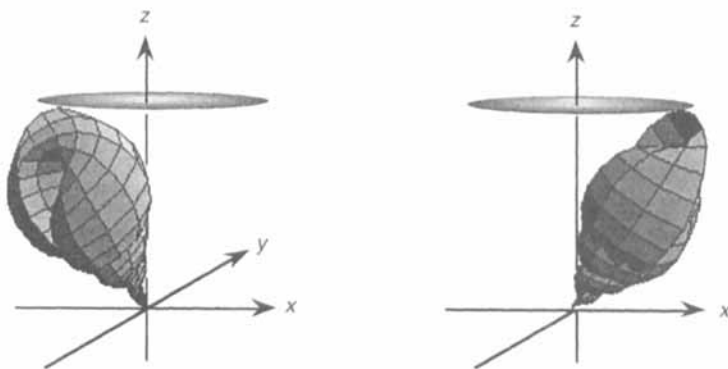


FIGURE 5.9 Precession of a top or helical shell about the z axis. In the vector model precession is uniform, so that the x and y components of angular momentum both have average value zero. (Adapted from *Mathematica* notebook `Precess`, which can animate the precession.)

To prepare the graphics to display such a precession requires using the matrices for rotations of coordinates, as described in Section 1.3.2. Problem 5.10 suggests how to derive the formulas in *Mathematica* notebook `Precess`, which can also animate the graphics.

5.3.2 Uses and Limitations of the Vector Model

The vector model nowadays serves mostly as a visual mnemonic for recalling the selection rules of angular momentum expectation values, but not for the off-diagonal matrix elements given in Section 3.4. Note also that the rotation operators depicted in Figure 5.8 act only on spatial functions and are therefore (according to Section 3.2) only *orbital* angular momentum operators. The vector model is particularly helpful in developing ideas about combining two angular momenta (Section 7.1). Again, it is limited because it fails to predict the phase rules for different orderings of coupling (Section 7.3).

Another limitation of the vector model is that it describes only expectation values, but not (for example) the mean-square fluctuations about these values. Therefore, most of our discussion in Section 5.2 on uncertainty relations for angular momentum is ignored in the vector model. Several other aspects that emphasize the limitations of the vector model are most easily made by comparison of the three sketches in Figure 5.8.

Connection of Rotations to Quantum Mechanics. In Figure 5.8 the left-hand and center sketches show the relation of operators and expectation values for infinitesimal rotations to Larmor precession in quantum mechanics. The major differences are the following.

For rotations the vector \mathbf{J} is an *operator*, as are its components such as J_z . For example, when acting on spatial functions $J_z = L_z = -i\partial/\partial\phi$. Therefore, it is not strictly correct to display \mathbf{J} and J_z as vectors, so quotation marks have been put around them in the figure. The expectation values of the operators *in a state of definite j and m* are as shown. Note that according to the derivations in Section 3.4, there are also off-diagonal elements of J_x and J_y , which are not included in this vector model.

Connection of Quantum Mechanics to Classical Mechanics. The center and right-hand sketches in Figure 5.8 show the following quantum-classical correspondences. The quantal expectation-value equation is correct for \mathbf{J}_q (and indeed for the geometrical \mathbf{J}), for an expectation value taken in *any* state and for any time dependence of \mathbf{B} , including directional changes with time. Only if \mathbf{B} is constant in direction and magnitude is the quantal-classical correspondence appropriate. An interesting example of a time-dependent \mathbf{B} is given in Section 8.4.

How Large Is j for the Classical Limit? By considering the relative spacing of operator eigenvalues, we can get a preliminary idea of what values of j are appropriate for assuming that numerical values computed in one of the three types of systems shown in Figure 5.8 agree closely enough for practical purposes. Since successive m values differ by unity, the cosine of the “angle” θ_m between the \mathbf{J} “vector” and the z axis is quantized in equal steps of

$$\delta(\cos\theta_m) = 1/\sqrt{j(j+1)} \approx 1/j \quad (5.60)$$

The smallest angle that “ \mathbf{J} ” makes with the z axis is about $1/\sqrt{j}$ radian. Similarly, the expectation value of \mathbf{J}^2 exceeds j^2 by the fraction $1/j$. Note that these estimates are completely independent of the value of Planck’s constant, since they are completely geometrical in origin.

We refine our discussion of the classical limits of angular momentum when discussing the classical limits of rotation matrices in Section 6.4.3 and of $3-j$ coefficients in Section 7.3.3. Especially for the rotation matrices, very small values of j (less than 10) are shown to effectively describe the classical limits.

5.4 ANGULAR MOMENTUM AND WAVE MECHANICS

In this section we develop the connection between angular momentum and waves, emphasizing the partial-wave expansion of plane waves in two and three dimensions. We make extensive analyses, both analytical and pictorial, of these expansions, including the radial functions appropriate for plane waves, which are the cylindrical and spherical Bessel functions. The results in Section 5.4.1 are appropriate for any plane scalar wave, be it a sound wave or a quantum scattering wave. For example, the centripetal barrier discussed there has its most useful interpretation in quantum mechanics, but it is not limited to this context.

Visualizing plane waves helps us to understand the relation between partial-wave components, angular momentum functions, and Bessel functions, which are combined to construct the wave. In Section 5.4.2 we therefore show several examples, and discuss the *Mathematica* notebooks in Appendix I that you can use to display the partial-wave expansions.

5.4.1 Plane Waves and Centripetal Barriers; Bessel Functions

The formulas for expansion of the spatial dependence of plane waves into partial waves are indispensable for wave descriptions of both quantal and classical scattering whenever the range of the interaction is comparable to the wavelength. The expansion is usually derived in a complicated way involving unfamiliar integrals [But68 p. 403; Wat44]. In the following we derive the basic formula concisely by using a simple method based on differentiation properties of Bessel functions, which I have given elsewhere [Tho92a] but with a different emphasis. This also brings in interesting analytical and numerical properties of Bessel functions that can be related to centripetal barriers.

Derivations are presented for waves in both three dimensions and two dimensions. After the derivations, the expansions are cast into various forms whose interpretation we then discuss, especially from the viewpoint of the centripetal barrier. These set the stage for the visualizations in Section 5.4.2.

Plane Waves in Three Dimensions. The form of the partial-wave expansion of a plane wave in three dimensions expressed in spherical polar coordinates is

$$e^{ikr\cos\theta} = \sum_{\ell=0}^{\infty} c_{\ell} j_{\ell}(kr) P_{\ell}(\cos\theta) \quad (5.61)$$

for a wave whose planes of constant phase are perpendicular to the z axis. Here k is the wavenumber, r the distance from the point about which the expansion is made, θ the angle between the wavevector and the radius vector, j_{ℓ} the *spherical* Bessel functions, and P_{ℓ} the familiar Legendre polynomial discussed and displayed in Section 4.1.2. The cylindrical symmetry about the z axis (thus $m = 0$) shows that Legendre polynomials, rather than spherical harmonics, are the appropriate angle functions. Our aim is to show that $c_{\ell} = i^{\ell}(2\ell + 1)$.

Expansion (5.61) is often called the Rayleigh expansion [Ral72] because of its extensive use by Baron Rayleigh (beginning in 1872) to describe scattering of sound waves, although the formula originated with the German mathematician Bauer in 1859 [Bau59]. Its extensive use in quantum scattering is of more recent origin, beginning with Faxen and Holtmark [Fax27].

Spherical Bessel functions as functions of $\rho = kr$ and ℓ are shown in Figure 5.10. You may make similar graphics by using *Mathematica* notebook BesL, as Problem 5.11 suggests.

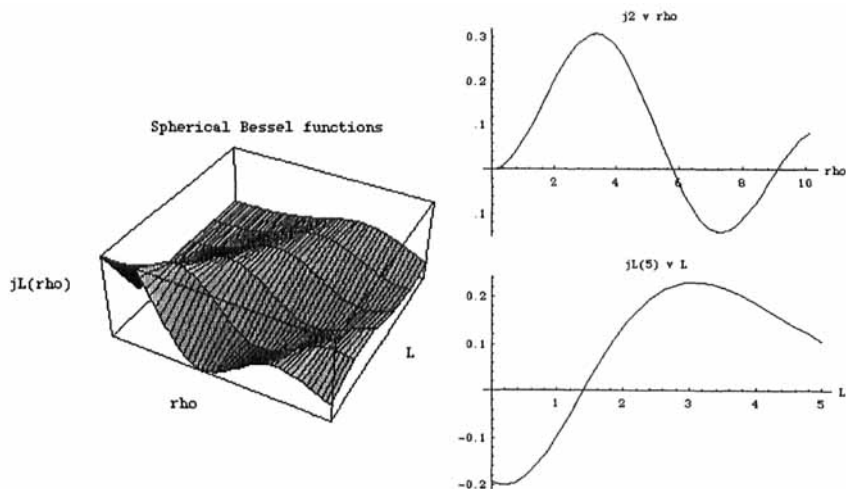


FIGURE 5.10 Spherical Bessel functions $j_L(\rho)$ in terms of $\rho = kr$ from 0 to 10 for $L = 0, 1, \dots, 5$ are shown as a surface at the left. The top right shows a section through this surface at $L = 2$. The bottom right shows a section at $\rho = 5$; for our purposes values at integer L are used. (*Mathematica* notebook BesL.)

The existence of a partial-wave expansion of the form (5.61) can easily be derived if the Legendre polynomials have been identified [But68, Won91] as solutions of the θ part of the Helmholtz wave equation

$$(\nabla^2 + k^2)\psi(\mathbf{r}) = 0 \quad (5.62)$$

and if the spherical Bessel functions have been shown [But68] to solve the radial part of the wave equation for the same value of ℓ . In order to specify the c_ℓ we recall the standardization of the Legendre polynomials from Section 4.1.1, namely

$$P_\ell(1) = 1 \quad (5.63)$$

and also the standardization (normalization) of the j_ℓ [But68]:

$$j_\ell(\rho) \rightarrow \frac{\rho^\ell}{(2\ell+1)!!} \left[1 - \frac{\rho^2}{2(2\ell+3)} \right] \quad \frac{\rho^2}{\ell} \ll 1 \quad (5.64)$$

where the double factorial of n is $n!! \equiv n(n-2)(n-4)\dots$. The conventional derivation of the formula for c_ℓ involves multiplying both sides of (5.61) by P_ℓ , then integrating over θ . This method requires knowing integrals of exponentials with Legendre polynomials as well as the integral definition of j_ℓ , which are hidden within Watson's treatise on Bessel functions [Wat44]. A much neater method is to use only the dependence of the expansion on $\rho = kr$, as follows. Since the c_ℓ are independent of θ , we may evaluate them at any convenient angle, such as $\theta = 0$, for which (5.63) allows (5.61) to be rewritten as

$$e^{i\rho} = \sum_{\ell=0}^{\infty} c_\ell j_\ell(\rho) \quad (5.65)$$

By invoking the parity symmetry of the Legendre polynomials from (4.4), $P_\ell(-1) = (-1)^\ell P_\ell(1)$, we can show quickly that $c_\ell^* = (-1)^\ell c_\ell$. Therefore, c_ℓ must be of the form

$$c_\ell = i^\ell a_\ell \quad (5.66)$$

where the a_ℓ are real amplitudes. This first step in the derivation is not essential but it simplifies the next step because it identifies the complex-number part of the expression.

To determine the a_ℓ , differentiate both sides of (5.65) with respect to ρ and use substitution (5.66) for c_ℓ . The resulting left-hand side is just i times the expansion (5.65), while the right-hand-side derivative can be expanded by using

$$\frac{d j_\ell(\rho)}{d\rho} = \frac{\ell}{2\ell+1} j_{\ell-1}(\rho) - \frac{\ell+1}{2\ell+1} j_{\ell+1}(\rho) \quad (5.67)$$

which follows readily from derivative and recurrence formulas for Bessel functions [But68, p.359]. If the partial-wave expansion is then rearranged to equate coefficients of the linearly-independent function $j_\ell(\rho)$ on both sides of the derivative relation, we find immediately the requirement that

$$a_\ell = (\ell+1) \frac{a_{\ell+1}}{2\ell+3} + \ell \frac{a_{\ell-1}}{2\ell-1} \quad (5.68)$$

This is a set of linear recurrence relations and may be rewritten to express successive coefficients in terms of the coefficients for the two previous partial waves. By expanding both sides of (5.65) through terms linear in ρ and using (5.64) for the lowest-order spherical Bessel functions, one readily finds that $a_0 = 1$ and $a_1 = 3$. Successive terms that satisfy (5.68) are then seen to be given by

$$a_\ell = 2\ell + 1 \quad (5.69)$$

Finally, by combining (5.69) and (5.66) and inserting into (5.61), we have derived simply the partial-wave expansion of a plane wave in three dimensions:

$$e^{ikr\cos\theta} = \sum_{\ell=0}^{\infty} i^\ell (2\ell + 1) j_\ell(kr) P_\ell(\cos\theta) \quad (5.70)$$

As a mnemonic, recall that $2\ell + 1$ is the number of angular momentum substates associated with partial wave ℓ . Visualization of this expansion is made in Section 5.4.2.

Plane Waves in Two Dimensions. The spatial part of a plane wave in two dimensions can be expanded in plane-polar coordinates, (r, ϕ) , with $x = r \cos \phi$, $y = r \sin \phi$. The expansion analogous to (5.70) in terms of cylindrical Bessel functions and complex exponentials of the angle ϕ is

$$e^{ikr\cos\phi} = \sum_{m=-\infty}^{\infty} i^m J_m(kr) e^{im\phi} \quad (5.71)$$

for a wave in which the lines of constant phase are perpendicular to the x axis. Notice that for two dimensions the complex-exponential functions are the analogues of the Legendre functions in three dimensions. This equation can alternatively be written in terms of cosines with non-negative m values.

In (5.71) J_m is the *cylindrical* Bessel function of order m , the analogue for two dimensions of the spherical Bessel functions required in three dimensions. The behavior of J_m as a function of $\rho = kr$ and of m is shown in Figure 5.11. Problem 5.12 invites you to examine relations between spherical and cylindrical Bessel functions and to visualize these by using *Mathematica* notebook `BesM`.

The derivation of the partial-wave expansion for two dimensions, (5.71), is suggested in Problem 5.12. The result is more than a curiosity for students of angular momentum, since steps analogous to those for three dimensions show that the operator

$$L_0 = -i \left(x \frac{\partial}{\partial y} - y \frac{\partial}{\partial x} \right) = -i \frac{\partial}{\partial \phi} \quad (5.72)$$

has eigenvalues m . Therefore, L_0 in two dimensions is the analogue of L_z in three dimensions, while the quantum numbers m take on the same values in both dimensions, namely the integers. Wave scattering in two dimensions is described with several examples in the articles by Adhikari [Adh86] and by Lapidus [Lap82].

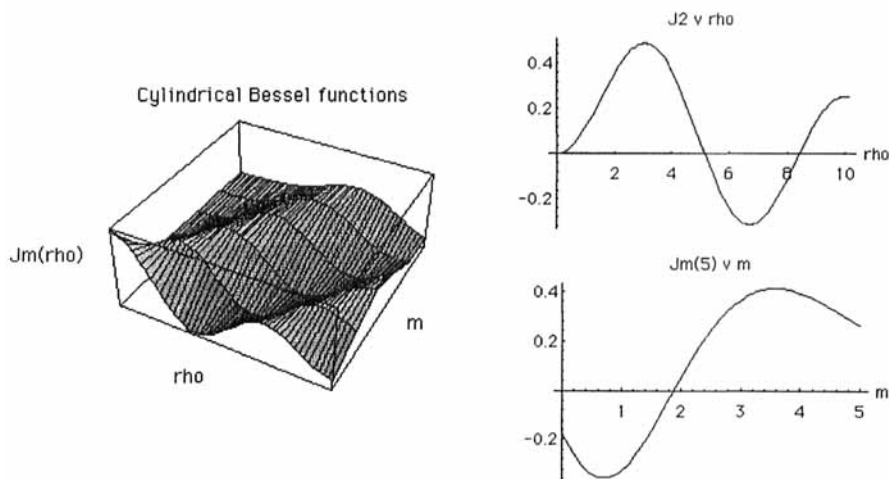


FIGURE 5.11 Cylindrical Bessel functions $J_m(\rho)$ displayed as functions of $\rho = \rho$ from 0 to 10 for $m = 0, 1, \dots, 5$ are shown as a surface at the left. Top right shows a section through this surface at $m = 2$. Bottom right shows a section at $\rho = 5$; for our purposes the values at integer m are used. (*Mathematica* notebook BesM.)

Expansion (5.71) may also be considered as a Fourier series expansion of the complex exponential on the left-hand side into its Fourier components $e^{im\phi}$ with m an integer. The Fourier coefficients are then $i^m J_m(\cos\phi)$, which depend on ρ because the left-hand side is a function of ρ as well as of ϕ . Techniques of Fourier expansions are covered—both analytically and numerically—in Thompson's text on computing [Tho92b].

One Dimension. For the spatial part of a wave in one dimension, say x , one has merely the two-term Euler formula

$$e^{ikx} = \cos(kx) + i \sin(kx) \quad (5.73)$$

in which the rotational symmetries occurring in two and three dimensions are replaced by the even and odd reflection symmetries under $x \rightarrow -x$ of the cosine and sine functions, respectively. A discussion of scattering and phase shifts in one dimension has been given by Formánek [For76]. Notice that in (5.70), (5.71), and (5.73) the $j_\ell(kr)$, $J_m(kr)$, and $\cos(kx)$ or $\sin(kx)$, respectively, are basis functions for the distance-dependent parts of the separated Helmholtz equation.

Convergence of Expansions. Convergence properties of plane-wave expansions such as (5.70) and (5.71), both analytical and numerical, are of interest. For example, analytical convergence of (5.70) can be examined by considering, for fixed kr , a partial wave which is large enough that (5.64) is a good approximation to the Bessel function. The ratio of the magnitude of successive partial-wave terms is then no larger than $\rho / (2\ell + 1)$ (recall that Legendre functions are bounded by ± 1). Thus, by comparison with successive terms in the exponential series, the expansion (5.70) is convergent.

Numerical convergence of the expansions can be visualized as follows. A spherical Bessel function of order ℓ satisfies the differential equation

$$\frac{d^2}{d\rho^2} [\rho j_\ell(\rho)] + \left[1 - \frac{\ell(\ell+1)}{\rho^2} \right] \rho j_\ell(\rho) = 0 \quad (5.74)$$

which has as solutions that are standardized according to (5.64):

$$j_0(\rho) = \frac{\sin \rho}{\rho} \quad j_1(\rho) = \frac{\sin \rho}{\rho^2} - \frac{\cos \rho}{\rho} \quad (5.75)$$

from which higher-order functions can be generated by the recurrence formula

$$j_{\ell+1}(\rho) = \frac{(2\ell+1)j_\ell(\rho)}{\rho} - j_{\ell-1}(\rho) \quad (5.76)$$

To check correct analytical application of (5.76), using (5.75) produces for $\ell = 2$

$$j_2(\rho) = \left(\frac{3}{\rho^3} - \frac{1}{\rho} \right) \sin \rho - \frac{3}{\rho^2} \cos \rho \quad (5.77)$$

which you will find to be correct.

The recurrence formula (5.76) is suitable for analytical work, but it does not provide a numerically stable way to generate the higher-order functions. Numerically, if one wants values of j_ℓ over a wide range of partial waves for ρ fixed one can use approximation (5.64) for a partial wave somewhat higher than one needs, then rewrite (5.76) to generate lower partial wave values by downward recurrence. Thereby the function values are increasing as ℓ decreases, so roundoff errors are relatively decreasing.

The so-called Riccati-Bessel function, $\rho j_\ell(\rho)$, corresponds to the radial wave functions that are most commonly used for solutions of wave equations of the Helmholtz and Schrödinger type in spherical-polar coordinates.

The convergence of partial-wave expansions of plane waves is to be contrasted with difficulties that arise in a similar expansion for wave scattering in a $1/r$ potential, typically the Coulomb-scattering problem. The expansion analogous to (5.61) with replacement of the spherical Bessel functions by the regular partial-wave Coulomb functions produces a nonconvergent expansion, as is carefully discussed by Marquez [Mar72], both analytically and numerically. In spite of these problems, a correct treatment of scattering by Coulomb plus short-range potentials is still possible. A clear discussion is provided in Landau's quantum mechanics text [Lan90].

Centripetal Barriers. Effects of the “centripetal barrier,” $\ell(\ell+1)/\rho^2$, in the radial Schrödinger equation in three dimensions can be seen in the spherical Bessel functions, analytically and numerically. According to (5.64), a partial-wave amplitude for $\ell > 0$ increases as ρ increases from zero. Using (5.74), we see that $\rho j_\ell(\rho)$ has a point of inflection (its slope starts to decrease) at $\rho = \rho_l = \sqrt{\ell(\ell+1)}$, which is within $1/(2\ell)$ of ℓ . Therefore the point of inflection of the wave function marks the classical value of $\rho = kr$ at which the particle would most probably be found if it had ℓ units of orbital angular momentum. For $\ell = 0$ the maximum of the spherical Bessel function $[\sin(\rho)/\rho]$ is at the origin (a classical particle and no lever arm) and the point of inflection of the zero-order Riccati-Bessel function is also there.

The factor ρ in (5.74) changes a cumbersome expression for the radial part of the ∇^2 operator, having both first and second radial derivatives, into a simple second derivative in ρ , as shown, so that the equation resembles that for Cartesian coordinates. A geometric interpretation of this simplification is that when the squares of the functions are used to construct probability densities (quantum mechanics) or energy densities (classical waves), the factor of ρ multiplying the function gives a density per unit $d\rho$ rather than per unit $\rho^2 d\rho$, which is proportional to the volume element in spherical-polar coordinates. Similar considerations hold for plane-polar coordinates, as you may derive in Problem 5.13.

In two dimensions we can identify the centripetal-barrier term in the radial Schrödinger or Helmholtz equations—here just the equation for the cylindrical Bessel function

$$J_m'' + \frac{1}{\rho} J_m' + \left(1 - \frac{m^2}{\rho^2}\right) J_m(\rho) = 0 \quad (5.78)$$

which can be compared with (5.74). Its solutions cannot be written in simple forms such as (5.75). Thus, m^2/ρ^2 is the analogue in two dimensions of $\ell(\ell+1)/\rho^2$ in three dimensions. This again provides a correspondence between the eigenvalue m in two dimensions and ℓ in three dimensions. By comparing Figures 5.10 and 5.11 we also see a similar behavior with increasing quantum number of the appropriate Bessel functions. This suggests, as the displays of partial-wave expansions in Section 5.4.2 show, that for the same number of partial waves in the expansions, the two- and three-dimensional expansions are remarkably similar.

5.4.2 Displaying Partial-Wave Expansions

Now that we understand the analysis behind partial-wave expansions in two and three dimensions, it is interesting to visualize the expansions carried out with a varying upper limit to the expansions. Such truncated partial-wave expansions are usually considered as purely mathematical results to be used in scattering theory. However, by displaying them we appreciate the angular momentum components contained within a plane wave.

Three Dimensions. For the three-dimensional wave we indicate the analytical and numerical steps; then the two-dimensional example may be done by analogy.

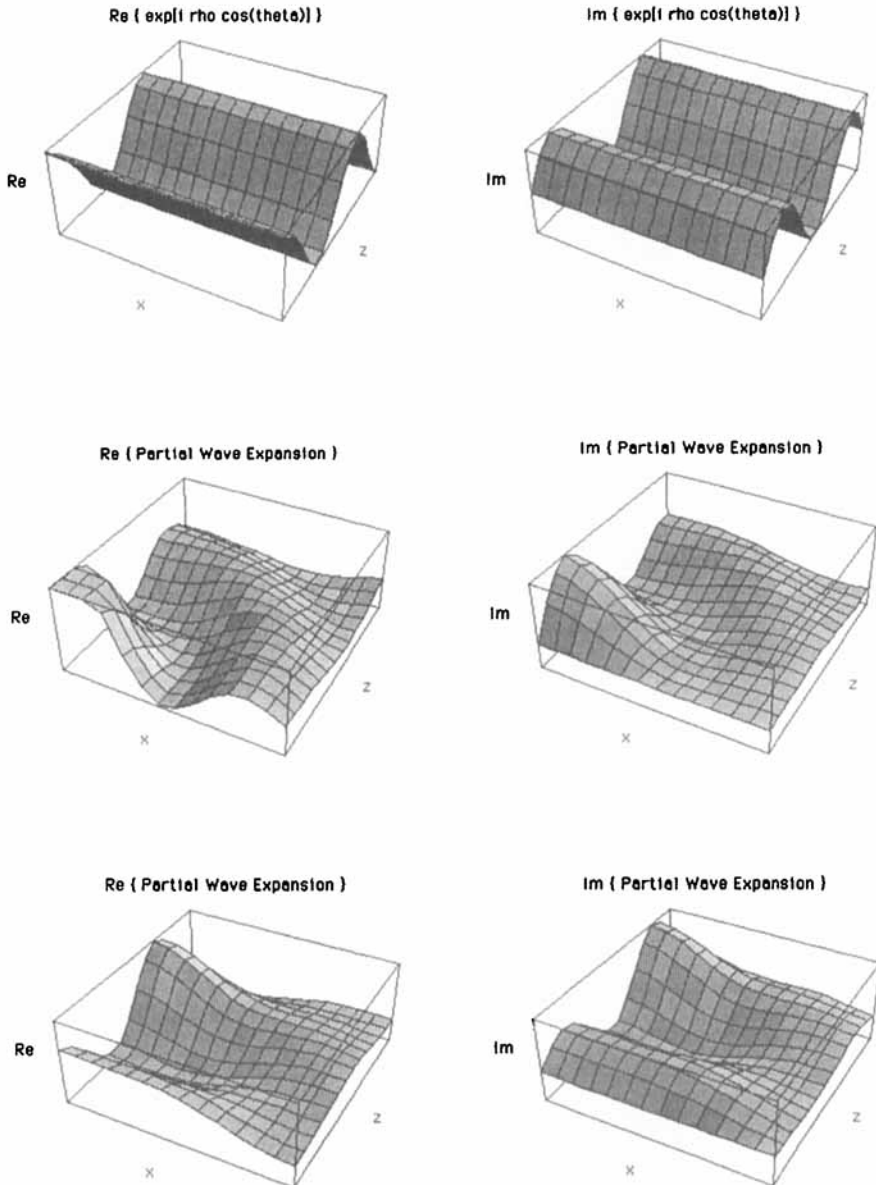


FIGURE 5.12 Partial-wave expansions in spherical-polar coordinates, with the origin of the coordinate system in the leftmost corner of each frame. Left-side panels show the real parts and right-side panels show the corresponding imaginary parts. Top panels show the complex exponential $\exp(i\rho\cos\theta)$, with ρ ranging from 0 to 10. Middle panels have summation upper limit $L=1$ (thus $\ell=0, 1$), and bottom panels have $L=5$. (Adapted from *Mathematica* notebook PW3D.)

For purposes of display, the expansion (5.70) to a finite upper limit L can be expressed in real and imaginary parts, with the real part describing the sum over even partial waves and the imaginary part the sum over odd partial waves, since this is just how i^ℓ (which is the only complex-number part of the expansion) alternates between even and odd ℓ . The steps for doing this are suggested as Problem 5.14, where the expressions are also given. One can compute these sums for a given L and range of ρ , then compare them with corresponding parts of the complex exponential, namely $\cos(\rho \cos \theta)$ and $\sin(\rho \cos \theta)$. This is done—using *Mathematica* to compute the spherical Bessel functions, Legendre polynomials, and graphics—in Figure 5.12. Problem 5.14 suggests that you use *Mathematica* notebook PW3D to explore the partial-wave expansion.

Since the wave is propagating in the z direction, there is no x dependence of the full waves (top two frames in Figure 5.12). In the partial-wave expansion, however, if we truncate the expansion at $\ell = L$, then higher angular momentum components are ignored, which produces an angle dependence (lower four frames in Figure 5.12) and an incorrect z dependence because the spherical Bessel functions (which carry the ρ dependence) are also omitted.

For $L = 1$ (middle two frames), $\ell = 0$ is the only contribution to the real part (note its independence of θ), while only $\ell = 1$ contributes to the imaginary part, which varies as $P_1(\cos \theta) = \cos \theta$. If the expansion is carried out to $L = 5$ (bottom two frames), the agreement with the exact result is good for small ρ but deteriorates as ρ increases because the contributions from higher-order terms then become more significant. By varying L and the maximum ρ value in *Mathematica* notebook PW3D, you can substantiate these claims.

Plane Waves in Two Dimensions. In two dimensions the partial-wave expansion in cylindrical coordinates, (5.71), can be developed similarly to that for three dimensions, but more simply. We consider a wave propagating in the x direction, with y as the other dimension, so the angle ϕ is measured from x toward y . A separation into even and odd m values again produces the real and imaginary parts of the expansion, as suggested in Problem 5.16, which gives the formulas when the upper limit on m is M . The resulting partial-wave surfaces, computed using *Mathematica*, are shown in Figure 5.13. You can produce such visualizations of partial-wave expansions by using *Mathematica* notebook PW2D, as Problem 5.15 suggests.

The expansions in two dimensions, Figure 5.13, are overall remarkably similar to those in three dimensions, Figure 5.12, because of the similarities of the Bessel functions describing the radial dependences, as discussed for the centripetal barriers in Section 5.4.1. The angular dependences, described by $\cos(m\phi)$ and $P_\ell(\cos \theta)$ for two or three dimensions, are substantially different, so as one moves away from $\phi = 0$ or $\theta = 0$ the discrepancies between the two figures increase. For the same upper limits in the partial-wave summations ($L = 1$ or $M = 1$ in middle panels, $L = 5$ or $M = 5$ in bottom panels), the reconstructions of the full waves are also similar.

Consider also the Fourier-expansion viewpoint, discussed for two dimensions in Section 5.4.1. The surfaces in the lowest four panels of Figure 5.13 are best-fit reconstructions of the surfaces in the top two panels for the given number of terms in

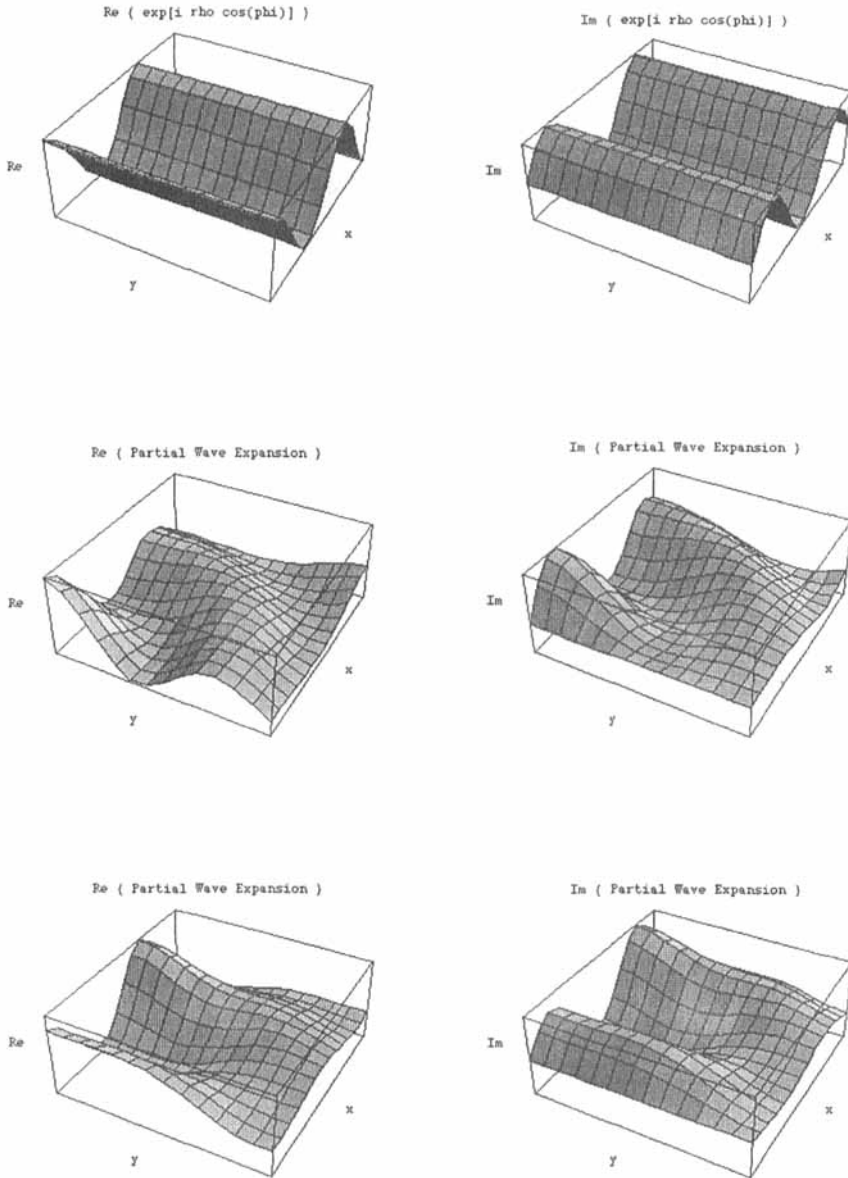


FIGURE 5.13 Partial-wave expansions in cylindrical coordinates, with the origin of the coordinate system in the leftmost corner of each frame. Left-side panels show the real parts, right-side panels show the imaginary parts. Top panels show the complex exponential $\exp(i\rho\cos\phi)$, with ρ ranging from 0 to 10. Middle panels have upper limit on the summation $M = 1$ (thus $m = 0, 1$), and bottom panels have $M = 5$. (Adapted from *Mathematica* notebook PW2D.)

the expansion ($M = 1$ in middle panels, $M = 5$ in bottom panels). In this context “best-fit” means the least-squares fitting criterion, which is what Fourier expansion coefficients provide, as described in Chapters 6 and 9 of Thompson [Tho92b].

5.5 THE CONCEPTUAL DEVELOPMENT OF ANGULAR MOMENTUM

We have now completed the foundations for understanding angular momentum and rotational symmetries for physical systems, comprising the first half of the book. In the second half we develop techniques and applications, which increase our expertise and reinforce our understanding, but contribute much less to conceptual development than do the topics in the first half.

At this juncture it is interesting to make an excursion to view the foundations of ideas about angular momentum, especially to show how the geometrical and dynamical aspects of the subject are bonded together. These two aspects are also discussed in Section 3.4.5, where we give examples clarifying the distinction between them, and in Section 5.1, where we characterize various distinctions between geometrical (rotational-symmetry) and dynamical (mechanical) viewpoints of angular momentum, emphasizing the role of Planck’s constant. We now summarize the conceptual development of angular momentum from a historical perspective.

A Brief History of Angular Momentum. The historical development of concepts in angular momentum and use of symmetry in the physical sciences, emphasizing rotational symmetry, is summarized in Figure 5.14. Scientists and their publications are selected under the criterion that in these works the key ideas are clearly expressed for the first time.

The earliest recognition of a conservation condition for rotational motion was probably by Kepler in 1609, with his empirical law of constant areal velocities for the motions of planets about the sun. Newton in *Principia Mathematica* (1686) showed that this law is a consequence of the central-force nature of gravitational attraction. Together with the fact that the orbits lie in a plane, we would nowadays call this the constancy of angular momentum for two-body central-force motion. Progress was from an essentially geometrical property (areal velocity) to a dynamical property (central forces). Such a progression is also discussed in Section 4.3.1.

Two centuries passed while the followers of Newton piled up layer upon layer of the consequences of his new mechanics, just as hosts of physicists and chemists in the second half of the twentieth century burden the libraries of the world with inferences from quantum mechanics. In 1848, Pasteur announced his discovery of a handedness in organic crystals, as discussed in Section 1.2.1. In two critical works in 1883 and 1901, Ernst Mach examined the foundations of mechanics and the relations between space and geometry. This work had significant influence on Einstein’s ideas about relativity of motion. About the same time, Pierre Curie presented his principles relating symmetries in causes and effects, as we discuss in Section 1.1.2. In 1918, Emmy Noether showed the necessary connections between continuous symmetries and conservation laws. Although (as discussed in Sec-

tion 1.1.2) this was interpreted in the context of classical mechanics, her theorem foreshadowed the extensive applications of group theory (Section 2.5) to physical systems.

Conceptual Development of Angular Momentum

- 1942 Racah: Complex spectra; angular momentum coupling [Rac42]
 1935 Condon and Shortley: Theory of atomic spectra [Con35]
 1930 Eckart, 1931 Wigner: Irreducible tensors [Eck30, Wig31]
 1927 Wigner: Rotation group applied to quantum mechanics [Wig27a,b]
 1926 Heisenberg and Jordan: Spin-1/2 angular momentum [Hei26]
 1926 Born et al.: Quantum angular momentum operators [Bor26]
 1919 Landé: Vector-addition model of angular momentum [Lan19]
 1918 Noether: Continuous symmetries and conservation laws [Noe18]
 1916 Sommerfeld: Spatial quantization of angular momentum [Som16]
 1913 Bohr: Quantized angular momentum for hydrogen atom [Boh13]
 1911 Nernst: Quantization of rotational motion [Ner11]
 1901 Mach: Space and geometry [Mac01]
 1894 Curie: Symmetry, causes and effects [Cur94]
 1883 Mach: Critique of classical mechanics [Mac83]
 1848 Pasteur: Discovery of handedness of organic molecules [Pas48]
 1686 Newton: Constancy of areal velocity for central forces [New86]
 1609 Kepler: Constancy of areal velocity for planetary orbits [Kep09]

FIGURE 5.14 Historical view of the foundations and conceptual development of angular momentum in its dynamical and rotational-symmetry aspects. As with geological strata, the vertical time scale is not uniform. In the text we summarize the significance of each publication.

Angular Momentum and the Development of Quantum Mechanics. While various symmetry topics were being developed in classical physics, the physicists were trying to complete the edifice of classical mechanics and electrodynamics. However, when Planck introduced the quantization of energy in 1900, cracks in the

foundation began to show. Twenty-five years passed as the scientists patched up the classical mechanics of atoms and their spectra by inventing various quantization conditions. In particular, the suggestion that rotational motion should be quantized was made by Nernst in 1911 and was used by Bohr in 1913 in his theory of the structure of the hydrogen atom. Sommerfeld suggested in 1916 that angular momenta should be quantized not only in their values but also spatially, which led to Landé's extensive use in 1919 of a vector-addition model for angular momentum (our Section 5.3).

The birth of modern quantum mechanics is usually dated to 1926, from several papers which appeared in that year. They are available in English translation in Van der Waerden's sourcebook [Van67]. Of particular importance to angular momentum are the papers by Born, Heisenberg, and Jordan [Bor26] and by Heisenberg and Jordan [Hei26]. They used the prescription for quantizing classical angular momentum, $\mathbf{p} \rightarrow -i\hbar\nabla$, to obtain an operator for dynamical angular momentum. Because they used the commutation relations to define angular momentum, they obtained half-integer as well as integer multiples of \hbar for the eigenvalues. Their use of \hbar (dynamical angular momentum in Figure 3.11) predisposed researchers and textbook authors to the dynamical viewpoint for the remainder of the twentieth century, as contrasted with the geometrical viewpoint we emphasize here.

This confluence of ideas in classical mechanics, symmetries, and quantum mechanics that underlie angular momentum and rotational symmetries is schematized in Figure 5.15.

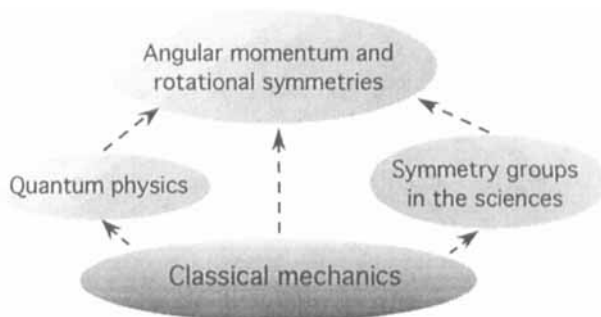


FIGURE 5.15 Ideas from classical mechanics, geometric symmetries, and quantum mechanics form the concepts underlying angular momentum and rotational symmetries.

Rotational Symmetry and Group Theory. The rotational-symmetry viewpoint and the use of group theory (Section 2.5) were emphasized by Wigner in a 1927 paper [Wig27b] and in his 1931 book [Wig31]. Eckart's 1930 paper foreshadowed Wigner's theory of irreducible tensor operators, particularly the Wigner-Eckart theorem on the magnetic-substate dependence of their matrix elements, which we derive in Section 8.3. The compendium on the theory of atomic spectra by Condon and Shortley (1935) and a series of papers by Racah beginning in 1942 presented many of the techniques of angular momentum by using algebraic methods rather than group theory techniques. Since then, the subject of angular momentum and its gen-

eralizations to other groups of continuous symmetries have grown in complexity and completeness, but their conceptual basis has not changed significantly.

An extensive history of the conceptual development of quantum mechanics in the first half of the twentieth century is given in the book by Jammer [Jam89], which also provides complete references. Several sources provide translated papers and reprints of obscure material on the development of angular momentum. Van der Waerden's book of sources in quantum mechanics [Van67] has a historical introduction and 17 key papers from 1917 through 1926, all of them in English. Biedenharn and Van Dam [Bie65] provide a historical survey in their collection of reprints and original papers. The two volumes on angular momentum theory by Biedenharn and Louck [Bie81a, Bie81b] are also mines of historical and technical information.

PROBLEMS ON ANGULAR MOMENTUM IN QUANTUM SYSTEMS

5.1 To derive the Ehrenfest theorem for orbital angular momentum, (5.5), consider a single component of \mathbf{L} , say L_x , and write this in Cartesian coordinates. Then consider the commutator $[L_x, H]f$, where f is any well-behaved function of the coordinates. Show that

$$[L_x, H]f = -i\hbar \left(y \frac{\partial V}{\partial z} - z \frac{\partial V}{\partial y} \right) f = -i\hbar (\mathbf{r} \times \nabla V)_x f \quad (5.79)$$

and thereby establish the correctness of (5.5).

5.2 To show the constancy of the quantal orbital angular momentum expectation values, $\langle L_i \rangle$ with $i = x, y, z$, for a particle experiencing a central force, $V(\mathbf{r}) = V(r)$, write out the derivative expression for a component (say the one in the x direction) of $\mathbf{r} \times \nabla V$. By showing that

$$\frac{\partial V}{\partial z} = \frac{z}{r} \frac{\partial V}{\partial r} \quad \frac{\partial V}{\partial y} = \frac{y}{r} \frac{\partial V}{\partial r} \quad r = \sqrt{x^2 + y^2 + z^2} \quad (5.80)$$

show that $(\mathbf{r} \times \nabla V)_z = 0$, and therefore that $\langle L_x \rangle$ is constant in time.

5.3 Derive formula (5.9) for the commutator of \mathbf{J} with $\mathbf{J} \cdot \mathbf{B}$ by considering a single component of the first appearance of \mathbf{J} , then using its commutator relations (3.6) with each of the \mathbf{J} components in $\mathbf{J} \cdot \mathbf{B}$. Because of the equivalence of the three components of \mathbf{J} , once you have the relation for one component you essentially have it for all three components.

5.4 In order to verify the Majorana formula (5.14), make the substitution of the expansion (5.16) of $U(t)$ in terms of the independent $U_k(t)$ in (5.17).

5.5 Derive the minimum-uncertainty equations for the state ψ_m by combining (5.23) and (5.27), reordering the Q and P in the latter by using the commutator in the text, then substituting the proportionality relation (5.26), to obtain (5.28).

5.6 Use (3.64) and (3.65) in the definitions (5.20) and (5.21) for uncertainties,

then multiply out the matrices for J_x^2 and J_y^2 to derive (5.40).

5.7 Carry out the derivation for the minimum-uncertainty states for L_{qx} and L_{qy} as follows.

(a) Substitute for the general operators P and Q in (5.32) the specific forms of L_{qx} and L_{qy} from (3.24), and note that their expectation values are zero for states of definite L_{qz} .

(b) Carry out the steps from (5.43) to (5.45) in order to verify the indicated θ and ϕ dependence of the wave function.

(c) Derive the normalization given in (5.45) by carrying out the integration over ϕ (0 to 2π) and over θ (0 to π). A method for the θ integration is indicated in Problem 4.4.

5.8 Consider the minimum-uncertainty states of L_{qz} with $\sin \phi$ as angle variable.

(a) Show that the requirement of periodic behavior of $\psi_{sm}(\phi)$ with period 2π reduces (5.56) to (5.57).

(b) Show by direct integration that the expectation value of L_{qz} in this state is $m\hbar$.

(c) Use symmetry arguments to show that the expectation value of $\sin \phi$ is zero in this state.

(d) Consider the behavior of the expectation values given in Table 5.3 for large μ and for small μ . For computing the matrix elements and state normalization for large μ , make a new variable of integration that is $\mu \cos \phi$ rather than ϕ . Thus produce the limiting cases for $\mu \rightarrow \infty$ in the table. For small μ , expand the exponential in the square of the wave function by a Maclaurin series, then evaluate integrals approximately, thus producing the $\mu \rightarrow 0$ cases in the table.

5.9 Show that if the expectation value $\langle \mathbf{J}^2 \rangle$ is estimated by integrating m^2 from $-j$ to j , with an average m estimated by its range, $2j$, then $\langle \mathbf{J}^2 \rangle \rightarrow j^2$.

5.10^M The vector model of angular momentum is illustrated in Figure 5.9 by showing a helical shell spinning on its tip about a central axis while this axis precesses uniformly on a cone about the z axis. To understand *Mathematica* notebook *Precess*, carry out the following geometry of rotations.

(a) If you have not worked Problem 1.2, show that a helical spiral centered vertically on the z axis can be generated by the equations

$$x = \phi \cos t \cos \phi \quad y = \phi \cos t \sin \phi \quad z = \phi \sin t + h \phi \quad (5.81)$$

where $0 \leq t \leq 2\pi$ generates the circular cross section of a spiral arm for given ϕ , and ϕ generates the twist about the central axis. For a spiral with r revolutions, $0 \leq \phi \leq 2\pi r$. The helicity $h = +1$ for a right-handed spiral (as shown) and $h = -1$ for a left-handed spiral. In the notebook ϕ is denoted by `ph`.

(b) Show that to tilt the spiral at an angle θ_s to the z axis, one can rotate it around the space-fixed y axis, using the matrix $A_y(\theta_s)$ given by (1.15) to transform the coordinates obtained in (a). In the notebook θ_s is denoted by `thS`.

(c) Show that to produce uniform precession of the tilted shell about the space-fixed z axis, the coordinates obtained in (b) should be rotated by using matrix $A_z(\phi_s)$ given by (1.14). In *Precess* ϕ_s is called `ps`, and it is varied in 8 uniform incre-

ments of $\pi/4$, $\{i, 0, 7, 1\}$ to make the object Shells. Note that in steps (b) and (c) you use Euler angles $\beta = \theta_s$ and $\gamma = \phi_s$.

(d) Run the notebook `Precess` to generate 8 views of the shell, then animate these views to show the uniform precession in time. The smoothness of this “movie” will depend upon the speed of your computer system, so you may need to adjust the number of views to get a smooth display, assuming that you do not have a way to adjust your own persistence of vision.

5.11^M Use *Mathematica* notebook `BesL` to visualize the spherical Bessel functions $j_\ell(\rho)$ as shown in Figure 5.10.

5.12^M Consider the plane wave in two dimensions, as discussed in Section 5.4.1.

(a) Derive the partial-wave expansion (5.71) by using a similar method to that for three dimensions.

(b) Use *Mathematica* notebook `BesM` to visualize the cylindrical Bessel functions $J_m(\rho)$, as shown in Figure 5.11.

5.13^M Consider the spherical Bessel function.

(a) Show that the analogue of the differential equation (5.74) is

$$\frac{d^2}{d\rho^2} [\sqrt{\rho} J_m(\rho)] + \left[1 - \frac{m^2 - 1/4}{\rho^2} \right] \sqrt{\rho} J_m(\rho) = 0 \quad (5.82)$$

and that therefore that the point of inflection of $\sqrt{\rho} J_m(\rho)$ is at $\rho_I = \sqrt{m^2 - 1/4}$.

(b) Following the arguments made for spherical-polar coordinates, show that the factor $\sqrt{\rho}$ in (5.82) takes care of the factor ρ in the surface element $\rho d\rho$ for plane-polar coordinates.

(c) Prepare graphics of the modified cylindrical Bessel functions, $\sqrt{\rho} J_m(\rho)$, similar to those for $\rho j_\ell(\rho)$ shown in Figure 5.10, then compare them with their analogues in three dimensions. The *Mathematica* notebook `BesM` that is used for Figure 5.11 may be modified for this.

5.14^M Consider the plane-wave expansion in spherical-polar coordinates, (5.70).

(a) Show that the real part of this expansion may be written as

$$\sum_{l=0}^{[L/2]} (-1)^l (4l+1) j_{2l}(\rho) P_{2l}(\cos\theta) \quad (5.83)$$

and that the imaginary part can be expressed as

$$\sum_{l=0}^{[(L-1)/2]} (-1)^l (4l+3) j_{2l+1}(\rho) P_{2l+1}(\cos\theta) \quad (5.84)$$

in both of which $[e]$ means “the integer part of expression e .”

(b) Use these two formulas in *Mathematica* notebook `PW3D` to visualize the real and imaginary parts of the partial-wave expansions shown in Figure 5.12.

5.15M Consider the expansion of a plane wave in two-dimensional cylindrical coordinates given by (5.71).

(a) Derive the expressions analogous to those in three dimensions for the real and imaginary parts, namely for the real part

$$J_0(\rho) + 2 \sum_{m'=1}^{[M/2]} (-1)^{m'} J_{2m'}(\rho) \cos(2m'\phi) \quad (5.85)$$

and for the imaginary part in cylindrical coordinates

$$2 \sum_{m'=0}^{[(M-1)/2]} (-1)^{m'} J_{2m'+1}(\rho) \cos[(2m'+1)\phi] \quad (5.86)$$

(b) Use these formulas in *Mathematica* notebook PW2D to compute the real and imaginary parts of the partial-wave expansions shown in Figure 5.13.



Chapter 6

FINITE ROTATIONS OF ANGULAR MOMENTUM EIGENSTATES

In Chapters 3, 4, and 5 we describe the behavior of systems under *small* rotations, and thus derive properties of angular momentum operators and their eigenstates $|jm\rangle$. Our main purpose in this chapter is more realistic—to understand the transformation of $|jm\rangle$ under *finite* rotations. The main topics covered are:

- The geometry of rotations is reviewed in Section 6.1, including the definition of the rotation matrices \mathbf{D}^j in terms of the Euler angles $(\alpha\beta\gamma)$.
- Determination of the rotation matrices is covered in Section 6.2, directly for spin-1 systems, then in more generality for arbitrary j .
- Interpreting rotated states and visualization of the matrix elements of the reduced rotation matrix, the $d_{m'm}^j$, are the main topics in Section 6.3.
- General properties of the rotation matrices, including symmetries and orthogonality properties, are derived in Section 6.4. Classical limits of rotation matrices are also considered in this section.
- Rigid-body rotations in quantum mechanics provide important connections between classical and quantum phenomena. We show in Section 6.5 how the rotation matrices are the eigenfunctions of the Hamiltonian of a rotator, then give examples of rotational spectra for molecular and nuclear systems.

The chapter concludes with problems to check your comprehension of the material on finite rotations of angular momentum eigenstates.

6.1 INTRODUCTION TO ROTATION MATRICES

As you begin this section you should review (Section 1.3.1) the confusing relations between active and passive rotations, as well as the definition of Euler angles for the active rotations that we use. It is very important to understand the conceptual and technical distinction between active and passive rotations. The main source of con-

fusion and error manifests itself as phase errors in algebraic expressions. Since, as discussed when presenting phase manipulation rules in Section 2.1.4, phases of ± 1 are often crucial to the interpretation of results in angular momentum—especially in its applications to quantum mechanics—it is necessary to distinguish phases that are consequences of rotational and other geometric symmetries of the system from phases arising from dynamical effects.

6.1.1 Review of Rotations and Angle Schemes

Chapter 3 begins by considering *full* rotations described by the unitary transformation operator, U , transforming states according to

$$U(\theta, \hat{\mathbf{n}}) = e^{-i\theta \hat{\mathbf{n}} \cdot \mathbf{J}} \quad (6.1)$$

in which $\hat{\mathbf{n}}$ is the unit normal to the direction of rotation and θ is the angle of rotation about this normal, as shown in Figure 3.1. In the remainder of Chapter 3 and in Chapter 4 we considered mainly *infinitesimal* rotations; that is, the properties of the operator \mathbf{J} and related eigenstates. Only for $j = 1/2$, where we could use the Pauli matrices directly in definition (6.1) to represent \mathbf{J} , did we make (Section 3.3.3) a matrix representation of U , given by (3.47). Our task in the present chapter is to construct such matrices for arbitrary j , with their elements labeled by the projection numbers.

The Euler Angles. To recall the scheme of Euler angles that we use to describe successive rotations of a system about space-fixed axes, look at Figure 6.1. We also show the detailed expression for the operator U , which is just the product of three U operators in (6.1) applied about the z axis (angle γ), then about the y axis (angle β), and finally about the z axis again (angle α). In Section 6.2 this angle scheme is used to construct matrix representations of U .

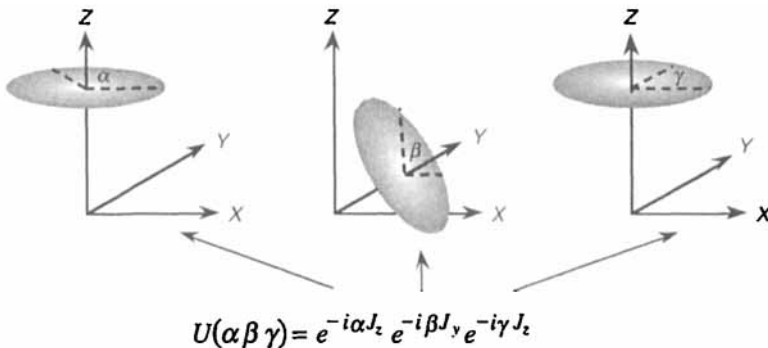


FIGURE 6.1 In the Euler-angle scheme for successive active rotations of a system about space-fixed axes, as shown, the rightmost rotation is applied first.

6.1.2 Group and Factorization Properties of Rotations

In Section 2.5 we provide an introduction to the key properties of groups, emphasizing their use for analyzing symmetry properties. We now summarize group properties of continuous rotations. Their representation matrices satisfy the same properties, since representations have the same group properties as the groups they represent, as explained in Section 2.5.3 and illustrated in Figure 2.14. The requirements that a set of elements and an operation between them must satisfy to form a group are summarized in Table 2.7.

Continuous Rotations Form a Group. In Example 4 in Section 2.5.1 we consider continuous rotations of an equilateral triangle about its center (Figure 2.12). In order to check that we have a group for our extended rotations in three dimensions, we must select group elements and a group “product.” The group elements are to consist of rotation operations U through sets of Euler angles $R_i = (\alpha_i, \beta_i, \gamma_i)$. Denote these elements by $U(R_i)$, $U(R_j)$, and so on. We are therefore dealing with a continuous group in the sense discussed in Section 2.5.4. The “multiplication” operation between elements is “successive rotations.” The notation $U(R_j)U(R_i)$ means “first rotate through angle set R_i , then rotate through angle set R_j . It is important to specify the order, since the rotations do not usually commute. Therefore, the three-dimension rotation group is non-Abelian (Section 2.5.2).

It is straightforward to verify that the group requirements given in Table 2.7 are satisfied for the above group elements and product rule. The identity element, E , is just a rotation with all angles zero, and the inverse of $U(\alpha, \beta, \gamma)$ is $U(-\gamma, -\beta, -\alpha)$, that is, rotations through the negative angles applied in the inverse order.

Representations of Continuous Rotations. Initial ideas on representing groups by mapping elements of groups onto matrices are described in Section 2.5.3. There the example of discrete rotations in a plane for the group C_3 is examined in detail and a matrix representation is described. Clearly, such rotations can be generalized to continuously variable angles and to three dimensions, with a corresponding generalization of the representation matrices. Such representations are described by the matrix groups (Table 2.12) identified by $SO(3)$, being Special because their determinant is +1, being Orthogonal, and being of dimension $N = 3$.

Another representation of rotations is based on spinors (Section 2.4), and involves 2×2 Unitary matrices with determinant +1, thus (in the nomenclature of Table 2.12) the matrix group is $SU(2)$. This representation is introduced in Section 3.3 in the context of the Pauli matrix representations of the \mathbf{J} operators. Most of our analysis in this chapter is based on $SU(2)$ representations.

6.2 DETERMINING ROTATION MATRICES

We determine the rotation matrices in a scheme where the total angular momentum j is fixed and the matrices are labeled by the projection number m . In Section 3.3.3

this is done explicitly for $j = 1/2$. We now do this more generally. First, we consider in Section 6.2.1 rotations about the z axis, the single axis chosen as the one with respect to which a component of \mathbf{J} has an eigenstate. (Recall that the fundamental commutation relations derived in Section 3.1.2 do not allow more than one component of \mathbf{J} to have eigenstates in a given representation.) This generalization of z -axis rotations to arbitrary j is straightforward and results in matrices that do not mix m values, that is, they are diagonal in m .

Rotation matrices for the y axis are more difficult to determine than for the z axis, since y -axis rotations mix m values; that is, they have off-diagonal elements. Although in Section 6.2.2 we use the direct matrix method of Section 3.3.3 for $j = 1$, such a method rapidly becomes cumbersome as j increases. For arbitrary j we therefore turn in Section 6.2.3 to the spinor representations introduced in Section 4.3.3, allowing a quick and intuitive derivation of the y -axis rotation matrices. Such matrices are called *reduced rotation matrices*, \mathbf{d}^j .

In Section 6.2.4 we show that when one of the m values labeling an element of \mathbf{d}^j is zero (which can happen only for j an integer), the matrix elements are simply related to Legendre functions. Finally in this section, we discuss practical ways to compute reduced rotation matrix elements.

6.2.1 Rotation of Eigenstates about z Axes

We begin by deriving the general formula for the matrix describing rotation of eigenstates (j, m) about the z axis, then we determine properties of this matrix.

Deriving the Rotation Matrix. We derive the matrix for z -axis rotations similarly to the derivation for spin 1/2 made in Section 3.3.3. The main difference is that there the Pauli matrix σ_z is used directly, whereas here we use the elements of the matrix. Consider a rotation about the z axis, with matrix elements computed between states $\langle j'm' |$ and $|jm\rangle$, as

$$\begin{aligned} \langle j'm' | e^{-i\gamma J_z} | jm \rangle &= \langle j'm' | \sum_{n=0}^{\infty} \frac{(-i\gamma J_z)^n}{n!} | jm \rangle \\ &= \langle j'm' | \sum_{n=0}^{\infty} \frac{(-i\gamma m)^n}{n!} | jm \rangle \\ &= e^{-i\gamma m} \langle j'm' | jm \rangle = e^{-i\gamma m} \delta_{j',j} \delta_{m',m} \end{aligned} \tag{6.2}$$

The first equality follows from the definition (2.38) of the exponential operator, the second equality arises because every application of J_z to a state with eigenvalue m produces just a factor m , and the third equality is from the definition of the exponential function. The final equality arises from the orthogonality relations for angular momentum eigenstates. Result (6.2) can be shown in matrix form as

$$\begin{bmatrix} e^{-i\gamma j} & 0 & 0 & \dots & 0 \\ 0 & e^{-i\gamma(j-1)} & 0 & \dots & 0 \\ 0 & 0 & \dots & \dots & 0 \\ 0 & \dots & \dots & \dots & 0 \\ 0 & \dots & \dots & 0 & e^{+i\gamma j} \end{bmatrix} \quad j=1: \begin{bmatrix} e^{-i\gamma} & 0 & 0 \\ 0 & 1 & 0 \\ 0 & 0 & e^{i\gamma} \end{bmatrix} \quad (6.3)$$

Here the labeling scheme has, as usual, the largest values of m' and m , namely j , in the top left-hand corner of the matrix, while the smallest values, namely $-j$, are in the lower right-hand corner. The particular case of $j = 1$ is shown on the right-hand side of (6.3). Note that we display a single block of a block-diagonal matrix (Section 2.1.3), with the value of j fixed. The block-diagonal property is required by the δ_{jj} in (6.2). In the example on the right-hand side of (6.3) the z -axis rotation matrix for $j = 1$ is 3×3 because there are $2j + 1 = 3$ values of each of m' and m . The form (6.3) is also exemplified by (3.43), derived explicitly for $j = 1/2$ by using the Pauli matrices.

Properties of z -axis Rotations. The general transformation matrices for z -axis rotations, (6.2), are explicitly unitary (as Problem 6.1 suggests you prove directly)—just as expected for a rotation, as discussed in Section 2.2.2. More particularly, z -axis rotations change only the *phase* of a state vector to which they are applied, without changing their magnitude. The consequences of such phase changes are usually nontrivial in quantum mechanics if there is more than one j or m value in a problem.

In the semiclassical vector model presented in Section 5.3, for a state of fixed j and m the angular momentum vector precesses *uniformly* around the z axis with a constant probability density along its orbit, as illustrated in Figure 6.2.

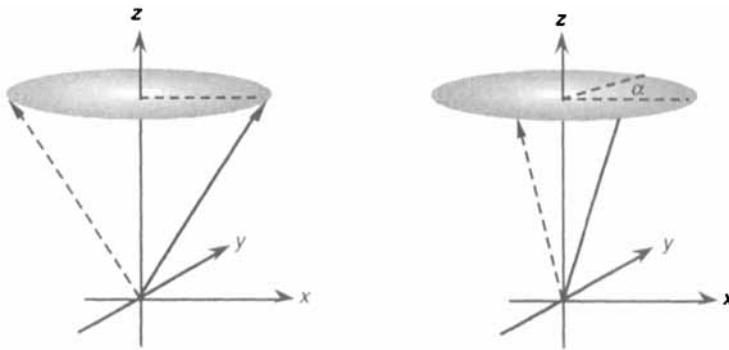


FIGURE 6.2 In the semiclassical vector model the angular momentum vector precesses uniformly around the z axis. The probability density is therefore not affected by a rotation through angle α about this axis.

The vector model is consistent with our algebraic result that z -axis rotations produce only phase changes, and thereby no change in probability density for each m value. We also see a limitation of the model; it is not able to depict such phase changes. The matrices (6.3) also show the property (to be derived in detail in Problem 6.1) that successive rotations about a z axis (without intermediate rotation about another axis) commute. Although such a property holds for *any* axis of rotation, its demonstration is particularly simple for z -axis rotations because the rotation matrices are diagonal.

Spinor Nature of z -Axis Rotations for Half-Integer Spins. We see immediately from (6.2) that when j is a half integer ($j = 1/2, 3/2, \dots$) every m value for this j is also half-integer, so a change of angle by 2π produces a sign change in every matrix element associated with that j . Therefore, we have a spinor nature for half-integer spins, according to the discussions in Sections 2.4 and 3.3.3.

Although experimentally, the spinor property is observed directly only for $j = 1/2$, namely with neutrons (Section 2.4), the correctness of the prediction that the property holds for *any* half-integer j is assured from consistency of calculations and measurements based on result (6.2), such as the properties of atoms and nuclei.

6.2.2 Rotations about the y Axis for $j = 1$

Rotations about the y axis are—as seen in Section 3.3.3 for $j = 1/2$ —more complicated to derive than are those for the z axis, but they are more interesting to understand and to apply. In this subsection we continue to use the direct matrix method used with the Pauli matrix σ_y for spin $1/2$ in Section 3.3.3.

Deriving the y -axis Rotation for $j = 1$. The calculation for $j = 1$ requires extension of the $j = 1/2$ treatment, but with the slight increase in complexity that the corresponding $3 \times 3 J_y$ matrix in Table 3.1 returns to J_y only after cubing, rather than after squaring. The details of the calculation of the operator exponential (3.1) using (2.38) are suggested as Problem 6.2. The result of this tedious calculation is

$$\mathbf{d}^1(\beta) = \begin{bmatrix} \cos^2(\beta/2) & -\frac{1}{\sqrt{2}}\sin\beta & \sin^2(\beta/2) \\ \frac{1}{\sqrt{2}}\sin\beta & \cos\beta & -\frac{1}{\sqrt{2}}\sin\beta \\ \sin^2(\beta/2) & \frac{1}{\sqrt{2}}\sin\beta & \cos^2(\beta/2) \end{bmatrix} \quad (6.4)$$

$$= \begin{bmatrix} c^2 & -\sqrt{2}cs & s^2 \\ \sqrt{2}cs & 1-2c^2 & -\sqrt{2}cs \\ s^2 & \sqrt{2}cs & c^2 \end{bmatrix} \quad c \equiv \cos(\beta/2) \quad s \equiv \sin(\beta/2)$$

Properties of the Spin-1 Matrix. It is quite clear to see that y -axis rotations for spin 1 do not have the simple phase relation that obtains for z -axis rotations. Moreover, incrementing β by any multiple of 2π leaves the matrix unchanged, so we do not have a spinor for this integer spin. However, as we know must hold for any rotation, \mathbf{d}^1 is a unitary matrix, as Problem 6.3 suggests that you verify. Indeed, since it is a real matrix, it is orthogonal.

A Worked Example for $j = 1$. As an example of y -axis rotation, consider a spin-1 system which is initially in state $m = 1$. What mixture of m values does it have after rotating it through angle β about the y axis? Following Table 3.2 or (4.70), the initial state can be described by the column matrix with 1 in the first position and 0 in the other two positions. After rotation we have the state vector

$$\begin{bmatrix} \cos^2(\beta/2) \\ \frac{1}{\sqrt{2}}\sin\beta \\ \sin^2(\beta/2) \end{bmatrix} = \begin{bmatrix} \cos^2(\beta/2) & -\frac{1}{\sqrt{2}}\sin\beta & \sin^2(\beta/2) \\ \frac{1}{\sqrt{2}}\sin\beta & \cos\beta & -\frac{1}{\sqrt{2}}\sin\beta \\ \sin^2(\beta/2) & \frac{1}{\sqrt{2}}\sin\beta & \cos^2(\beta/2) \end{bmatrix} \begin{bmatrix} 1 \\ 0 \\ 0 \end{bmatrix} \quad (6.5)$$

which is just the first column of the rotation matrix. Consider $\beta = \pi/2$, for which (6.5) produces amplitudes for $m = \pm 1$ projections both equal to $1/2$, while that for $m = 0$ is $1/\sqrt{2}$. If you make a sketch, as in Figure 6.3, you see that in the vector model (Section 5.3) the spin vector will be predominantly along the $-x$ axis, so $m = 0$ should have the largest amplitude, in agreement with (6.5). The $m = 0$ projection is twice as probable ($1/2$ rather than $1/4$) as the $m = \pm 1$ projections.

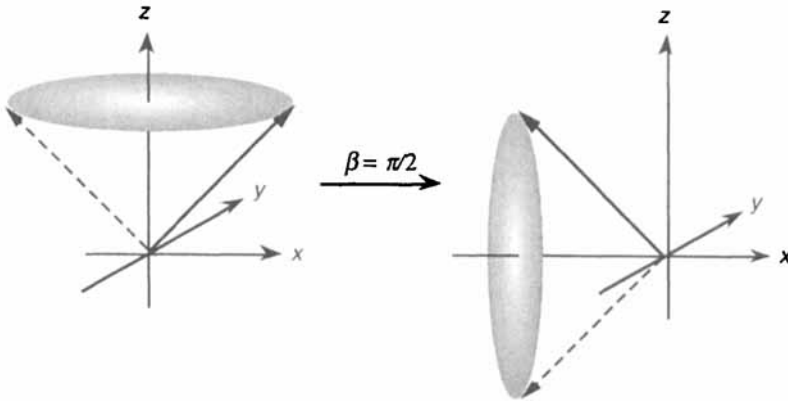


FIGURE 6.3 Semiclassical vector model viewpoint of rotation of an angular momentum vector through $\beta = \pi/2$ when the initial projection is $m = j$. The most probable projection is then $m' = 0$. The vector is drawn to scale for $j = 1$.

Also in Figure 6.3, $+z$ and $-z$ axes should be equivalent when $\beta = \pi/2$, and we see that they have equal amplitudes of $1/2$. Since $\cos^2[(\pi - \beta)/2] = \sin^2(\beta/2)$, we

see more generally from (6.5) that for $j = 1$ the $m = +1$ and $m = -1$ states interchange roles as $\beta \rightarrow \pi - \beta$. The sum over m of squares of amplitudes is unity before and after rotation, consistent with unitarity.

The matrix-expansion technique for deriving \mathbf{d}^j for $j = 1/2$ and 1 can be extended to arbitrary j , as shown by Lehrer-Ilamed [Leh64]. Although correct, the method is complicated and does not lead to insight, so we switch to another representation.

6.2.3 Constructing \mathbf{d}^j from Spinor Representations

We now turn to the challenge of deriving y -axis rotations for arbitrary j . For this we use the spinor-space representation introduced in Section 4.3.3. We show in Figure 6.4 how this representation can be visualized in the Majorana representation (Section 5.1.3) and in the semiclassical vector model (Section 5.3).

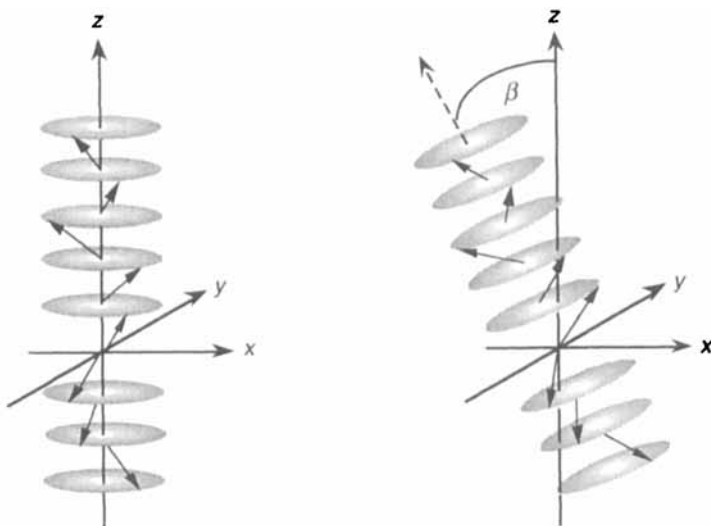


FIGURE 6.4 Semiclassical vector model view of the spinor-space representation (6.6), before the system is rotated (left-hand side) and after the system is rotated through β about the y axis (right-hand side). There are 5 spin-up spin- $1/2$ subsystems and 3 spin-down spin- $1/2$ subsystems. Therefore, the left-hand view represents a system with $m = (5 - 3)/2 = 1$ and $j = (5 + 3)/2 = 4$. In the right-hand view there is a range of m values but still $j = 4$.

In the spinor-space representation, to describe a system with total angular momentum number j and projection number m —labeled as (j, m) —we combine $j + m$ spin-up spinors and $j - m$ spin-down spinors. For example, in Figure 6.4 there are 5 spin-up and 3 spin-down subsystems. As justified in detail in Section 4.3.3, we have a state representation given by

$$u(jm, \beta) = \frac{[\chi_+(\beta)]^{j+m} [\chi_-(\beta)]^{j-m}}{\sqrt{(j+m)!(j-m)!}} \quad (6.6)$$

in which the rotated spin-1/2 spinors are obtained from the rotation matrix for a spin-1/2 system, (3.44), by

$$\begin{aligned} \chi_+(\beta) &= \cos(\beta/2)\chi_+(0) - \sin(\beta/2)\chi_-(0) \\ \chi_-(\beta) &= \sin(\beta/2)\chi_+(0) + \cos(\beta/2)\chi_-(0) \end{aligned} \quad (6.7)$$

in which the arguments of the χ_{\pm} indicate the angle of rotation of the system from the z axis (Figure 6.4). By using the definition of a rotated state and the reduced rotation matrix elements $d_{m'm}^j(\beta)$, we may also write (6.6) as

$$u(jm, \beta) = \sum_{m'=-j}^j u(jm', 0) d_{m'm}^j(\beta) \quad (6.8)$$

Thus, by substituting (6.7) into (6.6), expanding each power by the binomial theorem, then rearranging terms to identify the unrotated states that appear in (6.8), the resulting coefficients of these terms are just the required matrix elements. To carry out this procedure is straightforward but tedious, so it is relegated to Problem 6.4.

Finally, we have the *reduced rotation matrix elements* given by

$$\begin{aligned} d_{m'm}^j(\beta) &= \sqrt{(j+m')!(j-m')!(j+m)!(j-m)!} \\ &\times \sum_x \frac{(-1)^x [\cos(\beta/2)]^{2j+m'-m-2x} [\sin(\beta/2)]^{2x+m-m'}}{(j+m'-x)!(j-m-x)! x! (x+m-m')!} \end{aligned} \quad (6.9)$$

Here the summation is over all values of x for which the arguments of the factorials in the denominator are non-negative. Because there is an $x!$ in this formula, $x = 0$ is the smallest possible value, while the other factorial arguments impose the restrictions that $x \geq m' - m$, and $x \leq \min(j - m, j + m')$. The last two restrictions also guarantee that the cosine and sine powers are non-negative.

As we found for $j = 1/2$ (Section 3.3.3) and $j = 1$ (Section 6.2.2), the matrix elements for y -axis rotations are explicitly real. It is indeed worthwhile to verify agreement between (6.9) with these values of j and the independently derived expressions (3.44) and (6.4), as Problem 6.5 suggests that you do.

Formula (6.9) is the starting point for all our subsequent analyses of the reduced rotation matrix elements, which are related to the full rotation matrices in Sections 6.3 and 6.4.

Spinor Property of Rotations for Half-Integer j . In Section 3.3.3 the spinor nature of y -axis rotations for $j = 1/2$, namely sign reversal according to (2.74) for change of angle by 2π , was demonstrated explicitly by inspection of the rotation matrix (3.44). This property can be generalized to arbitrary j by considering the relation between the functions $d_{m',m}^j(\beta)$ and $d_{m',m}^j(\beta + 2\pi)$. Since both $\cos(\beta/2)$ and $\sin(\beta/2)$ change sign under $\beta \rightarrow \beta + 2\pi$, we see from (6.9) that each term in the summation undergoes a phase change which has as its exponent the term given by $(2j + m' - m + 2x) + (2x + m - m') = 2j + 4x$. Because x is an integer, the phase change is just that from $2j$, and this phase can be factored out of the sum. Thus

$$d_{m',m}^j(\beta + 2\pi) = (-1)^{2j} d_{m',m}^j(\beta) \tag{6.10}$$

Therefore, y -axis rotations describe spinors whenever j is a half-integer, such as $j = 1/2, 3/2, \text{ or } 49/2$. The same property is shown at the end of Section 6.2.1 for z -axis rotations. Thus, the spinor property—sign reversal under change of any Euler angle by 2π —holds for any system having half-integer total angular momentum number j .

6.2.4 Relation of d^j Elements to Other Functions

The full expression for the reduced rotation matrix elements describing y -axis rotations through angle β , given by (6.9), is quite complicated. It is therefore worthwhile, both for insight and for calculations, to simplify this expression whenever possible. We consider first the case when both projections, m' and m , are zero, which can occur only when $j = \ell$, an integer. This will show that d_{00}^ℓ is just a Legendre polynomial. Then we show that even if only one projection number is zero (still requiring $j = \ell$), then we get a Legendre function. Finally, the relation of the general reduced matrix element to Jacobi polynomials is derived, which is of interest for computing the rotation matrix elements. At this stage it would be worthwhile for you to review properties of Legendre functions, as in Sections 4.1.1 and 4.1.2.

The $d_{m',m}^j$ for Both Projections Zero. If in (6.9) we set $j = \ell$ and $m' = m = 0$, we certainly obtain an expression that looks simpler than the original, but the summation may not be immediately identified as a well-known function. However, by substituting $\ell = 0, \ell = 1, \text{ and } \ell = 2$ into this expression, we find in terms of the Legendre polynomials $P_\ell(\cos \beta)$, that

$$\begin{aligned} d_{00}^0(\beta) &= 1 = P_0(\cos \beta) & d_{00}^1(\beta) &= \cos \beta = P_1(\cos \beta) \\ d_{00}^2(\beta) &= \frac{1}{2}(3\cos^2 \beta - 1) = P_2(\cos \beta) \\ d_{00}^\ell(\beta) &= P_\ell(\cos \beta) \end{aligned} \tag{6.11}$$

in which the last conjecture is yet to be proven. To check this, note that Legendre polynomials satisfy the recurrence relation between three adjacent ℓ values given by [Won91, (5.8)]

$$(\ell + 1)P_{\ell+1}(x) - (2\ell + 1)xP_{\ell}(x) + \ell P_{\ell-1}(x) = 0 \quad (6.12)$$

Therefore, if d_{00}^{ℓ} satisfies this same relation with $x = \cos\beta$, then it must coincide with $P_{\ell}(\cos\beta)$, since it coincides for two adjacent ℓ values. The rather messy algebraic details of this method of proof are relegated to Problem 6.6. An alternative derivation is to verify that d_{00}^{ℓ} and $P_{\ell}(\cos\beta)$ satisfy the same linear second-order differential equation as functions of β , and that they coincide at two values of β , such as at $\beta = \pm\pi$. They must therefore be identical. This derivation is also suggested in Problem 6.6. The final result of such manipulations is the identity satisfied by reduced rotation matrices with both projection numbers zero:

$$\boxed{d_{00}^{\ell}(\beta) = P_{\ell}(\cos\beta)} \quad (6.13)$$

The physical interpretation of this result is given in Section 6.3.1.

The $d_{m'm}^j$ for One Projection Zero. You may suspect, indeed correctly, that if one of the projection numbers is zero (which again requires $j = \ell$, an integer) that the reduced rotation matrix elements are related to Legendre functions. As Problem 6.6 suggests that you prove by similar methods to those for both m values zero, the relation is

$$\boxed{d_{m'0}^{\ell}(\beta) = (-1)^{m'} \frac{(\ell - m')!}{\sqrt{(\ell + m')!}} P_{\ell}^{m'}(\cos\beta) \quad m' \geq 0} \quad (6.14)$$

in which $P_{\ell}^{m'}$ is the associated Legendre function. Indeed, (6.13) and its method of derivation are just special cases for $m' = 0$ of (6.14). The cases in which the zero occurs as the left-hand projection number or in which $m' < 0$ are handled by the symmetries of reduced rotation matrices derived in Section 6.4.1.

Relation of $d_{m'm}^j$ to Jacobi Polynomials. The general reduced rotation matrix element given by (6.9) can be related to Jacobi polynomials, which are discussed in the treatise on mathematical functions by Erdélyi et al. [Erd53]. Our main reason for doing this is to connect with the method used in the *Mathematica* notebook `Djm'm` used for computing rotation matrix elements in Section 6.2.5 and visualizing them in Section 6.3.3. Also, at a more advanced level, the connections between the two functions are discussed in several contexts in the angular momentum encyclopedia of Biedenharn and Louck [Bie81a].

The Jacobi polynomial may be defined (for integer n , α , and β) by

$$P_n^{(\alpha, \beta)}(x) = (n + \alpha)! (n + \beta)! \sum_s \frac{\left(\frac{x-1}{2}\right)^{n-s} \left(\frac{x+1}{2}\right)^s}{s! (n + \alpha - s)! (n - s)! (\beta + s)!} \quad (6.15)$$

By identifying $x = \cos \beta$, $n = j - m$, $\alpha = m - m'$, $\beta = m + m'$, and using trigonometric identities, we can match expansions (6.9) and (6.15) to show that

$$d_{m'm}^j(\beta) = \sqrt{\frac{(j+m)! (j-m)!}{(j+m')! (j-m')!}} \times [\cos(\beta/2)]^{m+m'} [\sin(\beta/2)]^{m-m'} P_{j-m}^{(m-m', m+m')}(\cos \beta) \quad (6.16)$$

This formula is used in notebook `Djm'm` in Appendix I to compute $d_{m'm}^j(\beta)$ in terms of *Mathematica* function `JacobiP`. In *Maple* the Jacobi polynomial can be computed symbolically or numerically by the function `Orthopoly[P]`.

By setting $m' = m = 0$ in (6.16) and comparing this with (6.13), you will be led to conclude that a special case of the Jacobi polynomial is

$$P_{\ell}^{(0,0)}(\cos \beta) = P_{\ell}(\cos \beta) \quad (6.17)$$

This may be useful when checking formulas for Legendre polynomials. Now that we have related reduced rotation matrix elements to other functions, we are ready to consider how to compute the $d_{m'm}^j(\beta)$.

6.2.5 Computing Reduced Rotation Matrix Elements

Although (6.9) gives the general formula for the reduced rotation matrix elements $d_{m'm}^j(\beta)$, it is interesting and useful to obtain explicit results and visualizations for small values of j . We discuss first analytical expressions, then summarize methods for numerical evaluation.

Analytical Expressions for Reduced Rotation Matrix Elements. Analytical expressions are easily derived by using on a computer the *Mathematica* notebook `Djm'm` in Appendix I, but it is not too painful to do the calculations by hand and brain for small values of j . The exercise is suggested as Problem 6.7. We give the matrices for $j \leq 2$ in Tables 6.1–6.3, with Table 6.2 showing a polar diagram of $d_{3/2,1/2}^{3/2}(\beta)$. This kind of diagram is discussed in detail in Sections 4.1.2 and 6.3.3. The notation used in the tables is $c = \cos(\beta/2)$, $s = \sin(\beta/2)$. In these tables the matrices demonstrate the symmetries that are derived generally in Section 6.4.1. Since rotation is a unitary transformation (Section 2.2.2), for any value of β the sum of squares of the elements in a given row or column is unity. Try it and see!

TABLE 6.1 Reduced rotation matrices, $d^j(\beta)$, as a function of polar rotation angle β for angular momenta $j = 0, 1/2$, and 1. The matrices are displayed in irreducible form, as discussed in Section 2.1. The sketch shows the relation between projections for an active rotation through (positive) angle β . The notation is $c = \cos(\beta/2)$, $s = \sin(\beta/2)$.

j	0	1/2	1
0	$ \begin{array}{c c} m' \setminus m & 0 \\ \hline 0 & 1 \end{array} $		
1/2		$ \begin{array}{c cc} m' \setminus m & 1/2 & -1/2 \\ \hline 1/2 & c & -s \\ -1/2 & s & c \end{array} $	
1	<div style="border: 1px solid black; padding: 5px; width: fit-content;"> $d_{-m',-m}^j(\beta) = d_{m',m}^j(-\beta)$ $d_{m',m}^j(-\beta) = d_{m',m}^j(\beta)$ $d_{m'm'}^j(\beta) = (-1)^{m-m'} d_{m',m}^j(\beta)$ $d_{m',m}^j(\pi - \beta) = (-1)^{j+m'} d_{m',-m}^j(\beta)$ </div>		$ \begin{array}{c ccc} m' \setminus m & 1 & 0 & -1 \\ \hline 1 & c^2 & -\sqrt{2}cs & s^2 \\ 0 & \frac{s}{\sqrt{2}} & 2cs & -\frac{s}{\sqrt{2}} \\ -1 & s^2 & -\sqrt{2}cs & c^2 \end{array} $

TABLE 6.2 Reduced rotation matrix $d^{3/2}(\beta)$ as a function of polar angle β . The notation is $c = \cos(\beta/2)$, $s = \sin(\beta/2)$. The sketch is a polar diagram (Section 4.1.2) of $d_{3/2,1/2}^{3/2}$, with positive values drawn with a solid curves and negative values drawn with dashed curves. Note that $d_{3/2,1/2}^{3/2}(2\pi) = -d_{3/2,1/2}^{3/2}(0) < 0$, which is correct for this half-integer spin, according to (6.10).

$j = 3/2$				
$m' \setminus m$	3/2	1/2	-1/2	-3/2
3/2	c^3	$-\sqrt{3}c^2s$	$\sqrt{3}cs^2$	$-s^3$
1/2	$\sqrt{3}c^2s$	$c(3c^2 - 2)$	$s(3s^2 - 2)$	$\sqrt{3}cs^2$
-1/2	$\sqrt{3}cs^2$	$-s(3s^2 - 2)$	$c(3c^2 - 2)$	$-\sqrt{3}c^2s$
-3/2	s^3	$\sqrt{3}cs^2$	$\sqrt{3}c^2s$	c^3

TABLE 6.3 Reduced rotation matrix $d^2(\beta)$ as a function of the polar rotation angle β . The notation is $c = \cos(\beta/2)$, $s = \sin(\beta/2)$.

		$j = 2$				
$m' \setminus m$	2	1	0	-1	-2	
2	c^4	$-2c^3s$	$\sqrt{\frac{3}{8}} \sin^2 \beta$	$-cs^3$	s^4	
1	$2c^3s$	$-2c^2s^2$	$-\sqrt{\frac{3}{2}} \sin \beta \cos \beta$	$c^2(2\cos \beta + 1)$	$-cs^3$	
0	$\sqrt{6} c^2 s^2$	$\sqrt{\frac{3}{2}} \sin \beta \cos \beta$	$\frac{1}{2}(3\cos^2 \beta - 1)$	$-\sqrt{\frac{3}{2}} \sin \beta \cos \beta$	$\sqrt{6} c^2 s^2$	
-1	cs^3	$c^2(2\cos \beta + 1)$	$\sqrt{\frac{3}{2}} \sin \beta \cos \beta$	$-2c^2s^2$	$-2c^3s$	
-2	s^4	cs^3	$\sqrt{\frac{3}{8}} \sin^2 \beta$	$2c^3s$	c^4	

The size of the reduced rotation matrices increases rapidly with j , since there are $(2j + 1)^2$ elements in d^j . By using phase relations under sign changes of m' or m and under interchanges of m' and m (as derived in Section 6.4.1), the number of elements with essentially different dependences on β is substantially reduced, as is clear by inspection. For example, if $j = 2$, among the 25 matrix elements there are just nine independent functions. By exploiting symmetries under $\beta \rightarrow \pi - \beta$, the number of functions can be further reduced. Such simplifications are also useful in discussing symmetry properties of expressions involving the $d_{m'm}^j(\beta)$.

Numerical Values of Reduced Rotation Matrix Elements. Although algebraic expressions for reduced rotation matrix elements are provided in Tables 6.1–6.3, numerical values are also needed. If you need such values for $j \leq 2$, just use the tables and program the algebraic expressions.

If you need a broad range of j , m' , m , and β values, then $d_{m'm}^j(\beta)$ can be obtained by using C-language program C1 in Appendix II. It implements efficiently formula (6.9). *Mathematica* notebook Djm'm in Appendix I can be modified to produce numerical values in addition to formulas and graphics of $d_{m'm}^j(\beta)$. In terms of computer effort—as contrasted to human effort—this is less efficient than using a compiled C function by several orders of magnitude.

6.3 INTERPRETING ROTATED STATES

In Sections 6.1 and 6.2 we emphasize determining matrix elements of operators for finite rotations of angular momentum eigenstates, the $D_{m'm}^j(\alpha\beta\gamma)$, whereas in this section our attention is on combining and interpreting such rotated states. To begin, we use the formalism of linear spaces, summarized in Section 2.1.1, writing the

rotated state as $|jm, \alpha\beta\gamma\rangle$, defined to be the state obtained by rotating through Euler angles (α, β, γ) the system that was in a state with angular momentum numbers (j, m) . The effect of rotating the state through these angles is to produce the ket $|jm, \alpha\beta\gamma\rangle$, given by

$$\begin{aligned}
 |jm, \alpha\beta\gamma\rangle &\equiv U(\alpha\beta\gamma)|jm\rangle \\
 &= \sum_{j'm'} |j'm'\rangle \langle j'm'|U(\alpha\beta\gamma)|jm\rangle \\
 &= \sum_{j'm'} |j'm'\rangle D_{m',m}^j(\alpha\beta\gamma) \delta_{j',j} \\
 &= \sum_{m'=-j}^j |jm'\rangle D_{m',m}^j(\alpha\beta\gamma)
 \end{aligned} \tag{6.18}$$

In the second line we use expansion (2.14) for the unit operator, in the third line we insert the definition of rotation matrix elements and use their irreducibility (Sections 2.5.5, 6.1.2), and in the fourth line we have the simplest form for the rotated state. The transformed state (the left-hand side) is a linear superposition of unrotated states having the same j value as on the right-hand side.

To summarize this key formula, the *rotated state* is given by

$$\boxed{|jm, \alpha\beta\gamma\rangle = \sum_{m'=-j}^j |jm', 000\rangle D_{m',m}^j(\alpha\beta\gamma)} \tag{6.19}$$

The rotated state usually does *not* have a unique projection, since the labeling in the ket on the left-hand side means “the projection *before* rotation is m .” After rotation, the amplitude with which the unrotated kets (Euler angles denoted 000) appear in the rotated ket is obtained from the right-hand side of (6.19) as $D_{m',m}^j(\alpha\beta\gamma)$.

In matrix form (6.19) appears in the form of *row-matrix* representations for the kets on the left- and right-hand sides and a square matrix for the rotation matrix \mathbf{D} . One way to remember this rule is that if one used instead a column-matrix form, the elements of \mathbf{D} would be on the left of the kets under the sum in (6.19), so that they might appear (erroneously) to be operators. Although you probably believe the algebra of the above arguments and discussion, we gain more insight by considering special examples of (6.19).

6.3.1 Orbital Angular Momentum States

To understand rotation formula (6.19) for angular momentum kets more concretely, consider the orbital angular momentum states introduced in Section 4.1. We divide the discussion into z-axis rotations and y-axis rotations.

Rotations about the z Axis. For the azimuthal part of a spherical harmonic—the operative factor for rotations about the z axis—we have

$$\langle(\phi)|\ell m, 000\rangle = e^{im\phi} \quad (6.20)$$

with m an integer, a formula that holds for any ℓ . Now rotate the *system* through angle γ about the z axis, as in Section 6.2.1. This is an *active* rotation, as discussed in Sections 1.3.1, and 3.1.1. For a z-axis rotation, (6.2) gives

$$D_{m'm}^j(00\gamma) = e^{-im\gamma} \delta_{m'm} \quad (6.21)$$

On projecting (6.18) into the space of angles ϕ and using (6.21), we have

$$\begin{aligned} \langle(\phi)|\ell m, 00\gamma\rangle &= \sum_{m'=-\ell}^{\ell} \langle(\phi)|\ell m, 00\gamma\rangle e^{-im'\gamma} \delta_{m'm} \\ &= e^{im(\phi-\gamma)} = \langle(\phi-\gamma)|\ell m, 000\rangle \end{aligned} \quad (6.22)$$

How should we interpret this result? The most instructive way is to draw a polar plot (Section 4.1.2) of the azimuthal part of the spherical harmonic, given by (6.20) for $m = 1$, say. It is sufficient to look at the real part, $\cos \phi$, because the imaginary part ($\sin \phi$) is just the same shape rotated through $\pi/2$. The left- and right-hand-side views in Figure 6.5 help you visualize the left- and right-hand sides of (6.22).

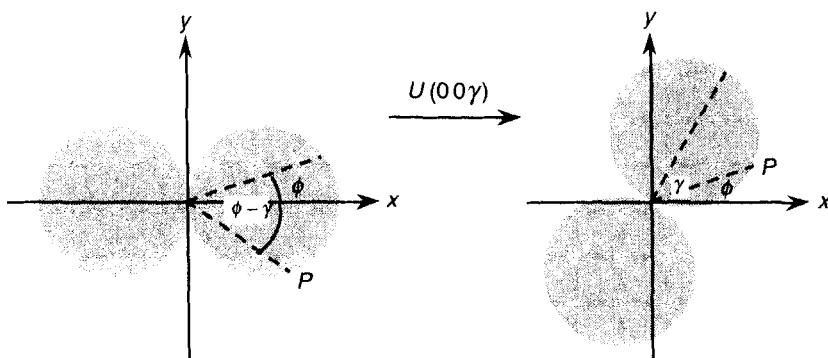


FIGURE 6.5 Effect of an active rotation through Euler angle γ of the function $\cos\phi$, shown in a polar plot. The value of the function at point P is unchanged by the rotation, in accord with (6.22).

In this example the interpretation is particularly simple because z-axis rotations do not change m values. The situation is immediately more complicated for y-axis rotations.

Rotations about the y Axis. For rotation of spherical harmonic $Y_{\ell m}(\theta, \phi)$ about the y-axis through Euler angle β , the D-matrix elements required in (6.18) are just the reduced rotation matrix elements $d_{m', m}^{\ell}(\beta)$, as described in Sections 6.2.2–6.2.5. The rotated spherical harmonic becomes

$$\langle(\theta\phi)|\ell m, 0\beta 0\rangle = \sum_{m'=-\ell}^{\ell} Y_{\ell m}(\theta, \phi) d_{m', m}^{\ell}(\beta) \quad (6.23)$$

This is usually *not* a single spherical harmonic, but rather, an expansion in terms of the complete set of functions in the space (θ, ϕ) , with the completeness being a consequence of the fact that the spherical harmonics on the right-hand side are eigenfunctions of the angular momentum operators, which are Hermitian.

To illustrate the result (6.23), consider the simplest nontrivial spherical harmonic, that for $\ell = 1, m = 0$, given explicitly in Table 4.2. The required $d_{m', 0}^1(\beta)$ are given by the third column of Table 6.1. After some simple manipulations that Problem 6.8 suggests you try, we obtain

$$\langle(\theta\phi)|10, 0\beta 0\rangle = \sqrt{\frac{3}{4\pi}} (\sin\theta \sin\beta \cos\phi + \cos\theta \cos\beta) \quad (6.24)$$

This rotated function is *not* usually a spherical harmonic because its dependence on ϕ is not of the form $e^{im\phi}$ required for such functions. For the case of no rotation, $\beta = 0$, we recover $Y_{10}(\theta, \phi)$, while for $\beta = \pi$, (6.24) produces the negative of this, in agreement with the negative parity of spherical harmonics having ℓ odd, as derived in Section 4.1.

When $\phi = 0$ the spherical harmonics collapse to functions proportional to associated Legendre functions and our particular example in (6.24) for $\ell = 1, m = 0$ simplifies to

$$\begin{aligned} \langle(\theta 0)|10, 0\beta 0\rangle &= \sqrt{\frac{3}{4\pi}} (\sin\theta \sin\beta + \cos\theta \cos\beta) \\ &= \sqrt{\frac{3}{4\pi}} \cos(\theta - \beta) = \langle(\theta - \beta, 0)|10, 000\rangle \end{aligned} \quad (6.25)$$

This result has a similar interpretation to that for z-axis rotation, as illustrated in Figure 6.5.

6.3.2 Transformation Amplitudes for Arbitrary j

Now that we understand how to interpret rotated states described in terms of orbital angular momentum, let us turn our attention to other descriptions of angular momentum states. We first review spin-1/2 states, then we consider transformation amplitudes for arbitrary j .

Interpreting Rotated States for $j = 1/2$. Rotations about the z and y axes for spin- $1/2$ states are derived in Section 3.3.3. There we show that the states denoted by $\chi_{\pm}(\beta) = |1/2, \pm 1/2, 0\rangle$ transform under y -axis rotations according to

$$\begin{aligned}\chi_+(\beta) &= \cos(\beta/2)\chi_+(0) - \sin(\beta/2)\chi_-(0) \\ \chi_-(\beta) &= \sin(\beta/2)\chi_+(0) + \cos(\beta/2)\chi_-(0)\end{aligned}\quad (6.26)$$

Consider the transformation of *amplitudes* for spin-up and spin-down states, $\chi_+(0)$ and $\chi_-(0)$, written as

$$\chi_{\pm}(\beta) = \sum_{m=-1/2}^{1/2} \chi_m(0) a_{\pm,m}(\beta) \quad (6.27)$$

The amplitudes $a_{\pm,m}(\beta)$ can be summarized in matrix form as

$$\mathbf{a}_{\pm}(\beta) = \mathbf{d}^{1/2}(\beta) \mathbf{a}_{\pm}(0) \quad (6.28)$$

where, according to (3.44), the rotation matrix is

$$\mathbf{d}^{1/2}(\beta) = \begin{bmatrix} \cos(\beta/2) & -\sin(\beta/2) \\ \sin(\beta/2) & \cos(\beta/2) \end{bmatrix} \quad (6.29)$$

and the unrotated amplitudes are given by

$$\mathbf{a}_+(0) = \begin{bmatrix} 1 \\ 0 \end{bmatrix} \quad \mathbf{a}_-(0) = \begin{bmatrix} 0 \\ 1 \end{bmatrix} \quad (6.30)$$

for spin-up and spin-down states, respectively.

To visualize the spin- $1/2$ rotations, look at the two polar diagrams in Figure 6.6, in which the left panel shows $d_{1/2,1/2}^{1/2}(\beta) = d_{-1/2,-1/2}^{1/2}(\beta) = \cos(\beta/2)$ while the right panel shows $d_{1/2,-1/2}^{1/2}(\beta) = -d_{-1/2,1/2}^{1/2}(\beta) = -\sin(\beta/2)$. Notice that in Figure 6.6, plotted for β in the range 0 to 2π , there is a sign switch at the apex of the polar plot on the left-hand side. This is correct, since half-integer j values (such as $j = 1/2$) are described by spinor functions (Section 2.4), which change sign under rotation through 2π .

Having understood interpretation of rotated states for spin $j = 1/2$, we now generalize these formulas for rotation of amplitudes to arbitrary spin.

Interpreting Rotated States for Arbitrary j . The rotational transformation of amplitudes just examined for spin- $1/2$ states can be generalized readily. Consider a system which before rotation has a unique j value but is in a superposition of magnetic substates; thus

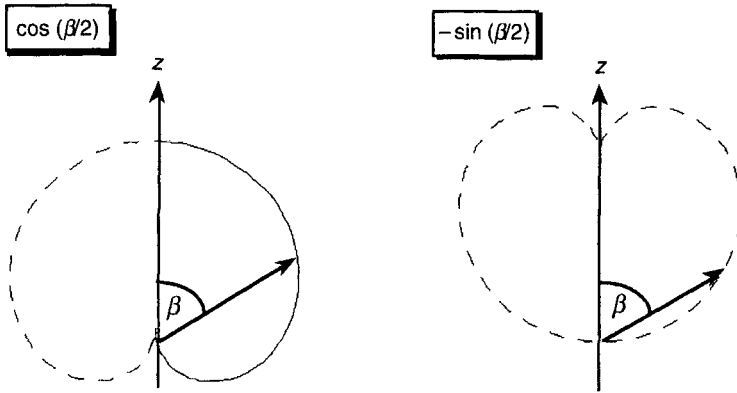


FIGURE 6.6 Polar plots of the reduced rotation matrix elements for transforming spin-1/2 states and amplitudes. Positive values are shown by solid curves and negative values are shown by dashed curves. (Adapted from *Mathematica* notebook Djm'm.)

$$|j, 000\rangle = \sum_{m=-j}^j |jm, 000\rangle a_m(000) \quad (6.31)$$

in which the a_m are the amplitudes whose rotational transformation we seek to determine. If the system is rotated through Euler angles (α, β, γ) , then the state described by (6.31) is transformed to $|j, \alpha\beta\gamma\rangle$, given by

$$|j, \alpha\beta\gamma\rangle = \sum_{m=-j}^j |jm, 000\rangle a_m(\alpha\beta\gamma) \quad (6.32)$$

in which the *transformed amplitudes* after rotation are given by

$$a_{m'}(\alpha\beta\gamma) = \sum_{m=-j}^j D_{m'm}^j(\alpha\beta\gamma) a_m(000) \quad (6.33)$$

This result can be derived by following the steps used for $j = 1/2$, as Problem 6.9 suggests that you do.

If we consider the amplitudes in (6.33) to form the elements of a *column* matrix $\mathbf{a}(\alpha\beta\gamma)$ having $2j + 1$ elements, as with the two-component matrices for spin-1/2 in (6.30), then (6.30) can be summarized as

$$\mathbf{a}(\alpha\beta\gamma) = \mathbf{D}^j(\alpha\beta\gamma) \mathbf{a}(000) \quad (6.34)$$

Notice that \mathbf{D} *pre*multiplies the amplitudes, whereas the rotated kets in (6.18) are *post*multiplied by \mathbf{D} .

Technically, a transformation of the kind (6.18), in which the transformation matrices *post*multiply a quantity, is called a *cogredient* transformation, whereas the amplitude transformation rule (6.34) is called a *contragredient* transformation, although this term is often used if \mathbf{D}^* rather than \mathbf{D} appears in (6.33).

The Case of Unique Initial Amplitudes. As an example of using (6.33), suppose that before rotation the system was in a *unique* substate m_0 , so that

$$a_m(000) = \delta_{m,m_0} \quad (6.35)$$

then, using (6.33), each amplitude after rotation is given simply by

$$a_{m'}(\alpha\beta\gamma) = D_{m'm_0}^j(\alpha\beta\gamma) \quad (6.36)$$

The probability for this amplitude, $P_{m'}(\alpha\beta\gamma)$, is therefore

$$P_{m'}(\alpha\beta\gamma) = |a_{m'}(\alpha\beta\gamma)|^2 = [d_{m'm_0}^j(\beta)]^2 \quad (6.37)$$

There is no effect on probabilities from z -axis rotations involving the angles α and γ , which contribute only phases to the amplitudes, as derived in Section 6.2.1. Interpreting a reduced rotation matrix element as a probability amplitude describing transformation under rotation is the main idea underlying angular-distribution schemes for determining j for a system, as discussed at the end of Section 7.5.2.

6.3.3 Visualizing Rotation Matrix Elements

How should we visualize the dependence of $d_{m'm}^j(\beta)$ on projection numbers m' and m ? We can figure this out by starting with examples in which m' is fixed and m varies. Consider $j = m' = 3$ for two values of m , namely $m = 3$ and $m = 0$. Their formulas are

$$d_{33}^3(\beta) = \cos^6(\beta/2) \quad d_{30}^3(\beta) = -2\sqrt{5} \cos^3(\beta/2) \sin^3(\beta/2) \quad (6.38)$$

and the corresponding polar diagrams are shown in Figure 6.7. For $m' = m = 3$ (left-hand side) we see that as β varies, the function varies slowly for small angles, then collapses for $\beta > \pi/2$, whereas if $m = 0$ (right-hand side), the function is small at angles away from $\beta = \pi/2$. Each behavior is as we should expect under the interpretation, derived in Section 6.3.2, that m gives the projection on the z axis *before* rotating the system, while m' , here equal to 3, gives the projection *after* rotation.

We display in Figure 6.8 as a function of polar angle β the reduced rotation matrix elements for $j = 3$ and positive values of m' and m . As derived in Section 6.4.1, the functions for negative projections are related by phases to those with positive projections.

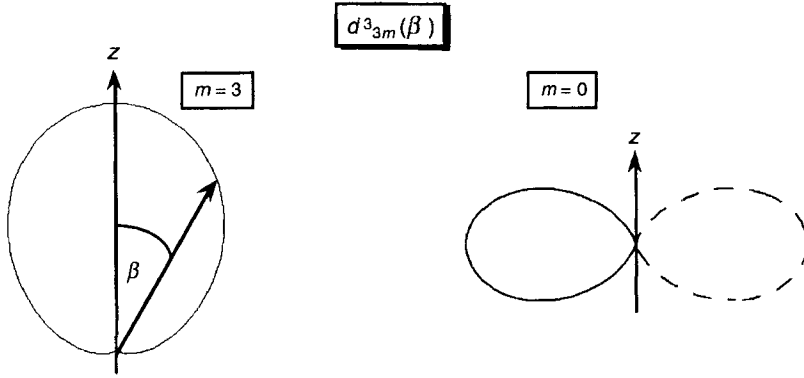


FIGURE 6.7 Reduced rotation functions for m values that are quite different, namely $m = 3$ in the left panel and $m = 0$ in the right panel. (Adapted from *Mathematica* notebook $D_{j m' m}$.)

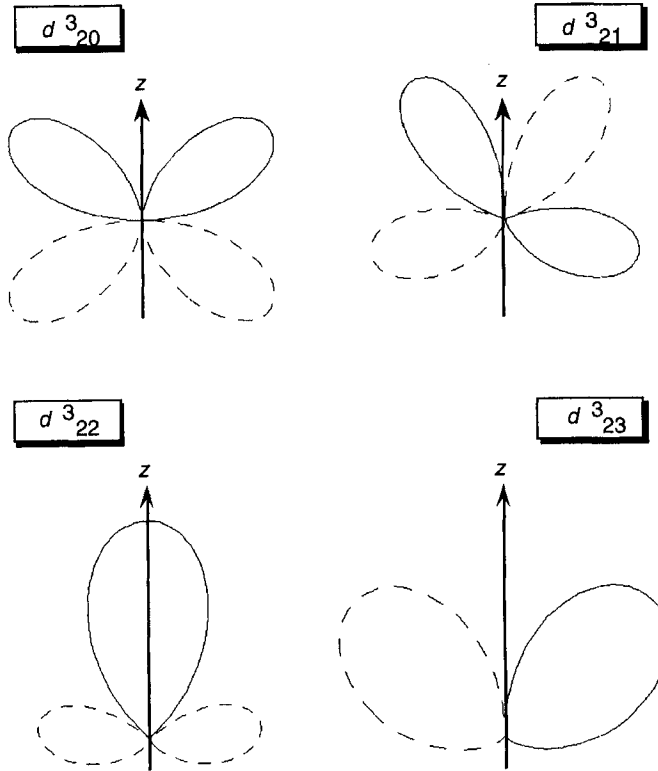


FIGURE 6.8 Reduced rotation matrix element functions for $j = 3$ and positive projections as a function of angle β from the z axis. Formulas for these functions are given in (6.39). (Adapted from *Mathematica* notebook $D_{j m' m}$.)

Formulas for the rotation functions in Figure 6.8 are in terms of $c = \cos(\beta/2)$ and $s = \sin(\beta/2)$ by

$$\begin{aligned} d_{20}^3(\beta) &= 4\sqrt{30}(2c^2 - 1)c^2s^2 & d_{21}^3(\beta) &= \sqrt{5/2}c^3(1 - 6cs^2) \\ d_{22}^3(\beta) &= c^4(6c^2 - 5) & d_{23}^3(\beta) &= \sqrt{6}c^5s \end{aligned} \quad (6.39)$$

as can be verified by running *Mathematica* notebook `Djm'm`, as suggested in Problem 6.10. The visualizations (also obtained from `Djm'm`) are in accord with the interpretation in terms of rotation of amplitudes that is derived in Section 6.3.2. Problem 6.10 also suggests that you describe fully the correspondence between the graphics in Figure 6.8 and this interpretation. From figures in this subsection we see that as functions of β the reduced rotation functions have many symmetry properties. The relation between m and m' being projection values before and after rotations implies symmetries relating the functions for β and $-\beta$ with those having interchanged m and m' values. Our examples thus far have not considered negative projections, which lead to further symmetries. It therefore behooves us to consider properties of rotation matrices in a systematic way.

6.4 PROPERTIES OF ROTATION MATRICES

In this section we emphasize algebraic and symmetry properties of rotation matrices. Having derived these properties, the graphic examples in Section 6.3.3 verify the properties explicitly. Algebraic expressions for $j = 0-2$ are given in Tables 6.1-6.3, while Figures 6.6-6.8 show the reduced rotation matrices in polar diagrams.

We derive in Section 6.4.1 symmetry properties of \mathbf{d}^j and \mathbf{D}^j matrix elements, then in Section 6.4.2 we show their unitarity and orthogonality properties. In Section 6.4.3 we discuss classical limits of rotation matrices, where we learn—perhaps with surprise—that even for angular momentum numbers as small as $j = 6$, their behavior is semiclassical. Finally, in Section 6.4.4 we derive relations between spherical harmonics (Section 4.1) and rotation matrix elements.

6.4.1 Symmetry Properties of \mathbf{d}^j and \mathbf{D}^j

We first derive symmetry properties of elements of the reduced rotation matrix, \mathbf{d}^j , then we derive symmetries of elements of the full rotation matrix, \mathbf{D}^j .

Symmetries of Reduced Rotation Matrix Elements. The formula for the matrix elements $d_{m'm}^j(\beta)$ is (6.9). The symmetries under sign changes of the projections m and m' and of the Euler angle β can be derived by writing out the expansions of the left- and right-hand sides in the following expressions in order to verify the phase relations given below. Since this is straightforward but tedious, we assign it to Problem 6.11. The diligent reader will verify the following symmetries:

$$d_{-m',-m}^j(\beta) = d_{m',m}^j(-\beta) \quad (6.40)$$

$$d_{m',m}^j(-\beta) = d_{mm'}^j(\beta) \quad (6.41)$$

$$d_{mm'}^j(\beta) = (-1)^{m-m'} d_{m',m}^j(\beta) \quad (6.42)$$

$$d_{m',m}^j(\pi - \beta) = (-1)^{j+m'} d_{m',-m}^j(\beta) \quad (6.43)$$

These symmetry relations are consistent with the semiclassical vector model, which predicts that each of the combinations of m' , m , and β should have the same probability distribution; that is, they should be related through a phase, which indeed they are. For $j = 1$ this connection is illustrated explicitly in Figure 6.3, while reduced rotation matrices for $j = 1/2, 1, 3/2,$ and 2 —given in Tables 6.1–6.3—also provide many examples of these symmetry properties.

Relations (6.40) and (6.41) connect active and passive rotations, since rotation through β in our active viewpoint (Sections 1.3.1, 3.1.1, and 6.1.1) is equivalent to $-\beta$ in the passive viewpoint. Symmetry (6.41) arises from the interpretation (Section 6.3.2) of m and m' labels as projection values before and after rotation. The last symmetry, (6.43), relates parity symmetry and reversal of the z axis.

Symmetries of Full Rotation Matrix Elements. The full rotation matrix elements, $D_{m',m}^j(\alpha\beta\gamma)$, are related to reduced rotation matrix elements, $d_{m',m}^j(\beta)$, by

$$D_{m',m}^j(\alpha\beta\gamma) = e^{-im'\alpha} d_{m',m}^j(\beta) e^{-im\gamma} \quad (6.44)$$

The symmetries of the full rotation (α, β, γ) can therefore be related to those of the reduced rotation (β) by using symmetries (6.40)–(6.43) of the latter. By this means, working out the details in Problem 6.12, we obtain

$$D_{-m',-m}^j(\alpha, \beta, \gamma) = D_{m',m}^j(-\alpha, -\beta, -\gamma) = [D_{m',m}^j(\alpha, -\beta, \gamma)]^* \quad (6.45)$$

$$D_{m',m}^j(-\alpha, -\beta, -\gamma) = D_{mm'}^j(\gamma, \beta, \alpha) = [D_{m',m}^j(-\gamma, -\beta, -\alpha)]^* \quad (6.46)$$

$$D_{mm'}^j(\alpha, \beta, \gamma) = (-1)^{m-m'} D_{m',m}^j(\gamma, \beta, \alpha) \quad (6.47)$$

$$D_{m',m}^j(\pi - \beta) = (-1)^{j+m'} D_{m',-m}^j(\alpha, \beta, -\gamma) \quad (6.48)$$

These relations by no means exhaust symmetries of the $D_{m',m}^j(\alpha\beta\gamma)$, but they follow directly from those for $d_{m',m}^j(\beta)$. By restricting the parameters m or m' and

the Euler angles, we can obtain further symmetries. Their consideration is postponed to Section 6.4.4, where we relate spherical harmonics to rotation matrix elements.

6.4.2 Unitarity and Orthogonality Properties

The unitarity and orthogonality properties of rotation matrix elements are useful for simplifying sums and integrals of these functions. We consider first summation properties involving matrix elements of \mathbf{D}^j and \mathbf{d}^j .

Unitarity and Orthogonality Sums. The unitarity of \mathbf{D}^j matrix elements is readily derived, as follows. From the discussion of unitarity in Section 2.2.2, we can write for the rotation operator $U(\alpha\beta\gamma)$,

$$\begin{aligned} \delta_{j'j} \delta_{m'm} &= \mathbf{1}_{j'm',m} \\ &= \langle j'm' | U(\alpha\beta\gamma) U^\dagger(\alpha\beta\gamma) | jm \rangle \\ &= \langle j'm' | U(\alpha\beta\gamma) \sum | j''m'' \rangle \langle j''m'' | U^\dagger(\alpha\beta\gamma) | jm \rangle \\ &= \delta_{j'j} \sum_{m''} D_{m'm''}^j(\alpha\beta\gamma) [D_{mm''}^j(\alpha\beta\gamma)]^* \end{aligned} \quad (6.49)$$

Here, the second line follows from the unitarity of rotations, in the third line we insert a complete set of states (Section 2.1.1), then in the fourth line we use (6.18) for the operator matrix elements. We therefore have the unitarity sum of the full rotation matrix elements

$$\sum_{m''} D_{m'm''}^j(\alpha\beta\gamma) [D_{mm''}^j(\alpha\beta\gamma)]^* = \delta_{m'm} \quad (6.50)$$

By setting $\alpha = 0$ and $\beta = 0$ we obtain a special case of this unitarity sum, namely the orthogonality sum of the (real) reduced rotation matrix elements

$$\sum_{m''} d_{m'm''}^j(\beta) d_{mm''}^j(\beta) = \delta_{m'm} \quad (6.51)$$

Unitarity and Orthogonality Integrals. Rotation matrix elements are angular momentum eigenfunctions, as is clear from the discussion in Section 6.3 and is shown in detail in Section 6.5.1. Since eigenfunctions of Hermitian operators such as \mathbf{J} are orthogonal with respect to integration over their range of definition, here (α, β, γ) , the $D_{m'm}^j(\alpha\beta\gamma)$ and $d_{m'm}^j(\beta)$ must also be orthogonal under such integration. Our task here is to determine the orthogonality integrals.

Consider the integral, I , given by

$$I \equiv \int_R \left[D_{m'_1 m_1}^{j_1}(\alpha \beta \gamma) \right]^* D_{m'_2 m_2}^{j_2}(\alpha \beta \gamma) d\alpha \sin \beta d\beta d\gamma \quad (6.52)$$

in which the region of integration, R , is yet to be specified. We can separate this into the product of three integrals, to obtain

$$I = \int e^{i(m'_1 - m'_2)\alpha} d\alpha \int e^{i(m_1 - m_2)\chi} d\chi \int d_{m'_1 m_1}^{j_1}(\beta) d_{m'_2 m_2}^{j_2}(\beta) \sin \beta d\beta \quad (6.53)$$

If we now choose the range of integration over angles appropriately, the integrals will vanish when the labels on the matrix elements are different. Consider integration over α . If the magnetic projections are both half integers or both integers (thus j_1 and j_2 have this property), the smallest interval over which the α integral vanishes is 0 to 2π . If, however, one projection is a half integer and the other is an integer, then the range of α integration cannot be smaller than 0 to 4π . For example, consider (6.53) for $j_1 = 1/2$, $m'_1 = m_1 = 1/2$, and $j_2 = 0$, so that $m'_2 = m_2 = 0$. Then for an α -integration range of 0 to $2n\pi$ with n an integer, a γ integration range of 0 to 2π , and a β range of 0 to π , we obtain, as Problem 6.13 suggests that you verify, $I = 64[\cos(n\pi) - 1]/3$. If $n = 1$ ($0 \leq \alpha \leq 2\pi$), then $I \neq 0$, but if $n = 2$ ($0 \leq \alpha \leq 4\pi$), then $I = 0$, as hoped for. Clearly, it is sufficient that only one of α or γ has the doubled range, and α is usually chosen.

These considerations have been ignored in most previous treatments of the rotation matrix elements, resulting in errors when half-integer and integer angular momentum orthogonality relations were used. The problem, its resolution, and its relation to the theory of the groups $SU(2)$ and $SO(3)$ introduced in Section 2.5.4 were pointed out by Jonkers and De Vries in 1967 [Jon67].

The orthogonality integral can now be expressed as

$$\begin{aligned} I &= \int_0^{4\pi} e^{i(m'_1 - m'_2)\alpha} d\alpha \int_0^{2\pi} e^{i(m_1 - m_2)\chi} d\chi \\ &\times \int_0^\pi d_{m'_1 m_1}^{j_1}(\beta) d_{m'_2 m_2}^{j_2}(\beta) \sin \beta d\beta \\ &= 8\pi^2 \delta_{m'_1 m'_2} \delta_{m_1 m_2} \int_0^\pi d_{m'_1 m_1}^{j_1}(\beta) d_{m'_2 m_2}^{j_2}(\beta) \sin \beta d\beta \end{aligned} \quad (6.54)$$

in which our choice of regions of integration has been made explicit. Notice that the choice of z -axis rotation angles, α and χ , has produced orthogonality in projection numbers. It remains to prove the orthogonality in total quantum numbers, j_1 and j_2 .

The orthogonality of the $d_{m'_1 m_1}^{j_1}(\beta)$ in integral (6.54) with weight factor $\sin \beta$ and range of integration 0 to π , as is usual for polar angles, is most simply obtained by relating these functions to Jacobi polynomials, as in Section 6.2.4. By consulting the treatise by Erdélyi et al. [Erd53], we are lead quite directly to

$$\int_0^\pi d_{m'_1 m_1}^{j_1}(\beta) d_{m'_2 m_2}^{j_2}(\beta) \sin \beta d\beta = \frac{2}{2j_1 + 1} \delta_{j_1 j_2} \quad (6.55)$$

Putting all the pieces together, we obtain the orthogonality relation for rotation matrix elements:

$$\begin{aligned}
 & \int_R \left[D_{m'_1 m_1}^{j_1}(\alpha\beta\gamma) \right]^* D_{m'_2 m_2}^{j_2}(\alpha\beta\gamma) d\alpha \sin\beta d\beta d\gamma \\
 & \quad = \frac{16\pi^2}{2j_1 + 1} \delta_{j_1 j_2} \delta_{m'_1 m'_2} \delta_{m_1 m_2} \\
 & \quad R: \quad 0 \leq \alpha \leq 4\pi \quad 0 \leq \beta \leq \pi \quad 0 \leq \gamma \leq 2\pi
 \end{aligned} \tag{6.56}$$

If j_1 and j_2 are both half integers (such as $1/2$ and $5/2$) or both integers, then orthogonality holds if the range of α integration is halved (0 to 2π). With the halved range of integration, the value of the integral is halved.

Orthogonality relations of the $D_{m'_m}^j(\alpha\beta\gamma)$ and $d_{m'_m}^j(\beta)$ with respect to summation and integration are of great utility in practical applications. Some of these are covered in Section 7.5, where we relate rotations and coupling coefficients.

6.4.3 Classical Limits of Rotation Matrices

Interpretation of rotated states in terms of probability amplitudes for projections before rotation (m) and after rotation (m'), as derived in Section 6.3, suggests that it is interesting to study the behavior of rotation matrices as j increases, the so-called classical limits. We should expect—and indeed find even for small j values—that the behavior predicted by the semiclassical vector model (Section 5.3) is realized.

Although a general treatment of the classical limits of rotation matrices has been given by Brussaard and Tolhoek [Bru57], it is most instructive to consider two special cases. The first case has, classically, the angular momentum of the system parallel to z , namely $m' = j$. This was first considered by Wigner in his classic treatise on group theory and its applications to quantum mechanics [Wig31]. The second case has a further restriction to $m = 0$.

Rotations with $m' = j$. We begin by simplifying the general expression for the reduced rotation function, (6.9), to that for $m' = j$, namely

$$d_{jm}^j(\beta) = (-1)^{j-m} \sqrt{\frac{(2j)!}{(j+m)!(j-m)!}} \left[\cos(\beta/2) \right]^{j+m} \left[\sin(\beta/2) \right]^{j-m} \tag{6.57}$$

From this we can calculate the probability density $P_m(\beta) = |d_{jm}^j(\beta)|^2$ relative to the value $P_{m_c}(\beta)$, which is expected to peak at the classically-unique value $m_c = j \cos\beta$. This has problems, in principle, because m_c can take on any value depending on the choice of angle β . A better way of considering this is to ask at what angle, β_c , the density is predicted to peak. This angle is just the solution of $\cos\beta_c = m/j$, which always has a solution for β_c because $|m| \leq j$.

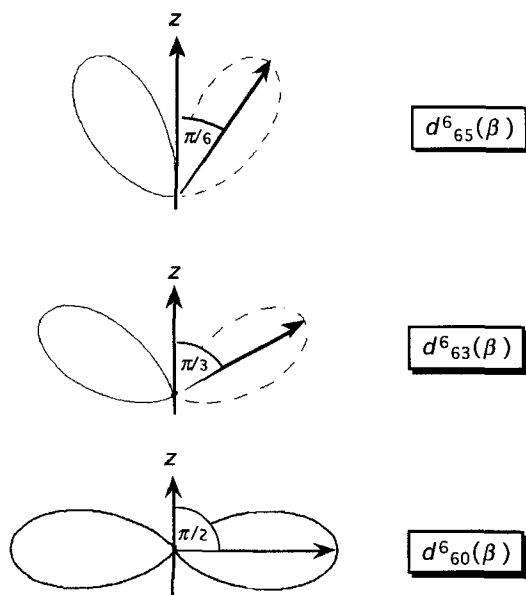


FIGURE 6.9 Reduced rotation functions for $j = m' = 6$ and three values of m as functions of rotation angle β . Indicated angles satisfy approximately the classical relation $\cos\beta_c = m/j$. Recall our convention for polar diagrams (Figure 4.4) that positive values are shown by solid curves and negative values are shown dashed. (Adapted from *Mathematica* notebook Djm'm.)

The semiclassical situation in Figure 6.9 can be analyzed in more detail by considering the probability density $P_m(\beta)$ that is the square of the rotation function (6.57). By following the steps indicated in Problem 6.14, you can readily show that at a fixed angle β , the m dependence of the density that satisfies $m_c = j \cos\beta$ is given approximately by

$$P_m \approx P_{m_c} e^{-(m-m_c)^2/(j-m_c^2/j)} \quad (6.58)$$

Thus, for $j \gg m_c$ this distribution is Gaussian (normal) with standard deviation of about $\sqrt{j/2}$. This value may seem inappropriate until we realize that the more relevant variable is m/j rather than m alone. By rewriting (6.58) in terms of this ratio, we see that the corresponding distribution has a standard deviation of about $1/\sqrt{2j}$, which indeed decreases with j .

These probability distributions from (6.57) and its approximation (6.58) can be visualized by plotting P_m against m for a given choice of j and m_c , as shown in Figure 6.10. As seen, there is very close agreement between the m dependences from the exact values—which are the squares from (6.57)—and approximation P_m from (6.58), even for as small a value as $j = 3$, which would not usually be considered

“classical.” For those who have access to *Mathematica*, further exploration of this topic is suggested as Problem 6.15.

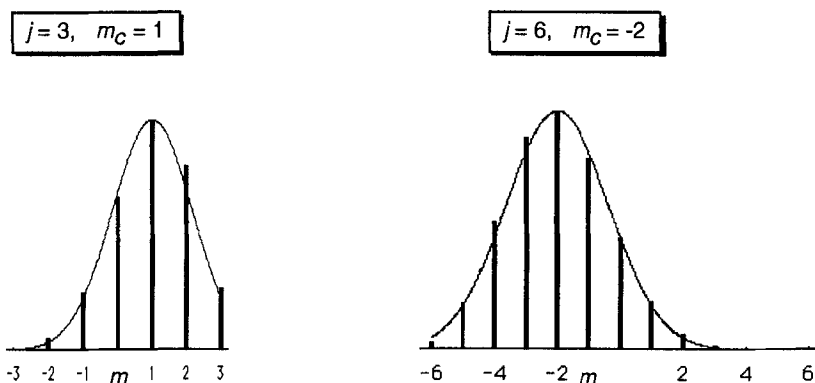


FIGURE 6.10 Probability densities corresponding to the square of the rotation matrix with final projection $m' = j$, (6.57), evaluated at the classical angle β such that $\cos\beta = m_c/j$. The densities are plotted as a function of the initial projection m . Bars show probabilities from (6.57) and curves show the approximation (6.58). Probabilities are normalized to have the same height at $m = m_c$. (Adapted from *Mathematica* notebook DjjmCPr.)

Rotations with $m = 0$. Another view of the classical limits of rotation matrices is obtained by considering projection $m' = j$, as above, but initial projection $m = 0$. Classically, if after rotating the system through β its projection on the z axis is $m' = j$ and it had $m = 0$ before rotation, then it must have been moving initially with its motion restricted to a plane perpendicular to the z axis. Is this prediction satisfied for small values of j ? Figure 6.11 helps to answer this question.

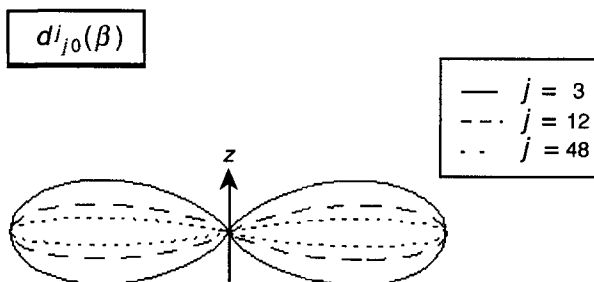


FIGURE 6.11 Probability densities for $m' = j$ and $m = 0$ as a function of polar angle β for three values of j , namely $j = 3, 12, 48$, which differ by factors of 4, so the angular widths of the distributions are predicted to differ by factors of 2, consistent with the figure. (Adapted from *Mathematica* notebook Djjj0.)

We can analyze the behavior of the probability densities in Figure 6.11 analytically by simplifying the general expression for a reduced rotation function, (6.9), to $m = 0$ and $m' = j$, in order to obtain

$$d_{j0}^j(\beta) \propto [\cos(\beta/2)]^j [\sin(\beta/2)]^j \propto [\sin \beta]^j \quad (6.59)$$

which clearly has its maximum value for any $j > 0$ at $\beta = \pi/2$, as in classical dynamics. Problem 6.16 suggests the steps by which you can show that when j increases, then the resulting probability distribution—the square of the amplitude in (6.59)—tends to a full width at half maximum (FWHM) of $2\sqrt{\ln 2/j}$. This property is indicated in Figure 6.11 for values of j that successively increase by factors of 4.

How Small Is j for the Classical Limit? From the preceding visualizations and analyses, we see clearly that the semiclassical limits of the rotation matrices meet all our expectations from classical mechanics. What you probably find very surprising is that the key elements of classical angular momentum are exhibited for small values of j , even as low as $j = 3$ or 6, as shown in Figures 6.10 and 6.11.

The classical-limit behavior is not at all conditional on the value of Planck's constant, but is, rather, a consequence of the fact that *angular momentum* is much more about *angles* and rotations than about *momentum*. This discovery notwithstanding, most texts on quantum mechanics lead one to believe that the classical limit of angular momentum is attained only for very large total angular momentum numbers, probably in the range $j \gg 100$, rather than $j \geq 10$.

6.4.4 Spherical Harmonics as Rotation Matrix Elements

As a final topic in the properties of rotation matrices, we discuss the relation between spherical harmonics, $Y_{\ell m}$, and rotation matrix elements $d_{m'm}^j(\beta)$. Spherical harmonics are related to Legendre functions, P_ℓ^m , through (4.18) in Section 4.1.3, while P_ℓ^m connects to d_{m0}^ℓ by (6.14) in Section 6.2.4. The required connection is therefore

$$\begin{aligned} Y_{\ell m}(\theta, \phi) &= \sqrt{\frac{2\ell+1}{4\pi}} d_{m0}^\ell(\theta) e^{im\phi} \\ Y_{\ell, -m}(\theta, \phi) &= (-1)^m [Y_{\ell m}(\theta, \phi)]^* \end{aligned} \quad m \geq 0 \quad (6.60)$$

We summarize in Table 6.4 the relations of rotation functions to spherical harmonics and Legendre functions under various conditions.

TABLE 6.4 Rotation matrix elements for special values of their parameters.

Under condition	$D_{m'm}^j(\alpha\beta\gamma)$ becomes	$d_{m'm}^j(\beta)$ becomes
$\alpha = 0 = \gamma$	$d_{m'm}^j(\beta)$	
$\gamma = 0, m = 0$ ($\therefore j = \ell$) $m' \geq 0$	$e^{-i\alpha m'} d_{m',0}^\ell(\beta)$ $= \sqrt{\frac{4\pi}{2\ell+1}} Y_{\ell m'}(\beta, -\alpha)$ $= \sqrt{\frac{4\pi}{2\ell+1}} Y_{\ell m'}^*(\beta, \alpha)$	$(-1)^{m'} \sqrt{\frac{(\ell-m')!}{(\ell+m')!}} P_\ell^{m'}(\cos\beta)$
$\alpha = 0, m' = 0$ ($\therefore j = \ell$) $m \geq 0$	$e^{-i\gamma m} d_{0m}^\ell(\beta)$ $= \sqrt{\frac{4\pi}{2\ell+1}} Y_{\ell m}(\beta, -\gamma)$ $= \sqrt{\frac{4\pi}{2\ell+1}} Y_{\ell m}^*(\beta, \gamma)$	$(-1)^m \sqrt{\frac{(\ell-m)!}{(\ell+m)!}} P_\ell^m(\cos\beta)$
$m' = 0 = m$ ($\therefore j = \ell$)	$P_\ell(\cos\beta)$	$P_\ell(\cos\beta)$

6.5 RIGID-BODY ROTATIONS IN QUANTUM MECHANICS

In this section we use our newly acquired understanding of finite rotations of angular momentum eigenstates to investigate the rotations of rigid bodies in quantum mechanics. We begin by characterizing rigid rotators, then in Section 6.5.1 discuss how rotation matrix elements serve as angular momentum eigenfunctions. Then we introduce the rotator Hamiltonian in Section 6.5.2 and show how to calculate its matrix elements between such eigenfunctions. Finally in this section, we discuss rotational states of molecules and nuclei.

What Is a Rigid Rotator? In classical mechanics, rigid rotators are introduced in the context of gyroscopes and tops. These spinning toys of delight and wonder in childhood become instruments of torture in advanced mechanics courses in early adulthood. Nevertheless, they are of such practical importance that their laborious study is worthwhile.

To summarize the essential ideas for describing a rigid rotator, look at Figure 6.12. One uses two sets of axes to describe a rigid rotator. One set, called the *body-fixed frame*, is locked into the body and completely characterizes rotations of

the body because of its rigidity. The second set of axes, the *space-fixed frame*, has an origin that coincides with the body-fixed frame, but which rotates as seen from this frame. The space-fixed axes are usually those in which observations are made.

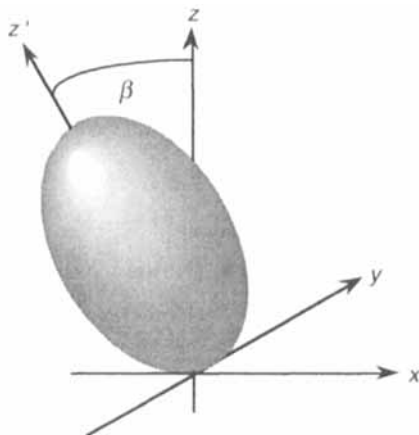


FIGURE 6.12 A rigid rotator is characterized primarily by angle β , the orientation of its z' (body-fixed) axis with respect to the z (space-fixed) axis.

For both classical macroscopic rotators (such as tops, gyroscopes, and space platforms) and quantum microscopic rotators (such as molecules and nuclei) the Euler angles (α, β, γ) , defined in Section 1.3.1 and reviewed in Section 6.1.1, are used to describe the orientation angles between the two frames. The y -axis rotation angle, β , is of major importance. Therefore, properties of the reduced rotation matrix elements derived in Sections 6.2–6.4 are often needed for rotational states.

To choose an appropriate body-fixed frame for molecules and nuclei in order to give the best approximation to a rigid rotator is far from straightforward, both conceptually and technically. It is discussed in great detail, and with much subtlety of reasoning, in Section 7.10 of Biedenharn and Louck's compendium on angular momentum [Bie81a].

6.5.1 The D^j as Angular Momentum Eigenfunctions

For discussing the quantized rigid rotator we need to involve the matrix elements of finite rotations. Consider the scalar products that are the projection of angular momentum kets onto the Euler-angle space, defined by

$$\langle (\alpha\beta\gamma) | jMK \rangle \equiv [D_{MK}^j(\alpha\beta\gamma)]^* = e^{iM\alpha} d_{MK}^j(\beta) e^{iK\gamma} \quad (6.61)$$

For integer values of $j = L$, say, we note that

$$\begin{aligned}
 L_z \langle (\alpha\beta\gamma) | LMK \rangle &= -i \frac{\partial}{\partial \alpha} \langle (\alpha\beta\gamma) | LMK \rangle = M \langle (\alpha\beta\gamma) | LMK \rangle \\
 L_{z'} \langle (\alpha\beta\gamma) | LMK \rangle &= -i \frac{\partial}{\partial \gamma} \langle (\alpha\beta\gamma) | LMK \rangle = K \langle (\alpha\beta\gamma) | LMK \rangle
 \end{aligned}
 \tag{6.62}$$

Thus, from (6.44), the complex conjugates of the rotation matrix elements with $j = L$ are eigenfunctions of the z components of the angular momentum operators in both the space-fixed and body-fixed frames, having eigenvalues M and K , respectively, as shown in Figure 6.13.

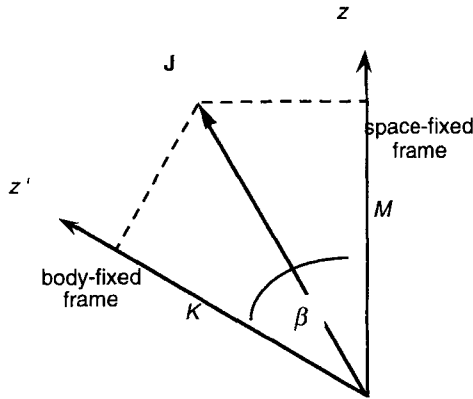


FIGURE 6.13 Rigid rotator projection numbers are M on the space-fixed axis, z , and K on the body-fixed axis, z' .

Therefore the visualizations of the rotation matrix elements in Section 6.3.3 are appropriate for the eigenfunctions that we have just determined. Our next task is to relate these functions to the eigenfunctions of a rigid rotator.

6.5.2 The Hamiltonian of a Rigid Rotator

The preceding developments provide the angular momentum states with respect to which we now calculate matrix elements of the Hamiltonian of the rigid rotator. We introduce the latter as follows.

The Classical Rotator. In classical mechanics one studies the rotational motions of rigid bodies in great detail, including the spinning of tops. It is shown in many mechanics texts, such as Sections 5–6 and 5–7 of Goldstein [Gol80], that the kinetic energy, T , is related to components of the angular momentum $\mathbf{L} = (L_{x'}, L_{y'}, L_{z'})$ in the principal-axes frame by

$$T = \frac{1}{2} \left[\frac{L_{x'}^2}{I_x} + \frac{L_{y'}^2}{I_y} + \frac{L_{z'}^2}{I_z} \right] \quad (6.63)$$

The principal moments of inertia in this frame are I_x, I_y, I_z (primes are conventionally omitted) and these are constants for each rotator. In most classical mechanics examples there are external torques, such as that due to gravity on a top. However, in the absence of such torques the Hamiltonian and the kinetic energy coincide. It is to the quantum mechanics version of this situation that we now turn our attention.

The Quantum-Mechanical Rotator. Consider the Hamiltonian operator, H_R , defined for a rigid rotator by

$$H_R \equiv \frac{1}{2} \left[\frac{J_{qx'}^2}{I_x} + \frac{J_{qy'}^2}{I_y} + \frac{J_{qz'}^2}{I_z} \right] \quad (6.64)$$

in which the quantum-mechanical angular momentum operator components in the body-fixed frame, (x', y', z') are $J_{qi} = \hbar J_i, i = x', y', z'$. One calls H_R the *rigid rotator Hamiltonian*, for reasons that will become clear immediately. Notice that between the classical mechanics (6.63) and the quantum mechanics (6.64) we have replaced angular momentum *values* by angular momentum *operators*.

What are the energy eigenvalues of the quantum-mechanical rigid rotator in terms of the principal moments of inertia and the angular momentum numbers J, M , and K ? To answer this, consider the matrix elements of H_R between the states described by (6.61). We then need to calculate the matrix elements of the *squares* of the angular momentum operators. Section 3.4.3 provides the matrix elements of the operators themselves, and for the squares we can use matrix multiplication rules, as Problem 6.17 suggests that you do. We thus obtain

$$\begin{aligned} & \langle JMK | J_{qx'}^2 | J'M'K' \rangle \\ &= \frac{\hbar^2}{2} \left\{ \begin{aligned} & [J(J+1) - K^2] \delta_{KK'} \\ & + \frac{1}{2} \sqrt{(J \pm K)(J \mp K + 1)(J \pm K - 1)(J \mp K + 2)} \delta_{KK' \pm 2} \end{aligned} \right\} \delta_{JJ'} \delta_{MM'} \\ & \langle JMK | J_{qy'}^2 | J'M'K' \rangle \\ &= \frac{\hbar^2}{2} \left\{ \begin{aligned} & [J(J+1) - K^2] \delta_{KK'} \\ & - \frac{1}{2} \sqrt{(J \pm K)(J \mp K + 1)(J \pm K - 1)(J \mp K + 2)} \delta_{KK' \pm 2} \end{aligned} \right\} \delta_{JJ'} \delta_{MM'} \\ & \langle JMK | J_{qz'}^2 | J'M'K' \rangle = \hbar^2 K^2 \delta_{KK'} \delta_{JJ'} \delta_{MM'} \end{aligned} \quad (6.65)$$

The nonzero matrix elements of the rigid rotator Hamiltonian are thus the elements that are diagonal in K , namely

$$\langle JMK|H_R|JMK\rangle = \frac{\hbar^2}{4} \left\{ \left(\frac{1}{I_x} + \frac{1}{I_y} \right) [J(J+1) - K^2] + \frac{2K^2}{I_z} \right\} \quad (6.66)$$

and those that are two steps removed from the diagonal in K . Such elements are given by

$$\begin{aligned} \langle JMK|H_R|JMK \pm 2\rangle &= \frac{\hbar^2}{8} \left(\frac{1}{I_x} - \frac{1}{I_y} \right) \\ &\times \sqrt{(J \pm K)(J \mp K + 1)(J \pm K - 1)(J \mp K + 2)} \end{aligned} \quad (6.67)$$

Note that the matrix elements are diagonal in the projection number M onto the space-fixed frame (Figure 6.13) and are independent of M (except that $|M| \leq J$ as usual). This property demonstrates that the rotator Hamiltonian is *intrinsic* to the body-fixed frame.

With the Hamiltonian matrix elements in hand, the energy eigenvalues are obtained by diagonalizing the matrix of H_R , as we now discuss.

Energy Eigenstates of the Symmetric Rigid Rotator. If the two principal moments of inertia I_x and I_y are equal, as in Figure 6.12, then one has a *symmetric rotator*. The off-diagonal matrix elements given by (6.67) become zero, so the matrix elements in (6.66) are just the energy eigenvalues, namely

$$E_J^{(sym)} = \hbar^2 \left[\frac{J(J+1)}{2I_x} + \left(\frac{1}{I_z} - \frac{1}{I_x} \right) \frac{K^2}{2} \right] \quad (6.68)$$

Therefore, these energy eigenvalues, $E_J^{(sym)}$, increase with K^2 for a fixed value of J if $I_z < I_x$. This is called a *prolate rotor* (or rotator), since a mechanical object of uniform mass density would have a prolate shape, like an American football or British rugby ball, as shown in Figure 6.14.

A symmetric rigid rotator for which $I_z > I_x$ is called an *oblate rotor* (or rotator), as shown on the right-hand side of Figure 6.14. The energy eigenvalues, $E_J^{(sym)}$, decrease with K^2 for a fixed value of J . Since K is a projection of J , for any rigid rotator one must have $J \geq K$ and there is also an energy degeneracy between $\pm K$ values, so one normally considers only the situation $K \geq 0$. A sequence of rotational energy levels for which K is fixed and J is varying is called a *rotational band*. The state of lowest energy for a given value of K , thus $J = K$, is termed the *bandhead*.

Asymmetric Rotators. If no two of the principal moments of inertia that appear in the rigid rotator Hamiltonian (6.64) are equal, then one has an asymmetric rotator,

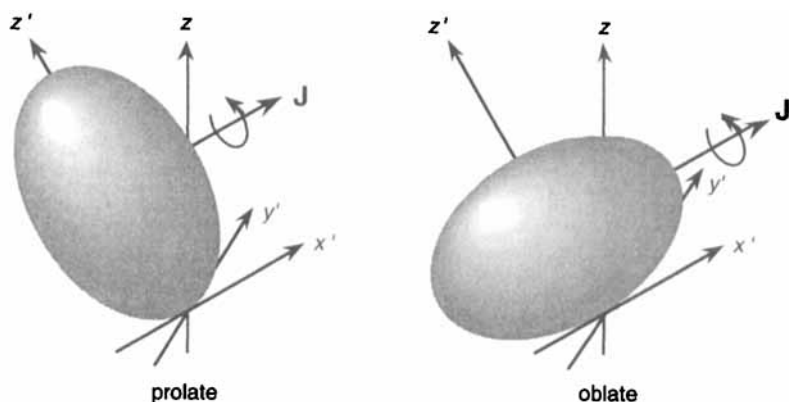


FIGURE 6.14 Symmetric rigid rotators of prolate shape (left) and oblate shape (right). The mechanical angular momentum \mathbf{J} is shown for the case $K = 0$, that is, for zero projection on the body-fixed axis, z' .

whose Hamiltonian matrix elements are given by (6.66). The most direct way to obtain the energy eigenvalues is to diagonalize the matrix numerically for a given choice of the three moments of inertia. The energy eigenfunctions of the asymmetric rotator can be expanded in terms of the basis states $D_{MK}^J(\alpha\beta\gamma)$. Because these are the eigenfunctions of the Hermitian angular momentum operators, they form a basis, according to the discussion in Section 2.3.3. Such an approach may be useful if the deviations from symmetry are relatively small, thus making perturbation methods appropriate.

6.5.3 Rotational States of Molecules and Nuclei

We now discuss examples of rotational bands in molecules and nuclei. These examples approximate those of symmetric rigid rotators. Since their bandheads are at $J = 0$, the rotational bands have $K = 0$, according to Figure 6.13.

Molecular Rotational States. The example from molecular spectra is LiF, for which the energy spacings between the lowest-lying levels are in the electromagnetic microwave spectrum. In the approximation that relevant properties of the constituent atoms are unaffected in different rotational states, J , the only question is the rigidity (constant length) of the interatomic spacing. Because the two atoms are distinct, the tumbling of the diatomic system about their center of mass can have both even and odd values of J . Thus $J = 0, 1, 2, \dots$, as seen in Figure 6.15. The ${}^6\text{LiF}$ molecule (the Li atom is the mass-6 isotope) is apparently very rigid under rotations, since its rotational energy levels coincide with those of the rigid rotator up to $J = 6$, for which the microwave-absorption measurements reported by Gordy and Cook [Gor70] were made.

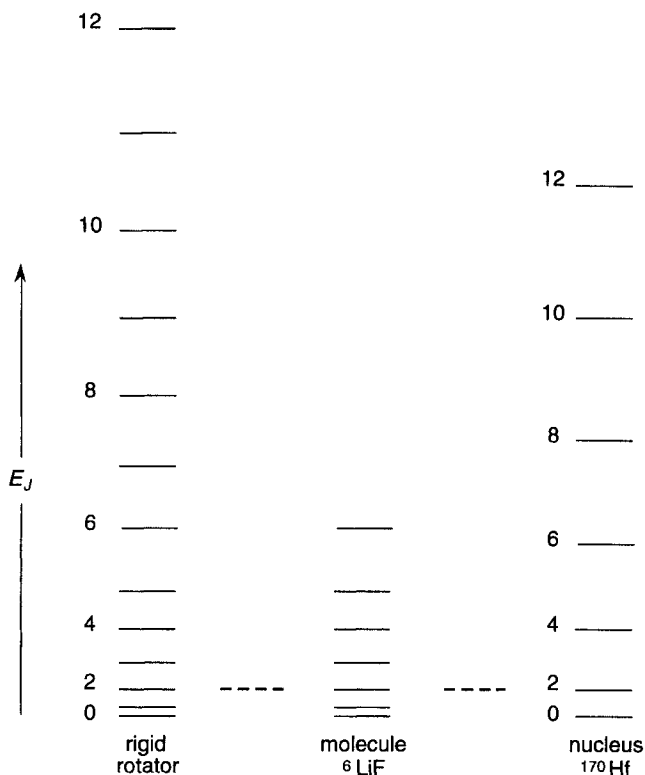


FIGURE 6.15 Energy spectra for rotators. The left-hand panel shows the idealized spectrum for a rigid symmetric rotator, $E_J \propto J(J+1)$, for $J = 0, 1, 2, \dots$. The center panel shows part of the spectrum of the LiF molecule [Gor70], and the right-hand panel is the spectrum of low-lying states in the reflection-symmetric nucleus ${}^{170}\text{Hf}$ [Won90], having $J = 0, 2, 4, \dots$. The energy scales of the latter two spectra have been chosen to coincide with the ideal spectrum at $J = 2$, as shown by the dashed lines.

Nuclear Rotational States. Many nuclei have energy levels that exhibit the characteristics of rigid rotators. For example, the nucleus of isotope ${}^{170}\text{Hf}$ has low-lying energy levels as shown in Figure 6.15. The energy levels now have spacing corresponding to the γ -ray region of the electromagnetic spectrum.

Since the ${}^{170}\text{Hf}$ nucleus is a many-body swarm of nucleons and the nuclear forces involved are parity invariant to a high degree of accuracy, the wave functions must have a definite parity, determined (as derived in Section 6.4.1) by $(-1)^J$. Therefore, given a ground-state spin of $J = 0$, the rotational band can consist only of even J values, $J = 0, 2, 4, \dots$, as shown in Figure 6.15.

The agreement for ${}^{170}\text{Hf}$ is actually better than the energy levels given in Section 6.3 of Wong's nuclear physics text [Won90] suggest, since the energy for

the $J = 6$ level reported there is misprinted. The accepted value, as given in [Nuc87], produces the good agreement shown in Figure 6.15. To spot such a misprint requires belief in the simplicity of such rotational spectra.

Notice that the nuclear energy levels observed gradually drop below those of a rigid rotator as J increases. One interpretation of this decrease is that the moments of inertia are gradually increasing as the mechanical angular momentum, $J\hbar$, increases. A moment of inertia can increase if nucleons are pulled apart because of centripetal forces. At this level of interpretation, we are making a correspondence between geometrical and dynamical angular momentum, in the senses discussed in Section 3.4.5. Such a correspondence is not unreasonable for $J > 6$, as justified in Section 6.4.3.

The examples of rotational spectra given here are for symmetric rotators having the projection quantum number K in Figure 6.13 equal to zero. For $K \neq 0$, as required when the principal moments of inertia are all different, the calculation of energy eigenvalues and the identification of the rotational spectra are more difficult, both for molecules and for nuclei. Introductory-level discussions are provided in [Gor70] and in [Won90].

Transition Energies Between Rotational States. As a final topic in our discussion of rigid rotators, consider the photon transition energies between rigid rotator energy eigenstates. For a given rotational band (K fixed), (6.68) shows that the photon transition energies, ΔE_J , form a uniformly spaced sequence. Considering the unit-step case, as for LiF above, we have

$$\begin{aligned}\Delta E_J &\equiv E_{J+1} - E_J \propto J + 1 \\ \Delta E_{J+1} - \Delta E_J &= \text{constant}\end{aligned}\tag{6.69}$$

with a similar result for J changing by steps of two, as for ^{170}Hf nuclei. Therefore, in a rotational band the photon energy spectrum will exhibit constant spacing between photon energies in emission or absorption. Transitions that break this pattern signal either new K bands, intruder energy levels, or artifacts of the experimental procedure.

PROBLEMS ON FINITE ROTATIONS OF ANGULAR MOMENTUM EIGENSTATES

6.1 Consider the matrices describing z -axis rotations in the (j, m) representation, given by (6.2).

(a) Show algebraically, by forming the product of the matrix with its Hermitian conjugate to produce the unit matrix of dimension $(2j + 1)$, that this rotation matrix is unitary.

(b) To prove that successive rotations about the z axis commute, write down the product of two such rotation matrices for angles γ_1 and γ_2 . Show that the order of writing down these angles, and thereby the order of the matrices, is not important.

6.2 For y -axis rotations of $j = 1$ states, consider the matrix for J_y given in Table 3.1.

(a) Show that for this matrix $\mathbf{J}_y^3 = \mathbf{J}_y$.

(b) Use this result in the exponential expansion (6.1) of the unitary matrix for y -axis rotation through angle β , then simplify the series that occur for each of the nine elements of the matrix in order to obtain (6.4).

6.3 Verify by direct multiplication of \mathbf{d}^1 with its transpose (equivalent to its Hermitian conjugate, since it is real) that \mathbf{d}^1 is a unitary matrix.

6.4 To derive formula (6.9) for the reduced rotation matrix elements, substitute (6.7) into (6.6), expand each power by using the binomial theorem, then rearrange terms to identify the unrotated states appearing in (6.8). The resulting coefficients of these terms are just the required matrix elements.

6.5 In order to check application of the general formula (6.9) for reduced rotation matrix elements, consider the following examples.

(a) Verify that for $j = 0$ there is a single y -axis rotation matrix element whose value is unity.

(b) Show that for $j = 1/2$ the y -axis rotation matrix agrees with (3.44).

(c) Repeat the calculation, but with $j = 1$, and verify agreement with (6.4). Notice that these nine calculations also show the symmetry properties of reduced matrix elements, there being only four independent expressions.

6.6 If a reduced rotation function $d_{m'm}^j$ has a projection number equal to zero (thus $j = \ell$, an integer), then we can relate it to Legendre functions, using the following methods of proof.

(a) Consider the recurrence relation satisfied by the Legendre polynomials, (6.12). By substituting series (6.9) for the reduced rotation matrix elements when $m' = m = 0$, show that d_{00}^ℓ satisfies the same recurrence relation. Since the functions coincide for $\ell = 0$ and for $\ell = 1$, they must agree for all values of ℓ .

(b) Repeat this analysis (or do it first) for only $m = 0$, in order to derive (6.13).

(c) As an alternative proof of (6.13), show that $d_{m'0}^\ell(\beta)$ and $P_m^\ell(\cos \beta)$ satisfy the same second-order differential equations in β , and that within the normalization factor and phase in (6.14), they coincide at two values of β , say at $\beta = \pm\pi$.

6.7^M Verify the formulas for the reduced rotation functions in Tables 6.1–6.3. This can be done longhand from (6.9) in terms of Jacobi polynomials, (6.16), or expeditiously by using *Mathematica* notebook Djm'm in Appendix I.

6.8 Consider rotation of a spherical harmonic with $\ell = 1$ about the y axis, as given by (6.23). By using the explicit expressions for $Y_{1m}(\theta, \phi)$ from Table 4.2 and for $d_{m'm}^1(\beta)$ from the third column of the matrix in Table 6.1, derive expression (6.24) for the rotated function.

6.9 Derive formula (6.33) for the transformation properties of magnetic substate amplitudes under rotations by following the steps for the $j = 1/2$ case.

6.10^M Consider interpretation of the reduced rotation matrices for $j = 3$.

- (a) Use *Mathematica* notebook `Djm'm` in Appendix I, or hand calculation from the general expression (6.9), to verify the formulas in (6.39).
- (b) Use the polar-plot option in `Djm'm`, or a simple calculator program, for each of the four functions in (6.39) to draw their polar diagrams, as in Figure 6.8.
- (c) Check the amplitude-rotation interpretation (6.36) for each value of initial projection, $m = 0, 1, 2, 3$, and the projection after rotation of the system, $m' = 2$. To do this, discuss how the amplitude changes with β for the four choices of m .

6.11 Verify the symmetry properties of the reduced rotation matrix elements $d_{m'm}^j(\beta)$ given in (6.40)–(6.43) by expressing both sides in the expansion (6.9). Rearrange the summations in order to verify the phase relations given.

6.12 Verify symmetries (6.45)–(6.48) of the full rotation matrix elements $D_{m'm}^j(\alpha\beta\gamma)$ by using the symmetries of the $d_{m'm}^j(\beta)$ given in (6.40)–(6.43) with the symmetries of the complex-exponential factors in (6.44).

6.13 For the orthogonality of the rotation matrix elements, consider (6.53) for $j_1 = 1/2$, $m'_1 = m_1 = 1/2$, and $j_2 = 0$ so that $m'_2 = m_2 = 0$, with an α -integration range 0 to $2n\pi$ with n an integer, a γ integration range 0 to 2π , and a β range 0 to π . Show that $I = 64[\cos(n\pi) - 1]/3$.

6.14 The classical limits of the reduced rotation matrix elements given in (6.58) may be approached as follows.

- (a) Use the square of the function in (6.57) to eliminate the angular variables in favor of the variable $m_c = j \cos\beta$ by using the relations

$$\tan^2(\beta/2) = (1 - \cos\beta)/(1 + \cos\beta) = (j - m_c)/(j + m_c) \tag{6.70}$$

Thereby derive the dependence of probability on the m value:

$$P_m/P_{m_c} = \left(1 - \frac{1}{j - m_c}\right) \left(1 - \frac{2}{j - m_c}\right) \dots \left(1 - \frac{m - m_c - 1}{j - m_c}\right) \tag{6.71}$$

$$\left(1 + \frac{1}{j + m_c}\right) \left(1 + \frac{2}{j + m_c}\right) \dots \left(1 + \frac{m - m_c}{j + m_c}\right)$$

Next use the result that

$$\prod_{n=1}^M \left(1 + \frac{n}{n'}\right) \approx 1 + \frac{1}{n'} \sum_{n=1}^M n = 1 + \frac{M(M+1)}{2n'} \approx e^{M^2/2n'} \tag{6.72}$$

when $M \ll n'$, in order to produce (6.58).

6.15^M Follow up the analysis in Problem 6.14 with visualization, as follows.

- (a) Use *Mathematica* notebook `Dj j m C p r` in Appendix I to calculate and display the squares of the reduced rotation matrix elements (6.57) and the approximation P_m , as shown in Figure 6.10. For computational convenience (avoidance of indeterminate forms) the notebook should not be run with $|m_c| = j$.

(b) Use (6.58) to explain this last remark.

(c) Show by running `Dj j m Cpx` for several values of j that if m_c is not too close to j , then the FWHM of the probability distribution scales approximately as \sqrt{j} , as discussed in the text.

6.16 The semiclassical limits of the reduced rotation functions for $m = 0$ and $m' = j$, given by (6.59), can be used to estimate the FWHM in angle β of the corresponding probability distribution $P_j(\beta) = |d'_{j0}(\beta)|^2$.

(a) Use (6.59) to show that

$$P_j(\beta) = P_j(\pi/2) [\sin \beta]^{2j} \quad (6.73)$$

(b) Write down the condition on the angle by which β must be displaced from $\pi/2$ for P_j to decrease by a factor 1/2, then use the approximation that $\ln(\cos \theta) \approx -\theta^2/2$ for $\theta \ll 1$ to show that the FWHM of the P_j distribution is approximately $2\sqrt{\ln 2/j}$.

6.17 Derive the rigid-rotator angular momentum matrix elements (6.66)–(6.67) in two ways:

(a) Use (3.64)–(3.66) for the matrix elements of the Cartesian components of the angular momentum operators. Then use the rules of matrix (inner product) multiplication, as in Section 2.1.2, to construct the formulas for the squares of the components.

(b) First show that the Cartesian operators can be expressed in terms of the ladder operators (3.9) by

$$\begin{aligned} J_x^2 &= \frac{1}{2}(\mathbf{J}^2 - J_0^2) + \frac{1}{4}(J_{+1}^2 + J_{-1}^2) \\ J_y^2 &= \frac{1}{2}(\mathbf{J}^2 - J_0^2) - \frac{1}{4}(J_{+1}^2 + J_{-1}^2) \\ J_z^2 &= J_0^2 \end{aligned} \quad (6.74)$$

Use the matrix elements of $J_{\pm 1}$, given by (3.63), to derive the matrix elements of their squares, then use (6.74) for the Cartesian components.



Chapter 7

COMBINING TWO ANGULAR MOMENTUM EIGENSTATES

Suppose that we have two subsystems, each characterized by angular momentum eigenvalues and eigenstates. In the preceding chapters, especially Chapters 3, 4, and 6, we developed the mathematics and interpretation appropriate to describing rotational properties of the subsystems. Now, however, let us look at the larger picture and ask about rotational properties of the total system.

In most of this chapter, we assume that the two subsystems are dynamically independent, in the sense that rotations of subsystem 1 could be made independently of rotations of subsystem 2. Analytically, this means that their rotation operators commute—a property that simplifies the operator algebra. For example, in Section 3.5 we stress the distinction between spin (subsystem 1) and orbital angular momentum (subsystem 2), so these would be appropriate to combine by using the algebra that follows. The idea of combining is sketched in Figure 7.1.

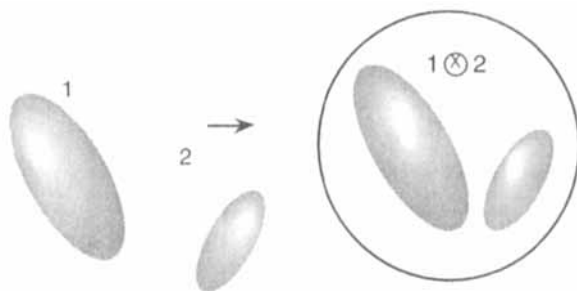


FIGURE 7.1 Subsystems 1 and 2 have their rotational properties, as indicated at the left. On the right the rotational properties of the whole system are to be considered.

An inappropriate application of the techniques derived here for combining two angular momentum eigenstates, if used directly, would be to combine the orbital angular momenta of two objects joined by a rigid rod—an idealized device constraining their angles of rotation to be identical. How to handle such a situation is derived in Section 7.5.

In spite of this warning about operators that may be combined using the following scheme, it is almost universal practice to use the term *coupling* rather than *combining*, which is the term used more often in this book. The conventional terminology is sometimes confusing in contexts such as *spin-orbit coupling*, as discussed in Section 7.1.3 and Chapter 9.

The outline of this chapter is as follows. In Section 7.1 we introduce the vector model for addition, we consider spin-orbit coupling as an example of coupling, and we use the operator algebra to investigate the degeneracy of energy states in the Coulomb potential. The angular momentum coupling of states is derived in Section 7.2, which introduces Clebsch-Gordan and $3-j$ coefficients. Formulas for the latter are derived in Section 7.3 and their properties are discussed. In Section 7.4 efficient methods for computing $3-j$ coefficients are presented. In Section 7.5 we bring together our expertise on rotation matrices from Chapter 6 with our newly acquired understanding of coupling. For example, we show how to evaluate readily complicated integrals involving spherical harmonics, whether they describe heavenly bodies or molecules. Problems to test your comprehension of combining angular momentum states round out the chapter.

7.1 THE SEMICLASSICAL VECTOR MODEL FOR ADDITION

The semiclassical vector model introduced in Section 5.3 helps one visualize the angular momentum operators \mathbf{J} , J_z and their eigenvalues, and it is of some help for calculations, especially as j becomes large. For combining two angular momenta, the so-called “vector addition” summarized in Section 7.1.1, the semiclassical model is of similar usefulness and limitation, being particularly useful as a mnemonic for the triangle and projection selection rules that we derive in Section 7.1.2. How to interpret angular momentum coupling, as introduced at the beginning of this chapter, is the topic in Section 7.1.3. In the final subsection we use our experience with combining angular momenta to derive in Section 7.1.4 the degeneracy of energy states in the Coulomb potential.

7.1.1 Vector-Addition Construction

The vector-addition construction for combining two angular momenta follows the vector model for a single angular momentum, as introduced in Section 5.3. Suppose that for system 1 the angular momentum “vector” (strictly speaking, a vector *operator*) is \mathbf{j}_1 and that the projection on the z axis (an eigenvalue of J_z) is m_1 , and similarly for system 2 the vector is \mathbf{j}_2 and its projection is m_2 . Figure 7.2 shows the vector-addition diagram for the vectors \mathbf{j}_1 and \mathbf{j}_2 combined to a resultant \mathbf{J} , with projection M . We are assuming that the vectors combine as in classical mechanics.

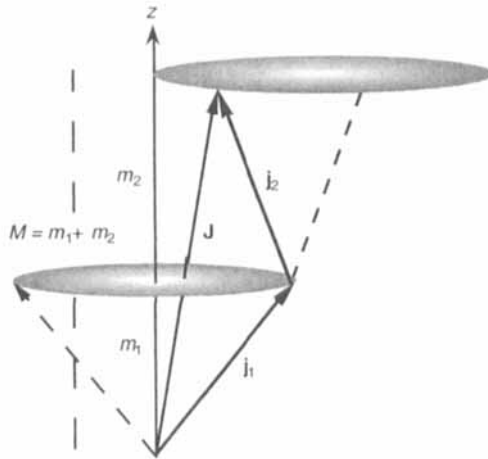


FIGURE 7.2 In classical mechanics two angular momenta \mathbf{j}_1 and \mathbf{j}_2 are combined to a resultant \mathbf{J} . Their projections on the axis z are m_1 , m_2 , and M , respectively. In the semiclassical model each vector precesses around the z axis.

Suppose, as in Figure 7.2, that the vector \mathbf{J} , its magnitude J , and its projection M , are given, and that the magnitudes j_1 and j_2 are also fixed. We write such a state as $|j_1 j_2 JM\rangle$. Even with these restrictions, the subsystem vectors (which both precess around the z axis) can have a range of projections consistent with conservation of the total projection, $M = m_1 + m_2$. There is therefore a range of subsystem kets $|j_1 m_1\rangle$ and $|j_2 m_2\rangle$ that can be combined to give the ket $|j_1 j_2 JM\rangle$. Classically, the range of projections may be interpreted as the two component vectors being in different phases of their precession cycles, but chosen in such a way that the projection, M , of their resultant, \mathbf{J} , is constant.

This vector-model description will also immediately suggest to you selection rules for the range of J , as we now derive in the full algebraic treatment of combining the two angular momenta.

7.1.2 Triangle and Projection Selection Rules

We now formalize the treatment of combining angular momenta introduced above in the vector model. First, we remark that subsystems 1 and 2 must describe *separate* systems. That is,

$$|j_1 m_1\rangle = |\alpha j_1 m_1\rangle \quad |j_2 m_2\rangle = |\beta j_2 m_2\rangle \quad \alpha \neq \beta \quad (7.1)$$

in which α and β are labels distinguishing the vector spaces to which the kets belong. Provided that this separateness is clear, we will usually drop the α and β labels. For example, for a single object α might label the spin space (internal degrees of freedom, according to Sections 3.5 and 4.3.1) and β might label the orbital angu-

lar momentum space, thus $\beta = (\theta, \phi)$. As another example, α and β might refer to different objects—such as two electrons—or a nucleus and an electron orbiting it.

At the macroscopic level, the first angular momentum may describe the shape of Earth's orbit around the sun (mostly $\ell_1 = 0$ because of the nearly circular orbit), while the second angular momentum may be the shape of the Moon's orbit around Earth (also mostly $\ell_2 = 0$). In this example, the coupled angular momentum would describe the shape of the Moon's orbit as viewed from the sun, which will be slightly less symmetric (larger maximum angular momentum from combining ℓ_1 and ℓ_2) than either orbit separately. If this example bothers you, because of the obviously huge dynamical angular momenta of the Earth and Moon in their orbits, review the discussion in Section 3.4.5, where we distinguish definitively between geometrical and dynamical angular momentum. Here we are discussing the geometry of orbits, so using small angular momentum numbers is appropriate.

Combining the Angular Momentum Operators. We now introduce the formalism for the addition of angular momenta. Consider the operator

$$\mathbf{J} \equiv \mathbf{J}_1 + \mathbf{J}_2 \quad (7.2)$$

If subsystems 1 and 2 are independent, then operators \mathbf{J}_1 and \mathbf{J}_2 commute. It is thus easy to see that if the basic commutation rule of angular momentum, (3.8), is satisfied by each operator separately, then it is satisfied by their sum:

$$\mathbf{J}_1 \times \mathbf{J}_1 = i\mathbf{J}_1 \quad \mathbf{J}_2 \times \mathbf{J}_2 = i\mathbf{J}_2 \quad \Rightarrow \quad \mathbf{J} \times \mathbf{J} = i\mathbf{J} \quad (7.3)$$

Conceptually, infinitesimal rotations of the whole system (\mathbf{J}) are compounded of infinitesimal rotations of the independent subsystems (\mathbf{J}_1 and \mathbf{J}_2), as sketched in Figure 7.1.

The space in which \mathbf{J} acts is a direct-product Hilbert space. Such direct products are introduced in the context of direct-product matrices in Section 2.1.2. Appropriate kets for components of \mathbf{J} , J_i , are therefore to be formed from products of the subsystem kets, as follows:

$$J_i |j_1 m_1\rangle |j_2 m_2\rangle = (J_{1i} |j_1 m_1\rangle) |j_2 m_2\rangle + |j_1 m_1\rangle (J_{2i} |j_2 m_2\rangle) \quad (7.4)$$

where i denotes a component of an operator, such as $i = x, y, z$ (Cartesian basis) or $i = +1, 0, -1$ (spherical basis). The ket from the subsystem to which the operator does not belong therefore acts like a multiplicative factor in the product space.

We determine the allowed range of eigenvalues of \mathbf{J}^2 by counting the range of independent combinations of m_1 and m_2 that give rise to each such eigenvalue. The upper limit to J , call it $J_>$, is readily obtained by noting that the biggest value of $M = m_1 + m_2$ is $j_1 + j_2$, so that $J_> = j_1 + j_2$. This so-called *stretched state* is very interesting in studying angular momenta of systems because it has a unique product-space representation, namely $|j_1 j_1\rangle |j_2 j_2\rangle$.

The next smaller value of M is $j_1 + j_2 - 1$, with one direct product state being

$|j_1 + j_2, j_1 + j_2 - 1\rangle$ and the other $|j_1 + j_2 - 1, j_1 + j_2 - 1\rangle$. The pattern is now clear: Each time M is reduced by unity, one of the coupled states belongs to a J value reduced by unity in which $M = J$, while one more product state is added to the growing list of product states associated with higher J values. The lower limit to this counting procedure is reached at $J_<$ when the number of product states is matched against the totality of uncombined states. Then we have

$$\sum_{J=J_<}^{J_>} (2J+1) = (2j_1+1)(2j_2+1) \quad (7.5)$$

By following the steps suggested in Problem 7.1, it is straightforward to show that the lower limit $J_< = |j_1 - j_2|$. This is called the *jackknife state*. It does not have the simplicity inherent in the stretched state.

In summary, the eigenvalues of the combined angular momenta are a total angular momentum J , given by the so-called *triangle condition*

$$|j_1 - j_2| \leq J \leq j_1 + j_2 \quad (7.6)$$

together with the *M-conservation condition*

$$M = m_1 + m_2 \quad (7.7)$$

These results, obtained after several detailed arguments, would seem obvious from the semiclassical vector model. Recall, however, that the model sketched in Figure 7.2 is of limited applicability overall, as stressed in Section 5.3. Although the model may suggest results such as the triangle condition (7.6), it cannot prove their correctness.

7.1.3 Interpreting Coupling: Spin-Orbit Interaction

We discussed in the introduction to this chapter the confusing use of the term “coupling” for combining of angular momentum as just described. Now we try to understand the reason for this term, we discuss spin-orbit interactions, and we summarize spectroscopic notation for coupled states.

Hamiltonians with Coupling. Angular momentum coupling is often used when calculating with Hamiltonians constructed from subsystem angular momentum operators. Suppose that the Hamiltonian is given—as discussed at the end of Section 4.3.1—by

$$H = H_0 + H_{so} \mathbf{L} \cdot \mathbf{S} \quad (7.8)$$

in which the spin-independent term is H_0 and the term with the factor H_{so} is called the spin-orbit part of the Hamiltonian. Both terms may be functions of position or momentum. For electrons, such a term was suggested as early as 1927 [Cou27]. The independent spaces are orbital angular momentum for operator \mathbf{L} and intrinsic spin for \mathbf{S} . Since the two operators commute, we may write either $\mathbf{L}\cdot\mathbf{S}$ or $\mathbf{S}\cdot\mathbf{L}$. Notice that—at least classically—if the projection of spin onto the “direction” of the orbital angular momentum is reversed, then the spin-orbit interaction effect changes sign.

Suppose that we combine the angular momentum operators by writing

$$\mathbf{J} = \mathbf{L} + \mathbf{S} \quad (7.9)$$

Note that according to the discussion in Section 4.3.1 about the nature of spin, this is an implicit definition of the spin operator. This “total” angular momentum operator is very useful for finding energy eigenvalues of H in (7.8), for the following reason. Form the operator combinations

$$\mathbf{J}^2 = (\mathbf{L} + \mathbf{S})^2 = \mathbf{L}^2 + \mathbf{S}^2 + 2\mathbf{L}\cdot\mathbf{S} \quad (7.10)$$

By solving for the scalar product and inserting the result in (7.8), we obtain

$$H = H_0 + H_{so} (\mathbf{J}^2 - \mathbf{L}^2 - \mathbf{S}^2)/2 \quad (7.11)$$

We see that by forming combined angular momentum states—eigenfunctions of \mathbf{J}^2 and J_z as well as of \mathbf{L}^2 and \mathbf{S}^2 — H has become diagonal in these angular momenta, so we can read off the energies directly:

$$\begin{aligned} E_{J\ell} &= \langle \ell s J | H | \ell s J \rangle \\ &= \langle H_0 \rangle + \langle H_{so} \rangle [J(J+1) - \ell(\ell+1) - s(s+1)]/2 \end{aligned} \quad (7.12)$$

Here we assume that s and ℓ are fixed and that J is variable. The expectation values of H_0 and H_{so} are taken with respect to the other degrees of freedom in the problem, such as radial coordinates. Note that (7.12) holds only for J in the range satisfying the triangle condition (7.6), namely $|\ell - s| \leq J \leq \ell + s$. In (7.12) there is no dependence of the energy on the projection quantum numbers, just as we expect, since the energy is a scalar quantity— independent of the orientation of axes.

Does the semiclassical prediction—that the effect of the spin-orbit interaction changes sign with reversal of spin projection—hold up? Consider the energy difference between the stretched case, $J = \ell + s$, and the jackknife case $J = |\ell - s|$. Directly from (7.12) we obtain (as Problem 7.2 suggests you verify) the ratio of the spin-orbit contributions to the energy:

$$\frac{E_{\ell+s,\ell} - \langle H_0 \rangle}{E_{|\ell-s|,\ell} - \langle H_0 \rangle} = -\frac{\max(\ell, s)}{\max(\ell, s) + 1} \quad (7.13)$$

where $\max(\ell, s)$ means “the larger of ℓ and s .” Therefore, except in the uninteresting case that one of ℓ or s is zero, there is indeed a sign reversal, but there is a complete reversal only in the limit that the larger of the two values (usually ℓ) greatly exceeds unity. We can also calculate the *spin-orbit splitting*, given by

$$\Delta E_{\ell s} \equiv E_{\ell+s, \ell} - E_{|\ell-s|, \ell} = \begin{cases} \langle H_{so} \rangle (2\ell + 1)s & \ell \geq s \\ \langle H_{so} \rangle (2s + 1)\ell & \ell \leq s \end{cases} \quad (7.14)$$

Spin-Orbit Energy Splitting in Atoms and Nuclei. The spin-orbit interaction in the Hamiltonian (7.8) is of major importance in the spectroscopy of atoms and nuclei. For a system with an odd number of electrons or of nucleons, a good approximation (called the *shell model*) is to assume that the angular momentum of the system, J , is that of the odd particle, and that the major spin-dependent term is of the form (7.8). Consider, for example, an electron or nucleon with orbital angular momentum number $\ell = 2$, a so-called D state. Since $s = 1/2$, the triangle condition (7.6) allows $J = 3/2$ or $5/2$. Figure 7.3 shows schematically the spin-orbit splitting of the energy spectrum of an atom or nucleus with such quantum numbers.

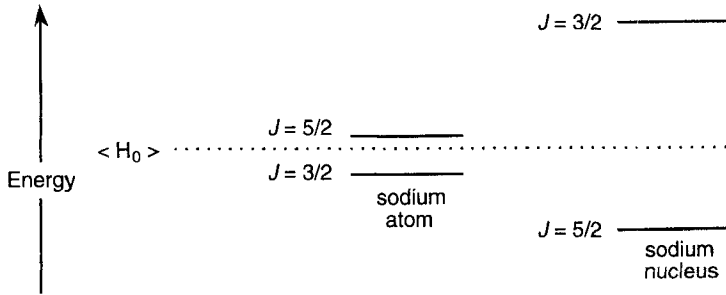


FIGURE 7.3 Schematic of spin-orbit splitting in atoms and nuclei. The D-line doublet in the visible spectrum of sodium (Na) arises from spin-orbit splitting of an $\ell = 2$ state into $J = 3/2$ and $5/2$ states, ordered as shown. In nuclei, the splitting is much larger in magnitude and of opposite sign, as indicated.

Notice in Figure 7.3 that the spin-orbit splitting relative to the unperturbed energy $\langle H_0 \rangle$ is asymmetric about this energy. For $\ell = 2$, $s = 1/2$ the splitting is in the ratio 2:3, according to (7.13). The energy scales are quite different for the two systems, with the splitting being of order meV in sodium atoms and of order MeV (10^9 times larger) in nuclei. Since typical energies of valence electrons in atoms are in the 10-eV range, while typical valence nucleon energies in nuclei are about 10 MeV, the fractional effect of the nuclear spin-orbit splitting is about an order of magnitude larger than in atoms. Note, however, that $\langle H_{so} \rangle$ in Figure 7.3 is indicated as being positive in the Na atom, whereas it is shown as negative for the Na nucleus.

The explanation of the dominant features of the energy spectra of many nuclei in terms of a shell model with a large spin-orbit coupling that is reversed in sign from that in atoms was realized by Maria Goeppert-Mayer (1906–1972), a nuclear scientist with extensive training in atomic spectroscopy. She was awarded a Nobel Prize in physics in 1963 for this discovery, and an award for outstanding young women in physics is named in her honor. For readable biographies, see the two books by Joan Dash [Das73, Das91].

A discussion of spectra in alkali atoms, including the sodium D lines and spin-orbit coupling, is given in Section 10-2 of Eisberg and Resnick's text on quantum physics [Eis85]. The origins of electron spin-orbit coupling in terms of the Dirac equation are derived in Section 15.E of Landau's text [Lan90]. At the end of Section 7.3.1 we show how to construct appropriate wave functions for Hamiltonians with spin-orbit coupling.

Spectroscopic Notation. We can extend the nomenclature for values of ℓ as s , p , d , f , etc. for $\ell = 0, 1, 2, 3$, etc. to include the total angular momentum number J of an electron or nucleon ($s = 1/2$) as a subscript on the orbital letter, thus $[\ell]_J$. For example, $d_{3/2}$ and $d_{5/2}$ are spectroscopic notation for the two angular momentum states that can be formed when combining $\ell = 2$ with $s = 1/2$. When we equate the total angular momentum number J of a system with the angular momentum of the odd particle, a model is assumed, since we are assuming—often with empirical evidence that is convincing enough for a Nobel Prize committee—that the remaining particles interact to produce complete rotational invariance, that is, zero angular momentum.

Elaborations of this spectroscopic notation abound in the various spectroscopies of molecules, atoms, nuclei, and fundamental particles. Indeed, it is one of the trials of initiation into these scientific subfields to be able to recite the appropriate spectroscopic notation rapidly and without error.

7.1.4 Degeneracy of Energy States in the Coulomb Potential

Now that we have experience with combining angular momentum operators, our aim is to show how combining two angular momenta can be used to prove the degeneracy of energy states in a Coulomb potential. We carry the development far enough to show that the energy is degenerate, but we do not investigate the nature of the degeneracy or properties of the energy eigenstates, which are much more complicated but fascinating in their own ways. Rather, we direct you to the extensive literature.

The main technical interest here is to show the correspondence between a classical mechanics problem and its quantum analog. Since our insight into classical mechanics is often well developed through everyday experience, it is helpful to set up quantum mechanics problems as analogues or extensions of classical problems. We have seen for angular momentum how fruitful this can be for the semiclassical vector model. Now we adapt this to Coulomb potentials. Many examples of classical-quantal analogues are given in the book by Park [Par90].

To develop the problem and its solution, we show that for inverse-square forces (as in Kepler's gravitational problem or Coulomb's electrical problem) there is an

additional conserved quantity, the Runge-Lenz (or eccentricity) vector. The existence of such a constant of the motion, in addition to the constancy of orbital angular momentum for *any* central force, suggests that there should be additional symmetry in the inverse-square problem, therefore additional degeneracies of quantities such as energy. We know from our discussion of Noether's theorem (Section 1.1.2) that a continuous symmetry implies a conservation law. The converse demonstrated here—conserved quantities in dynamical systems often imply symmetry relations—is a trustworthy guide to discovering new symmetry properties.

Classical Eccentricity Vector. We begin by using considerations from classical mechanics [Gol80] to establish the constancy of the eccentricity vector. Then we convert classical vectors into quantum operators to formulate the problem for one-electron, hydrogen-like atoms. For a central force between two particles with relative displacement \mathbf{r} , Newton's law for the time rate of change of their relative momentum \mathbf{p} may be written as

$$\dot{\mathbf{p}} = f(r)\hat{\mathbf{r}} \quad (7.15)$$

where $f(r)$ gives the dependence of the force on separation r . For *any* central force the time rate of change of the angular momentum $\mathbf{L} = \mathbf{r} \times \mathbf{p}$ is zero, that is, $\dot{\mathbf{L}} = 0$. Consider now the vector $\mathbf{L} \times \mathbf{p}$ and its time rate of change:

$$\frac{d\mathbf{L} \times \mathbf{p}}{dt} = \mathbf{L} \times \dot{\mathbf{p}} = m f(r) r^2 \frac{d\hat{\mathbf{r}}}{dt} \quad (7.16)$$

To obtain the second equality we use (as Problem 7.3 suggests you try) simple manipulation of vector cross products and express the result in terms of the unit vector $\hat{\mathbf{r}}$ describing the angle between them with respect to a reference frame and their reduced mass m . Equation (7.16) is true, but usually uninteresting. In the special case that the force law is inverse-square, namely

$$f(r) = -\frac{k}{r^2} \quad (7.17)$$

where $k = GMm$ for gravity and $k = Ze^2$ for a one-electron atom with nuclear charge Ze , the factor in (7.16) preceding the time derivative is a constant. The vector defined by

$$\mathbf{A}_c \equiv \mathbf{L} \times \mathbf{p} + mk\hat{\mathbf{r}} \quad (7.18)$$

is then a constant of the motion. We refer to \mathbf{A}_c as the *eccentricity vector*, for reasons that will become clear immediately.

To understand the properties of \mathbf{A}_c , apart from its constancy with time, we first find its orientation by noting that

$$\mathbf{A}_c \cdot \mathbf{L} = 0 \quad (7.19)$$

Since \mathbf{L} is perpendicular to the plane of the orbit, the eccentricity vector must lie in the plane of the orbit, but just *where* does it point in this plane? Consider the projection of \mathbf{r} onto \mathbf{A}_c :

$$\mathbf{A}_c \cdot \mathbf{r} = A_c r \cos \theta = \mathbf{L} \times \mathbf{p} \cdot \mathbf{r} + mkr = -L^2 + mkr \quad (7.20)$$

This is of maximum magnitude when r is smallest, that is, at perihelion for a planetary system. Therefore, the eccentricity vector lies along the line joining aphelion to perihelion. Equation (7.20) can be written as

$$\frac{1}{r} = \frac{mk}{L^2} \left(1 - \frac{A_c}{mk} \cos \theta \right) \quad (7.21)$$

By comparing this with the standard orbit equation—for example, equation (3-51) in [Gol80]—we see that the magnitude of the eccentricity vector is

$$A_c = mke \quad (7.22)$$

where e is the eccentricity of the orbit. For a bound orbit, the eccentricity is the fractional difference between major and minor axes of the orbit ellipse. Because \mathbf{A}_c is proportional to e for a given pair of particles and force relation (choice of k), it is appropriate to call it the eccentricity vector. Note that if the elliptical orbit degenerates into a circle (equal major and minor axes), then \mathbf{A}_c collapses to a null vector.

The properties of the eccentricity vector are summarized in Figure 7.4.

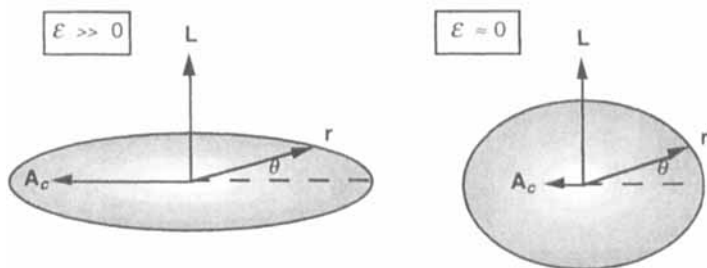


FIGURE 7.4 The eccentricity vector, \mathbf{A}_c , which is a constant of the motion for an inverse-square law of force. Examples of bound orbits of large eccentricity (left view) and of small eccentricity (right view) are shown in the center-of-mass frame.

To relate the eccentricity vector to the energy, E , from (7.20), one derives, as in [Gol80], the relation

$$A_c^2 = (mk)^2 \epsilon^2 = (mk)^2 + 2mL^2 E \quad (7.23)$$

which was published by Laplace in 1799 [Lap99]. By using this result we may take

a quantum leap into the twentieth century and write down the classical formula for the energy of a one-electron (hydrogenic) atom, namely

$$E = -\frac{mZ^2e^4}{2L^2} + \frac{m\epsilon^2}{2L^2} \quad (7.24)$$

This shows that for a fixed angular momentum, L , the energy decreases as the magnitude of the orbital eccentricity, ϵ , increases. Therefore, if the energy is the *same* for different values of L (as we are about to prove) the corresponding classical orbits must have different eccentricities.

The eccentricity vector, \mathbf{A}_c , has a long history in classical mechanics that has been traced back [Gol76] to J. Hermann in 1710. Laplace described it in his 1799 treatise on celestial mechanics [Lap99], and it became widely known through a 1919 text on vector analysis by Runge. It was used in the “old” (semiclassical) quantum theory by Lenz (1924) and in the “new” Heisenberg formulation of quantum mechanics by Pauli [Pau26] to prove the degeneracy of the energy states of the hydrogen spectrum. Although \mathbf{A}_c (or its negative) is often referred to as the “Runge-Lenz” vector, such attribution is not justified by its history, many details of which are provided in two articles by Goldstein [Gol75, Gol76].

Now that we understand the classical eccentricity vector, consider the situation for quantum mechanics.

Quantal Eccentricity Operator. The classical vectors in the preceding analysis are directly measurable quantities. In quantum mechanics one constructs corresponding Hermitean operators whose expectation values are measurable. Following the original treatment by Pauli [Pau26], we make the following correspondence:

$$\mathbf{A}_c = \mathbf{L} \times \mathbf{p} + mk\hat{\mathbf{r}} \quad \rightarrow \quad \mathbf{A}_q = \frac{1}{2}(\mathbf{L}_q \times \mathbf{p}_q - \mathbf{p}_q \times \mathbf{L}_q) + mk\hat{\mathbf{r}} \quad (7.25)$$

in which \mathbf{L}_q and \mathbf{p}_q are the quantum orbital angular momentum and linear momentum operators, respectively, and both contain factors of \hbar in their definitions. The more complicated form in the second line of (7.25) is necessary if the *quantal eccentricity operator*, \mathbf{A}_q , is to be Hermitean, and is thereby (Section 2.3) suitable to represent an observable.

Our goal is to relate properties of the operator \mathbf{A}_q to those of the Hamiltonian H . We will find representations in which combinations of \mathbf{A}_q , \mathbf{L}_q , and H are all diagonal. Thereby we relate energy (the expectation value of H in a diagonal representation) to angular momentum observables. To simplify the operator algebra, it is practical to introduce the dimensionless variables given in Table 7.1 which are commonly used in the quantum mechanics of one-electron atoms.

By using the system of units in Table 7.1, we can readily show (as Problem 7.3 suggests you try) that

$$\mathbf{A}_q^2 = \mathbf{A}_q \cdot \mathbf{A}_q = H(\mathbf{L}_q^2 + 1) + 1 \quad (7.26)$$

TABLE 7.1 Dimensionless variables for the quantum one-electron atom. The quantity a_0 is the Bohr radius for hydrogen ($Z = 1$).

Quantity	Unit
Length	a_0/Z
Dynamical angular momentum	\hbar
Momentum	$\hbar Z/a_0$
Energy	$Z^2 e^2 / 2a_0$

It is straightforward to show by analogy with the classical result that the eccentricity operator \mathbf{A}_q commutes with \mathbf{L}_q . Therefore, by diagonalizing \mathbf{A}_q^2 and \mathbf{L}_q^2 simultaneously we will have diagonalized H , that is, we will have the energy eigenvalues E . We consider only bound states, analogous to the closed classical orbits depicted in Figure 7.4. The more general case including scattering states is analyzed similarly but with some sign changes, as discussed on page 338 of [Bie81a].

To expedite the diagonalization, consider the operator \mathbf{A} defined so that $\mathbf{A}^2 H = -\mathbf{A}_q^2$, which allows (7.26) to be written simply as

$$(\mathbf{L}_q^2 + \mathbf{A}^2 + 1)H = -1 \quad (7.27)$$

To express this in terms of quantities that are more familiar, consider the operators

$$\mathbf{J}_1 \equiv \frac{1}{2}(\mathbf{L}_q + \mathbf{A}) \quad \mathbf{J}_2 \equiv \frac{1}{2}(\mathbf{L}_q - \mathbf{A}) \quad (7.28)$$

Problem 7.3 (b) suggests that you show that these quantities behave just like two independent angular momentum operators, namely

$$\mathbf{J}_k \times \mathbf{J}_k = i\mathbf{J}_k \quad k=1,2 \quad [\mathbf{J}_1, \mathbf{J}_2] = 0 \quad (7.29)$$

Further, it is interesting and relevant to show that

$$\mathbf{J}_1^2 = \mathbf{J}_2^2 = (\mathbf{L}_q^2 + \mathbf{A}^2) / 4 \quad (7.30)$$

We therefore know from Section 3.4.1 that diagonal representations of \mathbf{J}_1^2 and \mathbf{J}_2^2 have expectation values given by

$$\langle \mathbf{J}_1^2 \rangle = \langle \mathbf{J}_2^2 \rangle = j(j+1) \quad j = 0, 1/2, 1, \dots \quad (7.31)$$

By using this first in (7.27), then in the expectation values calculated using (7.31), we can write immediately (recalling that we are in a diagonal representation)

$$[4j(j+1)+1]\langle H \rangle = -1 \quad (7.32)$$

Therefore, the energies in dimensionless units are given by

$$\langle H \rangle = -\frac{1}{(2j+1)^2} \quad j = 0, 1/2, 1, \dots \quad (7.33)$$

Finally, replacing $2j+1$ by positive integers n and reverting to actual energy units by using the conversion from Table 7.1, we have the eigenenergies of the hydrogenlike, one-electron, atom

$$E_n = \langle H \rangle = -\frac{Z^2 e^4 m}{2\hbar^2 n^2} \quad n = 1, 2, \dots \quad (7.34)$$

which is the standard quantum-mechanical formula. We have obtained this result using only the conservation properties of the operators \mathbf{A}_q and \mathbf{L}_q , without requiring wave functions. Notice that eigenvalues of the orbital angular momentum operator \mathbf{L}_q do not appear in this formula, so we can say that the energy has degeneracy with respect to orbital angular momentum. From our discussion of (7.22), we would suspect that in the quantum-mechanical analysis for given E_n the most probable orbits become more eccentric as the total angular momentum number ℓ increases.

The quantum eccentricity operator, \mathbf{A}_q , can be used to develop hydrogenic-atom wave functions, as discussed in Section 7.4 of [Bie81a]. Englefield's monograph [Eng72]—especially Chapters 3 and 4—emphasizes group theoretical analysis. Both references describe how the wave functions in three-dimensional momentum space and the energy degeneracy can be viewed as arising from a symmetry in a four-dimensional space involving the group $O(4)$ introduced in Table 2.12.

In this section we have shown how to combine operators for angular momenta to obtain selection rules on eigenvalues, how to interpret such coupling, and how to apply operator properties to calculate spin-orbit and Coulomb energies. In the next two sections we emphasize properties of combined angular momentum eigenstates.

7.2 COUPLING COEFFICIENTS: DEFINITIONS AND GENERAL PROPERTIES

Our goal for this section is to construct eigenstates of \mathbf{J}^2 and J_z in terms of the direct-product states introduced at the beginning of Section 7.1.2. There we argue that if the angular momentum kets come from different Hilbert spaces, then we can combine their products to make coupled eigenstates. Clebsch-Gordan coefficients are introduced in Section 7.2.1, and in Section 7.2.2 their unitarity properties are determined. An explicit formula for the coefficients is derived in Section 7.2.3 by using the spinor representations developed in Section 4.3.3.

7.2.1 Combining Two Angular Momenta: Clebsch-Gordan Coefficients

To introduce the coupling coefficients, we begin at a formal level in terms of the kets (Sections 2.1, 2.3) that are eigenstates of the angular momentum operators. We write the unitary transformation connecting coupled and direct-product representations as

$$\boxed{|j_1 j_2 JM\rangle = \sum_{m_1, m_2} |j_1 j_2 m_1 m_2\rangle \langle j_1 j_2 m_1 m_2 | j_1 j_2 JM\rangle} \quad (7.35)$$

in which, technically, all we have done is to use the unit-operator expansion (2.14) in Section 2.1.2. The ket states are given in direct-product form as

$$|j_1 j_2 m_1 m_2\rangle = |\alpha j_1 m_1\rangle |\beta j_2 m_2\rangle = |j_1 m_1\rangle |j_2 m_2\rangle \quad (7.36)$$

in which the middle form reminds us that the states forming the direct product must be from different Hilbert spaces, as discussed in Section 7.1.2, while the last form is used whenever there is no ambiguity. Note that, at least for this reason, there is a difference between state $|j_1 m_1\rangle |j_2 m_2\rangle$ and state $|j_2 m_2\rangle |j_1 m_1\rangle$.

The coefficients $\langle j_1 j_2 m_1 m_2 | j_1 j_2 JM\rangle$ in (7.35) that give the amplitude for each product state in the combined state are called *Clebsch-Gordan* or *vector-coupling* coefficients. The first name is from use of similar coefficients in linear algebra in the nineteenth century by Clebsch [Cle72] and by Gordan [Gor75]. The second name is from association with the vector model (Section 7.1).

Direct-Product Expansions. In working with angular momentum, you will encounter the expansion (7.35) in various forms, in terms of the summation ranges and the notation for the coefficients. The range of summation over m_1 and m_2 depends somewhat on the properties one decides the coefficients must have. Especially in formal work, one sometimes wants the greatest possible freedom in the summations; then (7.35) can be written explicitly as

$$|j_1 j_2 JM\rangle = \sum_{m_1=-j_1}^{j_1} \sum_{m_2=-j_2}^{j_2} |j_1 m_1\rangle |j_2 m_2\rangle \delta_{m_1+m_2, M} \langle j_1 j_2 m_1 m_2 | j_1 j_2 JM\rangle \quad (7.37)$$

Sometimes the delta function is explicit, or it may be incorporated into the coupling coefficient. Note that M is fixed, as is explicit on the left-hand side.

7.2.2 Unitarity of Clebsch-Gordan Coefficients

We now derive from formal considerations, similar to those discussed for linear

vector spaces in Section 2.1, the unitarity of the Clebsch-Gordan coefficients for angular momentum coupling.

Unitarity J Sum. We know from the Hermitian property of angular momentum operators that the eigenfunctions are orthogonal, and may therefore be chosen to be orthonormal. Since this is true for both subsystem 1 and subsystem 2, it is true for their direct product. Therefore,

$$\begin{aligned} \langle j'_1 j'_2 m'_1 m'_2 | j_1 j_2 m_1 m_2 \rangle \\ = \langle j'_1 m'_1 | j_1 m_1 \rangle \langle j'_2 m'_2 | j_2 m_2 \rangle = \delta_{j'_1 j_1} \delta_{m'_1 m_1} \delta_{j'_2 j_2} \delta_{m'_2 m_2} \end{aligned} \tag{7.38}$$

Most of the time this is applied, you just get the true but interesting result $0 = 0$. However, by matching the j components and then inserting a unit operator expressed in terms of the (J, M) states, we obtain the *J-sum unitarity relation for Clebsch-Gordan coefficients*,

$$\sum_J \langle j_1 j_2 m'_1 m'_2 | j_1 j_2 JM \rangle \langle j_1 j_2 JM | j_1 j_2 m_1 m_2 \rangle = \delta_{m_1 m'_1} \delta_{m_2 m'_2} \tag{7.39}$$

In this there should be a sum over M , but such a sum contributes only one term, namely the term for which

$$m'_1 + m'_2 = M = m_1 + m_2 \tag{7.40}$$

As shown in Section 7.2.3, the coupling coefficients can be (and are) chosen to be real, so the second bra-ket in (7.39) can be flipped; then it becomes just a coupling coefficient. This relation therefore also expresses the *orthonormality* of Clebsch-Gordan coefficients.

Unitarity m-Component Sum. Another unitarity property of Clebsch-Gordan coefficients can be derived by considering the orthogonality of the coupled states $|JM\rangle$. By expanding these in bra and ket states and computing their scalar products in terms of the direct-product states, we obtain similarly to the preceding derivation (as Problem 7.4 suggests you verify) the *m-sum unitarity relation for Clebsch-Gordan coefficients*

$$\sum_{m_1 m_2} \langle j_1 j_2 J' M' | j_1 j_2 m_1 m_2 \rangle \langle j_1 j_2 m_1 m_2 | j_1 j_2 JM \rangle = \delta_{J' J} \delta_{M' M} \tag{7.41}$$

Again, this is a relation that is not of the uninteresting form $0 = 0$. With the use of real coupling coefficients, the first coefficient can be flipped, so we get an orthonormality m sum.

The results in this subsection are about as far as one can get from general considerations. We now derive explicit formulas for the coupling coefficients that enable us to put them to practical use and to find more of their properties.

7.2.3 Determining Coefficients from Spinor Representations

In order to derive formulas for the Clebsch-Gordan coefficients, we use the spinor-space representations of angular momentum states introduced in Section 4.3.3 and used in Section 6.2.3 to construct reduced rotation matrix elements. Our derivation therefore has a conceptual unity between the elementary spin-half states, χ_{\pm} , in Sections 2.4 and 3.3, the finite rotations of a single substate (Chapter 6), and the infinitesimal rotations of coupled states in this chapter. Our final triumph of reason over ignorance (at least for rotational symmetry) will be finite rotations and coupled states (Section 7.5).

Deriving the Coefficients by Using Spinors. We use a method based on that of Sharp [Sha60]. Recall from Section 4.3.3 that a spinor-space representation of angular momentum (j, m) is given by $u(jm)$, where

$$u(jm) = \frac{\chi_+^{j+m} \chi_-^{j-m}}{\sqrt{(j+m)!(j-m)!}} \quad (7.42)$$

This can be visualized (Figure 6.4) as $j+m$ spin-up states of a spin-1/2 system combined with $j-m$ spin-down states. Since in the present application angular dependence is not of immediate interest, we omit the label β in the spinors.

Our goal is to find the Clebsch-Gordan coefficients $\langle j_1 j_2 m_1 m_2 | j_1 j_2 JM \rangle$ such that

$$u(JM) = \sum_{m_1} \sum_{m_2} u(j_1 m_1) u(j_2 m_2) \langle j_1 j_2 m_1 m_2 | j_1 j_2 JM \rangle \quad (7.43)$$

in which each u is of the form (7.42). We first find the stretched- M eigenfunction $u(JJ)$ and its corresponding coefficient directly; then we make repeated applications of the lowering operator J_{-1} to get successively smaller M values. This is the same method as that used for spherical harmonics in Section 4.1.3. Spinor representations of angular momentum operators are discussed in Section 3.3.4. We extend the notation slightly to include the two subsystem spinors, which we denote by $\chi_{1\pm}$ and $\chi_{2\pm}$. Thereby the ladder operators for the combined system are

$$J_{\pm 1} = (\chi_{1\pm} \partial_{1\mp} + \chi_{2\pm} \partial_{2\mp}) \quad (7.44)$$

If we apply the raising operator to the stretched state we must get zero, so that

$$(\chi_{1\pm} \partial_{1\mp} + \chi_{2\pm} \partial_{2\mp}) u(JJ) = 0 \quad (7.45)$$

The solution of this equation is

$$u(JJ) = \phi(\chi_{1-}\chi_{2+} - \chi_{2-}\chi_{1+}, \chi_{1+}, \chi_{2+}) \quad (7.46)$$

where ϕ is any function of the indicated variables. However, $u(JJ)$ is homogeneous and of degree $2j_1$ in $\chi_{1+}\chi_{1-}$ and of degree $2j_2$ in $\chi_{2+}\chi_{2-}$, so it must be expressible in the form

$$u(JJ) = \sum_k (\chi_{1-}\chi_{2+} - \chi_{2-}\chi_{1+})^k \chi_{1+}^{2j_1-k} \chi_{2+}^{2j_2-k} C_k \quad (7.47)$$

in which the C_k are coefficients. By applying J_z, J_{1z}, J_{2z} , in each space, and noting that J_z commutes with the quantity in parentheses in (7.47), we see that $C_k = 0$ unless $k = j_1 + j_2 - J$. Thus, there is only one term in the sum in (7.47), which is therefore given by

$$u(JJ) = (\chi_{1-}\chi_{2+} - \chi_{2-}\chi_{1+})^{j_1+j_2-J} \chi_{1+}^{J+j_1-j_2} \chi_{2+}^{J-j_1+j_2} C \quad (7.48)$$

in terms a single coefficient, C , determined as follows. Expand the right-hand side of (7.47) and collect together terms corresponding to the subsystem eigenfunctions, of the form (7.42). You will then find (especially if you work Problem 7.5) the following expansion:

$$u(JJ) = C \sum_{m_1} (-1)^{j_1-m_1} \frac{\sqrt{(j_1+m_1)(j_2+J-m_1)!}}{\sqrt{(j_1-m_1)(j_2-J+m_1)!}} \times (j_1+j_2-J)! u(j_1 m_1) u(j_2 m_2) \quad (7.49)$$

By staring at this, we recognize that the coefficients of the subsystem states are just the required Clebsch-Gordan coefficients, according to (7.43). They are orthonormal, which enables C and the stretched- M coupling coefficient to be determined.

At this point we introduce the *Condon and Shortley phase convention*, namely that C in (7.49) is chosen to be real and positive. Thereby, all angular momentum coupling coefficients will be real and unitarity relations will become orthonormality relations. With this convention, whose use is worldwide (and probably universal), we find—working out the details in Problem 7.5—that C is given by

$$C = \sqrt{\frac{(2J+1)!}{(J+j_1-j_2)!(J-j_1+j_2)!(j_1+j_2-J)!(J+j_1+j_2+1)!}} \quad (7.50)$$

By factoring this into (7.49) we can identify the Clebsch-Gordan coefficients appropriate for $J = M$. But, let's dash on and derive the general coefficient.

The General Clebsch-Gordan Coefficient. Now that we essentially have the $J = M$ coefficients, we can produce the others by examining the effect of the lowering operator J_{-1} from (7.44) on $u(JJ)$. Applying the operator $J - M$ times produces the state $u(JM)$, whose expression in terms of the desired coupling coefficients is (7.43). After some algebraic sleight of hand that we suggest in Problem 7.5, one obtains the *standard Clebsch-Gordan coefficient* given by

$$\begin{aligned} \langle j_1 j_2 m_1 m_2 | j_1 j_2 JM \rangle &= \delta_{m_1 + m_2, M} \sqrt{2J + 1} \\ &\times \sqrt{\frac{(J + j_1 - j_2)!(J - j_1 + j_2)!(j_1 + j_2 - J)!(J + M)!(J - M)!}{(j_1 + j_2 + J + 1)!(j_1 - m_1)!(j_1 + m_1)!(j_2 - m_2)!(j_2 + m_2)!}} \\ &\times \sum_k \frac{(-1)^{k + j_2 + m_2} (j_2 + J + m_1 - k)!(j_1 - m_1 + k)!}{k!(J - j_1 + j_2 - k)!(J + M - k)!(k + j_1 - j_2 - M)!} \end{aligned} \quad (7.51)$$

The summation over k is over all integers for which the factorials are non-negative. We need immediately two special values for this coupling coefficient.

Clebsch-Gordan Coefficient for $j_2 = 0$. As one would hope, when the second angular momentum is zero, the triangle rule (7.6) and the vector-addition model (Section 7.1.1) both require that $J = j_1$ only, thence $M = m_1$. On substituting these values in the general formula (7.51), we obtain

$$\langle j_1 0 m_1 0 | j_1 0 J m_1 \rangle = 1 \quad (7.52)$$

a result consistent with the orthonormality condition (7.41), since there is only one term in the sum.

Clebsch-Gordan Coefficient for $J = 0$. Suppose that $J = 0$, which is possible, according to both the triangle rule (7.6) and the vector-addition model Figure 7.2, only if $j_2 = j_1$ and $m_2 = -m_1$. By substitution in the general formula (7.51), we find that only the $k = 0$ term survives in the sum, and we have

$$\langle j_1 j_1 m_1, -m_1 | j_1 j_1 0 0 \rangle = \frac{(-1)^{j_1 - m_1}}{\sqrt{2j_1 + 1}} \quad (7.53)$$

This gives a probability for this “antiparallel” coupling arrangement as just the reciprocal of the number of magnetic substates, $2j_1 + 1$, in the state with total angular momentum number j_1 .

Although use of the Clebsch-Gordan coefficients is quite common, a much more symmetrical form of the coupling coefficient is the 3- j coefficient, to which we now turn our attention.

7.3 THE 3-*j* COEFFICIENTS AND THEIR PROPERTIES

In our considerations of combining two angular momentum eigenstates, we have so far treated in a special way the third angular momentum, (J, M) . A more symmetric treatment in terms of 3-*j* coefficients considers the three angular momenta on equal terms. In Section 7.3.1 we derive the origin of the 3-*j* coefficients, we express them in terms of Clebsch-Gordan coefficients, and we write out analogous properties. Various ways of visualizing symmetry properties are presented in Section 7.3.2. As a diversion from heavy algebra and to help with interpretation, we discuss in Section 7.3.3 the classical limits of the coefficients. When one of the angular momenta in a coefficient is small, there are convenient algebraic expressions, a sampling of which is given in Section 7.3.4.

A Note on Symbols. So far, we have used the label j with various subscripts to refer to total angular momentum numbers and m with subscripts to indicate projection numbers. We continue this practice whenever angular momentum and rotational properties are being emphasized. On the other hand, for algebraic properties of coefficients, it is easier (for typesetters as well as readers) to use unsubscripted variables, such as a, b, c . Their projection quantum numbers are the corresponding Greek letters, such as α, β, γ .

7.3.1 Three Angular Momenta Coupled to Zero; 3-*j* Coefficients

Suppose that we combine two angular momentum states, j_1 and j_2 , to form a third, $(j_3, -m_3)$, then we combine this state with one of the same j_3 but opposite z projection, m_3 , so that now the total projection is zero. Let us also couple to the jack-knife state with total $j = 0$. We now have an isotropic quantity—a scalar—formed by coupling three angular momenta to zero. The corresponding coupling coefficient was invented by Wigner and is called a 3-*j* coefficient. Its symmetries under permutation of arguments are simpler than those of the Clebsch-Gordan coefficient.

*Deriving the 3-*j* Coefficient.* To derive the 3-*j* coefficient, let us perform the algebra of the angular momentum coupling described in the preceding paragraph. The first combination is

$$|(j_1 j_2) j_3, -m_3\rangle = \sum_{m_1, m_2} |j_1 m_1\rangle |j_2 m_2\rangle \langle j_1 j_2 m_1 m_2 | j_1 j_2 j_3, -m_3\rangle \quad (7.54)$$

The second combination, which produces state $(0, 0)$, is

$$|(j_1 j_2 j_3) 00\rangle = \sum_{m_3} |(j_1 j_2) j_3, -m_3\rangle |j_3 m_3\rangle \langle j_3 j_3, -m_3 m_3 | j_3 j_3 00\rangle \quad (7.55)$$

The needed coefficient is obtained from (7.53) as $(-1)^{j_3-m_3}/\sqrt{2j_3+1}$. If we now use this in (7.55) and combine with (7.54), we obtain the expression for three angular momenta coupled to zero, namely

$$|(j_1 j_2 j_3)00\rangle \propto \sum_{m_1, m_2, m_3} |j_1 m_1\rangle |j_2 m_2\rangle |j_3 m_3\rangle \begin{pmatrix} j_1 & j_2 & j_3 \\ m_1 & m_2 & m_3 \end{pmatrix} \quad (7.56)$$

in which the proportionality constant is just a phase. We have introduced the coefficient describing the combining of three angular momenta to zero, called Wigner's 3-*j* coefficient

$$\begin{pmatrix} j_1 & j_2 & j_3 \\ m_1 & m_2 & m_3 \end{pmatrix} \equiv (-1)^{j_1-j_2-m_3} \frac{\langle j_1 j_2 m_1 m_2 | j_1 j_2 j_3, -m_3 \rangle}{\sqrt{2j_3+1}} \quad (7.57)$$

The 3-*j* coefficient is zero unless

$$m_1 + m_2 + m_3 = 0 \quad (7.58)$$

and the triangle conditions (7.6) must also be satisfied.

By inserting formula (7.51) for the Clebsch-Gordan coefficient into (7.57), we obtain immediately a formula for the 3-*j* coefficient:

$$\begin{pmatrix} j_1 & j_2 & j_3 \\ m_1 & m_2 & m_3 \end{pmatrix} = \delta_{m_1+m_2+m_3,0} (-1)^{j_1-j_2-m_3} \times \sqrt{\frac{(j_3+j_1-j_2)!(j_3-j_1+j_2)!(j_1+j_2-j_3)!(j_3-m_3)!(j_3+m_3)!}{(j_1+j_2+j_3+1)!(j_1-m_1)!(j_1+m_1)!(j_2-m_2)!(j_2+m_2)!}} \times \sum_k \frac{(-1)^{k+j_2+m_2} (j_2+j_3+m_1-k)!(j_1-m_1+k)!}{k!(j_3-j_1+j_2-k)!(j_3-m_3-k)!(k+j_1-j_2+m_3)!} \quad (7.59)$$

From this formula we can derive various properties of the 3-*j* coefficient.

*Basic Formulas in 3-*j* Notation.* We now write down the basic formulas for combining two angular momenta using 3-*j* notation, since subsequent formulas will usually be given in this form. In 3-*j* notation the basic direct-product expansion (7.35) is expressed by

$$\begin{aligned}
 |j_1 j_2 JM\rangle &= \sum_{m_1=-j_1}^{j_1} \sum_{m_2=-j_2}^{j_2} |j_1 m_1\rangle |j_2 m_2\rangle \delta_{m_1+m_2, M} \\
 &\times (-1)^{j_1-j_2+M} \sqrt{2J+1} \begin{pmatrix} j_1 & j_2 & J \\ m_1 & m_2 & -M \end{pmatrix}
 \end{aligned} \tag{7.60}$$

Although this expression is initially more cumbersome than the Clebsch-Gordan expression (7.35), the greater symmetry of the 3- j coefficient makes it eventually more convenient.

The unitarity J sum is obtained by combining (7.39) and (7.57) as

$$\sum_{j_3} (2j_3+1) \begin{pmatrix} j_1 & j_2 & j_3 \\ m'_1 & m'_2 & m_3 \end{pmatrix} \begin{pmatrix} j_1 & j_2 & j_3 \\ m_1 & m_2 & m_3 \end{pmatrix} = \delta_{m_1 m'_1} \delta_{m_2 m'_2} \delta_{m_1+m_2, -m_3} \tag{7.61}$$

The unitarity m sum corresponding to (7.41) is

$$\sum_{m_1, m_2} (2j_3+1) \begin{pmatrix} j_1 & j_2 & j'_3 \\ m_1 & m_2 & m'_3 \end{pmatrix} \begin{pmatrix} j_1 & j_2 & j_3 \\ m_1 & m_2 & m_3 \end{pmatrix} = \delta_{j'_3 j_3} \delta_{m_3 m'_3} \tag{7.62}$$

Thus, in both J sum and m sum, the 3- j coefficient orthogonality conditions require weight factors of $2j_3+1$.

When one of the angular momenta in a 3- j coefficient is zero, say the first one, then we have the analogue of (7.53), which is

$$\begin{pmatrix} j_1 & 0 & j_3 \\ m_1 & 0 & m_3 \end{pmatrix} = \delta_{j_1 j_3} \delta_{m_1, -m_3} \frac{(-1)^{j_1-m_1}}{\sqrt{2j_1+1}} \tag{7.63}$$

Again, this is more complicated than the Clebsch-Gordan coefficient relation, but is simpler under exchange of j_1 and j_3 .

Comparing 3- j and Clebsch-Gordan Coefficients. To visualize the differences between the two coupling coefficients, apart from the algebraic relation (7.57), it is helpful to draw the semiclassical vector model (Section 7.1) for the respective combinations of angular momenta, as shown in Figure 7.5.

Given the claim that coupling to zero total angular momentum produces the 3- j coefficient that is more symmetric than the Clebsch-Gordan coefficient, we should derive symmetry properties of the 3- j coefficient.

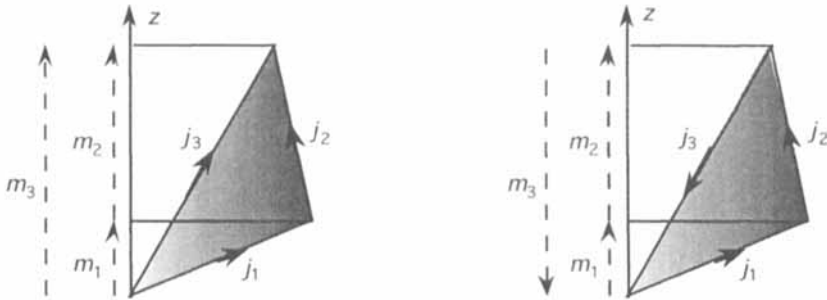


FIGURE 7.5 Visualizing the distinction between a Clebsch-Gordan coefficient (left) and a 3- j coefficient (right). Note particularly the reversed directions of the \mathbf{j}_3 and m_3 arrows between left and right and that the m -sum rules are different between the two coefficients.

Symmetries Under J Permutation and Projection Sign Change. Four symmetry properties of the 3- j coefficients that we now derive provide the greatest advantage of these coefficients over Clebsch-Gordan coefficients. First, by substituting in formula (7.59) for the 3- j coefficient $k' = k - j_1 + j_2 + m_1 + m_2$, then rearranging the summation, it can be seen directly (as Problem 7.6 suggests you verify) that

$$\begin{pmatrix} j_2 & j_1 & j_3 \\ -m_2 & -m_1 & -m_3 \end{pmatrix} = \begin{pmatrix} j_1 & j_2 & j_3 \\ m_1 & m_2 & m_3 \end{pmatrix} \quad (7.64)$$

The second symmetry property that can be derived similarly is

$$\begin{pmatrix} j_1 & j_3 & j_2 \\ m_1 & m_3 & m_2 \end{pmatrix} = (-1)^{j_1+j_2+j_3} \begin{pmatrix} j_1 & j_2 & j_3 \\ m_1 & m_2 & m_3 \end{pmatrix} \quad (7.65)$$

Third, by substituting in (7.59) $k' = j_2 + j_3 - j_1 - k$ and rearranging the sum, the diligent reader will verify that

$$\begin{pmatrix} j_1 & j_2 & j_3 \\ -m_1 & -m_2 & -m_3 \end{pmatrix} = (-1)^{j_1+j_2+j_3} \begin{pmatrix} j_1 & j_2 & j_3 \\ m_1 & m_2 & m_3 \end{pmatrix} \quad (7.66)$$

Besides being useful for manipulating expressions containing 3- j coefficients, this result will be used for coupling coefficients with all projections zero.

The fourth symmetry relation is obtained by combining (7.65) and (7.66). It is

$$\begin{pmatrix} j_2 & j_1 & j_3 \\ m_2 & m_1 & m_3 \end{pmatrix} = (-1)^{j_1+j_2+j_3} \begin{pmatrix} j_1 & j_2 & j_3 \\ m_1 & m_2 & m_3 \end{pmatrix} \quad (7.67)$$

This symmetry and (7.66) give the general symmetry condition for permutation of columns of a 3- j coefficient:

Even permutations of columns of a 3- j coefficient leave it unchanged.

Odd permutations of columns of a 3- j coefficient produce a phase change of $(-1)^{j_1+j_2+j_3}$.

(7.68)

The Order of Combining Angular Momenta is Significant. You might expect that the order of coupling, whether $|(j_1 j_2)JM\rangle$ or $|(j_2 j_1)JM\rangle$, should be unimportant. There is, however, often a difference. Problem 7.7 suggests that you use the permutation property (7.67) to show that

$$|(j_2 j_1)JM\rangle = (-1)^{j_1+j_2-J} |(j_1 j_2)JM\rangle \quad (7.69)$$

Therefore, *the order of combining two angular momenta is significant*, since interchanging the coupling order may produce a change of phase, dependent upon both the uncoupled and coupled total angular momenta. For example, suppose that we combine orbital (ℓ) and spin (s) eigenkets to form a total angular momentum (J). For the stretched and jackknife cases, respectively, we have

$$\begin{aligned} |(s\ell)J=\ell+s, M\rangle &= |(\ell s)J=\ell+s, M\rangle \\ |(s\ell)J=|\ell-s|, M\rangle &= (-1)^{2\min(\ell,s)} |(\ell s)J=|\ell-s|, M\rangle \end{aligned} \quad (7.70)$$

Therefore, for $s = 1/2$ (nucleons or electrons) the jackknife state does not change sign under interchanging the coupling order if $\ell = 0$, but it changes sign for all higher ℓ values.

Matrix elements of operators are also sensitive to the order of combining two angular momenta. For example, consider an operator O between states of the same J , but possibly different orbital angular momenta ℓ_1 and ℓ_2 . By using (7.69), we see immediately that

$$\langle (s\ell_1)JM' | O | (s\ell_2)JM \rangle = (-1)^{\ell_1-\ell_2} \langle (\ell_1 s)JM' | O | (\ell_2 s)JM \rangle \quad (7.71)$$

The effect of such a change of phase can be particularly confusing, since a similar

phase change in the matrix elements, namely $(-1)^{\ell_1 - \ell_2} \pi_O$ with π_O the parity of operator O , occurs under the parity operation. Changes of phase arising from reordering the coupling are no problem if one has a *consistent* order of coupling throughout a calculation. In big calculations, however, different parts of it may be done by different scientists without maintaining such consistency, especially within large computer programs. Thereby, spurious effects mimicking parity operations are easily introduced. When combining two angular momenta, the recoupling phase is mostly a nuisance. With three or more angular momenta, recoupling is a much more challenging problem, to which we devote Chapter 9.

Couplings with All Projections Zero. If a 3- j coefficient has all its magnetic substate projections (the bottom line) equal to zero then the general expression (7.59) collapses to a particularly simple form. First, the rule for change of sign of all m values, (7.66), produces the identical coupling coefficient if the m values are zero. Therefore, it must be that

$$\boxed{\begin{pmatrix} a & b & c \\ 0 & 0 & 0 \end{pmatrix} = 0 \quad a + b + c \text{ odd}} \quad (7.72)$$

This restriction on the nonzero coefficients reduces their number for given a and b from the usual $2 \min(a, b) + 1$ to $\min(a, b) + 1$, a result which Problem 7.8 suggests you prove. Included with the nonzero values are the jackknife case $c = |b - a|$ and the stretched case $c = a + b$.

Condition (7.72) on the coupling coefficient arguments leads to the term “parity-conservation” coupling coefficient, because this coefficient often appears as a factor in an amplitude related to parity conservation in a system. However, it is connected more with *rotational* symmetry than with *reflection* symmetry (Sections 1.2.1, 1.4.3). The connection of this coefficient with parity is that under $z \rightarrow -z$ we have $m \rightarrow -m$, so if $m = 0$ the coefficient is unchanged. One consequence of this condition is that rotational symmetry supersedes parity symmetry. Thereby, the simplest designs of experiments that aim to test parity conservation may often just be expensive ways of verifying the correctness of (7.72).

For the nonzero coefficients, by simplifying (7.59) for $a + b + c$ even, we have

$$\boxed{\begin{pmatrix} a & b & c \\ 0 & 0 & 0 \end{pmatrix} = (-1)^g \frac{g!}{(g-a)!(g-b)!(g-c)!} \times \sqrt{\frac{(2g-2a)!(2g-2b)!(2g-2c)!}{(2g+1)!}}}$$
(7.73)

in which $g = (a + b + c)/2$ is an integer. These 3- j coefficients with all projections zero occur so commonly in practical applications that it is worthwhile to tabulate their values for low values of angular momentum, as in Table 7.2.

TABLE 7.2 Squares of the nonzero 3-j coefficients $\begin{pmatrix} a & b & c \\ 0 & 0 & 0 \end{pmatrix}$ for which the two smallest angular momenta do not exceed 3. An asterisk indicates that the coefficient is negative. These can be computed by using *Mathematica* notebooks Num3j or 3j000.

a	b	c		a	b	c	
0	1	1	* 1/3	2	2	2	* 2/35
0	2	2	1/5	2	2	4	2/35
0	3	3	* 1/7	2	3	3	4/105
1	1	2	2/15	2	3	5	* 10/231
1	2	3	* 3/35	3	3	4	* 2/77
1	3	4	4/63	3	3	6	100/3003

As an example of using Table 7.2, we find $\begin{pmatrix} 1 & 2 & 3 \\ 0 & 0 & 0 \end{pmatrix} = -\sqrt{3/35} \approx -0.292770$. Any permutation of a, b, c , will produce the same coefficient. In Section 7.3.2 we present visualizations of these coefficients.

A Worked Example: Combining Spin and Orbital States. In Section 7.1.3 we discuss spin-orbit terms in a Hamiltonian and consequent spin-orbit splitting of energy levels in atoms and nuclei. Now that we have the techniques for combining two angular momentum states, it is interesting to combine spin and orbital states. We do this for the simplest case, $s = 1/2$, which is the most common case for atoms and nuclei. Introduce *combined spin and orbital states* as

$$Y_{\ell JM} \equiv \langle (\theta\phi) | (\ell 1/2) JM \rangle \quad (7.74)$$

with the understanding that spin states are expressed as χ_{\pm} , as in Section 3.3.4. By calculating the appropriate coupling coefficients from (7.59), or looking ahead to Table 7.3, it is then straightforward to derive (as Problem 7.9 suggests you do) the expressions for combined states:

$$\begin{aligned}
 & Y_{\ell, \ell+1/2, M} \\
 &= \sqrt{\frac{\ell - M + 1/2}{2\ell + 1}} Y_{\ell, M+1/2}(\theta\phi) \chi_{-} + \sqrt{\frac{\ell + M + 1/2}{2\ell + 1}} Y_{\ell, M-1/2}(\theta\phi) \chi_{+} \\
 & Y_{\ell, \ell-1/2, M} \\
 &= \sqrt{\frac{\ell + M + 1/2}{2\ell + 1}} Y_{\ell, M+1/2}(\theta\phi) \chi_{-} - \sqrt{\frac{\ell - M + 1/2}{2\ell + 1}} Y_{\ell, M-1/2}(\theta\phi) \chi_{+}
 \end{aligned} \quad (7.75)$$

Here it is assumed that the spherical harmonic $Y_{\ell m}(\theta\phi)$ vanishes if $|m| > \ell$.

For $\ell = 0$ the combined states are particularly simple, as one expects:

$$Y_{0,1/2,-1/2} = \chi_- \quad Y_{0,1/2,1/2} = \chi_+ \quad (7.76)$$

and jackknife states vanish. For any ℓ , the substates with $M = \ell + 1/2$ similarly contain only χ_+ and states with $M = -\ell - 1/2$ contain only the χ_- . In accord with the vector-addition construction (Section 7.1.1), for $M > 0$ the χ_+ state has the larger amplitude for $J = \ell + 1/2$, as does the χ_- state for $J = \ell - 1/2$. Notice the orthonormal nature of the combination of angular momenta in (7.75); if we set $\sin \xi = \sqrt{(\ell - M + 1/2)/(2\ell + 1)}$, we have a 2×2 matrix of rotation through ξ .

By construction, the combined “spin-orbit-coupled” states (7.75) are eigenfunctions of the Hamiltonian with spin-orbit coupling given by (7.8). Consequently, they are very useful for constructing wave functions with maximum rotational symmetry. We may use such combined states with or without a spin-orbit interaction.

7.3.2 Visualizing Symmetry Properties

Combination of angular momenta is often presented completely algebraically—a torment to tyros and a delight to experts. Interpreting the coupling in geometric and graphic terms can, however, often improve understanding of it. To visualize properties of 3- j coefficients, including the parity and j -permutation symmetries, it is appropriate to make two-dimensional graphics for various quantum numbers.

The simplest example is for the coupling $\mathbf{j} + \mathbf{j} = \mathbf{J}$, with each \mathbf{j} having the same projection m , so that \mathbf{J} has projection $2m$. This would be the combination for two equivalent electrons or nucleons in the same atomic or nuclear shell. A special case of the vector-addition construction Figure 7.2 is sketched in Figure 7.6.

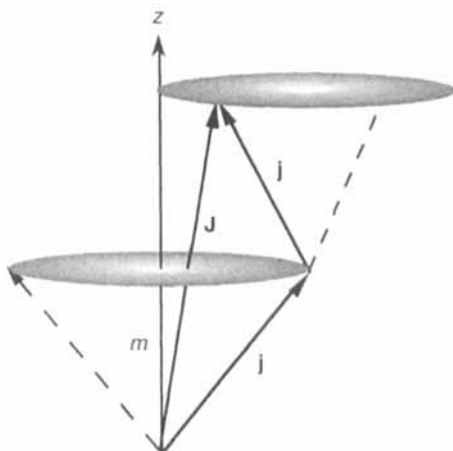


FIGURE 7.6 Vector-addition model for the coupling scheme $\mathbf{j} + \mathbf{j} = \mathbf{J}$ with both \mathbf{j} vectors having projection m . Their resultant is \mathbf{J} with projection $2m$.

The corresponding probability density for such a coupling is

$$\rho(J, m) = (2J + 1) \begin{pmatrix} j & j & J \\ m & m & -2m \end{pmatrix}^2 = \left(\langle j j m m | j j J 2m \rangle \right)^2 \quad (7.77)$$

which we may consider as a function of the coupled angular momentum J , with $0 \leq J \leq 2j$, and of m , with $-j \leq m \leq j$ and $-J \leq 2m \leq J$.

Figure 7.7 shows $\rho(J, m)$ on a gray-scale density plot for three values of j , two of which are small ($3/2$ and 2) and the third is semiclassical in the sense discussed in Section 6.4.3, namely $j = 6$. Clearly—as shown by the reflection symmetry about the midline of m —the probability density is independent of the sign of m . Because of the permutation symmetry (7.67) for the identical j values in (7.77), the coefficients and the densities are zero for $2j + J$ odd. To understand the pattern of increasing probability density in Figure 7.7 as m tends to $J/2$, note that this is the most favorable arrangement according to the vector-addition model sketched in Figure 7.6.

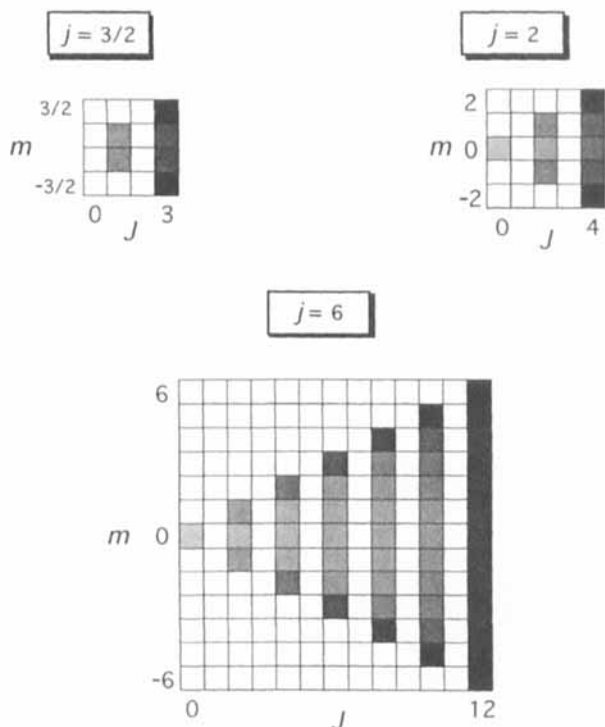


FIGURE 7.7 Density distributions $\rho(J, m)$ as a function of coupled angular momentum J and component (j) projection m , for $j = 3/2$, 2 , and 6 . Zero density is shown white, unity density is black, and intermediate densities are shades of gray. (Adapted from the *Mathematica* notebook *VccDnsty*.)

Coupling with All Projections Zero. It is interesting to plot the vector-addition diagrams for the special coupling coefficients with all projections on the z axis being zero. Formulas for these coefficients are derived in Section 7.3.1.

Since each angular momentum projection is zero, the diagrams correspond to the vectors lying in the x - y plane. The example shown in Figure 7.8 has $a = 2$, $b = 4$. The vector-addition triangles are drawn to scale for the nonzero 3 - j coefficients, whose values are given to the right of the triangles. There are $3 = \min(2, 4) + 1$ nonzero values, and two zero values—for $c = 3$ and $c = 5$. Both for $c = 2$ (the jack-knife case) and for $c = 4$ (the stretched case) the triangles have collapsed to lines. In the vector-addition model (Section 7.1.1) there is no explanation of why the coefficients for $c = 3$ and $c = 5$ vanish. Further exploration of these “parity conservation” 3 - j coefficients is suggested as Problem 7.8.

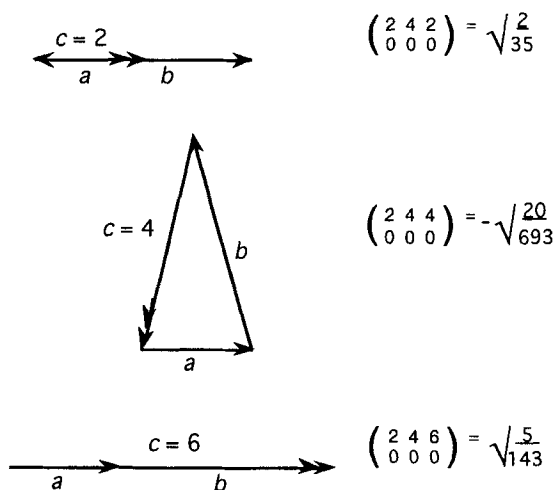


FIGURE 7.8 Coupling coefficients when all m values are zero. Here $a = 2$, $b = 4$, so the coefficients vanish when $c = 3$ or 5 , according to (7.72). (Coefficients evaluated using *Mathematica* notebook 3j000.)

7.3.3 Classical Limits of 3 - j Coefficients

Classical limits of rotation matrix elements (Section 6.4.3) provide further insight into their properties. Similarly, by considering the classical limits of 3 - j coefficients, we understand more about combining angular momenta. We combine the vector-addition construction (Section 7.1) with three angular momenta coupled to zero to discuss the behavior of 3 - j coefficients as their component angular momenta increase. Figure 7.9 repeats the construction shown in Figure 7.2, but it has more labeling because we want a quantitative interpretation.

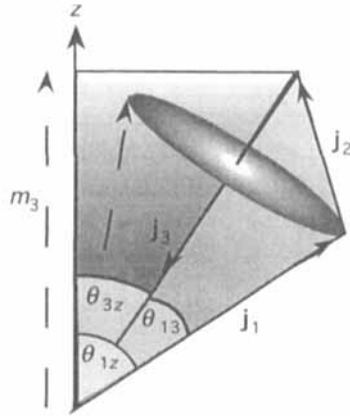


FIGURE 7.9 Vector-addition diagram for classical limits of 3- j coefficients. The projection of \mathbf{j}_3 onto the quantization axis, m_3 , is fixed, but the projections of \mathbf{j}_1 and \mathbf{j}_2 are variable, corresponding to different tilts and radii of their precession circles about \mathbf{j}_3 .

To quantify the discussion of the 3- j coefficients described by Figure 7.9, consider the interpretation of the quantity $P(m_1)$ given by

$$P(m_1) = \left| \langle j_1 j_2, m_1 m_2 | j_1 j_2 j_3 m_3 \rangle \right|^2 = (2j_3 + 1) \left| \begin{pmatrix} j_1 & j_2 & j_3 \\ m_1 & m_2 & m_3 \end{pmatrix} \right|^2 \quad (7.78)$$

which is the probability that the angular momentum projection on the z axis is m_1 , given that j_3 has projection m_3 , with the condition $m_1 + m_2 + m_3 = 0$ assumed. In the vector-addition model \mathbf{j}_3 has a uniform distribution around z , so this does not affect $P(m_1)$. We can therefore take the \mathbf{j}_3 - z plane in Figure 7.9 as the plane of the page. The plane \mathbf{j}_1 - \mathbf{j}_3 then makes an angle ϕ with this plane, and (corresponding to uniform precession) ϕ will have a uniform probability distribution P_ϕ . Since we may write by a change of variables $|P(m_1) dm_1| = |P_\phi d\phi|$, we have

$$P(m_1) \propto 1 \left| \frac{dm_1}{d\phi} \right| \quad (7.79)$$

From the trigonometry of the triangles in Figure 7.9 we can write

$$m_1 = j_1 \cos \theta_{1z} = j_1 (\cos \theta_{13} \cos \theta_{3z} + \sin \theta_{13} \sin \theta_{3z} \cos \phi) \quad (7.80)$$

thence we have

$$\left| \frac{dm_1}{d\phi} \right| = | -j_1 \sin \theta_{13} \sin \theta_{3z} \sin \phi | = | \mathbf{j}_1 \times \mathbf{j}_2 \cdot \hat{\mathbf{n}}_z | / | \mathbf{j}_3 | \quad (7.81)$$

The numerator in the last equality is just the area of the triangle formed by the three vectors projected onto the x - y plane, $\Delta(\mathbf{j}_1, \mathbf{j}_2, \mathbf{j}_3)$. By inserting this result in (7.81), we have

$$\left| \begin{pmatrix} j_1 & j_2 & j_3 \\ m_1 & m_2 & m_3 \end{pmatrix} \right|^2 = \frac{P(m_1)}{(2j_3 + 1)} \propto \frac{\sqrt{j_3(j_3 + 1)}}{(2j_3 + 1)\Delta(\mathbf{j}_1, \mathbf{j}_2, \mathbf{j}_3)} \approx \frac{1}{2\Delta(\mathbf{j}_1, \mathbf{j}_2, \mathbf{j}_3)} \quad (7.82)$$

in which the approximation holds with increasing accuracy as j_3 increases. Thus, we see that the semiclassical limit of the 3- j coefficient is a coupling invariant that depends upon the area of the coupling triangle—and is independent of the order of coupling.

In other presentations of this topic, for example Topic 9 in [Bie81b], the time variable is introduced in order to reinforce the analogy with the dynamical angular momentum aspect. In the development, however, this variable plays no role, as our treatment makes clear. The present treatment emphasizes the geometric (rotational symmetry) aspects of angular momentum. The distinction between geometrical and dynamical angular momentum is emphasized in Section 3.4.5.

The discussion given here for the 3- j coefficients can be extended to that for recouplings among three angular momenta (the 6- j coefficients, Chapter 9). Results with a similar interpretation can then be derived, as described in [Bie81b].

7.3.4 Expressions for One Angular Momentum Small

In Section 7.3.1 symmetry properties of the 3- j coefficient are derived. They may be used to put the smallest angular momentum into the first position. If this angular momentum is small, say less than 2, an algebraic expression for the coefficient may be practicable. Table 7.3 lists 3- j coefficients for this angular momentum ≤ 1 . It is much faster to evaluate particular algebraic expressions, as in Table 7.3, than to use general formula (7.59) for the coefficient.

7.4 COMPUTING COUPLING COEFFICIENTS

During the first 40 years of applied quantum mechanics—the major field in which coupling coefficients are used—it was usual to do as much as possible of a calculation analytically with pencil and paper, and only then to use numerical calculations. With the burgeoning availability of powerful, convenient, and modest-sized computers, the emphasis switched to performing more of the calculations by computer. We therefore describe methods of computing coupling coefficients by computer, either analytically (symbolic expressions) or numerically.

We begin by mentioning tabulations of coupling coefficients, whose main use nowadays is for pilot calculations and—in conjunction with the algebraic expressions given in Section 7.3.4—for checking computer programs. Regge symmetries

TABLE 7.3 The 3- j coefficients with the smallest angular momentum, s , less than or equal to 1. Related coefficients can be obtained by permutation of columns and sign changes of row elements. Note that a must be non-negative and $|\alpha| \leq a$; otherwise, the formulas do not apply. Coefficients are calculated by using the *Mathematica* notebook `Alg3j`.

$$\begin{pmatrix} 0 & a & a \\ 0 & \alpha & -\alpha \end{pmatrix} = (-1)^{a-\alpha} \frac{1}{\sqrt{1+2a}}$$

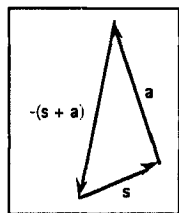
$$\begin{pmatrix} 1/2 & a & a+1/2 \\ 1/2 & \alpha & -1/2-\alpha \end{pmatrix} = (-1)^{1-a+\alpha} \sqrt{\frac{1+a+\alpha}{2(1+a)(1+2a)}}$$

$$\begin{pmatrix} 1 & a & a \\ 1 & \alpha & -1-\alpha \end{pmatrix} = \sqrt{\frac{(a-\alpha)(1+a+\alpha)}{2a(1+a)(1+2a)}}$$

$$\begin{pmatrix} 1 & a & a \\ 0 & \alpha & -\alpha \end{pmatrix} = (-1)^{a-\alpha} \frac{\alpha}{\sqrt{a(1+a)(1+2a)}}$$

$$\begin{pmatrix} 1 & a & a+1 \\ 1 & \alpha & -\alpha-1 \end{pmatrix} = (-1)^{a-\alpha} \sqrt{\frac{(a+\alpha+1)(a+\alpha+2)}{(2a+1)(2a+2)(2a+3)}}$$

$$\begin{pmatrix} 1 & a & a+1 \\ 0 & \alpha & -\alpha \end{pmatrix} = (-1)^{1-a+\alpha} \sqrt{\frac{(1+a-\alpha)(1+a+\alpha)}{(1+a)(1+2a)(3+2a)}}$$



presented in Section 7.4.2 often greatly speed up practical numerical calculations. Also in this section, we discuss methods for computing 3- j coefficients efficiently, including the use of rational fractions and prime factor representations in addition to conventional decimal representations.

7.4.1 Tabulations of Coupling Coefficients

The 3- j and Clebsch-Gordan coefficients have five arguments—the three angular momenta and the two independent projections. By using the triangle and m -selection rules (Section 7.1.2), it is straightforward to show (as Problem 7.10 suggests you verify) that for given j_1 and j_2 the number of coefficients for combining two angular momenta is $N_3(j_1, j_2) = (2j_1 + 1)(2j_2 + 1)[2 \min(j_1, j_2) + 1]$. For example, when $j_1 = j_2$ this number is $N_3(j_1, j_1) = (2j_1 + 1)^3$, which is 343 even for $j_1 = 3$. Although permutation and parity symmetries derived in Section 7.3.1 can be used to

reduce N_3 by nearly a factor of four, the number of table entries is still often formidable. There are two types of tables, algebraic and numerical.

Algebraic Tables. For algebraic tabulations of coupling coefficients, in addition to Table 7.3 for the smallest angular momentum less than or equal to unity, extensive tables of algebraic expressions for Clebsch-Gordan coefficients are available in [Bie81a] and in the angular momentum handbook by Varshalovich and coworkers [Var88].

Numerical Tables. The most widely available numerical tables of 3- j coefficients are those by Rotenberg et al. [Rot59]. Their use requires that the arguments of the coefficient be permuted to a specific order, then the coefficient is given in a prime-exponent notation described in Section 7.4.2. An advantage of this notation is that the squares of the coefficients are exact rational fractions. For all m values equal to zero, the tabulation has a largest j value of 16. For other m values the largest j value is 8. These tables were calculated by computer and their typesetting was done directly from the computer output. Therefore, the chance of errors in the Rotenberg tables is miniscule, unlike other published tables produced by hand calculation and manual typesetting.

Since the number of table entries for combining two angular momenta scales as the cube of the angular momenta, such printed tabulations rapidly become impracticable. Also, even for modest angular momentum values, in a computer program which uses angular momentum coupling as part of a much larger calculation, such table lookup (in either algebraic or numerical form) is often inefficient of programming effort, although it may be efficient in terms of computer time.

7.4.2 Computing 3- j Coefficients Efficiently

We discuss computing 3- j coefficients efficiently in some detail because many of the ideas are applicable to computing 6- j coefficients (Section 9.3.3) and 9- j coefficients (Section 9.5.1). In numerical work one may need either exact numerical expressions or decimal approximations. The former are most useful in theoretical analyses, while the latter are sufficient for analyzing experiments because the coefficients are usually combined with data of varying reliability. Programming of formulas for coupling coefficients is usually quite intricate, so we outline various possibilities, then direct you to references and sources of programs, such as our C-language program in Appendix II.

Regge Symmetries and 3- j Coefficients. In 1958, Regge [Reg58] discovered an unexpected type of symmetry of 3- j coefficients. There are 12 symmetries that we derive in Section 7.3.1, arising from 6 permutations among the three angular momenta and the sign change of the projections. Regge found a total of 72 symmetries of the coefficients, as we now summarize. Make the following correspondence between a 3- j coefficient and its "Regge symbol" R , given by

$$\begin{pmatrix} a & b & c \\ \alpha & \beta & \gamma \end{pmatrix} \sim R \begin{vmatrix} b+c-a & c+a-b & a+b-c \\ a-\alpha & b-\beta & c-\gamma \\ a+\alpha & b+\beta & c+\gamma \end{vmatrix} \quad (7.83)$$

Regge showed—and Bargmann later gave a more elegant proof [Bar62]—that the symmetries of R are similar to those of a determinant, in the sense that interchange of two rows or two columns produces a phase change $(-1)^{a+b+c}$. Further, rows and columns may be interchanged. The Regge symmetries may be used to combine angular momenta in the 3 - j coefficients to obtain parameters that are as small as possible, then permutation symmetries of the 3 - j coefficients (Section 7.3.1) allow the smallest parameter to be moved to a specific location within the coefficient in order to minimize the number of terms in the sum (7.59).

Coupling Coefficients by Computer Algebra. If the smallest angular momentum exceeds unity, so that Table 7.3 is not applicable, a symbolic-manipulation program—such as in the *Mathematica* notebook Alg3j in Appendix I—can be used to compute 3 - j (or Clebsch-Gordan) coefficients in either algebraic or exact rational fraction forms, as suggested in Problem 7.11. This is a general procedure, limited only by computer memory and computation time.

Algebraic forms are especially useful for generating expressions to be coded in a programming language such as C or Fortran, because conversion to coding statements may be done directly by using *Mathematica* functions CForm or FortranForm. Algebraic expressions for coupling coefficients are also useful for identifying errors in published algebraic or numerical tables, such as those described in Section 7.4.1.

Rational-Fraction and Prime-Factor Methods. Sometimes we need exact coupling coefficients. For example, when designing symmetry-violation experiments the symmetry-violating interactions lead to differences on the order of parts per million in observables, since the latter are dominated by symmetry-conserving interactions. One needs to be sure that roundoff in computing coupling coefficients does not simulate a symmetry-violation effect. The disadvantages of requiring exact coefficients are programming that is more complicated, and longer computing time.

Angular momentum coupling coefficients can be expressed exactly, since the square of each coefficient is rational, as (7.59) shows explicitly. Further, since any rational number can be specified by two integers and every positive integer has a unique factorization into primes, one can express a coupling coefficient in terms of prime factors and a phase of ± 1 . Computationally, this approach can be implemented by using primes and representing the coefficient by an array containing its phase and exponents of its prime factors. For example, consider the 3 - j coefficient

$$\begin{pmatrix} 2 & 2 & 2 \\ 1 & 1 & -2 \end{pmatrix} = -\sqrt{\frac{3}{35}} \quad (7.84)$$

Given that $3/35 = 3^1 5^{-1} 7^{-1}$, this coupling coefficient can be represented by an array $(-1, 0, 1, -1, -1, \dots)$, in which the initial -1 indicates the sign of the coefficient, the next four elements are the prime exponents in the square of the coefficient, and all elements in the ellipsis are zero. A similar representation is used in the computer-generated tables of Rotenberg et al. [Rot59].

Programming rational-fraction expressions requires defining arrays of primes for the rational-fraction variables and needs arithmetic on prime factors of numbers to be performed. A reasonable approach is to include the smallest primes in each array but to allow storage for including more primes if needed. An upper bound on the number of primes required, hence on array sizes, can be obtained from Legendre's result [Leg98] that the number of primes less than N is not more than $P = N / [(\log_{10} N) + 1]$ rounded upward to the nearest integer. If angular momenta a , b , and c are coupled, then the largest number that can occur in the coupling coefficient (7.59) is the factorial $(a + b + c + 1)!$, which has a maximum factor of $N = a + b + c + 1$. For example, if $a = b = 5$, then $c \leq 10$ and the prime array length does not exceed $P = 9$, but if $a = b = 50$, then $c \leq 100$ so an array of about 60 elements is needed.

For arithmetic using prime-exponent representation, multiplication or division in rational-fraction form is accomplished easily and efficiently by adding or subtracting the elements of their prime factor arrays—just the exponents in their prime representations. Such simplicity arises for the same reason that logarithms are used for efficient multiplication or division of numbers. Addition and subtraction of rational fractions are more difficult, just as when working with logarithms. One way around this difficulty is to convert prime factors to integer numerators and denominators, then to find the lowest common denominator, perform the standard combination to a single fraction, then convert the resulting numerator and denominator back to prime factors. Fang and Shriner [Fan92] discuss in detail implementing these ideas.

Decimal Approximations. Computer solutions are usually expressed as decimal approximations, so the finite number of bits in a computer word generally leads to roundoff errors. The impact of such errors can often be mitigated—up to some machine- or compiler-dependent limit—by choosing higher-precision arithmetic, albeit at the expense of more computation time. Our program for $3-j$ coefficients, given in Appendix II, uses double-precision decimal representation, and results are printed to six decimals.

Factorials and Computing Efficiency. When calculating coupling coefficients, no matter what numerical representation is used, the program must evaluate factorials of integers, as (7.59) shows. The sum over k in this formula includes all values such that none of the factorial arguments is negative. There are at least 16 factorials to be evaluated and the number needed may be much larger if several values of k are allowed. In example (7.84), in which all angular momentum numbers are small, $k = 1$ only. By contrast, for $a = b = 17$, $\alpha = 2$, $\beta = -2$, and $c = 15$, the k sum ranges over $0 \leq k \leq 15$.

Many of the factorial arguments occur repeatedly, so one can decrease computa-

tion time by precomputing and storing factorials in a table. For this to be efficient, one needs to ensure that the table is large enough to store most of the factorials that will be needed. For coupled angular momenta a , b , and c with $b = a$ the largest possible factorial is $(4a + 1)!$, so the factorial table is of length $4a + 2$, which is ≤ 200 for $a < 50$. In the rational-fraction representation, each table entry is a prime array, so from our discussion of Legendre's formula we see that about 200×60 integer elements are needed in the factorial table for this limit on a .

If factorials are represented by integers and are used directly, computer words will overflow very quickly. For example, $13!$ overflows a 32-bit word. If decimal representations are used, a maximum exponent of 100 is overflowed by about $70!$; that is, for angular momenta about $a = b = 17$ in our example above. Therefore, for decimal approximations logarithms of factorials are used to avoid overflow problems and to speed up multiplication and division. A table of log factorials can be computed efficiently using recurrence; $\ln(n + 1)! = \ln(n + 1) + \ln n!$, with $\ln 0! = 0$. This method for factorials is useful in any problem involving combinatorials.

Programs for 3-j Coefficients. Apart from the entry-level program in the C language that is given in Appendix II, you should probably not write your own program from scratch because there are now several published programs using various of the techniques outlined above. These programs are summarized in Table 7.4.

TABLE 7.4 Programs for the 3-j coefficients.

Source	Method	Remarks
<i>Mathematica</i>	Symbolic	Algebraic or numerical values
[Rao78]	Decimal	Clebsch-Gordan coefficients
[Lai90]	Prime and decimal	Prime for $j \leq 30$
[Fan92]	Prime	Workstation version available

Programs using the rational-fraction (prime) form include those by Lai and Chiu [Lai90] and by Fang and Shriner [Fan92], although Lai and Chiu's program switches to decimal approximations for large angular momenta in the 3-j coefficient. In Table 7.4, except for the *Mathematica* choice, these programs are written in Fortran. Details are given in the references.

Once you have a program installed in a computer, a practical way to check that it is correct and numerical accurate is to use the orthogonality relations for different total angular momenta, (7.61), and for different m values, (7.62). Initial checks can be made by verifying orthogonality for the squares of coefficients, and if this is successful, you can check the correctness of relative phases by choosing one of the arguments to be different, which should give zero for the sum of products. Problem 7.12 offers such a programming exercise for 3-j coefficients.

7.5 ROTATION MATRICES AND COUPLING COEFFICIENTS

In Chapter 4 we consider the eigenstates (j, m) of infinitesimal rotations—the angular momentum eigenstates. In Chapter 6 finite rotations of these eigenstates are derived, leading to the \mathbf{D}^j matrices and to the reduced rotation matrix elements $d_{m'm}^j$. Now that we have learned in the preceding sections of this chapter how to combine pairs of angular momentum eigenstates, we can round out our understanding of this subject by relating rotation matrices and coupling coefficients.

We first derive the important Clebsch-Gordan series for combining rotation matrix elements that have the *same* angles and which therefore do *not* satisfy our previous condition of coming from separate state spaces. In Section 7.5.2 we present special cases of the Clebsch-Gordan series, then in Section 7.5.3 we use the series to perform integrals over rotation functions and spherical harmonics. Integration examples from celestial mechanics and from quantum-mechanical rotators (Section 6.5) are given in Section 7.5.4.

7.5.1 Clebsch-Gordan Series for Combining D^j Elements

By considering the relations for combining two angular momenta to form a third for systems each of which undergoes the *same* rotation, we derive two very useful relations between rotation matrix elements, as follows.

Inverse Clebsch-Gordan Series. Consider the combination of angular momenta given by (7.60), written as

$$\begin{aligned}
 |j_1 j_2 j_3 m_3, 000\rangle &= \sum |j_1 m_1, 000\rangle |j_2 m_2, 000\rangle \\
 &\times (-1)^{j_1 - j_2 + m_3} \sqrt{2j_3 + 1} \begin{pmatrix} j_1 & j_2 & j_3 \\ m_1 & m_2 & -m_3 \end{pmatrix}
 \end{aligned}
 \tag{7.85}$$

This relation is valid for any orientation of the system relative to the reference frame. Suppose that the system is rotated through Euler angles (α, β, γ) in the active viewpoint discussed in Sections 1.3.1 and 6.1.1. Each angular momentum state is transformed—according to (6.19)—as

$$|jm, \alpha\beta\gamma\rangle = \sum_{m'} |jm', 000\rangle D_{m'm}^j(\alpha\beta\gamma)
 \tag{7.86}$$

If (7.85) is written for the rotated system, so that $(000) \rightarrow (\alpha\beta\gamma)$, and three substitutions of the kind (7.86) are made, then orthonormality of the angular momentum eigenkets can be used (as Problem 7.13 suggests you show) to derive a relation between rotation matrix elements, called the *inverse Clebsch-Gordan series*:

$$\begin{aligned}
 D_{m'_1 m_3}^{j_3}(\alpha\beta\gamma) &= (-1)^{m'_3 - m_3} (2j_3 + 1) \\
 &\times \sum_{\substack{m'_1 m'_2 \\ m_1 m_2}} \begin{pmatrix} j_1 & j_2 & j_3 \\ m'_1 & m'_2 & m'_3 \end{pmatrix} D_{m'_1 m_1}^{j_1}(\alpha\beta\gamma) D_{m'_2 m_2}^{j_2}(\alpha\beta\gamma) \begin{pmatrix} j_1 & j_2 & j_3 \\ m_1 & m_2 & m_3 \end{pmatrix}
 \end{aligned} \quad (7.87)$$

Note that in the summation there are only two independent summation variables because of the requirements in the 3- j coefficients that

$$m'_1 + m'_2 + m'_3 = 0 = m_1 + m_2 + m_3 \quad (7.88)$$

in which m'_3 and m_3 are fixed, since they are parameters on the left-hand side of (7.87). Similarly, the three total angular momenta must be constrained by the triangle rule (7.6) in order that the orthonormality relations of the angular momentum eigenkets can be used.

The inverse Clebsch-Gordan series may be used as a starting point to derive angular momentum coupling coefficients. The coefficients are then the matrix elements of the unitary transformation (7.85) that transforms the direct product of two \mathbf{D} matrices into a form diagonal in J and M . If one has good command of direct-product groups, then this provides an effective way to derive the coupling coefficients, as shown in Wigner's book [Wig31].

One use of the inverse series (7.87) is to build up rotation matrix elements from the spin-1/2 elements by choosing $j_1 = 1/2$, then $j_2 = 1/2, 1, \dots$, and the stretched value $j_3 = j_2 + 1/2$. The required 3- j coefficients are given by (7.59). For example, the elements of \mathbf{D}^1 can be obtained from those of $\mathbf{D}^{1/2}$, then $\mathbf{D}^{3/2}$ can be obtained from $\mathbf{D}^{1/2}$ and \mathbf{D}^1 , and so on.

The Clebsch-Gordan Series. A very useful formula relating products of rotation matrix elements to sums over single matrix elements is obtained by starting with the direct-product formula (7.85) for the rotated and unrotated states, then applying orthogonality relations as used in deriving (7.87). By relegating the details to Problem 7.13, we obtain quickly the *Clebsch-Gordan series*:

$$\begin{aligned}
 D_{m'_1 m_1}^{j_1}(\alpha\beta\gamma) D_{m'_2 m_2}^{j_2}(\alpha\beta\gamma) &= (-1)^{m'_3 - m_3} \delta_{m'_3, -(m'_1 + m'_2)} \delta_{m_3, -(m_1 + m_2)} \\
 &\times \sum_{j_3} (2j_3 + 1) \begin{pmatrix} j_1 & j_2 & j_3 \\ m'_1 & m'_2 & m'_3 \end{pmatrix} D_{m'_3 m_3}^{j_3}(\alpha\beta\gamma) \begin{pmatrix} j_1 & j_2 & j_3 \\ m_1 & m_2 & m_3 \end{pmatrix}
 \end{aligned} \quad (7.89)$$

The summation is over all j_3 consistent with the triangle rule (7.6).

Note that in both this series and in the inverse series (7.87) there are *two* 3- j coefficients in each term rather than a single coefficient that you might expect. After all—as derived in Section 6.5.1—the $D_{m' m}^j$ are angular momentum eigenfunctions,

so why is a single coupling coefficient not sufficient? The answer is that the rotation matrix elements in both (7.87) and (7.89) have the *same* arguments (α, β, γ) and therefore refer to the same Hilbert space. However, the combination formulas for angular momenta derived in Section 7.1.2 require that the two subsystems be from *separate* Hilbert spaces. For the particular case of the $D_{m',m}^j$ it is sufficient to insert an extra coupling coefficient to overcome this problem, as we have just proved.

7.5.2 Special Cases of Clebsch-Gordan Series

Both forms of Clebsch-Gordan series have interesting special cases. The first is obtained by setting $\alpha = 0 = \gamma$ in (7.89), when—according to Table 6.4—the D-matrix elements become d-matrix elements, so that for the product of two reduced matrix elements evaluated at the *same* angle β , we have

$$d_{m'_1, m_1}^{j_1}(\beta) d_{m'_2, m_2}^{j_2}(\beta) = (-1)^{m'_3 - m_3} \delta_{m'_3, -(m'_1 + m'_2)} \delta_{m_3, -(m_1 + m_2)} \times \sum_{j_3} (2j_3 + 1) \begin{pmatrix} j_1 & j_2 & j_3 \\ m'_1 & m'_2 & m'_3 \end{pmatrix} d_{m'_3, m_3}^{j_3}(\beta) \begin{pmatrix} j_1 & j_2 & j_3 \\ m_1 & m_2 & m_3 \end{pmatrix} \quad (7.90)$$

From this we derive, by setting the m values to zero, the following case.

Legendre Polynomials and the Clebsch-Gordan Series. The Clebsch-Gordan series (7.89) provides a convenient way to collapse products of pairs of Legendre polynomials into a series of single polynomials. To do this, set the m values on the left-hand side of (7.89) all to zero, so the j values must be integers (reabeled as ℓ values) and the $d_{m',m}^j$ collapse to Legendre polynomials, according to Table 6.4. The series (7.89) then gives immediately

$$P_{\ell_1}(\cos \beta) P_{\ell_2}(\cos \beta) = \sum_{\ell_3} (2\ell_3 + 1) \begin{pmatrix} \ell_1 & \ell_2 & \ell_3 \\ 0 & 0 & 0 \end{pmatrix}^2 P_{\ell_3}(\cos \beta) \quad (7.91)$$

Parity considerations are relevant here. From Section 4.1 we have under parity $\beta \rightarrow \pi - \beta$. Thereby, according to (4.8), the parity of any $P_\ell(\cos \beta)$ is $(-1)^\ell$. The parity of the left-hand side of (7.91) is therefore $(-1)^{\ell_1 + \ell_2}$, also the parity of the right-hand side, as guaranteed by vanishing of the 3- j coefficient unless $\ell_1 + \ell_2 + \ell_3$ is even. Thus, in the expansion there are only even terms or only odd terms.

As a worked example, suppose that in (7.91) $\ell_1 = 2$ and $\ell_2 = 3$. We can look up the appropriate 3- j coefficients in Table 7.2 to obtain

$$P_2(\cos \beta) P_3(\cos \beta) = \frac{9}{35} P_1(\cos \beta) + \frac{4}{15} P_3(\cos \beta) + \frac{10}{21} P_5(\cos \beta) \quad (7.92)$$

To visualize this relationship, look at Figure 7.10, where we show polar diagrams of the polynomials, and the product on the left-hand side of (7.92). As is clear from the figure, the odd parity of the product $P_2 P_3$ (solid and dashed curves interchange across the horizontal at $\beta = \pi/2$ and $3\pi/2$) produces an expansion in terms of odd-order polynomials only.

By exploring with the *Mathematica* notebook LegProd, you can draw all the functions appearing in (7.92) and can determine decimal approximations to the Clebsch-Gordan series coefficients on its right-hand side. Such exercises are suggested in Problem 7.14. As a check on the correctness of the coefficients, note that they must sum to unity because of unitarity condition (7.61). Indeed, the coefficients in example (7.92) satisfy this condition if computed exactly by using the rational-fraction values obtained from Table 7.2.

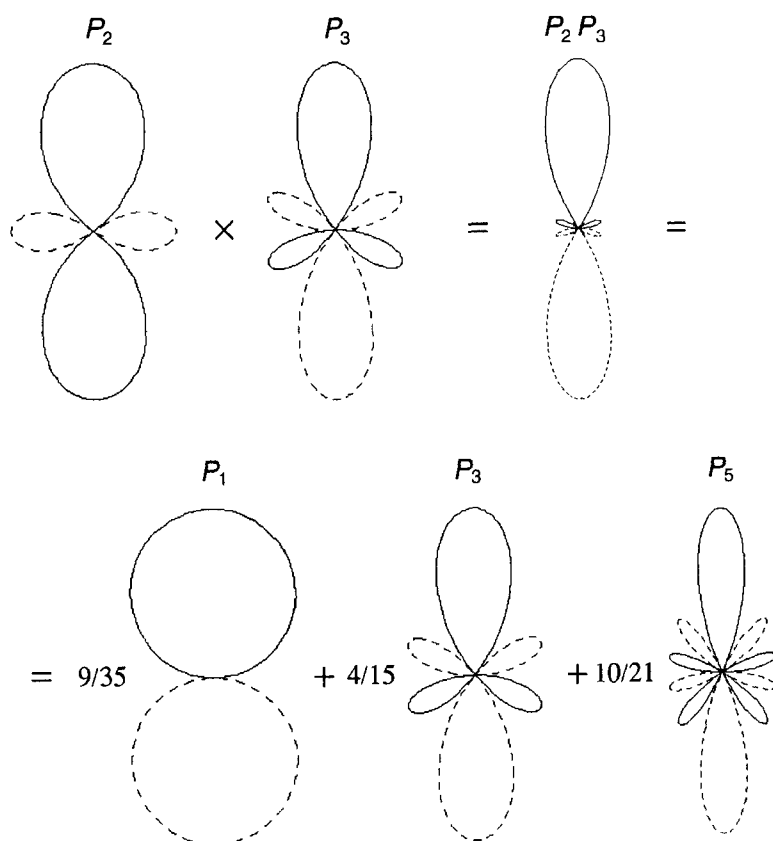


FIGURE 7.10 Visualizing the Clebsch-Gordan series, (7.91), using polar diagrams (Section 4.1.2) for P_2 and P_3 , for their product, and for the expansion in terms of P_1 , P_3 and P_5 on the right-hand side. Positive values are shown as solid curves and negative values are dashed. (Adapted from *Mathematica* notebook LegProd.)

Scattering Cross Sections and the Clebsch-Gordan Series. A practical use of the result (7.91)—providing a simple example of selection rules in scattering that are imposed by angular momentum conservation—is in fitting scattering differential cross sections, $\sigma(\theta)$, as a function of the scattering angle, θ , when the scattering amplitude has been expanded into partial waves (Section 5.4). For example, in nonrelativistic quantum mechanics with spin-independent interactions, $\sigma(\theta)$ is given in terms of (complex) partial-wave scattering amplitudes α_ℓ by

$$\sigma(\theta) = \left| \sum_{\ell=0}^L \alpha_\ell P_\ell(\cos\theta) \right|^2 \quad (7.93)$$

as derived, for example, in Landau [Lan90, Section 3.B]. The upper limit to the summation, L , is the highest partial wave for which α_L is significantly different from zero. By expanding out the absolute-value squared and using (7.91), you will find readily (as suggested in Problem 7.15) the Legendre polynomial expansion for the differential cross section

$$\sigma(\theta) = \sum_{\ell''=0}^{2L} A_{\ell''} P_{\ell''}(\cos\theta) \quad (7.94)$$

in which there are $(2L+1)$ expansion coefficients $A_{\ell''}$, given by

$$A_{\ell''} = \sum_{\ell=0, \ell'=0}^{L, L} \text{Re}(\alpha_\ell \alpha_{\ell'}^*) (2\ell''+1) \begin{pmatrix} \ell & \ell' & \ell'' \\ 0 & 0 & 0 \end{pmatrix}^2 \quad (7.95)$$

The result that the complexity of the differential cross section goes up to terms of order $\ell'' = 2L$ if the partial wave expansion goes up to partial wave $\ell = L$ is an example of *Yang's theorem* on the complexity of angular distributions in quantum scattering [Yan48].

C. N. Yang—who wrote his Ph.D. thesis on this topic—also investigated with T. D. Lee the evidence for parity conservation in β decay (Section 1.4.1). They published their conclusions in 1956 [Yan56]; parity violation in β decay was observed by Wu et al. in 1957 [Wu57]. Lee and Yang were awarded the 1957 Nobel Prize in physics for their analysis.

An elementary way to convince yourself of the correctness of Yang's theorem is to recall that the Legendre polynomial $P_\ell(\cos\theta)$ has a highest power $\cos^\ell\theta$. Upon squaring a sum of such polynomials going up to $\ell = L$, the highest power of $\cos\theta$ that appears is $2L$, which is the highest power in $P_{2L}(\cos\theta)$, as (7.94) indicates.

Yang's theorem is most often used in reverse, as follows. Suppose that we fit an experimental angular distribution in terms of Legendre polynomials, according to (7.94). If we find (within the uncertainties of fitting imprecise data) that the $A_{\ell''}$ are insignificant after some value $\ell'' = K$, then the amplitudes of physical relevance, the

α_ℓ , are negligible for $\ell \geq K/2$. A detailed example of a fitting procedure using the least-squares criterion and the Legendre expansion (7.94) is given in Section 7.3 of Bevington and Robinson's book on data analysis techniques for the physical sciences [Bev92]. Of course, as we continually emphasize throughout this book, these formulas in no way rely for their validity on the correctness of quantum mechanics. They are applicable to most phenomena described by waves, such as the scattering of sound.

To visualize and verify the equality of relations (7.93) and (7.94), consider Figure 7.11, in which the partial wave amplitudes and their squares are shown. The *Mathematica* notebook YngThm in Appendix I allows both expressions (7.93) and (7.94) to be computed, visualized in polar plots, and compared. Within the accuracy of drawing, they are identical, as you will find if you work Problem 7.16. Amazingly, even though both the amplitudes $A_{\ell'}$ and the Legendre polynomials $P_{\ell'}(\cos\theta)$ may be of either sign, the equivalence of (7.93) and (7.94) shows that analytically the sum (7.94) must be non-negative. Within roundoff errors in the various computations, this must also hold for the numerical sum.

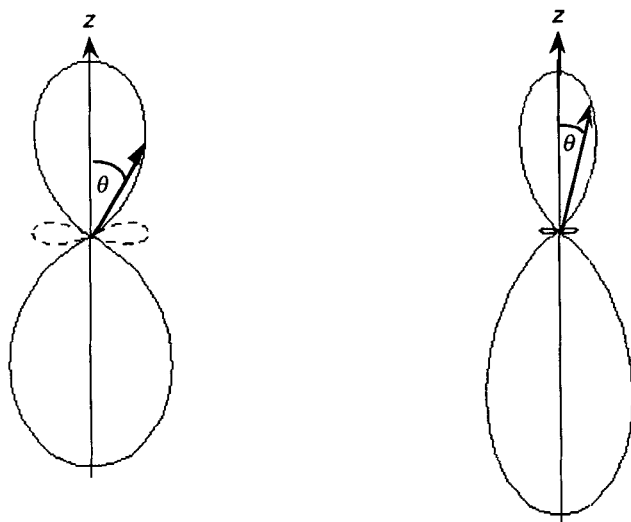


FIGURE 7.11 Partial-wave-sum amplitude (7.93) for $L = 2$, with $\alpha_0 = 1$, $\alpha_1 = -1$, $\alpha_2 = 6$, shown in the left-side polar diagram (positive values solid, negative values dashed). Its square shown in the right-side diagram agrees with the result calculated using the Legendre polynomial expansion (7.94), as can be verified by running *Mathematica* notebook YngThm. (Adapted from notebook YngThm.)

Now that we have seen the usefulness of Clebsch-Gordan series for simplifying summations, it is interesting to apply them to help perform integrations.

7.5.3 Integrals of Rotation Functions

The Clebsch-Gordan series (7.89) provides quick methods of evaluating integrals involving D-matrix and d-matrix elements, as we now derive and illustrate by examples. We consider first general integrals, then we specialize to integrals over three spherical harmonics—the so-called Gaunt integrals. Then follow two examples; the first relates to the figures of equilibrium of celestial bodies, while the second comes from the theory of wave scattering by rigid rotators.

Orthogonality of D-matrix Elements. The Clebsch-Gordan series allows direct proof of the orthogonality of the product of two rotation matrix elements over a suitable range of Euler angles, as derived in Section 6.4.2. In (7.89) the symmetry (6.45) may be used to produce a complex conjugate for the first function. On the right-hand side of (7.89) there is a sum over integrals over a single matrix element. As in Section 6.4.2, the integral over α requires $m'_3 = 0$ and gives 4π , while j_3 and m_3 must also be integers. The integral over γ must therefore also be zero unless $m_3 = 0$, when it becomes 2π . The remaining integral, over β , is just that over the Legendre polynomial $P_{j_3}(\cos \beta)$, which is just $2\delta_{j_3,0}$. Finally, (7.63) can be used for the 3- j coefficients. By carrying through these steps, as Problem 7.17 suggests, it is straightforward to show that

$$\int_R [D_{m'_1 m_1}^{j_1}(\alpha\beta\gamma)]^* D_{m'_2 m_2}^{j_2}(\alpha\beta\gamma) d\alpha \sin \beta d\beta d\gamma$$

$$= \frac{16\pi^2}{2j_1 + 1} \delta_{j_1 j_2} \delta_{m'_1 m'_2} \delta_{m_1 m_2} \tag{7.96}$$

$R: \quad 0 \leq \alpha \leq 4\pi \quad 0 \leq \beta \leq \pi \quad 0 \leq \gamma \leq 2\pi$

in agreement with (6.56). The technique used here can readily be extended to integrals over several matrix elements, as we now show.

Integrals of the Product of Several D-matrix Elements. A powerful application of the Clebsch-Gordan series (7.89) is to reduce the integral over the product of several D-matrix elements to sums of products of 3- j coefficients. Every pair of elements produces a sum over two coefficients. We indicate this schematically as

$$\int_R d\Omega D^{j_1}(\alpha\beta\gamma) D^{j_2}(\alpha\beta\gamma) \dots D^{j_N}(\alpha\beta\gamma)$$

$$= \sum_{j_{12} \dots} (12)' (34)' \dots \int_R d\Omega D^{j_{12 \dots N}}(\alpha\beta\gamma) (12)(34) \dots \tag{7.97}$$

in which (12)' and (12) represent the coupling coefficients, with appropriate m values assumed throughout, and $j_{12 \dots N}$ is the resultant of all the couplings.

The simplest example of this procedure is for integrals over the product of three

D-matrix elements, which requires use of (7.89) only once, followed by the orthogonality (7.96) of the matrix elements. Thus, the integral is given by

$$\int_R D_{m'_1 m_1}^{j_1}(\alpha\beta\gamma) D_{m'_2 m_2}^{j_2}(\alpha\beta\gamma) D_{m'_3 m_3}^{j_3}(\alpha\beta\gamma) d\alpha \sin \beta d\beta d\gamma$$

$$= 16\pi^2 \begin{pmatrix} j_1 & j_2 & j_3 \\ m'_1 & m'_2 & m'_3 \end{pmatrix} \begin{pmatrix} j_1 & j_2 & j_3 \\ m_1 & m_2 & m_3 \end{pmatrix} \quad (7.98)$$

R: $0 \leq \alpha \leq 4\pi \quad 0 \leq \beta \leq \pi \quad 0 \leq \gamma \leq 2\pi$

The range of α integration may be reduced to 2π and the integral halved if the conditions on half-integer properties of $j_1, j_2,$ and j_3 (Section 6.4.2) are satisfied.

Note that relation (7.90) for *reduced* rotation matrix elements does not always simplify the integration over β of products of such matrix elements. To understand why, note that the α and γ integrals produce most of the simplification after the Clebsch-Gordan series has been used. If, however, both the m' and m sums are zero, then the integral over α in (7.98) gives 4π and the integral over γ gives another factor of 2π . We can therefore write an analogous result for the integral of the product of three d-matrix elements:

$$\int_0^\pi d_{m'_1 m_1}^{j_1}(\beta) d_{m'_2 m_2}^{j_2}(\beta) d_{m'_3 m_3}^{j_3}(\beta) \sin \beta d\beta \delta_{m'_1+m'_2+m'_3,0} \delta_{m_1+m_2+m_3,0}$$

$$= 2 \begin{pmatrix} j_1 & j_2 & j_3 \\ m'_1 & m'_2 & m'_3 \end{pmatrix} \begin{pmatrix} j_1 & j_2 & j_3 \\ m_1 & m_2 & m_3 \end{pmatrix} \quad (7.99)$$

Whenever this does not lead to the result $0 = 0$, it is useful for evaluating the integral. In particular, since Table 6.4 shows that a reduced rotation matrix element collapses to a Legendre polynomial when both its m values are zero, we have immediately from (7.99) the integral

$$\int_0^\pi P_{\ell_1}(\cos \beta) P_{\ell_2}(\cos \beta) P_{\ell_3}(\cos \beta) \sin \beta d\beta = 2 \begin{pmatrix} \ell_1 & \ell_2 & \ell_3 \\ 0 & 0 & 0 \end{pmatrix}^2 \quad (7.100)$$

The same result may be deduced from (7.91) by using the orthogonality of Legendre polynomials. Note that the 3- j coefficient is given simply by (7.73) and that it is zero unless $\ell_1 + \ell_2 + \ell_3$ is even. This requirement is consistent with the parity symmetry of $P_\ell(\cos \theta)$, namely $(-1)^\ell$.

A Worked Example for Three Reduced Rotation Matrix Elements. Suppose that $j_1 = j_2 = j_3 = 2$, and that one wishes to perform an integral of the kind (7.99).

If $m'_1 = m'_2 = 1$ and $m'_3 = -2$, then the first Kronecker δ is satisfied. If $m_1 = 2$ and $m_2 = m_3 = -1$, then the second Kronecker δ is also satisfied. We therefore have nonzero values on both sides of (7.99), so the integral is given by

$$\int_0^\pi d_{1,2}^2(\beta) d_{1,-1}^2(\beta) d_{-2,-1}^2(\beta) \sin \beta \, d\beta = 2 \begin{pmatrix} 2 & 2 & 2 \\ 1 & 1 & -2 \end{pmatrix} \begin{pmatrix} 2 & 2 & 2 \\ 2 & -1 & -1 \end{pmatrix} = \frac{6}{35} \tag{7.101}$$

in which the 3- j coefficients are equal because of the permutation symmetry (7.64), and their value is given by (7.84). The alternative method of evaluating the integral—by substituting from Table 6.3 the expressions for the three functions, multiplying out the factors, and integrating termbyterm—is both tedious and error-prone. If one can obtain readily the 3- j coefficients, as described in Sections 7.3.4 and 7.4, then such integrals are performed most easily by using (7.99).

Integrals over Three Spherical Harmonics; Gaunt Integrals. The integral over the product of three D-matrix elements given by (7.98) can be specialized to a case that is frequently required, namely when the j values are integers and one of the m values in each element is zero. Then—according to Table 6.4—we have an integral over quantities proportional to spherical harmonics. It is then straightforward to show that the integral over the unit sphere, R' , of the product of three spherical harmonics is given by

$$\int_{R'} Y_{LM}^*(\theta\phi) Y_{\ell_1 m_1}(\theta\phi) Y_{\ell_2 m_2}(\theta\phi) \, d\phi \sin \theta \, d\theta = (-1)^M \sqrt{\frac{(2\ell_1 + 1)(2\ell_2 + 1)(2L + 1)}{4\pi}} \begin{pmatrix} \ell_1 & \ell_2 & L \\ m_1 & m_2 & -M \end{pmatrix} \begin{pmatrix} \ell_1 & \ell_2 & L \\ 0 & 0 & 0 \end{pmatrix} \tag{7.102}$$

$R' : \quad 0 \leq \phi \leq 2\pi \quad 0 \leq \theta \leq \pi$

Here it is appropriate to halve the range of integration over $\alpha = \phi$, since the total angular momentum numbers are integers. Note the three conditions that are necessary for the integral to be nonzero:

$$\Delta(\ell_1 \ell_2 L) \quad \ell_1 + \ell_2 + L \text{ even} \quad m_1 + m_2 = M \tag{7.103}$$

The result (7.102) is usually called the *Gaunt integral* [Gau29]. The integral over the product of three Legendre polynomials, (7.100), being a special case of this formula.

7.5.4 Examples: Celestial Bodies and Rotator Matrix Elements

We now develop two examples—from celestial mechanics and from molecular and nuclear scattering—that illustrate using the Gaunt integrals.

Figures of Equilibrium of Celestial Bodies. A long-term problem in celestial mechanics is to determine the dynamics of planetary and binary-star systems. Indeed, many of the techniques developed in applied mathematics from the eighteenth century onward—by such luminaries as Laplace, Legendre, Gauss, and Poincaré—have been motivated by such problems. In the second half of the twentieth century the deployment of artificial satellites around Earth and the other planets has enabled precise determination of their mass distributions from measurements of perturbations of satellite orbits because of departures of the gravitational potential from spherical symmetry.

In the following we illustrate how a complicated angular integral over Legendre functions that appears in the theory of interactions between planetary or stellar rotations and the tides induced by a nearby celestial body can be performed simply by using the techniques developed in this chapter and Chapter 6. It is traditional in celestial mechanics to use tedious brute-force methods for almost all analyses. The details of setting up the integral are described by Kopal in a monograph on the figures of equilibrium of celestial bodies [Kop60, Section IV-1]. Introductory material on celestial mechanics is given in the text by Danby [Dan62], while a more advanced presentation for practical calculations is given by Taff [Taf85].

The geometry of the problem is shown in Figure 7.12, in which the larger body is the one whose shape (including surface fluids such as water and atmosphere) is affected by the body centered at $\mathbf{r}'' = (r'', \theta'', \phi'')$.

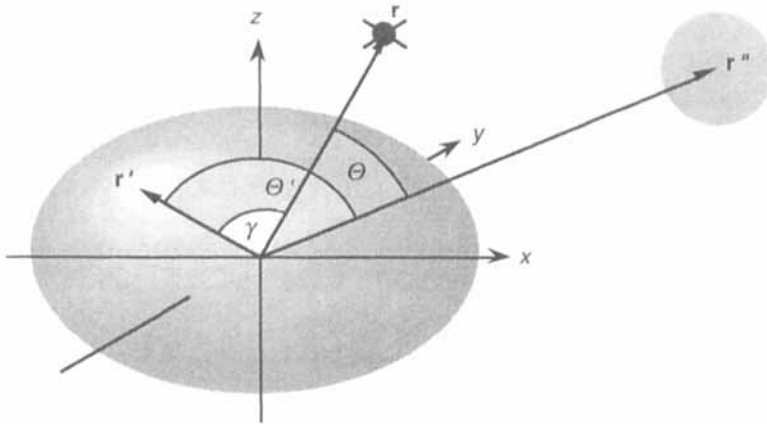


FIGURE 7.12 A rotating celestial body, shown by the ellipsoid at left, contains representative mass elements at points \mathbf{r}' . It interacts gravitationally with another body at \mathbf{r}'' that causes tidal forces on it. To calculate the gravitational potential at a point \mathbf{r} outside the first body requires the angular integral (7.104).

In Figure 7.12, vector $\mathbf{r} = (r, \theta, \phi)$ is drawn from the center of the coordinate system (x, y, z) to a point at which the gravitational potential is required. Typically, \mathbf{r} is the instantaneous position of an artificial satellite. The positions of the mass points exerting the gravitational pull are denoted by $\mathbf{r}' = (r', \theta', \phi')$ and are to be integrated over, including the following integration over angles:

$$P_n^{(j)}(\hat{\mathbf{r}}, \hat{\mathbf{r}}'') \equiv \frac{2n+1}{4\pi} \int P_j(\hat{\mathbf{r}}' \cdot \hat{\mathbf{r}}'') P_n(\hat{\mathbf{r}} \cdot \hat{\mathbf{r}}') P_2^2(\cos \theta') \sin \theta' d\theta' d\phi' \quad (7.104)$$

Here j and n (in the notation used by Kopal) are non-negative integers.

The strategy for performing such integrals over Legendre functions of angles between two vectors (Θ' and γ , respectively, in Figure 7.12) is to use the spherical harmonic addition theorem (4.23) to expand into spherical harmonics of the component angles, then to use the Gaunt integral (7.102) to integrate over three spherical harmonics after writing the P_2^2 in terms of Y_{22} by using (4.18). By carrying out the details of this in Problem 7.18, you will discover easily that

$$\begin{aligned} P_n^{(j)}(\hat{\mathbf{r}}, \hat{\mathbf{r}}'') &= 2P_j(\cos \Theta) \delta_{jn} - 8\pi \sqrt{\frac{2n+1}{2j+1}} \begin{pmatrix} 2 & j & n \\ 0 & 0 & 0 \end{pmatrix} \\ &\times \sum_m \begin{pmatrix} 2 & j & n \\ 0 & m & -m \end{pmatrix} Y_{jm}(\theta'' \phi'') Y_{n,-m}(\theta' \phi') \end{aligned} \quad (7.105)$$

Kopal [Kop60, page 91] tabulates the integrals (evaluated “after a considerable amount of algebra”) for $0 \leq j \leq 4$ and $0 \leq n \leq 7$ and suggests a general relation:

$$\sum_n P_n^{(j)}(\hat{\mathbf{r}}, \hat{\mathbf{r}}'') = P_2^2(\cos \theta) P_j(\cos \Theta) \quad (7.106)$$

As you may verify in Problem 7.18, this result follows rather directly by using the Clebsch-Gordan series (7.89). The symmetry

$$(2j+1)P_n^{(j)}(\hat{\mathbf{r}}, \hat{\mathbf{r}}'') = (2n+1)P_j^{(n)}(\hat{\mathbf{r}}'', \hat{\mathbf{r}}) \quad (7.107)$$

follows directly from (7.105) by using symmetries of the 3- j coefficients.

Now that we know how to apply rotational-symmetry techniques to simplify angular integrals in macroscopic systems such as binary stars or artificial satellites, let us focus on an example of what is often a microscopic system—wave scattering by a rigid rotator, as occurs in molecular and nuclear physics. The method is, in essence, also applicable to scattering of sound waves by a spheroidal object.

An Integral from the Theory of Scattering by a Rigid Rotator. In Section 6.5 we discuss rigid-body rotations in quantum mechanics and find that the complex conjugates of rotation-matrix elements describe angular momentum eigenstates.

Those developments emphasize the energy states, whereas now we discuss the matrix elements for scattering by such a rotator. We follow an article by Arthurs and Dalgarno [Art60] on scattering of a quantum wave by a molecule approximated as a rigid rotator, using their notation. Although described in this context, the angular integrals are also applicable to scattering of waves by any object whose Hamiltonian approximates that of a rigid rotator. Since our emphasis is on showing how to do angular integrals, whenever clarity and simplicity are served we drop overall proportionality factors.

Suppose that a rigid rotator, such as the diatomic molecule sketched in Figure 7.13, interacts with a wave with representative point $\mathbf{r} = (r, \theta, \phi)$. Our aim is to calculate for given angular momentum states the effective potential at r averaged over all points of the rotator. This requires wave functions, interaction potentials, then matrix elements. We develop the angle-dependent parts of each of these in turn.

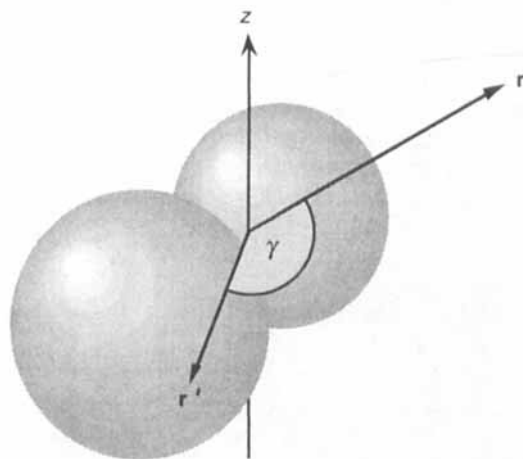


FIGURE 7.13 A rigid rotator interacts with a wave, of which a representative point is \mathbf{r} . The matrix elements of the multipole elements of the potential, (7.110), are to be evaluated. Integration is over all points \mathbf{r}' of the molecule that contribute to the potential at \mathbf{r} .

Coupled Wave Functions. First, we make appropriately coupled wave functions. For the scattered wave, as discussed in Section 5.4, a given partial wave ℓ has an angular dependence proportional to $P_\ell(\cos\theta)$ if it is a plane wave directed along the z axis. More generally, for a wave at an arbitrary orientation the angular dependence is $Y_{\ell m}(\theta, \phi)$. For the rotator wave function, suppose that it is symmetric ($K = 0$ on the body-fixed symmetry axis, Figure 7.13), with angular momentum number j and projection on the space-fixed z axis of m_j . Table 6.4 shows that the complex-conjugated D-matrix element is just proportional to $Y_{jm_j}(\theta', \phi')$, where $\mathbf{r}' = (r', \theta', \phi')$ is a representative point of the rotator. The combined system in the state (J, M) is then given by sums of products with $3-j$ coefficients and is proportional to $Y_{Jj\ell}^M(\hat{\mathbf{r}}, \hat{\mathbf{r}}')$ defined by

$$\begin{aligned}
 Y_{j\ell}^M(\hat{\mathbf{r}}, \hat{\mathbf{r}}') &\equiv \langle (\theta' \phi')(\theta \phi) | j \ell; JM \rangle \\
 &= \sum \begin{pmatrix} j & \ell & J \\ m_j & m & -M \end{pmatrix} Y_{jm}(\hat{\mathbf{r}}') Y_{\ell m}(\hat{\mathbf{r}})
 \end{aligned} \tag{7.108}$$

in which the summation is over those m_j and m values whose sum is the given M .

Multipole Expansion of the Interaction. We assume that the interaction $V(\mathbf{r}, \mathbf{r}')$ of the scattered wave with the scatterer is spin-independent, depending only on position. Because we calculate the effective potential at r , without regard to the orientation of the rotator, it is convenient to make a multipole expansion, as follows:

$$\int V(\mathbf{r}, \mathbf{r}') r'^2 dr' = \sum_{\mu} v_{\mu}(r) P_{\mu}(\cos \gamma) \tag{7.109}$$

in terms of the angle γ between \mathbf{r} and \mathbf{r}' shown in Figure 7.13. This expansion separates out the distance dependence (r) from the angle dependence (γ), which is especially convenient for doing subsequently angle integrations. The *multipole moment* of order μ , $v_{\mu}(r)$, is given by inverting (7.109), using the orthogonality relation (4.3) for the Legendre polynomials. Thus

$$v_{\mu}(r) = \frac{2\mu+1}{2} \int \left[\int V(\mathbf{r}, \mathbf{r}') r'^2 dr' \right] P_{\mu}(\cos \gamma) \sin \gamma d\gamma \tag{7.110}$$

for $\mu = 0, 1, 2, \dots$ until the expansion when inserted in the subsequent matrix elements is sufficiently accurately converged.

As an example of the multipole expansion, suppose that the interaction is purely electrostatic, that the scattered object has a spherically symmetric charge distribution with total charge Ze , and that the two scatterers do not interpenetrate ($r > r'$). Starting from Coulomb's law, we have that an element of charge in a small volume element $d\mathbf{r}'$ at \mathbf{r}' in the scatterer where the density is $\rho(\mathbf{r}')$ contributes to the potential at \mathbf{r} an amount of dV , given by

$$\begin{aligned}
 dV(\mathbf{r}, \mathbf{r}') &= \frac{Ze\rho(\mathbf{r}')d\mathbf{r}'}{|\mathbf{r}-\mathbf{r}'|} \\
 &= \frac{Ze}{r} \sum_{\mu} \rho(\mathbf{r}') d\mathbf{r}' \left(\frac{r'}{r}\right)^{\mu} P_{\mu}(\cos \gamma)
 \end{aligned} \tag{7.111}$$

In the second line we used the familiar Legendre expansion [Won91, Section 5.2] for the inverse of the separation. By comparing the last two equations, we have immediately for electrostatic interactions the multipole expansion coefficients given by

$$v_{\mu}(r) = \frac{ZeQ_{\mu}}{r^{\mu+1}} \tag{7.112}$$

in which the Q_μ are the charge multipole moments of the rotator, given by

$$Q_\mu \equiv \int \rho(r') (r')^{\mu+2} dr' \quad (7.113)$$

For other forms of the interaction—for example, a nucleon-nucleon potential if the rotator describes an atomic nucleus such as ^{170}Hf (Section 6.5.3)—the multipole moments are usually computed numerically in terms of the definition (7.110).

Matrix Elements in the Multipole Expansion. Now that we have the ingredients for calculating the angular integrals for interaction matrix elements, we have to sandwich the interaction V between the bread and butter of the wave functions (7.108). Since V is scalar, the matrix elements are diagonal in the total angular momentum J and its projection M on a chosen z axis, so it is sufficient to calculate the matrix elements given by

$$\langle j'' \ell''; JM | V | j' \ell'; JM \rangle = \sum \begin{pmatrix} j'' & \ell'' & J \\ m_{j''} & m'' & M \end{pmatrix} \begin{pmatrix} j & \ell & J \\ m_{j'} & m' & M \end{pmatrix} \sum_{\mu} v_{\mu}(r) I_{\mu} \quad (7.114)$$

in which the first summation is over projections that sum to M , and the second sum is over μ values consistent with these for the matrix elements I_{μ} . As Problem 7.19 suggests you verify, these matrix elements are given by

$$\begin{aligned} I_{\mu} &= \frac{4\pi}{2\mu+1} \sum_m \int Y_{\ell'' m''}^*(\hat{r}) Y_{\mu m}^*(\hat{r}) Y_{\ell' m'}(\hat{r}) d\hat{r} \\ &\quad \times \int Y_{j'' m_{j''}}^*(\hat{r}') Y_{\mu m}(\hat{r}') Y_{j' m_{j'}}(\hat{r}') d\hat{r}' \\ &= \frac{1}{2\mu+1} \sum_m \sqrt{(2\ell''+1)(2\mu+1)(2\ell'+1)(2j''+1)(2\mu+1)(2j'+1)} \\ &\quad \times \begin{pmatrix} \ell'' & \mu & \ell' \\ m'' & m & m' \end{pmatrix} \begin{pmatrix} \ell'' & \mu & \ell' \\ 0 & 0 & 0 \end{pmatrix} \begin{pmatrix} j'' & \mu & j' \\ m_{j''} & m & m_{j'} \end{pmatrix} \begin{pmatrix} j'' & \mu & j' \\ 0 & 0 & 0 \end{pmatrix} \end{aligned} \quad (7.115)$$

The matrix element (7.114) therefore reduces to

$$\begin{aligned} \langle j'' \ell''; JM | V | j' \ell'; JM \rangle &= 4\pi \sqrt{(2\ell''+1)(2\ell'+1)(2j''+1)(2j'+1)} \\ &\quad \times \sum_{\mu} v_{\mu}(r) \begin{pmatrix} \ell'' & \mu & \ell' \\ 0 & 0 & 0 \end{pmatrix} \begin{pmatrix} j'' & \mu & j' \\ 0 & 0 & 0 \end{pmatrix} S_{\mu} \end{aligned} \quad (7.116)$$

in which the sum over magnetic-substate projections is

$$S_{\mu} = \sum \begin{pmatrix} \ell'' & \mu & \ell' \\ m'' & m & m' \end{pmatrix} \begin{pmatrix} j'' & \mu & j' \\ m_{j''} & m & m_{j'} \end{pmatrix} \begin{pmatrix} j'' & \ell'' & J \\ m_{j''} & m'' & M \end{pmatrix} \begin{pmatrix} j & \ell' & J \\ m_{j'} & m' & M \end{pmatrix} \quad (7.117)$$

The sum is over all m values except M . Thus, we have reduced the problem of integration over angles to summations over products of 3- j coefficients. The geometric (rotational symmetry) aspects in the coupling coefficients have also been clearly separated from the dynamical aspects, the $v_\mu(r)$. In formula (7.117) the m -value summation is tedious to perform directly, but in Section 9.4.2 we show how it can be simplified in terms of 6- j coefficients.

A major advantage of formulas (7.116) and (7.117) over other methods of simplifying the calculation of matrix elements is that angular momentum selection rules are immediately evident in the 3- j coefficients. For example, suppose that the scatterer is a diatomic homonuclear molecule—such as N_2 —approximated as a rigid rotator. Then the reflection symmetry of this system about its center allows only even angular momentum states j'' and j' . From the parity conservation 3- j coefficients in (7.116) that contain j'' and j' , we therefore have that μ must be even; that is, only even multipole moments contribute to the scattering. Thence, from the parity conservation 3- j coefficient with ℓ'' and ℓ' , the difference between the incident partial wave ℓ' and outgoing partial wave ℓ'' must be even. For example, scattering from p wave to f wave, but not p wave to d wave.

In both examples of the use of Gaunt integrals, the rotational symmetry aspect of angular momentum is paramount. Thus, we use *geometrical* angular momentum rather than *dynamical* angular momentum—making the distinction established in Section 3.4.5 and developed in Section 5.1.

PROBLEMS ON COMBINING TWO ANGULAR MOMENTUM EIGENSTATES

7.1 In combining angular momenta, we have formula (7.5), which determines the lower limit on the coupled angular momentum, $J_<$. Use the formula for the sum

$$\sum_{j=\alpha}^{\beta} j = \frac{1}{2} [\beta(\beta+1) - \alpha(\alpha+1)] \quad (7.118)$$

which is valid for integer or half-integer j values, together with the upper limit $\beta = J_> = j_1 + j_2$, in order to derive the lower limit $J_< = |j_1 - j_2|$.

7.2 Verify the spin-orbit energy formulas (7.13) and (7.14), starting with relation (7.12).

7.3 For the Coulomb problem in Section 7.1.4 derive in detail the following:

(a) Demonstrate that for an inverse-square force the classical eccentricity vector, \mathbf{A}_c , is a constant of the motion; that is, show in detail the steps between equations (7.15) through (7.18).

(b) Derive the quantal operator properties (7.26) through (7.29) by starting with the definitions and commutation properties of the operators for orbital angular momentum and linear momentum.

7.4 Derive the m -sum unitarity property of Clebsch-Gordan coefficients, (7.41),

by following through steps similar to those used for J -sum unitarity.

7.5 Carry out the algebraic steps leading to formula (7.51) for the Clebsch-Gordan coefficients, as follows.

- (a) Apply the binomial expansion to (7.48) and collect terms to obtain (7.49).
- (b) Use the orthogonality condition (7.39) to obtain the C coefficient given by (7.50). To collapse the sum, use the combinatorial identities

$$\sum_k \binom{a}{k} \binom{b}{c-k} = \binom{a+b}{c} \quad \binom{u}{v} = (-1)^v \binom{v-u-1}{v} \quad (7.119)$$

where the combinatorial

$$\binom{a}{x} \equiv \frac{a!}{x!(a-x)!} \quad (7.120)$$

- (c) To obtain the general coefficient, apply J_{-1} operator $J-M$ times to (7.49), expand terms by using the binomial theorem and the analogue of the Leibnitz theorem for the action of ∂_{\pm} . Then identify the coefficient of the product of each subsystem eigenstate, as in (7.43), to obtain (7.51).

7.6 Verify the symmetry properties of the 3- j coefficients, (7.64) and (7.65), by making the substitutions indicated in the general formula (7.59).

7.7 Verify the phase relation (7.69) for interchanging the order of combining two angular momenta. To do this, use the combination rule (7.60), the symmetry relation (7.67), and the phase-manipulation rules in Section 2.1.4.

7.8^M The 3- j coefficients with all magnetic substate values zero have several simplifications over the general coefficients.

- (a) Show that the number of such coefficients for a and b fixed is $\min(a, b) + 1$.
- (b) Show that the jackknife case, $c = |b - a|$, and the stretched case, $c = a + b$, have nonzero coefficients.
- (c) Derive formula (7.43) for the “parity-conservation” coupling coefficients by specializing (7.59) to the case with each m value zero.
- (d) Prove that the signs of the nonzero coefficients alternate for successive allowed values of c with a and b fixed.
- (e) Use *Mathematica* notebook 3j000 in Appendix I to verify the numerical values of the coefficients in Figure 7.2. Check the orthogonality condition (7.61) using these values.

7.9 Derive the combined spin and orbital states for $s = 1/2$, as given by (7.75), by substituting the orbital spherical harmonics and the spin states χ_{\pm} for the component angular momentum states, then using the general expression (7.59) or Table 7.3 for spin 1/2 for the coupling coefficients.

7.10 Show that for given j_1 and j_2 the number of coefficients for combining two angular momenta is $N_3(j_1, j_2) = (2j_1 + 1)(2j_2 + 1)[2\min(j_1, j_2) + 1]$. To do this,

count the number of m_1 and m_2 values, as well as the number of combined angular momenta by using the triangle and projection selection rules in Section 7.1.2.

7.11^M Algebraic expressions for 3- j coefficients can be obtained by using *Mathematica* notebook `Alg3j` in Appendix I. (Note that function `ThreeJSymbol` checks the triangle and m -sum selection rules only if *numerical* arguments are given.)

- (a) Enter and check `Alg3j` by computing a few of the values given in Table 7.3.
- (b) Generate the four independent algebraic 3- j coefficients corresponding to the smallest angular momentum being $3/2$. Check the column-permutation symmetries and orthogonality of the resulting coefficients.
- (c) For a small angular momentum of your choice, say $1/2$, modify the notebook so that it applies the function `CForm` or `FortranForm` to the algebraic 3- j coefficient generated by *Mathematica*. Then use this code as part of a small C or Fortran program that computes the coefficient numerically. Check its results against the program for 3- j coefficients given in Appendix II.
- (d) Time the special-purpose program from (c) and the general-purpose program from Appendix II, measuring only the execution times of the coefficients, not the times for input and output. What is the speedup factor in your computing system? Would this produce significant savings in typical calculations where you use these coefficients?

7.12 With a computer program for 3- j coefficients that you have chosen (for example, `C2` in Appendix II), modify the program to verify orthogonality condition (7.61). Note that—unless you compute the coefficients symbolically or with exact rational-fraction arithmetic—the orthogonality will be satisfied only within the roundoff errors of your computation.

7.13 Consider the two types of Clebsch-Gordan series.

- (a) Derive the inverse Clebsch-Gordan series (7.87) by following along the steps indicated in the text.
- (b) Make a similar derivation of the Clebsch-Gordan series (7.89).

7.14^M Use *Mathematica* notebook `LegProd` with various choices of ℓ_1 and ℓ_2 in (7.91) to explore the Clebsch-Gordan series expansion for products of Legendre polynomials. `LegProd` draws the functions appearing in (7.91) and displays decimal approximations to the Clebsch-Gordan series coefficients on its right-hand side.

7.15 Use the Clebsch-Gordan series (7.89) and the steps indicated in the text to derive the angular distribution formulas (7.94) and (7.95).

7.16^M Use *Mathematica* notebook `YngThm` in Appendix I to verify graphically the equivalence of expressions (7.93) and (7.94) for several choices of real values of the amplitudes α_ℓ . The choice of real amplitudes is for simplification only.

7.17 To derive the orthogonality relation for D-matrix elements (7.96), show the details of the steps indicated in Section 7.5.3.

7.18 Investigate the celestial-mechanics integral (7.104) as follows.

- (a) Use the spherical harmonic addition theorem (4.23) to expand the first two Leg-

endre polynomials into spherical harmonics of the component angles, then use the Gaunt integral (7.102) to integrate over three spherical harmonics of the angles $(\theta'\phi')$ after writing the P_2^2 in terms of Y_{22} by using (4.18).

(b) By using the Clebsch-Gordan series (7.89) applied to the special case of rotation matrix elements as spherical harmonics, then using the spherical harmonic addition theorem (4.23), derive the sum rule (7.106).

(c) Derive the symmetry relation (7.107) by using the permutation symmetries of the 3- j coefficients.

7.19 Calculate expression (7.115) for the rigid rotator multipole matrix elements by using the spherical-harmonic addition theorem (4.23) in (7.110), then use the Gaunt integral formula (7.102) to obtain the second equality in (7.115).



Chapter 8

IRREDUCIBLE SPHERICAL TENSORS AND SPIN

In the preceding chapters we have developed rotational properties of angular momentum eigenstates, both under infinitesimal rotations (\mathbf{J} operators, Chapters 3 and 4) and under finite rotations (D-matrix elements, Chapter 6). Our emphasis in this chapter is on constructing operators whose properties under rotations are similar to those of such eigenstates. Figure 8.1 summarizes correspondences that we derive between angular momentum and spherical tensors.

ANGULAR MOMENTUM AND SPHERICAL TENSORS	
<i>Angular momentum operators, J_i, and eigenstates $jm\rangle$</i>	<i>Irreducible spherical tensor operator components T_{kq}</i>
Spherical-basis operators, J_σ , $\sigma = \pm 1, 0$ Commutation relations; [3.1.2, 3.1.3]	Commutation relations of J_σ with T_{kq} ; [8.1.2]
Angular momentum eigenvalues (j, m) and matrix elements; [3.4]	Tensor (k, q) and matrix elements; Wigner-Eckart theorem; [8.3]
Angular momentum eigenstates, $ jm\rangle$; [4]	Tensor components, T_{kq} ; [8.1, 8.2]
Rotations of $ jm\rangle$ by $D_{m'm}^j$; [6]	Rotations of T_{kq} by $D_{q'q}^k$; [8.1]
Combining angular momenta; [7, 9]	Combining tensors; [8.2, 9.4, 9.5]
Spin angular momentum; [3.5, 4.3]	Spin tensors; [8.4]

FIGURE 8.1 Correspondences between angular momentum and irreducible spherical tensors. Relevant sections are indicated in brackets.

Before studying this chapter, it would be worthwhile for you to review the sections on angular momentum in Chapters 2–7 that are indicated in Figure 8.1.

We begin the chapter by defining irreducible tensor operators and explaining their power (Section 8.1), then we show in Section 8.2 how tensors may be combined, either to produce tensors of higher rank or to produce scalars (zero-rank tensors). The Wigner-Eckart theorem for irreducible spherical tensors—surely the most powerful and useful result in this field—separates dynamics from geometry. We derive it in Section 8.3, where we also show how to determine and interpret reduced matrix elements. Tensors for spin polarization are related to density matrices in Section 8.4, which also has a treatment of spin transport through magnetic field gradients that illustrates using various angular momentum techniques.

In Chapter 9, after developing the 6- j and 9- j coefficients for combining three and four angular momentum eigenstates, we return to irreducible tensors, devising formulas for their scalar products (Section 9.4) and for their matrix elements in coupled schemes (Section 9.5).

Tensors in the Physical Sciences. Tensors appear in a variety of contexts and terminologies in the physical sciences. Probably familiar to you are the stress-energy tensor in classical mechanics [Gol80, Section 12-3] and the field tensor in electromagnetism [Gol80, Section 12-6]. Both of these are second-rank tensors, which are often just called “tensors.” Surely even more familiar are rank-zero tensors, called scalars, and rank-one tensors, called vectors. Tensor nomenclature is summarized in Table 8.1.

TABLE 8.1 Notation for tensors and examples of tensors.

Tensor rank, k	Type of tensor	Example
0	Scalar	Hamiltonian, $V_{so}(r)\mathbf{L}\cdot\mathbf{S}$
1	Vector	Angular momentum, \mathbf{J}
2	“Tensor”	Inertia tensor, \mathbf{I}
$k \geq 3$	k th-Rank tensor	\mathbf{T}_k

Tensors of rank higher than two occur frequently in areas such as piezoelectricity, the Hall effect, and the characterization of electro-optical devices such as Pockels and Kerr cells. The physical properties of the materials used in such devices are highly anisotropic, so corresponding high-order tensors are needed to describe them. An introduction to Cartesian tensors in this context is given in Lovett’s book [Lov89], while a more advanced treatment using group theory methods (Section 2.5) is given in the monograph by Wooster [Woo73].

Note some ambiguity in the examples of tensors in Table 8.1. In classical mechanics (as well as in electromagnetism) quantities such as angular momentum (\mathbf{L}_c in Section 3.4.5) and the inertia tensor are directly observable. On the other hand, in quantum mechanics $\mathbf{J}_q = \hbar\mathbf{J}$ is an *operator* whose expectation values follow

(according to the Ehrenfest's theorems, Section 5.1) classical equations of motion. One generalization made in the following when developing irreducible tensors is that such tensors may be composed of operators as well as of numbers.

Rotations of Scalars and Vectors. If we rotate something (an object, a function that depends on coordinates, or an operator) and find that it is *invariant* under rotations, then—by definition—we have a *scalar*, S . On the other hand, for a *vector*, \mathbf{V} , under rotation its components transform according to

$$V'_q = \sum_{q'} V_{q'} a_{q'q} \quad q' = 1, 2, 3 = x, y, z \quad (8.1)$$

for $q = 1, 2, 3$ or x, y, z . The unconventional labeling in (8.1) facilitates comparison with formulas for irreducible spherical tensors. For rotations the $a_{q'q}$ form the elements of an orthogonal 3×3 matrix, as shown for coordinate rotations in Section 1.3. More generally, if the elements of \mathbf{V} are allowed to be complex, then the matrix is unitary.

We may cast the rotational invariance of a scalar trivially into a form analogous to (8.1) by writing

$$S' = \sum_{q'} S_{q'} a_{q'} = S \quad q' = 0 \quad a_{q'} = 1 \quad (8.2)$$

so the “transformation” element a_0 is automatically a 1×1 unitary matrix.

Second-Rank Tensors and Rotations. Consider the inertia tensor \mathbf{I} in classical mechanics, or the analogous quadrupole-moment tensor in electrostatics. For a system of mass points m_α at $\mathbf{r}_\alpha = (r_{\alpha 1}, r_{\alpha 2}, r_{\alpha 3})$ the elements of the inertia tensor are given by

$$I_{ij} = \sum_{\alpha} m_{\alpha} r_{\alpha i} r_{\alpha j} \quad i, j = 1, 2, 3 \quad (8.3)$$

in which the sum is over all mass points in the system. The inertia tensor is said to be of second rank because the coordinate components appear bilinearly for each mass point. Generally, there are nine combinations of i and j , but since this tensor is symmetric, $I_{ji} = I_{ij}$, there are six linearly independent components of \mathbf{I} . Under rotations, the inertia tensor transforms as

$$I'_{p'q'} = \sum_{p'q} I_{p'q} a_{p'p} a_{q'q} \quad p', q' = 1, 2, 3 \quad (8.4)$$

which is the transformation property for any second-rank tensor \mathbf{T} constructed from coordinates.

In the terminology of groups (Section 2.5), the rotational-transformation coefficients for a second-rank tensor form a 9×9 matrix that is a 9-dimensional repre-

sentation (Section 2.5.3) of the rotation group, just as the vector transformation produces a 3-dimensional representation and the invariant scalar is a 1-dimensional representation. The nine components of a general second-rank tensor can be expressed in terms of one scalar, $T^{(0)}$, given by

$$T^{(0)} = \sum_p T_{pp} \quad (8.5)$$

plus three antisymmetric tensor components

$$T_{pq}^{(a)} = \frac{1}{2}(T_{pq} - T_{qp}) \quad (8.6)$$

plus a symmetric tensor with five independent components and zero trace

$$T_{pq}^{(s)} = \frac{1}{2}(T_{pq} + T_{qp}) - \frac{1}{3}T^{(0)}\delta_{pq} \quad (8.7)$$

Under rotations, each set of components transforms within the same set, thus forming an *irreducible representation* (Section 2.5.5) of the rotation group.

These considerations of familiar scalars, vectors, and second-rank tensors—especially their properties under rotations—lead us to irreducible tensor operators.

8.1 DEFINITION OF IRREDUCIBLE TENSOR OPERATORS

There are two primary definitions of irreducible spherical tensor operators. The first is in terms of properties under finite rotations, while the second—due to Racah—is in terms of infinitesimal rotations through the commutation properties of the tensor elements with angular momentum operators. We examine both of these in turn.

One impediment to developing irreducible tensors is that both definitions are implicit rather than constructive. That is, they specify what properties the tensor must have, rather than providing a prescription for generating the elements of the tensor. An exception to this is in Racah's definition, which requires one element to initiate the construction, as shown in Section 8.1.2.

8.1.1 Defining Irreducible Spherical Tensors

The nomenclature commonly used for the tensor operators is that each quantity T_{kq} ($q = -k, -k+1, \dots, k-1, k$) is one of $2k+1$ *elements* of the rank- k tensor \mathbf{T}_k , just as V_i is one of three elements of the vector \mathbf{V} . (Note that—rather than wrestling with the Greco-Roman convention—we use q rather than κ for the projection of k .) The components of the irreducible spherical tensor operator \mathbf{T}_k (often just called a “tensor operator”) transform under rotation through the Euler angles (Section 1.3.1) of $(\alpha\beta\gamma)$ according to

$$T_{kq}(\alpha\beta\gamma) = \sum_{q'=-k}^k T_{kq'}(0) D_{q'q}^k(\alpha\beta\gamma) \quad (8.8)$$

where the $D_{q'q}^k$ are the rotation matrix elements (Chapter 6) associated with total angular momentum k . Note that even though the $T_{kq'}$ often involve differential operators, they do not act on the D -matrix elements. The correspondence between this relation and the transformation of angular momentum eigenstates (j, m) under rotations is $k \sim j$ and $q \sim m$.

The *irreducibility* in relation (8.8) is that rotations maintain the rank of the tensor (same unique k on both sides), just as for the irreducibility of a group representation (Section 2.5.5) and the j representations of angular momentum operators (Section 3.4.1). A matrix representation (in the group sense discussed in Section 2.5.3) will therefore be block-diagonal in k , and each block will be of size $(2k+1) \times (2k+1)$, corresponding to the allowed range of q values. Thus, as shown by the examples in the introduction to this chapter, there are 1-, 3-, and 5-dimensional representations for scalars, vectors, and (second-rank) tensors, respectively.

The overall normalization of the tensor, including complex phases that are independent of q , does not affect its rotation properties, since relation (8.8) is linear. Indeed, confusion as to normalization of tensors whose properties are otherwise similar is a constant problem.

8.1.2 Racah's Definition and Its Applications

In his pioneering work on rotational symmetry in atomic spectroscopy, Racah [Rac42] introduced alternative requirements that a set of $2k+1$ quantities, T_{kq} with $q = -k, -k+1, \dots, k-1, k$, must satisfy to qualify as a rank- k irreducible spherical tensor. Racah's requirements are that the commutators

$$[J_0, T_{kq}] = [J_z, T_{kq}] = q T_{kq} \quad q = -k, -k+1, \dots, k-1, k \quad (8.9)$$

and that with the ladder operators for angular momentum the commutators

$$[J_{\pm 1}, T_{kq}] = \sqrt{(k \mp q)(k \pm q + 1)} T_{kq \pm 1} \quad q = -k, -k+1, \dots, k-1, k \quad (8.10)$$

in which the $J_{\pm 1}$ are also the angular momentum operator components in the spherical basis (Sections 3.1.3, 3.4.2). Note the similarity of requirements (8.9) and (8.10) to the properties of angular momentum eigenstates in Section 3.4, again suggesting the close correspondence between spherical tensor operators and state vectors.

Proof of Equivalence. To show that the original definition, (8.8), is equivalent to Racah's rules, consider first an infinitesimal rotation about the z axis through angle δ_z . The Euler angles describing the rotation are thus $\alpha = \delta_z$, $\beta = 0 = \gamma$. The right-hand side of (8.8) is then

$$\sum_{q'} T_{kq'}(0) D_{q'q}^k(\delta_z 00) = e^{-iqz} T_{kq}(0) \tag{8.11}$$

in which the single zero in the tensor abbreviates (000) for the Euler angles. The left-hand side of (8.8) becomes the rotated operator

$$T_{kq}(\delta_z 00) = e^{-i\delta_z J_z} T_{kq}(0) e^{i\delta_z J_z} \tag{8.12}$$

If we now expand these last two equations through first order in δ_z , we find that they are equal provided that (8.9) is satisfied.

Having seen the method of proof for the easiest rotation axis, namely the eigenvalue axis z , we can extend it for x and y axis rotations, as follows. Let λ denote either x or y ; then the operator for an infinitesimal rotation about the λ axis through angle δ_λ can be approximated by $I - i\delta_\lambda J_\lambda$ and its Hermitian conjugate requires just a sign change of the second term. The operator matrix elements are approximated by

$$D_{q'q}^k(\delta_\lambda) \approx \delta_{q'q} - i\delta_\lambda \langle kq' | J_\lambda | kq \rangle \tag{8.13}$$

By inserting the operators and matrix elements in the definition, then simplifying and taking the limit $\delta_\lambda \rightarrow 0$, it is straightforward to show (as Problem 8.1 suggests doing) that

$$[J_\lambda, T_{kq}] = \sum_{q'} T_{kq'} \langle kq' | J_\lambda | kq \rangle \tag{8.14}$$

The Racah definition (8.10) follows upon combining J_x and J_y to give $J_{\pm 1}$ and substituting for the matrix elements. The two conditions (8.9) and (8.10) can be summarized as

$$\begin{aligned}
 [J_\sigma, T_{kq}] &= \frac{1}{\sqrt{2}} \sqrt{k(k+1)} \langle 1k\sigma q | 1k1\sigma+q \rangle \\
 &= \frac{1}{\sqrt{2}} (-1)^{k-q-\sigma} \sqrt{k(k+1)(2k+1)} \begin{pmatrix} 1 & k & k \\ \sigma & q & -\sigma-q \end{pmatrix} T_{k\sigma+q} \\
 \sigma &= \pm 1, 0
 \end{aligned}
 \tag{8.15}$$

As a mnemonic for the 3- j coefficient, note that J_σ is a vector (rank 1), that there is

rank- k T_{kq} on the left-hand side, and that they combine to $T_{k,q+\sigma}$ on the right-hand side. Spherical tensors can be either generated or tested by using the Racah definition, as we now show for several practical examples.

Vectors as Spherical Tensors by the Racah Definition. Since the z component of a vector \mathbf{V} commutes with J_z , (8.9) shows that $V_z = V_0$, the $q = 0$ component of a $k = 1$ tensor. The other two tensor components, $V_{\pm 1}$, can therefore be generated by using (8.10). From the commutation relations of V_z with the angular momentum operators, it is straightforward to show that

$$V_{\pm 1} = \mp (V_x \pm iV_y) \quad (8.16)$$

in agreement with (4.44), apart from a different choice of normalization. The set of angular momentum operators when expressed in the spherical basis, as in Section 3.1.3, provide an example of vector operators.

Spherical Harmonics and Irreducible Tensors. Spherical and solid harmonics (Sections 4.1.3 and 4.1.4, respectively) are examples of irreducible tensors, in the following sense. The spherical harmonic Y_{kq} (k a non-negative integer) satisfies transformation property (8.8), being an angular momentum eigenstate. Therefore, the set $\{Y_{kq}, q = -k, \dots, k\}$ gives the components of a rank- k tensor. The Racah definition is just the way we generate the spherical harmonics in Section 4.1.3. Here the “operators” are just number operators in an angle space.

Angular Momentum Operators as Tensors. As an example of testing a set of operators to see whether they compose a spherical tensor, consider the angular momentum operators in the spherical basis, J_q with $q = \pm 1, 0$, themselves. As Problem 8.2 suggests that you show in detail, these form the components of a rank-1 tensor operator. The spherical-basis unit vectors $\hat{\mathbf{e}}_\sigma$ given by (4.38) and the angular momentum basis vectors \mathbf{S}_σ defined by (4.46), where $\sigma = \pm 1, 0$, can be tested similarly to show that they are rank-1 tensor operators.

Gradient Operator in Spherical Basis as a Rank-1 Spherical Tensor. Suppose that we construct the gradient operator, ∇ , with its components ∇_q given in the spherical basis. Since we have a function only of coordinates, the general considerations in Section 3.2 show that $J_\sigma \rightarrow L_\sigma$. It is straightforward but tedious (so deferred to Problem 8.3) to show that the components of the gradient satisfy

$$\begin{aligned} [L_\sigma, \nabla_q] &= (-1)^\sigma \sqrt{2} \langle 11q + \sigma, -\sigma | 111q \rangle \nabla_{\sigma+q} \\ &= (-1)^{\sigma+q} \sqrt{6} \begin{pmatrix} 1 & 1 & 1 \\ \sigma & q & -\sigma - q \end{pmatrix} \nabla_{\sigma+q} \end{aligned} \quad (8.17)$$

This result is particularly useful for electromagnetic multipole fields [Ros57, Section 25].

Adjoint of a Tensor Operator. To find the adjoint (Hermitian conjugate) of a tensor operator, consider the Racah definitions (8.9) and (8.10), then take the Hermitian conjugate (\dagger) on both sides. By using (2.45) to relate commutators and adjoints, then (3.10) for the adjoint of the spherical-basis angular momentum operators, we find the requirement that

$$\begin{aligned} [J_0, T_{kq}^\dagger] &= -qT_{kq}^\dagger \\ [J_{\pm 1}, T_{kq}^\dagger] &= -\sqrt{(k \pm q)(k \mp q + 1)} T_{kq}^\dagger \end{aligned} \tag{8.18}$$

which is satisfied by

$$T_{kq}^\dagger = (-1)^{p-q} T_{k,-q} \tag{8.19}$$

for any exponent p . For example, the choice $p = 0$ is appropriate for the angular momentum operators and the spherical harmonics.

Matrix elements of tensor operators and their adjoints that are related by (8.19) are connected by

$$\langle jm | T_{kq} | j'm' \rangle = (-1)^{p-q} \langle j'm' | T_{k,-q} | jm \rangle^* \tag{8.20}$$

So a consistent choice of p is required when matrix elements are calculated and combined. We usually leave p as a variable.

8.2 COMBINING IRREDUCIBLE TENSORS

In Chapter 7 we develop techniques for combining the eigenstates of angular momentum operators. Now that we have devised spherical tensor operators, which transform under rotations just like wave functions, we develop combinations of these operators. We first discover a general procedure (Section 8.2.1), then we specialize in Section 8.2.2 to the case of building a scalar ($k = 0$ tensor) from two tensors of the same rank, analogous to the scalar product of two vectors. In both sections we develop several applications of coupled tensors.

8.2.1 Building Up Irreducible Spherical Tensors

The correspondence between irreducible tensor operators and angular momentum eigenstates exhibited in Figure 8.1 becomes even more apparent when coupling of tensors is considered. Let $T_{k_1q_1}(A_1)$ and $T_{k_2q_2}(A_2)$ be elements of irreducible tensor operators of ranks k_1 and k_2 , respectively. It does *not* need to be assumed—unlike in Section 7.1.2 for combining two angular momentum eigenstates—that labels A_1 and A_2 indicate distinct systems. When no ambiguity is likely, we omit the

labels. Ordering of the operators $T_{k_1, q_1}(A_1)$ and $T_{k_2, q_2}(A_2)$ is significant, however.

The Building-Up Formula. Consider the direct-product combination of tensor operators formed in exact analogy to the combination of independent angular momenta given by (7.60), namely:

$$\begin{aligned}
 T_{KQ}(A_1, A_2) &= \sum_{q_1, q_2} T_{k_1, q_1}(A_1) T_{k_2, q_2}(A_2) \\
 &\times (-1)^{k_1 - k_2 + Q} \sqrt{2K + 1} \begin{pmatrix} k_1 & k_2 & K \\ q_1 & q_2 & -Q \end{pmatrix}
 \end{aligned} \tag{8.21}$$

in which the sum over q_1 and q_2 is constrained to values for which $q_1 + q_2 = Q$. To prove that the left-hand side really is a tensor operator of rank K and projection Q , consider a rotation of each of the component tensors through the *same* Euler angles, just as for the rotation matrices in Section 7.5. Each component tensor is transformed according to (8.8). By following through the algebraic steps suggested in Problem 8.4, you can show directly that the expression on the right-hand side of (8.21) transforms under rotations with $D_{Q'Q}^K$, so it is (by definition) a tensor of rank K with components Q . Since only a single value of K is required for this rotation, (8.21) really does define a component of an *irreducible* tensor.

Thus, merely by using the machinery of angular momentum coupling developed in Chapter 7 and extended in Chapter 9, we can take two tensors of ranks k_1 and k_2 then use them to build up tensors of all ranks K between $|k_1 - k_2|$ and $k_1 + k_2$. Although we use the term "building up," a useful special case of (8.21) is to contract two tensors of the same rank to a scalar, rank $K = 0$. This case we develop in detail in Section 8.2.2.

Note that there is generally no simple relationship between $T_{KQ}(A_1, A_2)$ and $T_{KQ}(A_2, A_1)$, unless the component operators commute. In this case we have

$$\begin{aligned}
 T_{KQ}(A_2, A_1) &= (-1)^{k_1 + k_2 + K - 2Q} T_{KQ}(A_1, A_2) \\
 &\text{if component tensors commute}
 \end{aligned} \tag{8.22}$$

We now give several examples of using the tensor coupling formula (8.21) to construct tensors of rank higher than zero that are interesting for the physical sciences. The rank of the irreducible tensors formed generally increases from example to example.

Vector Cross Products in Spherical Tensor Representation. Suppose that we have two conventional vectors, **A** and **B**. Convert them first to their rank-1 complex spherical basis components, as derived in Section 4.2.1. Then combine them to form another rank-1 tensor ($K = 0$) by using (8.21). After some tedious algebra, deferred to Problem 8.5, you may find that

$$\begin{aligned}
 X_{1\sigma}(\mathbf{A}, \mathbf{B}) &\equiv \sum_{\sigma_1, \sigma_2} A_{\sigma_1} B_{\sigma_2} (-1)^\sigma \sqrt{3} \begin{pmatrix} 1 & 1 & 1 \\ \sigma_1 & \sigma_2 & -\sigma \end{pmatrix} \\
 &= \frac{i}{\sqrt{2}} (\mathbf{A} \times \mathbf{B})_\sigma
 \end{aligned} \tag{8.23}$$

Note that \mathbf{X} reverses sign if \mathbf{A} and \mathbf{B} are interchanged, as we expect for a cross product and as agrees with (8.22) for $k_1 = k_2 = K = 1$ and $Q = \sigma$ an integer. Generally, \mathbf{X} is complex even if the components of \mathbf{A} and \mathbf{B} in the Cartesian basis are real.

Rank-2 Tensors from Vectors. Suppose that we follow a similar procedure as when deriving (8.23), but now combine the vectors to form a $K = 2$ tensor. Thus

$$T_{2\sigma}(\mathbf{A}, \mathbf{B}) \equiv \sum_{\sigma_1, \sigma_2} A_{\sigma_1} B_{\sigma_2} (-1)^\sigma \sqrt{5} \begin{pmatrix} 1 & 1 & 2 \\ \sigma_1 & \sigma_2 & -\sigma \end{pmatrix} \tag{8.24}$$

After a little busywork, one finds the second-rank tensor components

$$\begin{aligned}
 T_{2, \pm 2} &= A_{\pm 1} B_{\pm 1} & T_{2, \pm 1} &= \frac{1}{\sqrt{2}} (A_{\pm 1} B_0 + A_0 B_{\pm 1}) \\
 T_{20} &= \frac{1}{\sqrt{6}} (A_1 B_{-1} + 2A_0 B_0 + A_{-1} B_1) = \frac{1}{\sqrt{6}} (3A_z B_z - \mathbf{A} \cdot \mathbf{B})
 \end{aligned} \tag{8.25}$$

only the last of which is simple in terms of Cartesian-coordinate components of \mathbf{A} and \mathbf{B} . Notice that T_{2q} is symmetric with respect to interchange of \mathbf{A} and \mathbf{B} . As you can see by inspection of T_{20} , it will transform under rotations by the Legendre polynomial P_2 , as the primary definition (8.8) requires. The advantage of casting familiar vector relations into the unfamiliar spherical tensor forms is that the tensors so formed have the simple rotation property (8.8).

Bipolar Harmonics. As pointed out in Section 8.1.1, spherical harmonics of a given k with q varying form components of a rank- k spherical tensor. We can therefore combine products of spherical harmonics with angles that may differ. Let $\Omega = (\theta\phi)$ and $\Omega' = (\theta'\phi')$, then we construct the bipolar harmonic B_{LM} as

$$\begin{aligned}
 B_{LM}(\Omega, \Omega') &= \sum_{m_1, m_2} Y_{\ell_1 m_1}(\Omega) Y_{\ell_2 m_2}(\Omega') \\
 &\times (-1)^{\ell_1 - \ell_2 + M} \sqrt{2L+1} \begin{pmatrix} \ell_1 & \ell_2 & L \\ m_1 & m_2 & -M \end{pmatrix}
 \end{aligned} \tag{8.26}$$

As an example of using bipolar harmonics, suppose that two particles are in orbital angular momentum states ℓ_1 and ℓ_2 . The two-particle system state constructed

using (8.26) is then in a definite orbital state L . Most commonly, the particles will be quarks, nucleons, or electrons in atoms, but (heaven forbid!) they may also be astronomical objects with small values for their geometrical angular momentum, as in the example in Section 7.5.4.

Vector Spherical Harmonics. When considering a scalar field equation—such as the Schrödinger equation for the probability amplitude ψ in Chapter 5—it is sufficient to use the orbital angular momentum eigenfunctions $Y_{\ell m}(\theta\phi)$ (Section 4.1). However, with vector field equations—such as the Maxwell equations for the electromagnetic field (Sections 1.4.3, 4.2.3)—the spherical harmonics have to be combined with vectors to indicate directions. This is the purpose of the *vector spherical harmonics*, defined by

$$\mathbf{Y}_{L\ell,M}(\theta\phi) = \sum_{\sigma} Y_{\ell,M-\sigma}(\theta\phi) \hat{\mathbf{e}}_{\sigma} (-1)^{\ell-1+M} \sqrt{2L+1} \begin{pmatrix} \ell & 1 & L \\ M-\sigma & \sigma & -M \end{pmatrix} \quad (8.27)$$

in which $\hat{\mathbf{e}}_{\sigma}$ with $\sigma = \pm 1, 0$ is a spherical-basis unit vector (Section 4.2.1). Note that the factors after the unit vector comprise the Clebsch-Gordan coefficient for combining angular momenta ℓ and unity to make L . The so-called *multipolarity* of the vector field, L , is thus $L = |\ell - 1|$, ℓ , or $\ell + 1$, having three values if $\ell > 0$.

Notations for vector spherical harmonics are quite variable. That used in (8.27) indicates their essential character, namely that $\mathbf{Y}_{L\ell,M}(\theta\phi)$ is a vector depending on angles $(\theta\phi)$ with respect to the unit vectors and that it is a component of a rank- L tensor of $2L + 1$ components having projection number M .

Vector spherical harmonics are used extensively to discuss the electromagnetic field—as in Rose’s monograph [Ros55], in Section 7.6 of Biedenharn and Louck [Bie81a], and in Section 6.1 of the handbook by Brink and Satchler [Bri94]. These harmonics—and generalizations of them to higher-rank tensor harmonics—are also useful in geophysics and fluid dynamics, as developed in Jones’ monograph on spherical harmonics and tensors for classical field theory [Jon85].

8.2.2 Contraction of Irreducible Tensors to Scalars

In the physical sciences, interactions within a system are almost always described in terms of scalars, since it is assumed that the system is isolated and that space is isotropic. A primary construction involving spherical tensors is therefore contraction to a scalar tensor, $K = 0$. The general building-up formula therefore requires that $k_1 = k_2 = k$, say. From (8.21) and the 3- j coefficient with $K = 0$ it is easy to show (as Problem 8.6 suggests doing) that

$$T_{00}(A_1, A_2) = \frac{1}{\sqrt{2k+1}} \sum_q (-1)^{k-q} T_{kq}(A_1) T_{k-q}(A_2) \quad (8.28)$$

Note that T_{00} is rotationally invariant. In practical examples of tensors k (and therefore q) is an integer, as seen in Section 8.2.1. Then, by the phase manipulation rules (Section 2.1.4), we can factor $(-1)^k$ out of the sum. This leads to the definition of the *scalar product* $\mathbf{T}_k(A_1) \cdot \mathbf{T}_k(A_2)$ of two irreducible tensors:

$$\begin{aligned} \mathbf{T}_k(A_1) \cdot \mathbf{T}_k(A_2) &\equiv (-1)^k \sqrt{2k+1} T_{00}(A_1, A_2) \\ &= \sum_q (-1)^q T_{kq}(A_1) T_{k-q}(A_2) \end{aligned} \quad (8.29)$$

Unlike general rule (8.21) for combining tensors, the scalar product is independent of the order of the two tensors if they commute. In terms of Hermitian conjugates of tensors, the scalar product may be rewritten by using (8.19) as

$$\begin{aligned} \mathbf{T}_k(A_1) \cdot \mathbf{T}_k(A_2) &= (-1)^p \sum_q T_{kq}(A_1) T_{kq}^\dagger(A_2) \\ &= (-1)^p \sum_q T_{kq}^\dagger(A_1) T_{kq}(A_2) \end{aligned} \quad (8.30)$$

The equivalence of these two forms does not require commutation of operators.

Examples of Scalar Products. The first example of scalar products is from Section 4.2.1, where we form the scalar product of two spherical-basis vectors as (4.40) and (4.41), which involves the complex conjugate of one of them. We now see that this illustrates the property (8.30) with $k = 1$ and p chosen to be zero.

The second example is to choose the two T_{kq} as spherical harmonics with different angles $A_1 = \Omega'$, $A_2 = \Omega$. Their scalar product is proportional to the Legendre polynomial, P_k , of the angle between A_1 and A_2 , as shown in Figure 4.6 and derived as the spherical harmonic addition theorem (4.23).

What is the rotational invariance of this scalar product? It is that the value depends only upon ω , the angle *between* A_1 and A_2 and is therefore independent of orientation of the coordinate system. Indeed, we anticipated this property in order to derive the theorem. It is perhaps puzzling—yet still true—that $P_k(\cos \omega)$ is a scalar (rank of zero) but also has angular momentum numbers $j = k$ and $m = 0$, as discussed in Section 4.1. The latter properties, however, assume that the orbital angular momentum operators are expressed in terms of ω rather than $(\theta'\phi')$ and $(\theta\phi)$. Notice that—within proportionality factors—the bipolar harmonic of rank zero in Section 8.2.1 also just expresses the spherical harmonic addition theorem.

8.3 WIGNER-ECKART THEOREM; REDUCED MATRIX ELEMENTS

We now come to one of the most remarkable results in rotational symmetries for physical systems: the Wigner-Eckart theorem. For an operator given in irreducible spherical tensor form, the theorem allows separation between geometrical and dy-

namical aspects of matrix elements of the operator taken between angular momentum eigenstates. The truth of the theorem (like most results in angular momentum) does not depend upon quantum mechanics, although the Wigner-Eckart theorem finds very fruitful application in that discipline.

The Wigner-Eckart theorem—like many a beautiful flower—was born to blush unseen. Wigner anticipated it in a remark made in a 1927 paper on atomic spectroscopy [Wig27b, below equation (16e)]. In his 1930 article [Eck30] Eckart obtained the result in Section 24 by using group theory methods, but did not emphasize its importance. Wigner in his 1931 book [Wig31] mentioned the theorem in passing, below equation (21.19), and attributed it to Eckart.

In Section 8.3.1 we derive the theorem and discuss its interpretation, then in Section 8.3.2 we discuss conventions used for the reduced matrix elements which appear in its statement. Finally in this section, several examples of determining and using reduced matrix elements are worked out in Section 8.3.3.

8.3.1 Geometry and Dynamics: The Wigner-Eckart Theorem

Deriving the Wigner-Eckart Theorem. A simple way to derive the theorem is to use rotational invariance of matrix elements with both states and operators rotated. We can write

$$\langle jm|T_{kq}|j'm'\rangle = \langle jm|U^\dagger U T_{kq} U^\dagger U|j'm'\rangle \quad U = U(\alpha\beta\gamma) \quad (8.31)$$

in which U is the unitary rotation operator ($U^\dagger U = I$) for Euler angles $(\alpha \beta \gamma)$, as shown in Figure 6.1. By applying the rotations to each of the three quantities—bra, operator, and ket—using (6.19) or (8.8), one obtains (as you may show in Problem 8.7) a complicated expansion into products of three D-matrix elements, valid for all Euler angles. By integrating over these angles through the range R given in (7.98), a factor of $16\pi^2$ is obtained on both the left- and right-hand sides. The resulting expression is an identity only if the tensor matrix elements satisfy the *Wigner-Eckart theorem*

$$\langle jm|T_{kq}|j'm'\rangle = (-1)^{2k} \langle j'km'q|j'kjm\rangle \langle j||\mathbf{T}_k||j'\rangle \quad (8.32)$$

Here $\langle j||\mathbf{T}_k||j'\rangle$ is called the *reduced matrix element* of operator \mathbf{T}_k . It is conventional to state the theorem in terms of a Clebsch-Gordan coefficient rather than a 3- j coefficient, an unfortunate practice to which we defer.

Irreducible spherical tensor operators therefore have matrix elements in the angular momentum basis in which the dependence on projection numbers is completely contained in a coupling coefficient. Thus, if the quantization axis is changed by rotating the system, then only this coefficient changes, but the reduced matrix element is unchanged. The Wigner-Eckart theorem factors matrix elements of spherical tensors into a geometrical part (the coupling coefficient) and a dynamical part (the reduced matrix element). We make a similar distinction between

geometry and dynamics in Section 3.4.5 when discussing the interpretation of angular momentum.

Another way to derive the Wigner-Eckart theorem is to show the proportionality of the matrix elements in an angular momentum basis to the Clebsch-Gordan coefficient by showing that they satisfy the same selection rules and recurrence relations. The Racah rules (8.9) and (8.10) are convenient for this. Consider the matrix elements of the commutation of T_{kq} with J_0 , given as

$$\langle jm|J_0 T_{kq}|j'm'\rangle - \langle jm|T_{kq} J_0|j'm'\rangle = q \langle jm|T_{kq}|j'm'\rangle \tag{8.33}$$

Operating with $J_0 = J_z$ to the left and right in the two matrix elements produces

$$(m - q - m') \langle jm|T_{kq}|j'm'\rangle = 0 \tag{8.34}$$

so the nonzero matrix elements satisfy the same m -selection rule as the Clebsch-Gordan coefficient with $q + m' = m$. Next, by considering similarly the matrix elements of the second commutator (8.10) it is straightforward to show (as you may do in Problem 8.8) that the T_{kq} satisfy the same recurrence relations for k fixed and q varying as the Clebsch-Gordan coefficient with the same total and projection numbers, thus proving the theorem.

The Wigner-Eckart theorem can also be derived by using methods of group theory (Section 2.5), as in Eckart's [Eck30] and Wigner's [Wig31] original treatments, and in Sections 4.20 and 7.4 of Elliott and Dawber [Ell79] or in Sections 6.2 and 11.3 of Ludwig and Falter [Lud88].

A Simple Example of the Theorem. Before continuing with generalities, consider a concrete example of (8.32). As discussed in Section 8.1.2, the set of spherical harmonics $\mathbf{Y}_k(\Omega) \equiv \{Y_{kq}(\Omega), q = -k, \dots, k\}$ is a rank- k irreducible spherical tensor having multiplication as its operation. The Gaunt integral formula (7.102) gives the integral over the product of three spherical harmonic functions. We identify the outer functions as the orthonormal eigenstates for orbital angular momentum (Section 4.1) and the middle function as an element of the \mathbf{Y}_k tensor. From (7.102) we make the transcriptions $LM \rightarrow \ell m$, $\ell_1 m_1 \rightarrow kq$, and $\ell_2 m_2 \rightarrow \ell' m'$. After some manipulations from 3- j to Clebsch-Gordan coefficients (as suggested in Problem 8.9), we identify by inspection the reduced matrix element for the spherical harmonic tensor \mathbf{Y}_k as

$$\begin{aligned} \langle \ell \| \mathbf{Y}_k \| \ell' \rangle &= \sqrt{\frac{2k+1}{4\pi}} (-1)^k \langle k\ell 00 | k\ell\ell' 0 \rangle \\ &= \sqrt{\frac{(2k+1)(2\ell+1)}{4\pi}} (-1)^\ell \begin{pmatrix} \ell & k & \ell' \\ 0 & 0 & 0 \end{pmatrix} \end{aligned} \tag{8.35}$$

Notice that because of the occurrence of the parity-conservation coefficient with

all projections zero (discussed in Sections 7.3.1, 7.3.2), the reduced matrix element is zero unless $\ell + k + \ell'$ is even. The nonzero matrix elements can be obtained in terms of expression (7.73) for a 3- j coefficient with all projections zero.

Selection Rules for Irreducible Tensor Matrix Elements. Immediately from the Wigner-Eckart theorem (8.32) we see selection rules on matrix elements of an operator T_{kq} between angular momentum eigenstates. Namely:

$$\begin{array}{l}
 m \neq q + m' \quad \Rightarrow \quad \langle jm | T_{kq} | j' m' \rangle = 0 \\
 k < |j - j'| \quad \text{or} \quad k > j + j' \quad \Rightarrow \quad \langle jm | T_{kq} | j' m' \rangle = 0
 \end{array}
 \tag{8.36}$$

The first necessary condition is just conservation of projections, since we can consider that T_{kq} acts on the state with projection m' to give projection $q + m'$, which must match the m in the bra state. For the second condition, it can be considered that, for example, k and j' combine to form total angular momentum states of which the one with a total angular momentum j must be a member, so the three angular momenta must comprise the sides of a triangle.

The rules in (8.36) are necessary for nonzero matrix elements, but are far from sufficient, since other symmetries—such as “parity conservation” discussed below (8.35)—may require zero matrix elements.

Using the Wigner-Eckart Theorem. We now summarize in words and pictures (Figure 8.2) general procedures for using the Wigner-Eckart theorem. Three major steps are involved in applying the theorem. First, the state vectors of the system under investigation (wave functions in quantum mechanics) must be expanded into angular momentum bases, such as the partial-wave expansion in scattering (Section 5.4). Second, one must discover the irreducible tensor expansion of the operators, as we do for some common operators in Sections 8.1.2 and 8.2.1.

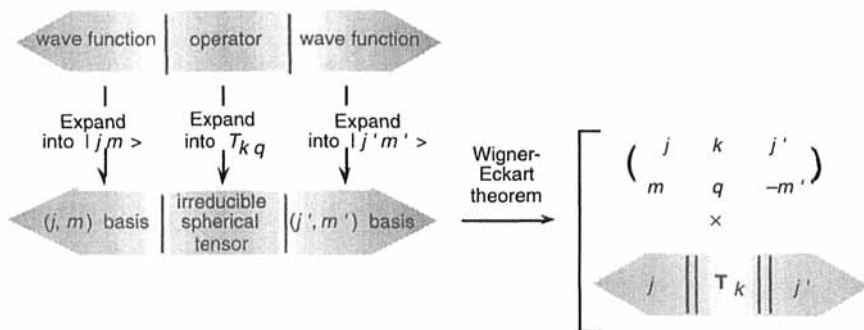


FIGURE 8.2 Schematic of the process of reducing calculation of a matrix element to use of the Wigner-Eckart theorem.

The third step in using the Wigner-Eckart theorem is to identify the reduced matrix elements of the operators, as for the spherical harmonics in (8.35).

In Section 8.3.3 we continue this procedure for basic operators in simple angular momentum states, then we develop formulas for combined states in Sections 9.4 and 9.5. Given this overview of using the Wigner-Eckart theorem, it is necessary to be aware of conventions for reduced matrix elements.

8.3.2 Conventions for Reduced Matrix Elements

The reduced matrix elements $\langle j \| \mathbf{T}_k \| j' \rangle$ appearing in the Wigner-Eckart theorem, (8.32), are subject to considerable ambiguity, arising from three sources. First, for a given type of operator and rank k , linearity of the definitions (8.15), or (8.9) and (8.10), allows an overall normalization factor for the operator. This factor may depend on k but it must be independent of q for this k .

Second, the normalization of the bra and ket states needs to be specified through the representation space used and (in configuration space, for example) the range of integrations. For example, the states may be normalized to unity.

Third, in the reduced matrix element factorization on the right-hand side of (8.32) the factoring between the matrix elements, the phases, and the normalization differences that arise from rearranging arguments in the Clebsch-Gordan coefficient is not always uniform. A definition using 3- j coefficients is awkward because in (8.32) it introduces a phase that depends upon the projection number q .

The convention that we adopt for reduced matrix elements is the same as that of Brink and Satchler [Bri94], which explains the phase of $(-1)^{2k}$ inserted in the defining (8.32) and the order of the arguments in the Clebsch-Gordan coefficient. The phase is significant only for the unusual case that k is not an integer.

8.3.3 Determining and Using Reduced Matrix Elements

We now determine and show how to use reduced matrix elements for several interesting operators occurring in the physical sciences. Then we derive some general formulas for reduced matrix elements. To give you practice, our first example is worked in detail.

A Worked Example: Quadrupole Moments. The electric quadrupole moment of an assembly of charges with charge density $\rho(\mathbf{r})$ is given classically by

$$Q_0 = e \int (3z^2 - r^2) \rho(\mathbf{r}) d\mathbf{r} \quad (8.37)$$

in which the integral is over all space, or effectively that region in which the charge density is nonzero. The situation is sketched in Figure 8.3.

In the quantum mechanics version of (8.37) one writes the factor before the density as the *quadrupole operator*, $Q_0^{(2)}$, defined by

$$Q_0^{(2)} \equiv 3z^2 - r^2 = r^2 \sqrt{\frac{16\pi}{5}} Y_{2,0}(\theta, \phi) \quad (8.38)$$

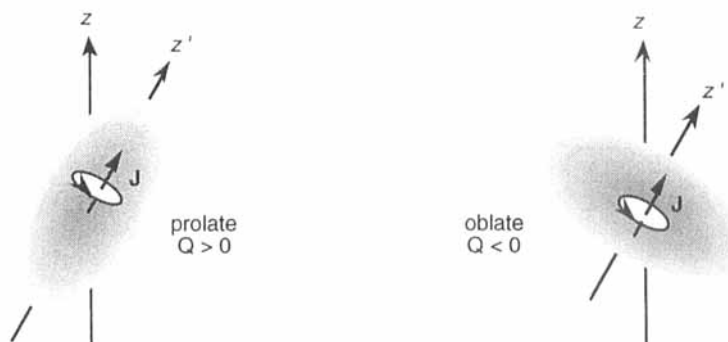


FIGURE 8.3 Charge distributions for prolate and oblate spheroids, having quadrupole moments (for $j > 1/2$) of $Q > 0$ and $Q < 0$, respectively.

In (8.38) we have expressed z in terms of polar-coordinate angles in a reference frame as yet undefined. The density becomes

$$\rho(\mathbf{r}) = e |\psi_{jm}|^2 \quad (8.39)$$

in which ψ_{jm} is the wave function of the state for which the quadrupole moment is to be measured. This state is assumed to have unique total angular momentum j and projection m onto the space-fixed axis z in Figure 8.3. If the object is a rigid body then, as in Section 6.5, we can associate with it a body-fixed axis, z' in Figure 8.3. We now calculate how the expectation value of $Q_0^{(2)}$ in the space-fixed frame depends on m and j .

From (8.38) we see that $Q_0^{(2)}$ is the $q = 0$ element of a rank $k = 2$ irreducible tensor. Using the Wigner-Eckart theorem, (8.32), we write

$$\begin{aligned} \langle jm | Q_0^{(2)} | jm \rangle &= \langle j 2 m 0 | j 2 jm \rangle \langle j || Q^{(2)} || j' \rangle \\ &= (-1)^{j-2+m} \sqrt{2j+1} \begin{pmatrix} j & 2 & j \\ m & 0 & -m \end{pmatrix} \langle j || Q^{(2)} || j' \rangle \end{aligned} \quad (8.40)$$

Immediately, from the triangle condition in (8.40) we see that this space-fixed-frame quadrupole moment is zero unless $j \geq 1$. In the semiclassical model of angular momentum (Section 5.3) this would be explained as saying that for states with $j = 0$ and $j = 1/2$ the “precession” of the angular momentum vector about the z axis averages to zero the quadrupole moment observed from this frame.

There is no denying that the quadrupole moment in the body-fixed frame may be nonzero. Indeed, if we replace charge density by mass density, then we are cal-

culating components of the inertia tensor in this frame, as discussed for the rigid rotator in Section 6.5. The result analogous to (8.40) is the vanishing of the inertia tensor in the *space-fixed* frame if $j < 1$.

Given that the triangle condition is satisfied ($j \geq 1$), there is no case for $-j \leq m \leq j$ when (8.40) predicts a zero result, since when $m = 0$ we have the parity-conservation 3- j coefficient (7.73) and j must be an integer with the sum of the total angular momenta in the coefficient—just $2j + 2$ —sure to be even. Indeed, the coupling coefficients in (8.40) can be evaluated as suggested in Problem 8.10 to produce

$$\langle jm|Q_0^{(2)}|jm\rangle = \frac{3m^2 - j(j+1)}{\sqrt{j(j+1)(2j-1)(2j+3)}} \langle j\|Q^{(2)}\|j\rangle \quad j \geq 1 \quad (8.41)$$

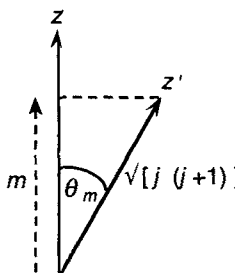
The (atomic) *spectroscopic quadrupole moment*, Q , is defined as $\langle jj|Q_0^{(2)}|jj\rangle$, so from (8.41) we deduce that

$$Q = \sqrt{\frac{j(2j-1)}{(j+1)(2j+3)}} \langle j\|Q^{(2)}\|j\rangle \quad (8.42)$$

which is consistent with vanishing matrix elements in the space-fixed frame for $j = 0$ and $j = 1/2$. The m dependence in (8.41) can then be simplified to

$$\begin{aligned} \langle jm|Q_0^{(2)}|jm\rangle &= \frac{3m^2 - j(j+1)}{j(2j-1)} Q \\ &= (3 \cos^2 \theta_m - 1) \frac{j+1}{2j-1} Q \quad j \geq 1 \end{aligned} \quad (8.43)$$

where θ_m is a quantized angle given by



$$\cos \theta_m = \frac{m}{\sqrt{j(j+1)}} \quad (8.44)$$

as sketched. The range of the cosine is $\pm\sqrt{j/(j+1)} < 1$, so that it is never quite aligned with the z axis, but approaches it as j increases. Thus, for $j = 6$, θ_j is about 0.4 rad (25 degree). Noting that the angle factor in (8.43) varies proportionally to $P_2(\cos \theta_m)$, we could in a semiclassical model interpret this as the conversion factor between the reference frames.

Now that we see how simple reduced matrix elements can be calculated and interpreted, there are several more matrix elements that are interesting and useful.

Position Operator Reduced Matrix Elements. The position operator $\mathbf{r} = r\hat{\mathbf{r}}$, where $\hat{\mathbf{r}}$ is the unit vector. Since the matrix elements in an orbital angular momentum basis involve only angles, r is just an overall factor in the matrix elements, so we set it to unity. Then (as you may verify in Problem 8.11) we have the following chain of equalities:

$$\begin{aligned}
 \langle \ell \| \hat{\mathbf{r}} \| \ell' \rangle &= \langle \ell \| r_0 \| \ell' \rangle = \langle \ell \| \cos \theta \| \ell' \rangle \\
 &= \sqrt{\frac{4\pi}{3}} \langle \ell \| Y_{10} \| \ell' \rangle = \sqrt{\frac{4\pi}{3}} \langle \ell \| \mathbf{Y}_1 \| \ell' \rangle \\
 &= -\langle 1\ell 0 0 | 1\ell \ell' 0 \rangle = (-1)^\ell \sqrt{2\ell'+1} \begin{pmatrix} 1 & \ell & \ell' \\ 0 & 0 & 0 \end{pmatrix}
 \end{aligned} \tag{8.45}$$

By using the algebraic expressions in Table 7.2 for the 3- j coefficients, we obtain

$$\langle \ell \| \hat{\mathbf{r}} \| \ell' \rangle = \begin{cases} -\sqrt{\frac{\ell+1}{2\ell+1}} & \ell' = \ell+1 \\ 0 & \ell' = \ell \\ \sqrt{\frac{\ell}{2\ell+1}} & \ell' = \ell-1 \end{cases} \tag{8.46}$$

Is it surprising that the reduced matrix element of \mathbf{r} —and therefore all its matrix elements—vanish for $\ell' = \ell$? Notice that (8.45) contains the parity conservation coupling coefficient discussed below (7.72), which vanishes for $\ell' = \ell$. To see why, note that in this case the product of angular momentum functions in the bra-ket is proportional to the absolute square of $Y_{\ell m}$, which has even parity because $Y_{\ell m}$ has a definite parity, whereas $\hat{\mathbf{r}} = \cos \theta$ has odd parity (Section 1.4.1, $P\theta = \pi - \theta$). The integral over θ is therefore zero.

Angular Momentum Operator Reduced Matrix Elements. To find the reduced matrix elements of \mathbf{J} it is easiest to consider its $q = 0$ component, namely $J_0 = J_z$, since this operator is diagonal in both j and m . Thus

$$\begin{aligned}
 \langle jm | J_0 | j' m' \rangle &= \langle jm | J_z | j' m' \rangle = m \delta_{jj'} \delta_{mm'} \\
 &= \langle j' 1 m' 0 | j' 1 j 0 \rangle \langle j \| \mathbf{J} \| j' \rangle \\
 &= (-1)^{j-m} \sqrt{2j+1} \begin{pmatrix} 1 & j & j \\ 0 & m & -m \end{pmatrix} \langle j \| \mathbf{J} \| j' \rangle
 \end{aligned} \tag{8.47}$$

To obtain this result, we use the Wigner-Eckart theorem in the second line and assume that only $j' = j$ is required for the third line. By looking up in Table 7.3 the 3- j coefficient then solving for the reduced matrix element, one readily finds

$$\langle j \| \mathbf{J} \| j' \rangle = \sqrt{j(j+1)} \delta_{jj'} \quad (8.48)$$

The selection rule on j is reasonable—since rotations conserve j , therefore certainly an infinitesimal rotation generated by \mathbf{J} leaves it unchanged. Note that this formula holds for any type of angular momentum, whether orbital (\mathbf{L} , Sections 3.2, 4.1) or spin (\mathbf{S} , Sections 3.5, 4.3).

More formulas for explicit reduced matrix elements are given in Table 8 of the appendix to [Bie81a].

General Formulas for Reduced Matrix Elements. There are three general formulas for reduced matrix elements, of which our examples above use only the first. The first general formula is

$$\langle j \| \mathbf{T}_k \| j' \rangle = (-1)^{2k} \langle jm | T_{kq} | j' m' \rangle / \langle j' k m' q | j' k j m \rangle \quad (8.49)$$

for any matrix element with nonzero Clebsch-Gordan coefficient

This is useful if one of the matrix elements is easy to calculate, as in our derivations of formulas (8.46) and (8.48).

The second general formula obtains the reduced matrix element from the sum rule for irreducible tensor matrix elements

$$\langle j \| \mathbf{T}_k \| j' \rangle = (-1)^{2k} \sum_{m'q} \langle j' k m' q | j' k j m \rangle \langle jm | T_{kq} | j' m' \rangle \quad (8.50)$$

while a similar formula that is less informative is

$$\langle j \| \mathbf{T}_k \| j' \rangle^2 = \sum_{m'q} |\langle jm | T_{kq} | j' m' \rangle|^2 \quad (8.51)$$

Although this expression cannot produce the phase of the reduced matrix element, it corresponds to a common experimental situation in which one averages uniformly over all magnetic substates when making a measurement. Thus, magnitudes of reduced matrix elements can be obtained. Problem 8.12 suggests that you derive formulas (8.50) and (8.51).

Reduced Matrix Elements for Hermitian Irreducible Tensors. Relation (8.20) can be used to relate reduced matrix elements for the usual case that the spherical tensor operator is Hermitian. By applying the Wigner-Eckart theorem to each side

of (8.20), then relating the coupling coefficients, it is easy to show (for example, by doing Problem 8.13) that

$$\boxed{\begin{aligned} \sqrt{2j+1} \langle j \| \mathbf{T}_k \| j' \rangle &= (-1)^{j-j'-p} \sqrt{2j'+1} \langle j' \| \mathbf{T}_k \| j \rangle^* \\ &\text{for } \mathbf{T}_k \text{ Hermitian} \end{aligned}} \quad (8.52)$$

in which p is often chosen as zero, as discussed below (8.20). Indeed, p must be zero if the operator has nonzero diagonal matrix elements. Examples satisfying (8.52) with $p = 0$ are the spherical harmonic tensor, \mathbf{Y}_k in (8.35), and the unit vector, $\hat{\mathbf{r}}$ in (8.46).

8.4 DENSITY MATRICES AND POLARIZATION TENSORS

Our goals in this section are twofold. First, in Section 8.4.1 we develop and apply some of the technology of density matrices in the context of intrinsic spins and relate this to irreducible spherical tensors for spin, such as polarization tensors. Second, as a relief from formalism, in Sections 8.4.2 and 8.4.3 we show how spin wave functions in quantum mechanics evolve in time, how the rotating-frame transformation can simplify the description of spin evolution, and how the problem of the transport of beam of spin-polarized particles through a magnetic field gradient can be solved using angular momentum techniques that we have developed.

8.4.1 Spin Density Matrices and Spin Tensors

In this section we review relevant properties of describing quantal systems by density matrices and we give examples of how such density matrices transform under rotations of a system relative to the reference frame. We then introduce spin tensors, which are irreducible spherical tensors used to describe ensembles of particles with spin. This leads to the concept of spin-polarization tensors, of which we give several examples.

An extensive treatment of angular momentum techniques using density matrices is given in Section 7.7 of [Bie81a]. Applications to polarized light and to polarization of ensembles of spin-1/2 or spin-1 particles (including relativistic treatment) are given in the monograph by Robson [Rob74]. A general treatment relating Cartesian and spherical components of tensors for spin polarization has been given by Normand and Raynal [Nor82].

The Density Matrix for Spin. In our descriptions of quantum-mechanical systems in previous chapters, particularly in Chapter 5, we use a *wave function* to characterize a state. According to the standard interpretation of quantum mechanics, this provides the maximum information that can be obtained about the system,

which is said to be in a *pure state*. Note that for such a state, there are still uncertainties for noncommuting variables measured in the same state, as we show for angular momentum in Section 5.2. Therefore, maximal information should not be equated with complete information.

Consider an ensemble, in the sense used in statistical mechanics. For a pure state, all components of the ensemble are described by the same wave function, usually expanded in terms of an appropriate basis. For present purposes, the ensemble is assumed to consist of particles all of which have the same spin, s , but a variety of projections, σ , consistent with this, namely $-s \leq \sigma \leq s$. A basis of spin states—which is complete, according to (2.73)—can be used to describe this ensemble of spins. Thus, the spin wave function for such a pure state is

$$|s, \nu\rangle = \sum_{\sigma=-s}^s a_{\sigma}^{(\nu)} |s\sigma\rangle \quad (8.53)$$

in which the label ν describes other properties of the system.

Pure states are the playgrounds of theorists, a nirvana devoutly to be wished. The reality of experiments in the physical sciences is that information about an ensemble is seldom maximal in the quantum-mechanical sense, but there is an averaging over at least some of the variables ν . The ensemble is then said to be in a *mixed state* (or *general state*), and it is characterized by a density matrix ρ , whose elements are defined by

$$\rho_{\sigma\sigma'} \equiv \sum_{\nu} a_{\sigma}^{(\nu)} [a_{\sigma'}^{(\nu)}]^* \quad (8.54)$$

where the sum (or an integral) is over all unobserved variables ν . This may be, for example, a distribution of temperatures or velocities—in which case summation in (8.54) would be replaced by integration. It is usual for the amplitudes $a_{\sigma}^{(\nu)}$ to be normalized—to describe a probability distribution, for example.

Density matrices are Hermitian (Section 2.1.3):

$$\rho_{\sigma\sigma'} = \rho_{\sigma'\sigma}^* \quad (8.55)$$

as can readily be seen by inspection of the definition (8.54). Thus, according to theorem (2.70), there is a unitary transformation that diagonalizes it. In our context, in which rows and columns are labeled by spin projections, this transformation is a rotation. In the diagonal representation, the nonzero elements are proportional to the populations in each magnetic substate:

$$P_{\sigma} = |a_{\sigma}|^2 \quad \text{in diagonal representation} \quad (8.56)$$

For example, for a spin $s = 1$ system, we have $P_{\pm} = P_{\pm 1}$ and P_0 as the populations of the three possible magnetic substates. It is usual to choose normalizations such that these populations are actually fractions with a sum of unity.

Operator Expectation Values. The expectation value of an operator, P , in an ensemble characterized by density matrix ρ is given by

$$\langle P \rangle = \sum_{\sigma, \sigma'} \rho_{\sigma\sigma'} P_{\sigma'\sigma} = \text{Tr}(\rho P) = \text{Tr}(P\rho) \quad (8.57)$$

where, from the discussion below (2.34), recall that the order of the matrices in the trace does not matter and that the expectation value is invariant under symmetry transformations, such as rotations. Note also that the expectation value, $\langle \rangle$, has a different meaning from our previous usage in this book, since it is taken in a mixed state rather than the pure angular momentum states, such as (j, m) , used elsewhere.

In the following developments we introduce the use of density matrix and irreducible spherical tensor methods to characterize ensembles of spins.

Spin Polarizations and Density Matrices. For a typical system that is close to thermal equilibrium, the distribution of spin substates is very close to equality, $P_{\sigma} = 1/(2s+1)$. What are convenient ways to describe departures from such equality? This is typically required if one devises a polarized beam or a polarized target in order to study interactions that depend sensitively on the spin s .

Consider *vector polarization*, defined—for spins zero and one—by

$$\begin{aligned} P_z &= P_{+1/2} - P_{-1/2} & s &= 1/2 \\ P_z &= P_{+1} - P_{-1} & s &= 1 \end{aligned} \quad (8.58)$$

which is just the fractional difference between spin populations parallel (+) and antiparallel (−) to the quantization axis. Spins $s = 1/2$ (electrons and nucleons) and $s = 1$ (deuterons) are most common. For higher spins there is no convention for specifying vector polarization. To visualize vector polarization, look at the motif at the beginning of this chapter, then work Problem 8.14.

The vector polarization takes no significant account of population of the $\sigma = 0$ state, which occurs for any integer spin. For example, in a spin-1 system if spin-plus and spin-minus populations are equal, there will be zero vector polarization according to (8.58), but the fraction of spins with zero projection can be different than $1/3$. The simplest component that takes account of this is the *tensor polarization* z component P_{zz} , defined by

$$P_{zz} \equiv 1 - 3P_0 \quad (8.59)$$

If all spin substates are equally populated, then $P_{zz} = 0$, which is sensible. As P_0 ranges over 0 to 1, P_{zz} ranges from 1 to -2 , a rather asymmetric quantity. As we show below, P_{zz} transforms under rotations like the $q = 0$ component of a rank $k = 2$ spherical tensor.

Transforming the Density Matrix. Consider how the density matrix transforms under rotation of the spin ensemble by polar angle θ . The case of spin-1 particles

is sufficiently complicated—but not algebraically overwhelming—to show the features. The $s = 1/2$ case is much simpler and can be done by analogy, as suggested in Problem 8.15. Suppose that an ensemble of spin-1 particles, such as a beam of deuterium atoms, is initially polarized with density matrix

$$\rho_0 = \begin{bmatrix} P_+ & 0 & 0 \\ 0 & P_0 & 0 \\ 0 & 0 & P_- \end{bmatrix} \quad (8.60)$$

in which the populations of the magnetic substates, P_+ , P_0 , and P_- , satisfy

$$\text{Tr} \rho_0 = P_+ + P_0 + P_- = 1 \quad (8.61)$$

Rotation of an ensemble of spin- s particles is described by the matrix with elements $d_{m',m}^s(\theta)$, where θ is the usual polar angle. The reduced rotation matrix for $s = 1$ is (Table 6.1)

$$\mathbf{d}^1(\theta) = \begin{bmatrix} c^2 & -\sqrt{2}cs & s^2 \\ \sqrt{2}cs & c_2 & -\sqrt{2}cs \\ s^2 & \sqrt{2}cs & c^2 \end{bmatrix} \quad (8.62)$$

which uses the abbreviations

$$c = \cos(\theta/2) \quad s = \sin(\theta/2) \quad c_2 = \cos \theta \quad (8.63)$$

Several identities used extensively to simplify expressions are:

$$\begin{aligned} c^2 + s^2 &= 1 & c^2 - s^2 &= 2c^2 - 1 = 1 - 2s^2 = c_2 = \cos \theta \\ c^4 - s^4 &= c_2 & P_2(c_2) &= (3c_2^2 - 1)/2 \end{aligned} \quad (8.64)$$

in which P_2 is a Legendre polynomial, as discussed in Section 4.1.2.

Suppose that the ensemble is rotated through polar angle θ , about the quantization axis. The spin density matrix transforms into $\rho(\theta)$ given by

$$\rho(\theta) = \mathbf{d}(\theta)\rho_0\mathbf{d}^{-1}(\theta) = \mathbf{d}(\theta)\rho_0\mathbf{d}(-\theta) \quad (8.65)$$

After some tedious algebra, we find that

$$\rho(\theta) = \frac{1}{3} \mathbf{1}_3 + \rho'(\theta) \quad (8.66)$$

in which the first matrix is a 3×3 unit matrix representing an unpolarized beam and the density matrix describing the polarization components is

$$\rho'(\theta) = \begin{bmatrix} c^4 P'_+ + 2c^2 s^2 P'_0 + s^4 P'_- & \sqrt{2}cs \left[c^2 P'_+ - (2c^2 - 1)P'_0 - s^2 P'_- \right] & c^2 s^2 (P'_+ - 2P'_0 + P'_-) \\ \dots & 2c^2 s^2 P'_+ + (2c^2 - 1)^2 P'_0 + 2c^2 s^2 P'_- & \dots \\ \dots & \sqrt{2}cs \left[s^2 P'_+ + (2c^2 - 1)P'_0 - c^2 P'_- \right] & s^4 P'_+ + 2c^2 s^2 P'_0 + c^4 P'_- \end{bmatrix} \quad (8.67)$$

where omitted off-diagonal elements can be inferred from symmetry of the matrix. (Generally, a density matrix is Hermitian, but these density matrices are also real.) The primed quantities in (8.67) are the excess populations above the unpolarized-beam populations:

$$P'_m = P_m - \frac{1}{3} \quad P'_+ + P'_0 + P'_- = 0 \quad (8.68)$$

Diagonal elements of ρ' are the populations of magnetic substates observed in simple measurements, while off-diagonal elements describe other spin properties of the ensemble.

Several intuitive checks of the correctness of (8.67) can be made:

(1) For an unpolarized initial beam, $P'_m = 0$, so $\rho' = 0$ and the beam remains unpolarized after rotation. Although this may not be obvious from the active viewpoint, consider it from the passive viewpoint, as follows. If merely rotating reference frames *could* alter the relative populations, then an ensemble could be polarized merely by walking around it!

(2) Under $\theta \rightarrow \pi - \theta$ the c^2 and s^2 terms interchange, as do the $m = +1$ and $m = -1$ states. This symmetry, which is equivalent (in the passive viewpoint) to flipping the direction of the quantization axis, can be verified directly in (8.67) and serves to check the off-diagonal elements.

(3) Since a rotation is a unitary transformation, not changing total probabilities, the trace of the density matrix must be independent of θ . By summing the diagonal elements in (8.67) we find—after extensive use of (8.64)—that

$$\text{Tr } \rho'(\theta) = P'_+ + P'_0 + P'_- = \text{Tr } \rho'_0 = 0 \quad (8.69)$$

where the difference between the polarized and unpolarized situations is

$$\rho'_0 = \rho_0 - \frac{1}{3} \mathbf{1}_3 \quad (8.70)$$

From the diagonal elements in (8.67), after a little algebra and use of (8.58), we find that the vector polarization after rotation is $P_z(\theta)$, given by

$$P_z(\theta) \equiv P'_+(\theta) - P'_-(\theta) = P_1(\cos\theta)P_z(0) \quad (8.71)$$

Thus, vector polarization transforms under rotations as a rank-1 tensor.

The rotational transformation of the spin-1 second-rank tensor component P_{zz} , given by (8.59), can be obtained by following steps similar to those for the vector polarization. Thus, we obtain the angular dependence of this tensor component as

$$P_{zz}(\theta) = P_2(\cos\theta)P_{zz}(0) \quad (8.72)$$

In the last step of this equation the central element of (8.62) is used with the identities in (8.64). Now we can see why the term *tensor* is appropriate, since P_{zz} transforms under θ rotations with $k = 2$; that is, the tensor is irreducible and of *second rank*.

In Figure 8.4 we use polar diagrams (in the convention of Section 4.1.2) to compare the dependences of vector (first-rank tensor) and (second-rank) tensor polarizations on polar angle θ for rotation of the z axis.

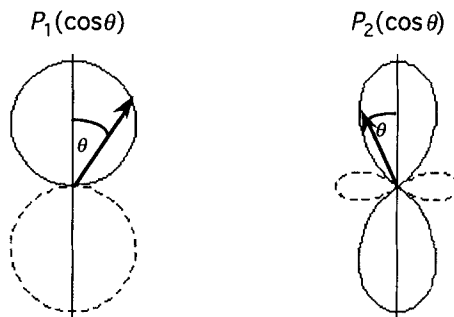


FIGURE 8.4 As the system is rotated through polar angle θ , the vector polarization changes proportionally to $P_1(\cos\theta)$ (left-hand panel) and the simplest second-rank tensor polarization changes as $P_2(\cos\theta)$ (right-hand panel). Positive values are indicated by solid lines and negative values are shown dashed. (Adapted from *Mathematica* notebook PL.)

So far we have discussed rotations of an initially diagonal density matrix through Euler angle $\beta = \theta$. What about the rotations through angles α or γ , which leave the z axis unchanged? As you might guess, they leave a diagonal density matrix unchanged, that is, they do not mix magnetic substate populations because m values do not change under such simple rotations.

8.4.2 Spin Precession in Magnetic Fields: Rotating Frames

In this subsection and the next we study the behavior of particle spins when their magnetic moment interacts with simple magnetic-field configurations—first, a constant field (producing Larmor precession), then a field changing uniformly with time, which produces interesting spin effects. In Section 5.1.3 we also develop spin precession, but emphasize correspondences between rotational symmetry and dynamical angular momentum as well as between quantal and

classical mechanics aspects of the latter. Here we emphasize the development of wave functions and spin for polarized ensembles. We first set up the Schrödinger equation for a magnetic-field Hamiltonian and use this to show Larmor precession described by quantum mechanics. Then we derive the rotating-frame transformation, which is especially useful in NMR studies.

Magnetic-Field Hamiltonian. We revisit the problem of evolution of the spin state of a particle having spin s and magnetic moment $\boldsymbol{\mu}$ in a magnetic field \mathbf{B} . In NMR the nuclei are usually stationary in the laboratory frame (except for thermal vibrations) while time-dependent but spatially homogeneous magnetic fields are used to induce resonant transitions between magnetic substates. An alternative scenario, which is important for beams of particles, is that particles move through a spatially-dependent magnetic field. As a function of distance moved through the field, the magnetic-substate populations will change, since in the rest frame of the particles the field is time-dependent. We calculate this case in detail.

The time-dependent Schrödinger equation for the spin state vector χ of a particle interacting with magnetic field \mathbf{B} is

$$i\hbar \frac{\partial \chi}{\partial t} = H \chi = -\boldsymbol{\mu} \cdot \mathbf{B} \chi = -g\mu_0 \mathbf{S} \cdot \mathbf{B} \chi \quad (8.73)$$

in which g is the g -factor of the particle and μ_0 is the appropriate magnetic moment unit. Some relevant values are given in Table 5.2. In (8.73) \mathbf{S} denotes the spin operator for the particle. For electrons in atoms the electron angular momentum operator is usually denoted by \mathbf{J} , whereas for nuclei it is usually denoted \mathbf{I} . The Hamiltonian used for modeling atomic hyperfine structure contains contributions from both electron and nuclear spins, as discussed in Woodgate's text on atomic structure [Woo80]. Measurement of magnetic moments and g -factors for nuclei is described in detail in Krane's text [Kra88].

The basic method of solving (8.73) is to expand $\mathbf{S} \cdot \mathbf{B}$ into spherical-basis components (Section 3.1.3), as

$$\mathbf{S} \cdot \mathbf{B} = S_{+1} B_{-} + S_{-1} B_{+} + S_0 B_z \quad (8.74)$$

Note that spin quantities are operators on the χ in (8.73), whereas magnetic-field components are conventional numbers. Spherical-basis components are given in terms of Cartesian components by

$$B_{\pm} = \frac{1}{2} (B_x \pm iB_y) \quad (8.75)$$

Assume that the z axis can be chosen so that \mathbf{B} has cylindrical symmetry about this axis. For example, in a conventional NMR apparatus the static (and usually homogeneous) field determines an appropriate z axis and a time-dependent probe field is arranged to have cylindrical symmetry about this direction. For a beam of particles the beam direction (assumed locally uniform) usually coincides with the direction of the largest magnetic field component, called B_z . If this field is

provided by a solenoid, with the beam flow centered on the solenoid axis, then transverse fields are purely radial, of magnitude B_r , say, as sketched in Figure 8.5.

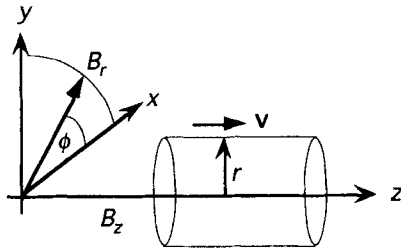


FIGURE 8.5 Arrangement of magnetic-field components B_z and B_r for cylindrically-symmetric fields. A particle trajectory is assumed to be parallel to the axis at representative radius r .

From the condition of cylindrical symmetry for the magnetic field we obtain

$$B_x = B_r \cos \phi \quad B_y = B_r \sin \phi \quad B_{\pm} = \frac{B_r}{2} e^{\pm i\phi} \quad (8.76)$$

The Hamiltonian thus becomes

$$H = -g\mu_0 \left[B_0 S_0 + \frac{B_r}{2} (e^{i\phi} S_{+1} + \text{h.c.}) \right] \quad (8.77)$$

where “h.c.” is the Hermitian conjugate of the immediately preceding expression.

Larmor Precession. If the particle is in a *uniform* field, B_0 , directed along the z axis, the solution of (8.73) is

$$\chi(t) = e^{-\frac{i}{\hbar} H(t)t} \chi(0) = e^{+i\omega_L t S_z} \chi(0) \quad (8.78)$$

where ω_L is the *Larmor precession frequency* introduced in Section 5.1.3. From the magnetic moments in Table 5.2, using $\hbar = 1.054 \times 10^{-34}$ J s and the field strength, B_0 , the precession frequency may be calculated. Solution (8.78) for the spin state gives the wave function for Larmor precession, as we now demonstrate. Consider the expansion of $\chi(t)$ into the complete set of time-independent magnetic substates $|\sigma\rangle$ by

$$\chi(t) = \sum_{\sigma=-s}^s a_{\sigma}(t) |\sigma\rangle \quad (8.79)$$

Noting that S_z in (8.78) produces σ each time it is applied to $|\sigma\rangle$ and that these states are orthogonal, we can immediately write down the solution for the time dependence of the amplitude for a given σ , namely

$$a_{\sigma}(t) = a_{\sigma}(0)e^{i\omega_L\sigma t} \quad -s \leq \sigma \leq s \quad (8.80)$$

In the semiclassical picture of angular momentum in Section 5.1.3 the spin vector, $\langle s \rangle$, precesses about the z axis with a selected projection σ and corresponding angular frequency $\omega_L\sigma$, as sketched in Figure 8.6. The probability of this arrangement is time-independent because $|a_{\sigma}(t)|^2 = |a_{\sigma}(0)|^2$ according to (8.80).

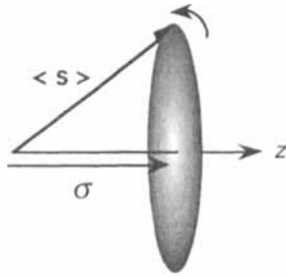


FIGURE 8.6 Semiclassical picture of the spin-amplitude relation (8.80) for uniform Larmor precession at angular frequency ω_L about the z axis. The opening angle of the precession cone is that for $s = 1/2$, $\sigma = 1/2$, namely 55° .

There are $2s + 1$ such pictures, one for each σ . For an arbitrary state, pure or mixed, there is a superposition of such precessions, with weights depending on the $a_{\sigma}(0)$. Note that positive and negative σ substates “rotate” in opposite directions. In particular, if $\sigma = 0$ (only for s an integer!) there is a constant vector standing perpendicular to the z axis. In this situation, both classically and quantumly the magnetic dipole is perpendicular to \mathbf{B} , so $\boldsymbol{\mu} \cdot \mathbf{B} = 0$.

Rotating-Frame Transformation. The precession phase in (8.80) often dominates the time dependence of the amplitude, so it is practical to hide it by making a unitary transformation, as we now describe. To undo the rotation factors in (8.79), consider the operator for the *rotating-frame transformation*

$$U \equiv e^{-i\omega_L t S_z} \quad (8.81)$$

which is unitary because (Section 2.2.3) S_z is Hermitian. Its action on spin state $\chi(t)$ produces the spin state in the rotating frame, $\chi_R(t)$, given by

$$\chi_R(t) \equiv U\chi(t) \quad (8.82)$$

For uniform precession at angular frequency ω_L this transformation completely undoes the precession, producing

$$\chi_R(t) = \chi_R(0) = \chi(0) \quad (8.83)$$

This result holds for any mixture of amplitudes in state χ . The time-independent state is, however, produced only if the precession frequency is constant. Equation (8.83) states that if we can transform our (passive) viewpoint to a frame precessing about the z axis at ω_L , then the state will be time-independent, consistent with the semiclassical picture in Figure 8.6.

To emphasize the simplicity often gained by using the rotating-frame viewpoint, we display in Figure 8.7 precessional motions from this frame and from the laboratory frame for two different Larmor frequencies.

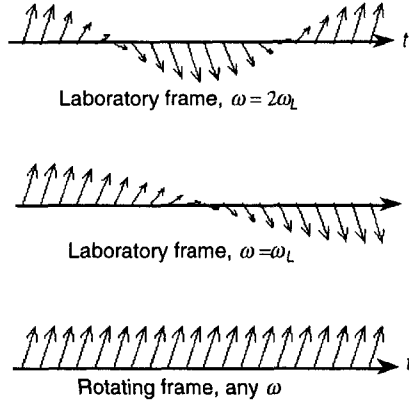


FIGURE 8.7 Precession as a function of time, t , viewed in the rotating frame at any frequency (lower panel), and as viewed in the laboratory frame for two frequencies ω differing by a factor of 2 (upper two panels).

Spin Equation in Rotating Frame. How does the spin transform under the rotating-frame transformation (8.81)? We begin with a general Hamiltonian, H , and general unitary transformation, U , then gradually specialize to operators of interest. Given

$$i\hbar \frac{\partial \chi}{\partial t} = H \chi \tag{8.84}$$

the transformed state vector satisfies the rotating-frame equation

$$i\hbar \frac{\partial \chi_R}{\partial t} = H_R \chi_R + i\hbar \frac{\partial U}{\partial t} U^{-1} \chi \tag{8.85}$$

in which the Hamiltonian after transformation is

$$H_R \equiv U H U^{-1} \tag{8.86}$$

Now, specializing U to the rotating-frame transformation, we find that

$$\frac{\partial U}{\partial t} U^{-1} = -i\omega_0 S_z \tag{8.87}$$

Since this U involves only the S_z operator,

$$US_zU^{-1} = S_z \quad (8.88)$$

The equation of motion in the rotating frame is therefore

$$\boxed{i\hbar \frac{\partial \chi_R}{\partial t} = (H_R + i\hbar\omega_0)\chi_R} \quad (8.89)$$

If we choose a particular arrangement of magnetic fields, and thereby a spin Hamiltonian, we can compute H_R and thence the spin motion in the rotating frame. The solution in the original, "laboratory," frame is obtained from the inverse of (8.82).

A common application of the rotating-frame transformation is to describe the effects of time-dependent magnetic fields applied transversely to the z -axis field B_0 . Such use in NMR for research and applications is described in detail in several monographs on magnetic resonance, such as Slichter's [Sli89]. Here we explore an application to a beam of particles moving through a magnetic field gradient and show how this effects spin polarization. Other techniques for polarization, relying on NMR effects in stationary samples, are described in Chapter 15 of Poole and Farach [Poo87].

8.4.3 Spin Transport through Magnetic Field Gradients

Our goal now is to apply the general rotating-frame equation (8.89) to a simple but realistic system, particles moving at constant speed through magnetic fields with uniform gradient. We derive the coupled differential equations describing the precession and mixing of substates, we introduce the precession length, then we show how the motion of the spin vectors can be visualized. A summary of the following is given elsewhere [Tho93] in a description of depolarization effects in atomic-beam polarized-ion sources.

Equations for a Uniform Gradient. Suppose that the magnetic field along the direction of flow of a beam of particles all having spin s is constant up to a certain point, then changes linearly with z , that is,

$$B_z = \begin{cases} B_0 & z \leq 0 \\ B_0 - B'z & z \geq 0 \end{cases} \quad (8.90)$$

in which B' is constant. In many situations of experimental interest the field decreases as z increases (as in emerging from a solenoid); then $B' > 0$ in the convention of (8.90). If the field arrangement is more complicated, a good approximation is to divide the z axis into segments within each of which the field gradient is nearly constant, then to patch together solutions for each segment. Now we set up and solve the equation of motion for spin transport in such a field gradient.

Equation of Motion. We use the conservation equation for magnetic fields, $\nabla \cdot \mathbf{B} = 0$, and the expression for divergence in cylindrical coordinates to obtain

$$B_r = -\frac{r}{2} B' \quad (8.91)$$

which is independent of z for our model magnetic field. The equation of motion in the rotating frame, (8.89), now simplifies to

$$i\hbar \frac{\partial \chi_R}{\partial t} = g\mu_0 B' \left[zS_z + \frac{r}{2} \left(e^{i\phi} U S_{+1} U^{-1} + \text{h.c.} \right) \right] \chi_R \quad (8.92)$$

in which the energy term corresponding to Larmor precession does not appear. Therefore only if the field gradient B' is nonzero does the state χ_R change with time when viewed in this frame.

In (8.92) the only complicated-looking term is the one involving the raising operator, S_{+1} , and in the Hermitian conjugate S_{-1} . Instead of spinning our wheels, let us develop this directly as

$$S_{R\pm} \equiv U S_{\pm 1} U^{-1} = e^{-i\tau S_z} S_{\pm 1} e^{i\tau S_z} \quad (8.93)$$

in which 2π times the number of precessions in B_0 within time t is the dimensionless time variable τ given by

$$\tau \equiv \omega_L t \quad (8.94)$$

Relating the ladder operators (Sections 2.2.4, 3.1.3) in the rotating frame, $S_{R\pm}$, to spin operators in the original frame is slightly tricky. Take the derivative of $S_{R\pm}$ in (8.93) and use the commutator of $S_{\pm 1}$ with S_z , (3.11), to obtain

$$\frac{dS_{R\pm}}{d\tau} = \mp S_{R\pm} \quad (8.95)$$

By repeating this step we obtain easily

$$\frac{d^2 S_{R\pm}}{d\tau^2} = -S_{R\pm} \quad (8.96)$$

which is just the harmonic oscillator differential equation, with general solution

$$S_{R\pm}(\tau) = A \cos \tau + B \sin \tau \quad (8.97)$$

By choosing $S_{R\pm}$ to coincide with $S_{\pm 1}$ at $\tau = t = 0$, and using (8.95) for the derivative, we find that

$$S_{R\pm}(\tau) = S_{\pm 1} e^{\mp i\tau} = S_{\pm 1} e^{\mp i\omega_L t} \quad (8.98)$$

Thus, rotating-frame raising and lowering operators rotate at the Larmor precession frequency relative to laboratory-frame operators—a result that is expected.

Returning to our rotating-frame equation of motion, (8.92), it now becomes

$$i\hbar \frac{\partial \chi_R}{\partial t} = g\mu B' \left\{ zS_z + \frac{r}{2} \left[e^{i(\phi-\tau)} S_{+1} + \text{h.c.} \right] \right\} \chi_R \quad (8.99)$$

in which all operators are in the laboratory frame, and the spin-state vector in this frame is obtained by inverting (8.82):

$$\chi(t) = e^{i\omega_L t S_z} \chi_R(t) \quad (8.100)$$

To continue our study of the effects of a uniformly changing field, (8.90), it is simplest to use as variable the distance along the axis, z , so that (8.92) is transformed to the spin equation in the rotating frame:

$$\boxed{\frac{\partial \chi_R}{\partial z} = -i \frac{\omega_L}{v} \frac{B'}{B_0} \left\{ zS_z + \frac{r}{2} \left[e^{i(\phi-\tau)} S_{+1} + \text{h.c.} \right] \right\} \chi_R} \quad (8.101)$$

Magnetic Substates. To make progress toward solving (8.101), expand χ_R into the complete set of time-independent laboratory-frame magnetic substates:

$$\chi_R = \sum_{\sigma'=-s}^s a_{R\sigma'} |\sigma'\rangle \quad (8.102)$$

By substituting this into (8.101) then taking the scalar product with a representative state having projection σ , we obtain the time evolution of the amplitude $a_{R\sigma}$:

$$\begin{aligned} \frac{da_{R\sigma}}{dz} = & -i \frac{\omega_L}{v} \frac{B'}{B_0} \\ & \times \left\{ z\sigma a_{R\sigma} + \frac{r}{2} \left[e^{i(\phi-\tau)} a_{R\sigma-1} \Gamma_+(\sigma) + e^{-i(\phi-\tau)} a_{R\sigma+1} \Gamma_-(\sigma) \right] \right\} \end{aligned} \quad (8.103)$$

in which the matrix elements of the ladder operators are, from (3.62),

$$\Gamma_{\pm}(\sigma) = \sqrt{(s \pm \sigma)(s \mp \sigma + 1)} \quad (8.104)$$

Amplitudes in the laboratory frame are obtained by applying (8.100), thus producing the expansion of the spin state in the laboratory frame

$$\chi = \sum_{\sigma=-s}^s a_{\sigma} |\sigma\rangle \quad (8.105)$$

where the time-dependent amplitudes in this frame are

$$a_{\sigma} = e^{i\omega_L \sigma t} a_{R\sigma} \quad (8.106)$$

Notice that stationary- and rotating-frame amplitudes differ only by time-dependent phases, so *probabilities* for a given magnetic substate are the same in both frames. In general, (8.103) can be written as a matrix first-order differential equation in which the amplitudes are the elements of a column matrix and the coupling matrix formed from elements on the right-hand side is tridiagonal, having nonzero elements only on the diagonal and one removed from it. This property is independent of the particle spin s .

Precession Length. Equation (8.103) may be written in another form, emphasizing the dependence of amplitudes on distance for a beam of particles. Define in terms of speed, v , and precession frequency, ω_L , the *precession length*, L_p , by

$$L_p \equiv \frac{v}{\omega_L} \quad (8.107)$$

This is the distance along the axis in which the spin would precess 1 radian in a constant magnetic field of strength B_0 . Now define distances and field gradients in terms of L_p and B_0 by

$$z_p = z/L_p \quad r_p = r/L_p \quad B'_p = L_p B'/B_0 \quad (8.108)$$

Indeed, $z_p = \tau$, connects space and time dimensionless variables. The equation of motion for the spin amplitude evolution in a linear field gradient is then

$$\boxed{\frac{da_{R\sigma}}{dz_p} = -iB'_p \times \left\{ z_p \sigma a_{R\sigma} + \frac{r_p}{2} \left[e^{i(\phi - z_p)} a_{R\sigma-1} \Gamma_+(\sigma) + e^{-i(\phi - z_p)} a_{R\sigma+1} \Gamma_-(\sigma) \right] \right\}} \quad (8.109)$$

In the precession-length system of units two parameters control the spin evolution and coupling—the rate of decrease of the axial magnetic field relative to the original field B_0 , which is B'_p , and a radial coupling strength proportional to $B'_p r_p$. On the z axis $r_p = 0$, so there is no coupling of spins but only precession whose rate varies with time because the magnetic field is changing steadily.

Broken Symmetry. It is instructive to examine in detail the effects of a broken symmetry (Section 1.5) of a geometric kind on coupling between magnetic substates. Particles moving along the axis of cylindrical symmetry of the field ($r_p = 0$) do not break this symmetry of the physical system (left panel in Figure 8.8). Therefore their spin projections are constants of the motion for each particle.

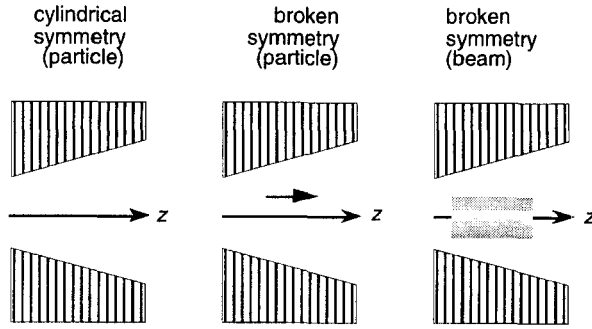


FIGURE 8.8 Cylindrical and broken symmetries for particles moving in a magnetic field having cylindrical symmetry about the z axis. For an on-axis particle (left panel) the symmetry is conserved so magnetic substates do not mix. For off-axis particles (center panel) the symmetry is broken, so substates mix. Thus, even for a beam of particles with overall cylindrical symmetry (right panel), substates become mixed.

Particles moving off-axis (center panel of Figure 8.8) break the symmetry of the overall system of particle plus field, so σ is *not* a constant of their motion. Thus, even if a beam has cylindrical symmetry about the magnetic-field axis (right panel of Figure 8.8), the magnetic substates of particles in the beam are mixed. This is an example of an ensemble (Section 8.4.1) which has macroscopic geometric symmetry but whose underlying states have broken dynamical symmetry.

Spin-1/2 Systems. The general result (8.109) for spin transport in a uniformly changing magnetic field is most easily studied for $s = 1/2$, since there are only two substates. Denoting, as usual, $a_+ = a_{R,1/2}$ and $a_- = a_{R,-1/2}$, (8.109) simplifies to a pair of equations written concisely as

$$\frac{da_{\pm}}{dz_p} = i \frac{B'_p}{2} \left[\mp z_p a_{\pm} - r_p e^{i(\phi - z_p)} a_{\mp} \right] \tag{8.110}$$

Although these equations are for the rotating frame, the probabilities may be used in the laboratory frame because of (8.106). There are several ways that equations (8.110) may be explored. Here we visualize results from numerical direct computation of the amplitudes, as Problem 8.16 suggests you do by using *Mathematica*.

It is interesting to use the numerical solutions to calculate spin-component expectation values and then to display the spin vectors. Problem 8.17 outlines the steps needed to derive the following results, which are valid for any spin:

$$\langle S_x \rangle = \frac{1}{2} \sum_{\sigma=-s}^s a_{\sigma}^* [\Gamma_+(\sigma) a_{\sigma-1} + \Gamma_-(\sigma) a_{\sigma+1}] \tag{8.111}$$

$$\langle S_y \rangle = \frac{-i}{2} \sum_{\sigma=-s}^s a_{\sigma}^* [\Gamma_+(\sigma) a_{\sigma-1} - \Gamma_-(\sigma) a_{\sigma+1}] \tag{8.112}$$

$$\langle S_z \rangle = \sum_{\sigma=-s}^s \sigma |a_\sigma|^2 \tag{8.113}$$

in which the $\Gamma_{\pm}(\sigma)$ are given by (8.104) For the simplest case, $s = 1/2$, after transforming the amplitudes to the laboratory frame by using (8.106), these become our working equations

$$\begin{aligned} \langle S_x \rangle &= \text{Re} \left[e^{iz_p} a_{R+} a_{R-}^* \right] & \langle S_y \rangle &= \text{Im} \left[e^{iz_p} a_{R+} a_{R-}^* \right] \\ \langle S_z \rangle &= \frac{1}{2} (|a_{R+}|^2 - |a_{R-}|^2) \end{aligned}$$

(8.114)

With the amplitudes $a_{R\sigma}$ in the form of numerical tables as a function of z_p and r_p for a chosen field gradient B'_p , we are able to calculate and display these spin expectation values. They are shown in Figure 8.9 for a scaled field gradient that has a large effect on the polarization (proportional to $\langle S_z \rangle$), namely $B'_p = -0.5$ (field strength increasing as z increases) for a range of scaled radii $r_p = 0, 1, 2, 3$.

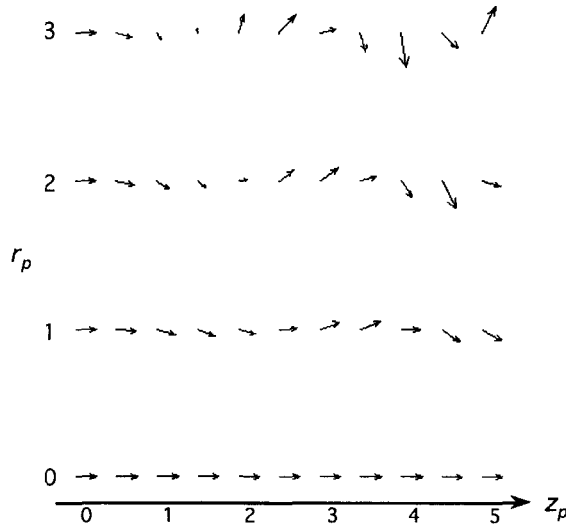


FIGURE 8.9 Spin expectation value in the rotating frame projected onto the x - z plane for spin-1/2 particles at four scaled radii, r_p , and distance along the symmetry axis of the magnetic field, z_p , calculated for an increasing magnetic field with $B'_p = -0.5$. At left a particle enters the field gradient with $\sigma = 1/2$. For $r_p = 0$ it experiences no coupling between substates. For $r_p > 0$ the radial component of the magnetic field couples the substates according to (8.110).

The consequences of spin substate mixing for practical devices producing spin-polarized beams of protons and deuterons are described in [Tho93].

PROBLEMS ON IRREDUCIBLE SPHERICAL TENSORS AND SPIN

8.1 In the derivation of the Racah definition of an irreducible tensor, (8.9) and (8.10), check out the following:

- (a) Work through the steps from (8.13) to (8.14) for arbitrary rotation axis λ .
- (b) Substitute in (8.14) the matrix elements for J_z to verify (8.9).
- (c) Combine the x and y -axis rotations, then use the matrix elements of the ladder operators given by (3.63) to derive (8.10).

8.2 Consider the Racah conditions—(8.9) and (8.10)—as tests for the angular momentum operators in the spherical basis to be irreducible spherical tensors with $k = 1$. There are three checks to be made for each of the three components.

- (a) Verify the conditions for each of the spherical basis operators J_{+1}, J_0, J_{-1} , by using the commutation relations (3.6).
- (b) Check the conditions for the three components of the unit coordinate vectors defined by (4.38).
- (c) Show that the three angular momentum basis vectors defined by (4.46) satisfy the Racah conditions.

8.3 To show that the gradient operator in the spherical basis is a rank-1 spherical tensor, construct the commutators $[L_\sigma, \nabla_q]$ for $\sigma = \pm 1, 0$ and $q = \pm 1, 0$, then use the explicit formula for coupling three angular momenta of unity (obtained from Table 7.3) to show that the commutators satisfy (8.17).

8.4 To prove that (8.21) defines the components of an irreducible tensor of rank K and projection Q , carry out the following steps:

- (a) Rotate each tensor on the right-hand side of (8.21) through the same Euler angles $(\alpha\beta\gamma)$, using the appropriate D-matrix elements.
- (b) Use the Clebsch-Gordan series (7.89) to replace the product of D-matrix elements by a sum over single elements.
- (c) Invoke the orthogonality of the 3- j coefficients, (7.61), so that only a sum over single 3- j coefficients appears. Identify the result as a rotated tensor defined according to (8.21).

8.5 For the combination of the spherical-basis components of vectors **A** and **B** to form a third rank-1 vector, show as follows that they form a cross-product vector in the spherical basis, as given by (8.23).

- (a) First show that spherical-basis components are related as

$$\begin{aligned} (\mathbf{A} \times \mathbf{B})_{\pm 1} &= \mp i(A_1 B_0 - A_0 B_1) \\ (\mathbf{A} \times \mathbf{B})_0 &= i(A_{-1} B_1 - A_1 B_{-1}) \end{aligned} \tag{8.115}$$

- (b) In the tensor-combination relation (8.21) set $k_1 = k_2 = K = 1$, and let the component tensors be **A** and **B** in the spherical basis. Use from Table 7.3 the 3- j coefficients for the first argument unity and write out each of three expansions in (8.21) for $Q = \pm 1, 0$. Thus verify (8.23).

8.6 Derive the following results for spherical-tensor scalar products:

- (a) Carry out the reduction from the general coupling form (8.21) to the scalar-product form (8.28), assuming that k is an integer.
- (b) Show that if two tensor operators commute then their scalar product is independent of their ordering.
- (c) Use expression (8.19) for the adjoint of a tensor to derive (8.30). Show the equivalence of the two forms in this expression.

8.7 To derive the Wigner-Eckart theorem, rotate each of bra, operator, and ket by using (6.19) or (8.8) to obtain an expansion into products of three D-matrix elements. Integrate over these angles through range R given in (7.98). Show that the resulting expression is an identity if the tensor matrix elements satisfy the Wigner-Eckart theorem (8.32).

8.8 For an alternative proof of the Wigner-Eckart theorem, evaluate the matrix elements of the commutator (8.10) as done in the text for (8.9), then show that the recurrence relation obtained is the same as that for the coupling coefficient.

8.9 Obtain the reduced matrix elements for the spherical harmonic tensor \mathbf{Y}_k by starting with (7.102) and making the identifications and transcriptions suggested in the text. Convert from 3- j to Clebsch-Gordan coefficients by using (7.57), then identify the reduced matrix element in the general expression (8.32) to get (8.35).

8.10^M To obtain the quadrupole moment formulas (8.41) – (8.43), produce an algebraic expression for the coupling coefficients either by plugging into (7.59) and simplifying or by using *Mathematica* notebook Alg3j in Appendix I. Manipulate these to produce the given relations between Q and the reduced matrix element as well as that between Q and the m -dependence of the quadrupole matrix element.

8.11 Consider the reduced matrix elements of \mathbf{r} .

- (a) Trace through the chain of equalities in (8.45), justifying each step.
- (b) Substitute the 3- j coefficients to obtain the final result, (8.46).

8.12 Derive the sum-rule relations (8.50) and (8.51) for reduced matrix elements by using orthogonality of the Clebsch-Gordan coefficients in conjunction with the Wigner-Eckart theorem (8.32).

8.13 Consider the reduced matrix elements of Hermitian spherical tensors that satisfy (8.20).

(a) Use the Wigner-Eckart theorem to write down the relation between the matrix elements of T_{kq} and its Hermitian conjugate. Transform the Clebsch-Gordan coefficients to 3- j coefficients and use the symmetry properties of the latter, plus some phase manipulations, to verify (8.20).

(b) Show that the reduced matrix elements of both the spherical harmonic tensor, \mathbf{Y}_k in (8.35), and of the unit vector, $\hat{\mathbf{r}}$ in (8.46), satisfy (8.52).

8.14 The motif of shells at the beginning of this chapter may be interpreted as an ensemble of spin-1/2 particles with spins up and down.

- (a) What is the polarization of this ensemble for a vertical quantization axis?

- (b) If the polarization were 80%, what would be the smallest possible number of spins in the ensemble?
- (c) What is the minimum number of shells you would have to collect before you could have a polarization of 90%?

8.15 Consider a polarized ensemble of spin-1/2 particles, such as a beam or target of hydrogen atoms. Investigate its properties under polar-angle rotations as follows.

- (a) By analogy with the development for spin-1 ensembles, and using the reduced rotation matrix for $s = 1/2$ given in Table 6.1, show that after rotation by polar angle θ the density matrix that is initially

$$\rho_0 = \begin{bmatrix} P_+ & 0 \\ 0 & P_- \end{bmatrix} \tag{8.116}$$

is transformed into

$$\rho(\theta) = \begin{bmatrix} c^2 P_+ + s^2 P_- & cs(P_+ - P_-) \\ cs(P_+ - P_-) & s^2 P_+ + c^2 P_- \end{bmatrix} \tag{8.117}$$

in which the half-angle function abbreviations in (8.63) have been made.

- (b) Show that if the ensemble is initially unpolarized, $P_+ = P_- = 1/2$, so that $\rho_0 = (1/2) \mathbf{1}_2$, then it is unpolarized after the rotation, thus $\rho(\theta) = \rho_0$.
- (c) Show that under $\theta \rightarrow \pi - \theta$ the c^2 and s^2 terms interchange, as do the roles of the $\sigma = +1/2$ and $\sigma = -1/2$ states. Explain this in physical terms.
- (d) A unitary transformation, such as a rotation, cannot change total probabilities. Verify this general result by showing that the trace of the density matrix (8.117) is independent of θ .
- (e) Consider the vector polarization for a spin-1/2 ensemble given by (8.58). Using $\rho(\theta)$ from (8.117), show that after rotation the polarization becomes

$$P_z(\theta) = P_1(\cos\theta)P_z(0) \tag{8.118}$$

Explain from the viewpoint of irreducible spherical tensors why this result is the same as for the vector polarization of a spin-1 ensemble, as given by (8.71).

8.16^M Consider the numerical solution of the pair of coupled differential equations for the spin amplitudes a_+ and a_- , as given by (8.110).

- (a) Use the *Mathematica* function `NDSolve` with initial conditions $a_+ = 1, a_- = 0$, to solve for the evolution of the spin amplitudes as a function of z_p .
- (b) By using the formulas in (8.114) for the spin expectation values, make a table of the x and z components of the spin as a function of z_p .
- (c) In *Mathematica* package `Graphics`PlotField`` use function `PlotVectorField` to visualize the spin mixing, as in the graphics for a given value of

scaled radius r_p in Figure 8.9.

8.17 Show that spin expectation values of a spin- s system can be calculated in terms of magnetic-substate amplitudes in the expansion (8.102) by inserting operators S_z and $S_{\pm 1}$ between such bra-ket expansion states, then using relation (3.63) for the ladder operators and the orthonormality of σ eigenstates to simplify the double magnetic-substate sums. Finally, convert to x and y components to verify (8.111)–(8.113).

8.18 The evolution of the vector polarization for a spin-1/2 beam, P_z , in a uniform magnetic field gradient satisfies a differential equation that can be constructed by taking the following steps.

(a) Note that the populations of the spin-parallel and spin-antiparallel substates are given by $P_{\pm} = |a_{\pm}|^2 = a_{\pm}^* a_{\pm}$, and use this to construct from the differential equation for a_{\pm} the first derivatives of P_{\pm} with respect to z_p .

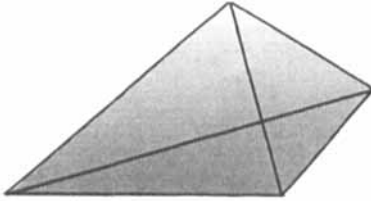
(b) Show that the derivative of $P_+ + P_-$ with respect to z_p is zero, so the effects of the transverse coupling do not change the total substate projection for each particle as a function of time, with time being proportional to z_p because the speed is constant.

(c) Now take second and third derivatives of P_+ , say, in order to derive a third-order differential equation for P_+ containing only the magnetic-field parameters and z_p . In particular, the reference-frame angle ϕ no longer appears.

(d) By using (b) to argue that P_- satisfies the same equation as P_+ , write down the third-order equation satisfied by their difference, which is P_z , namely

$$(1-u)P_z''' + P_z'' + (1-u) \left[\frac{r_p^2}{4} + \frac{(1-u)^2}{B_p'^2} \right] P_z' + \frac{r_p^2}{4} P_z = 0 \quad B_p' \neq 0 \quad (8.119)$$

where $u = B_p' z_p$ and derivatives are with respect to this variable. This equation, with appropriate initial conditions, gives the same numerical values for P_z as do the amplitude equations, and it is independent of the azimuthal angle ϕ .



Chapter 9

RECOMBINING SEVERAL ANGULAR MOMENTUM EIGENSTATES

As a grand finale to this book, we present the algebraically quite formidable problem of recombining several angular momentum eigenstates. At this level we provide just the overture. A complete treatment—as of a decade ago—occupies 500 pages in the work on the Racah-Wigner algebra by Biedenharn and Louck [Bie81b].

We begin by introducing in Sections 9.1 and 9.2 the Racah and $6-j$ coefficients, which describe recouplings of three angular momenta to form a fourth. In Section 9.3 we emphasize the unitarity and symmetry properties of the $6-j$ coefficients, and discuss how to use them and compute them efficiently. The relation of the coupling coefficients to the irreducible tensors introduced in Chapter 8 is the topic of Section 9.4. In the final section of this chapter we derive properties and applications of $9-j$ coefficients, which describe recouplings among four angular momenta.

9.1 RECOUPLING THREE ANGULAR MOMENTA

We now discuss the various coupling schemes by which three angular momenta can be combined to form a fourth. Clearly, understanding the relation between such coupling schemes is important in practical calculations, since otherwise the whole calculation has to be redone if the order of coupling is altered. Our initial approach in Section 9.1.1 is algebraic and formal, whereas in Section 9.1.2 we provide a geometric and informal viewpoint.

9.1.1 Racah and $6-j$ Coefficients for Three Angular Momenta

Here we set up the problem of describing recouplings among three angular momenta to form a fourth. Since the distinction between components and resultants soon be-

comes irrelevant, we do not use the j labels and subscripts used in some of Chapter 7, but rather just the letters of the Roman alphabet (a, b, c, d, \dots) for total angular momenta and their Greek counterparts ($\alpha, \beta, \gamma, \delta, \dots$) for projections.

Recoupling Two Angular Momenta. When deriving the coupling of two angular momenta, a and b , we show in Section 7.3 that interchanging a and b changes the phase of the coupled state, c by $(-1)^{a+b-c}$, according to (7.69). This phase, although simple, should not be neglected. It is also implicit in the following discussion, in which it is understood that, for example, the coupling scheme $\mathbf{J}_a + \mathbf{J}_b$ need not give an identical state to that from $\mathbf{J}_b + \mathbf{J}_a$.

Recoupling Three Angular Momenta. Consider the combination of three angular momentum operators:

$$\mathbf{J}_c = \mathbf{J}_a + \mathbf{J}_b + \mathbf{J}_d \tag{9.1}$$

in which it is assumed—as when combining two angular momenta using 3- j coefficients—that all three operators act in different Hilbert spaces, such as spin and orbital angular momentum or independent orbital angular momenta. Clearly, \mathbf{J}_c is an angular momentum operator. To see this, consider

$$\mathbf{J}_e = \mathbf{J}_a + \mathbf{J}_b \tag{9.2}$$

with eigenstates constructed using (7.60) for coupling in terms of 3- j coefficients:

$$|(ab)e\varepsilon\rangle = \sum |a\alpha\rangle|b\beta\rangle (-1)^{a-b+\varepsilon} \sqrt{2\varepsilon+1} \begin{pmatrix} a & b & e \\ \alpha & \beta & -\varepsilon \end{pmatrix} \tag{9.3}$$

in which the summation is over α and β such that $\alpha + \beta = \varepsilon$. Next consider the angular momentum operator constructed as

$$\mathbf{J}_c = \mathbf{J}_e + \mathbf{J}_d \tag{9.4}$$

This has eigenstates

$$|(ed)c\gamma\rangle = \sum |e\varepsilon\rangle|d\delta\rangle (-1)^{e-d+\gamma} \sqrt{2c+1} \begin{pmatrix} e & d & c \\ \varepsilon & \delta & -\gamma \end{pmatrix} \tag{9.5}$$

Why do we not choose a different combination of operators and eigenstates? There is no particular reason, and we could choose

$$\mathbf{J}_f = \mathbf{J}_b + \mathbf{J}_d \tag{9.6}$$

with eigenstates constructed as

$$|(bd)f\phi\rangle = \sum |b\beta\rangle |d\delta\rangle (-1)^{b-d+\phi} \sqrt{2f+1} \begin{pmatrix} b & d & f \\ \beta & \delta & -\phi \end{pmatrix} \quad (9.7)$$

with the sum over β and δ such that $\beta + \delta = \phi$. Then the total angular momentum operator is

$$\mathbf{J}_c = \mathbf{J}_a + \mathbf{J}_f \quad (9.8)$$

with eigenstates

$$|(af)c\gamma\rangle = \sum |a\alpha\rangle |f\phi\rangle (-1)^{a-f+\gamma} \sqrt{2c+1} \begin{pmatrix} a & f & c \\ \alpha & \phi & -\gamma \end{pmatrix} \quad (9.9)$$

Definition of Racah and 6-j Coefficients. What is the relation between eigenkets $|(ed)c\gamma\rangle$ and $|(af)c\gamma\rangle$ in (9.5) and (9.9)? Since each coupling is described by a unitary transformation, there must be a unitary transformation between the two coupling schemes. Following Racah, we write the relation in terms of *Racah coefficients*, W , as

$$|(ed)c\gamma\rangle = \sum_f |(af)c\gamma\rangle \sqrt{(2e+1)(2f+1)} W(abcd;ef) \quad (9.10)$$

In terms of Racah coefficients, the *Wigner 6-j coefficients* are defined as

$$\left\{ \begin{matrix} a & b & e \\ d & c & f \end{matrix} \right\} \equiv (-1)^\Sigma W(abcd;ef) \quad (9.11)$$

in which the phase exponent Σ is given by

$$\Sigma \equiv a + b + c + d \quad (9.12)$$

Thus, the unitary relation between the two recouplings with intermediaries e and f is

$$|(ed)c\gamma\rangle = \sum_f |(af)c\gamma\rangle \sqrt{(2e+1)(2f+1)} (-1)^\Sigma \left\{ \begin{matrix} a & b & e \\ d & c & f \end{matrix} \right\} \quad (9.13)$$

Although this second expansion is slightly more complicated to write down (but the phase can be factored out of the sum), the 6-j coefficient is more symmetric than the W coefficient, as shown in Section 9.3.2.

The treatment so far is heavily algebraic, so let us step back and look at geometric views of recoupling transformations.

9.1.2 Recoupling Tetrahedra, Quadrilaterals, and Trees

When combining two angular momenta to form a third (Clebsch-Gordan coefficients) or combining three angular momenta to zero ($3-j$ coefficients) in Section 7.1 we show how representation in terms of triangles summarizes the properties, especially the symmetries of these coefficients. We now use similar geometrical representations to visualize and suggest properties for recouplings among three angular momenta. This involves a total of six angular momenta because there are also two intermediaries and a resultant.

Recouplings of a , b , and d through intermediaries e or f to form a resultant angular momentum c , as given in (9.12) – (9.13), involve four coupling triangles, as shown in Figure 9.1.

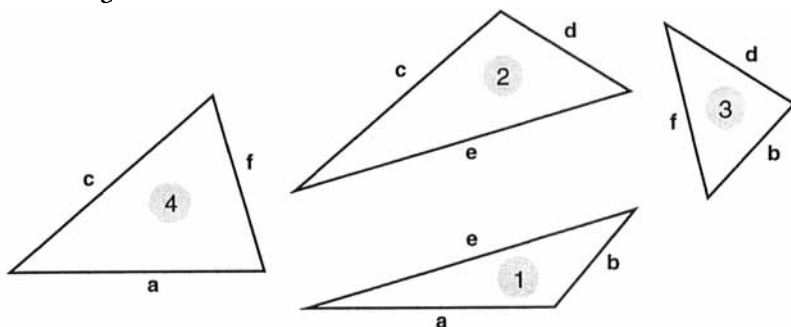


FIGURE 9.1 The four coupling triangles corresponding to coupling three angular momenta a , b , d to form a resultant c , with intermediary angular momenta e or f .

The four triangles are labeled in the order 1, 2, 3, 4 in which the coupling is performed in (9.2) – (9.8).

Tetrahedron and Quadrilateral Representations. For Racah or $6-j$ coefficients there are two visualizations of the recoupling coefficients. One is a three-dimensional *tetrahedron* and its projection onto a plane, while the other is a *quadrilateral* with diagonals. Both contain six interconnected lines and can be used to represent the $6-j$ coefficients and to summarize their symmetry properties. They are formed by glueing together the four triangles in Figure 9.1, as shown in Figure 9.2.

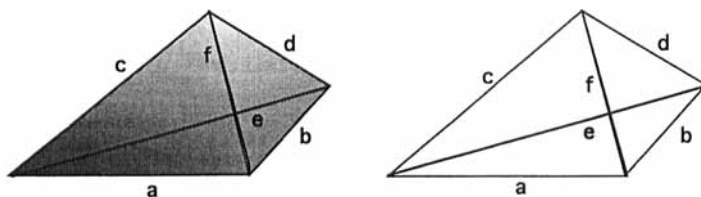


FIGURE 9.2 Geometric representations of Racah and $6-j$ coefficients, either as a tetrahedral solid (left) or a quadrilateral and its diagonals (right).

In Figure 9.2 the figures may represent the Racah coefficient $W(abcd;ef)$ with its triangles $\Delta(a b e)$, $\Delta(e d c)$, $\Delta(b d f)$, $\Delta(a f c)$. Equivalently, they represent the 6- j coefficient $\{a b e, d c f\}$, where for typographical convenience we have separated the second row of the coefficient from the first by a comma. The beauty and utility (since these may coexist) of the tetrahedron representation are that all rotations of this solid that interchange vertices represent the same coupling coefficient, except possibly for phase differences. If you need to manipulate these coupling coefficients frequently, it is worthwhile to construct a wire-frame tetrahedron with its edges labeled as shown in Figure 9.2, then to use this tetrahedron to relate recoupling coefficients. We develop this geometrical relationship in Section 9.3.2 when discussing symmetries of the recoupling coefficients.

Tree Representation. Another graphical representation of recoupling coefficients is in terms of a tree structure, as used in mathematics and computer science. An example is shown in Figure 9.3.

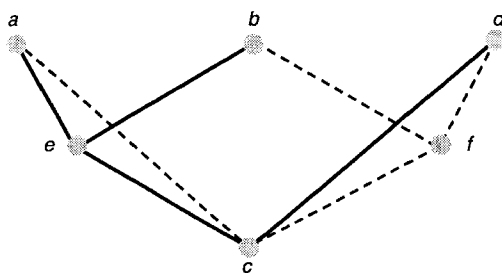


FIGURE 9.3 Tree representation for coupling of six angular momenta corresponding to Racah and 6- j coefficients. The tree with solid branches corresponds to the ket on the left-hand side of (9.10), while the tree with dashed branches corresponds to a ket on the right-hand side.

Although the tree representation has no particular advantage in this context, it is very useful for visualizing the coupling of nine angular momenta (Section 9.5).

The Triangle Conditions. Four triangle-closure conditions have to be satisfied for each nonzero Racah or 6- j coefficient, as sketched for the latter in Figure 9.4. Each of the four triplets of Δ values in this figure must form a closed triangle for the coefficient to be nonzero, as also shown geometrically in Figure 9.2.

$$\begin{array}{c}
 \left. \begin{array}{ccc} a & b & e \\ d & c & f \end{array} \right\} \\
 \left\{ \begin{array}{ccc} \Delta & \Delta & \Delta \end{array} \right\} \quad \left\{ \begin{array}{ccc} & & \Delta \end{array} \right\} \quad \left\{ \begin{array}{ccc} & \Delta & \end{array} \right\} \quad \left\{ \begin{array}{ccc} \Delta & & \end{array} \right\} \\
 \left\{ \begin{array}{ccc} \Delta & \Delta & \end{array} \right\} \quad \left\{ \begin{array}{ccc} & & \Delta \end{array} \right\} \quad \left\{ \begin{array}{ccc} \Delta & & \Delta \end{array} \right\} \quad \left\{ \begin{array}{ccc} \Delta & & \Delta \end{array} \right\}
 \end{array}$$

FIGURE 9.4 The four triangle conditions for a 6- j coefficient.

9.2 FORMULAS FOR 6-*j* COEFFICIENTS

In this section we first derive (Section 9.2.1) relations between 6-*j* and 3-*j* coefficients by using the defining relation (9.13). These relations may be used to simplify sums over products of 3-*j* coefficients, as we do for the matrix element expansion (7.117) for scattering by a rigid rotator. In Section 9.2.2 we give a useful algebraic expression for 6-*j* coefficients, and in Section 9.2.3 we summarize tabulations.

9.2.1 Expansion in Terms of 3-*j* Coefficients

We now derive in progression several expansions over products of 3-*j* and 6-*j* coefficients that progressively isolate the latter. The intermediate results are interesting, however, because they can be used to simplify such expansions, as we subsequently demonstrate.

Basic Expansion Formulas. The primary expansion begins with defining relation (9.13). We expand each state into the original states, $|a\alpha\rangle$, $|b\beta\rangle$, and $|d\delta\rangle$, which involves a pair of 3-*j* coefficients on each side. Since each state is drawn from a different Hilbert space and in each space the angular momentum eigenstates are orthogonal, we can equate the coefficients of their products on both sides and manipulate the phases (as suggested in Problem 9.1). We thus obtain the first rule:

$$\sum_f (2f+1)(-1)^\Sigma \begin{Bmatrix} a & b & e \\ d & c & f \end{Bmatrix} \begin{pmatrix} b & d & f \\ \beta & \delta & -\phi \end{pmatrix} \begin{pmatrix} a & f & c \\ \alpha & \phi & -\gamma \end{pmatrix} (-1)^{f-e-\alpha-\delta} \quad (9.14)$$

$$= \begin{pmatrix} a & b & e \\ \alpha & \beta & -\varepsilon \end{pmatrix} \begin{pmatrix} e & d & c \\ \varepsilon & \delta & -\gamma \end{pmatrix}$$

In this formula the projections α , β , and γ are given, whereas ϕ , γ , and ε are derived from them by means of the *m*-sum condition for 3-*j* coefficients, (7.58). Note that the phase multiplying the 6-*j* coefficient is just that needed to convert it into the *W* coefficient, following (9.12). In the following formulas the *m*-sum conditions and this connection between 6-*j* and *W* coefficients are maintained.

The second expansion formula removes one 3-*j* coefficient and the *f* sum from the left-hand side of (9.14) and produces a sum over 3-*j* coefficients on the right-hand side through use of the *m*-orthogonality condition (7.62). Thus, we obtain the second rule:

$$(-1)^\Sigma \begin{Bmatrix} a & b & e \\ d & c & f \end{Bmatrix} \begin{pmatrix} a & f & c \\ \alpha & \phi & -\gamma \end{pmatrix} \quad (9.15)$$

$$= \sum_{\beta\delta} (-1)^{f-e-\alpha-\delta} \begin{pmatrix} a & b & e \\ \alpha & \beta & -\varepsilon \end{pmatrix} \begin{pmatrix} e & d & c \\ \varepsilon & \delta & -\gamma \end{pmatrix} \begin{pmatrix} b & d & f \\ \beta & \delta & -\phi \end{pmatrix}$$

This is sometimes convenient for summing over products of three 3-*j* coefficients. Our final sum rule is an explicit expression for the 6-*j* coefficient:

$$\begin{aligned}
 & (-1)^\Sigma \begin{Bmatrix} a & b & e \\ d & c & f \end{Bmatrix} \\
 &= \sum_{\alpha\beta\delta} (-1)^{f-e-\alpha-\delta} (2c+1) \begin{pmatrix} a & b & e \\ \alpha & \beta & -\varepsilon \end{pmatrix} \begin{pmatrix} e & d & c \\ \varepsilon & \delta & -\gamma \end{pmatrix} \\
 & \times \begin{pmatrix} b & d & f \\ \beta & \delta & -\phi \end{pmatrix} \begin{pmatrix} a & f & c \\ \alpha & \phi & -\gamma \end{pmatrix} \quad \Sigma = a + b + c + d
 \end{aligned} \tag{9.16}$$

in which the summation over α , β , and δ is constrained by the requirement of a fixed sum, γ . As you can see by inspection of the original definition (9.13) and can verify by working Problem 9.2, this is the same result as obtained by taking the bra-ket of the two coupled states expanded into their component states. As you can see by this method, the 6-*j* coefficient is independent of magnetic substates; that is, it does not depend what direction is chosen for the *z* axis.

There are many other sum rules satisfied by 6-*j* coefficients. Many of these are given in the two-volume work of Biedenharn and Louck [Bie81a, Bie81b], in the compendium by Varshalovich et al. [Var88], and in the angular momentum handbook of Brink and Satchler [Bri94].

Example: Matrix Elements for Rigid-Rotator Scattering. In Section 7.5.4 we derive matrix elements in the partial-wave expansion for scattering by a rigid rotator. Although we have the formally correct expression, (7.117), it is given as the rather complicated function

$$S_\mu = \sum \begin{pmatrix} \ell'' & \mu & \ell' \\ m'' & m & m' \end{pmatrix} \begin{pmatrix} j'' & \mu & j' \\ m_{j''} & m & m_{j'} \end{pmatrix} \begin{pmatrix} j'' & \ell'' & J \\ m_{j''} & m'' & M \end{pmatrix} \begin{pmatrix} j' & \ell' & J \\ m_{j'} & m' & M \end{pmatrix} \tag{9.17}$$

(3)
(4)
(2)
(1)

with a sum over all the *m* values except *M*. We now show how this summation can be written in terms of a 6-*j* coefficient.

To see whether this is plausible by sketching the triangles of angular momentum numbers for the 3-*j* coefficients, similarly to Figure 9.1, as shown in Figure 9.5. Having convinced ourselves that we really have something proportional to a 6-*j* coefficient, it requires merely some permuting of arguments in (9.17) to get the same order as in (9.16), so this chore is relegated to Problem 9.3. The result is the very compact expression

$$S_\mu = \frac{(-1)^{j''+\ell'}}{2j''+1} \begin{Bmatrix} j' & \ell' & J \\ \ell'' & j'' & \mu \end{Bmatrix} \tag{9.18}$$

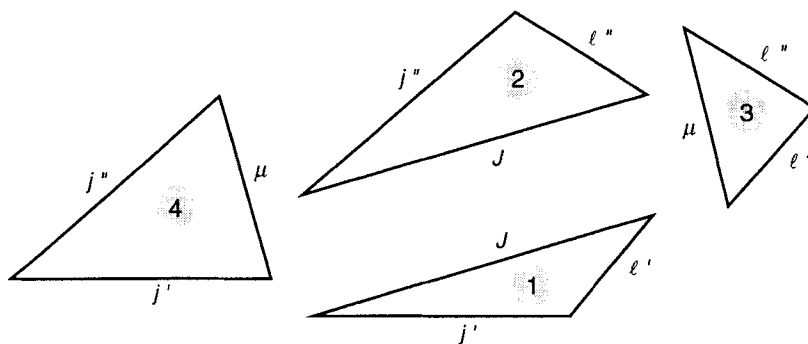


FIGURE 9.5 Coupling triangles corresponding to the four 3- j coefficients in (9.17).

This nice result is not useful unless compact expressions can be found for 6- j coefficients. This can be done, as we now describe.

9.2.2 Algebraic Expressions for 6- j Coefficients

Although the expansion of a 6- j coefficient as a sum over products of four 3- j coefficients is desirable in formal manipulations, such as the sum (9.16), it is not efficient for numerical work. In his pioneering work on angular momentum in atomic spectroscopy discussed in Section 5.5, Racah [Rac42] succeeded in reducing the equivalent relation between Clebsch-Gordan and Racah coefficients to a single algebraic sum. This can be written in terms of the Δ function defined by

$$\Delta(abc) \equiv \sqrt{\frac{(a+b-c)!(a+c-b)!(b+c-a)!}{(a+b+c+1)!}} \quad (9.19)$$

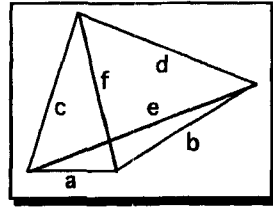
In this and the following expression it is assumed that the six arguments of the coefficient satisfy the triangle relations in Section 9.1.2. For example, in the C program `_6j` in Appendix II these conditions are checked before the 6- j function is called. The 6- j coefficient is then expressed as

$$\begin{aligned} \left\{ \begin{matrix} a & b & e \\ d & c & f \end{matrix} \right\} &= (-1)^{a+b+c+d} \Delta(abe) \Delta(acf) \Delta(bdf) \Delta(cde) \\ &\times \sum_k (-1)^k (a+b+c+d+1-k)! \\ &\times [k!(e+f-a-d+k)!(e+f-b-c+k)!]^{-1} \\ &\times [(a+b-e-k)!(c+d-e-k)!(a+c-f-k)!(b+d-f-k)!]^{-1} \end{aligned} \quad (9.20)$$

The range of summation over *k* in (9.20) is to be chosen so that no factorial argument in the sum is negative. If the initial phase factor in (9.20) is omitted, one has an expression for the Racah coefficient $W(abcd;ef)$.

TABLE 9.1 The 6-*j* coefficients with the smallest angular momentum $a = 0, 1/2, \text{ or } 1$. Related coefficients are obtained by permuting columns and by pairwise row and column interchanges. Variables in the coefficients must be chosen to satisfy the triangle rules and must be non-negative; otherwise, the formulas given do not apply. (Coefficients calculated by using *Mathematica* notebook Alg6j.)

$$\begin{Bmatrix} 0 & b & b \\ d & c & c \end{Bmatrix} = \frac{(-1)^{b+c+d}}{\sqrt{(1+2b)(1+2c)}}$$



$$\begin{Bmatrix} 1/2 & b & b+1/2 \\ d & c & c+1/2 \end{Bmatrix} = (-1)^{1/2+b+c+d} \sqrt{\frac{(1/2+b-c+d)(1/2-b+c+d)}{(1+2b)(2+2b)(1+2c)(2+2c)}}$$

$$\begin{Bmatrix} 1/2 & b & b+1/2 \\ d & c & c-1/2 \end{Bmatrix} = (-1)^{1/2+b+c+d} \sqrt{\frac{(1/2+b+c-d)(3/2+b+c+d)}{(1+2b)(2+2b)2c(1+2c)}}$$

$$\begin{Bmatrix} 1 & b & b+1 \\ d & c & c+1 \end{Bmatrix} = (-1)^{1+b+c+d} \sqrt{\frac{(b-c+d)(1+b-c+d)(-b+c+d)(1-b+c+d)}{(1+2b)(2+2b)(3+2b)(1+2c)(2+2c)(3+2c)}}$$

$$\begin{Bmatrix} 1 & b & b+1 \\ d & c & c \end{Bmatrix} = (-1)^{1+b+c+d} \sqrt{\frac{(1+b+c-d)(1+b-c+d)(-b+c+d)(2+b+c+d)}{(1+2b)(2+2b)(3+2b)c(1+2c)(2+2c)}}$$

$$\begin{Bmatrix} 1 & b & b+1 \\ d & c & c-1 \end{Bmatrix} = (-1)^{b+c+d} \sqrt{\frac{(b+c-d)(1+b-c+d)(-b+c+d)(1+b+c+d)}{2b(1+2b)(2+2b)c(-1+2c)(1+2c)}}$$

$$\begin{Bmatrix} 1 & b & b \\ d & c & c \end{Bmatrix} = (-1)^{1+b+c+d} \frac{b(1+b)+c(1+c)-d(1+d)}{\sqrt{b(1+2b)(2+2b)c(1+2c)(2+2c)}}$$

Expressions for One Angular Momentum Small. Although these expressions look formidable, if one of the angular momenta in the $6-j$ coefficient is very small (such as 0, $1/2$, or 1), then simple algebraic expressions for the coefficient are practicable. Such coefficients are given in Table 9.1. By applying exchange symmetries of $6-j$ coefficients derived in Section 9.3.2, you can produce from the entries in Table 9.1 all the $6-j$ coefficients that have 0, $1/2$, or 1 in at least one position.

The *Mathematica* system can be used to compute $6-j$ coefficients in algebraic form, as suggested in Problem 9.4. The algebraic forms obtained by using notebook `Alg6j` in Appendix I may be converted to the programming languages C or Fortran by using functions `CForm` or `FortranForm` in *Mathematica*. We discuss this further in Section 9.3.3.

9.2.3 Tabulations of $6-j$ Coefficients

It is useful to have available tabulations of Racah or $6-j$ coefficients, both algebraic (as in Table 9.1) and numerical. We postpone discussion of computing $6-j$ coefficients efficiently until Section 9.3.3. By then we have developed their symmetry properties, which greatly reduce the range of tables needed. In the meantime, here is a catalog of tables that are generally accurate and that are not in specialized technical reports and research journals.

Algebraic Expressions. Extensive tables of algebraic expressions for Clebsch-Gordan and Racah coefficients are available in Biedenharn and Louck [Bie81a] and in the recent tome by Varshalovich et al. [Var88]. Such tables were developed by hand calculation and the formulas were typeset by hand. Because both procedures have possibilities for errors in the relatively complicated expressions involved, it is advisable to check their correctness against computer-generated expressions, such as we describe in Section 9.2.2 and Problem 9.4.

Numerical tables. Extensive numerical tables of $6-j$ coefficients as exact rational fractions (Section 7.4.2) were computer-generated and typeset for the publication of Rotenberg et al. [Rot59]. Within the limitations of the tabulation (largest angular momentum equal to 8), these are the most useful numerical tables.

Biedenharn and Louck [Bie81a] provide a bibliography of tables produced through about 1975. Given the widespread availability of portable computer programs for coupling coefficients (recent programs are summarized in Section 9.3.3), the earlier work is now most useful for checking the correctness of programs.

9.3 PROPERTIES OF RECOUPLING COEFFICIENTS

Although we have derived expressions for the $6-j$ coefficients, the large number of arguments in the coefficients makes their use very unwieldy unless some simplifications can be introduced, for example through use of orthogonality and symmetry relations. These are the topics of the following two subsections.

9.3.1 Orthogonality Relations of 6-j Coefficients

In Section 7.2.2 we derive j -sum orthogonality relation of 3- j coefficients, (7.61), by considering orthogonality of coupled states. By a similar analysis of the coupled state $|c\gamma\rangle$ with states $|e\mathcal{E}\rangle$ making the unit operator, then—as Problem 9.5 suggests showing in detail—one gets an orthogonality relation between 6- j coefficients:

$$\sum_e (2e+1)(2f+1) \begin{Bmatrix} a & b & e \\ d & c & f \end{Bmatrix} \begin{Bmatrix} a & b & e \\ d & c & g \end{Bmatrix} = \delta_{fg} \quad (9.21)$$

If each 6- j coefficient is replaced by its corresponding Racah coefficient then the same sum rule results, since W and 6- j coefficients differ only by the phase (9.12), which is the same in both factors in (9.21). By using various intermediate states for the summation, one can obtain a multitude of sum rules for products of 6- j and Racah coefficients. Many of these are in Brink and Satchler’s handbook [Bri94].

9.3.2 Symmetries and Special Values of 6-j Coefficients

Very few functions that you encounter have *six* arguments that (for nonzero function values) are constrained by complicated relations, such as the triangle rules Figure 9.4. It is therefore important for simplifying calculations to understand symmetry relations under changes of arguments of the 6- j coefficients. As mentioned in Section 9.2.3, such symmetries reduce the number of independent coefficients to be tabulated. Finally, we give a simple numerical example of using explicit 6- j coefficients to relate wave functions in different coupling schemes.

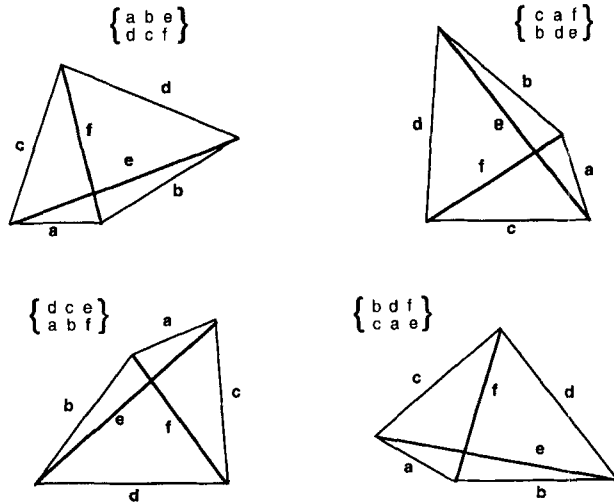


FIGURE 9.6 Quadrilaterals related by rotations in the plane of the page. Each describes the same recoupling associated with the 6- j coefficients labeling the quadrilaterals.

Symmetries from Geometry. To explain the symmetry relations, we make a geometrical analysis of the recoupling quadrilateral in Section 9.1.2. From a geometric perspective, it is the same coupling coefficient no matter what its orientation in the plane. Four such orientations are shown in Figure 9.6. By rotating the coupling quadrilaterals, each outer edge, a , b , c , or d , is chosen to occupy the lowest horizontal position. By comparing the new labels with those on the original quadrilateral at top left, we see that the four $6-j$ coefficients given must describe an equivalent recoupling. Indeed, the four coefficients in Figure 9.6 are equal to each other, rather than being just proportional. This can be verified by substitution in the expansion formula (9.16) for $6-j$ coefficients in terms of $3-j$ coefficients, as suggested in Problem 9.6.

In the quadrilateral diagrams for $6-j$ coefficients (Figures 9.2 and 9.6) the diagonals e and f represent the intermediate angular momenta. Symmetries involving two of the other four angular momenta can be visualized by rotating the coupling tetrahedron in three dimensions so that when projected onto a quadrilateral there are different diagonals. Figures analogous to Figure 9.6 can then be drawn and the symmetries deduced. There are six choices of diagonals and four figures for each choice, thus generating 24 symmetries of the $6-j$ coefficient. By this means one can deduce the following symmetry rule:

<p>A $6-j$ coefficient is invariant under interchange of any two columns and under interchange of the upper and lower arguments in each of any two columns.</p>	(9.22)
--	--------

Relations between the geometry of tetrahedra and their projected quadrilaterals have been developed by several authors, as summarized in Topics 8 and 9 in Biedenharn and Louck [Bie81b].

Examples of the Permutation Symmetries. For $6-j$ coefficients there are 24 symmetries of the kind depicted in Figure 9.6. For example, corresponding to the crossed quadrilateral in that figure which has e and f as diagonals, we have that

$$\begin{Bmatrix} a & b & e \\ d & c & f \end{Bmatrix} = \begin{Bmatrix} c & a & f \\ b & d & e \end{Bmatrix} = \begin{Bmatrix} d & c & e \\ a & b & f \end{Bmatrix} = \begin{Bmatrix} b & d & f \\ c & a & e \end{Bmatrix} \quad (9.23)$$

Note that the phase factor between the Racah coefficient, W , and the $6-j$ coefficient, as given by (9.12), makes the Racah coefficient less symmetric, because phase factors appear when its arguments are permuted.

Besides the mathematical beauty of these symmetries, what is their usefulness? Their most practical use is for reducing the range of tabulations of $6-j$ coefficients. For example, the tables of Rotenberg et al. [Rot59] assume "odometer" ordering of the arguments. That is, like the odometer (distance meter) of an automobile, the smallest arguments are put in the top row and in leftmost positions as much as

possible consistent with maintaining the triangle conditions. An example of such a reordering is shown in Figure 9.7.

$$\left\{ \begin{matrix} 8 & 6 & 3 \\ 4 & 2 & 8 \end{matrix} \right\} = \left\{ \begin{matrix} \overleftarrow{4} & \overleftarrow{2} & \overleftarrow{3} \\ \overleftarrow{8} & \overleftarrow{6} & \overleftarrow{8} \end{matrix} \right\} = \left\{ \begin{matrix} 2 & 3 & 4 \\ 6 & 8 & 8 \end{matrix} \right\} = -\sqrt{\frac{11}{3808}}$$

FIGURE 9.7 The process of permuting arguments of a 6- j coefficients into odometer order. The left-pointing arrows in the middle 6- j coefficient indicate cyclic substitution.

As you may verify by running *Mathematica* notebook Num6j, all three forms give identical results when the arithmetic is done exactly. In the *Mathematica* system the running time for each coefficient is about the same. (The first call of SixJSymbol in a *Mathematica* session involves some setup time, so the 6- j coefficient that is computed first will take longest.)

A Numerical Example of Using 6- j Coefficients. Suppose that a proton (spin, $a = 1/2$) interacts with a deuteron (spin, $d = 1$), and that the relative orbital angular momentum in their center of mass is ℓ . We might be describing a configuration in the ${}^3\text{He}$ nucleus (for negative total energy), or in p - d scattering (for positive total energy). The situation is sketched in Figure 9.8.

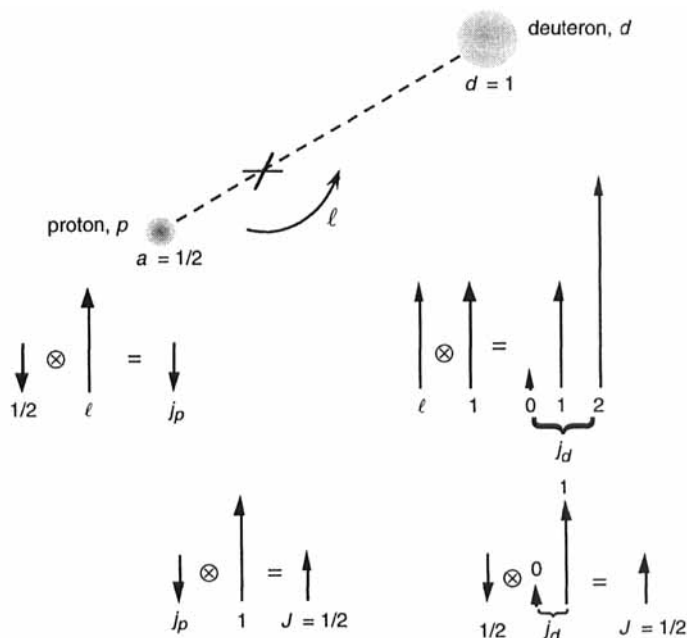


FIGURE 9.8 In the p - d interaction with relative orbital angular momentum ℓ one can either couple the spin of p to ℓ , then couple this to the spin of d , or the d spin may be coupled to ℓ first. The lower part of the figure indicates the coupling schemes in (9.24) with $\ell = 1$, $J = 1/2$.

The relative orbital angular momentum, ℓ , is common to both particles; therefore, it should make no real difference whether proton spin is coupled to ℓ , then this is coupled to deuteron spin, or whether ℓ is coupled to deuteron spin then this coupled to proton spin. That is, wave functions from the two coupling schemes should be related by a unitary transformation. To express the states of angular momentum J and projection M formed in the first coupling scheme in terms of those in the second scheme, we go directly to the definition (9.10). Choose $a = 1/2$, $b = \ell$, $e = j_p$ as the proton total angular momentum. With the deuteron spin as $d = 1$, then $f = j_d$ as the deuteron total angular momentum, with $c = J$ being the system angular momentum. Thus, by direct substitution, we have

$$\begin{aligned} & \left| \left\{ \left[\left(\frac{1}{2}, \ell \right) j_p \right] 1 \right\} J M \right\rangle \\ &= \sum_{j_d = \ell - 1}^{\ell + 1} \left| \left\{ \frac{1}{2} \left[\left(\ell, 1 \right) j_d \right] \right\} J M \right\rangle \sqrt{[2(1/2) + 1][2j_d + 1]} \\ & \quad \times (-1)^{3/2 + \ell + J} \begin{Bmatrix} 1/2 & \ell & j_p \\ 1 & J & j_d \end{Bmatrix} \end{aligned} \quad (9.24)$$

For clarity, we expand the labels identifying intermediate states $e = j_p$ and $f = j_d$.

Consider the simplest nontrivial case, $\ell = 1$ and $j_p = 1/2$, so the proton spin is “antiparallel” in the semiclassical vector model (Sections 5.3, 7.1). Further, choose the case $J = 1/2$, corresponding in the vector model to proton spin antiparallel to the orbital angular momentum. These arrangements are shown schematically in the lower part of Figure 9.8. We do not show any tilt to the coupling vectors; that is, we approximate their values by their projections. Given the angular momentum values, there are no free quantities in (9.24). It reduces to

$$\begin{aligned} & \left| \left\{ \left[\left(\frac{1}{2}, 1 \right) 1/2 \right] 1 \right\} 1/2, M \right\rangle \\ &= - \sum_{j_d = 0, 1, 2} \left| \left\{ \frac{1}{2} \left[\left(1, 1 \right) j_d \right] \right\} 1/2, M \right\rangle \sqrt{2(2j_d + 1)} \begin{Bmatrix} 1/2 & 1 & 1/2 \\ 1 & 1/2 & 1 \end{Bmatrix} \\ &= \frac{-1}{\sqrt{3}} \left| \left\{ \frac{1}{2} \left[\left(1, 1 \right) 0 \right] \right\} 1/2, M \right\rangle + \sqrt{\frac{2}{3}} \left| \left\{ \frac{1}{2} \left[\left(1, 1 \right) 1 \right] \right\} 1/2, M \right\rangle \end{aligned} \quad (9.25)$$

in which either Table 9.1 or *Mathematica* notebook Num6j in Appendix I can be used to find the two 6- j coefficients required. Note that $j_d = 2$ does not contribute for the given coupling states, as you can see by sketching the coupling vectors.

Is result (9.25) reasonable? It claims that the second contribution ($j_d = 1$) is twice as probable ($2/3$) as the first contribution ($j_d = 0$), which has just $1/3$. If you sketch the coupling vectors more carefully than in Figure 9.8, you will see that this is plausible. The relative negative sign is just a requirement of unitarity for a system with two components. Starting from (9.24), you can make other choices of angular momenta to investigate various recoupling schemes, as suggested in Problem 9.7.

Although these analyses are tedious as well as error-prone, such direct expansions seldom have to be done by hand. There are two alternatives: either the manipulations are done algebraically and a final compact expression for matrix elements or other observables is produced, or steps corresponding to the expansion (9.24) are coded in computer programs that crunch out the numbers without human intervention. Whatever way one uses, there is a premium on efficient computation of 6- j coefficients, a topic to which we now turn.

9.3.3 Computing 6- j Coefficients Efficiently

In Section 7.4.3 we discussed efficient computation of numerical values of 3- j coefficients. Our purpose here is to extend the discussion to 6- j coefficients. Again, because of the complexity of writing such programs (beyond the entry-level program in Appendix II) we outline the options, then direct you to references and sources of improved programs.

Algebraic Expressions. If one angular momenta in the 6- j coefficient is small (say, 2 or less), then an algebraic expression for the coefficient may be practicable. We give such expressions in Section 9.2.2. Using these expressions for numerical work is much faster than using the general formula for the coefficient, (9.20), no matter in what form—rational-fraction or decimal—the coefficient is expressed. The *Mathematica* system can compute 6- j coefficients in algebraic form, for example, by using notebook Alg6j in Appendix I. *Mathematica* can then generate expressions coded in C or Fortran by using functions CForm or FortranForm. Such computer-generated algebraic forms are also useful for identifying errors in published tables of algebraic expressions, as discussed in Sections 9.2.2 and 9.2.3.

Numerical Expression for 6- j Coefficients. We show two general formulas for the 6- j coefficient, namely the expansion as sums of products of 3- j coefficients, (9.16), and the direct summation in terms of factorials, (9.20). Experience shows that the latter is more practicable and efficient for numerical work.

Just as discussed for the 3- j coefficient in Section 7.4.2, for 6- j coefficients there is a choice between exact rational-fraction (prime-exponent) expressions and decimal approximations. Similarly, the disadvantages of requiring exact coefficients are programming that is more complicated and longer computing time. An array of primes must be used for each rational fraction, and factorials should be precomputed and stored in tables. Such a prime-exponent representation (Section 7.4.2) is used in the computer-generated tables of Rotenberg et al. [Rot59].

Computer Programs for 6- j Coefficients. The *Mathematica* notebook Num6j in Appendix I may be used to compute exact rational-fraction expressions for 6- j coefficients. We also give in C3 of Appendix II an entry-level program for 6- j coefficients, coded in the C language. This program, _6j, uses expression (9.20) to calculate decimal values in double-precision arithmetic and it outputs the values to

six decimal digits. The *Mathematica* program is about two orders of magnitude slower than the C program when run on the same workstation. Although these two programs are suitable for exploratory work, they use none of the methods discussed in Section 7.4.2 for improving efficiency or accuracy. If you plan to do extensive calculations requiring 6- j coefficients, you should read on.

There are Regge symmetries for 6- j coefficients depending upon linear combinations of the arguments, similar to the Regge symmetries for 3- j coefficients given in Section 7.4.2. These symmetries for 6- j coefficients are discussed, for example, in Section 3.18 of [Bie81a]. Regge symmetries may be used to combine angular momenta in a 6- j coefficient to obtain parameters that are as small as possible, then the permutation symmetries (9.22) allow the smallest angular momentum to be moved to a specific location within the coefficient. Thus, one can express a coefficient in its computationally simplest form. The complicated programming logic required is justified only if many 6- j coefficients with large arguments are to be calculated.

Several authors have published programs for 6- j coefficients, including Lai and Chiu [Lai90] and Fang and Shriner [Fan92]. Both programs yield exact rational-fraction values, although Lai and Chiu's program switches to decimal approximations when the angular momenta in the coefficient exceed 20. Programs by Rao and Venkatesh [Rao78] compute Racah coefficients in decimal approximation. The programs summarized in Table 9.2 are in Fortran, except for the *Mathematica* option. Program details are given in the references.

TABLE 9.2 Published programs for 6- j coefficients.

Source	Method	Remarks
<i>Mathematica</i>	Symbolic	Algebraic or numerical values
[Rao78]	Decimal	Racah coefficients
[Lai90]	Prime and decimal	Prime for $j \leq 20$
[Fan92]	Prime	Workstation version available

A practical way to check program correctness and numerical accuracy for 6- j coefficients is to use the orthogonality relation (9.21). Initial checks can be made by verifying orthogonality for the squares of coefficients, then you can check the correctness of relative phases by choosing one argument to be different, which should give zero for the sum of products of 6- j coefficients appropriately weighted. Such checks are suggested as Problem 9.8.

As shown in Section 9.5.1, the 9- j coefficients are usually computed as a sum over products of three 6- j coefficients, so efficiency in calculating the latter is important for this purpose.

9.4 SCALAR PRODUCTS OF IRREDUCIBLE TENSORS

In Chapter 8 we introduce irreducible spherical tensors, particularly how to combine them to form scalars (Section 8.2.2). We also show the power of the Wigner-Eckart theorem (Section 8.3) and the related reduced matrix elements. Our purpose in this section is to apply our newfound skills in techniques of recoupling three angular momenta (Sections 9.1–9.3) with results from Sections 8.1–8.3 in order to obtain formulas that are especially suitable for describing scalar quantities such as Hamiltonians in quantum mechanics.

We begin by deriving in Section 9.4.1 factorization and projection theorems for tensors, which is especially useful for calculating matrix elements of scalar products of a system in terms of reduced matrix elements of its constituents. We then use the factorization theorem in Section 9.4.2 to derive formulas for matrix elements of multipole expansions, which is a generalization of the Gaunt-integral formulas for three spherical harmonics in Section 7.5.3 and of the example of quadrupole-moment reduced matrix elements in Section 8.3.3. The last topic in this section—but not the least—is a discussion of tensor matrix elements in L - S and j - j coupling schemes. This topic sets the scene for consideration of recouplings among four angular momenta in Section 9.5.

9.4.1 Factorization and Projection Theorems for Tensors

In the following we derive two theorems that can greatly simplify calculations involving irreducible tensors.

Factorization Theorem. In Section 8.2.2 we learn how to contract irreducible tensors to form scalars, with the scalar product of two irreducible tensors, $\mathbf{T}_k(A_1)$ and $\mathbf{T}_k(A_2)$, being given by

$$\begin{aligned} \mathbf{T}_k(A_1) \cdot \mathbf{T}_k(A_2) &\equiv (-1)^k \sqrt{2k+1} T_{00}(A_1, A_2) \\ &= \sum_q (-1)^q T_{kq}(A_1) T_{k-q}(A_2) \end{aligned} \quad (9.26)$$

Note that the k on the left-hand side of this definition indicates the rank of the two components rather than the rank of their scalar product, which is—of course—zero.

Matrix elements of the scalar product, which is typically an *operator*, are most readily determined in an angular momentum representation in which the systems characterized by the labels A_1 and A_2 are combined—in the sense described in Chapter 7. The tensors on the right-hand side of (9.26) are, however, most likely to be evaluated in the uncoupled representation. We therefore calculate the matrix elements $\langle (j_1 j_2) JM | \mathbf{T}_k(A_1) \cdot \mathbf{T}_k(A_2) | (j_1' j_2') J' M' \rangle$ in terms of those of the states before combining, namely $\langle j_i m_i | \mathbf{T}_k(A_i) | j_i' m_i' \rangle$ with $i = 1, 2$. To do this, the coupled states are expanded in terms of Clebsch-Gordan coefficients by using the basic formula

(7.35). Since we are dealing with irreducible tensors, m dependences of corresponding matrix elements can be expressed in terms of Clebsch-Gordan coefficients by using the Wigner-Eckart theorem, (8.32). Since this is easier to do than to typeset, we defer details to Problem 9.9. The result is the *factorization theorem in the coupled representation* :

$$\begin{aligned}
 & \langle (j_1 j_2) J M | \mathbf{T}_k(A_1) \cdot \mathbf{T}_k(A_2) | (j'_1 j'_2) J' M' \rangle \\
 &= \delta_{JJ'} \delta_{MM'} \langle (j_1 j_2) J \| \mathbf{T}_k(A_1) \cdot \mathbf{T}_k(A_2) \| (j'_1 j'_2) J' \rangle \\
 &= \delta_{JJ'} \delta_{MM'} (-1)^{j'_1 + j_2 + J} \sqrt{(2j_1 + 1)(2j_2 + 1)} \begin{Bmatrix} j_1 & j_2 & J \\ j_2 & j'_1 & k \end{Bmatrix} \\
 & \quad \times \langle j_1 \| \mathbf{T}_k(A_1) \| j'_1 \rangle \langle j_2 \| \mathbf{T}_k(A_2) \| j'_2 \rangle
 \end{aligned} \tag{9.27}$$

In the factorization theorem formula there are two delta functions, as expected, since the scalar operator cannot change the total angular momentum J or its projection M . The 6- j coefficient gives the probability amplitude for coupling among the angular momenta involved, of which we show a simple example immediately below. Finally, in (9.27), we have the reduced matrix elements of the two rank- k operators composing the scalar product.

A Simple Example of the Factorization Theorem. To illustrate use of (9.27), consider the scalar product $\mathbf{L} \cdot \mathbf{S}$, which is the spin-orbit operator discussed in Sections 4.3.1 and 7.1.3. It is composed of two rank-1 operators, \mathbf{L} and \mathbf{S} , whose reduced matrix elements are obtained from (8.48). These matrix elements are diagonal in the corresponding total angular momenta, ℓ and s , respectively. If (8.48) is used twice on the right-hand side of (9.27), if the 6- j coefficient is manipulated by using the symmetry rule (9.22) to the form given as the last equation in Table 9.1, then (as Problem 9.10 suggests that you show) we obtain

$$\langle (\ell s) J \| \mathbf{L} \cdot \mathbf{S} \| (\ell' s') J' \rangle = \delta_{JJ'} \delta_{\ell\ell'} \delta_{ss'} [J(J+1) - \ell(\ell+1) - s(s+1)] \tag{9.28}$$

This result is just as expected from the simple derivation in Section 7.1.3. If (7.12) is taken as given, then use of (9.27) provides a heavy-handed way of deriving the simple expression in Table 9.1 for the 6- j coefficient $\{1 b b, d c c\}$.

Projection Theorem for Rank-1 Operators. Suppose that we have a rank-1 (vector) operator \mathbf{T}_1 . In the semiclassical vector model of angular momentum (Section 5.3), and ignoring for the moment the distinction between a classical vector and a vector operator such as \mathbf{T}_1 , we would expect the situation sketched in Figure 9.9.

According to this picture, which relates to expectation values in angular momentum eigenstates (j, m) , the precession of \mathbf{T}_1 about \mathbf{J} averages its transverse component about \mathbf{J} to zero. The *projection theorem* that we derive is

$$\langle jm | \mathbf{T}_1 | j'm' \rangle = \frac{\langle jm | \mathbf{J} (\mathbf{J} \cdot \mathbf{T}_1) | j'm' \rangle}{j(j+1)} \delta_{jj'} \quad (9.29)$$

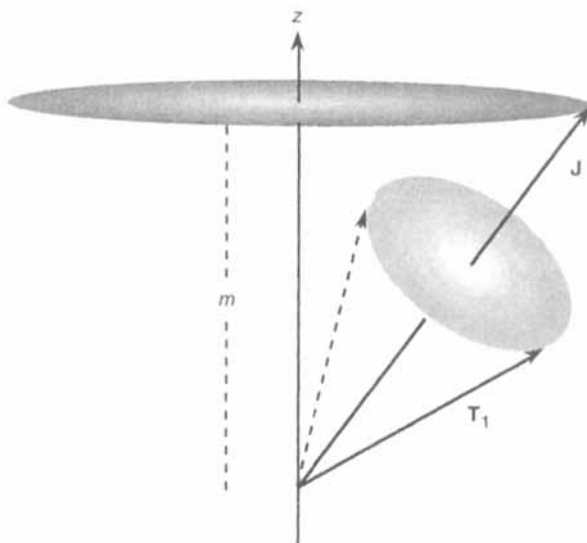


FIGURE 9.9 A vector operator \mathbf{T}_1 , treated as a classical vector, precesses about the angular momentum \mathbf{J} , also treated classically. The z component of \mathbf{T}_1 is determined by its projection along \mathbf{J} and by the direction of \mathbf{J} .

Our proof of (9.29) proceeds as follows. Consider a representative component of \mathbf{J} on the right-hand side of (9.29), say J_σ with $\sigma = \pm 1, 0$ for the spherical basis. We can write the matrix element as

$$\langle jm | J_\sigma (\mathbf{J} \cdot \mathbf{T}_1) | j'm' \rangle = \sum_q (-1)^q \langle jm | J_\sigma J_q T_{1,-q} | j'm' \rangle \quad (9.30)$$

in which we use definition (8.29) for the scalar product. By writing

$$J_q T_{1,-q} = T_{1,-q} J_q + [J_q, T_{1,-q}] \quad (9.31)$$

we can split each matrix element in the sum in (9.30) into one contribution from the first term in (9.31) and one from the commutator term. As you can verify by working Problem 9.11, the commutator matrix elements are zero, corresponding (in the semiclassical viewpoint Figure 9.9) to vanishing of the averaged components of \mathbf{T}_1 that are orthogonal to \mathbf{J} . There remains the matrix elements

$$\langle jm|J_\sigma(\mathbf{J}\cdot\mathbf{T}_1)|j'm'\rangle = \sum_q (-1)^q \langle jm|J_\sigma T_{1,-q} J_q|j'm'\rangle \quad (9.32)$$

This can be simplified by inserting a unit operator between J_σ and $T_{1,-q}$ with a second unit operator between $T_{1,-q}$ and J_q , according to (2.14), with the complete set of states being (j,m'') and (j,m''') states, respectively. It is sufficient to keep the same label j throughout, since angular momentum operators do not change this eigenvalue. Matrix elements of the angular momentum components can be expressed by using the Wigner-Eckart theorem (8.32) with $k = 1$ and the reduced matrix element (8.48). The resulting sum over products of two Clebsch-Gordan coefficients can be collapsed by using orthogonality relation (7.41). Finally, the Wigner-Eckart theorem is used again to produce (9.29) for a given choice of σ . Since this choice is arbitrary, the relation holds for the vectors \mathbf{T}_1 and \mathbf{J} , as written.

Continuing our excursion in abstraction in order to produce practical formulas, consider the matrix elements on the right-hand side of (9.29) for a representative angular momentum component σ . Using the trick of inserting a complete set of states, we have

$$\begin{aligned} \langle jm|J_\sigma(\mathbf{J}\cdot\mathbf{T}_1)|j'm'\rangle &= \sum_{m''} \langle jm|J_\sigma|jm''\rangle \langle jm''|\mathbf{J}\cdot\mathbf{T}_1|j'm'\rangle \\ &= \langle jm|J_\sigma|j'm'\rangle \langle j\|\mathbf{J}\cdot\mathbf{T}_1\|j\rangle \delta_{jj'} \end{aligned} \quad (9.33)$$

in which the second line follows by noticing that the second operator is a scalar, $k = 0$, so by (8.32) its matrix elements cannot change the projection and must be identical to its reduced matrix elements, as written. Expressing (9.33) in vector form gives a *factorization theorem in uncoupled representation*:

$$\langle jm|\mathbf{J}(\mathbf{J}\cdot\mathbf{T}_1)|j'm'\rangle = \langle jm|\mathbf{J}|jm'\rangle \langle j\|\mathbf{J}\cdot\mathbf{T}_1\|j\rangle \delta_{jj'} \quad (9.34)$$

Finally, by combining (9.29) and (9.34) we have for any rank-1 tensor operator the *decomposition theorem*:

$$\langle jm|\mathbf{T}_1|j'm'\rangle = \frac{\langle jm|\mathbf{J}|jm'\rangle \langle j\|\mathbf{J}\cdot\mathbf{T}_1\|j\rangle}{j(j+1)} \delta_{jj'} \quad (9.35)$$

which can be written for its reduced matrix elements as

$$\langle j\|\mathbf{T}_1\|j'\rangle = \frac{\langle j\|\mathbf{J}\cdot\mathbf{T}_1\|j\rangle}{\sqrt{j(j+1)}} \delta_{jj'} \quad (9.36)$$

These results can be applied immediately to a practical example.

The Landé g-factor Formula. Suppose that we have a single particle (typically an electron, a nucleon, or a quark) in a state of well-defined ℓ , s , and j . We want to calculate matrix elements of the magnetic moment operator

$$\boldsymbol{\mu} = \mu_0(g_L \mathbf{L} + g_s \mathbf{S}) \quad (9.37)$$

in which μ_0 is the appropriate magnetic moment unit (Table 5.2), g_L is the g -factor for orbital motion, and g_s is the spin g -factor. In the decomposition theorem (9.35) we set $\mathbf{T}_1 = \boldsymbol{\mu}$, a vector operator because of (9.37). The scalar product $\boldsymbol{\mu} \cdot \mathbf{J} = \mathbf{J} \cdot \boldsymbol{\mu}$ can be manipulated simply into

$$\begin{aligned} \boldsymbol{\mu} \cdot \mathbf{J} &= \mu_0(g_L \mathbf{L} + g_s \mathbf{S}) \cdot (\mathbf{L} + \mathbf{S}) \\ &= \mu_0 \left[g_L \mathbf{L}^2 + g_s \mathbf{S}^2 + \frac{1}{2}(g_L + g_s)(\mathbf{J}^2 - \mathbf{L}^2 - \mathbf{S}^2) \right] \end{aligned} \quad (9.38)$$

in which we have used $\mathbf{J} = \mathbf{L} + \mathbf{S}$ and, as in the step between (7.10) and (7.11), we have expressed $\mathbf{L} \cdot \mathbf{S} = \mathbf{S} \cdot \mathbf{L}$ in terms of operators for which the bra-kets are eigenstates. This completes the operator algebra.

Matrix elements in a state of definite ℓ , s , and j are now simply obtained by using (9.38) in (9.35). If we require the expectation value of $\boldsymbol{\mu}$, then $m' = m$ and the first matrix element on the right-hand side is nonzero only for $\sigma = 0$ (the z component) and its value is m . Thus we have the *Landé g-factor formula*:

$$\langle (\ell s) j m | \mu_\sigma | (\ell s) j m \rangle = g \mu_0 m \delta_{\sigma,0} \quad (9.39)$$

in which the g -factor is given by

$$g = \frac{1}{2} \left[(g_L + g_s) + (g_L - g_s) \frac{\ell(\ell+1) - s(s+1)}{j(j+1)} \right] \quad (9.40)$$

Note that—given the assumption of definite ℓ , s , and j values—only rotational symmetry (geometrical angular momentum, Section 3.4.5) is used to derive these formulas. The dynamics (primarily as quantum mechanics) is manifested in the origin of the primary g -factors (g_L and g_s) and in comparison with experiments to check the assumption and then to assign the total angular momenta ℓ and j .

9.4.2 Matrix Elements of Multipole Expansions

In this section we illustrate using the factorization theorem in the coupled representation, (9.27), to calculate two-particle central interactions V_{12} when the two particles are characterized by their orbital angular momenta ℓ_1 and ℓ_2 , which are combined to give total angular momentum number L . Our methods and results are essentially generalizations of those in Section 7.5.4 for rotator matrix elements.

Suppose that we have two particles with coordinates \mathbf{r}_1 and \mathbf{r}_2 , as shown in Figure 9.10, with an interaction $V_{12}(r_{12})$ that depends upon their separation r_{12} .

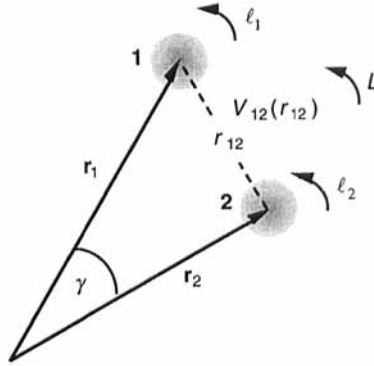


FIGURE 9.10 Matrix elements of the two-particle central interaction V_{12} are to be calculated in the coupled representation, with the two particles having definite orbital angular momenta, as shown.

We make a multipole expansion of V_{12} analogously to (7.109), namely:

$$V_{12}(r_{12}) = \sum_{\mu=0}^{\infty} v_{\mu}(r_1, r_2) P_{\mu}(\cos \gamma) \quad (9.41)$$

in terms of the angle γ between \mathbf{r}_1 and \mathbf{r}_2 , as shown in Figure 9.10. In (9.41) the μ th multipole moment v_{μ} is given from the orthogonality relation of Legendre polynomials, (4.3), by

$$v_{\mu}(r_1, r_2) = \frac{2\mu + 1}{2} \int_{-1}^1 V_{12}(r_{12}) P_{\mu}(\cos \gamma) d(\cos \gamma) \quad (9.42)$$

$$r_{12} = \sqrt{r_1^2 + r_2^2 - 2r_1 r_2 \cos \gamma}$$

For example, as in the discussion below (7.111), for the Coulomb interaction $V_{12}(r_{12}) = e^2/r_{12}$ we have

$$v_{\mu}(r_1, r_2) = \frac{e^2}{r_{>}} \left(\frac{r_{<}}{r_{>}} \right)^{\mu} \quad r_{<} = \min(r_1, r_2) \quad r_{>} = \max(r_1, r_2) \quad (9.43)$$

Notice that this decreases at least as fast as the Coulomb potential that would be experienced by the particle that is more distant from the center ($r_{>}$) if there were a charge e at the origin. For any interaction, (9.42) can be evaluated by numerical integration if necessary.

The states between which the multipole matrix elements are taken are the coupled orbital states with representative kets projected into configuration space given by

$$\langle(\Omega_1 \Omega_2) | (\ell_1 \ell_2) LM \rangle = \sum_{m_1, m_2} Y_{\ell_1}(\Omega_1) Y_{\ell_2}(\Omega_2) \langle \ell_1 \ell_2 m_1 m_2 | \ell_1 \ell_2 LM \rangle \quad (9.44)$$

The Legendre polynomials in (9.41) can be expanded by using the spherical-harmonic addition theorem (4.23), which the discussion at the end of Section 8.2.2 identifies as an example of a scalar product. Therefore, the factorization theorem in the coupled representation, (9.27), can be used immediately to obtain

$$\begin{aligned} & \langle (\ell_1 \ell_2) L \| P_\mu \| (\ell'_1 \ell'_2) L' \rangle \\ &= \frac{4\pi \sqrt{(2\ell_1 + 1)(2\ell_2 + 1)} (-1)^{\ell'_1 + \ell_2 + L}}{2\mu + 1} \begin{Bmatrix} \ell_1 & \ell_2 & L \\ \ell'_2 & \ell'_1 & \mu \end{Bmatrix} \\ & \times \langle \ell_1 \| Y_\mu \| \ell'_1 \rangle \langle \ell_2 \| Y_\mu \| \ell'_2 \rangle \delta_{LL'} \end{aligned} \quad (9.45)$$

By using expression (8.35) for the two reduced matrix elements then simplifying and using phase-manipulation rules (Section 2.1.4), we obtain a very compact expression for the reduced matrix element

$$\begin{aligned} & \langle (\ell_1 \ell_2) L \| P_\mu \| (\ell'_1 \ell'_2) L' \rangle = (-1)^{\mu + L} (2\ell_1 + 1)(2\ell_2 + 1) \\ & \times \begin{pmatrix} \ell_1 & \mu & \ell'_1 \\ 0 & 0 & 0 \end{pmatrix} \begin{pmatrix} \ell_2 & \mu & \ell'_2 \\ 0 & 0 & 0 \end{pmatrix} \begin{Bmatrix} \ell_1 & \ell_2 & L \\ \ell'_2 & \ell'_1 & \mu \end{Bmatrix} \delta_{LL'} \end{aligned} \quad (9.46)$$

From (9.41) it follows that the angular momentum dependence of the reduced matrix elements of interaction V_{12} is a sum over μ of reduced matrix elements of the form (9.46), weighted by the multipole moments v_μ .

Selection rules for reduced matrix elements of V_{12} follow immediately from those inferred from (9.46). From the two “parity-conservation” 3- j coefficients we see that not only must the “orbital angular momentum transfer,” μ , conserve relative parity between primed and unprimed states, but if $\ell_1 + \ell_2$ is even (odd), then $\ell'_1 + \ell'_2$ must be even (odd) or else the matrix elements vanish. In this example—in the absence of spins—many matrix elements will vanish because of rotational symmetry requirements and will enforce parity conservation, even if V_{12} is not a parity-conserving interaction. This exemplifies the remarks made below (7.72) relative to tests of parity conservation.

9.4.3 The L - S and j - j Coupling Schemes

Suppose that we have systems 1 and 2, for example—when investigating the atomic hyperfine interaction—an electron and a nucleus. The description of each has some symmetry relative to rotation of its center of mass about some point in space, thus

orbital angular momentum numbers ℓ_i , $i = 1, 2$, as introduced in Sections 3.2 and 4.1. Each system may have internal rotational symmetries, thus a *spin*—as discussed in Sections 3.5 and 4.3.1—with values s_i , $i = 1, 2$, such as $s_1 = 1/2$ for an electron and $s_2 = 1$ for a deuteron. With four angular momenta being involved, there are at least two ways of combining operators and eigenstates.

In the L - S coupling scheme one combines the operators as:

$$\mathbf{L} = \mathbf{L}_1 + \mathbf{L}_2; \quad \mathbf{S} = \mathbf{S}_1 + \mathbf{S}_2; \quad \mathbf{J} = \mathbf{L} + \mathbf{S} \quad (9.47)$$

whereas in the j - j scheme the order of combining operators is

$$\mathbf{j}_1 = \mathbf{L}_1 + \mathbf{S}_1; \quad \mathbf{j}_2 = \mathbf{L}_2 + \mathbf{S}_2; \quad \mathbf{J} = \mathbf{j}_1 + \mathbf{j}_2 \quad (9.48)$$

These two schemes for combining angular momentum operators are illustrated in Figure 9.11, which uses the tree representation (Section 9.1.2).

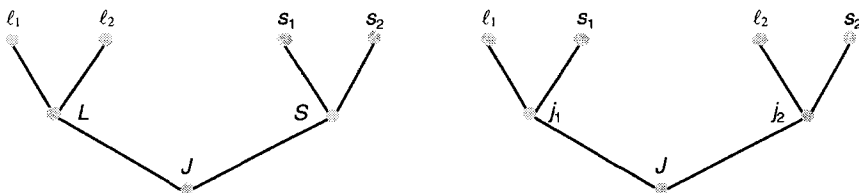


FIGURE 9.11 The L - S coupling scheme (left) and j - j coupling (right) in tree representations.

Why should one prefer one coupling scheme over the other? From a mathematical viewpoint—given enough brain power and computer power—it makes absolutely no difference which scheme is used if the calculation is made without approximation. From a physical viewpoint, calculations and model approximations will often be easier and more realistic if one of the schemes is used.

For example, suppose that the Hamiltonian of the system is modeled by central interactions plus a spin-orbit interaction for each particle, proportional to the (scalar) spin-orbit operator $\mathbf{L}_i \cdot \mathbf{S}_i$, $i = 1, 2$. As derived in Section 7.1.3, the system energies—the eigenvalues of the Hamiltonian—are given immediately from the angular momentum numbers ℓ_i , s_i , and j_i , provided that the j - j scheme is used, since the spin-orbit operators are diagonal in this representation. On the other hand, if the Hamiltonian has a spin-orbit interaction proportional to $\mathbf{L} \cdot \mathbf{S}$, where the two operators are as in (9.47), then the L - S scheme is preferred. Notice that a Hamiltonian containing both types of spin-orbit interaction—so-called *intermediate coupling*—will be computationally rather messy. In either scheme, after appropriate relabeling, reduced matrix elements of the spin-orbit operator are given by (9.28).

In the following, we specify angular momentum eigenstates in the two coupling schemes, thus preparing for Section 9.5, which emphasizes how to convert matrix elements between the two representations.

The L-S Coupling Scheme. We can visualize this coupling scheme by using the tree representation (Section 9.1.2) shown as the left-hand tree in Figure 9.11. Angular momentum eigenkets corresponding to the operators in (9.47) are formed following the combination rule (7.60). For the combined orbital states we have

$$|(\ell_1 \ell_2) L \Lambda\rangle = \sum_{\lambda_1, \lambda_2} |\ell_1 \lambda_1\rangle |\ell_2 \lambda_2\rangle (-1)^{\ell_1 - \ell_2 + \Lambda} \sqrt{2L+1} \begin{pmatrix} \ell_1 & \ell_2 & L \\ \lambda_1 & \lambda_2 & -\Lambda \end{pmatrix} \quad (9.49)$$

while for the combined spin states

$$|(s_1 s_2) S \Sigma\rangle = \sum_{\sigma_1, \sigma_2} |s_1 \sigma_1\rangle |s_2 \sigma_2\rangle (-1)^{s_1 - s_2 + \Sigma} \sqrt{2S+1} \begin{pmatrix} s_1 & s_2 & S \\ \sigma_1 & \sigma_2 & -\Sigma \end{pmatrix} \quad (9.50)$$

Finally, we have the total angular momentum state

$$|(LS) JM\rangle = \sum_{\Lambda, \Sigma} |L \Lambda\rangle |S \Sigma\rangle (-1)^{L-S+M} \sqrt{2J+1} \begin{pmatrix} L & S & J \\ \Lambda & \Sigma & -M \end{pmatrix} \quad (9.51)$$

in which—let it be clearly understood—the resulting ket depends upon the components making up L and S , and also—according to (7.69)—on the ordering (1, 2 \neq 2, 1, and $L, S \neq S, L$) of the pairwise combinations. This coupling scheme is most applicable for small and medium-sized atoms.

The j-j Coupling Scheme. This coupling scheme can be visualized using the right-hand tree in Figure 9.11. For the combined orbital-spin states we have, by using (7.60), the eigenkets

$$|(\ell_i s_i) j_i m_i\rangle = \sum_{\lambda_i, \sigma_i} |\ell_i \lambda_i\rangle |s_i \sigma_i\rangle (-1)^{\ell_i - s_i + j_i} \sqrt{2j_i+1} \begin{pmatrix} \ell_i & s_i & j_i \\ \lambda_i & \sigma_i & -m_i \end{pmatrix} \quad (9.52)$$

$j = 1, 2$

The consequences of reversing the coupling order to s followed by ℓ are detailed in (7.70) and (7.71). The total angular momentum state is now formed as

$$|(j_1 j_2) JM\rangle = \sum_{m_1, m_2} |j_1 m_1\rangle |j_2 m_2\rangle (-1)^{j_1 - j_2 + M} \sqrt{2J+1} \begin{pmatrix} j_1 & j_2 & J \\ m_1 & m_2 & -M \end{pmatrix} \quad (9.53)$$

This coupling scheme is most applicable for large atoms and for nuclei.

Clearly, it would be tedious and therefore prone to considerable error if each time we decided to use a different coupling scheme among four angular momenta we had to go through the algebra of angular momentum eigenstates. Just as for recombining three angular momenta (Sections 9.1–9.3), an algebra for recombining four angular momenta can also be devised, as we do in the following section.

9.5 RECOUPLING FOUR ANGULAR MOMENTA

Now that we have met the challenge of understanding recouplings among three angular momenta, we confront the problem of recoupling four angular momenta. This is more complicated because there are nine arguments rather than six. However, the 9- j coefficient is algebraically more symmetric than the 6- j coefficient, which partially compensates for the increased number of arguments.

We begin this section by defining 9- j coefficients and describing how to compute them conveniently and efficiently, then in Section 9.5.2 we discuss their symmetries and special values. We return in Section 9.5.3 to discuss tensor matrix elements in coupled schemes, a topic introduced in Section 9.4.3. In Section 9.5.4 we show how to make transformations between L - S and j - j coupling schemes, which is an important part of the technology of atomic and nuclear spectroscopy. Finally in this section, we give references to graphical and automated methods for performing the algebra of the functions considered in this section.

9.5.1 Definition and Computation of 9- j Coefficients

Suppose that we have four angular momentum operators summed to a total, \mathbf{J} , as

$$\mathbf{J}_i = \mathbf{J}_a + \mathbf{J}_b + \mathbf{J}_d + \mathbf{J}_e \quad (9.54)$$

in which the operators act in different Hilbert spaces, so that the operators on the left-hand side commute with each other. For example, we may have the orbital angular momentum and the spin operators both for two particles, as in Section 9.4.3. Two distinct coupling schemes are

$$\begin{aligned} \mathbf{J}_c = \mathbf{J}_a + \mathbf{J}_b & & \mathbf{J}_f = \mathbf{J}_d + \mathbf{J}_e & & \mathbf{J}_i = \mathbf{J}_c + \mathbf{J}_f \\ \mathbf{J}_g = \mathbf{J}_a + \mathbf{J}_d & & \mathbf{J}_h = \mathbf{J}_b + \mathbf{J}_e & & \mathbf{J}_i = \mathbf{J}_g + \mathbf{J}_h \end{aligned} \quad (9.55)$$

We can represent this scheme by a tree representation, as shown in Figure 9.12.

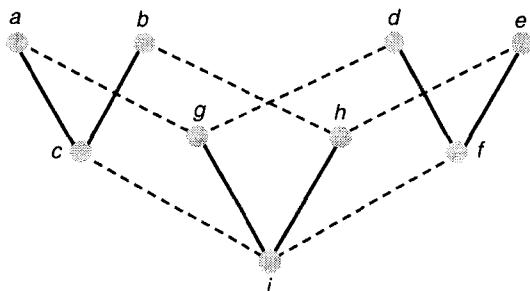


FIGURE 9.12 Six couplings among nine angular momenta in the tree representation. Solid lines indicate couplings across rows and dashed lines indicate couplings down columns in the 9- j coefficient.

Defining the 9-j Coefficient. The unitary transformation between the angular momentum eigenkets in the two coupling schemes depicted in Figure 9.12 is written, similarly to (9.13) for 6-j coefficients, as

$$\begin{aligned}
 |(ad)g,(be)h;im\rangle &= \sum_{cf} |(ab)c,(de)f;im\rangle \\
 &\times \sqrt{(2c+1)(2f+1)(2g+1)(2h+1)} \begin{Bmatrix} a & b & c \\ d & e & f \\ g & h & i \end{Bmatrix} \quad (9.56)
 \end{aligned}$$

which introduces the 9-j coefficient as the transformation coefficient in the braces {...}. Giving no iota for our Greco-Roman convention between projections and total angular momenta, we use the symbol m in this equation for the projection of i on the quantization axis. For typographical convenience the 9-j coefficient is often written as the identical coefficient $X(abc, def, ghi)$.

The complete symmetry of the coupling scheme (9.56) and its graphical representation (Figure 9.12) upon interchange of elements between rows and columns of the 9-j coefficient, indicate that the coefficient is completely symmetric under such interchange.

Formula (9.56) is useful for obtaining one set of coupled states in terms of the other, provided that one knows the 9-j coefficients. However, like much fine mathematics, it does not immediately solve the problem of knowing values of these coefficients. This problem is formally solved just by writing

$$\begin{aligned}
 &\sqrt{(2c+1)(2f+1)(2g+1)(2h+1)} \begin{Bmatrix} a & b & c \\ d & e & f \\ g & h & i \end{Bmatrix} \\
 &= \langle (ab)c,(de)f;im | (ad)g,(be)h;im \rangle \quad (9.57)
 \end{aligned}$$

which follows from the unitarity of the recoupling transformation (orthonormality of the eigenkets). If formulas for the bra-ket on the right-hand side of (9.57) can be found, we have expressions for the 9-j coefficient.

Expansions for 9-j Coefficients. Several expansion formulas for 9-j coefficients can be produced. The basic one is obtained by expanding the bra-ket in (9.57) into sums of products of 3-j coefficients, as Problem 9.12 suggests you do. A model for such an expansion is provided by the L - S and j - j coupling scheme expansions given by (9.49)–(9.53). Thus one obtains, essentially by inspection, the expression

$$\left\{ \begin{matrix} a & b & c \\ d & e & f \\ g & h & i \end{matrix} \right\} = \sum \left(\begin{matrix} a & b & c \\ \alpha & \beta & \gamma \end{matrix} \right) \left(\begin{matrix} d & e & f \\ \delta & \varepsilon & \phi \end{matrix} \right) \left(\begin{matrix} g & h & i \\ \gamma & \eta & m \end{matrix} \right) \quad (9.58)$$

$$\times \left(\begin{matrix} a & d & g \\ \alpha & \delta & \gamma \end{matrix} \right) \left(\begin{matrix} b & e & h \\ \beta & \varepsilon & \eta \end{matrix} \right) \left(\begin{matrix} c & f & i \\ \gamma & \phi & m \end{matrix} \right)$$

in which the summation is over all projection numbers except m . This form is suitable for determining symmetries of 9- j coefficients, as we derive in Section 9.5.2. Note the direct correspondence between this formula and the tree representation in Figure 9.12, with the first row of 3- j coefficients being the couplings shown by solid lines in the figure and the second row of coefficients corresponding to the couplings shown by dashed lines.

The form (9.58) is less efficient for computation than the expression in terms of 6- j coefficients:

$$\left\{ \begin{matrix} a & b & c \\ d & e & f \\ g & h & i \end{matrix} \right\} = \sum_k (2k+1) \left\{ \begin{matrix} a & i & k \\ h & d & g \end{matrix} \right\} \left\{ \begin{matrix} b & f & k \\ d & h & e \end{matrix} \right\} \left\{ \begin{matrix} a & i & k \\ f & b & c \end{matrix} \right\} \quad (9.59)$$

To obtain this expression, pairs of 3- j coefficients are collapsed using (9.14), to obtain 6- j coefficients. As Problem 9.12 suggests verifying, the product of six 3- j coefficients becomes the product of just three 6- j coefficients, summed over a single variable, k . Since the algebraic expression for a 6- j coefficient, (9.20), takes only about as long to compute as expression (7.59) for a 3- j coefficient, a great savings in time is realized by using (9.59) rather than (9.58) to compute 9- j coefficients.

Algorithms for 9- j Coefficients. Algebraic expressions for 9- j coefficients might be desirable, but nine arguments are required to define the coefficients, so their analysis is very complicated. On the other hand, exact numerical expressions—as rational fractions or decimal approximations (as discussed in Section 7.4.2)—are of great utility, because there are few published tables of the coefficients, and these are only over very small values of the nine j arguments. Here we outline options for computing 9- j coefficients, then direct you to references and sources of programs.

Permutational symmetries of the 9- j coefficients—(9.60) and (9.61) below—allow the smallest angular momentum to be moved to a specific location within the coefficient. By doing this, one can express the coefficient in its computationally simplest form. As when computing the 3- j and 6- j coefficients (Sections 7.4.2 and 9.3.3), rational-fraction expressions in prime-exponent notation may be used for 9- j coefficients. The many factorials required should be precomputed and saved in a lookup table.

Although the $9-j$ coefficient is commonly evaluated as a sum over the product of three $6-j$ coefficients, (9.59), other algorithms are available and often significantly improve the efficiency of computation. This is especially important for $9-j$ coefficients, because for a workstation to evaluate a single coefficient typically takes from a fraction of a second (decimal approximation) up to about one minute (rational-fraction form) and may require hundreds to tens of thousands of factorials.

Alisauskas and Jucys [Ali71] derived a formula for $9-j$ coefficients as a triple sum over factorials instead of a single sum over products of three $6-j$ coefficients. Zhao and Zare [Zha88] tested the computational efficiency of this formula and concluded that generally the triple-sum formula is inferior. However, Rao, Rajeswari, and Chiu [Rao89] showed that the optimal method depends on the number of terms to be summed. Their program determines this number and chooses the evaluation method accordingly. Still another approach, discussed by Rao and coworkers, is to use hypergeometric functions to evaluate the $9-j$ coefficients, which they found also increases the speed.

Parallel Processing. All the algorithms discussed above were implemented on serial-processing computers. Implementation on parallel processors has been developed by Fack, Van der Jeugt, and Rao [Fac92], using a network of transputers organized as indicated in Figure 9.13.

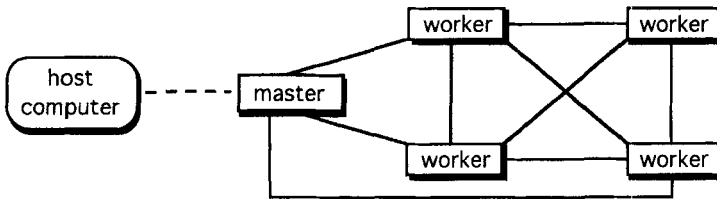


FIGURE 9.13 Network of master and worker transputers used by [Fac92] for efficient computation of $9-j$ coefficients.

Fack and colleagues found that the $9-j$ coefficient is the first angular momentum coupling coefficient for which parallelization has a remarkable impact. For their transputer configuration, the most appropriate algorithm was a sum over products of three $6-j$ coefficients, as in (9.59). Each “worker” transputer computes the product for a given summation variable, k , and returns the product to the “master” transputer for summing. They explored how the speed of computing the $9-j$ coefficient depends upon the number of transputers and found that for their system an average speedup of a factor of 4 was obtained with four worker transputers (Figure 9.13). Little was gained by using eight cross-linked worker transputers because of increased communication overhead between them.

Programs for $9-j$ Coefficients. Our programs for $9-j$ coefficients are the *Mathematica* notebook Num9j in Appendix I and the C-language program _9j in Appendix II. Both use expansion (9.59) into products of three $6-j$ coefficients after

checking the six triangle conditions on rows and columns. The *Mathematica* version provides exact rational-fraction value (Section 7.4.2), but with a very large increase in running time compared with the decimal approximations in the C program `_9j`. For example, to compute $X(2, 1, 2, 3/2, 3/2, 1, 1/2, 1/2, 1) = -1/(10\sqrt{6})$ on my workstation using the *Mathematica* version takes about 7 seconds, but the C version needs only about 0.01 second for the decimal approximation.

Published programs using the 6- j expansion, (9.59), include those by Lai and Chiu [Lai92] and by Fang and Shriner [Fan92]. Both yield exact rational-fraction values, although Lai and Chiu's program switches from the Alisaukas-Jucys triple-sum formula to decimal approximations when the angular momenta in the coefficient exceed 10. Programs by Rao et al. [Rao89] are available for decimal approximations. We summarize these recent programs in Table 9.3.

TABLE 9.3 Published programs for 9- j coefficients.

Source	Method	Remarks
[Rao89]	Decimal	Workstation version available
[Lai92]	Prime and decimal	Prime for $j \leq 10$
[Fan92]	Prime	Workstation version available
[Fac92]	Decimal	Parallel-processing version

These programs for 9- j coefficients are in Fortran, except for the version of Fack et al. [Fac92] for parallel processing, which is in C. Details about the programs are available in the references. If you wish to check out such a program installed in your computer, a practical way to check its correctness and numerical accuracy (for decimal versions) is to use the orthogonality relation (9.65) below. Initial checks can be made by verifying orthogonality for the squares of coefficients. If this is successful, check the correctness of relative phases by choosing one of the arguments to be different, which should give zero for the orthogonality sum. Such checks are suggested as Problem 9.13.

Now that we appreciate how the 3 n - j coefficients with $n = 1, 2, 3$ can be computed efficiently, we derive some more symmetries of the 9- j coefficients before discussing uses of the coefficients.

9.5.2 Symmetries, Special Values, and Sum Rules of 9- j Coefficients

We discuss in Section 9.3.2 the complexity of 6- j coefficients because of their six arguments. The problem is more severe for recoupling among four angular momenta there are nine arguments. Fortunately, the 9- j coefficient appears very symmetric when displayed in matrix form and its symmetries under permutations of rows and columns are like those of the corresponding determinant, as we now derive.

Symmetries of 9-j Coefficients. To visualize symmetry relations of 9-j coefficients, consider its tree representation in Figure 9.12. The probability of a recoupling should not change if rows and columns (solid and dashed lines) are interchanged, or if rows (or columns) are interchanged with each other, since any of these interchanges preserves the couplings between triads of angular momenta.

To quantify these claims, consider the expansion into 3-j coefficients, as given by (9.58). The coefficients in the first row of the product are those from the row couplings in the 9-j coefficient, while in the second row of the product the 3-j coefficients come from column couplings. Since the ordering of 3-j coefficients in the product is not important, we have the first symmetry rule:

Under interchange of all rows with all columns a 9-j coefficient is invariant.	(9.60)
---	--------

Now consider interchanging the first and second rows, so that $X(abc, def, ghi) \rightarrow X(def, abc, ghi)$. The 3-j coefficients in the first row of (9.58) are unaltered, while in the second row each of the coefficients has its first and second columns interchanged, introducing an overall phase change as the sum of all total angular momenta in the second row. Since this property holds for any two rows or columns, we have the second symmetry rule:

Under interchange of two rows or two columns a 9-j coefficient is multiplied by the phase $(-1)^P$ where $P = a + b + c + d + e + f + g + h + i$.	(9.61)
--	--------

Note that P must be an integer if the triangle rules for each coupling of triplets is satisfied. Isn't that beautifully simple?

Special Values of 9-j Coefficients. Because of the high symmetry of the 9-j coefficients, any one argument can be moved to a special position—such as the top-left corner—and this will at most introduce a phase change. For $a = 0$, using the expansion (9.59) and simplifying (as suggested in Problem 9.14), one obtains

$\left\{ \begin{matrix} 0 & b & c \\ d & e & f \\ g & h & i \end{matrix} \right\} = \frac{(-1)^{b+d+f+h}}{\sqrt{(2b+1)(2d+1)}} \left\{ \begin{matrix} d & e & f \\ b & i & h \end{matrix} \right\} \delta_{bc} \delta_{dg}$	(9.62)
---	--------

A particular case of this coefficient is for $b = c = 1/2$, which—upon rearranging the 6-j coefficient by using (9.22)—becomes

$$\boxed{\begin{Bmatrix} 0 & 1/2 & 1/2 \\ d & e & f \\ g & h & i \end{Bmatrix}} = \frac{(-1)^{1/2+d+f+h}}{\sqrt{2(2d+1)}} \begin{Bmatrix} 1/2 & i & f \\ d & e & h \end{Bmatrix} \delta_{dg} \quad (9.63)$$

in which the special 6- j coefficient is given in Table 9.1. Formula (9.63) is useful for describing the transformation between L - S and j - j coupling in Section 9.5.3. Another formula that is useful for the same purpose can also be derived from (9.59) by substituting for the special 6- j coefficients (as suggested in Problem 9.14), namely

$$\boxed{\begin{Bmatrix} 1 & b & b \\ d & e & f \\ d & h & i \end{Bmatrix}} = \frac{[e(e+1)+i(i+1)-f(f+1)-h(h+1)]}{\sqrt{4b(b+1)(2b+1)d(d+1)(2d+1)}} \times (-1)^{b+d+f+h} \begin{Bmatrix} d & e & f \\ b & i & h \end{Bmatrix} \quad (9.64)$$

Many other special cases of the 9- j coefficient are given in Appendix III of Brink and Satchler [Bri94] and in the work of Varshalovich et al. [Var88].

Sum Rule for 9- j Coefficients. The simplest sum rule expresses the unitarity (orthogonality, since the coefficients are real) of the recoupling transformation (9.57). The sum rule is given by

$$\boxed{\sum_{cf} (2c+1)(2f+1) \begin{Bmatrix} a & b & c \\ d & e & f \\ g & h & i \end{Bmatrix} \begin{Bmatrix} a & b & c \\ d & e & f \\ j & k & i \end{Bmatrix}} = \frac{\delta_{gj} \delta_{hk}}{(2g+1)(2h+1)} \quad (9.65)$$

Sum rules of great variety and some utility are given in sources such as [Bri94, Var88, Bie81a, Bie81b].

9.5.3 Tensor Matrix Elements in Coupled Schemes

In the quantum mechanics of atomic and subatomic systems a frequent problem is to understand a composite system, say two particles, in terms of its constituent particles. Typically, one has operators acting on each particle and an angular momentum state formed by combining the angular momenta of the two particles. We are therefore led to consider matrix elements of composite irreducible spherical tensors, as in Section 8.2.1, taken between coupled states, as in Chapter 7.

Consider the building-up formula for tensors, (8.21), expressed for temporary convenience in terms of Clebsch-Gordan coefficients as

$$T_{KQ}(A_1, A_2) = \sum_{q_1, q_2} T_{k_1 q_1}(A_1) T_{k_2 q_2}(A_2) \langle k_1 k_2 q_1 q_2 | k_1 k_2 K Q \rangle \quad (9.66)$$

The reduced matrix elements of this tensor in the composite system with $\mathbf{J} = \mathbf{J}_1 + \mathbf{J}_2$ can be expressed by using the sum rule (8.50):

$$\begin{aligned} & \langle (j_1 j_2) J \| \mathbf{T}_K(A_1, A_2) \| (j'_1 j'_2) J' \rangle \\ &= \sum_{M', Q} \langle J' K M' Q | J' K J M \rangle \langle (j_1 j_2) J M | \mathbf{T}_{KQ}(A_1, A_2) | (j'_1 j'_2) J' \rangle \end{aligned} \quad (9.67)$$

The bras and kets can be expanded by using basic combination formula (7.35), the operator can be expressed by using (9.66), and the matrix elements in the uncoupled representation can be written in terms of their reduced matrix elements by using the Wigner-Eckart theorem. Amid the chaos of coupling coefficients you may recognize (especially by working Problem 9.15) that the magnetic substate summations produce a quantity proportional to a $9-j$ coefficient. Thus, we obtain the formula for tensor matrix elements in the coupled scheme:

$$\begin{aligned} & \langle (j_1 j_2) J \| \mathbf{T}_K(A_1, A_2) \| (j'_1 j'_2) J' \rangle \\ &= \sqrt{(2j_1 + 1)(2j_2 + 1)(2J + 1)(2J' + 1)(2K + 1)} \\ & \times \begin{Bmatrix} j_1 & j'_1 & k_1 \\ j_2 & j'_2 & k_2 \\ J & J' & K \end{Bmatrix} \langle j_1 \| \mathbf{T}_{k_1}(A_1) \| j'_1 \rangle \langle j_2 \| \mathbf{T}_{k_2}(A_2) \| j'_2 \rangle \end{aligned} \quad (9.68)$$

In this formula it is understood but not expressed that the rank- K tensor is formed from coupling of a rank- k_1 and rank- k_2 tensors. The spaces A_1 and A_2 must be disjoint because this theorem relies on disjointness for constructing the states involved, as explained at the beginning of Section 7.1.2.

If in (9.68) we set $K = 0$, so that the left-hand side becomes the reduced matrix element of the scalar product (thus, $k_1 = k_2 = k$), then (as you may verify in Problem 9.15) we recover the factorization theorem, (9.27).

9.5.4 Transformations between L - S and j - j Coupling

In Section 9.4.3 we discuss the advantages and differences between L - S and j - j coupling schemes. Suppose that part of a calculation or an analysis of data has used the L - S scheme and we want to transform to the j - j scheme. The $9-j$ coefficients

are immediately usable for this purpose, especially if eigenstates are to be converted. If we merge the two trees in Figure 9.11, taking care to distinguish their branches, as in Figure 9.12, then we obtain representation of the relation between L - S and j - j coupling schemes, as shown in Figure 9.14.

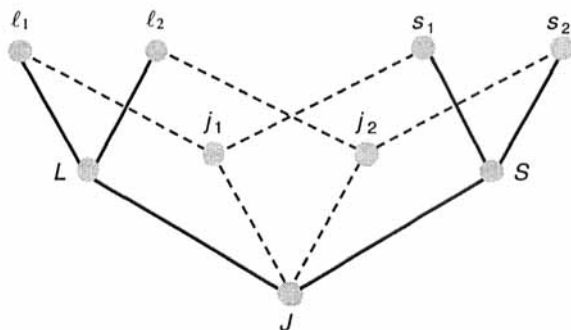


FIGURE 9.14 The tree representation for transforming between L - S and j - j coupling schemes. Solid lines indicate couplings across the rows and dashed lines indicate couplings down the columns.

We obtain eigenkets in the j - j scheme merely by comparing labels between Figures 9.12 and 9.14, then rewriting (9.56), to obtain

$$\left| (\ell_1 s_1) j_1, (\ell_2 s_2) j_2; JM \right\rangle = \sum_{LS} \left| (\ell_1 \ell_2) L, (s_1 s_2) S; JM \right\rangle \times \sqrt{(2L+1)(2S+1)(2j_1+1)(2j_2+1)} \begin{Bmatrix} \ell_1 & \ell_2 & L \\ s_1 & s_2 & S \\ j_1 & j_2 & J \end{Bmatrix} \quad (9.69)$$

Because of the row-column symmetry (9.60) of 9 - j coefficients and the invariance of the factor under the radical in (9.69) under row and column interchange, eigenkets in the L - S scheme can be put on the left-hand side if those of the j - j scheme are put on the right-hand side and the summation is made over j_1 and j_2 .

To make this plethora of symbols more realistic, we now consider a concrete example.

L - S and j - j Coupling for Spin-1/2 Particles. In calculations of atomic and nuclear structure or in the quark model of hadrons, the intrinsic spins of the particles (electrons, nucleons, or quarks) are $1/2$. Thus, transformation (9.69) between coupling schemes has $s_1 = s_2 = 1/2$; thus $S = 0$ (singlet state) or $S = 1$ (triplet state).

The singlet-state contribution in (9.69) can be simplified by noting that the 9 - j coefficient with $S = 0$ can be manipulated to the form (9.63) by using rule (9.61) for

interchanges of rows and columns, then the resulting 6- j coefficient can be manipulated by using (9.22) to produce the singlet-state contribution

$$\begin{aligned} |(\ell_1 s_1)j_1, (\ell_2 s_2)j_2; JM\rangle_{S=0} &= |(\ell_1 \ell_2)L, (s_1 s_2)0; JM\rangle \\ &\times \sqrt{\frac{(2j_1+1)(2j_2+1)}{2}} (-1)^{J+1/2-\ell_1-j_2} \begin{Bmatrix} 1/2 & \ell_1 & j_1 \\ J & j_2 & \ell_2 \end{Bmatrix} \delta_{L,J} \end{aligned} \quad (9.70)$$

Table 9.1 gives the required 6- j coefficients.

The triplet-state contribution in (9.69) contains, in general, contributions from three values of L , namely the sum

$$\begin{aligned} |(\ell_1 s_1)j_1, (\ell_2 s_2)j_2; JM\rangle_{S=1} &= \sum_{L=J-1}^{J+1} |(\ell_1 \ell_2)L, (s_1 s_2)1; JM\rangle \\ &\times \sqrt{3(2L+1)(2j_1+1)(2j_2+1)} \begin{Bmatrix} \ell_1 & \ell_2 & L \\ 1/2 & 1/2 & 1 \\ j_1 & j_2 & J \end{Bmatrix} \end{aligned} \quad (9.71)$$

In the common situation that both particles are in the same shell—so that $\ell_2 = \ell_1$ and $j_2 = j_1$ —the 9- j coefficient in (9.71) changes by the phase $P = 1 + L + J$ if the first and second columns—which are identical—are interchanged, as can be shown by using the phase-change rule (9.61) and simplifying by using the phase manipulation rules in Section 2.1.4. Therefore, the coupled orbital state that has $L = J$ does not contribute to the triplet state in this case, as we see in the following example. This condition, which arises from rotational symmetries only, could easily be confused with the Pauli principle, which (9.71) does not invoke.

A Worked Example of L - S and j - j Coupling. To see expansion (9.69) in explicit action, consider the simplest nontrivial example, having $\ell_2 = \ell_1 = 1$ and $j_2 = j_1 = 1/2$. To avoid confusion from effects of the Pauli principle, imagine that system 1 describes an electron, system 2 describes a proton, and their orbital angular momenta are referred to the center of a molecule of which this “hydrogen” is an atom. The j - j state is then obtained from L - S states as

$$\begin{aligned} |(1,1/2)1/2, (1,1/2)1/2; JM\rangle \\ = 2 \sum_{LS} |(11)L, (1/2 1/2)S; JM\rangle \sqrt{(2L+1)(2S+1)} \begin{Bmatrix} 1 & 1 & L \\ 1/2 & 1/2 & S \\ 1/2 & 1/2 & J \end{Bmatrix} \end{aligned} \quad (9.72)$$

We can now commit to a choice of J on the left-hand side, say $J = 1$, which the bottom row of the 9- j coefficient shows is the largest possible value. Table 9.4 lists the appropriate 9- j (X) coefficients, which you can obtain when working Problem 9.16 by using *Mathematica* notebook Num9j in Appendix I.

TABLE 9.4 Values of 9-*j* coefficients for expansion (9.72).

<i>L</i>	<i>S</i>	$X\{1,1,L; 1/2,1/2,S; 1/2,1/2,J\}$
0	1	-1/18
1	0	1/(3√6)
1	1	0
2	1	1/9

By using these coefficients, expansion (9.72) reduces to

$$\begin{aligned}
 & |(1,1/2)1/2,(1,1/2)1/2;1M\rangle \\
 &= \frac{-1}{\sqrt{27}}|01;1M\rangle + \sqrt{\frac{6}{27}}|10;1M\rangle + \sqrt{\frac{20}{27}}|21;1M\rangle
 \end{aligned} \tag{9.73}$$

in which the kets have been abbreviated to $|LS;JM\rangle$. The state $|11;1M\rangle$ does not contribute because the symmetry rule (9.61) makes the phase exponent in the 9-*j* coefficient odd for $L = 1 = S$, yet two of its rows are identical, so it must be zero.

As a partial check on the correctness of this expansion (it does not check correctness of signs), notice that the sum of the squares of the expansion coefficients is unity, consistent with (9.65). States with largest *L* and *S* are favored in this expansion, with $L = 2, S = 1$ being more than three times as probable (20/6) as $L = 1, S = 0$. As continually emphasized throughout this book, these properties arise from rotational symmetries, not from dynamics, once angular momenta are chosen.

Extensive applications of the theory of recoupling angular momenta to atomic spectroscopy are given in Section 7.5 of Biedenharn and Louck [Bie81a] and in the monograph by Judd [Jud63]. Applications to the nuclear shell model are given in Section 7.9 of [Bie81a] and in the monograph by de-Shalit and Talmi [de-S63]. Recoupling techniques for angular momentum in nuclear reactions are developed in Chapters X and XI of Rose's book [Ros57] and in Section 7.8 of [Bie81a]. In all these applications the Pauli principle (Sections 1.4.3, 1.4.4) has a significant influence. The inclusion of the identity of the fermions involved is emphasized in Chapter XII of [Ros57].

Group theory (introduced in Section 2.5) provides an alternative methodology and emphasis to that used here and in the references of the preceding paragraph. Group theory for atomic and nuclear structure is presented in Chapter 8 of Elliott and Dawber [Ell79] and in Chapter 13 of Ludwig and Falter [Lud88]. Related applications to models of elementary particles are given in Chapters 10–12 of [Ell79] and in Chapter 13 of [Lud88].

9.5.5 Graphical and Automated Methods

As computers become more suitable for symbolic as well as numerical computation, more of the algebraic tedium of angular momentum coupling can be assigned to ma-

chines for processing while humans think about the science.

One often begins by describing a graphical method, such as extension of the coupling triangles (for 3- j coefficients) and coupling quadrilaterals (for 6- j coefficients), as in Brink and Satchler's monograph [Bri94] or in the book by Danos and Gillet [Dan90], which provides a complete treatment. General methods for diagram techniques in group theory, including the 6- j and 9- j coupling coefficients, are described in Stedman's monograph [Ste90]. Given the method, it can either be used by hand and brain or it can be implemented into a computer program, such as that published by Williams and Silbar [Wil92]. The logic of their program organizes the angular momentum couplings according to a tree structure—similar to Figures 9.3 and 9.12—and uses several heuristic rules for simplifying solutions. Their program also simplifies expressions for reduced matrix elements.

Alternatively, one can use a symbolic-processing system to compute directly the algebraic expressions for the results of coupling. When supplemented by some simplification rules, such an approach can be very effective. An example of such an application in atomic physics, using *Mathematica*, is given in the article by Way and Williams [Way93].

PROBLEMS ON RECOMBINING SEVERAL ANGULAR MOMENTUM EIGENSTATES

9.1 Derive the sum rule (9.14) between 3- j and 6- j coefficients by expanding the left-hand and right-hand sides of defining relation (9.13) into the basic states $|a\alpha\rangle$, $|b\beta\rangle$, and $|d\delta\rangle$, by using the coupling formula (7.60) twice on each side. Equate coefficients of these orthogonal states on each side, and assume that the 3- j coefficients do not vanish because of violating the m -sum rules. Simplify the phases by using the phase-manipulation rules (Section 2.1.4), in order to obtain (9.14).

9.2 Verify directly the explicit formula for the 6- j coefficient, (9.16), by expanding the bra-ket of the coupled states in the definition (9.13) into uncoupled states by using 3- j coefficients.

9.3 To show the reduction of the sum (9.17) to (9.18), first identify the angular momenta between Figures 9.5 and 9.1. Next, use the permutation symmetry rule for 3- j coefficients, (7.68), to interchange the second and third arguments in coefficients (4) and (2). Finally, simplify the phases and identify the part of the sum that agrees with the 6- j expansion (9.16).

9.4^M Algebraic expressions for 6- j coefficients can be obtained by using *Mathematica* notebook Alg6j in Appendix I. By this means you can extend Table 9.1 if necessary. (Be careful when assigning symbols because of the symbol-replacement rules in *Mathematica*. Also note that SixJSymbol checks the triangle and m -sum selection rules *only* if all its arguments are numerical.)

(a) Enter and check Alg6j by running a few of the values given in Table 9.1.

(b) Generate all the independent algebraic 6- j coefficients corresponding to the smallest angular momentum being 3/2.

(c) For a small angular momentum of your choice, say $a = 1/2$, modify the notebook so that it applies functions `CForm` or `FortranForm` to the algebraic 6- j coefficient generated by *Mathematica*. Then use these coding statements to build a small program that computes the coefficient numerically. Check its results against the C-language program for 6- j coefficients given as C3 in Appendix II.

(d) Time the special-purpose program from (c) and the general-purpose program from Appendix II, measuring only the execution times of the coefficients, not the times for input and output. What is the speedup factor for your computing system? Would this produce a significant saving in typical calculations in which you use these coefficients?

9.5 Derive the orthogonality relation for 6- j coefficients, (9.21), by using unitarity of the coupling, with state (e, ϵ) as intermediate state. The derivation of (7.61) for 3- j coefficients may serve as a model.

9.6 Derive one of the symmetry conditions for 6- j coefficients that satisfies (9.22) by using expression (9.16) for its expansion as a sum of products of 3- j coefficients then using the symmetries of these coefficients as given in Section 7.3.1.

9.7 Investigate the recoupling schemes for wave functions given in (9.24) by giving the detailed expansions, analogous to (9.25), for the two cases with proton angular momentum $j_p = 3/2$ combined to total $J = 1/2$ and to $J = 3/2$.

9.8 With a numerical program that computes 6- j coefficients, for example `_6j` in Appendix II, check its accuracy by computing and printing the orthogonality sum (9.21) for a range of the six parameters over which you are likely to use the program. If feasible with your computer system, run the program in single- and double-precision modes in order to estimate how the accuracy of the results depends on roundoff errors in the floating-point arithmetic.

9.9 Consider the matrix elements $\langle (j_1 j_2) JM | \mathbf{T}_k(A_1) \cdot \mathbf{T}_k(A_2) | (j'_1 j'_2) J' M' \rangle$ for the scalar product in terms of matrix elements of the separate operators between uncoupled states.

(a) Expand the coupled states in terms of uncoupled states and Clebsch-Gordan coefficients by using the basic formula (7.35).

(b) Use the Wigner-Eckart theorem, (8.32), to express the m dependences of the corresponding matrix elements in terms of Clebsch-Gordan coefficients.

(c) Identify the resulting magnetic substate summation as proportional to a 6- j coefficient in order to derive (9.27).

9.10 For reduced matrix elements of the spin-orbit operator, carry out the details of the steps from (9.27) to (9.28), as indicated above the latter equation.

9.11 Prove the projection theorem (9.29) for a representative component J_σ with $\sigma = \pm 1, 0$. To do this, verify the following steps.

(a) Write the matrix element as in (9.30), then use (9.31). Use the Racah condition (8.15) with $k = 1$ to simplify the commutator. Show that the sum over Clebsch-Gordan coefficients with all total angular momenta is zero, by using connection (7.57) to 3- j coefficients then explicit expressions in Table 7.3 for the latter.

(b) For the matrix element sum in (9.32), insert unit operators as suggested in the text, then use the Wigner-Eckart theorem with $k = 1$ and reduced matrix element (8.48). Simplify the sum over products of two Clebsch-Gordan coefficients by using their orthogonality relation (7.41).

(c) Apply the Wigner-Eckart theorem again to produce (9.29).

9.12 Consider the expansion formulas for $9-j$ coefficients.

(a) To derive expansion (9.58) into $3-j$ coefficients, make the complete expansion of the bra-ket in (9.57) into combining pairs of angular momenta according to (7.60), then cancel common factors and simplify the phases.

(b) To obtain (9.59), collapse pairs of $3-j$ coefficients using (9.14) to get $6-j$ coefficients. Thus produce the product of three $6-j$ coefficients summed over k .

9.13^M The orthogonality sum for $9-j$ coefficients, (9.65), can be used to check a numerical program for computing $9-j$ coefficients, for example `_9j` in Appendix II.

(a) Check the program accuracy by computing and printing the coefficient for a range of the nine parameters over which you intend to use the program. If feasible, run the program in single- and double-precision modes and estimate how the accuracy of the calculations depends on roundoff errors.

(b) Use *Mathematica* notebook `Num9j` in Appendix I to get exact $9-j$ coefficients. Compare these with values from decimal approximation results in (a).

9.14^M Consider the special values $a = 0$ and $a = 1$ in a $9-j$ coefficient.

(a) Derive (9.62) by using expansion (9.59), then simplifying the two $6-j$ coefficients by using the first entry in Table 9.1.

(b) Verify the correctness of (9.62) by adding to *Mathematica* notebook `Num9j` a cell that evaluates the right-hand side of (9.62), then compares this with the result of evaluating the $9-j$ coefficient with $a = 0$. Run this for several values of the remaining eight arguments that are consistent with the triangle rules.

(c) Make a similar analysis for $a = 1$, $c = b$, and $g = d$, in order to obtain (9.64).

9.15 To derive (9.68) for tensor matrix elements in the coupled scheme, expand the bras and kets by using basic combination formula (7.35), express the operator by using (9.66), and write the matrix elements in the uncoupled representation by using the Wigner-Eckart theorem. Show that the magnetic substate summations produce a quantity proportional to a $9-j$ coefficient, thereby (9.68).

9.16^M For example (9.72), relating $L-S$ and $j-j$ coupling, use *Mathematica* notebook `Num9j` in Appendix I to calculate the $9-j$ coefficients for the L and S values in Table 9.4.



Myself when young did eagerly frequent
 Doctor and saint, and heard great argument
 About it and about: but evermore
 Came out by the same door as in I went.

With them the seed of wisdom did I sow,
 And with my own hand labour'd it to grow:
 And this was all the harvest that I reap'd –
 "I came like water, and like wind I go."

The Rubaiyat of Omar Khayyam, trans. Edward FitzGerald

EPILOGUE

We have now completed our introduction to rotational symmetries for physical systems. As summarized in Section 1.3.3 (Figure 1.15), there are many interrelations among topics in angular momentum theory—geometrical and dynamical, classical and quantal. Aspects of angular momentum theory pertaining most nearly to mathematical physics are presented in the two-volume encyclopedic works by Biedenharn and Louck [Bie81a, Bie81b], with the first volume emphasizing the standard treatment of angular momentum theory and its applications, and the second dealing in depth with fundamental concepts of the subject and interrelations of the theory with other areas of mathematics. The handbook by Brink and Satchler [Bri94] and the compendium by Varshalovich et al. [Var88] are useful sources of formulas and further developments.

Starting from macrosystems and turning inward to microsystems, applications of spherical harmonics and tensors to classical field theory (especially geophysics and fluid dynamics) are emphasized in the monograph by Jones [Jon85], angular momentum theory for diatomic molecules is the subject of a text by Judd [Jud75], applications in chemistry are emphasized in the book by Zare [Zar87], while nuclear physics applications (including electromagnetic multipole fields) are described in the two books by Rose [Ros55, Ros57]. More general aspects of symmetries relevant to nuclear and particle physics are catalogued in the text by Greiner and Müller [Gre89]. Group-theoretical approaches to symmetry are made in several of the references indicated in Section 2.5.

As we have continually emphasized throughout this book, rotations in the three dimensions of configuration space often provide the most concrete example of a continuous symmetry operation. The more abstract symmetries, such as isospin (Section 3.4.3) and its generalizations, can therefore usually be most easily understood by comparison and analogy with angular momentum.



APPENDIX I

NOTEBOOKS FOR *MATHEMATICA*

Here we provide *Mathematica* notebooks that you can use to visualize rotational symmetries and compute other quantities in *Angular Momentum*. The notebooks were used to produce many of the figures in the text, as indicated in figure captions, which give the names of the notebooks used. First, we summarize the purpose of the notebooks, the computer requirements to run them, their arrangement, the programming conventions used, and some suggestions for animating the graphics. Next come the notebooks in alphabetic order. Finally, there is a table that indexes the notebooks. Of the 135 problems at the end of the chapters, 27 suggest using *Mathematica* to help with their solution.

Purpose of the Notebooks. The *Mathematica* notebooks enable you to explore analytical, numerical, and graphical properties of objects occurring in the study of angular momentum and rotational symmetries for physical systems. Visualization is especially important for understanding rotational properties. Since *Mathematica* is especially adept at graphics, the programs are easily written, compact, and usually simple to understand—hence my choice of this system for doing mathematics by computer.

It is especially important for understanding angular momentum that once you have the notebook running on your computer you should use it extensively and thoughtfully in order to explore the fascinating world of rotations. Do not be afraid to stress the system, since the notebooks and the *Mathematica* system will usually protect against inappropriate input. The three-dimensional graphics typically require the most memory and time for completion. Once the graphic object is completed, however, on most computers you can easily view it from different orientations by using the 3D ViewPoint Selector command in the Prepare Input submenu of the Action menu.

Computer Requirements. The notebooks were prepared on an Apple Macintosh IIsi computer with accelerator board, RAM cache, and floating-point unit. The effective speed of the machine when running *Mathematica* is about 35 MHz, and the time required to execute most cells was a few seconds to a minute. The RAM required was usually about 4 Mbyte, with a few notebooks needing 6 Mbyte. The simplest way to free up unneeded memory is to save the notebook after a run, then quit and relaunch *Mathematica* before making the next run. Displays that by default display color will show in color on appropriate monitors but will also produce satisfactory black-and-white or gray-scale displays without modification.

As the angular momentum numbers that you input increase, so do the time and memory required to execute the notebook cells. Also, for two-dimensional graphics (such as polar diagrams, Section 4.1.2) time and memory needs increase roughly linearly with the number of display points. For three-dimensional graphics both the time and memory required increase roughly quadratically with the number of display points in each dimension. If you have a smaller computer than mine or want more speed, you can run the kernels on a remote computer, with only the *Mathematica* front end on the local computer. Various means for doing this are described in books about the *Mathematica* system, such as [Mae91] and [Wol91].

The version of *Mathematica* used for the notebooks given here is version 2.2. Different versions have different requirements as to whether a built-in function or a package is used and will sometimes have different default values for options. Notebook user interfaces are available (as of this writing) on Macintosh, Microsoft Windows, NeXT systems, and on the X Window System on Unix operating systems.

Arrangement of the Angular Momentum Notebooks. The notebook contents usually include only the program cells, without output. To see sample output, look at the section and figure or table numbers indicated at the start of each notebook listing. The programs are listed in full at the end of this appendix and are arranged by order of appearance by notebook name.

You can also use Table A.I.1 to locate the chapter and section of the text in which the notebook is first used. Each figure in the book indicates if a *Mathematica* notebook was used to help prepare the figure. Most such figures were enhanced by using an illustration and layout program with *Mathematica* PostScript graphics as its input; if so, the figure caption gives the notebook name and is annotated with "Adapted from". The graphics, usually without lettering, should look like your notebook output cell, which you can use to test that your program is executing appropriately.

For a few of the figures that were prepared with help from *Mathematica*, I do not provide the notebooks used. Some were too small and some were too large and cumbersome. Those that I include will be just right for you to learn about rotational symmetries.

Programming Conventions. In these notebooks I use a consistent programming style, with the following programming conventions to keep the notebooks compact.

- Built-in functions (in version 2.2 used) are preferred over packages or my own programming constructions. Repetitive coding is often avoided by using functions defined within each notebook.
- Options in functions are changed from default values as little as necessary to produce clear results. You may wish to change these options.
- Lettering is kept to the minimum needed to identify output clearly.
- Verbose output is suppressed by using the “;” code at the end of most expressions. Further suppression can be obtained by turning off Show In/Out Names in the File menu. This is recommended except if you need to debug a notebook.

Animated Visualizations. On several computer systems that run *Mathematica*, it is possible and straightforward to animate the graphics displays. For many of the notebooks in *Angular Momentum* this is worth the time and small extra programming effort involved. Particularly effective is animation of three-dimensional displays of rotation functions used to describe objects whose state is time-dependent, such as precessing tops (notebook *Precess* in Section 5.3.1) and rigid rotators (Section 6.5). Animation can usually be added to each appropriate notebook by writing a new cell and running it after the notebook cell provided here.

The Mathematica Notebooks. The notebooks are listed by order of their appearance in the book. This order is specified by the section number and figure following the notebook name. All this information is summarized in Table A.I.1.

Notebook Shell (Section 1.2.1, Figure 1.7)

```
Print["\nANGULAR MOMENTUM: Rotational Symmetries\n"]
Print["Notebook Shell: Helical Shell\n"]
Unprotect[In, Out]; Clear[In, Out]; Protect[In, Out];
Clear[h, r];

h = 2 ; r = 7/4 ;
```

```
Conch = ParametricPlot3D[{phi Cos[phi] Cos[t],
  phi Sin[phi] Cos[t], phi Sin[t] + h phi},
  {t, 0, 2 Pi}, {phi, 0, 2 Pi r},
  PlotPoints->(*4*)20, DisplayFunction->Identity];
Unprotect[In, Out]; Clear[In, Out]; Protect[In, Out];
ShowSurf = Show[Conch, Boxed->False, Axes->False,
  DisplayFunction->${DisplayFunction}];
```

Notebook Polyhedra (Section 1.2.2, Figure 1.9)

```
(* Regular polyhedra filling 3-space *)
Print["\nANGULAR MOMENTUM: Rotational Symmetries\n"]
Print["Notebook Polyhedra: The five regular polyhedra\n"]
<<Graphics`Polyhedra` ;

Solid[name_] := Show[Graphics3D[name,
  Axes->False, Boxed->False]];
```



```
Solid[Tetrahedron[]];Solid[Cube[]];
Solid[Octahedron[]];Solid[Dodecahedron[]];
Solid[Icosahedron[]];
```

Notebook WorldView (Section 1.3.2, Figure 1.14)

```
Print["\nANGULAR MOMENTUM: Rotational Symmetries\n"]
Print["Notebook WorldView: World views\n"]
<<Miscellaneous`WorldPlot`
(* To suppress irrelevant error messages *)
Off[Power::infy,Infinity::indet,Graphics::gptn];

WPeasy = WorldPlot[{World, RandomGrays},
  WorldRotation->{0,0,0},
  WorldRange->{{-90,90}, {-180,180}},
  WorldProjection->LambertAzimuthal];
```

Notebook Ppsi (Section 1.4.1, Figure 1.19)

```
Print["\nANGULAR MOMENTUM: Rotational Symmetries\n"];
Print["Notebook Ppsi: Parity and wave functions\n"];

(* Sample wave function, psi *)
psi[x_] := Cos[x]+0.5*(x+2)*Sin[x];

(* Functions for plotting *)

DashIt := {Dashing[{0.02,0.02}]} (* short dash *)
WFPlot[sign_,pwr_,style_] :=
  Plot[{(psi[x]+sign*psi[-x])^pwr},{x,-3,3},
  PlotStyle->style, DisplayFunction->Identity];

(* Execution *)

(* psi and its square *)
psiShow = Show[WFPlot[0,1,DashIt],
  WFPlot[0,2,Automatic],
  DisplayFunction->${DisplayFunction}];

psiPlot = Plot[{psi[x]^2 + psi[-x]^2},{x,-3,3}];

(* Even-parity; psi+ and square *)
EvenShow = Show[WFPlot[1,1,DashIt],
  WFPlot[1,2,Automatic],
  DisplayFunction->${DisplayFunction}];

(* Odd-parity; psi- and square *)
OddShow = Show[WFPlot[-1,1,DashIt],
  WFPlot[-1,2,Automatic],
  DisplayFunction->${DisplayFunction}];
```

Notebook PauliCC (Section 1.4.5, Figure 1.22)

```
Print["\nANGULAR MOMENTUM: Rotational Symmetries\n"]
Print["Notebook PauliCC: Coulomb scattering of C nuclei\n"]
```

```
(* Functions for Coulomb-scattering amplitudes *)
fR[th_,sgn_] := Exp[2I*eta*Log[Sin[th/2]]]
/Sin[th/2]^2
fSym[th_,sgn_] := fR[th,sgn] + sgn*fR[Pi-th,sgn]
SigPlot[F_,sgn_] := Plot[ Log[Abs[F[th,sgn]]^2],
  {th, Pi/9, 2*Pi/3}, PlotPoints->80, Ticks->None,
  Axes->None, DisplayFunction->Identity];
Clear[eta]; eta = 15; (* Sommerfeld parameter *)
(* Execution *)
C12w12C = SigPlot[fSym,+1];
C13w12C = SigPlot[fR,0];
C13w13C = SigPlot[fSym,-1];
Show[GraphicsArray[{C12w12C,C13w12C,C13w13C}],
  DisplayFunction->${DisplayFunction}];
```

Notebook PL (Section 4.1.2, Figure 4.2)

```
Print["\nANGULAR MOMENTUM: Rotational Symmetries\n"]
Print["Notebook PL: Legendre polynomials\n"]
(* To suppress irrelevant error messages *)
Off[General::spell1];
stepTheta = 0.10; LMx = 6;
PLSurf = Table[N[LegendreP[L,Cos[theta]]],
  {L,0,LMx}, {theta,0,Pi,stepTheta}];
PLGraphS = ListPlot3D[PLSurf, Ticks->None,
  ViewPoint->{1.3, -2.4, 2.0},
  AxesLabel->{"theta", "L", "PL"},
  PlotLabel->"PL:
  L=0-<>ToString[LMx]<>", theta=0-Pi"];
PLGraphTheta =
Plot[N[LegendreP[LMx/2,Cos[theta]]],
  {theta,0,Pi}, Ticks->Automatic,
  AxesLabel->{"theta", ""},
  PlotLabel->"P<>ToString[LMx/2]<>" v theta"];
PLGraphL = Plot[N[LegendreP[L,0]], {L,0,LMx},
  Ticks->Automatic,
  AxesLabel->{"L", ""},
  PlotLabel->"PL(cos Pi/2) v L"];

```

Notebook PLM (Section 4.1.2, Figure 4.4)

```
Print["\nANGULAR MOMENTUM: Rotational Symmetries\n"]
Print["Notebook PLM : \n Legendre functions ( L >= 0, 0 <= m <= L )\n"]
(* Functions *)
pos[x_] := If[ x>0, x, 0]
```

```

neg[x_] := -If[ x<0, x, 0]
signedPoints[pn_,AutoOrDash_] :=
  ParametricPlot[{pn[dL]*Sin[theta],pn[dL]*
  Cos[theta]},{theta,0,2 Pi},PlotPoints->points,
  PlotDivision->points, Axes->{False,True},
  AspectRatio->Automatic, Ticks->None,
  PlotStyle->AutoOrDash,
  DisplayFunction->Identity]

(* Execution *)
L = Input["Legendre functions, P(L)m.
  Enter L ( >=0 ):"];
m = Input[" Enter m ( 0 <= m <= L ):"];
If[ m<0, Print["\n!!m < 0; Using |m|\n"];
  m = -m; ];
Print[" ",m]
Print["P (Cos[theta]) = "]
Print[" ",L ]

dL = Factor[Simplify[((L+m)!/(2^m (L!))*
  ((Sin[theta])^m)* JacobiP[L-m,m,m,Cos[theta]]]]
dLsin = dL Sin[theta];
points = Max[8,Min[2*L+8,20]];
If[Input["For 2D x-y Plot enter non-zero:"] != 0,
  Plot[dL, {theta, 0, Pi},
  PlotPoints->points, PlotDivision->points,
  AxesLabel->{"theta",""}];
]
If[Input["For 2D Polar Plot enter non-zero:"]
!= 0,
(
  (* positive values as solid curves *)
  posPoints = signedPoints[pos,Automatic];
  (* negative values as dashed curves *)
  negPoints = signedPoints[neg,
  {Dashing[{0.05,0.05}]}];
  Show[posPoints,negPoints,
  DisplayFunction->$DisplayFunction];
) ]

```

Notebook YLMabs (Section 4.1.3, Figure 4.7)

```

Print["\nANGULAR MOMENTUM: Rotational Symmetries\n"]
Print["Notebook YLMabs: Plot |Spherical harmonic|\n"]
DeclarePackage["Global`",{"SphericalHarmonicY"}]
(*loads function if needed. *)

(* Function *)
absYLM[theta_,phi_] := ComplexExpand[Abs[
  SphericalHarmonicY[L,m,theta,phi]];

(* Input *)
L=Input["Spherical harmonic YLm. Enter L (>=0):"];
m=Input[" Enter m (|m|<=L):"];

```

```
Print["Y ",L," ",m," (theta,phi) ="]
(* Execution *)
Clear[PointYLM]; PointYLM = 24;
yLm = SphericalHarmonicY[L,m,theta,phi]
g = SphericalPlot3D[Evaluate[absYLM[theta,phi]],
  {theta, 0, Pi, Pi/(PointYLM-1)},
  {phi, Pi/6,11 Pi/6,10 Pi/(6*(PointYLM-1))},
  ViewPoint->{3.0, 0.0, 1.5},
  Boxed->False,Axes->False];
```

Notebook EXPimPHI (Section 4.1.3, Figure 4.8)

```
Print["\nANGULAR MOMENTUM: Rotational Symmetries\n"]
Print["Notebook ExpimPhi: Re[exp(i m phi)] = cos (m phi)\n"]
Unprotect [In,Out];Clear [In, Out];Protect [In,Out];

(* Functions *)
(* Phi dependence has a small offset *)
rfatCos[phi_,t_] :=
  Cos[phi]*(R+(Cos[m*phi]+0.05)*Cos[t]);
rfatSin[phi_,t_] :=
  Sin[phi]*(R+(Cos[m*phi]+0.05)*Cos[t]);
rfat[phi_,t_] := (Cos[m*phi] + 0.05)*Sin[t];

(* Execution:
  Very slow for m > 0 *)
Clear[m, R]; m = 1; R = 3;

Print["exp(i ", m, " phi)\n"]
Surf = ParametricPlot3D[
  {Evaluate[rfatCos[phi,t]],
   Evaluate[rfatSin[phi,t]],
   Evaluate[rfat[phi,t]]},
  {t, 0, 2*Pi}, {phi, 0, 2*Pi},
  PlotPoints->15,Boxed->False,Axes->False];
```

Notebook Precess (Section 5.3.1, Figure 5.9)

```
(* Precessing shell *)
(* Needs about 4 Mbyte for Mathematica
  plus about 7 Mbyte for kernel *)
Print["\nANGULAR MOMENTUM: Rotational Symmetries\n"]
Print["Notebook Precess: Uniform Precession\n"]

Unprotect [In,Out];Clear [In,Out];Protect [In,Out];
(* To suppress irrelevant error messages *)
Off[General::spell1,General::spell,
  Set::write,SetDelayed::write];

(*Functions *)
(* Define shell with axis along z, vertical,
  helix pitch h *)
```

```

xV[ph_,t_] := ph*Cos[ph]*Cos[t];
yV[ph_,t_] := ph*Sin[ph]*Cos[t];
zV[ph_,t_] := ph*Sin[t] + h*ph;

(* Rotate around y by thS *)
xYthS[ph_,t_] := xV[ph,t]*Cos[thS]-zV[ph,t]*
  Sin[thS];
yYthS[ph_,t_] := yV[ph,t];
zYthS[ph_,t_] := xV[ph,t]*Sin[thS]+zV[ph,t]*
  Cos[thS];

(* Then rotate around z by pS for precession *)
xZphS[ph_,t_,pS_] := xYthS[ph,t]*
  Cos[pS]-yYthS[ph,t]*Sin[pS];
yZphS[ph_,t_,pS_] := xYthS[ph,t]*
  Sin[pS]+yYthS[ph,t]*Cos[pS];
zZphS[ph_,t_,pS_] := zYthS[ph,t];

Conch[pS_] := ParametricPlot3D[
  {Evaluate[xZphS[ph,t,pS]],
   Evaluate[yZphS[ph,t,pS]],
   Evaluate[zZphS[ph,t,pS]]},
  {t, 0, 2*Pi}, {ph, 0, 2*Pi*r },
  Boxed->False, Axes->False, SphericalRegion->True,
  ViewCenter->{1/2,1/2,1/2},
  PlotRange->{{-20,20},{-20,20},{0,30}},
  DisplayFunction->Identity, PlotPoints->15];

(* Execution *)
Clear[h,r,thS];
h = 2 (* helix pitch *); r = 7/4 (* phi range *);
thS = Pi/6 (* shell angle to z axis *);

Shells = Table[Conch[i*Pi/4],{i,0,7,1}];
<<Graphics`Animation`
Precess = ShowAnimation[Shells,
  DisplayFunction->$DisplayFunction];

```

Notebook BesL (Section 5.4.1, Figure 5.10)

```

Print["\nANGULAR MOMENTUM: Rotational Symmetries\n"]
Print["Notebook BesL: Spherical Bessel functions\n"]
(* To suppress irrelevant error message *)
Off[General::spell1];

(* Function *)
jL[L_,rho_] :=
  Sqrt[Pi/(2*rho)]*BesselJ[L+(1/2),rho]

(* Execution *)
rhoMx = 10.1; stepRho = 0.2; LMx = 5;
jLSurf = Table[N[jL[L,rho]],
  {L,0,LMx}, {rho,0.001,rhoMx,stepRho}];

```

```

jLGraphS = ListPlot3D[jLSurf, Ticks->None,
  ViewPoint->{1.3, -2.4, 2.0},
  AxesLabel->{"rho", "L", "jL(rho) "},
  PlotLabel->"Spherical Bessel functions"];
jLGraphRho =
  Plot[N[jL[Floor[LMx/2], rho]], {rho, 0.001, rhoMx},
  Ticks->Automatic, AxesLabel->{"rho", ""},
  PlotLabel->
  "j"<>ToString[Floor[LMx/2]]<>" v rho"];
jLGraphL = Plot[N[jL[L, Floor[rhoMx/2]]], {L, 0, LMx},
  Ticks->Automatic, AxesLabel->{"L", ""},
  PlotLabel->
  "jL("<>ToString[Floor[rhoMx/2]]<>") v L"];

```

Notebook BesM (Section 5.4.1, Figure 5.11)

```

Print["\nANGULAR MOMENTUM: Rotational Symmetries\n"]
Print["Notebook BesM: Cylindrical Bessel functions\n"]

(* Execution *)

rhoMx = 10.1; stepRho = 0.2; mMx = 5;

JmSurf = Table[N[BesselJ[m, rho]],
  {m, 0, mMx}, {rho, 0.001, rhoMx, stepRho}];
JmGraphSurf = ListPlot3D[JmSurf, Ticks->None,
  ViewPoint->{1.3, -2.4, 2.0},
  AxesLabel->{"rho", "m", "Jm(rho) "},
  PlotLabel->"Cylindrical Bessel functions"];
JmGraphRho = Plot[N[BesselJ[Floor[mMx/2], rho]],
  {rho, 0.001, rhoMx},
  Ticks->Automatic, AxesLabel->{"rho", ""},
  PlotLabel->
  "J"<>ToString[Floor[mMx/2]]<>" v rho"];
JmGraphM = Plot[N[BesselJ[m, Floor[rhoMx/2]]],
  {m, 0, mMx},
  Ticks->Automatic, AxesLabel->{"m", ""},
  PlotLabel->
  "Jm("<>ToString[Floor[rhoMx/2]]<>") v m"];

```

Notebook PW3D (Section 5.4.2, Figure 5.12)

```

Print["\nANGULAR MOMENTUM: Rotational Symmetries\n"]
Print["Notebook PW3D: Plane waves in 3 dimensions\n"]

(* Functions *)
rho:=Sqrt[z^2+x^2](* Cartesian->plane polar *)
theta:=ArcTan[z,x](* define spherical Bessel *)
jL[L_,rho_] :=
  Sqrt[Pi/(2*rho)]*BesselJ[L+(1/2),rho]

(* Execution *)

LL = Input["Maximum L value ( >=0 )"];

```

```

rL = Floor[LL/2]; iL = Floor[(LL-1)/2];
rhoMx = Input["Max rho (=kr) value ( >0 )"];

NumZX = 15; (* points in z & x directions *)
stepZX = rhoMx/(NumZX-1);

(* Real part of complex exponential *)
ReExp3D = Table[N[Cos[rho*Cos[theta]]],
  {z,0.00001,rhoMx,stepZX},
  {x,0.00001,rhoMx,stepZX}];
(* Real part of partial-wave sum up to LL *)
RePW3D = Table[NSum[(-1)^L*(4*L+1)*jL[2*L,rho]*
  LegendreP[2*L,Cos[theta]],{L,0,rL}],
  {z,0.00001,rhoMx,stepZX},
  {x,0.00001,rhoMx,stepZX}];
ReExpGraph = ListPlot3D[ReExp3D,
  Ticks->None, AxesLabel->{"x","z","Re"},
  PlotLabel->"Re { exp[i rho cos(theta)] }"];
RePWGraph = ListPlot3D[RePW3D,
  Ticks->None, AxesLabel->{"x","z","Re"},
  PlotLabel->"Re { Partial Wave Expansion }"];

(* Imaginary part of complex exponential *)
ImExp3D = Table[N[Sin[rho*Cos[theta]]],
  {z,0.00001,rhoMx,stepZX},
  {x,0.00001,rhoMx,stepZX}];
(* Imaginary part of partial-wave sum to LL *)
ImpW3D = Table[NSum[(-1)^L*
  (4*L+3)*jL[2*L+1,rho]*
  LegendreP[2*L+1,Cos[theta]],{L,0,iL}],
  {z,0.00001,rhoMx,stepZX},
  {x,0.00001,rhoMx,stepZX}];
ImExpGraph = ListPlot3D[ImExp3D,
  Ticks->None, AxesLabel->{"x","z","Im"},
  PlotLabel->"Im { exp[i rho cos(theta)] }"];
ImpWGraph = ListPlot3D[ImpW3D,
  Ticks->None, AxesLabel->{"x","z","Im"},
  PlotLabel->"Im { Partial Wave Expansion }"];

```

Notebook PW2D (Section 5.4.2, Figure 5.13)

```

Print["\nANGULAR MOMENTUM: Rotational Symmetries\n"]
Print["Notebook PW2D: Plane waves in 2 dimensions\n"]

(* Functions *)

rho := Sqrt[x^2+y^2](* Cartesian->plane polar *)
phi := ArcTan[x,y]

(* Execution *)

M = Input["Maximum m value ( >=0 )"];
rM = Floor[M/2]; iM = Floor[(M-1)/2];
rhoMx = Input["Max rho (=kr) value ( >0 )"];

```

```

NumXY = 15; (* points in x & y directions *)
stepXY = rhoMx/(NumXY-1);

(* Real part of complex exponential *)
ReExp2D = Table[N[Cos[rho*Cos[phi]]],
  {x,0.00001,rhoMx,stepXY},
  {y,0.00001,rhoMx,stepXY}];
(* Real part of partial-wave sum to M *)
RePW2D = Table[N[BesselJ[0,rho]] +
  2*NSum[(-1)^m*BesselJ[2*m,rho] *
  Cos[2*m*phi],{m,1,rM}],
  {x,0.00001,rhoMx,stepXY},
  {y,0.00001,rhoMx,stepXY}];
ReExpGraph = ListPlot3D[ReExp2D,
  Ticks->None, AxesLabel->{"y","x","Re"},
  PlotLabel->"Re { exp[i rho cos(phi)] }"];
RePWGraph = ListPlot3D[RePW2D,
  Ticks->None, AxesLabel->{"y","x","Re"},
  PlotLabel->"Re { Partial Wave Expansion }"];

(* Imaginary part of complex exponential *)
ImExp2D = Table[N[Sin[rho*Cos[phi]]],
  {x,0.00001,rhoMx,stepXY},
  {y,0.00001,rhoMx,stepXY}];
(* Imaginary part of partial-wave sum to M *)
ImpPW2D = Table[2*NSum[(-1)^m*BesselJ[2*m+1,rho]
  Cos[(2*m+1)*phi], {m,0,iM}],
  {x,0.00001,rhoMx,stepXY},
  {y,0.00001,rhoMx,stepXY}];
ImExpGraph = ListPlot3D[ImExp2D,
  Ticks->None, AxesLabel->{"y","x","Im"},
  PlotLabel->"Im { exp[i rho cos(phi)] }"];
ImpPWGraph = ListPlot3D[ImpPW2D,
  Ticks->None, AxesLabel->{"y","x","Im"},
  PlotLabel->"Im { Partial Wave Expansion }"];

```

Notebook Djm'm (Section 6.3.3, Figure 6.7)

```

Print["\nANGULAR MOMENTUM: Rotational Symmetries\n"]
Print["Notebook Djm'm: Reduced rotation matrix elements\n"]

(* Functions *)
pos[x_] := If[ x>0, x, 0]
neg[x_] := -If[ x<0, x, 0]

signedPoints[pn_,AutoOrDash_] :=
  ParametricPlot[{pn[dj]*Sin[B], pn[dj]*Cos[B]},
  {B,0,2*Pi}, PlotPoints->points, Axes->False,
  PlotDivision->points, AspectRatio->Automatic,
  Ticks->None, PlotStyle->AutoOrDash,
  DisplayFunction->Identity]

(* Execution *)
j = Input["Reduced rotation matrix, d(j)m'm."]

```



```

Enter j ( >=0 ):"];
mp = Input[" Enter m' ( |m'|<=j ):"];
m = Input[" Enter m ( |m|<=j ):"];
Print[" ",j]; Print["d (B) ="];
Print[" ",mp,"",m ];

dj = Factor[Simplify[
  Sqrt[(j+m)!(j-m)!/((j+mp)!(j-mp)!)]*
  ((Sin[B/2])^(m-mp))*((Cos[B/2])^(m+mp))*
  JacobiP[j-m,m-mp,m+mp,Cos[B]] ]]
djsin = dj*Sin[B];
points = Max[10,Min[6*j+10,40]];
If[ Input[
  "For 2D Cartesian Plot enter non-zero:"] != 0,
  Plot[dj, {B, 0, Pi}, AxesLabel->{"B",""},
  PlotPoints->points, PlotDivision->points];
]
If[ Input["For 2D Polar Plot enter non-zero:"]
  != 0,
  (
    (* positive values as solid curves *)
    posPoints = signedPoints[pos,Automatic];
    (* negative values as dashed curves *)
    negPoints = signedPoints[neg,
      {Dashing[{0.05,0.05}]}];
    Show[posPoints,negPoints,
      DisplayFunction->$DisplayFunction];
  ) ]

```

Notebook DjjmCpr (Section 6.4.3, Figure 6.10)

```

Print["\nANGULAR MOMENTUM: Rotational Symmetries\n"]
Print["Notebook: DjjmCpr: Rotation functions; \n
Compare djjm (bars) and classical (curve)"]

(* Functions *)
<<Graphics`Graphics`
Probjj[m_] := (2j/((j+m)!*(j-m)!))*
  (Cos[b/2])^(2*(j+m))*(Sin[b/2])^(2*(j-m))
ProbClass[m_] := Exp[-(m-mc)^2/(j-mc^2/j)];

(* Execution *)
Clear[j,mc,b];

(* Total angular momentum *)          j = 6;
(* Classical m value (|mc|<j) *)      mc = -2;

Print[" for j = ",j," & mc = ",mc,"\n\n"]
b = N[ArcCos[mc/j]]; (* Classical angle *)
ProbTable = Table[
  {m, Probjj[m]/Probjj[mc], 0.1},
  {m, -j, j, 1}];
Plotjjm = GeneralizedBarChart[ProbTable,

```

```

Axes->{True, False},
DisplayFunction->Identity];
ClassTable = Table[{m, N[ProbClass[m]]},
                  {m, -j, j, 0.02}];
PlotClass = ListPlot[ClassTable,
                    PlotJoined->True,
                    DisplayFunction->Identity];
Compare = Show[Plotjjm,PlotClass,
              DisplayFunction->$DisplayFunction];

```

Notebook Djjo (Section 6.4.3, Figure 6.11)

```

Print["\nANGULAR MOMENTUM: Rotational
Symmetries\n"]
Print["Notebook Djjo: Rotation functions;\n
Probabilities for m=0, m'=j=3,12,48\n"]

(* Functions *)
Prob[j_] := (Sin[B])^(2*j)

probDen[j_,AutoOrDash_] := ParametricPlot[
  {Prob[j]*Sin[B], Prob[j]*Cos[B]},{B,0,2*Pi},
  PlotPoints->points, PlotDivision->points,
  AspectRatio->Automatic, Axes->False,
  Ticks->None, PlotStyle->AutoOrDash,
  DisplayFunction->Identity]

(* Execution *)

points = 100;
prob3 = probDen[3, Automatic];
prob12 = probDen[12, {Dashing[{0.04, 0.04}]}];
prob48 = probDen[48, {Dashing[{0.005, 0.02}]}];
PlotAll = Show[prob3, prob12, prob48,
              DisplayFunction->$DisplayFunction];

```

Notebook Num3j (Section 7.3.1, Table 7.2)

```

Print["\nANGULAR MOMENTUM: Rotational Symmetries\n"]
Print["Notebook Num3j: Numerical 3-j coefficients\n"]

(* Execution *)

Clear[a, b, c, ma, mb];
a = Input["Enter a:"]; b = Input["Enter b:"];
c = Input["Enter c:"]; ma = Input["Enter ma:"];
mb = Input["Enter mb:"]; mc = -ma-mb;
Print["(", a, "      ", b, "      ", c, ") = ";
Print["(", ma, "      ", mb, "      ", mc, ")"];

ThreeJay = ThreeJSymbol[{a, ma}, {b, mb}, {c, mc}]

```

Notebook 3j000 (Section 7.3.1, Table 7.2)

```

Print["\nANGULAR MOMENTUM: Rotational Symmetries\n"]

```

```
Print["Notebook 3j000:\n
3-j coefficients with all m values zero\n"]

(* Function *)
JaySpec[gg_,g_] :=
(((1-Mod[gg,2])*(-1)^g)*g!/((g-a)!*(g-b)!*(g-
c)!))*
Sqrt[(gg-2a)!*(gg-2b)!*(gg-2c)!/(gg+1)!]

(* Execution *)
Clear[a,b,c];
a = Input["Enter a (number):"];
b = Input["Enter b (number):"];
c = Input["Enter c (number):"];

gg = a+b+c; g = gg/2;

Print["(",a," ",b," ",c,") = ",JaySpec[gg,g]];
Print["(",0," ",0," ",0,")"];
```

Notebook VccDnsty (Section 7.3.2, Figure 7.7)

```
Print["\nANGULAR MOMENTUM: Rotational Symmetries\n"]
Print["Notebook VccDnsty:\n
Density plots:<jj mmljjJ 2m>|^2, j=3/2,2,6\n"]
(* Suppress irrelevant error message *)
Off[ClebschGordan::phy];

(* Function *)
DPjj[j_] := DensityPlot[
1-(ClebschGordan[{j,m},{j,m},{J,2 m}]^2,
{J, 0, 2*j},{m, -j, j},
PlotPoints->2*j+1, Frame->False];

(* Execution *)
DPjj[3/2]; DPjj[2]; DPjj[6];
```

Notebook Alg3j (Section 7.3.4, Table 7.3)

```
Print["\nANGULAR MOMENTUM: Rotational Symmetries\n"]
Print["Notebook Alg3j:\n
Algebraic 3-j coefficients for first j small\n"]

(* Execution *)
Clear[s,a,as,ms,ma,mas];
s = Input["Enter smallest j (number):"];
a = Input["Enter next j (symbol):"];
as = Input["Enter resulting j (symbols):"];
ms = Input["Enter smallest m (number):"];
ma = Input["Enter next m (symbol):"];
mas = -ms-ma;
```

```
Print["(",s,"      ",a,"      ",as,")      = ";
Print["(",ms,"      ",ma,"      ",mas,")"];

ThreeJay = ThreeJSymbol[{s,ms},{a,ma},{as,mas}]
```

Notebook LegProd (Section 7.5.2, Figure 7.10)

```
Print["\nANGULAR MOMENTUM: Rotational Symmetries\n"]
Print["Notebook LegProd: Product of Legendre polynomials\n"]
Off[General::spell1];

(* Functions *)

(* Abbreviated Legendre polynomial *)
PL[eL_] := LegendreP[eL,Cos[beta]]
PLp[one_] := PL[L1]*PL[L2]*one (* and product *)
pos[x_] := If[x>0, x, 0] (* select positive *)
neg[x_] := -If[x<0, x, 0] (* select negative *)
(* For plotting signed points *)
signedPoints[fn_,eL_,pn_,AutoOrDash_] :=
  ParametricPlot[
    {pn[fn[eL]]*Sin[beta],pn[fn[eL]]*Cos[beta]},
    {beta,0,2*Pi}, PlotPoints->points,
    PlotDivision->points, PlotRange->All,
    AspectRatio->Automatic, Axes->False, Ticks->None,
    PlotStyle->AutoOrDash,
    DisplayFunction->Identity]
ShowBoth[fn_,LV_] := Show[
  signedPoints[fn,LV,pos,Automatic],
  signedPoints[fn,LV,neg,{Dashing[{0.05,0.05}]}],
  DisplayFunction->${DisplayFunction}]

(* Execution *)

Clear[L1,L2];
(* Sample input *)
L1 = 2; L2 = 3;

(* Number of plotting points *)
points = Max[20,Min[5*Max[L1,L2]+15,40]];
(* First Legendre *)
Print["P ",L1," [cos(beta)] = ",PL[L1]," \n"]
(* Second Legendre *)
Print["P ",L2," [cos(beta)] = ",PL[L2]," \n"]
(* Combined + & - points for PL1, PL2, PL1*PL2 *)
ShowBoth[PL,L1]; ShowBoth[PL,L2]; ShowBoth[PLp,1];

(* Clebsch-Gordan series coefficients *)
L3min = Max[L1-L2,L2-L1]; L3max = L1+L2;
Print[
"\n {L3, Clebsch-Gordan coefficient for L3}",
  Table[{L3,(2*L3+1)*(N[ThreeJSymbol[
    {L1,0},{L2,0},{L3,0}]]^2),
    {L3,L3min,L3max}}]
```

```
(* and series Legendre polar plots*)
Do[ShowBoth[PL, L3], {L3, L3min, L3max, 2}]
```

Notebook YngThm (Section 7.5.2, Figure 7.11)

```
Print["\nANGULAR MOMENTUM: Rotational Symmetries\n"]
Print["Notebook YngThm: Yang's theorem\n"];
(* To suppress nuisance error messages *)
Off[ClebschGordan::tri];

(* Functions *)

pos[x_] := If[ x>0, x, 0]
neg[x_] := -If[ x<0, x, 0]
signedPntPW[pn_, AutoOrDash_] :=
  ParametricPlot[{pn[PWamp]*Sin[theta],
  pn[PWamp]*Cos[theta]}, {theta, 0, 2*Pi},
  PlotPoints->points, Axes->{False, True},
  PlotDivision->points, AspectRatio->Automatic,
  Ticks->None, PlotStyle->AutoOrDash,
  DisplayFunction->Identity]

(* Execution *)

Clear[L, alf];
(* Sample input *)
L = 2; alf[1] = 1; alf[2] = -1; alf[3] = 6;

(* Number of plotting points *)
points = Max[10, Min[3*L+10, 30]];

(* Direct method; amplitude *)
Print["PW = "]
PWamp = Sum[alf[elv+1]*
  LegendreP[elv, Cos[theta]], {elv, 0, L}]

(* Positive values solid curves *)
posPntPW = signedPntPW[pos, Automatic];
(* Negative values dashed curves *)
negPntPW = signedPntPW[neg,
  {Dashing[{0.05, 0.05}]}];
Show[posPntPW, negPntPW, (* combined plots *)
  DisplayFunction->${DisplayFunction}];

(* Direct method; cross section *)
PWSq = PWamp*PWamp;
ParametricPlot[
  {pos[PWSq]*Sin[theta], pos[PWSq]*Cos[theta]},
  {theta, 0, 2 Pi}, PlotPoints->points,
  PlotDivision->points, AspectRatio->Automatic,
  Axes->{False, True}, Ticks->None,
  PlotLabel->"PW^2"];

(* Clebsch-Gordan expansion method; *)
(* Expansion coefficients *)
```

```
ALP=Table[Sum[alf[el+1]*alf[elp+1]*(2*elpp+1)*
  (N[ThreeJSymbol[{el,0},{elp,0},{elpp,0}]]^2,
  {el,0,L},{elp,0,L}},{elpp,0,2*L}];
(* Differential cross section *)
sigma = Sum[ALP[[bigL+1]]*
  N[LegendreP[bigL,Cos[theta]],{bigL,0,2*L}];
ParametricPlot[
  {sigma*Sin[theta],sigma*Cos[theta]},
  {theta,0,2*Pi}, PlotPoints->points,
  PlotDivision->points,AspectRatio->Automatic,
  Axes->{False,True},Ticks->None,
  PlotLabel->"By expansion:"];

```

Notebook Alg6j (Section 9.2.2, Table 9.1)

```
Print["\nANGULAR MOMENTUM: Rotational Symmetries\n"]
Print["Notebook Alg6j:\n
Algebraic 6-j; no triangle condition checks\n"]

Clear[a,b,c,d,e,f,g,h,i];

(* Substitute symbols of your choice *)
TopRow = {1,b,b+1};
BottomRow = {d,c,c+1};

SixJay = SixJSymbol[TopRow,BottomRow];
Print[TableForm[{TopRow, BottomRow}]]
Print["\n = "]
Print[SixJay]

```

Notebook Num6j (Section 9.3.2)

```
Print["\nANGULAR MOMENTUM: Rotational Symmetries\n"]
Print["Notebook Num6j:\n
Numerical 6-j coefficients\n"]

Print["Be careful assigning values\n"]
Clear[a,b,c,d,e,f];
a = Input["Enter a:"];
b = Input["Enter b:"];
e = Input["Enter intermediate, e:"];
d = Input["Enter d:"];
c = Input["Enter c:"];
f = Input["Enter other intermediate, f:"];

Print[{"a," "b," "e,"}];
Print[{"d," "c," "f,"} = "];
SixJay = SixJSymbol[{a,b,e},{d,c,f}]

```

Notebook Num9j (Section 9.5.1)

```
Print["\nANGULAR MOMENTUM: Rotational Symmetries\n"]
Print["Notebook Num9j:\n"]

```

```

Numerical 9-j coefficients\n"]
(* Triangle condition definition *)
Tri[x_,y_,z_] := (Abs[x-z] <= y) && (y <= x+z);

(* Execution *)

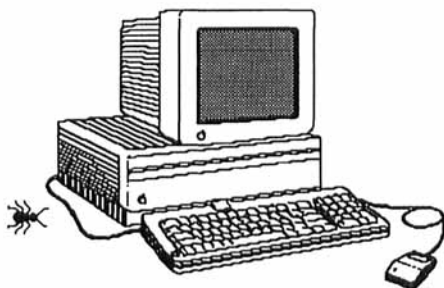
Clear[a,b,c,d,e,f,g,h,i];
a = Input["First row; enter a:"];
b = Input["enter b:"]; c = Input["enter c:"];
d = Input["Second row; enter d:"];
e = Input["enter e:"]; f = Input["enter f:"];
g = Input["Third row; enter g:"];
h = Input["enter h:"]; i = Input["enter i:"];
Print["{",a," ",b," ",c,"}"]; Print[" "];
Print["{",d," ",e," ",f,"}"]; Print[" "];
Print["{",g," ",h," ",i,"} = "];

If[ Tri[a,b,c] && Tri[d,e,f] && Tri[g,h,i]
  && Tri[a,d,g] && Tri[b,e,h] && Tri[c,f,i]
,
(* Sum over 6-j products from kmin to kmax *)
kmin = Max[Abs[a-i], Abs[h-d], Abs[b-f]];
kmax = Min[a+i, h+d, b+f];
NineJ = Sum[ (2*k+1)*
  SixJSymbol[{a,i,k},{h,d,g}]*
  SixJSymbol[{b,f,k},{d,h,e}]*
  SixJSymbol[{a,i,k},{f,b,c}],
  {k, kmin, kmax} ]
,
Print["\n!! A triangle rule is broken:"];
NineJ = 0
]

```

TABLE A.I.1 Index by chapter of *Mathematica* notebooks. Notebook names are listed by order of first application in each chapter.

Chapter	Notebook / section	Subject of the <i>Mathematica</i> notebook
1	Shell / 1.2.1	Generating a spiral shell; graphics
	Polyhedra / 1.2.2	Platonic solids; graphics
	WorldView / 1.3.2	Earth sphere in latitude and longitude; graphics
	Ppsi / 1.4.1	Parity in quantum mechanics; formulas and graphics
	PauliCC / 1.4.5 /Problems	Pauli principle in scattering; formulas and graphics
2	No notebooks	
3	No notebooks /Problems	
4	PL / 4.1.2	Legendre polynomials; formulas and graphics
	PLM / 4.1.2	Associated Legendre functions; formulas and graphics
	YLMabs / 4.1.3	Spherical harmonics; formulas and 3-D views
	EXPimPHI / 4.1.3 /Problems	Cosine of $m\phi$ modulating a torus; 3-D views
5	Precess / 5.3.1	Precession of a top; animated graphics
	BesL / 5.4.1	Spherical Bessel functions; graphics
	BesM / 5.4.1	Cylindrical Bessel functions; graphics
	PW3D / 5.4.2	Plane waves in 3 dimensions; 3-D views
	PW2D / 5.4.2 /Problems	Plane waves in 2 dimensions; 3-D views
6	Djm'm / 6.3.3	Reduced rotation functions; formulas and graphics
	DjjmCpr / 6.4.3	Probability density classical limits; graphics
	Djj0 / 6.4.3 /Problems	Reduced rotation functions, $m' = j$ and $m = 0$; graphics
7	Num3j / 7.3.1	Numerical 3- j coefficients
	3j000 / 7.3.1	3- j coefficients with m values zero; formulas
	VccDnsty / 7.3.2	Density distribution of coupled states; graphics
	Alg3j / 7.3.4	Algebraic 3- j coefficients; formulas
	LegProd / 7.5.2	Clebsch-Gordan series; formulas and graphics
	YngThm / 7.5.2 /Problems	Yang's theorem for distributions; formulas and graphics
8	PL / 8.4.1 /Problems	Legendre polynomials to transform polarizations; graphics
9	Alg6j / 9.2.2	Algebraic 6- j coefficients; formulas
	Num6j / 9.3.2	Numerical 6- j coefficients
	Num9j / 9.5.1 /Problems	Numerical 9- j coefficients



APPENDIX II

NUMERICAL COMPUTER PROGRAMS IN C

In the book we discuss reduced rotation matrix elements (the $d_{m'm}^j$, Chapter 6), coefficients for coupling two angular momenta (the 3- j coefficients, Chapter 7), and coefficients for recombining angular momenta (the 6- j and 9- j coefficients, Chapter 9). Here we provide computer programs in the C programming language to evaluate these coefficients numerically. All except the 9- j coefficient are also provided in *Mathematica* notebooks (Appendix I), which emphasize algebraic and graphical properties. In practical work, however, relatively efficient numerical routines are desirable. For example, on the same workstation the 3- j and 6- j coupling coefficients programmed below evaluate about two orders of magnitude faster than the *Mathematica* versions, albeit with slightly less accuracy.

In the following, we provide four simple C programs for the above functions. These are not optimized in the ways discussed in the text, but are intended to be easy to understand and moderately efficient. We describe first the common features of the programs and their coding, then how they can be translated directly to Fortran or Pascal, and how several multi-use functions are to be used with the programs. Sections C1 to C4 describe the programs individually, in terms of formulas used, coding, and tests of correctness.

The programs are provided on the diskette accompanying this book. This 3.5-inch diskette can be read by Apple computers, including Macintosh. Suggestions for converting the programs on diskette for other computers are suggested in The Computer Interface, page xiii.

Programming the Functions. The four programs are prepared in a uniform way, so they are easy to use and understand. For the user, all angular momentum numbers are to be entered as decimals. For example, $a = 3/2$ is entered as 1.5 and $m_b = -2$ is entered as -2., in which the decimal point may be optional for some computer systems. Program execution is terminated if the first variable entered (which should be non-negative) is entered as a negative number. Otherwise, the

program stays in a loop in the main program that inputs arguments, tests selection rules, then computes and prints a function value.

Before a function is executed, its arguments are checked within the main program to see whether the function is automatically zero because of violation of selection rules on m ($|m| \leq j$) or between j values (the triangle selection rules). No such testing is done within the function itself. Therefore, if you wish to use the function apart from the main program, you should probably include these checks.

We adopt the following conventions for coding the functions. ANSI-standard C is used. A variable name that begins with “t” indicates *twice* an angular momentum number, such as t_j for $2j$ or t_e for $2e$. After this has been done, there is a one-to-one correspondence between program variables and formula variables, with the exception that m' is replaced by mp . Function names that are capitalized—such as Max or Min—are functions provided in this appendix, not part of the C standard libraries. The first line after the main program declaration is a comment line (`/* Complete program uses ... */`) giving the names of all these capitalized functions that are needed.

Fortran and Pascal Compatibility. The programs given here can be translated readily to Fortran or to Pascal, usually through line-by-line transliteration. A summary of translating between C, Fortran, and Pascal languages is given in the appendix to my textbook on computing (with C programs) for scientists and engineers [Tho92b]. The C language is described for Fortran programmers in the book by Kerrigan [Ker91], and an introduction to C for Pascal programmers is given in the book by Shammas [Sha88].

The Multi-Use C Functions. There are six multi-use functions that are used by more than one main program: Fctrl, Max, Min, Power, TriangleBroken, and Twice. They are listed here and reside in the file AM.h on the diskette, while the programs get these source programs through the `#include "AM.h"` at the top of each program. In the comment line after the declaration of each main program the names of all functions needed by that program are given. Here is the multi-use function file AM.h, with a description of the purpose of each function inserted.

```
#define TRUE 1
#define FALSE 0
```

Fctrl. This computes the factorial function for non-negative integer arguments. There is no check on overflow for this double-precision floating-point function.

```
double Fctrl(N)
/* Factorial function; assumes N >= 0 */
int N;
{
double product;
int i;
product = 1;
```

```

if ( N <= 1 ) return product;
else
{
  for ( i = 2; i <= N; i++ )
    { product = product*i; }
  return product;
}
}

```

Max. This function returns the biggest of the N elements that are stored in array. The [0] element of the array is not used.

```

int Max(array,N)
/* Maximum of first N elements; array [1]...[N] */
int array[],N;
{
  int big,i;
  big = array[1];
  for ( i = 2; i <= N; i++ )
    {
      if ( array[i] > big ) big = array[i];
    }
  return big;
}

```

Min. This function returns the smallest of the N elements that are stored in array. The [0] element of the array is not used.

```

int Min(array,N)
/* Minimum of first N elements; array [1]...[N] */
int array[],N;
{
  int small,i;
  small = array[1];
  for ( i = 2; i <= N; i++ )
    {
      if ( array[i] < small ) small = array[i];
    }
  return small;
}

```

Power. The Power function returns x^i , in which i is an integer. The C library function `pow(x,y)` assumes that x and y are double variables. Also, if $x = 0$ and $y \leq 0$, the function returns negative infinity. However, as every school-child knows, $x^0 \equiv 1$, so Power traps for $i = 0$, in which case it returns 1. Here's the power play:

```

double Power(x,i) /* x to integer power */
double x; int i;
{

```

```
double floati;
/* always return 1.0 for i=0 */
if ( i == 0 ) return 1.0;
floati = i; return pow(x, floati);
}
```

TriangleBroken. This function tests the triangle condition, using *twice* each of the three angular momenta. Therefore, the sum of the three function arguments must be even. A TRUE (=1) is returned if either this condition or the triangle rule is broken, else a FALSE (=0) is returned. The calling functions then test for a 1 or a 0 being returned.

```
int TriangleBroken(tj1,tj2,tj3)
/* tests the triangle condition */
int tj1,tj2,tj3;
{
int sum;
sum = tj1+tj2+tj3;
if ( sum != 2*(sum/2) ||
    tj2 < abs(tj1-tj3) || tj2 > tj1+tj3 )
{
printf
("\n!! (%i,%i,%i) breaks triangle rule:",
tj1,tj2,tj3);
return TRUE;
}
else return FALSE;
}
```

Twice. This function converts a decimal half integer, such as 1.5 or -2.0, to an integer that is twice this. The possibility that the decimal representation is imprecise is allowed for by adding the roundoff term 0.01.

```
int Twice(x)
/* Converts to integer(2*x) */
double x;
{
int int2x;
if ( x < 0 ) int2x = -2*(fabs(x)+0.01);
else int2x = 2*(x+0.01);
return int2x;
}
```

We now describe each of the angular momentum functions.

C1 PROGRAM FOR REDUCED ROTATION MATRIX ELEMENTS

Formulas and Coding for Reduced Rotation Matrix Elements. We use a direct implementation of formula (6.9), after making the checks that $|m| \leq j$ and

$|m| \leq j$. The rotation angle β is entered in radian measure. Coding is straightforward. The range of the sum over x is obtained by finding what extreme values of x would make any argument in the factorials within the summation equal to zero. The phase factor $(-1)^x$ is accounted for by changing the sign of the terms for which x is odd; that is, $2x$ is not exactly divisible by 4.

Testing Reduced Rotation Matrix Elements. Tables 6.1–6.3 give several formulas for $d_{m,m}^j(\beta)$ for $j \leq 2$. Spot checks using these formulas are easily made. *Mathematica* notebook *Dj_m'_m* that computes algebraic expressions for $d_{m,m}^j(\beta)$ can also be adapted to calculate numerical values.

PROGRAM C.1 The reduced rotation matrix elements.

```
#include <stdio.h>
#include <math.h>
#include "AM.h"

main() /* Reduced rotation matrix elements */
/* Complete program uses Djmpm given here,
   plus Fctrl,Max,Min,Power,Twice
   from AM.h file */
{
double beta,dj,j,mp,m;
int tj,tmp,tm;
double Djmpm();

printf("Angular Momentum\n");
printf("Reduced rotation matrix elements\n");
tj = 0;
while ( tj >= 0 )
{
printf("\n\nInput j (<0 to end): ");
scanf("%lf",&j);    tj = Twice(j);
if ( tj < 0 )
{
printf("\nEnd rotation matrix elements\n");
exit(0);
}
printf("\nInput m', m, beta (radian): ");
printf("\n(Use only spaces to separate values) ");
scanf("%lf%lf%lf",&mp,&m,&beta);
/* Convert to integers that are twice input values */
tmp = Twice(mp);    tm = Twice(m);
if ( abs(tmp) > tj || abs(tm) > tj )
printf("\n!m' or m is too big; try again");
else
{
dj = Djmpm(tj,tmp,tm,beta);
printf("\n djm'm(beta) = %lf",dj);
}
}
}
```

```

double Djmpm(tj,tmp,tm,beta)
/* Reduced rotation matrix element */
double beta;    int tj,tmp,tm;
{
double norm,cb2,sb2,sum,term;
int minmax[3],txmin,txmax,tx;

norm = sqrt(Fctrl((tj+tmp)/2)*Fctrl((tj-tmp)/2)*
           Fctrl((tj+tm)/2)*Fctrl((tj-tm)/2));
cb2 = cos(beta/2);  sb2 = sin(beta/2);
minmax[1] = 0; minmax[2] = tmp-tm;
txmin = Max(minmax,2); /* smallest x */
minmax[1] = tj+tmp; minmax[2] = tj-tm;
txmax = Min(minmax,2); /* largest x */
sum = 0;
for ( tx = txmin; tx <= txmax; tx = tx+2 )
{
term = Power(cb2,tj-tx+(tmp-tm)/2)*
       Power(sb2,tx+(tm-tmp)/2)/
       (Fctrl((tj+tmp-tx)/2)*
        Fctrl((tj-tm-tx)/2)*Fctrl(tx/2)*
        Fctrl((tx+tm-tmp)/2));
if ( tx != 4*(tx/4) )
term = -term; /* for x odd */
sum = sum+norm*term;
}
return sum;
}

```

C2 PROGRAM FOR 3-*j* COEFFICIENTS

*Formulas and Coding for 3-*j* Coefficients.* Formula (7.59) is used for the 3-*j* coefficient. The formula is not computed if the sum of the *m* values is nonzero or if the magnitude of any *m* value exceeds its matching *j* value.

*Testing the 3-*j* Coefficients.* Spot checks for a range of angular momenta can be made by comparing the results from `_3j` with those from the *Mathematica* notebook `Num3j` in Appendix I. A testing method that is more complete is to check the orthogonality conditions (7.61) and (7.62). Such tests are also useful for checking the numerical accuracy of the 3-*j* coefficients.

PROGRAM C.2 The 3-*j* coefficients.

```

#include <stdio.h>
#include <math.h>
#include "AM.h"

main() /* 3-j coupling coefficients */
/* Complete program uses _3j,EvenOrOdd given here,

```

```

    plus Fctrl,Max,Min,Power,TriangleBroken,Twice
    from AM.h file */
{
double a,b,c,ma,mb,mc,Three_j;
int ta,tb,tc,tma,tmb,tmc;
double _3j();
int EvenOrOdd();

printf("Angular Momentum\n");
printf("3-j coupling coefficients\n");
ta = 0;
while ( ta >= 0 )
{
    printf("\n\nInput a as 0.5, etc (<0 to end): ");
    scanf("%lf",&a);
    if ( a < 0 )
    {
        printf("\nEnd 3-j coupling coefficients\n");
        exit(0);
    }
    printf("\nInput b, c, ma, mb, mc: ");
    printf("\n(Use only spaces to separate values) ");
    scanf("%lf%lf%lf%lf%lf",&b,&c,&ma,&mb,&mc);
    /* Convert to integers that are twice input values */
    ta = Twice(a);    tb = Twice(b);    tc = Twice(c);
    tma = Twice(ma); tmb = Twice(mb);  tmc = Twice(mc);
    /* Testing for zero coefficient */
    if ( tma+tmb+tmc != 0 )
    { printf("\n!!ma+mb+mc not zero; try again");    }
    else
    {
        if ( TriangleBroken(ta,tb,tc) != 0 )
            printf(" try again");
        else
        {
            if ( abs(tma) > ta ||
                abs(tmb) > tb ||
                abs(tmc) > tc )
                printf("\n!!An m value is too big; try again");
            else
            {
                if ( EvenOrOdd(ta,tma) ||
                    EvenOrOdd(tb,tmb) ||
                    EvenOrOdd(tc,tmc) > 0 )
                    printf("\n!!An m doesn't match a j; try again");
                else
                {
                    Three_j = _3j(ta,tb,tc,tma,tmb,tmc);
                    printf("\n 3-j coefficient = %lf",Three_j);
                }
            }
        }
    }
}
}

```

```

    }
}

double _3j(ta,tb,tc,tma,tmb,tmc)
/* 3-j coupling coefficient */
int ta,tb,tc,tma,tmb,tmc;

{
double n1,n2,n3,d1,d2,d3,norm,sum,phase,term;
int minmax[3],tkmin,tkmax,tk;

/* Normalization factorials */
n1 = Fctrl((tc+ta-tb)/2)*Fctrl((tc-ta+tb)/2);
n2 = Fctrl((ta+tb-tc)/2);
n3 = Fctrl((tc-tmc)/2)*Fctrl((tc+tmc)/2);
d1 = Fctrl((ta+tb+tc)/2+1);
d2 = Fctrl((ta-tma)/2)*Fctrl((ta+tma)/2);
d3 = Fctrl((tb-tmb)/2)*Fctrl((tb+tmb)/2);
norm = Power(-1.0,(ta-tb-tmc)/2)*
      sqrt(n1*n2*n3/(d1*d2*d3));

minmax[1] = 0; minmax[2] = tb-ta-tmc;
tkmin = Max(minmax,2);
minmax[1] = tc-ta+tb; minmax[2] = tc-tmc;
tkmax = Min(minmax,2);
sum = 0;
phase = Power(-1.0,(tkmin+tb+tmb)/2);
for ( tk = tkmin; tk <= tkmax; tk = tk+2 )
{
  n1 = Fctrl((tb+tc+tma-tk)/2);
  n2 = Fctrl((ta-tma+tk)/2);
  d1 = Fctrl(tk/2)*Fctrl((tc-ta+tb-tk)/2);
  d2 = Fctrl((tc-tmc-tk)/2);
  d3 = Fctrl((tk+ta-tb+tmc)/2);
  term = phase*n1*n2/(d1*d2*d3);
  phase = -phase;
  sum = sum+norm*term;
}
return sum;
}

int EvenOrOdd(tj,tm) /* tests for tj+tm even */
int tj,tm;
{
int sum;

sum = tj+tm;
if ( sum != 2*(sum/2) ) return 1;
else return 0;
}

```


C3 PROGRAM FOR 6-j COEFFICIENTS

Formulas and Coding for 6-j Coefficients. Formula (9.20) is used for the 6-j coefficient. The formula is not computed if any of the four triangles of the tetrahedron, Figure 9.2, is not closed.

Testing the 6-j Coefficients. Spot checks for a range of angular momenta can be made by comparing results from `_6j` with those from *Mathematica* notebook `Num6j` in Appendix I. A more complete testing method is to check orthogonality condition (9.21). Such tests are also useful for checking numerical accuracy.

PROGRAM C.3 The 6-j coefficients.

```
#include <stdio.h>
#include <math.h>
#include "AM.h"

main() /* 6-j recoupling coefficients */
/* Complete program uses _6j,Delt given here
   plus Fctrl,Max,Min,Power,TriangleBroken,Twice
   from AM.h file */
{
double a,b,c,d,e,f,Six_j;
int ta,tb,tc,td,te,tf;

printf("Angular Momentum\n");
printf("6-j recoupling coefficients\n");
ta = 0;
while ( ta >= 0 )
{
printf("\n\nInput a as 0.5, etc (<0 to end): ");
scanf("%lf",&a); ta = Twice(a);
if ( ta < 0 )
{
printf("\nEnd 6-j recoupling coefficients\n");
exit(0);
}
printf("\nInput b, c, d, e, f: ");
printf("\n(Use only spaces to separate values) ");
scanf("%lf%lf%lf%lf%lf",&b,&c,&d,&e,&f);
/* Convert to integers that are twice input values */
tb = Twice(b); tc = Twice(c);
td = Twice(d); te = Twice(e); tf = Twice(f);

/* Testing for zero coefficient */
if ( TriangleBroken(ta,tb,te) != 0 ||
    TriangleBroken(ta,tc,tf) != 0 ||
    TriangleBroken(tb,td,tf) != 0 ||
    TriangleBroken(tc,td,te) != 0 )
printf(" try again");
else
```

```

    {
        Six_j = _6j(ta,tb,tc,td,te,tf);
        printf("\n 6-j coefficient = %lf",Six_j);
    }
}

double _6j(ta,tb,tc,td,te,tf)
/* 6-j recoupling coefficient */
int ta,tb,tc,td,te,tf;
{
    double norm,sum,phase,n1,d1,d2,d3,d4,d5,d6,term;
    int minray[4],maxray[6],tkmin,tkmax,tk;
    double Delt();

    /* Normalization factorials */
    norm = sqrt(Delt(ta,tb,te)*Delt(ta,tc,tf)*
                Delt(tb,td,tf)*Delt(tc,td,te));
    /* Minimum summation index */
    minray[1] = 0;          minray[2] = ta+td-te-tf;
    minray[3] = tb+tc-te-tf; tkmin = Max(minray,3);
    /* Maximum summation index */
    maxray[1] = ta+tb+tc+td+2; maxray[2] = ta+tb-te;
    maxray[3] = tc+td-te;      maxray[4] = ta+tc-tf;
    maxray[5] = tb+td-tf;      tkmax = Min(maxray,5);
    sum = 0;                  /* Phase of 6-j */
    phase = Power(-1.0,(ta+tb+tc+td+tkmin)/2);
    for ( tk = tkmin; tk <= tkmax; tk = tk+2 )
    {
        n1 = Fctrl((ta+tb+tc+td-tk)/2+1);
        d1 = Fctrl(tk/2)*Fctrl((te+tf-ta-td+tk)/2);
        d2 = Fctrl((te+tf-tb-tc+tk)/2);
        d3 = Fctrl((ta+tb-te-tk)/2);
        d4 = Fctrl((tc+td-te-tk)/2);
        d5 = Fctrl((ta+tc-tf-tk)/2);
        d6 = Fctrl((tb+td-tf-tk)/2);
        term = phase*n1/(d1*d2*d3*d4*d5*d6);
        phase = -phase;
        sum = sum+norm*term;
    }
    return sum;
}

double Delt(ta,tb,tc)
/* Square of delta factor */
int ta,tb,tc;
{
    return Fctrl((ta+tb-tc)/2)*
           Fctrl((ta+tc-tb)/2)*Fctrl((tb+tc-ta)/2)/
           Fctrl((ta+tb+tc)/2+1);
}

```

C4 PROGRAM FOR 9-j COEFFICIENTS

Formulas and Coding for 9-j Coefficients. Formula (9.59)—expansion in terms of 6-j coefficients—is used for the 9-j coefficients. The formula is not computed if any of the six independent triangle conditions is not satisfied. The function `_6j` is obtained from Section C3.

Testing the 9-j Coefficients. Spot checks can be made by comparing the results from `_9j` with those in Matsunobu and Takebe [Mat55] and with exact numerical values from *Mathematica* notebook Num9j in Appendix I. For example,

$$\left\{ \begin{array}{ccc} 2 & 1 & 2 \\ 3/2 & 3/2 & 1 \\ 1/2 & 1/2 & 1 \end{array} \right\} = -\frac{1}{2.5\sqrt{6}} \qquad \left\{ \begin{array}{ccc} 4 & 2 & 5 \\ 7/2 & 3/2 & 4 \\ 1/2 & 1/2 & 1 \end{array} \right\} = \frac{\sqrt{7}}{4.3.5\sqrt{3}}$$

A more complete testing method is to check the orthogonality condition (9.65), which is also useful for checking the numerical accuracy of the coefficients.

PROGRAM C.4 The 9-j coefficients.

```
#include <stdio.h>
#include <math.h>
#include "AM.h"

main() /* 9-j recoupling coefficients */
/* Complete program uses _6j,_9j,Delt given here,
   plus Fctrl,Max,Min,Power,TriangleBroken,Twice
   from AM.h file */
{
double Nine_j;
int ta,tb,tc,td,te,tf,tg,th,ti;
double a,b,c,d,e,f,g,h,i,_6j(),_9j();

printf("Angular Momentum\n");
printf("9-j recoupling coefficients\n");
ta = 0;
while ( ta >= 0 )
{
printf("\n\nInput a (<0 to end): ");
scanf("%lf",&a);   ta = Twice(a);
if ( ta < 0 )
{
printf("\nEnd 9-j recoupling coefficients\n");
exit(0);
}
printf("\nInput b, c: ");
printf("\n(Use only spaces to separate values) ");
scanf("%lf%lf",&b,&c);
printf("\nInput d, e, f: ");
```

```

scanf("%lf%lf%lf",&d,&e,&f);
printf("\nInput g, h, i: ");
scanf("%lf%lf%lf",&g,&h,&i);
        tb = Twice(b);  tc = Twice(c);
td = Twice(d);  te = Twice(e);  tf = Twice(f);
tg = Twice(g);  th = Twice(h);  ti = Twice(i);
/* Testing for zero coefficient */
if ( TriangleBroken(ta,tb,tc) != 0 ||
    TriangleBroken(td,te,tf) != 0 ||
    TriangleBroken(tg,th,ti) != 0 ||
    TriangleBroken(ta,td,tg) != 0 ||
    TriangleBroken(tb,te,th) != 0 ||
    TriangleBroken(tc,tf,ti) != 0 )
    printf(" try again");
else
    {
    Nine_j = _9j(ta,tb,tc, td,te,tf, tg,th,ti);
    printf("\n 9-j coefficient = %lf",Nine_j);
    }
}
}

double _6j(ta,tb,tc, td,te,tf)
/* 6-j recoupling coefficient */
int ta,tb,tc,td,te,tf;
{
double norm,sum,phase,n1,d1,d2,d3,d4,d5,d6,term;
int minray[4],maxray[6],tkmin,tkmax,tk;
double Delt();

/* Normalization factorials */
norm = sqrt(Delt(ta,tb,te)*Delt(ta,tc,tf)*
            Delt(tb,td,tf)*Delt(tc,td,te));
/* Minimum summation index */
minray[1] = 0;          minray[2] = ta+td-te-tf;
minray[3] = tb+tc-te-tf; tkmin = Max(minray,3);
/* Maximum summation index */
maxray[1] = ta+tb+tc+td+2; maxray[2] = ta+tb-te;
maxray[3] = tc+td-te;      maxray[4] = ta+tc-tf;
maxray[5] = tb+td-tf;      tkmax = Min(maxray,5);
sum = 0;                  /* Phase of 6-j */
phase = Power(-1.0, (ta+tb+tc+td+tkmin)/2);
for ( tk = tkmin; tk <= tkmax; tk = tk+2 )
    {
    n1 = Fctrl((ta+tb+tc+td-tk)/2+1);
    d1 = Fctrl(tk/2)*Fctrl((te+tf-ta-td+tk)/2);
    d2 = Fctrl((te+tf-tb-tc+tk)/2);
    d3 = Fctrl((ta+tb-te-tk)/2);
    d4 = Fctrl((tc+td-te-tk)/2);
    d5 = Fctrl((ta+tc-tf-tk)/2);
    d6 = Fctrl((tb+td-tf-tk)/2);
    term = phase*n1/(d1*d2*d3*d4*d5*d6);
    phase = -phase;
    }
}

```

```

    sum = sum+norm*term;
  }
return sum;
}

double _9j(ta,tb,tc, td,te,tf, tg,th,ti)
/* 9-j recoupling coefficient */
int ta,tb,tc,td,te,tf,tg,th,ti;
{
double sum,term,_6j();
double term1,term2,term3;
int minmax[4],tkmin,tkmax,tk;

/* Minimum summation index */
minmax[1] = abs(ta-ti);  minmax[2] = abs(th-td);
minmax[3] = abs(tb-tf); tkmin = Max(minmax,3);
/* Maximum summation index */
minmax[1] = ta+ti;      minmax[2] = th+td;
minmax[3] = tb+tf;      tkmax = Min(minmax,3);
sum = 0;
for ( tk = tkmin; tk <= tkmax; tk = tk+2 )
  {
    term = _6j(ta,ti,td, th,tk,tg)*
           _6j(tb,tf,th, td,tk,te)*
           _6j(ta,ti,tb, tf,tk,tc);
    sum = sum+(tk+1)*term;
  }
return sum;
}

double Delt(ta,tb,tc)
/* Square of delta factor */
int ta,tb,tc;
{
double Fctrl();
return Fctrl((ta+tb-tc)/2)*
       Fctrl((ta+tc-tb)/2)*Fctrl((tb+tc-ta)/2)/
       Fctrl((ta+tb+tc)/2+1);
}

```



APPENDIX III

TABLES OF FORMULAS

In this appendix we tabulate formulas that are primarily of practical use in angular momentum calculations rather than being key formulas for understanding the subject. You can therefore use the tables for ready reference. If you wish to understand the origins and uses of a formula in more detail, look for it in the text under the equation number given here. Also, the formulas given here appear in the text with a box around them, but not all boxed formulas appear here. The order of presentation of formulas is by increasing equation number.

T1 LEGENDRE FUNCTIONS AND SPHERICAL HARMONICS

Tables of Formulas

Legendre functions $\ell \leq 4$, Table 4.1, p. 131.

Spherical harmonics $\ell \leq 4$, Table 4.2, p. 139.

Solid harmonics $\ell \leq 4$, Tables 4.4, 4.5, pp. 145, 146.

Legendre Functions

Integral property:

$$\int_0^\pi P_{\ell'}^m(\cos\theta) P_\ell^m(\cos\theta) \sin\theta \, d\theta = \frac{2(\ell+m)! \delta_{\ell'\ell}}{(2\ell+1)(\ell-m)!} \quad (4.6)$$

Parity:

$$P_\ell^m(-\cos\theta) = (-1)^{\ell-m} P_\ell^m(\cos\theta) \quad (4.8)$$

Spherical HarmonicsStretched- m value:

$$Y_{\ell\ell}(\theta, \phi) = (-1)^\ell \sqrt{\frac{(2\ell+1)!}{2^{2\ell+2}(\ell!)^2\pi}} \sin^\ell \theta e^{i\ell\phi} \quad (4.14)$$

General formula ($m \geq 0$):

$$Y_{\ell m}(\theta, \phi) = (-1)^m \sqrt{\frac{(2\ell+1)(\ell+m)!(\ell-m)!}{4\pi}} e^{im\phi} \\ \times \sum_x \frac{(-1)^x (\sin \theta)^{2x+m} (\cos \theta)^{\ell-2x-m}}{2^{2x+m} (m+x)! x! (\ell-m-2x)!} \quad (4.15)$$

Parity:

$$PY_{\ell m}(\theta, \phi) = Y_{\ell m}(\pi - \theta, \pi + \phi) = (-1)^\ell Y_{\ell m}(\theta, \phi) \quad (4.16)$$

Relation to Legendre functions:

$$Y_{\ell m}(\theta, \phi) = (-1)^m \sqrt{\frac{(2\ell+1)(\ell-m)!}{4\pi(\ell+m)!}} P_\ell^m(\cos \theta) e^{im\phi} \quad m \geq 0 \quad (4.18)$$

Spherical harmonic for $m < 0$:

$$Y_{\ell, -|m|}(\theta, \phi) = (-1)^{|m|} Y_{\ell, |m|}^*(\theta, \phi) \quad (4.19)$$

Relation to Legendre polynomials for $m = 0$:

$$Y_{\ell 0}(\theta, \phi) = Y_{\ell 0}(\theta, 0) = \sqrt{\frac{2\ell+1}{4\pi}} P_\ell(\cos \theta) \quad (4.20)$$

Values at $\theta = 0, \pi$:

$$Y_{\ell m}(0, \phi) = \sqrt{\frac{2\ell+1}{4\pi}} \delta_{m,0} \quad Y_{\ell m}(\pi, \phi) = (-1)^\ell \sqrt{\frac{2\ell+1}{4\pi}} \delta_{m,0} \quad (4.21)$$

Spherical harmonic addition theorem:

$$\sum_m Y_{\ell m}^*(\theta', \phi') Y_{\ell m}(\theta, \phi) = \frac{2\ell+1}{4\pi} P_\ell(\cos \omega) \quad (4.23)$$

Solid harmonic formulas:

$$\begin{aligned}
 Y_{\ell m}(\mathbf{r}) &\equiv r^\ell Y_{\ell m}(\theta\phi) \\
 &= (-1)^m \sqrt{\frac{(2\ell+1)(\ell+m)!(\ell-m)!}{4\pi}} \\
 &\quad \times \sum_{x'} \frac{(-1)^{x'} (x+iy)^{x'+m} (x-iy)^{x'} z^{\ell-2x'-m}}{2^{2x'+m} (m+x')! x'! (\ell-m-2x')!}
 \end{aligned} \tag{4.28}$$

Real forms of spherical harmonics:

$$\begin{aligned}
 Z_\ell(\theta\phi) &\equiv \sqrt{\frac{2\ell+1}{4\pi}} P_\ell(\cos\theta) \\
 Z_{\ell m}^c(\theta\phi) &\equiv \sqrt{\frac{(2\ell+1)(\ell-m)!}{2\pi(\ell+m)!}} P_\ell^m(\cos\theta) \cos m\phi \quad m \geq 0 \\
 Z_{\ell m}^s(\theta\phi) &\equiv \sqrt{\frac{(2\ell+1)(\ell-m)!}{2\pi(\ell+m)!}} P_\ell^m(\cos\theta) \sin m\phi \quad m \geq 0
 \end{aligned} \tag{4.32}$$

Real spherical harmonic addition theorem:

$$\sum_{\kappa=0,c,s} \sum_{m=0}^{\ell} Z_{\ell m}^\kappa(\theta'\phi') Z_{\ell m}^\kappa(\theta\phi) = \frac{2\ell+1}{4\pi} P_\ell(\cos\omega) \tag{4.34}$$

T2 ROTATION MATRIX ELEMENTS

Tables of Formulas

Reduced rotation matrices $j \leq 2$, Tables 6.1 – 6.3, pp. 223, 224.
 Rotation matrix elements for special parameters, Table 6.4, p. 240.

Reduced Rotation Matrix Elements

General formula:

$$\begin{aligned}
 d_{m'm}^j(\beta) &= \sqrt{\frac{(j+m')!(j-m')!(j+m)!(j-m)!}{(j+m'-x)!(j-m-x)! x! (x+m-m')!}} \\
 &\quad \times \sum_x \frac{(-1)^x [\cos(\beta/2)]^{2j+m'-m-2x} [\sin(\beta/2)]^{2x+m-m'}}{(j+m'-x)!(j-m-x)! x! (x+m-m')!}
 \end{aligned} \tag{6.9}$$

Reduced rotation matrix element with both projection numbers zero:

$$d_{00}^\ell(\beta) = P_\ell(\cos\beta) \tag{6.13}$$

Reduced rotation matrix element with first projection number zero:

$$d_{m'0}^{\ell}(\beta) = (-1)^{m'} \sqrt{\frac{(\ell - m')!}{(\ell + m')!}} P_{\ell}^{m'}(\cos \beta) \quad m' \geq 0 \quad (6.14)$$

Rotated state ket:

$$|jm, \alpha\beta\gamma\rangle = \sum_{m'=-j}^j |jm', 000\rangle D_{m'm}^j(\alpha\beta\gamma) \quad (6.19)$$

Transformed amplitudes after rotation:

$$a_{m'}(\alpha\beta\gamma) = \sum_{m=-j}^j D_{m'm}^j(\alpha\beta\gamma) a_m(000) \quad (6.33)$$

Symmetries of reduced rotation matrix elements:

$$d_{-m', -m}^j(\beta) = d_{m'm}^j(-\beta) \quad (6.40)$$

$$d_{m'm}^j(-\beta) = d_{mm'}^j(\beta) \quad (6.41)$$

$$d_{mm'}^j(\beta) = (-1)^{m-m'} d_{m'm}^j(\beta) \quad (6.42)$$

$$d_{m'm}^j(\pi - \beta) = (-1)^{j+m'} d_{m', -m}^j(\beta) \quad (6.43)$$

Relation of reduced and full rotation matrix elements:

$$D_{m'm}^j(\alpha\beta\gamma) = e^{-im'\alpha} d_{m'm}^j(\beta) e^{-im\gamma} \quad (6.44)$$

Symmetries of full rotation matrix elements:

$$D_{-m', -m}^j(\alpha, \beta, \gamma) = D_{m'm}^j(-\alpha, -\beta, -\gamma) = [D_{m'm}^j(\alpha, -\beta, \gamma)]^* \quad (6.45)$$

$$D_{m'm}^j(-\alpha, -\beta, -\gamma) = D_{mm'}^j(\gamma, \beta, \alpha) = [D_{m'm}^j(-\gamma, -\beta, -\alpha)]^* \quad (6.46)$$

$$D_{mm'}^j(\alpha, \beta, \gamma) = (-1)^{m-m'} D_{m'm}^j(\gamma, \beta, \alpha) \quad (6.47)$$

$$D_{m'm}^j(\pi - \beta) = (-1)^{j+m'} D_{m', -m}^j(\alpha, \beta, -\gamma) \quad (6.48)$$

Unitarity sum for full rotation matrix elements:

$$\sum_{m''} D_{m', m''}^j(\alpha\beta\gamma) [D_{m'' m}^j(\alpha\beta\gamma)]^* = \delta_{m' m} \quad (6.50)$$

Orthogonality sum for reduced rotation matrix elements:

$$\sum_{m''} d_{m' m''}^j(\beta) d_{m m''}^j(\beta) = \delta_{m' m} \quad (6.51)$$

Orthogonality integral for rotation matrix elements:

$$\begin{aligned} \int_R [D_{m'_1 m_1}^{j_1}(\alpha\beta\gamma)]^* D_{m'_2 m_2}^{j_2}(\alpha\beta\gamma) d\alpha \sin\beta d\beta d\gamma \\ = \frac{16\pi^2}{2j_1+1} \delta_{j_1 j_2} \delta_{m'_1 m'_2} \delta_{m_1 m_2} \quad (6.56) \\ R: \quad 0 \leq \alpha \leq 4\pi \quad 0 \leq \beta \leq \pi \quad 0 \leq \gamma \leq 2\pi \end{aligned}$$

Spherical harmonics and reduced rotation matrix elements:

$$\begin{aligned} Y_{\ell m}(\theta, \phi) = \sqrt{\frac{2\ell+1}{4\pi}} d_{m0}^\ell(\theta) e^{im\phi} \\ Y_{\ell, -m}(\theta, \phi) = (-1)^m [Y_{\ell m}(\theta, \phi)]^* \quad m \geq 0 \quad (6.60) \end{aligned}$$

T3 THE 3-*j* COEFFICIENTS

Tables of Formulas

3-*j* with all *m* zero and smallest *j* ≤ 3 (numerical), Table 7.2, p. 275.

3-*j* coefficients with smallest *j* ≤ 1 (algebraic), Table 7.3, p. 281.

Clebsch-Gordan Coefficients

Clebsch-Gordan transformation between coupled and direct-product representations:

$$|j_1 j_2 JM\rangle = \sum_{m_1 m_2} |j_1 j_2 m_1 m_2\rangle \langle j_1 j_2 m_1 m_2 | j_1 j_2 JM\rangle \quad (7.35)$$

J-sum unitarity for Clebsch-Gordan coefficients:

$$\sum_J \langle j_1 j_2 m'_1 m'_2 | j_1 j_2 JM\rangle \langle j_1 j_2 JM | j_1 j_2 m_1 m_2\rangle = \delta_{m_1 m'_1} \delta_{m_2 m'_2} \quad (7.39)$$

M-sum unitarity for Clebsch-Gordan coefficients:

$$\sum_{m_1 m_2} \langle j_1 j_2 J' M' | j_1 j_2 m_1 m_2\rangle \langle j_1 j_2 m_1 m_2 | j_1 j_2 JM\rangle = \delta_{J' J} \delta_{M' M} \quad (7.41)$$

The 3- j Coefficients

Definition in terms of Clebsch-Gordan coefficients:

$$\begin{pmatrix} j_1 & j_2 & j_3 \\ m_1 & m_2 & m_3 \end{pmatrix} \equiv (-1)^{j_1 - j_2 - m_3} \frac{\langle j_1 j_2 m_1 m_2 | j_1 j_2 j_3, -m_3 \rangle}{\sqrt{2j_3 + 1}} \quad (7.57)$$

$$m_1 + m_2 + m_3 = 0 \quad (7.58)$$

General formula for 3- j coefficient:

$$\begin{aligned} \begin{pmatrix} j_1 & j_2 & j_3 \\ m_1 & m_2 & m_3 \end{pmatrix} &= \delta_{m_1 + m_2 + m_3, 0} (-1)^{j_1 - j_2 - m_3} \\ &\times \sqrt{\frac{(j_3 + j_1 - j_2)!(j_3 - j_1 + j_2)!(j_1 + j_2 - j_3)!(j_3 - m_3)!(j_3 + m_3)!}{(j_1 + j_2 + j_3 + 1)!(j_1 - m_1)!(j_1 + m_1)!(j_2 - m_2)!(j_2 + m_2)!}} \\ &\times \sum_k \frac{(-1)^{k + j_2 + m_2} (j_2 + j_3 + m_1 - k)!(j_1 - m_1 + k)!}{k!(j_3 - j_1 + j_2 - k)!(j_3 - m_3 - k)!(k + j_1 - j_2 + m_3)!} \end{aligned} \quad (7.59)$$

3- j transformation between coupled and direct-product representations:

$$\begin{aligned} |j_1 j_2 JM\rangle &= \sum_{m_1 = -j_1}^{j_1} \sum_{m_2 = -j_2}^{j_2} |j_1 m_1\rangle |j_2 m_2\rangle \delta_{m_1 + m_2, M} \\ &\times (-1)^{j_1 - j_2 + M} \sqrt{2J + 1} \begin{pmatrix} j_1 & j_2 & J \\ m_1 & m_2 & -M \end{pmatrix} \end{aligned} \quad (7.60)$$

 J -sum unitarity for 3- j coefficients:

$$\sum_{j_3} (2j_3 + 1) \begin{pmatrix} j_1 & j_2 & j_3 \\ m'_1 & m'_2 & m_3 \end{pmatrix} \begin{pmatrix} j_1 & j_2 & j_3 \\ m_1 & m_2 & m_3 \end{pmatrix} = \delta_{m_1 m'_1} \delta_{m_2 m'_2} \delta_{m_1 + m_2, -m_3} \quad (7.61)$$

 M -sum unitarity for 3- j coefficients:

$$\sum_{m_1, m_2} (2j_3 + 1) \begin{pmatrix} j_1 & j_2 & j'_3 \\ m_1 & m_2 & m'_3 \end{pmatrix} \begin{pmatrix} j_1 & j_2 & j_3 \\ m_1 & m_2 & m_3 \end{pmatrix} = \delta_{j'_3 j_3} \delta_{m_3 m'_3} \quad (7.62)$$

3- j coefficient with one j zero:

$$\begin{pmatrix} j_1 & 0 & j_3 \\ m_1 & 0 & m_3 \end{pmatrix} = \delta_{j_1 j_3} \delta_{m_1, -m_3} \frac{(-1)^{j_1 - m_1}}{\sqrt{2j_1 + 1}} \quad (7.63)$$

Symmetry under reversal of all m values:

$$\begin{pmatrix} j_2 & j_1 & j_3 \\ -m_2 & -m_1 & -m_3 \end{pmatrix} = \begin{pmatrix} j_1 & j_2 & j_3 \\ m_1 & m_2 & m_3 \end{pmatrix} \quad (7.64)$$

Even permutations of columns of a 3-j coefficient leave it unchanged.
 Odd permutations of columns of a 3-j coefficient produce a phase change of $(-1)^{j_1+j_2+j_3}$. (7.68)

3-j coefficient with all m values zero:

$$\begin{pmatrix} a & b & c \\ 0 & 0 & 0 \end{pmatrix} = 0 \quad a+b+c \text{ odd} \quad (7.72)$$

$$\begin{aligned} \begin{pmatrix} a & b & c \\ 0 & 0 & 0 \end{pmatrix} &= (-1)^g \frac{g!}{(g-a)!(g-b)!(g-c)!} \\ &\times \sqrt{\frac{(2g-2a)!(2g-2b)!(2g-2c)!}{(2g+1)!}} \quad a+b+c \text{ even} \end{aligned} \quad (7.73)$$

Combined spin and orbital states:

$$Y_{\ell, \ell+1/2, M} = \sqrt{\frac{\ell-M+1/2}{2\ell+1}} Y_{\ell, M+1/2}(\theta\phi) \chi_- + \sqrt{\frac{\ell+M+1/2}{2\ell+1}} Y_{\ell, M-1/2}(\theta\phi) \chi_+ \quad (7.75)$$

$$Y_{\ell, \ell-1/2, M} = \sqrt{\frac{\ell+M+1/2}{2\ell+1}} Y_{\ell, M+1/2}(\theta\phi) \chi_- - \sqrt{\frac{\ell-M+1/2}{2\ell+1}} Y_{\ell, M-1/2}(\theta\phi) \chi_+$$

Inverse Clebsch-Gordan series:

$$\begin{aligned} D_{m'_3 m_3}^{j_3}(\alpha\beta\gamma) &= (-1)^{m'_3 - m_3} (2j_3 + 1) \\ &\times \sum_{\substack{m'_1 m'_2 \\ m_1 m_2}} \begin{pmatrix} j_1 & j_2 & j_3 \\ m'_1 & m'_2 & m'_3 \end{pmatrix} D_{m'_1 m_1}^{j_1}(\alpha\beta\gamma) D_{m'_2 m_2}^{j_2}(\alpha\beta\gamma) \begin{pmatrix} j_1 & j_2 & j_3 \\ m_1 & m_2 & m_3 \end{pmatrix} \end{aligned} \quad (7.87)$$

Clebsch-Gordan series for D-matrix elements:

$$\begin{aligned} D_{m'_1 m_1}^{j_1}(\alpha\beta\gamma) D_{m'_2 m_2}^{j_2}(\alpha\beta\gamma) &= (-1)^{m'_3 - m_3} \delta_{m'_3, -(m'_1+m'_2)} \delta_{m_3, -(m_1+m_2)} \\ &\times \sum_{j_3} (2j_3 + 1) \begin{pmatrix} j_1 & j_2 & j_3 \\ m'_1 & m'_2 & m'_3 \end{pmatrix} D_{m'_3 m_3}^{j_3}(\alpha\beta\gamma) \begin{pmatrix} j_1 & j_2 & j_3 \\ m_1 & m_2 & m_3 \end{pmatrix} \end{aligned} \quad (7.89)$$

Clebsch-Gordan series for reduced rotation matrix elements:

$$\begin{aligned}
 d_{m'_1 m_1}^{j_1}(\beta) d_{m'_2 m_2}^{j_2}(\beta) &= (-1)^{m'_3 - m_3} \delta_{m'_3, -(m'_1 + m'_2)} \delta_{m_3, -(m_1 + m_2)} \\
 &\times \sum_{j_3} (2j_3 + 1) \begin{pmatrix} j_1 & j_2 & j_3 \\ m'_1 & m'_2 & m'_3 \end{pmatrix} d_{m'_3 m_3}^{j_3}(\beta) \begin{pmatrix} j_1 & j_2 & j_3 \\ m_1 & m_2 & m_3 \end{pmatrix}
 \end{aligned} \quad (7.90)$$

Clebsch-Gordan series for Legendre polynomials:

$$P_{\ell_1}(\cos\beta) P_{\ell_2}(\cos\beta) = \sum_{\ell_3} (2\ell_3 + 1) \begin{pmatrix} \ell_1 & \ell_2 & \ell_3 \\ 0 & 0 & 0 \end{pmatrix}^2 P_{\ell_3}(\cos\beta) \quad (7.91)$$

Integral of the product of three D-matrix elements:

$$\begin{aligned}
 \int_R D_{m'_1 m_1}^{j_1}(\alpha\beta\gamma) D_{m'_2 m_2}^{j_2}(\alpha\beta\gamma) D_{m'_3 m_3}^{j_3}(\alpha\beta\gamma) d\alpha \sin\beta d\beta d\gamma \\
 = 16\pi^2 \begin{pmatrix} j_1 & j_2 & j_3 \\ m'_1 & m'_2 & m'_3 \end{pmatrix} \begin{pmatrix} j_1 & j_2 & j_3 \\ m_1 & m_2 & m_3 \end{pmatrix} \\
 R: \quad 0 \leq \alpha \leq 4\pi \quad 0 \leq \beta \leq \pi \quad 0 \leq \gamma \leq 2\pi
 \end{aligned} \quad (7.98)$$

Integral of the product of three reduced rotation matrix elements:

$$\begin{aligned}
 \int_0^\pi d_{m'_1 m_1}^{j_1}(\beta) d_{m'_2 m_2}^{j_2}(\beta) d_{m'_3 m_3}^{j_3}(\beta) \sin\beta d\beta \delta_{m'_1 + m'_2 + m'_3, 0} \delta_{m_1 + m_2 + m_3, 0} \\
 = 2 \begin{pmatrix} j_1 & j_2 & j_3 \\ m'_1 & m'_2 & m'_3 \end{pmatrix} \begin{pmatrix} j_1 & j_2 & j_3 \\ m_1 & m_2 & m_3 \end{pmatrix}
 \end{aligned} \quad (7.99)$$

Integral over the product of three Legendre polynomials:

$$\int_0^\pi P_{\ell_1}(\cos\beta) P_{\ell_2}(\cos\beta) P_{\ell_3}(\cos\beta) \sin\beta d\beta = 2 \begin{pmatrix} \ell_1 & \ell_2 & \ell_3 \\ 0 & 0 & 0 \end{pmatrix}^2 \quad (7.100)$$

Integral of the product of three spherical harmonics (Gaunt integral):

$$\begin{aligned}
 \int_{R'} Y_{LM}^*(\theta\phi) Y_{\ell_1 m_1}(\theta\phi) Y_{\ell_2 m_2}(\theta\phi) d\phi \sin\theta d\theta \\
 = (-1)^M \sqrt{\frac{(2\ell_1 + 1)(2\ell_2 + 1)(2L + 1)}{4\pi}} \begin{pmatrix} \ell_1 & \ell_2 & L \\ m_1 & m_2 & -M \end{pmatrix} \begin{pmatrix} \ell_1 & \ell_2 & L \\ 0 & 0 & 0 \end{pmatrix}
 \end{aligned} \quad (7.102)$$

$$R': \quad 0 \leq \phi \leq 2\pi \quad 0 \leq \theta \leq \pi$$

$$\Delta(\ell_1 \ell_2 L) \quad \ell_1 + \ell_2 + L \text{ even} \quad m_1 + m_2 = M \quad (7.103)$$

T4 IRREDUCIBLE SPHERICAL TENSOR OPERATORS

Irreducible Spherical Tensors

Basic definition of irreducible tensors:

$$T_{kq}(\alpha\beta\gamma) = \sum_{q'=-k}^k T_{kq'}(0) D_{q'q}^k(\alpha\beta\gamma) \quad (8.8)$$

Racah's requirements on commutators:

$$[J_0, T_{kq}] = [J_z, T_{kq}] = q T_{kq} \quad q = -k, -k+1, \dots, k-1, k \quad (8.9)$$

$$[J_{\pm 1}, T_{kq}] = \sqrt{(k \mp q)(k \pm q + 1)} T_{k, q \pm 1} \quad q = -k, -k+1, \dots, k-1, k \quad (8.10)$$

Gradient operator commutators:

$$\begin{aligned} [L_\sigma, \nabla_q] &= (-1)^\sigma \sqrt{2} \langle 11q + \sigma, -\sigma | 111q \rangle \nabla_{\sigma+q} \\ &= (-1)^{\sigma+q} \sqrt{6} \begin{pmatrix} 1 & 1 & 1 \\ \sigma & q & -\sigma - q \end{pmatrix} \nabla_{\sigma+q} \end{aligned} \quad (8.17)$$

Hermitian adjoint of a tensor component:

$$T_{kq}^\dagger = (-1)^{p-q} T_{k, -q} \quad (8.19)$$

Matrix elements of tensor operators and adjoints:

$$\langle jm | T_{kq} | j' m' \rangle = (-1)^{p-q} \langle j' m' | T_{k, -q} | jm \rangle^* \quad (8.20)$$

Building-up formula for tensors:

$$\begin{aligned} T_{KQ}(A_1, A_2) &= \sum_{q_1, q_2} T_{k_1, q_1}(A_1) T_{k_2, q_2}(A_2) \\ &\times (-1)^{k_1 - k_2 + Q} \sqrt{2K+1} \begin{pmatrix} k_1 & k_2 & K \\ q_1 & q_2 & -Q \end{pmatrix} \end{aligned} \quad (8.21)$$

Bipolar harmonics:

$$\begin{aligned} B_{LM}(\Omega, \Omega') &= \sum_{m_1, m_2} Y_{\ell_1, m_1}(\Omega) Y_{\ell_2, m_2}(\Omega') \\ &\times (-1)^{\ell_1 - \ell_2 + M} \sqrt{2L+1} \begin{pmatrix} \ell_1 & \ell_2 & L \\ m_1 & m_2 & -M \end{pmatrix} \end{aligned} \quad (8.26)$$

Vector spherical harmonics:

$$\mathbf{Y}_{L\ell M}(\theta\phi) = \sum_{\sigma} Y_{\ell, M-\sigma}(\theta\phi) \hat{\mathbf{e}}_{\sigma} (-1)^{\ell-1+M} \sqrt{2L+1} \begin{pmatrix} \ell & 1 & L \\ M-\sigma & \sigma & -M \end{pmatrix} \quad (8.27)$$

Scalar product of two irreducible tensors:

$$\begin{aligned} \mathbf{T}_k(A_1) \cdot \mathbf{T}_k(A_2) &\equiv (-1)^k \sqrt{2k+1} T_{00}(A_1, A_2) \\ &= \sum_q (-1)^q T_{kq}(A_1) T_{k-q}(A_2) \end{aligned} \quad (8.29)$$

Wigner-Eckart theorem:

$$\langle jm | T_{kq} | j' m' \rangle = (-1)^{2k} \langle j' k m' q | j' k j m \rangle \langle j | \mathbf{T}_k | j' \rangle \quad (8.32)$$

Reduced Matrix Elements

Spherical harmonic tensor:

$$\begin{aligned} \langle \ell | \mathbf{Y}_k | \ell' \rangle &= \sqrt{\frac{2k+1}{4\pi}} (-1)^k \langle k \ell 0 0 | k \ell \ell' 0 \rangle \\ &= \sqrt{\frac{(2k+1)(2\ell+1)}{4\pi}} (-1)^{\ell} \begin{pmatrix} \ell & k & \ell' \\ 0 & 0 & 0 \end{pmatrix} \end{aligned} \quad (8.35)$$

Angular momentum operator:

$$\langle j | \mathbf{J} | j' \rangle = \sqrt{j(j+1)} \delta_{jj'} \quad (8.48)$$

Formula for reduced matrix element (for nonzero Clebsch-Gordan coefficient):

$$\langle j | \mathbf{T}_k | j' \rangle = (-1)^{2k} \langle jm | T_{kq} | j' m' \rangle / \langle j' k m' q | j' k j m \rangle \quad (8.49)$$

Reduced matrix element from sum rule:

$$\langle j | \mathbf{T}_k | j' \rangle = (-1)^{2k} \sum_{m'q} \langle j' k m' q | j' k j m \rangle \langle jm | T_{kq} | j' m' \rangle \quad (8.50)$$

Absolute square of reduced matrix element:

$$|\langle j | \mathbf{T}_k | j' \rangle|^2 = \sum_{m'q} |\langle jm | T_{kq} | j' m' \rangle|^2 \quad (8.51)$$

For \mathbf{T}_k Hermitian:

$$\sqrt{2j+1} \langle j | \mathbf{T}_k | j' \rangle = (-1)^{j-j'-k} \sqrt{2j'+1} \langle j' | \mathbf{T}_k | j \rangle^* \quad (8.52)$$

T5 THE 6-*j* COEFFICIENTS

Table of Formulas

6-*j* coefficients with smallest $j \leq 1$ (algebraic), Table 9.1, p. 353.

Recoupling transformation in terms of Racah coefficients:

$$|(ed)c\gamma\rangle = \sum_f |(af)c\gamma\rangle \sqrt{(2e+1)(2f+1)} W(abcd;ef) \tag{9.10}$$

6-*j* coefficients in terms of Racah coefficients:

$$\begin{aligned} \left\{ \begin{matrix} a & b & e \\ d & c & f \end{matrix} \right\} &\equiv (-1)^\Sigma W(abcd;ef) \\ \Sigma &\equiv a+b+c+d \end{aligned} \tag{9.11}$$

Recoupling transformation in terms of 6-*j* coefficients:

$$|(ed)c\gamma\rangle = \sum_f |(af)c\gamma\rangle \sqrt{(2e+1)(2f+1)} (-1)^\Sigma \left\{ \begin{matrix} a & b & e \\ d & c & f \end{matrix} \right\} \tag{9.13}$$

Triangle conditions for nonzero Racah or 6-*j* coefficient:

$$\begin{matrix} & \left\{ \begin{matrix} a & b & e \\ d & c & f \end{matrix} \right\} \\ \left\{ \begin{matrix} \Delta & \Delta & \Delta \end{matrix} \right\} & \left\{ \begin{matrix} \Delta & \Delta & \Delta \end{matrix} \right\} & \left\{ \begin{matrix} \Delta & \Delta & \Delta \end{matrix} \right\} & \left\{ \begin{matrix} \Delta & \Delta & \Delta \end{matrix} \right\} \end{matrix}$$

First expansion rule for 6-*j* coefficients:

$$\begin{aligned} \sum_f (2f+1) (-1)^\Sigma \left\{ \begin{matrix} a & b & e \\ d & c & f \end{matrix} \right\} \begin{pmatrix} b & d & f \\ \beta & \delta & -\phi \end{pmatrix} \begin{pmatrix} a & f & c \\ \alpha & \phi & -\gamma \end{pmatrix} (-1)^{f-e-\alpha-\delta} \\ = \begin{pmatrix} a & b & e \\ \alpha & \beta & -\varepsilon \end{pmatrix} \begin{pmatrix} e & d & c \\ \varepsilon & \delta & -\gamma \end{pmatrix} \end{aligned} \tag{9.14}$$

Second expansion rule for 6-*j* coefficients:

$$\begin{aligned} (-1)^\Sigma \left\{ \begin{matrix} a & b & e \\ d & c & f \end{matrix} \right\} \begin{pmatrix} a & f & c \\ \alpha & \phi & -\gamma \end{pmatrix} \\ = \sum_{\beta\delta} (-1)^{f-e-\alpha-\delta} \begin{pmatrix} a & b & e \\ \alpha & \beta & -\varepsilon \end{pmatrix} \begin{pmatrix} e & d & c \\ \varepsilon & \delta & -\gamma \end{pmatrix} \begin{pmatrix} b & d & f \\ \beta & \delta & -\phi \end{pmatrix} \end{aligned} \tag{9.15}$$

6-*j* coefficients in terms of 3-*j* coefficients:

$$\begin{aligned}
 & (-1)^\Sigma \left\{ \begin{matrix} a & b & e \\ d & c & f \end{matrix} \right\} \\
 &= \sum_{\alpha\beta\delta} (-1)^{f-e-\alpha-\delta} (2c+1) \begin{pmatrix} a & b & e \\ \alpha & \beta & -\varepsilon \end{pmatrix} \begin{pmatrix} e & d & c \\ \varepsilon & \delta & -\gamma \end{pmatrix} \\
 & \times \begin{pmatrix} b & d & f \\ \beta & \delta & -\phi \end{pmatrix} \begin{pmatrix} a & f & c \\ \alpha & \phi & -\gamma \end{pmatrix} \quad \Sigma = a+b+c+d
 \end{aligned} \tag{9.16}$$

General formula for 6-*j* coefficient:

$$\begin{aligned}
 \left\{ \begin{matrix} a & b & e \\ d & c & f \end{matrix} \right\} &= (-1)^{a+b+c+d} \Delta(abe) \Delta(acf) \Delta(bdf) \Delta(cde) \\
 & \times \sum_k (-1)^k (a+b+c+d+1-k)! \\
 & \times [k!(e+f-a-d+k)!(e+f-b-c+k)!]^{-1} \\
 & \times [(a+b-e-k)!(c+d-e-k)!(a+c-f-k)!(b+d-f-k)!]^{-1}
 \end{aligned} \tag{9.20}$$

$$\Delta(abc) \equiv \sqrt{\frac{(a+b-c)!(a+c-b)!(b+c-a)!}{(a+b+c+1)!}}$$

Orthogonality relations of 6-*j* coefficients:

$$\sum_e (2e+1)(2f+1) \left\{ \begin{matrix} a & b & e \\ d & c & f \end{matrix} \right\} \left\{ \begin{matrix} a & b & e \\ d & c & g \end{matrix} \right\} = \delta_{fg} \tag{9.21}$$

Symmetry properties of 6-*j* coefficient:

A 6-*j* coefficient is invariant under interchange of any two columns and under interchange of the upper and lower arguments in each of any two columns.

(9.22)

Scalar Products of Irreducible Tensors

Scalar product of two irreducible tensors:

$$\begin{aligned}
 \mathbf{T}_k(A_1) \cdot \mathbf{T}_k(A_2) &\equiv (-1)^k \sqrt{2k+1} T_{00}(A_1, A_2) \\
 &= \sum_q (-1)^q T_{kq}(A_1) T_{k-q}(A_2)
 \end{aligned} \tag{9.26}$$

Factorization theorem in coupled representation:

$$\begin{aligned}
 & \langle (j_1 j_2) JM | \mathbf{T}_k(A_1) \cdot \mathbf{T}_k(A_2) | (j'_1 j'_2) J' M' \rangle \\
 &= \delta_{JJ'} \delta_{MM'} \langle (j_1 j_2) J \| \mathbf{T}_k(A_1) \cdot \mathbf{T}_k(A_2) \| (j'_1 j'_2) J' \rangle \\
 &= \delta_{JJ'} \delta_{MM'} (-1)^{j'_1 + j_2 + J} \sqrt{(2j_1 + 1)(2j_2 + 1)} \begin{Bmatrix} j_1 & j_2 & J \\ j_2 & j'_1 & k \end{Bmatrix} \\
 & \quad \times \langle j_1 \| \mathbf{T}_k(A_1) \| j'_1 \rangle \langle j_2 \| \mathbf{T}_k(A_2) \| j'_2 \rangle
 \end{aligned} \tag{9.27}$$

Projection theorem for rank-1 tensors:

$$\langle jm | \mathbf{T}_1 | j' m' \rangle = \frac{\langle jm | \mathbf{J}(\mathbf{J} \cdot \mathbf{T}_1) | jm' \rangle}{j(j+1)} \delta_{jj'} \tag{9.29}$$

Factorization theorem for rank-1 tensors in uncoupled representation:

$$\langle jm | \mathbf{J}(\mathbf{J} \cdot \mathbf{T}_1) | j' m' \rangle = \langle jm | \mathbf{J} | jm' \rangle \langle j \| \mathbf{J} \cdot \mathbf{T}_1 \| j \rangle \delta_{jj'} \tag{9.34}$$

Decomposition theorem for rank-1 tensor operator:

$$\langle jm | \mathbf{T}_1 | j' m' \rangle = \frac{\langle jm | \mathbf{J} | jm' \rangle \langle j \| \mathbf{J} \cdot \mathbf{T}_1 \| j \rangle}{j(j+1)} \delta_{jj'} \tag{9.35}$$

Reduced matrix element of rank-1 tensor operator:

$$\langle j \| \mathbf{T}_1 \| j' \rangle = \frac{\langle j \| \mathbf{J} \cdot \mathbf{T}_1 \| j \rangle}{\sqrt{j(j+1)}} \delta_{jj'} \tag{9.36}$$

Reduced matrix element of Legendre polynomial:

$$\begin{aligned}
 & \langle (\ell_1 \ell_2) L \| P_\mu \| (\ell'_1 \ell'_2) L' \rangle = (-1)^{\mu+L} (2\ell_1 + 1)(2\ell_2 + 1) \\
 & \quad \times \begin{pmatrix} \ell_1 & \mu & \ell'_1 \\ 0 & 0 & 0 \end{pmatrix} \begin{pmatrix} \ell_2 & \mu & \ell'_2 \\ 0 & 0 & 0 \end{pmatrix} \begin{Bmatrix} \ell_1 & \ell_2 & L \\ \ell'_2 & \ell'_1 & \mu \end{Bmatrix} \delta_{LL'}
 \end{aligned} \tag{9.46}$$

T6 THE 9- j COEFFICIENTS

9- j coefficients in terms of 3- j coefficients:

$$\begin{aligned}
 \begin{Bmatrix} a & b & c \\ d & e & f \\ g & h & i \end{Bmatrix} &= \sum \begin{pmatrix} a & b & c \\ \alpha & \beta & \gamma \end{pmatrix} \begin{pmatrix} d & e & f \\ \delta & \varepsilon & \phi \end{pmatrix} \begin{pmatrix} g & h & i \\ \gamma & \eta & m \end{pmatrix} \\
 & \quad \times \begin{pmatrix} a & d & g \\ \alpha & \delta & \gamma \end{pmatrix} \begin{pmatrix} b & e & h \\ \beta & \varepsilon & \eta \end{pmatrix} \begin{pmatrix} c & f & i \\ \gamma & \phi & m \end{pmatrix}
 \end{aligned} \tag{9.58}$$

Symmetry properties of 9-*j* coefficients:

Under interchange of all rows with all columns a 9- <i>j</i> coefficient is invariant.	(9.60)
---	--------

Under interchange of two rows or two columns a 9- <i>j</i> coefficient is multiplied by the phase $(-1)^P$ where $P = a + b + c + d + e + f + g + h + i$.	(9.61)
--	--------

9-*j* coefficient with one argument zero:

$$\left\{ \begin{matrix} 0 & b & c \\ d & e & f \\ g & h & i \end{matrix} \right\} = \frac{(-1)^{b+d+f+h}}{\sqrt{(2b+1)(2d+1)}} \left\{ \begin{matrix} d & e & f \\ b & i & h \end{matrix} \right\} \delta_{bc} \delta_{dg} \quad (9.62)$$

9-*j* coefficient with one argument unity:

$$\left\{ \begin{matrix} 1 & b & b \\ d & e & f \\ d & h & i \end{matrix} \right\} = \frac{[e(e+1)+i(i+1)-f(f+1)-h(h+1)]}{\sqrt{4b(b+1)(2b+1)d(d+1)(2d+1)}} \times (-1)^{b+d+f+h} \left\{ \begin{matrix} d & e & f \\ b & i & h \end{matrix} \right\} \quad (9.64)$$

Orthogonality sum rule for 9-*j* coefficients:

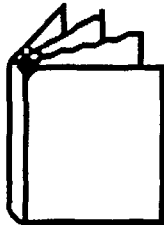
$$\sum_{cf} (2c+1)(2f+1) \left\{ \begin{matrix} a & b & c \\ d & e & f \\ g & h & i \end{matrix} \right\} \left\{ \begin{matrix} a & b & c \\ d & e & f \\ j & k & i \end{matrix} \right\} = \frac{\delta_{gj} \delta_{hk}}{(2g+1)(2h+1)} \quad (9.65)$$

Tensor matrix elements in the coupled scheme:

$$\begin{aligned} & \langle (j_1 j_2) J \| \mathbf{T}_K(A_1, A_2) \| (j'_1 j'_2) J' \rangle \\ & = \sqrt{(2j_1+1)(2j_2+1)(2J+1)(2J'+1)(2K+1)} \\ & \quad \times \left\{ \begin{matrix} j_1 & j'_1 & k_1 \\ j_2 & j'_2 & k_2 \\ J & J' & K \end{matrix} \right\} \langle j_1 \| \mathbf{T}_{k_1}(A_1) \| j'_1 \rangle \langle j_2 \| \mathbf{T}_{k_2}(A_2) \| j'_2 \rangle \end{aligned} \quad (9.68)$$

States in j - j scheme in terms of L - S scheme:

$$\begin{aligned}
 |(\ell_1 s_1)j_1, (\ell_2 s_2)j_2; JM\rangle &= \sum_{LS} |(\ell_1 \ell_2)L, (s_1 s_2)S; JM\rangle \\
 &\times \sqrt{(2L+1)(2S+1)(2j_1+1)(2j_2+1)} \begin{Bmatrix} \ell_1 & \ell_2 & L \\ s_1 & s_2 & S \\ j_1 & j_2 & J \end{Bmatrix} \quad (9.69)
 \end{aligned}$$



REFERENCES

- [Ada71] Adams, D. A., U.S. Patent 3 586 413, June 22, 1971.
- [Adh86] Adhikari, S. K., "Quantum Scattering in Two Dimensions," *American Journal of Physics*, **54**, 362 (1986).
- [Ali71] Alisaukas, S. J., and A. P. Jucys, "Weight Lowering Operators and the Multiplicity-Free Isoscalar Factors for the Group R_5 ," *Journal of Mathematical Physics*, **12**, 594 (1971).
- [Alt86] Altmann, S. L., *Rotations, Quaternions, and Double Groups*, Clarendon Press, Oxford, 1986.
- [And79] Andrews, M., "Vector Operators and Spherical Harmonics in Quantum Mechanics," *American Journal of Physics*, **47**, 274 (1979).
- [Arf85] Arfken, G., *Mathematical Methods for Physicists*, Academic Press, New York, third edition, 1985.
- [Arm88] Armstrong, M. A., *Groups and Symmetry*, Springer-Verlag, New York, 1988.
- [Art60] Arthurs, A. M., and A. Dalgarno, "Theory of Scattering by a Rigid Rotator," *Proceedings of the Royal Society (London)*, **A256**, 540 (1960).
- [Ave89] Avery, J., *Hyperspherical Harmonics: Applications in Quantum Theory*, Kluwer, Dordrecht, The Netherlands, 1989.
- [Ave91] Avetisov, V. A., V. I. Goldanskii, and V. V. Kuz'min, "Handedness, Origin of Life, and Evolution," *Physics Today*, July 1991, p. 33.
- [Bar62] Bargmann, V., "On the Representations of the Rotation Group," *Reviews of Modern Physics*, **34**, 300 (1962).
- [Bau59] Bauer, G., "Von dem Coefficienten der Reihen von Kugelfunctionen einer Variablen," *Journal für die Reine und Angewandte Mathematik*, **6**, 101 (1859).

- [Bel54] Bell, D. G., "Group Theory and Crystal Lattices," *Reviews of Modern Physics*, **26**, 311 (1954).
- [Ber72] Bernal, I., W. C. Hamilton, and J. S. Ricci, *Symmetry: A Stereoscopic Guide for Chemists*, W. H. Freeman, San Francisco, 1972.
- [Bet36] Beth, R. A., "Mechanical Detection and Measurement of the Angular Momentum of Light," *Physical Review*, **50**, 115 (1936).
- [Bev92] Bevington, P. R., and D. K. Robinson, *Data Reduction and Error Analysis for the Physical Sciences*, McGraw-Hill, New York, second edition, 1992.
- [Bia92] Bialynicki-Birula, I., M. Cieplak, and J. Kaminski, *Theory of Quanta*, Oxford University Press, New York, 1992.
- [Bie65] Biedenharn, L. C., and H. Van Dam, *Quantum Theory of Angular Momentum*, Academic Press, New York, 1965.
- [Bie81a] Biedenharn, L. C., and J. D. Louck, *Angular Momentum in Quantum Physics*, Addison-Wesley, Reading, Massachusetts, 1981.
- [Bie81b] Biedenharn, L. C., and J. D. Louck, *The Racah-Wigner Algebra in Quantum Theory*, Addison-Wesley, Reading, Massachusetts, 1981.
- [Boh13] Bohr, N., "On the Constitution of Atoms and Molecules," *Philosophical Magazine*, **26**, 1, 476, 857 (1913).
- [Bol73] Bolker, E. D., "The Spinor Spanner," *American Mathematical Monthly*, **80**, 977 (1973).
- [Bor26] Born, M., W. Heisenberg, and P. Jordan, "Zur Quantenmechanik II," *Zeitschrift für Physik*, **35**, 557 (1926); translated as "On Quantum Mechanics II," in *Sources of Quantum Mechanics*, B. L. Van der Waerden (ed.), North-Holland, Amsterdam, 1967.
- [Bou69] Bouten, M., "On the Rotation Operators in Quantum Mechanics," *Physica*, **42**, 572 (1969).
- [Bre81] Brewer, J. W., and M. K. Smith, *Emmy Noether: A Tribute to Her Life and Work*, Marcel Dekker, New York, 1981.
- [Bri94] Brink, D. M., and G. R. Satchler, *Angular Momentum*, Clarendon Press, Oxford, third edition, 1994.
- [Bru57] Brussaard, P. J., and H. A. Tolhoek, "Classical Limits of Clebsch-Gordan Coefficients, Racah Coefficients and D_{mn}^{ℓ} Functions," *Physica*, **23**, 955 (1957).
- [Bun89] Bunch, B., *Reality's Mirror: Exploring the Mathematics of Symmetry*, Wiley, New York, 1989.
- [Bur90] Burns, G., and A. M. Glazer, *Space Groups for Solid State Scientists*, Academic Press, New York, second edition, 1990.
- [But68] Butkov, E., *Mathematical Physics*, Addison-Wesley, Reading, Massachusetts, 1968.
- [Car65] Carroll, L. (C. L. Dodgson), *Alice's Adventures in Wonderland*, Macmillan, London, 1865.

- [Car66] Cartan, E., *The Theory of Spinors*, M.I.T. Press, Cambridge, Massachusetts, 1966.
- [Cha92] Char, B. W. et al., *First Leaves: A Tutorial Introduction to Maple V*, Springer-Verlag, New York, 1992.
- [Chu93] Chung, F., and S. Sternberg, "Mathematics and the Buckyball," *Scientific American*, **81**, 56 (1993).
- [Cle72] Clebsch, A., "Theorie der binären algebraischen Formen," Teubner, Leipzig, 1872.
- [Coh77] Cohen-Tannoudji, C., B. Diu, and F. Laloë, *Quantum Mechanics*, Wiley, New York, 1977.
- [Com93] Commins, E. D., "Resource Letter ETDSTS-1: Experimental Tests of the Discrete Space-Time Symmetries," *American Journal of Physics*, **61**, 778 (1993).
- [Con35] Condon, E. U., and G. H. Shortley, *The Theory of Atomic Spectra*, Cambridge University Press, London, 1935.
- [Cor84] Cornwell, J. F., *Group Theory in Physics*, Vols. I and II, Academic Press, London, 1984.
- [Cou27] Coupling, L. S., and J. J. Thomson, "On Spin-Dependent Interactions in Atoms," *Philosophical Magazine*, **137**, 731 (1927).
- [Cur94] Curie, P., "Symétrie dans les Phénomènes Physiques, Symétrie d'un Champ Electrique et d'un Champ Magnétique," *Journal de Physique* **3**, 393 (1894); reprinted in *Oeuvres de Pierre Curie*, Gauthier-Villars, Paris, 1908, p. 118.
- [Dan62] Danby, J. M., *Fundamentals of Celestial Mechanics*, Macmillan, New York, 1962.
- [Dan90] Danos, M., and V. Gillet, *Angular Momentum Calculus in Quantum Physics*, World Scientific, Singapore, 1990.
- [Das73] Dash, J., *A Life of One's Own: Three Gifted Women and the Men They Married*, Harper & Row, New York, 1973.
- [Das91] Dash, J., *The Triumph of Discovery: Women Scientists Who Won the Nobel Prize*, Messner, Englewoods Cliffs, New Jersey, 1991.
- [Dav74] Davies, P. C. W., *The Physics of Time Asymmetry*, University of California Press, Berkeley, 1974.
- [DeL91] De Lange, O. L., and R. E. Raab, *Operator Methods in Quantum Mechanics*, Clarendon Press, Oxford, 1991.
- [de-S63] de-Shalit, A., and I. Talmi, *Nuclear Shell Theory*, Academic Press, New York, 1963.
- [Dir28] Dirac, P. A. M., "The Quantum Theory of the Electron," *Proceedings of the Royal Society of London*, **A117**, 610 (1928); *ibid.*, **A118**, 351 (1928).
- [Dod91] Dodd, J. N., *Atoms and Light*, Plenum Press, New York, 1991.
- [Dub76] Dubos, R., *Louis Pasteur, Free Lance of Science*, Scribner, New York, 1976.

- [Dup91] Duplessy, J.-C., L. Labeyrie, A. Juillet-Leclerc, F. Maitre, J. Duprat, and M. Sarnthein, "Surface Salinity Reconstruction of the N. Atlantic Ocean During the Last Glacial Maximum," *Oceanologica Acta*, **14**, 311 (1991).
- [Eck30] Eckart, C., "The Application of Group Theory to the Quantum Dynamics of Monatomic Systems," *Reviews of Modern Physics*, **2**, 305 (1930).
- [Ehr27] Ehrenfest, P., "Bemerkung über die angenäherte Gültigkeit der klassischen Mechanik innerhalb der Quantenmechanik," *Zeitschrift für Physik*, **45**, 455 (1927).
- [Ein54] Einstein, A., *Ideas and Opinions*, Ways Books, Avenal, New Jersey, 1954, p. 232.
- [Eis85] Eisberg, R., and R. Resnick, *Quantum Physics of Atoms, Molecules, Solids, Nuclei, and Particles*, Wiley, New York, second edition, 1985.
- [Ell79] Elliott, J. P., and P. G. Dawber, *Symmetry in Physics*, Vols. 1 and 2, Macmillan, London, 1979.
- [Eng72] Englefield, M. J., *Group Theory and the Coulomb Problem*, Wiley, New York, 1972.
- [Erd53] Erdélyi, A., W. Magnus, F. Oberhettinger, and G. F. Tricomi, *Higher Transcendental Functions*, Vol. I, McGraw-Hill, New York, 1953.
- [Fac92] Fack, V., J. Van der Jeugt, and K. S. Rao, "Parallel Computation of Recoupling Coefficients Using Transputers," *Computer Physics Communications*, **71**, 285 (1992).
- [Fan92] Fang, D. F., and J. F. Shriner, Jr., "A Computer Program for the Calculation of Angular-Momentum Coupling Coefficients," *Computer Physics Communications*, **70**, 147 (1992).
- [Fax27] Faxen, H., and J. Holtsmark, "Beitrag zur Theorie des Durchganges langsamer Elektronen durch Gase," *Zeitschrift für Physik*, **45**, 307 (1927).
- [Fer75] Ferraro, J. R., and J. S. Ziomek, *Introductory Group Theory and Its Application to Molecular Structure*, Plenum Press, New York, second edition, 1975.
- [Fey63] Feynman, R. P., *Feynman Lectures on Physics*, Addison-Wesley, Reading, Massachusetts, 1963, Chapter 34.
- [Flo86] Flood, R., and M. Lockwood, *The Nature of Time*, Basil Blackwell, Oxford, 1986.
- [For76] Formánec, J., "On Phase Shift Analysis of One-Dimensional Scattering," *American Journal of Physics*, **44**, 778 (1976).
- [Fre81] Frescura, F. A. M., and B. J. Hiley, "Geometrical Interpretation of the Pauli Spinor," *American Journal of Physics*, **49**, 152 (1981).
- [Fri49] von Frisch, K., "Die Polarisation des Himmelslichtes als Orientierender Faktor bei den Tänzen der Bienen," *Experientia*, **4**, 142 (1949).
- [Fro91] Froggatt, C. D., and H. B. Nielsen, *Origin of Symmetries*, World Scientific, Singapore, 1991.

- [Gal90] Gallian, J. A., "Symmetry in Logos and Hubcaps," *American Mathematical Monthly*, **97**, 235 (1990).
- [Gar90] Gardner, M., *The New Ambidextrous Universe*, W.H. Freeman, New York, third revised edition, 1990.
- [Gau29] Gaunt, J. A., "The Triplets of Helium," *Transactions of the Royal Society (London)*, **A228**, 151 (1929).
- [Geo82] Georgi, H., *Lie Algebras in Particle Physics: From Isospin to Unified Theories*, W. A. Benjamin, Menlo Park, California, 1982.
- [Gib76] Gibson, W. M., and B. R. Pollard, *Symmetry Principles in Elementary Particle Physics*, Cambridge University Press, Cambridge, 1976.
- [Gol75] Goldstein, H., "Prehistory of the Runge-Lenz Vector," *American Journal of Physics*, **43**, 737 (1975).
- [Gol76] Goldstein, H., "More on the Prehistory of the Laplace or Runge-Lenz Vector," *American Journal of Physics*, **44**, 1123 (1976).
- [Gol80] Goldstein, H., *Classical Mechanics*, Addison-Wesley, Reading, Massachusetts, second edition, 1980.
- [Gor70] Gordy, W., and R. L. Cook, *Microwave Molecular Spectra*, Wiley, New York, 1970, Table 4.2.
- [Gor75] Gordan, P., "Über das Formensystem binärer Formen," Teubner, Leipzig, 1875.
- [Gor85] Gorenstein, D., "The Enormous Theorem," *Scientific American*, **253**, 104 (1985).
- [Gre89] Greiner, W., and B. Müller, *Quantum Mechanics: Symmetries*, Springer-Verlag, Berlin, 1989.
- [Gri87] Grinstein, L. S., and P. J. Campbell (eds.), *Women of Mathematics*, Greenwood Press, New York, 1987.
- [Hal78] Halprin, A., "Pedagogy of Spin in Nonrelativistic Quantum Mechanics," *American Journal of Physics*, **46**, 768 (1978).
- [Ham62] Hamermesh, M., *Group Theory and Its Application to Physical Problems*, Addison-Wesley, Reading, Massachusetts, 1962.
- [Har92] Hargittai, I. (ed.), *Fivefold Symmetry*, World Scientific, Singapore, 1992.
- [Haw92] Hawryshyn, C. W., "Polarization Vision in Fish," *American Scientist*, **80**, 164 (1992).
- [Hec92] Heck, A., *Introduction to Maple*, Springer-Verlag, New York, 1992.
- [Hei26] Heisenberg, W., and P. Jordan, "Anwendung der Quantenmechanik auf das Problem der anomalen Zeemaneffekte," *Zeitschrift für Physik*, **37**, 263 (1926).
- [Hob31] Hobson, E. W., *The Theory of Spherical and Ellipsoidal Harmonics*, Cambridge University Press, London, 1931.
- [Hou65] Houtappel, R. M. F., H. van Dam, and E. P. Wigner, "The Conceptual Basis and Use of the Geometric Invariance Principles," *Reviews of Modern Physics*, **37**, 595 (1965).

- [Jac59] Jacob, M., and G.-C. Wick, "On the General Theory of Collisions for Particles with Spin," *Annals of Physics (New York)*, **7**, 404 (1959).
- [Jam89] Jammer, M., *The Conceptual Development of Quantum Mechanics*, American Institute of Physics, New York, 1989.
- [Jon67] Jonkers, J. E., and E. De Vries, "A Note on Orthogonality and Completeness of the Rotation Matrices," *Nuclear Physics*, **A105**, 621 (1967).
- [Jon85] Jones, M. N., *Spherical Harmonics and Tensors for Classical Field Theory*, Research Studies Press, Letchworth, England, 1985.
- [Jor69] Jordan, T. F., *Linear Operators for Quantum Mechanics*, Wiley, New York, 1969.
- [Jud63] Judd, B. R., *Operator Techniques in Atomic Spectroscopy*, McGraw-Hill, New York, 1963.
- [Jud75] Judd, B. R., *Angular Momentum Theory for Diatomic Molecules*, Academic Press, New York, 1975.
- [Kep09] Kepler, J., *Astronomia Nova*, Prague, 1609.
- [Ker91] Kerrigan, J. F., *From Fortran to C*, Windcrest Books, Blue Ridge Summit, Pennsylvania, 1991.
- [Kob86] Kobe, D. H., "Active and Passive Views of Gauge Invariance in Quantum Mechanics," *American Journal of Physics*, **54**, 77 (1986).
- [Kop60] Kopal, Z., *Figures of Equilibrium of Celestial Bodies*, University of Wisconsin Press, Madison, 1960.
- [Kra30] Kramers, H. A., "General Theory of Paramagnetic Rotation in Crystals," *Koninklijke Nederlandse Akademie van Wetenschappen*, **33**, 959 (1930).
- [Kra88] Krane, K. S., *Introductory Nuclear Physics*, Wiley, New York, 1988.
- [Lai90] Lai, S.-T., and Y.-N. Chiu, "Exact Computation of the 3- j and 6- j Symbols," *Computer Physics Communications*, **61**, 350 (1990).
- [Lai92] Lai, S.-T., and Y.-N. Chiu, "Exact Computation of the 9- j Symbols," *Computer Physics Communications*, **70**, 544 (1992).
- [Lan19] Landé, A., "Eine Quantenregel für die räumliche Orientierung von Elektronen-ringen," *Verhandlungen der Deutschen Physikalischen Gesellschaft*, **21**, 585 (1919).
- [Lan82] Landsberg, P. T., *The Enigma of Time*, Adam Hilger, Bristol, England, 1982.
- [Lan90] Landau, R. H., *Quantum Mechanics II: A Second Course in Quantum Theory*, Wiley, New York, 1990.
- [Lap82] Lapidus, I. R., "Quantum-Mechanical Scattering in Two Dimensions," *American Journal of Physics*, **50**, 45 (1982).
- [Lap99] Laplace, P. S., *Traité de Mécanique Celeste*, Tome I, Première Partie, Livre II, 1799, p. 165 ff.
- [Leg98] Legendre, A. M., *Théorie des Nombres*, Courcier, Paris, 1798.

- [Leh64] Lehrer-Ilamed, Y., "On the Direct Calculations of the Representations of the Three Dimensional Pure Rotation Group," *Proceedings of the Cambridge Philosophical Society*, **60**, 61 (1964).
- [Len24] Lenz, W., "Über den Bewegungsverlauf und die Quantenzustände der gestörten Keplerbewegung," *Zeitschrift für Physik*, **24**, 197 (1924).
- [Lev79] Lvinger, J. S., and R. M. Lichtenstein, "Intuitive Understanding of Pauli's σ Matrices," *American Journal of Physics*, **47**, 744 (1979).
- [Lév71] Lévy-Leblond, J.-M., "Galilei Group and Galilean Invariance," in E. M. LoebI (ed.), *Group Theory and Its Applications*, Academic Press, New York, 1971, Vol. II, pp. 222–299.
- [Lév82] Lévy-Leblond, J.-M., "Commuting Functions of Noncommuting Operators," *American Journal of Physics*, **50**, 657 (1982).
- [Lip73] Lipkin, H. J., *Quantum Mechanics: New Approaches to Selected Topics*, North-Holland, Amsterdam, 1973.
- [Lov89] Lovett, D. R., *Tensor Properties of Crystals*, Adam Hilger, Bristol, England, 1989.
- [Lub42] Lubanski, J. K., "Sur la Theorie des Particules Elementaires de Spin Quelconque," *Physica*, **9**, 310 (1942).
- [Lüd57] Lüders, G., "Proof of the TCP Theorem," *Annals of Physics*, **2**, 1 (1957).
- [Lud88] Ludwig, W., and C. Falter, *Symmetries in Physics: Group Theory Applied to Physical Problems*, Springer-Verlag, Berlin, 1988.
- [Mac01] Mach, E., *Space and Geometry*, Open Court, Chicago, 1901.
- [Mac83] Mach, E., *Die Mechanik in Ihrer Entwicklung Historisch-Kritisch Dargestellt*, 1883; translated as *The Science of Mechanics: A Critical and Historical Account of Its Development*, Open Court, LaSalle, Illinois, third paperback edition, 1974.
- [Mae91] Maeder, R., *Programming in Mathematica*, Addison-Wesley, Redwood City, California, second edition, 1991.
- [Maj32] Majorana, E., "Atomi Orientati in Campo Magnetico Variabile," *Nuovo Cimento* [8], **9**, 43 (1932).
- [Mar72] Marquez, L., "On the Divergence of the Rutherford Scattering Amplitude in Terms of Coulomb Phase Shifts," *American Journal of Physics*, **40**, 1420 (1972).
- [Mar91] Martin, G. E., *Polyominoes*, Mathematical Association of America, Washington, D.C., 1991.
- [Mat55] Matsunobu, H., and H. Takebe, *Progress of Theoretical Physics*, **14**, 589 (1955).
- [Mei87] Meiring, W. J., "Nuclear β -Decay and the Origin of Biomolecular Chirality," *Nature*, **329**, 712 (1987).
- [Mis73] Misner, C. W., K. S. Thorne, and J. A. Wheeler, *Gravitation*, W. H. Freeman, San Francisco, 1973.

- [Mor53a] Morse, P. M., and H. Feshbach, *Methods of Theoretical Physics*, McGraw-Hill, New York, 1953.
- [Mor53b] Morette-de Witt, C., and J. H. D. Jensen, "Über den Dreimpuls der Multipolstrahlung," *Zeitschrift für Naturforschung*, **8a**, 267 (1953).
- [Ner11] Nernst, W., "Zur Theorie der spezifischen Wärme und über die Anwendung der Lehre von den Energiequanten auf physikalisch-chemische Fragen überhaupt," *Zeitschrift für Elektrochemie*, **17**, 265 (1911).
- [New86] Newton, I., *Philosophiae Naturalis Principia Mathematica*, London, 1686; translated as *Mathematical Principles of Natural Philosophy and His System of the World*, University of California Press, Berkeley, 1971. Vols. 1 and 2.
- [Noe18] Noether, E., "Invariante Variationsprobleme," *Göttinger Nachrichtung*, **5**, 235 (1918).
- [Nol91] Nolte, E., et al., "Test of the Pauli Exclusion Principle for Nucleons and Atomic Electrons by Accelerator Mass Spectrometry," *Zeitschrift für Physik*, **A340**, 411 (1991).
- [Nor82] Normand, J. M., and J. Raynal, "Relations Between Cartesian and Spherical Components of Irreducible Cartesian Tensors," *Journal of Physics* **A15**, 1437 (1982).
- [Nuc87] Nuclear Data Sheets, Academic Press, New York, **50**, 370 (1987).
- [Oha86] Ohanian, H. C., "What is Spin?" *American Journal of Physics*, **54**, 500 (1986).
- [Par90] Park, D. A., *Classical Dynamics and Its Quantum Analogues*, Springer-Verlag, New York, second edition, 1990.
- [Pas48] Pasteur, L., "Recherches sur le Dimorphism," *Annales de Chimie et de Physique*, **23**, 267 (1848); "Recherches sur les Relations qui Peuvent Exister entre la Forme Cristalline, la Composition Chimique et le Sens de la Polarisation Rotatoire," *ibid.*, **24**, 442 (1848).
- [Pau26] Pauli, W., "On the Hydrogen Spectrum from the Standpoint of the New Quantum Mechanics," *Zeitschrift für Physik*, **36**, 336 (1926); translated in *Sources of Quantum Mechanics*, B. L. Van der Waerden (ed.), Dover, New York, 1968.
- [Pau27] Pauli, W., "Zur Quantenmechanik des magnetischen Elektrons," *Zeitschrift für Physik*, **43**, 601 (1927).
- [Pau55] Pauli, W., "Exclusion Principle, Lorentz Group, and Reflexion of Space-Time and Charge," in *Niels Bohr and the Development of Physics*, Pergamon Press, London, 1955, p. 30.
- [Pay52] Payne, W. T., "Elementary Spinor Theory," *American Journal of Physics*, **20**, 253 (1952).
- [Pen80] de la Peña, L., and R. Montemayor, "Raising and Lowering Operators and Spectral Structure: A Concise Algebraic Technique," *American Journal of Physics*, **48**, 855 (1980).

- [Pla81] Plattner, G.-R., and I. Sick, "Coherence, Interference and the Pauli Principle: Coulomb Scattering of Carbon from Carbon," *European Journal of Physics*, **2**, 109 (1981).
- [Poo87] Poole, C. P., and H. A. Farach, *Theory of Magnetic Resonance*, Wiley, New York, second edition, 1987.
- [Rac42] Racah, G., "Theory of Complex Spectra I," *Physical Review*, **62**, 186 (1942); "Theory of Complex Spectra," *ibid.*, **62**, 438 (1942).
- [Ral72] Strutt, J. W., "Investigation of the Disturbance Produced by a Spherical Obstacle on the Waves of Sound," *Proceedings of the London Mathematical Society*, **4**, 253 (1872); J. W. Strutt (Baron Rayleigh), *The Theory of Sound*, Dover, New York, 1945, Section 334.
- [Rao78] Rao, K. S., and K. Venkatesh, "New Fortran Programs for Angular Momentum Coefficients," *Computer Physics Communications*, **15**, 227 (1978).
- [Rao81] Rao, K. S., "Computation of Angular-Momentum Coefficients Using Sets of Generalized Hypergeometric Functions," *Computer Physics Communications*, **22**, 297 (1981).
- [Rao89] Rao, K. S., V. Rajeswari, and C. B. Chiu, "A New Fortran Program for the 9 - j Angular Momentum Coefficient," *Computer Physics Communications*, **56**, 231 (1989).
- [Rau75] Rauch, H., A. Zeilinger, G. Badurek, A. Wilfing, W. Bauspiess, and U. Bouse, "Verification of Coherent Spinor Rotation of Fermions," *Physics Letters*, **A54**, 427 (1975).
- [Reg58] Regge, T., "Symmetry Properties of Clebsch-Gordan's Coefficients," *Il Nuovo Cimento*, **10**, 544 (1958).
- [Ren35] Renaud, P., "Sur une Généralisation du Principe de Symétrie de Curie," *Comptes Rendues Academie Sciences de Paris*, **200**, 531 (1935).
- [Rie79] Rieflin, E., "Some Mechanisms Related to Dirac's Strings," *American Journal of Physics*, **47**, 379 (1979).
- [Rob74] Robson, B. A., *The Theory of Polarization Phenomena*, Clarendon Press, Oxford, 1974.
- [Rom61] Roman, P., *Theory of Elementary Particles*, North-Holland, Amsterdam, 1961.
- [Ros55] Rose, M. E., *Multipole Fields*, Wiley, New York, 1955.
- [Ros57] Rose, M. E., *Elementary Theory of Angular Momentum*, Wiley, New York, 1957.
- [Ros73] Rosen, J., "Transformation Properties of Electromagnetic Quantities Under Space Inversion, Time Reversal, and Charge Conjugation," *American Journal of Physics*, **41**, 586 (1973).
- [Ros83] Rosen, J., *A Symmetry Primer for Scientists*, Wiley, New York, 1983.
- [Rot59] Rotenberg, M., R. Bivins, N. Metropolis, and J. K. Wooten, Jr., *The 3-j and 6-j Symbols*, Technology Press, M.I.T., Cambridge, Massachusetts, 1959.
- [Sak94] Sakurai, J. J., *Modern Quantum Mechanics*, S. F. Tuan (ed.), W. A. Benjamin, Menlo Park, California, revised edition, 1994.

- [Sch51] Schwinger, J., "Theory of Quantized Fields. I," *Physical Review*, **82**, 914 (1951).
- [Sch53] Schwinger, J., "Theory of Quantized Fields. II, III," *Physical Review*, **91**, 713, 728 (1953).
- [Sha60] Sharp, R. T., "Simple Derivation of the Clebsch-Gordan Coefficients," *American Journal of Physics*, **28**, 116 (1960).
- [Sha80] Shankar, R., *Principles of Quantum Mechanics*, Plenum Press, New York, 1980.
- [Sha88] Shamma, N., *Introducing C to Pascal Programmers*, Wiley, New York, 1988.
- [Sli89] Slichter, C. P., *Principles of Magnetic Resonance*, Springer-Verlag, Berlin, third edition, 1989.
- [Som16] Sommerfeld, A., "Zur Quantentheorie der Spektrallinien," *Annalen der Physik*, **51**, 1, 125 (1916).
- [Ste90] Stedman, G. E., *Diagram Techniques in Group Theory*, Cambridge University Press, Cambridge, England, 1990.
- [Taf85] Taff, L. G., *Celestial Mechanics: A Computational Guide for the Practitioner*, Wiley, New York, 1985.
- [Tho43] Thompson, D. W., *On Growth and Form*, Cambridge University Press, New York, 1943.
- [Tho92a] Thompson, W. J., "A Concise Derivation of the Plane-Wave Partial-Wave Expansion," *American Journal of Physics*, **60**, 378 (1992).
- [Tho92b] Thompson, W. J., *Computing for Scientists and Engineers*, Wiley, New York, 1992.
- [Tho93] Thompson, W. J., "Spin Mixing in Magnetic Field Gradients," *Nuclear Instruments and Methods*, **A333**, 443 (1993).
- [Tin64] Tinkham, M., *Group Theory and Quantum Mechanics*, McGraw-Hill, New York, 1964.
- [Van67] Van der Waerden, B. L., *Sources of Quantum Mechanics*, North-Holland, Amsterdam, 1967.
- [Var88] Varshalovich, D. A., A. N. Moskalev, and V. K. Khersonskii, *Quantum Theory of Angular Momentum*, World Scientific, Singapore, 1988.
- [Vin77] Vincent, A., *Molecular Symmetry and Group Theory*, Wiley, London, 1977.
- [Wat44] Watson, G. N., *Theory of Bessel Functions*, Cambridge University Press, New York, 1944, Section 11.5.
- [Way93] Way, J. B., and J. F. Williams, "A Study of the Helium $3^1D \rightarrow 2^1P \rightarrow 1^1S$ Cascade with Algebraic Computing," *Computer Physics Communications*, **75**, 275 (1993).

- [Wer75] Werner, S. A., R. Colella, A. W. Overhauser, and C. F. Eagen, "Observation of the Phase Shift of a Neutron Due to Precession in a Magnetic Field," *Physical Review Letters*, **35**, 1053 (1975).
- [Wig27a] Wigner, E. P., "Einige Folgerungen aus der Schrödingerschen Theorie für die Termstrukturen," *Zeitschrift für Physik*, **43**, 624 (1927); *ibid.*, **45**, 601 (1927); an expanded treatment is in [Wig31].
- [Wig27b] Wigner, E. P., "Über die Erhaltungssätze in der Quantenmechanik," *Göttingen Nachricht*, 375 (1927).
- [Wig31] Wigner, E. P., *Gruppentheorie und ihre Anwendung auf die Quantenmechanik der Atomspektren*, Vieweg, Braunschweig, 1931. Translated by J. J. Griffin as *Group Theory and Its Application to the Quantum Mechanics of Atomic Spectra*, Academic Press, New York, 1959.
- [Wig67] Wigner, E. P., *Symmetries and Reflections*, Indiana University Press, Bloomington, 1967.
- [Wil92] Williams, H. T., and R. R. Silbar, "Automated Angular Momentum Recoupling Algebra," *Journal of Computational Physics*, **99**, 299 (1992).
- [Wol69] Wolf, A. A., "Rotation Operators," *American Journal of Physics*, **37**, 531 (1969).
- [Wol77] Wolbarst, A. B., *Symmetry and Quantum Systems*, Van Nostrand Reinhold, New York, 1977; "An Intuitive Approach to Group Representation Theory," *American Journal of Physics*, **45**, 803 (1977).
- [Wol79] Wolbarst, A. B., "An Intuitive Approach to Group Representation Theory. II," *American Journal of Physics*, **47**, 103 (1979).
- [Wol91] Wolfram, S., *Mathematica: A System for Doing Mathematics by Computer*, Addison-Wesley, Redwood City, California, second edition, 1991.
- [Won90] Wong, S. S. M., *Introductory Nuclear Physics*, Prentice Hall, Englewood Cliffs, New Jersey, 1990, Section 6.3.
- [Won91] Wong, C. W., *Introduction to Mathematical Physics*, Oxford University Press, New York, 1991.
- [Woo73] Wooster, W. A., *Tensors and Group Theory for the Physical Properties of Crystals*, Oxford University Press, London, 1973.
- [Woo80] Woodgate, G. L., *Elementary Atomic Structure*, Clarendon Press, Oxford, 1980.
- [Wu57] Wu, C. S., et al., "Experimental Test of Parity Conservation in Beta Decay," *Physical Review*, **105**, 1413 (1957).
- [Yan48] Yang, C. N., "On the Angular Distribution in Nuclear Reactions and Coincidence Measurements," *Physical Review*, **74**, 361 (1948).
- [Yan56] Yang, C. N., and T. D. Lee, "Question of Parity Conservation in Weak Interactions," *Physical Review*, **104**, 254 (1956).
- [Zar87] Zare, R. N., *Angular Momentum*, Wiley, New York, 1987.

- [Zeh89] Zeh, H.-D., *The Physical Basis of the Direction of Time*, Springer-Verlag, New York, 1989.
- [Zha88] Zhao, D., and R. N. Zare, "Numerical Computation of 9-*j* Symbols," *Molecular Physics*, **65**, 1263 (1988).



INDEX

- 3-*j* coefficients, 269–285
 algebraic values for, 281
 and rotation matrix elements, 286–300
 basic formulas in terms of, 270–271
 by computer algebra, 283
 classical limits of, 278–280
 compared to Clebsch-Gordans, 271
 computation of, 280–285
 derivation of, 269–270
 in rational-fraction form, 283–284
 key formulas for, 425–428
 parity-conservation coefficients, 274
 programs for, 285
 Regge symmetries for, 282–283
 symmetries of, 272–273
 tabulations of, 281–282
 visualizing, 272, 276–278
 with all projections zero, 274–275, 278
- 6-*j* coefficients, 345–360
 algebraic expressions for, 352–354
 computation of, 359–360
 definition of, 347
 deriving formulas for, 350–354
 expansion formulas involving, 350–351
 key formulas for, 431–433
 Mathematica notebook Alg6j, 354
 numerical example of using, 357–358
 orthogonality relations, 355
 properties of, 354–360
- Regge symmetries for, 360
 symmetries of, 355–357
 tabulations of, 354
 triangle conditions, 349
- 9-*j* coefficients, 370–380
 algorithms for, 372–374
 definition of, 370–371
 expansion formulas involving, 371–372
 key formulas for, 433–435
 parallel processing to compute, 373
 programs for, 373–374
 special values of, 375–376
 sum rules for, 376
 symmetries of, 375
- Abelian group, 79
 active rotations, 13–15
 active transformations, 54
 Adams, D. A., 72, 437
 addition theorem
 for spherical harmonics, 138
 Adhikari, S. K., 197, 437
 adjoint, *see* Hermitian conjugate
 alias rotations, *see* passive rotations
 alibi rotations, *see* active rotations
 Alisauskas, S. J., 373, 437
 Altmann, S. L., 72, 437
 ammonia molecule symmetry group, 73, 83
 Andrews, M., 135, 437

First authors are referenced in full on the pages with numbers printed in italics.

- angular momentum:
 and development of quantum mechanics, 204–206
 and spherical tensors, 305
 and time reversal symmetry, 29
 atomic, 121
 ball bearing, 121
 classical limit, 172
 combining vs. coupling, 252
 commutation relations, 97–99
 conceptual and historical development, 203–206
 dimensions of, 171
 dimensions of operators, 96
 Earth, 121
 eigenvectors for $j = 0, 1/2, 1, 3/2$, 119
 galactic, 121
 geometrical and dynamical, 120–122
 graphical methods for recoupling, 380–381
 interpreting coupling, 255–258
 jackknife case, 256
 of displacement vector, 151
 of light, 155
 operator representations, 96, 105–113
 operators as spinors, 112
 orbital, *see* orbital angular momentum
 Pauli matrix representation, 105–111
 role of Planck's constant in, 171–172
 semiclassical vector model, 189
 stretched case, 256
 triangle rules for combining, 253–255
 uncertainties in quantal, 179–189
 uncertainty with angles, 186–189
 waves and, 193–203
- angular momentum basis, 151
- angular momentum conservation, 4
 in central potential, 4
 Noether's theorem for, 4
- angular momentum eigenstates, 127–165
 recoupling four, 370–381
 recoupling three, 345–354
 rotation matrix elements as, 241–242
- angular momentum eigenvalues, 113–116
- angular momentum matrix elements, 116
 for $j = 1/2, 1, 3/2$, 119–120
- angular momentum operators:
 as tensors, 311
 in Cartesian basis, 97
 in spherical basis, 99
 reduced matrix elements, 323
- antenna pattern, *see* polar diagrams
- antilinear operators and time reversal, 45
- antiparticles and charge conjugation, 25
- Arfken, G., 41, 437
- Armstrong, M. A., 73, 437
- arrow of time, 27
 and time-reversal symmetry, 26
 in microworld, 30
- Arthurs, A. M., 297, 437
- associated Legendre functions,
see Legendre functions
- asymmetric rotator, 244
- Australia, 19
- Avery, J., 149, 437
- Avetisov, V. A., 36, 437
- ball bearing angular momenta, 121
- bandhead, 244
- Bargmann, V., 283, 437
- Bauer, G., 194, 437
- Bell, D. G., 149, 438
- Bernal, I., 73, 438
- Bessel functions:
 cylindrical, 196–197
 spherical, 194–195
 visualizing cylindrical, 197
 visualizing spherical, 194
- Beth, R. A., 156, 438
- Bevington, P. R., 291, 438
- Bialynicki-Birula, I., 159, 438
- Biedenharn, L. C., 25, 72, 124, 135, 156, 187, 189, 206, 241, 315, 351, 356, 385, 438
- biological systems, 35
- bipolar harmonics, 314
- block-diagonal matrices, 51
- body-fixed frame, 240–241
 quadrupole moment in, 321
- Bohr, N., 205, 438
- Bohr magneton, 175
- Bolker, E. D., 72, 438
- Born, M., 205, 438
- Bouten, M., 16, 438
- bra space, 43
- Brewer, J. W., 6, 438
- Brink, D. M., 163, 315, 320, 351, 376, 381, 385, 438
- broken symmetries, 34–36
 and organic molecules, 36
 in biological systems, 35
 in spin transport, 338
- Brussaard, P. J., 236, 438
- buckminsterfullerene, 12
- buckyball, 12
- Bunch, B., 438

- Burns, G., 73, 438
 Butkov, E., 41, 193–195, 438
- C programs, 407–419
 3- j coefficients, 282, 284, 285, 302, 412
 6- j coefficients, 352, 359, 415
 9- j coefficients, 373, 383, 417
 compared with Fortran and Pascal, 408
 multi-use C functions, 408
 reduced rotation matrix elements, 224, 410
- canonical transformations, 55
 Carroll, L., 157, 438
 Cartan, E., 72, 439
 celestial bodies, integrals for, 295–296
 central potential, 4
 angular momentum conservation in, 4, 173, 206
 centripetal barrier:
 in partial-wave expansion, 199
 Char, B. W., xiv, 439
 charge conjugation symmetry, 21, 25
 and antiparticles, 25
 Cheshire cat, 157
 chirality, 8
 of *Neogloboquadrina pachyderma*, 35
 Chung, F., 12, 439
 classical limits:
 Ehrenfest theorems and, 172–174
 of 3- j coefficients, 278–280
 of angular momentum, 172
 of rotation matrix elements, 236, 239
 size of j for, 192, 239
 classical mechanics:
 and parity symmetry, 23
 quantum analogues for precession, 190–192
 quantum analogues of, 172–173, 258
 Clebsch, A., 48, 264, 439
 Clebsch-Gordan coefficients, 48, 264–268,
 see also 3- j coefficients
 definition of, 264
 derivation from spinor representations, 266–268
 for $J = 0$, 268
 for $j_2 = 0$, 268
 unitarity properties, 264–265
 Clebsch-Gordan series, 286–291
 and differential cross sections, 290–291
 for integrals of rotation functions, 292–294
 Legendre polynomials and, 288–289
 special cases of, 288–291
 Cohen-Tannoudji, C., 41, 439
 combining angular momenta, 252
 density distributions for, 277
 importance of phases, 273–274
 Commins, E. D., 33, 439
 commutation and Hermitian matrices, 66
 commutator:
 and exponentials, 58
 and Hermitian conjugate, 59
 and uncertainties, 180
 classical limit and, 172
 of angular momenta, 97, 124
 spherical tensor and angular momentum, 309
 complex conjugation
 and time-reversal symmetry, 28
 composite groups, 86–87
 computer programs in C:
 for 3- j , 6- j , 9- j coefficients, 407–408
 for reduced rotation matrix elements, 407–408
 computer requirements
 for *Mathematica* notebooks, 388
 Condon, E. U., 136, 205, 439
 Condon and Shortley phase convention, 267
 connections between angular momenta;
 geometrical, quantal, classical, 171
 continuous groups, 84–85
 contraction of spherical tensors, 315
 Cornwell, J. F., 73, 81, 89, 439
 cosmetology, 35
 cosmos, 35
 Coulomb parameter, 38
 Coulomb potential and degeneracy
 of energy states in, 258–263
 Coulomb scattering, 34, 38
 partial-wave expansion, 198
 Coupling, L. S., 256, 439
 coupling angular momenta,
 see combining angular momenta
 coupling coefficients, definitions
 and general properties, 263–268
 coupling schemes
 see L - S and j - j coupling
 Crick, F., 9
 crystals, 11
 Curie, Marie, 7
 Curie, Pierre, 7, 203, 439
 Curie's principle, 6
 cyclic group, 84
 cylindrical Bessel functions, 196–197
 visualizing, 197, 208

- Danby, J. M., 295, 439
 Danos, M., 381, 439
 Dash, J., 258, 439
 Davies, P. C. W., 27, 439
 De Lange, O. L., 42, 439
 de-Shalit, A., 380, 439
 decomposition theorem
 for spherical tensors, 364
 density distributions
 for combining angular momenta, 277
 density matrices for spins, 325–330
 rotation of, 327–330
 spin polarizations, 327
 determinants, 23
 for rotations and reflections, 38
 diagonal matrices, 64–66
 and eigenvectors, 66
 and Hermitian matrices, 66
 differential cross sections
 and Clebsch-Gordan series, 290–291
 dihedral group, 84
 dimension of a representation, 81
 dimensions of angular momentum, 96, 171
 Dirac, P. A. M., 158, 439
 Dirac equation, 25, 159
 and time reversal symmetry, 30
 Dirac strings, 72
 direct products, 47–49
 and separable Hamiltonians, 49
 and spin, 48
 compared with inner products, 49
 of groups, 80
 of matrices, 90
 discrete rotations and groups, 74
 discrete symmetries, 21–34
 and quantum systems, 21
 displacement vector angular momentum, 151
 DNA molecules, 9, 36
 Dodd, J. N., 155, 439
 Down Under, 19
 Dubos, R., 9, 439
 Duplessy, J.-C., 35, 440
 dynamical angular momentum, 122
 rotational symmetries and, 170–179
 Earth's angular momentum, 121
 eccentricity vector:
 classical, 259–261
 history of, 261
 quantal operator, 261–263
 Eckart, C., 205, 317, 318, 440
 Egyptian pyramids, 8
 Ehrenfest, P., 172, 440
 Ehrenfest theorems, 172–174
 and three types of angular momentum,
 174
 for momentum, 172
 for orbital angular momentum, 173, 206
 eigenstates, 63–67
 of angular momentum, 127–165
 of orbital angular momentum, 127–149
 of rigid rotator, 244–245
 of spin, 156–165
 with spin-orbit interaction, 256
 eigenvalues, 63–67
 degeneracy of
 in Coulomb potential, 258–263
 etymology of, 64
 eigenvectors:
 and diagonal matrices, 66
 as basis states, 66
 of Pauli matrices, 108
 of vector spin, 154
 Einstein, A., 8, 203, 440
 Einstein summation convention, 98
 Eisberg, R., 258, 440
 electromagnetic field intrinsic spin, 155
 Elliott, J. P., 30, 57, 73, 81, 163, 318,
 380, 440
 ellipsoidal harmonics, 149
 enantiomers, 9
 energy conservation, 3
 Noether's theorem for, 3
 Englefield, M. J., 87, 263, 440
 Erdélyi, A., 221, 235, 440
 Euclidean group, 87
 Euler angles, 14, 97, 212
 expectation value in mixed state, 327
 exponentials:
 and commutators, 58, 91
 of operators, 58, 91
 of Pauli matrices, 125
 extraterrestrial life, 9
 Fack, V., 373, 440
 factorials for efficient computing, 284–285
 factorization theorem:
 example of using, 362
 for spherical tensors, 361–362, 364
 faithful representation, 82
 Fang, D. F., 285, 360, 374, 440
 Faxen, H., 194, 440
 Ferraro, J. R., 73, 440
 Feynman, R. P., 191, 440
 Fitzgerald, E., 385
 Flood, R., 30, 440

- Formánek, J., 197, 440
- formulas:
 tables of key, 421–435
- Fourier expansions, 197
- Frescura, F. A. M., 72, 440
- friendly-giant group, 79
- Froggatt, C. D., 87, 440
- Frisch, K., 35, 440
- g -factor, 175
 Landé formula for, 365
- galaxy
 angular momenta of, 121, 122
- Galilean invariance:
 and electron g -factor, 159
 and spin, 159
- Gallian, J. A., 35, 441
- Gardner, M., 9, 25, 27, 441
- gauge invariance, 17
- Gaunt integrals, 294
 examples of, 295–300
- Gaunt, J. A., 294, 441
- generalized coordinates, 54
- geometric symmetry, 7
- geometrical angular momentum, 120
- Georgi, H., 158, 441
- Gibson, W. M., 88, 441
- giraffe, and shirt-and-tie theorem, 47
- Goepfert-Mayer, M., 258
- Goldstein, H., 65, 66, 176, 242, 261, 441
- Gordan, P., 48, 264, 441
- Gordy, W., 245, 441
- Gorenstein, D., 79, 441
- gradient operator as a rank-1 tensor, 311
- graphical methods for angular momentum
 recoupling, 380–381
- Greiner, W., 385, 441
- Grinstein, L. S., 6, 441
- groups, 72–89
 Abelian, 79
 and continuous rotations, 77, 213
 and discrete rotations, 74
 and permutations, 75
 and reflections, 75
 as measuring symmetry, 90
 composite, 86–87
 continuous, 84–85
 definition of, 73–79
 direct product, 80
 Euclidean, 87
 examples, 73–79
 for Coulomb problem, 263
 for subatomic physics, 87
 formal definition of, 78
 homomorphisms of, 79
 isomorphisms of, 79
 Lorentz, 87, 92
 matrix, 85
 order of, 79
 orthogonal, 86
 Poincaré, 87
 point, 84–85
 representations of, 80–84
 special, 86
 subgroup of a, 79
 symmetry examples, 74–78
 terminology for, 79–80
 unitary, 86
 used in physical sciences, 86–87
- Halprin, A., 158, 441
- Hamermesh, M., 73, 441
- Hamiltonian of rigid rotator, 242–244
- handedness, 8
see also helicity
- handwaving in angular momentum, 8
- Hargittai, I., 11, 441
- harmonic oscillator
 and ladder operators, 62
- Hawryshyn, C. W., 35, 441
- Heck, A., xiv, 441
- Heisenberg, W., 205, 441
- Heisenberg uncertainty relations
see uncertainties
- helicity, 9
 of shell, 36
- Hermitian conjugate, 50
 of commutator, 59
- Hermitian matrices:
 and diagonal matrices, 66
 and eigenfunctions, 67
- Hobson, E. W., 129, 149, 441
- homomorphisms:
 and group representations, 81
 of groups, 79
- Houtappel, R. M. F., 25, 441
- hyperspherical harmonics, 149
- Indians, 18
- inertia tensor, 307
- infinitesimal rotations:
 and angular momentum, 97–98
 applied to spatial functions, 100–103
 of vectors, 152–155
- initiation rites and spectroscopic
 notation, 258

- inner products, 44
 - compared with direct products, 49
 - of matrices, 45–47
- integrals of rotation functions, 292–294
- intermediate coupling, 368
- intrinsic spin:
 - of electromagnetic field, 155
 - of vectors, 154
 - see also* spin
- inverse Clebsch-Gordan series
 - for rotation matrix elements, 286–287
- irreducibility:
 - of a representation, 88–89
 - of \mathbf{J}^2 and J_z matrices, 115
 - of matrices, 52
- irreducible spherical tensor operators
 - see* spherical tensors
- isomorphisms of groups, 79
- isospin operators, 118
- isotropy of space, 12
- j - j coupling, 369
- jackknife case:
 - 3- j with all projections zero, 274
 - for angular momentum, 256
- Jacob, M., 124, 442
- Jacobi polynomials and reduced rotation matrix elements, 221–222
- Jammer, M., 206, 442
- Jones, M. N., 149, 315, 385, 442
- Jonkers, J. E., 235, 442
- Jordan, T. F., 42, 45, 54, 67, 111, 442
- Judd, B. R., 380, 385, 442
- Kepler, J., 203, 442
- Kerrigan, J. F., 408, 442
- ket space, 42
- Khayyam, O., 385
- Kobe, D. H., 17, 442
- Kopal, Z., 295, 442
- Kramer's degeneracy, 164
- Kramers, H. A., 165, 442
- Krane, K. S., 331, 442
- Kronecker product, *see* direct products
- Kubic harmonics, 149
- L - S and j - j coupling, 367–369
 - transformations between, 377–380
 - transforming between for spin 1/2, 378–379
 - worked example of transforming between, 379–380
- ladder operators, 59–63, 91
 - and harmonic oscillator, 62
 - angular momentum eigenvalues from, 113–115
 - spectrum of, 61
 - spherical harmonics by, 136–137
- Lai, S.-T., 285, 360, 374, 442
- Landau, R. H., 25, 124, 159, 198, 258, 290, 442
- Landé, A., 190, 205, 442
- Landé g -factor formula, 365
- Landsberg, P. T., 30, 442
- Lapidus, I. R., 197, 442
- Laplace, P. S., 260, 442
- Laplace equation, 127–129
- Larmor precession, 175–179, 332
 - frequency, 176
 - visualizing, 177, 190
- latitude, 17
- Lee, T. D., 10, 290
- Legendre, A. M., 284, 442
- Legendre functions, 129–135, 165
 - and reduced rotation matrix elements, 221
 - displaying, 131–135
 - formulas for, 130–131
 - key formulas for, 421
 - orthogonality of, 130
 - parity of, 130
 - stretched in m , 131
- Legendre polynomials, 129–130, 194
 - and Clebsch-Gordan series, 288–289
 - integral of product of three, 293
- Legendre's formula for primes, 284
- Lenz, W., 261, 443
- Levinger, J. S., 106, 443
- Lévy-Leblond, J.-M., 59, 159, 443
- light, angular momentum of, 155
- linear operators, 45
- linear spaces, 42–45
 - and conventional vectors, 43
 - scalar products in, 44
- Lipkin, H. J., 53, 443
- longitude, 17
- Lorentz group, 85, 87, 92
- Lovett, D. R., 306, 443
- lowering operator, *see* ladder operators
- Lubanski, J. K., 124, 443
- Lüder's theorem, 32–33
- Lüders, G., 32, 443
- Ludwig, W., 318, 380, 443
- Mach, E., 203, 443
- Maeder, R., xiii, 443
- magnetic fields:
 - Hamiltonian in, 331

- spin precession in, 330–335
- spin transport through gradients, 335–340
- magnetic moment, 175
- Majorana, E., 177, 443
- Majorana formulation of spin precession, 177–179
 - rotational symmetries and, 179
 - spinor representations and, 177
 - time-evolution operator, 178
 - visualizing, 178
- Marquez, L., 198, 443
- Martin, G. E., 11, 443
- Mathematica*, 387–389
- Mathematica* notebooks, 387
 - 3j000, 278, 399
 - Alg3j, 281, 283, 342, 400
 - Alg6j, 353, 359, 381, 403
 - animated visualizations, 389
 - BesL, 194, 208, 394
 - BesM, 197, 208, 395
 - Djj0, 238, 399
 - DjjmCpr, 238, 249, 398
 - Djm'm, 221, 222, 224, 229, 231, 232, 237, 248, 249, 397
 - EXPimPHI, 141, 166, 393
 - index of topics, 405
 - LegProd, 289, 401
 - Num3j, 275, 399
 - Num6j, 357–359, 403
 - Num9j, 373, 379, 383, 403
 - PauliCC, 34, 390
 - PL, 132, 133, 391
 - PLM, 133, 134, 165, 166, 391
 - Polyhedra, 11, 389
 - Ppsi, 24, 390
 - Precess, 191, 207, 393
 - programming conventions, 388
 - purpose of, 387
 - PW2D, 201, 202, 209, 396
 - PW3D, 200, 208, 395
 - Shell, 10, 389
 - VccDnsty, 277, 400
 - WorldView, 18, 390
 - YLMabs, 140, 392
 - YngThm, 291, 402
- mathematics; relation to physics, 169–170
- matrices:
 - block-diagonal, 51
 - diagonal, 64–66
 - irreducible, 52
 - operations on, 50
 - symmetry properties of, 51
- matrix elements of operators, 45
- matrix groups, 85
- matrix products:
 - see direct products, 45
 - see inner products, 45
- Maxwell equations:
 - and PCT, 30–32, 38
 - and vector spherical harmonics, 315
 - intrinsic spin, 155
- Meiring, W. J., 36, 443
- mindset in mathematics
 - and physical sciences, 89
- minimum-uncertainty state, 182
 - for angular momentum and angle function, 187–189
 - for momentum and position, 182
 - for orbital angular momenta 185, 207
 - visualizing, 186, 188
- Misner, C. W., 72, 443
- mixed state, 326
- molecular rotational states, 245
- momentum conservation, 2
 - Noether's theorem for, 2
- monster group, 79
- Morette-de Witt, C., 156, 444
- Morse, P. M., 149, 444
- mosaics, 10
- multipole expansion:
 - for scattering interaction, 298
 - matrix elements of, 365–367
- multipole moments, 298
 - matrix elements of, 299
- Neogloboquadrina pachyderma*, 35
- Nernst, W., 205, 444
- Neumann's principle, 6
- New Zealand, 19
- Newton, I., 203, 444
- nirvana, 326
- Noether, E., 6, 203, 444
- Noether's theorem, 5, 36
 - and conservation of
 - angular momentum, 4
 - and energy conservation, 3
- Nolte, E., 33, 444
- noncommuting of rotations, 19
- norm of a vector, 44
- normal modes, 66
- Normand, J. M., 325, 444
- notebooks for *Mathematica*, 387–389
- Nuclear Data Sheets, 247, 444
- nuclear magnetic resonance, 175
- nuclear magneton, 175
- nuclear rotational states, 246

- oblate rotator, 244
 - charge distribution of, 321
- Ohanian, H. C., 156, 160, 444
- operations on matrices, 50–52
- operators, 53–63
 - angular momentum, 96
 - antilinear, 45
 - exponential of, 58
 - linear, 45
 - noncommuting and uncertainties, 180–181
- orbital angular momentum:
 - connection to mechanics, 102–103
 - Ehrenfest theorems for, 173
 - eigenstates of, 127–149
 - operators, 100–105
 - operators in spherical basis, 104–105
 - operators in spherical polar coordinates, 103–104
 - quantum-mechanical, 102
 - reference frames and, 122–124
 - special role of z component, 105
- orthogonal group, 86
- orthogonal transformation, 57
- Ozma problem, 9

- parallel processing for $9-j$ coefficients, 373
- parity symmetry, 21, 22–25
 - and rotations, 22
 - in classical mechanics, 23
 - in quantum mechanics, 24, 38
 - of Legendre functions, 130
 - of spherical harmonics, 137
- Park, D. A., 258, 444
- partial-wave expansion:
 - centripetal barrier in, 199
 - convergence of, 198
 - for Coulomb scattering, 198
 - in three dimensions, 193–196
 - in two dimensions, 196–197
 - visualizing, 199–203
- passive rotations, 16
- passive transformations, 54
- Pasteur, L., 9, 203, 444
- Pauli, W., 159, 261, 444
- Pauli equation, 159
- Pauli matrices:
 - anticommutation property of, 106
 - as angular momentum operators, 105–111
 - eigenvectors of, 108
 - exponentials of, 125
 - finite rotations and, 109–110
 - in Cartesian coordinates, 106
 - in spherical basis, 107
 - properties of, 106
- Pauli principle, 33–34
 - in scattering, 33, 38
 - limits on validity of, 33
- Payne, W. T., 72, 444
- PCT:
 - and Maxwell equations, 30–32
 - and Pauli principle, 32–33
- pearls dissolve in vinegar, 25
- Peña, L., 59, 444
- permutation symbol, 98
- permutations and groups, 75
- phase factors, 52
 - z -axis rotations and, 110
- phase-manipulation rules, 52–53
- phases when combining angular momenta, 273–274
- photon spin, 155
- physics relation to mathematics, 169–170
- Planck's constant:
 - distinguishes geometrical from dynamical angular momentum, 171
 - dynamical angular momentum and, 171–172
- plane waves, 193–203
 - in one dimension, 197
 - in three dimensions, 193–196
 - in two dimensions, 196–197
 - partial-wave expansion, 193, 196
- planetary rings, spin and, 123
- Platonic solid, 11
 - and groups, 84
- Plattner, G.-R., 34, 445
- Poincaré group, 87
- point groups, 84–85
- polar diagrams, 133
 - for associated Legendre functions, 134
 - for Legendre polynomial, 133
- polyominoes, 11
- Poole, C. P., 176, 335, 445
- position operator
 - reduced matrix elements, 323
- positive-definite norm, 44
- precession, 190
 - see also* Larmor precession
 - of spins in magnetic fields, 330–335
 - visualizing, 191
- precession length, 338
- prime-factor forms:
 - for $3-j$ coefficients, 283–284
 - for $6-j$ coefficients, 359
- primes, Legendre's formula for, 284

- principal axes frame, 242
 principal-axis transformation, 65
 projection theorem
 for spherical tensors, 362–364
 prolate rotator, 244
 charge distribution of, 321
 pure state, 326
 see also nirvana
- quadrilaterals for recoupling, 348–349
 quadrupole moment:
 in body-fixed frame, 321
 reduced matrix elements, 320–322
 spectroscopic, 322
 quantum analogues of classical mechanics,
 172–173, 190–192
 quantum mechanics:
 and parity symmetry, 24–25
 classical analogues of, 258
 development of, and angular momentum
 204–206
 history of, 206
 rigid rotator in, 240–247
 spin and, 124
 uncertainty relations in, 180–183
 quantum-mechanical orbital angular
 momentum, 102
- Racah, G., 204, 309, 445
 Racah coefficients
 see 6- j coefficients
 Racah definition of spherical tensors,
 309–312
 Racah-Wigner algebra, 345
 racemic mixture, 9
 radiation pattern, *see* polar diagrams
 raising operator, *see* ladder operators
 Rao, K. S., 360, 373, 374, 445
 rational-fraction forms:
 for 3- j coefficients, 283–284
 for 6- j coefficients, 359
 Rauch, H., 68, 445
 Rayleigh expansion
 see partial-wave expansion
 recoupling tetrahedra, quadrilaterals,
 and trees, 348–349
 reduced matrix elements:
 conventions for, 320
 for angular momentum operators, 323
 for Hermitian spherical tensors, 324
 general formulas, 324
 how to determine and use, 320–325
 key formulas for, 430
 of position operator, 323
 of quadrupole moment, 320, 322
 selection rules for, 319
 reduced rotation matrix elements, 216–224
 analytical expressions for, 222–224
 computing, 222–224
 numerical values of, 224
 relation to other functions, 220–222
 reference frames:
 orbital angular momentum and, 122–124
 spin and, 122–124
 reflection symmetry, 8
 and groups, 75
 Regge, T., 282, 445
 Regge symmetries
 for 3- j coefficients, 282–283
 regular polygons, 10, 37
 regular polyhedron, 11, 37
 Renaud, P., 7, 445
 representations of groups, 80–84
 examples of, 82–83
 faithful, 82
 identity, 82
 of continuous rotations, 213
 tensors and, 307
 Riccati-Bessel function, 198, 199
 Rieflin, E., 72, 445
 rigid rotator, 240–241
 coupled wave functions, 297
 energy eigenstates of, 244–245
 Hamiltonian of, 242–244
 rigid rotators:
 integrals for scattering by, 296–300
 matrix elements for scattering by, 351
 rigid-body rotations in quantum mechanics
 240–247
 Robson, B. A., 325, 445
 Roman, P., 5, 25, 30, 33, 124, 445
 Rose, M. E., 135, 315, 380, 385, 445
 Rosen, J., 7, 32, 445
 rotated states:
 interpreting, 224–230
 interpreting for any j , 228–230
 interpreting for $j = 1/2$, 228
 orbital angular momentum, 225–227
 rotating-frame transformation, 333–334
 for spin transport in uniform field
 gradient, 336
 spin equation in, 334
 visualizing, 334
 rotation matrices for spin- $1/2$, 111
 rotation matrix elements:
 and coupling coefficients, 286–300

- rotation matrix elements (*continued*)
 arbitrary j , 213–224
 as angular-momentum eigenfunctions, 241–242
 classical limits of, 236–239
 Clebsch-Gordan series, 286, 287–291
 for y -axis rotations, 216–218
 for z -axis rotations, 214–216
 integrals of, 292–294
 integrals of their products, 292–294
 inverse Clebsch-Gordan series, 286–287
 key formulas for, 423
 symmetry properties, 232–234
 unitarity and orthogonality, 234–236
 unitarity integrals, 234–236, 292
 visualizing, 230–232
- rotational band, 244
- rotational invariance, 5
- rotational states of molecules and nuclei, 245–247
- rotational symmetries, 12–19
 and group theory, 205
 and Majorana formulation, 179
 and shells, 10
 dynamical angular momentum and, 170–179
- rotations:
 and groups, 77, 213
 and parity symmetry, 22
 and semiclassical vector model, 218
 angle schemes for, 212
 of density matrices for spin, 327, 330
 Pauli matrix representation, 109–110
 schemes for describing, 96–97
- Rotenberg, M., 282, 354, 445
- Runge–Lenz vector
see eccentricity vector
- Sakurai, J. J., 41–43, 445
- Saturn, 123
 spin of, 156
- scalar products, 44–45
 in linear spaces, 44
 of spherical tensors, 316, 361–365
- scattering:
 in one dimension, 197
 in two dimensions, 197
- Schrödinger equation:
 and parity symmetry, 24
 and time-reversal symmetry, 27–29
 spin in, 158–159
 time-dependent, 172
- Schwarz inequality, 180
- Schwinger, J., 33, 446
- sectorial harmonic, 142–143
- semiclassical vector model, 189–193
 analogies, 190
 and rotations, 218
 and z -axis rotations, 215–216
 for combining angular momenta, 263
 uses and limitations of, 192–193
 visualizing with spinning shell, 207
- Shammas, N., 406, 446
- Shankar, R., 41, 446
- Sharp, R. T., 446
- shell, 10, 36
- shell model, 257
- shift operator, *see* ladder operators
- shirt-and-tie theorem, 46
 and quantum mechanics, 47
- similarity transformations, 54–57
 and unitarity, 57
- Slichter, C. P., 176, 335, 446
- sodium D-line doublet, 257
- solid harmonics, 143–146
- Sommerfeld, A., 190, 205, 446
- Sommerfeld Coulomb parameter, 38
- space, isotropy of, 12
- space-fixed frame, 241
- spatial symmetries, 7–12
- special group, 86
- spectroscopic calculations, 380
- spectroscopic notation, 258
- spectroscopic quadrupole moment, 322
- spherical basis:
 angular momentum matrix elements in, 116–117
 angular momentum operators, 99
 orbital operators in, 104–105
 spherical harmonics in, 144–145
 unit vectors, 150–151
- spherical Bessel functions, 194
 visualizing, 194, 208
- spherical harmonics:
 addition theorem for, 138, 166
 as irreducible tensors, 311
 as rotation matrix elements, 239–240
 calculating, 135–137
 for negative m , 137
 formulas for, 139–140
 in spherical basis, 144–145
 integral over product of three, 294
 key formulas for, 422
 parity of, 137
 properties of, 137–138
 real form of, 146–148

- visualizing, 140–141
- spherical polar coordinates, 103, 128
- spherical tensors:
 - adjoint of, 312
 - and angular momentum, 305
 - and commutators, 309
 - and irreducibility, 309
 - and Maxwell equations, 315
 - and vector spherical harmonics, 315
 - and Wigner-Eckart theorem, 316–320
 - bipolar harmonics, 314
 - building up, 312–315
 - classical field theory and, 315
 - combining, 312–316
 - contraction to scalars, 315
 - decomposition theorem for, 364
 - definitions of, 308–312
 - factorization theorem for, 361–362, 364
 - key formulas for, 429–430, 432–433
 - matrix elements in coupled schemes, 376–377
 - projection theorem for, 362–364
 - Racah definition, 309, 312
 - reduced matrix elements, 317
 - scalar products of, 361–365
 - second-rank from vectors, 314
- spin:
 - and Cheshire cat, 157
 - and conservation of angular momentum, 160
 - and direct products, 48
 - combining with orbital states, 161
 - Dirac equation and wave field, 160
 - eigenstates, 156–165
 - eigenstates of, 160–161
 - Galilean invariance and, 159
 - in Schrödinger equation, 158–159
 - interpretation of, 156–158
 - Kramer's degeneracy, 164
 - matrices for eigenstates, 161
 - planetary rings and, 123
 - quantal systems and, 124
 - reference frames and, 122–124
 - time-reversal symmetry and, 163–165
- spin polarizations, 327
- spin precession:
 - in magnetic field, 176–177
 - Majorana formulation of, 177–179
- spin transport in magnetic field gradients, 335–340
 - for spin-1/2 systems, 339–340
 - vector polarization for spin 1/2, 344
 - visualizing, 340
- spin-orbit interaction, 160, 256–258
 - combining spin and orbital states for, 275–276
 - in atoms and nuclei, 257–258
- spin-orbit splitting, 257
- spin-statistics theorem, 32–33
- spinor representations, 111
 - and Majorana formulation, 177
 - for Clebsch-Gordan coefficients, 266–268
 - for constructing rotation matrix elements, 218–219
 - of angular momentum eigenstates, 162–163
 - visualizing, 178
- spinors, 67–72
 - and rotations through 2π , 72
 - definition of, 67
 - neutron experiment demonstrating, 68
 - representation space, 111–113
 - representing, 69–70
 - rotation of, 70–71
 - spin-1/2 rotations and, 110
 - wave functions and, 68–69
 - y-axis rotations and half-integer spins, 220
 - z-axis rotations and half-integer spins, 216
- standard deviation, 180
- Stedman, G. E., 381, 446
- stretched case:
 - 3-*j* with all projections zero, 274
 - for angular momentum, 256
- Strutt, J. W. (Baron Rayleigh), 194, 445
- Sturm-Liouville differential operators, 67
- subatomic physics, 87
- subgroup, 79
- superposition principle, 24
- symbols in coupling coefficients, 269, 346
- symmetric rotator, 244
- symmetries:
 - and groups, 74–78
 - and humans, 34
 - groups for subatomic physics, 87
 - in logos and hubcaps, 34
 - of matrices, 51
 - reflection, 8
 - see also* parity symmetry
- symmetries and conservation laws, 2–7
- tables of formulas, 421–435
- Taff, L. G., 295, 446
- tensor harmonics, 149
- tensor polarization, 327

- tensors:
 as representations of rotation group, 307
 in physical sciences, 306–307
 nomenclature, 306
 scalars and vectors as, 307
 second-rank, 307
- tesseral harmonic, 142–143
- tetrahedra for recoupling, 348–349
- thermodynamics and time-reversal symmetry, 26
- Thompson, D. W., 35, 446
- Thompson, W. J., 197, 203, 408, 446
- tiles, *see* mosaics
- time reversal operator, 45
- time reversal symmetry, 21, 25–30
 and angular momentum, 29
 and arrow of time, 26
 and complex conjugation, 28
 and Schrödinger equation, 27–29
 and spin, 163–165
 and thermodynamics, 26
- time-evolution operator
 for spin precession, 178
- Tinkham, M., 73, 446
- torture in advanced mechanics courses, 240
- transformations, 53–63
 active, 54
 canonical, 55
 orthogonal, 57
 passive, 54
 similarity, 54–57
- translation symmetry, 10
- transputer, 373
- trees for recoupling, 348–349
- triangle rules:
 for combining two angular momenta, 253–255
 for recombining three angular momenta, 349
- uncertainties:
 between angular momentum and angles, 186–189
 for angular momentum, 179–189
 for momentum and position, 181
 in quantal angular momentum, 183–189
 in simultaneous measurement of angular momenta, 184
 orbital angular momentum and angle functions, 187
 orbital angular momentum and angles, 186
 states with minimal, 181–182
- unit vectors in spherical basis, 150–151
- unit-operator expansion, 46
- unitarity:
 and diagonal matrices, 64
 and similarity transformations, 57
 of rotation matrix elements, 234–236
- unitary group, 86
- Van der Waerden, B. L., 205, 446
- Varshalovich, D. A., 282, 351, 354, 376, 385, 446
- vector
 angular momentum of, 152–155
 as a spherical tensor, 311
- vector cross product
 as spherical tensor, 313
- vector harmonics, 149
- vector model
see semiclassical vector model
- vector polarization, 327
 visualizing rotation of, 330
- vector spherical harmonics, 315
- vector-addition construction for
 combining angular momenta, 252–253
- vector-coupling coefficients
see Clebsch-Gordan coefficients
- Vincent, A., 73, 446
- visualization and symmetries, 90
- visualizing spherical harmonics, 140–141
- Watson, G. N., 9, 195, 446
- waves,
 angular momentum and, 193–203
- Way, J. B., 381, 446
- weak interaction, 10
- Werner, S. A., 68, 447
- Wigner, E. P., 5, 6, 25, 65, 90, 163, 205, 236, 287, 317, 318, 447
- Wigner-Eckart theorem, 316–325
 derivation of, 317–318
 derivation using group theory, 318
 geometry and dynamics, 317
 reduced matrix elements, 317
 schematic of use, 319
- Williams, H. T., 381, 447
- Wolbarst, A. B., 83, 447
- Wolf, A. A., 16, 447
- Wolfram, S., xiii, 447
- Wong, C. W., 41, 42, 67, 99, 128, 129, 143, 443
- Wong, S. S. M., 246, 247, 447
- Woodgate, G. L., 331, 447
- Wooster, W. A., 306, 447

Wu, C. S., 10, 290, 447

Yang, C. N., 10, 290, 447

Yang's theorem, 290

Zare, R. N., 385, 447

Zeh, H.-D., 30, 448

Zhao, D., 373, 448

zonal harmonic, 141–142